ORGANOMETALLICS

Volume 2, Number 5, May 1983

Multistep Cyclometalation of Solid *trans*-Dichloro[3,3′-oxybis[((diphenylphosphino)methyl)-benzene]]platinum(II)

Urs Baltensperger,[1a] John R. Günter,[1a] Stephan Kägi,[1b] Günter Kahr,[1c] and Werner Marty*[1b,2]

Laboratorium für Anorganische Chemie ETH and Tonmineralogisches Labor, ETH Zürich, CH-8092 Zürich, Switzerland, Anorganisch-chemisches Institut, Universität Zürich-Irchel, CH-8057 Zürich, Switzerland, and Institut de chimie, Université de Neuchâtel, CH-2000 Neuchâtel, Switzerland

Received March 30, 1982

A solid complex of a new trans-spanning bis(phosphine) ligand, *trans*-dichloro[3,3′-oxybis[((diphenylphosphino)methyl)benzene]]platinum(II), *trans*-$PtCl_2$(PoP), I, undergoes thermolysis at ca. 250 °C with evolution of 2 mol of HCl to form a doubly cyclometalated complex, [3,3′-oxybis[((diphenylphosphino)methyl)benzen]ato(2−)-C^2,$C^{2'}$,P,P']platinum(II), Pt(PoP-2H), II. Deuterium labeling in different positions (Chart I) shows that during thermolysis, approximately one ortho hydrogen of the phosphino phenyl groups is replaced by a H_A proton (Chart I). This rearrangement is interpreted by a sequence of cyclometalation steps (Figure 5), one of which leads to an intermediate four-membered metallacycle. The reacting solid was investigated by thermogravimetry (TG), derivative thermogravimetry (DTG), differential thermal analysis (DTA), and differential scanning calorimetry (DSC), partly with on-line mass spectral monitoring of the gaseous reaction product, by heating X-ray powder diffraction, and by optical microscopy. The results indicate that a short-lived fluid phase is involved when the reaction is carried out under optimal conditions.

Introduction

Cyclometalations have rapidly become familiar reactions in organometallic chemistry, and this fast growing field has been reviewed several times in the last few years.[3-6] In most of the known examples, an organic molecule is coordinated via an aromatic or aliphatic carbon that has lost a hydrogen atom and via a second donor atom to form one five-membered or, less commonly, a four-membered chelate ring. In some presently less abundant examples, tetradentate ligands are formed in reactions that may be visualized as a sequence of two consecutive cyclometalation steps.

An apparent limitation to such sequential cyclometalations arises when additional rearrangement steps are required for structural reasons. Such limitations will appear even more severe if the cyclometalation steps are irreversible, e.g. in those cases where volatile reaction products (HCl, CH_4, or others) are continuously removed from the reaction mixture. This paper shows that no such limitations exist in the reaction I → II (Figure 1) where a doubly cyclometalated product is formed in high yield from the solid starting material. This transformation requires a trans to cis rearrangement of two phosphorus donor atoms at some stage of the reaction.

The success of this reaction raises the following questions: "what chemical mechanisms can accommodate this complicated sequence of steps?" and "which physical state of the reaction mixture is able to accommodate this process in the absence of solvent?". This paper accordingly presents the results of a series of deuterium-labeling experiments to elucidate the nature of some intermediates of this transformation as well as experiments designed to characterize intermediate physical states of the reacting material.

Experimental Section

Physical Methods. ^1H and ^{31}P NMR spectra were measured at ambient temperature on a Bruker HX90 instrument in the FT mode at 90 and 36.43 MHz relative to internal Me_4Si and external H_3PO_4 standards, respectively. IR spectra were recorded on a Beckman IR 4250 instrument to ±5 cm^{-1}. Mass spectra were run on a Hitachi Perkin-Elmer RMV 6M instrument at probe temperatures between 130 and 200 °C and at an acceleration voltage of 4.2 kV. In the elemental analyses of deuterated samples, H and D were determined as H_2O and the theoretical values were

(1) (a) Universität Zürich. (b) Laboratorium für Anorganische Chemie, ETH. (c) Tonmineralogisches Labor, ETH.
(2) To whom correspondence should be addressed at Institut de chimie, Université de Neuchâtel, CH-2000 Neuchâtel, Switzerland.
(3) Omae, I. *Coord. Chem. Rev.* **1980**, *32*, 235.
(4) Bruce, M. I. *Angew. Chem., Int. Ed. Engl.* **1977**, *16*, 73.
(5) Dehand, J.; Pfeffer, M. *Coord. Chem. Rev.* **1976**, *18*, 327.
(6) Parshall, G. W. *Acc. Chem. Res.* **1975**, *8*, 113.

0276-7333/83/2302-0571$01.50/0

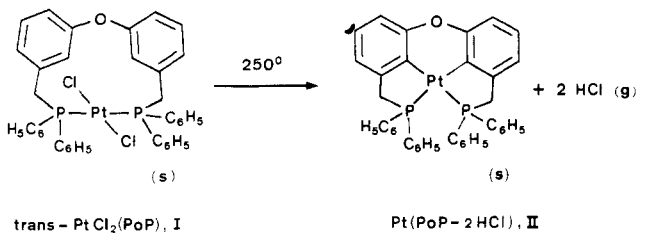

Figure 1. Thermal dehydrohalogenation of *trans*-$PtCl_2$(PoP) (I) to Pt(PoP-2H) (II).

determined on this basis. Molecular masses were determined by vapor pressure osmometry. Thermal analyses were carried out on 20-mg samples of I on a Mettler thermoanalyzer TA-1 or on a Perkin-Elmer thermogravimetric system TGS-2 either statically in air or under streaming nitrogen (1.9 dm^3/h, heating rate 10 °C/min to 230 °C and then 1 °C/min to 300 °C). Thermoanalysis coupled to mass spectroscopy was performed on a Mettler TM 1 thermobalance coupled to a Balzers Quadrupole QMG 101 mass spectrograph system via a steel capillary.[7] A Perkin-Elmer differential scanning calorimeter DSC-2 was used in the DSC measurements. Heating X-ray powder photographs were taken on a "Nonius" Guinier-Lenné camera,[8] using Cu K_α radiation. The heating rates were varied for all methods used: 1–5 °C/min in TG, DTA, and DSC and 0.5 °C/h–1 °C/min in X-ray diffraction.

Materials and Preparations. All commercial chemicals used were of purum, puriss. or analytical grade. 3,3′-Oxybis[(bromomethyl)benzene] was prepared as described.[9] Chlorobis(pentadeuteriophenyl)phosphine was prepared from benzene-d_6 (>99% D) according to Horner et al.:[10] yield 29–42% based on benzene-d_6. Bis(pentadeuteriophenyl)phosphine was prepared from the chlorophosphine by $LiAlH_4$ reduction:[11] bp 77–79 °C (0.03–0.05 torr); yield 62%; ^1H NMR (1 ± 1)% aromatic proton intensity relative to the P–H proton intensity; IR (cm^{-1}) ν_{C-D} and ν_{P-H} at 2270 (br). Bis(2,6-dideuteriophenyl)phosphine was prepared according to Parshall et al.[12] from triphenylphosphine and deuterium gas (>99.5% D) by using $RuHCl[P(C_6H_5)_3]_3$ catalyst.[12,13] Tris(3,4,5-trideuteriophenyl)phosphine was prepared from (perdeuteriotriphenyl)phosphine[14] and hydrogen gas by using perdeuterated Ru catalyst. The corresponding labeled diphenylphosphines were prepared by reductive cleavage with sodium.[15]

3,3′-Oxybis[(methoxycarbonyl)benzene]. 3,3′-Oxybis[(carboxy)benzene][16] (0.5 g, 1.94 mmol) was suspended in thionyl chloride (8 mL) and heated under reflux (1 h) until the solution became homogeneous. Excess thionyl chloride was evaporated (0.01 torr, 12 h, 20 °C). The residue of solid dicarboxylic acid dichloride was converted into the dimethyl ester as its direct reduction to the diol proved unsatisfactory. It was thus treated (3 h) with pyridine (1 mL) and methanol (30 mL). Crystals of the ester precipitated (300 mg) that were recrystallized once from methanol–benzene and once from methanol alone: mp 126–127 °C; 130 mg (23%); IR (cm^{-1}) 1725, 1715 ($\nu_{C=O}$); ^1H NMR ($CDCl_3$) δ 7.5–7.6 (m, 8 H), 3.46 (s, 6 H). Anal. Calcd for $C_{16}H_{14}O_5$: C, 67.13; H, 4.92. Found: C, 67.07; H, 4.98.

3,3′-Oxybis[(hydroxymethyl)benzene] and 3,3′-Oxybis[(hydroxydideuteriomethyl)benzene]. A solution of the above ester (290 mg, 1 mmol in anhydrous ether (30 mL) was stirred with lithium aluminum hydride (70 mg, 1.84 mmol) in a stoppered flask (5 days, 20 °C). The mixture was then treated with ice and hydrochloric acid. Extraction with chloroform (5 × 20 mL) and removal of solvent gave the solid diol (192 mg, 82%) that was recrystallized from chloroform–petroleum ether: mp 87–88 °C; IR (cm^{-1}) 3260 (ν_{O-H}); ^1H NMR ($CDCl_3$) δ 7.3–6.5 (m, 8 H), 4.65 (s, 4 H), 1.93 (s, br, 2 H). The deuterated compound was prepared by $LiAlD_4$ (>99% D) reduction (crude yield 94%, mp 87–88 °C after one recrystallization): IR (cm^{-1}) 3260 (ν_{O-H}), 3050 (ν_{C-D}). ^1H NMR residual signal at δ 4.65 integrates corresponding to >97% deuteration. Anal. Calcd for $C_{14}H_{14}O_3$: C, 73.03; H, 6.13. Found: C, 72.48; H, 6.16. Calcd for $C_{14}H_{10}D_4O_3$: C, 71.77; H, 7.74. Found: C, 71.58; H, 6.08.

3,3′-Oxybis[(chlorodideuteriomethyl)benzene]. The above deuterated alcohol (2.93 g, 12.5 mmol) was heated with thionyl chloride (15 g, 55 mmol) in chloroform (50 mL) under reflux (2 h). The oil remaining after evaporation (10 torr, 80 °C) was treated with methanol–benzene (12 h) and evaporated to remove residual thionyl chloride. Chromatography (silica gel, benzene) gave 2.5 g (74%) of nearly pure product that was directly used in the ligand synthesis: IR no ν_{O-H} absorption.

3,3′-Oxybis[((diphenylphosphino)methyl)benzene-d_0, -d_4, -d_8, -d_{12}, -d_{12}, -d_{20}, and d_{24}] (PoP-d_0, -d_4, -d_8, -d_{12}, -d_{20}, and -d_{24}; Chart I). All ligands were prepared according to the following procedure for PoP-d_0 from the appropriately labeled diphenylphosphines and 3,3′-oxybis[(halogenomethyl)benzene]. Diphenylphosphine (2.22 g, 11.9 mmol) and butyllithium (5.6 mL, 2.6 M, 11.7 mmol) were added from a syringe to deoxygenated, anhydrous tetrahydrofuran (50 mL) with stirring at 0 °C under nitrogen. 3,3′-Oxybis[(bromomethyl)benzene] (2.08 g, 5.84 mmol) in deoxygenated benzene (12 mL) was then added within 20 min. After the mixture was stirred at room temperature (30 min), the solvent was removed under reduced pressure at 20–40 °C. The residue was distributed between water and chloroform, and the water layer was discarded. The chloroform phase was evaporated in vacuo, and the remaining oil was kept at 10^{-3} torr overnight. Hot, deoxygenated ethanol (10 mL) was added, and the ligand crystallized at 0 °C on constant stirring: yield 2.7 g (80%); mp 87 °C. **PoP-d_0**: IR (cm^{-1}) 3080–3000 (ν_{C-H} aromatic), 2920 (ν_{C-H} aliphatic), 1255 (ν_{C-O}); ^1H NMR ($CDCl_3$) δ 7.9–6.6 (aromatic protons, 28 H), 3.2 (s, 4 H). Anal. Calcd for $C_{38}H_{32}OP_2$: C, 80.55; H, 5.69; P, 10.94. Found: C, 80.38; H, 5.70; P, 10.64. **PoP-d_8**: IR (cm^{-1}) 3065 (ν_{C-H} aromatic), 2920 (ν_{C-H} aliphatic), 2270 (ν_{C-D} aromatic), 1250 (ν_{C-O}); ^1H NMR (CD_2Cl_2) δ 7.35–6.60 (aromatic protons, 20 H), 3.35 (s, 4 H). Anal. Calcd for $C_{38}H_{24}D_8OP_2$: C, 79.44; H, 5.72. Found: C, 78.87; H, 5.54. **PoP-d_{12}**: ^1H NMR (CD_2Cl_2) δ 7.72–6.55 (aromatic protons, 16 H), 3.35 (s, 4 H). **PoP-d_{20}**: IR (cm^{-1}) 3060 (ν_{C-H} aromatic), 2940–2900 (ν_{C-H} aliphatic), 2270 (ν_{C-D} aromatic), 1260 (ν_{C-O}); ^1H NMR (CD_2Cl_2) δ 7.12 (t, $^3J_{H-H}$ = 7.8 Hz, 2 H), 6.85 (d, $^3J_{H-H}$ = 6.5 Hz, 2 H), 6.60 (d + s, 4 H), 3.40 (s, 4 H). Anal. Calcd for $C_{38}H_{12}D_{20}OP_2$: C, 77.82; H, 5.50; P, 10.56. Found: C, 77.82; H, 5.63; P, 10.40. The ligands PoP-d_4 and PoP-d_{24} were not crystallized and were used in situ to prepare the corresponding $PtCl_2$ complexes.

***trans*-Dichloro[3,3′-oxybis((diphenylphosphino)methyl)benzene-d_0, -d_4, -d_8, -d_{12}, -d_{20}, and -d_{24}]platinum(II) ($PtCl_2$(PoP-d_n)).** To a deoxygenated solution of *cis*-$PtCl_2(CH_3CN)_2$[15] (2 g, 5.75 mmol) in acetonitrile (2 mL)–toluene (200 mL) at 80 °C was added the appropriate PoP ligand, e.g., PoP-d_0 (3.2 g, 5.65 mmol). The temperature was kept at 80 °C (2 h) and then at 100 °C (2 h). The resulting clear yellow solution was evaporated to dryness. The residue was dissolved in the minimal amount of methylene chloride and chromatographed on Merck silica gel 60 (70–230 mesh), 4 × 40 cm, with benzene. The product was eluted as a fast moving yellow band, and it was recovered when the solvent was evaporated to dryness. Samples for elemental analysis were dried in vacuo (120 °C, 140 h): yield 4.09 g (87%). ***trans*-$PtCl_2$(PoP-d_n)**: Anal. Calcd for $C_{38}H_{32}OP_2Cl_2Pt$ (η = 0): C, 54.82; H, 3.87; M_r 833. Found: C, 54.63; H, 3.95; M_r (CH_2Cl_2) 853. Calcd for $C_{38}H_{28}D_4OP_2Cl_2Pt$ (n = 4): 54.54; H, 3.91. Found: C, 55.11; H, 4.16. Calcd for $C_{38}H_{24}D_8OP_2Cl_2Pt$ (n = 8): C, 54.36; H, 3.95. Found: C, 54.28; H, 4.04. Calcd for $C_{38}H_{20}D_{12}OP_2Cl_2Pt$ (n = 12): C, 54.04; H, 3.97. Found: C, 54.11; H, 3.99. Calcd for $C_{38}H_{12}D_{20}OP_2Cl_2Pt$ (n = 20): C, 53.52; H, 4.03; P, 8.31. Found: C, 53.59; H, 4.00; P, 8.47. Calcd for $C_{38}H_8D_{24}OP_2Cl_2Pt$ (n = 24): C, 53.27; H, 4.07. Found: C, 53.35; H, 3.95.

Thermal Cyclometalation Reactions on *trans*-$PtCl_2$(PoP-d_n). In a typical preparation, finely crystallized *trans*-$PtCl_2$(PoP-d_0) (73 mg, 0.086 mmol) was placed at the bottom of

(7) Müller-Vonmoos, M.; Kahr, G.; Rub, A. *Thermochim. Acta* **1977**, *20*, 387.
(8) Lenné, H.-U. *Z. Kristallogr.* **1961**, *116*, 190.
(9) Marty, W.; Espenson, J. H. *Inorg. Chem.* **1979**, *18*, 1246.
(10) Horner, L.; Beck, P.; Toscano, V. *Chem. Ber.* **1969**, *94*, 2122.
(11) Kuchen, W.; Buchwald, H. *Chem. Ber.* **1958**, *91*, 2871.
(12) (a) Parshall, G. W.; Knoth, W. H.; Schunn, R. A. *J. Am. Chem. Soc.* **1969**, *91*, 4990. (b) Hallman, P. S.; Stephenson, T. A.; Wilkinson, G. *Inorg. Synth.* **1970**, *12*, 237.
(13) Schunn, R. A.; Wonchoba, E. R. *Inorg. Synth.* **1972**, *13*, 131.
(14) Hamid, A. M.; Trippett, S. *J. Chem. Soc. C* **1967**, 2625.
(15) Gee, W.; Shaw, R. A.; Smith, B. C. *Inorg. Synth.* **1967**, *9*, 19.
(16) v. Schickh, O. *Ber. Deutsch. Chem. Ges.* **1936**, *69*, 242.

a Schlenk tube and covered with a quartz wool plug. A slow stream of nitrogen was passed through the tube via a gas inlet tube. The bottom of the tube was slowly heated to 250 ± 10 °C (2 h) and then to 270 °C (2 h). After this treatment, the remaining off-white powder was recrystallized from methylene chloride–petroleum ether to give colorless crystals (62 mg, 94%). **Pt(PoP-2H,d_0)**: Anal. Calcd for $C_{38}H_{30}OP_2Pt$: C, 60.07; H, 3.98; P, 8.15; M_r 760. Found: C, 60.35; H, 4.12; P, 8.03; M_r (CH_2Cl_2) 771. **Pt(PoP-2H,d_4)**: Anal. Calcd for $C_{38}H_{26}D_4OP_2Pt$: C, 59.70; H, 4.02. Found: C, 59.62; H, 4.22. **Pt(PoP-H-D,d_7)**: Anal. Calcd for $C_{38}H_{23}D_7OP_2Pt$: C, 59.53; H, 4.04. Found: C, 59.45; H, 4.09. **Pt(PoP-2H,d_{12})**: Anal. Calcd for $C_{38}H_{18}D_{12}OP_2Pt$: C, 59.15; H, 4.09. Found: C, 58.70; H, 3.83. **Pt(PoP-H-D,d_{19})**: Anal. Calcd for $C_{38}H_{11}D_{19}OP_2Pt$: C, 58.60; H, 4.14. Found: C, 58.36; H, 3.96. **Pt(PoP-H-D,d_{23})**: Anal. Calcd for $C_{38}H_7D_{23}OP_2Pt$: C, 58.22; H, 4.19. Found: C, 57.63; H, 4.16.

Attempted Cyclometalation of *trans*-PtCl₂ (PoP) in Solution. Portions of the complex (20–100 mg) were heated under reflux or to a maximal temperature of 150 °C for hours to days while nitrogen was bubbled through the solutions. Enough solvent was used to ensure complete dissolution of the solid. The following solvents were used: decahydronaphthalene, dioxane, chlorobenzene, pyridine, and 1,3-dimethylisoquinoline. In no case were detectable amounts of II formed and most of the starting material was recovered. Further experiments were done to study the solution reactivity of I at temperatures where solid I would be converted into 2. A sample of I was heated to 250 °C in decahydronaphthalene in a sealed tube that was contained in an autoclave. A metallic mirror formed, indicating extensive decomposition of the starting material and/or the pyrolysis product. In this experiment, any HCl evolved cannot escape from the system so further experiments were done in solvents with boiling points >250 °C. Samples of I were heated to 250 °C in triethylene glycol and triethylenetetramine, respectively, while a stream of nitrogen was passed through the solution. Darkening of the solutions occurred at >200–220 °C within a few minutes, and extensive decomposition of the complex was suggested by the appearance of a fine, black precipitate. No II was detected in the residue left after these solvents were distilled under reduced pressure.

Results and Discussion

The Structures of Reactant I and Product II and the Reaction Stoichiometry. The new ligand PoP, owing to its "bite" of 11 atoms, is capable of spanning trans positions when acting as a bidentate ligand in square-planar complexes. The presence of two 1,3-disubstituted phenyl rings in the ligand backbone reduces its flexibility such as to favor the formation of a 12-membered trans-chelate ring. Indeed, space-filling models suggest greater strain and nonbonded interactions in a cis chelate than in a trans chelate. The structure of PoP resembles that of the less readily accessible ligand 2,11-bis((diphenylphosphino)methyl)benzo[*c*]phenanthrene, III,[17] the main difference being the greater flexibility of the PoP backbone.

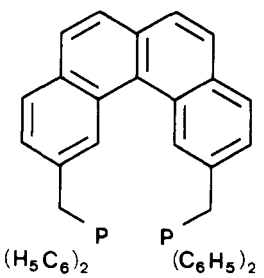

III

The configuration of the main product (87%) of the reaction between PoP and *cis*-$PtCl_2(CH_3CN)_2$, viz., the trans monomer I, is deduced from its ^1H and ^{31}P NMR spectra: the ^1H NMR spectrum (Figure 2 shows the analogous spectrum of *trans*-$PtCl_2$(PoP-d_{20})) features a three-line pattern with Pt satellites ($|^3J_{Pt-H}|$ = 28.4 Hz) for the methylene protons. Such patterns have been observed previously[17,18] and are considered to be due to "virtual" coupling ($|^2J_{P-H} + {}^4J_{P-H}|$ = 9 Hz) characteristic of two P donors in trans position. The aromatic protons appear as three complex patterns (δ 6.25–6.45 (2 H), 7.1–7.25 (4 H), and 7.25–7.6 (20 H) and one moderately broad signal at low field (δ 8.30 (2 H)). The latter is assigned to the H_A protons, and their observed deshielding is characteristic of the monomeric trans-spanning and cis chelations of the ligand as it is not observed in any of the known polymeric species.[19] An appreciable deshielding effect is also observed in analogous trans chelate complexes of III.[17] The ^{31}P NMR shift (δ 16.5 ($CDCl_3$)), and the Pt coupling ($|^1J_{Pt-P}|$ = 2610 Hz) are also consistent with a *trans*-PtP_2Cl_2 central coordination unit.[18,20] The asserted trans structure is also consistent with the IR spectrum (one ν_{Pt-Cl} at 343 cm^{-1}, no band at this position in the analogous bromo compound).

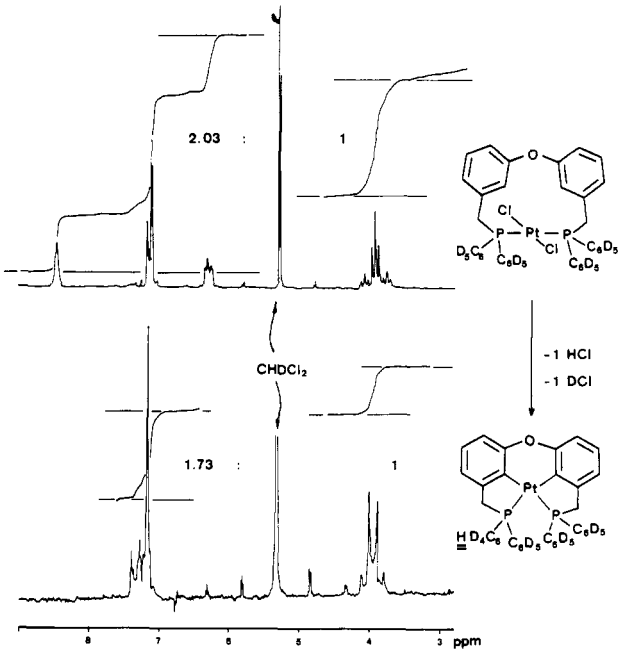

Figure 2. ^1H NMR spectra of *trans*-$PtCl_2$(PoP-d_{20}) and of Pt(PoP-H-D,d_{19}) at 90 MHz in CD_2Cl_2. Chemical shifts in δ units, relative to internal Me_4Si.

The thermal reaction I → II is accompanied by HCl evolution as shown by thermal analysis with on-line mass spectral monitoring of the gas phase that gave peaks at *m/e* 36 and 38 (natural abundance ratio, 3.09, found $H^{35}Cl/H^{37}Cl$, 3.21; Figure 3). Neither H_2 nor Cl_2 were detected among the gaseous reaction products. The proposed reaction stoichiometry (2 mol of HCl/mol of I) was confirmed by the weight loss as determined by thermogravimetry (1.95–2.16 mol of HCl/mol of I). In other experiments, the evolved HCl was absorbed in NaOH and titrated with $AgNO_3$ or HNO_3. These titrations are more precise and do not suffer from interference by sublimation

(17) DeStefano, N. J.; Johnson, D. K.; Venanzi, L. M. *Helv. Chim. Acta* **1976**, *59*, 2683.

(18) Nixon, J. F.; Pidcock, A. *Ann. Rev. NMR Spectrosc.* **1969**, *2*, 381.

(19) These are (*trans*-$PtCl_2$(PoP))$_2$ and (*cis*-$PtCl_2$(PoP))$_n$ (n > 2). Monomeric *cis*-$PtCl_2$(PoP) is not formed in detectable quantities by reacting Pt compounds with the ligand PoP: Kägi, St.; Marty, W., unpublished results.

(20) (a) Reference 18, p 373. (b) Pregosin, P. S.; Kunz, R. W. "NMR Basic Principles and Progress"; Springer Verlag, Berlin, Heidelberg, New York, 1979; 94.

Chart I

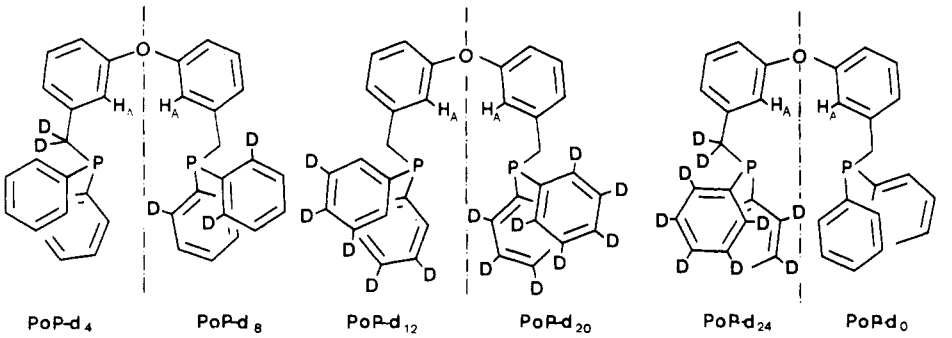

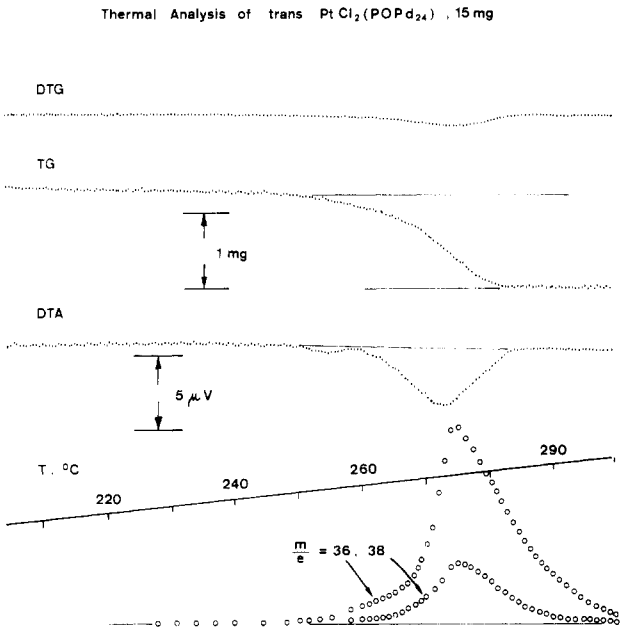

Figure 3. Typical thermogram of thermal dehydrohalogenation reaction I → II. Sample: 15 mg of $PtCl_2(PoP\text{-}d_{24})$. At the bottom is shown the relative mass peak intensity of $H^{35}Cl$ and $H^{37}Cl$ in function of temperature.

or secondary reactions of II; 1.84–1.94 mol of HCl/mol of I were found. Despite many attempts, the transformation I → II was never observed so far in homogeneous solution (see below).

The ^1H NMR spectrum of pyrolysis product II (Figure 2 shows the spectrum of the pyrolysis product of *trans*-$PtCl_2(PoP\text{-}d_{20})$, viz., $Pt(PoP\text{-}H\text{-}D,d_{19})$) shows a different, higher order pattern for the CH_2 protons and there is no low-field proton signal. The ^{31}P NMR chemical shift (δ 39.57) is consistent with the strong deshielding expected for the formation of five-membered chelate rings by cyclometalation.[21,22] The small coupling $|^2J_{Pt-P}| = 2067$ Hz is consistent with σ-bonded carbon trans to the phosphorus nuclei such as in *cis*-$Pt(C_6H_5)_2[P(C_2H_5)_3]_2$ ($|^2J_{Pt-P}| = 1705$ Hz[23]) and in *cis*-$Pt(CH_3)_2(PoP)$ ($|^2J_{Pt-P}| = 1930$ Hz[24]). Two alternative structures for the thermolysis product, viz., IV and V, are ruled out on the basis of the observed strong

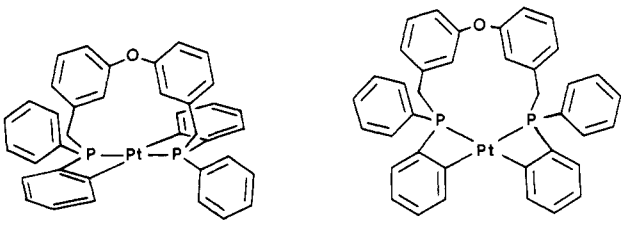

IV V

^{31}P deshielding since formation of four-membered chelate rings by cyclometalation is expected to give a shielding effect.[21] Compound II reacts with bromine to form a tetrabromo compound: two bromine atoms are oxydatively added to Pt and another two substitute aromatic hydrogens in the backbone of the PoP ligand.[27] The X-ray molecular structure of this tetrabromoplatinum(IV) compound has been determined[32] and shows the same arrangement of PoP as proposed for II.

Deuterium-Labeling Studies. The syntheses of the specifically deuterated PoP ligands d_4, d_8, d_{12}, d_{20}, and d_{24} (Chart I) involved the use of differently labeled diphenylphosphines and of 3,3′-oxybis[(chlorodideuteriomethyl)benzene], all of which were prepared following known methods outlined in the Experimental Section. As shown by appropriate blank experiments, our preparative method for *trans*-$PtCl_2$ ($PoP\text{-}d_n$) did not result in detectable loss or scrambling of deuterium. The pyrolysis experiment on *trans*-$PtCl_2(PoP\text{-}d_{20})$ was originally designed to provide an independent means of discriminating between structure II and IV/V. For the formation of II, two hydrogen atoms would be lost (as HCl), but formation of IV or V would require evolution of 2DCl. Rather than determining HCl and DCl in the gas evolved, the resulting complex may be analyzed for its deuterium content by ^1H NMR integration and by mass spectroscopical determination of its molecular mass.[25] In the case of *trans*-$PtCl_2(PoP\text{-}d_{20})$, the observed integral ratio (aromatic H: aliphatic H = 1.73, ≃7:4) is almost exactly intermediate between that anticipated for direct loss of the two H_A protons (6:4) and that for exclusive elimination of two deuterium atoms from the phosphino phenyl groups (8:4). Thus, *one hydrogen and one deuterium are lost from the*

(21) Garrou, P. E. *Chem. Rev.* **1981**, *81*, 229.
(22) Abicht, H. P.; Issleib, K. *J. Organomet. Chem.* **1980**, *185*, 265.
(23) Allen, F. H.; Pidcock, A. *J. Chem. Soc. A* **1968**, 2700.
(24) Kägi, St., unpublished work.
(25) Quantitative determination of DCl and HCl during coupled thermogravimetry/gas-phase mass spectrometry is not possible owing to rapid scrambling DCl + H_2O ⇄ HCl + HDO with traces of humidity in the system. Attempts after extreme drying of the system showed at least qualitatively that DCl was among the gaseous reaction products.
(26) In $(H_5C_6)_3P$, the coupling constants are $^3J_{P-H_2} = 7.5$ Hz, $^4J_{P-H_3} = 1.4$ Hz, and $^5J_{P-H_4} = 0.7$ Hz: (a) Sørensen, S.; Jakobsen, H. J. *Acta Chem. Scand., Ser. A* **1974**, *A28*, 248. (b) Radics, L.; Baitz-Gacs, E.; Neszmelyi, A. *Org. Magn. Res.* **1974**, *6*, 60.
(27) Kägi, St.; Marty, W., to be submitted for publication.
(28) Clerici, M. G.; Shaw, B. L.; Weeks, B. *J. Chem. Soc., Chem. Commun.* **1973**, 516.
(29) Galwey, A. K. "Chemistry of Solids"; Chapman and Hall: London, 1967; Chapter 5.
(30) Günter, J. R.; Bischof, R.; Oswald, H. R. *J. Solid State Chem.* **1982**, *41*, 205.
(31) It may be possible that the reaction occurs in a liquid crystalline phase, but the present experiments do not provide specific evidence for this.
(32) Bürgi, H.-B.; Kägi, St.; Marty, W.; Parvez, M., unpublished work.

starting material. The observed deviations (~±10%) are within the error. The mass spectrum of the pyrolysis product (M^+, *m/e* 778) is consistent with the NMR result; abstraction of 2HCl or 2DCl would require M^+ at *m/e* 777 or 779, respectively. Further confirmation of the *migration* of a proton into a phosphino phenyl group comes from the following observations. The ^{31}P NMR spectrum of the pyrolysis product indicates the presence of two chemically equivalent phosphorus nuclei so that any type of mixed four-membered/five-membered chelate ring structure is ruled out. On the basis of the above ring current argument that supports structure II, the loss of one hydrogen and one deuterium indicates a hydrogen migration from position A to a phosphino phenyl ring. The rearranged proton was observed as a doublet in the 360-MHz ^{1}H NMR spectrum (δ 8.09 (1.0 ± 0.1 H, $^3J_{P-H}$ = 11.7 Hz)). The large P–H coupling constant is indicative of an ortho proton.[26] The assignment of this coupling was checked by its {^{31}P}^{1}H NMR spectrum which showed collapse of the original doublet into a single line.

Pyrolysis reactions on *trans*-PtCl$_2$(PoP-d_8) and on *trans*-PtCl$_2$(PoP-d_{12}) were carried out as an independent check of the ortho regiospecificity in the postulated hydrogen migration to one phosphino phenyl group. In the former, the anticipated loss of an ortho deuterium was verified by ^{1}H NMR (integral ratio aromatic H:aliphatic H = 4.80. Substitution of one D by H requires a ratio of 19:4 = 4.75) and by mass spectroscopy (M^+, *m/e* 766. Pt(PoP-H-D, d_7) requires *m/e* 766). The dodecadeuterio compound did not react with substitution of deuterium by light hydrogen as expected for H_A being transferred into the ortho position of the phosphino phenyl group. (^{1}H NMR integral ratio aromatic H:aliphatic H = 3.51. Calculated ratio for the absence of isotopic rearrangement: 14:4 = 3.50. Mass spectrum: M^+, *m/e* 771. Pt(PoP-2H,d_{12}) requires *m/e* 771). Within experimental error, complete ortho regiospecificity of the hydrogen migration is obtained. Finally, possible participation in hydrogen exchange of the methylene group of the PoP ligand is ruled out by the observation that pyrolysis of *trans*-PtCl$_2$(PoP-d_4) and of *trans*-PtCl$_2$(PoP-d_{24}) did not lead to an increase of the weak residual ^{1}H NMR signals for the deuterated methylene group in the products.

The pyrolysis of *trans*-PtCl$_2$(PoP-d_0) was also carried out under an atmosphere of DCl (~1 atm) to see whether incorporation of deuterium is possible from the gaseous reaction product. The mass spectrum of the resulting product distinctly differs from that of Pt(PoP-2H) prepared under nitrogen. The most intense line of the M^+ pattern is shifted from *m/e* 759 to *m/e* 762, and a detailed analysis of the pattern intensities gave the best fit for an average degree of deuteration of 3.36 D/molecule and for an irregular distribution of d_n species (n = 0–8). Thus deuterium is incorporated from gaseous DCl, and this observation is interpreted below.

Analysis of Mass Spectral Intensity Patterns: Intermediate and Product Formation in the Gas Phase. The intensity patterns of the M^+ ions of the starting materials and of the pyrolysis products were calculated on the basis of the natural isotope abundances for Pt and Cl, whereas the contributions from the ligands were matched against the experimental spectra of the free ligands. The latter spectra show the effects of hydrogenation and dehydrogenation reactions and of incomplete isotopic purity in the case of deuterated species. The spectra of Pt(PoP-2H,d_n) (n = 0, 12) agree satisfactorily with those calculated on this basis (Table I). However, in all cases where loss of one HCl and one DCl is inferred, the agreement is not as good for all lines with $m/e > (M^+ + 2)$ and $m/e < (M^+ - 2)$, and possible reasons for these discrepancies will be discussed below.

The mass spectra of the *trans*-PtCl$_2$(PoP-d_n) species provide a clue to possible intermediates in the transformation I → II in the gas phase. The stability of such intermediates may be judged from their relative pattern intensity. *trans*-PtCl$_2$(PoP-d_0) shows its most intense pattern at *m/e* 795 (M^+ – HCl) and *m/e* 759 (M^+ – 2HCl). Agreement between observed and calculated isotope distribution patterns is good, suggesting no significant source of interference in these dehydrohalogenation reactions (Table I). A broad signal representing a metastable fragment occurred at *m/e* 725, arising from *m/e* (795 – 36) = 759, i.e., [PtCl(PoP-H)]$^+$ or [HPtCl(PoP-2H)]$^+$ producing [Pt(PoP-2H)]$^+$. Clearly, loss of one molecule of HCl leads to an intermediate that reacts directly to form the product in the gas phase reaction.

We now return to the discrepancies between observed and calculated isotope intensity patterns in the pyrolysis products formed with simultaneous HCl/DCl elimination. As suggested by the pyrolysis experiment in DCl atmosphere, these deviations may be due to to random loss of zero, one, or two DCl per molecule and a mixture of differently labeled species of the proper total composition could be formed. Even in the absence of excess hydrogen chloride, such scrambling could occur by a reversible HCl/DCl elimination–addition sequence in the physical state of the reacting system (see below). For comparison, the mass spectrum of *trans*-PtCl$_2$(PoP-d_8) was studied. Here, the intense fragment corresponding to double dehydrohalogenation [PtCl$_2$(PoP-d_8)-2HCl]$^+$ occurs reproducibly at m/e 767, i.e., one unit higher than the mass peak of the solid-state pyrolysis product, [Pt(PoP-H-D,d_7)]$^+$. Thus, the mass spectrometer reaction does not involve a proton migration and follows a mechanism different of that of pyrolysis of the solid. The *isotope intensity distribution patterns* in Table I and Figure 4 show the following characteristics for the mass peaks of the pyrolysis products [Pt(PoP-2H,d_n)]$^+$ and [Pt(PoP-H-D,d_7)]$^+$ and the corresponding gas phase pyrolysis product peaks [PtCl$_2$(PoP-d_n)-2HCl]$^+$.

(i) There is good to reasonable agreement between [Pt(PoP-2H,d_n)]$^+$ and [PtCl$_2$(PoP-d_n)-2HCl]$^+$ for n = 0 and 12, i.e., where there is exclusive loss of HCl. These patterns all show a sharp drop in peak intensity between *m/e* $(M^+ - 1)^+$ and m/e ≤ $(M^+ - 2)^+$ (where M stands also for the doubly dehydrohalogenated fragments of I).

(ii) In contrast with the calculated patterns, this intensity drop is not found in [Pt(PoP-H-D,d_7)]$^+$ and this may at first sight appear characteristic of the situation where there is loss of deuterium.

(iii) Surprisingly, this intensity drop is not found either in [PtCl$_2$(PoP-d_8)-2HCl]$^+$ despite the fact that formation of this fragment is not accompanied by loss of deuterium. This shows that lack of this intensity drop is linked with the presence of ortho deuterium in the phosphino phenyl groups and not necessarily with its abstraction. H/D randomization during pyrolysis that would give rise to a higher intensity of the $(M - 2)^+$ peak is therefore not a satisfactory explanation, and the origin of the $(M - 2)^+$ intensity discrepancy remains unknown. This problem does not, however, affect the mechanistic conclusions for the gas-phase dehydrohalogenation of the M^+ ion.

Mechanistic Interpretation. Chemical Mechanism. The observed migration of one hydrogen atom from position H_A into an ortho position of the phosphino phenyl groups in the course of five-membered metallacycle for-

Table I. Mass Spectra of *trans*-$PtCl_2(PoP\text{-}d_n)$ Species and Their Pyrolysis Products: Observed and Calculated Isotope Abundance Patterns for Selected Fragments[a]

m^+/e	828	829	830	831	832	833	834	835	836	837	838	839	840	841	842	843	844	845	846	847	848	849	850	851
	(a) M^+ Ions																							
$PtCl_2(PoP)$	...	...	58	84	*100*	73	64	27	19	7	(2.3)		*100*	73	62	29	18	6	3	1				
	(1.2)	(0.5)	(52.2)	(75.2)	(100)	(70.5)	(63.8)	(27.5)	(18.0)	(5.9)	60	84	(100)	(71.3)	(60.4)	(26.0)	(16.6)	(5.0)	(2.1)	(0.5)				
$PtCl_2(PoP\text{-}d_8)$									...	10	(59.6)	(82.0)	2, 6	6	52	79	*100*	78	67	34	20	9	4	...
									(2.5)	(9.9)			(1.1)	(3.5)	(48.3)	(74.7)	(100)	(78.8)	(68.9)	(34.8)	(21.8)	(8.2)	(3.4)	(1.0)
$PtCl_2(PoP\text{-}d_{12})$																								
	(b) $M - HCl^+$ Fragments																							
m^+/e	794	795	796	797	798	799	800	801	802	803	804	805	806	807	808	809	810	811	812	813				
$PtCl_2(PoP)\text{-}HCl$	81	100	*100*	59	44	13	6																	
	(62.4)	(90.0)	(100)	(55.6)	(44.7)	(14.9)	(7.2)																	
$PtCl_2(PoP\text{-}d_8)\text{-}HCl$							5	21	78	100	95	56	41	15	5	...								
							(3.1)	(12.2)	(72.7)	(97.4)	(100)	(56.6)	(42.2)	(13.8)	(6.8)	(1.7)								
$PtCl_2(PoP\text{-}d_{12})\text{-}HCl$											8	18	70	98	*100*	66	45	20	9	...				
											1.3	(4.1)	(56.8)	(87.2)	(100)	(64.9)	(49.2)	(20.2)	(9.8)	(3.2)				
	(c) $M - 2HCl^+$ Fragments (First Line) and M^+ of Solid Pyrolysis Product (Second Line)																							
m^+/e	754	755	756	757	758	759	760	761	762	763	764	765	766	767	768	769	770	771	772	773	774	775	776	
$PtCl_2(PoP)$	1	2		5	73	*100*	85	32	22	7														
			4	8	74	*100*	86	29	21	6	1													
$PtCl_2(PoP\text{-}d_8)$			(1.6)	(7.0)	(69.0)	(100)	(89.1)	(29.5)	(20.6)	(7.0)	(1.3)	23	76	*100*	84	37	22	9	3					
										5	10	82	*100*	3	42	22	9	3						
$PtCl_2(PoP\text{-}d_{12})$								3	7	17	37	76.6	(100)	(82.1)	(28.1)	(18.6)	(5.6)	(1.3)	98	52	29	14	5	
										(3.3)	(13.0)				7	14	64	*100*	92	38	23	10	2.5	
																13	71	*100*	(95.2)	(43.2)	(26.4)	(9.5)	(2.9)	
																(4.7)	(65.7)	(100)						

[a] Calculated values in parentheses.

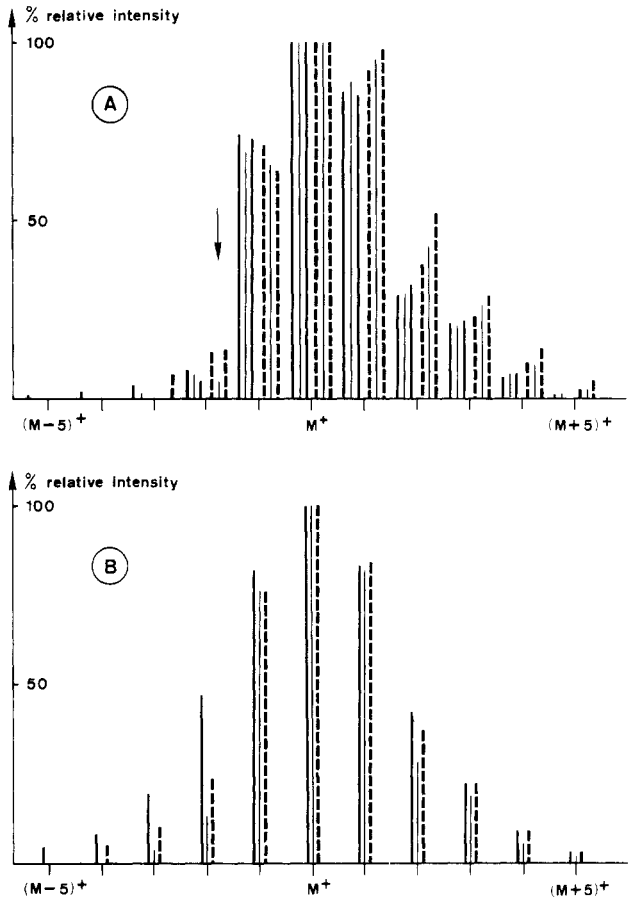

Figure 4. Isotope intensity distribution patterns for mass peaks and fragments arising from double dehydrohalogenation (both abbreviated by M^+): (A) observed pattern (—) for $[Pt(PoP\text{-}2H,d_0)]^+$ on left-hand side and for $[PtCl_2(PoP\text{-}d_0)\text{-}2HCl]^+$ on right-hand side (calculated pattern, thin middle lines); observed pattern (- - -) for $Pt(PoP\text{-}2H,d_{12})$ on left-hand side and for $[PtCl_2(PoP\text{-}d_{12})\text{-}2HCl]^+$ on right-hand side (calculated pattern, thin middle lines); (B) observed pattern (—) for $[Pt(PoP\text{-}H\text{-}D,d_7)]^+$; observed pattern for (- - -) for $[PtCl_2(PoP\text{-}d_8)\text{-}2HCl]^+$ calculated pattern, thin middle line). Note that there is *one mass unit difference in M^+* for the two observed patterns.

mation is unexpected and, to our knowledge unprecedented. It may be interpreted mechanistically as a sequence of two cyclometalation steps. (i) Formation of a four-membered metallacycle that is subsequently opened by the migrating H_A proton. (ii) The carbon from which the migrating proton originated becomes a donor atom in a five-membered metallacycle. Inspection of space-filling models suggests that the ortho positions of the phosphino phenyl groups are well buried inside the complex and that formation of a four-membered metallacycle is more likely than intermolecular metalation unless one phosphine donor is completely detached at some stage of the reaction. However, the exclusive formation of mononuclear pyrolysis product makes this an unlikely prospect. The deuterium scrambling in the pyrolysis under DCl of *trans*-$PtCl_2(PoP\text{-}d_0)$ suggests more than one act of formation of the four-membered metallacycle for any one act of product formation.

The transformation I → II requires trans to cis isomerization of the phosphine donors in addition to hydrogen chloride elimination, most probably in several elementary steps. It is somewhere within this series of events that the inferred formation of a four-membered metallacycle must be placed. The following, additional observations enable us to propose a sequence for these steps. Solid *cis*-$PtCl_2(PoP)$ (prepared by HCl addition to Pt(PoP-2H))

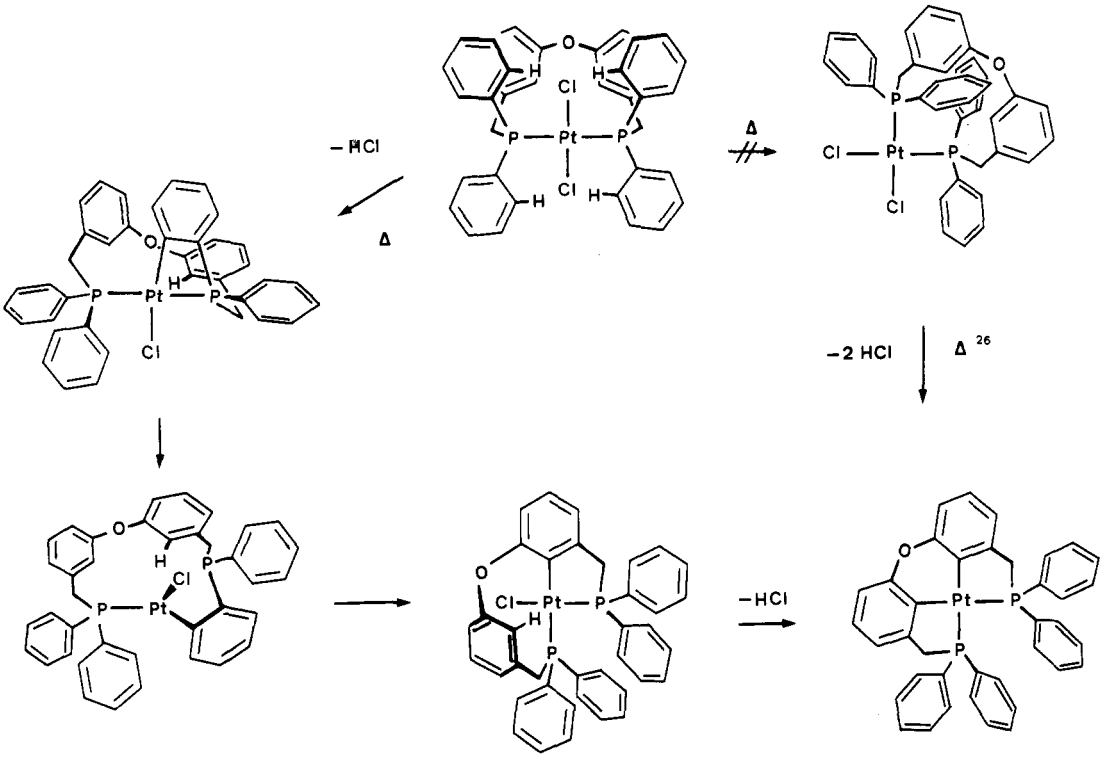

Figure 5. Proposed sequence of mechanistic steps in the thermal dehydrohalogenation of $PtCl_2(PoP)$.

undergoes thermal dehydrohalogenation at ≳250 °C to form II. This isomer therefore fulfills important necessary conditions for being an intermediate in the sequence I → II. However, a pyrolysis experiment on appropriately deuterated *cis*-$PtCl_2(PoP)$ showed the absence of proton migration.[27] From this, we conclude that *cis*-$PtCl_2(PoP)$ is not a likely intermediate of the sequence since its formation would have to precede HCl elimination. This is inconsistent with the observed retention of deuterium in *cis*-$PtCl_2(PoP)$ pyrolysis. Formation of the four-membered metallacycle with HCl elimination is therefore likely to precede or to accompany the trans–cis rearrangement process. We may interpret the formation of a four-membered metallacycle by speculating that its formation assists rearrangement of the phosphine donors. Once this metallacycle is formed, the adjacent phosphine donor may dissociate in order to relieve strain. In this loose arrangement, a first five-membered metallacycle can form while the P donors move into cis positions, and during this process, the proton released from the ligand backbone is inserted into the C–Pt bond of the phosphino phenyl group. In another series of experiments, samples of solid *trans*-$PtCl_2(PoP\text{-}d_{20})$ were heated to 250 °C and rapidly cooled. All these samples showed only the ^{31}P NMR resonances of I and II, and the ^{1}H NMR of recovered starting material showed no evidence for proton migration without dehydrohalogenation. Although these experiments are not particularly sensitive, they argue against the building up of significant concentrations of an intermediate and a fast, reversible proton migration as the initial step of the sequence. The proposed mechanism (Figure 5) accounts for all available information. We finally note that the reaction temperature, while common to the trans and cis isomers, is not very likely to indicate a common intermediate state for the two systems as also solid $Pt(CH_3)_2(o\text{-tolyl})_2PCH_2CH_2CH_2P(o\text{-tolyl})_2$ has been reported to undergo cyclometalation with methane evolution at ≳250 °C.[28]

Solid-State Investigation of the Pyrolysis Reaction. Physical Mechanism. In the course of this work it became ever more evident that the success of reaction I → II depended on a number of subtle variables. We did not vary the reaction conditions systematically beyond the variations described below, and we are therefore not sure whether there are no further variables of which we remain unaware. However, when strictly adhering to the procedures given in the Experimental Section, the preparation of II (from free ligand via I) worked reliably in the hands of several of us. All attempts to produce II in homogeneous solution were unsuccessful. The crystalline modification of I is critical; the crystalline powder obtained by rapid evaporation of the eluate from chromatography reproducibly gave II in >85% yield. On the other hand, samples of I from this source, when recrystallized from ethanol-containing solvent mixtures, gave crystals of essentially the same analytical composition and with identical spectra but with a slightly different X-ray powder diffraction pattern. They decomposed with some HCl evolution at 250 °C, leaving a brownish, glassy residue that was insoluble in the common solvents. The heating rate and the size of the crystals are also important:[29] fast heating (5–10 °C/min) or the use of finely powdered starting material led to complete melting and the product yield was greatly reduced.

The reaction was investigated by the heating X-ray powder diffraction technique.[8] Figure 6 shows a typical run at a heating rate of 1 °C/min. The powder diffraction lines of I remain essentially unchanged up to ca. 250 °C. At very slow heating rates (0.5–2.5 °C/h) the reaction temperature was lowered to ca. 200 °C. Near these temperatures most of the lines fade gradually with new lines growing in. The overlapping of reactant and product lines indicates that there is always a solid phase (I and/or II) present at any temperature. There are no additional lines of an intermediate. The observed influence of the crystal modification and the heating X-ray powder pattern may suggest a genuine solid-state transformation. This possibility is, however, ruled out by observations made on the reacting complex under a hot-stage optical microscope. When a heating rate of 1 °C/min is used at or near 253

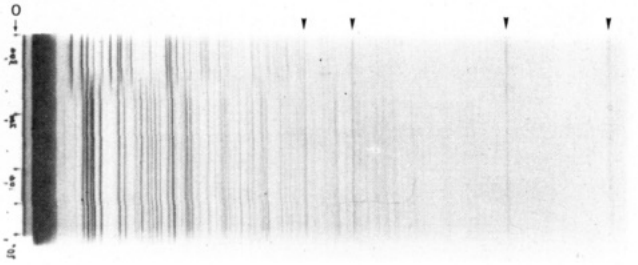

Figure 6. Heating X-ray powder diffraction diagram for thermal reaction I → II. Ordinate: temperature in °C; marks on left margin, 20, 100, 200, and 300 °C from bottom. Abscissa: $d = \lambda/2 \sin \theta$, Å. Arrows: calibration lines from internal Pt standard; from left to right, 2.265, 1.387, and 1.1826 Å; λ = 1.5405 Å.

°C larger crystals of the starting material showed the beginning of a melting process that gradually stopped during the transformation to leave the solid final product. In another experiment, larger crystals were heated to 254 °C at 1 °C/min for a short time to show melting at edges and corners. Heating was then interrupted for 30 min and then continued to higher temperature to cause once more partial melting on the surface of the crystals. Once the reaction was finished, no melting was observed on further heating below the melting point of II. The diffraction pattern of this product is identical with that of a molten (349 °C) and solidified sample. These results show that melting of the reactant is crucial to the reaction. The melt could act as a fluid reaction medium or, less likely, as a catalyst to trigger a solid-state transformation. The observation that some of the powder lines remain essentially unchanged during the reaction is not inconsistent with a melt as the reaction medium since the structures of I and II are similar enough to give rise to coincidence of some powder lines.

The pyrolysis reaction was finally investigated by thermal analysis (TG, DTG, DTA, and DSC). Figure 3 shows a typical run. There was up to 5.3% excess weight loss in the runs and this is explained by sublimation of II under atmospheric pressure as shown by the appearance of crystals of II outside the crucible. While only a single enthalpy effect and one burst of HCl formation are seen in the TG/DTA/MS experiments, two separate, though appreciably smaller enthalpy effects become apparent in the DSC runs, both of which are irreversible. These two peaks are not unambiguously assigned, but one possible interpretation is that in the first process melting occurs along with some chemical step, followed by another chemical reaction. This is supported by the observation that the starting material was never recovered unchanged after melting had taken place.

Attempted Dehydrohalogenation in Solution. Many attempts were made to carry out transformation I → II thermally in homogeneous solution. Solvents of quite different polarity and basicity (see Experimental Section) were used as well as different temperatures up to 150 °C. In every except one experiment (decahydronaphthalene at 250 °C), nitrogen was passed through the solutions to remove rapidly any HCl evolved. Under this range of conditions, a major part of the known cyclometalation reactions would occur but no reaction was observed in all above mentioned experiments.

In three different solvents (decahydronaphthalene, triethylenetetramine, and triethylene glycol), rapid and extensive decomposition of I was found in the temperature range 200–250 °C. We estimate that ca. 10% of II could have gone undetected in these experiments. These experiments are clearly not definitive, but they suggest that reaction I → II is more difficult to achieve in solution than by using solid I.

Conclusions. A novel and interesting concept in preparative chemistry begins to emerge from the present work. The mechanistic studies indicate that the transformation I → II is a complicated multistep sequence that has very little probability to occur via a topotactic[30] or more complex solid-solid transformation process. Indeed, a melting process (only detected by optical microscopy) accompanies the chemical changes and under optimal reaction conditions (i.e., a moderately slow heating rate, the proper crystalline phase, optimal crystal size), the molten phase must be highly unstable with respect to solid product II. This becomes apparent from the heating X-ray powder diffraction as well as from microscopical observations on intermediate-size reacting crystals. Such a short-lived molten phase allows for the extensive internal molecular motion required in the series of proposed mechanistic steps and yet it may not correspond to a homogeneous,[31] thermally equilibrated fluid phase (such as a homogeneous melt or solution); this potentially minimizes certain undesired side reactions, viz., intermolecular reaction with solvent or other solutes. At the same time, the high reaction temperature will ensure rapid transformation into products. The observation that reaction I → II is very difficult if not impossible to achieve in homogeneous solution lends support to the idea that such a highly unstable melt provides a unique reaction medium. The success of this reaction may be due to the following constellation of crucial events: a solid starting material is first transformed into a melt. Under ideal conditions, the lifetime of this melt is kept very short by its high reactivity and by rapid crystallization of the final product. While rapid reaction is favored by the high melting temperature, the last condition is fulfilled by the melting point difference between the starting material and the final product of ca. 100 °C. If a short lifetime of the melt is important, then isothermal heating at a temperature as close as possible to the melting point will give higher product yields than rapid, nonisothermal heating, and this has been confirmed by our experiments. Other factors important to the heat flow in the reacting system are the crystal size and modification of the starting material, both of which have been shown to influence the yield. Clearly, the conditions for a successful reaction in an unstable melt, as restrictive as they may appear, still allow for more molecular motion than a proper solid-state reaction and this reaction type seems therefore more widely applicable than the last.

Acknowledgment. This work was supported by ETH through Grant 13622/41-0410.5. We acknowledge discussions with Professor J. Seibl of ETH on the mass spectra. Drs. G. Balimann and R. W. Kunz kindly recorded the NMR spectra.

Registry No. I, 84369-28-8; II, 84393-87-3; PoP-d_0, 84369-34-6; PoP-d_4, 84369-35-7; PoP-d_8, 84393-93-1; PoP-d_{12}, 84369-36-8; PoP-d_{20}, 84369-37-9; PoP-d_{24}, 84369-38-0; *trans*-$PtCl_2$(PoP-d_4), 84369-29-9; *trans*-$PtCl_2$(PoP-d_8), 84369-30-2; *trans*-$PtCl_2$(PoP-d_{12}), 84369-31-3; *trans*-$PtCl_2$(PoP-d_{20}), 84369-32-4; *trans*-$PtCl_2$(PoP-d_{24}), 84369-33-5; Pt(PoP-2H,d_4), 84393-88-4; Pt(PoP-H-D,d_7), 84393-89-5; Pt(PoP-2H,d_{12}), 84393-90-8; Pt(PoP-H-D,d_{19}), 84393-91-9; Pt(PoP-H-D,d_{23}), 84393-92-0; *cis*-$PtCl_2(CH_3CN)_2$, 21264-32-4; 3,3′-oxybis[(methoxycarbonyl)benzene], 74302-26-4; 3,3′-oxybis[carboxybenzene], 15791-89-6; 3,3′-oxybis[benzenecarbonyl chloride], 19434-44-7; 3,3′-oxybis[(hydroxymethyl)benzene], 84369-39-1; 3,3′-oxybis[(hydroxydideuteriomethyl)benzene], 84369-40-4; 3,3′-oxybis[(chlorodideuteriomethyl)benzene], 84369-41-5; diphenylphosphine, 829-85-6; 3,3′-oxybis[(bromomethyl)benzene], 69484-03-3; chlorobis(pentadeuteriophenyl)phosphine, 72142-98-4; bis(pentadeuteriophenyl)phosphine, 72142-99-5; bis(2,6-dideuteriophenyl)phosphine, 84369-42-6; tris(3,4,5-trideuteriophenyl)phosphine, 84369-43-7.

Chemistry of Boron. 130.[1] The Reaction of Organolithium Compounds with Borane Donors. Preparation and Isolation of Lithium Monoorganotrihydroborates

Werner Biffar, Heinrich Nöth,* and Dieter Sedlak

Institut für Anorganische Chemie der Universität München, D-8000 München 2, F.R.G.

Received August 9, 1982

The reactions of a series of organolithium compounds with the borane donors BH_3·THF, BH_3·SMe_2, and BH_3·NMe_3 have been studied in order to develop a general synthesis of lithium organotrihydroborates, $LiRBH_3$. Starting from RLi and BH_3 in THF, all members of the series $LiR_{4-n}BH_n$ are formed irrespective of reaction conditions. Bulky substituents R prevent the formation of $LiBR_4$, with BR_3 being produced instead. Much higher proportions of $LiRBH_3$ result from the interaction of RLi and BH_3·SMe_2, with low temperature favoring their formation. Crystalline $LiMe_2CHBH_3$ and $LiMe_3CBH_3$ can be obtained by this method in good yield. However, $LiBH_4$ is an inevitable byproduct. Other compounds are also formed in minor quantities. Temperatures of >80 °C are required for the reaction of RLi with BH_3·NMe_3, and $LiPhBH_3$·TMEDA and $LiPhCH_2BH_3$·TMEDA were isolated in 35 and 90% yield, respectively. Increasing the bulkiness of R (e.g., CMe_3) favors deprotonation of BH_3·NMe_3 over amine displacement. Either $LiMe_2NCH_2BH_3$ or $[Me_2NCH_2BH_2]_2$ is formed depending on the reaction conditions.

Introduction

Tetrahydroborates as well as trialkylhydroborates of alkali metals are very versatile reducing agents, the latter being the much stronger ones. Moreover, use of the anions R_3BH^- results in a much higher regio- and stereoselectivity than with BH_4^-.[2,3] In contrast, comparatively little was known about alkali-metal mono- and diorganohydroborates until recently. The main reason for this was that they were not readily accessible. Although this difficulty has now been overcome, most of these compounds have so far been characterized in solution only.[4,5]

The first preparation of a lithium monoorganotrihydroborate originated from the classical studies of complex metal hydrides by H. I. Schlesinger.[6] $LiMeBH_3$ was obtained in the solvent-free reaction (1). This route has

$$LiAlH_4 + B(CH_3)_3 \rightarrow LiCH_3BH_3 + Al(CH_3)_2H \quad (1)$$

$$2C_6H_5Li + B_2H_6 \rightarrow 2LiC_6H_5BH_3 \quad (2)$$

$$Li[(CH_3)_2CH]_3BH + 3[(CH_3)_2CH_2B]_2H \rightarrow LiBH_4 + 3B[(CHCH_3)_2]_3 \quad (3)$$

$$Na(C_2H_5)_3BH + 2(C_2H_5)_2BH \rightarrow NaC_2H_5BH_3 + 2B(C_2H_5)_3 \quad (4)$$

$$MH + B[CH_2CH(CH_3)_2]_3 \xrightarrow{150\ °C} M(CH_3)_2CHCH_2BH_3 + 2(CH_3)_2C{=}CH_2 \quad (5)$$

not yet been reinvestigated in order to test its general applicability. However, a modification using a solvent system has now been developed.[5] Wiberg et al.,[7] in 1958, described the formation of $LiPhBH_3$ in diethyl ether as a solvent by several routes. The compound was obtained free of solvent, but ether and dioxane adducts also were reported, and it has been noted that $LiBH_4$ is readily formed in reaction 2 in the presence of an excess of diborane. The fairly rapid alkyl–hydride exchange among organohydroborates and organoboranes has been used successfully by Köster et al.[8] to prepare both $LiBH_4$ according to (3) or sodium ethyltrihydroborate as described by eq 4 in nearly quantitative yield. $NaC_2H_5BH_3$ is fairly insoluble in hexane, and this contributes to its easy preparation. It decomposes at 100 °C to give $NaBH_4$. The thermal instability of alkali-metal triorganohydroborates has been used by Zakharkin[10] to obtain the Li or Na salt of $(CH_3)_2CHCH_2BH_3^-$ by heating LiH or NaH with triisobutylborane. Under these conditions dehydroboration occurs according to eq 5.

This short survey on monoorganohydroborates shows that this type of compounds was known for some time, in contrast to a recent claim.[4] Finally, the formation of a mixture of $LiR_{4-n}BH_n$ in the reaction of *n*-BuLi with BH_3 in tetrahydrofuran has been reported, but without details concerning the product distribution.[11a] This also holds for the reaction of *n*-BuLi with H_3B·SMe_2.[11b] However, we can confirm these findings, and since our results are complementary, we will include them in the discussion. The present study was initiated by attempts to prepare Me_3N·$BH_2CH_2SCH_3$ as an intermediate en route to boraacetylcholin.[9] This required $Li(CH_3SCH_2)BH_3$ as another precursor. In order to find an effective reaction to produce this monoorganotrihydroborate, we studied the interaction of various organolithium reagents with suitable BH_3 donors, and BH_3·THF, BH_3·SMe_2, and BH_3·NMe_3 were chosen for this purpose.

The Reactions of Alkyllithium Compounds with Borane–Tetrahydrofuran. Considering the large number of known organolithium compounds, reactions according to eq 6 would be the most convenient for preparing lithium monoorganotrihydroborates. This equation rep-

(1) Contribution 129: K. Niedenzu and H. Nöth, *Chem. Ber.*, in press.
(2) S. Krishnamurty, F. Vogel, and H. C. Brown, *J. Org. Chem.*, **42**, 2534 (1977) and literature cited therein.
(3) S. Krishnamurty, *Aldrichchimica Acta*, **7**, 55 (1974).
(4) H. C. Brown, B. Singaram, and P. C. Mathew, *J. Org. Chem.*, **46**, 2712 (1981).
(5) H. C. Brown, B. Singaram, and P. C. Mathew, *J. Org. Chem.*, **46**, 4541 (1981).
(6) Th. Wartik and H. I. Schlesinger, *J. Am. Chem. Soc.*, **75**, 835 (1953).
(7) E. Wiberg, J. E. F. Evans, B: and H. Nöth, *Z. Naturforsch., B: Anorg. Chem., Org. Chem., Biochem., Biophys., Biol.*, **13B**, 265 (1958).
(8) P. Binger, G. Benedikt, G. W. Rothermund, and R. Köster, *Justus Liebigs Ann. Chem.*, **717**, 21 (1968).
(9) D. Sedlak, Ph.D. Thesis, University of München, 1982.
(10) L. I. Zakharkin, USSR Patent 125548 (1960); *Chem. Abstr.* **1960**, 14125.
(11) a) H. C. Brown and E. Negishi, unpublished results cited in E. Negishi, M. J. Idacavage, K.-W. Chu, A. Abramovitch, M. E. Goetter, A. Silveira, Jr., and H. D. Bretherick, *J. Chem. Soc., Perkin Trans. 2*, **1978**, 1225; (b) E. J. Corey, L. O. Weigel, A. R. Chamberlin, and B. Lipshutz, *J. Am. Chem. Soc.*, **102**, 1439 (1980).

0276-7333/83/2302-0579$01.50/0

Table I. Product Distribution (mol %) as Observed by ^{11}B NMR Spectroscopy for Solutions Obtained by Reacting Equivalent Amounts of RLi and BH_3 in Tetrahydrofuran

R	Me[a]	CH_2-$SiMe_3$[b]	n-Bu[b]	sec-Bu[d]	t-Bu[d]
$LiBH_4$	74	62	77	55	41
LiR_3BH	3	14	13	13	35
LiR_2BH_2	1		3	30[d]	24[d]
$LiRBH_3$		21[c]		2	
$LiBR_4$	22		7		

[a] No phase separation was observed. [b] No phase separation observed but the solution went slightly turbid. This could indicate LiH formation. [c] Arising from $B[CH_2SiMe_3]_3$ that is taken here as the substitute for $LiHB(CH_2SiMe_3)_3$. [d] Phase separation occurred in these instances. Some solid was also formed.

resents a simple base displacement. However, the situation is more complex as will be demonstrated, and this renders this approach less general. Reactions of RLi with BH_3

$$RLi + H_3B{\cdot}D \rightarrow LiRBH_3 + D \quad (6)$$

in tetrahydrofuran proceed rapidly even at low temperatures. However, under these conditions and independent of the mode of addition, practically all members of the series $Li(R_{4-n})BH_n$ are produced as shown by ^{11}B NMR spectra of the solutions obtained. This is in accord with the report on the reaction of *n*-butyllithium with diborane in THF.[11a] Table I summarizes typical product distributions.

These data reveal an increasing tendency to produce $LiBH_4$ and $LiBR_4$ with decreasing bulkiness of the organic group. In contrast, a fair quantity of $LiRBH_3$ is only formed with *tert*-butyllithium, while a minimum amount of this type is observed for methyllithium. Also, little LiR_3BH is present in any of the systems, but these species were always detected in NMR spectra at appropriate amplification.

Since organohydroborates are perfectly stable toward disproportionation into BR_4^- and BH_4^- in the absence of a catalyst, the product distribution will not reflect an equilibrium situation. It appears, therefore, that the data represent a situation in which the catalyst is used up in the process. The following series of reactions (eq 7–13) is suggested to explain the results. They are characterized by rapid hydride abstraction reactions.[12]

$$RLi + H_3B{\cdot}THF \rightarrow LiRBH_3 + THF \quad (7)$$

$$LiRBH_3 + H_3B{\cdot}THF \rightarrow LiBH_4 + RBH_2 + THF \quad (8)$$

$$RLi + RBH_2 \rightarrow LiR_2BH_2 \quad (9)$$

$$LiR_2BH_2 + H_3B{\cdot}THF \rightarrow LiBH_4 + R_2BH + THF \quad (10)$$

$$RLi + R_2BH \rightarrow LiR_3BH \quad (11)$$

$$LiR_3BH + BH_3{\cdot}THF \rightarrow LiBH_4 + BR_3 + THF \quad (12)$$

$$RLi + BR_3 \rightarrow LiBR_4 \quad (13)$$

As we progress in the series $R_{4-n}BH_n^-$ from the trihydro- to the monohydroborates, the BH bond becomes weaker,[4] i.e., more hydridic, and we may, therefore, expect more facile hydride abstraction by BH_3. On the other hand, $BH_3{\cdot}THF$ is also consumed by LiR addition according to eq 7 and this holds also for the proposed alkylborane intermediates (eq 9, 11, 13). The net result, then, depends

(12) For the use of hydride abstraction reactions in preparative boron hydride chemistry, see: M. Toft, K. Himpsel, and S. Shore, *Inorg. Chem.* in press.

Table II. ^{11}B NMR Chemical Shift Values (ppm) in Hexane/THF Solution and Coupling Constants (^1J(BH) in Hz) of Organoborates[a]

R	$LiRBH_3$	LiR_2BH_2	LiR_3BH	$LiBR_4$
Me	−31.4	−23.6	−21.0	−20.7
J	70.3	66.6	66.6	
n-Bu	−29.0	−19.2	−14.4	−17.5
J	74	70	75	
sec-Bu	−25.3	−11.9	−6.7	
J	77	74	73	
CH_2SiMe_3	−31.7			
J	78			
t-Bu	−21.2	−6.4	−2.3	
J	77.7	70.3	83	

[a] The intensities of the various lines of multiplets are as expected.

on the relative rates of these reactions, which in turn should also be influenced by the state of association of RLi. If the hydride abstractions proceed much faster than the addition reactions, then it is to be expected that only $LiBH_4$ and $LiBR_4$ should be the products, and this situation is apparently realized for MeLi. An inspection of the data of Table I shows that more $LiBH_4$ is formed than is to be expected from the observed amounts of $LiRBH_3$, LiR_2BH_2, and LiR_3BH. This is especially evident for reactions with *n*-butyllithium and isobutyllithium. In these cases phase separations occurred[13] due to the fact that these LiR compounds were used in hexane solution. Therefore, the estimated product distribution can only be a crude approximation. Inspite of this uncertainty, more $LiRBH_3$ and LiR_2BH_2 are formed with these RLi compounds than in the MeLi case.

No $LiBR_4$ was detected in the reaction of Me_3SiCH_2Li with BH_3 in THF. Also, only a minute amount of the respective LiR_3BH was present according to the ^{11}B NMR spectrum. Instead, $B(CH_2SiMe_3)_3$ had formed, and this organoborane was isolated in 33% yield.

The fairly high proportion of $LiRBH_3$ formed in the reaction of *t*-BuLi with $H_3B{\cdot}THF$ is a notable feature, and isomerization of the *tert*-butyl group is another interesting aspect. This isomerization occurs on the way to LiR_2BH_2 since no lithium isobutyltrihydroborate was detected. Following the generally accepted view that isomerization of organoboranes proceeds via dehydroboration–hydroboration, the observation of this isomerization lends credence to organoboranes as reaction intermediates. The dehydroboration product, in this specific case BH_3, may be responsible for the somewhat higher yield of $LiBH_4$, because under these circumstances it will be the relative rates of hydroboration and hydride abstraction that will determine the yield of $LiRR'BH_2$. Since about twice as much $LiRR'BH_2$ is present among the reaction products as LiR_2BH_2 and since the excess of $LiBH_4$ is not too significant, it seems that hydroboration competes well with hydride abstraction in this case. Table II lists chemical shifts as well as coupling constants for the products.

Reactions of Organolithium Compounds with Borane–Dimethyl Sulfide. Provided that the sequence (7)–(13) describes reactions in the $RLi/BH_3/THF$ systems correctly, one expects reaction 9 to become dominant if the hydride abstractions (8), (10), and (12) can be supressed. Obviously a less active borane-donating agent than $H_3B{\cdot}THF$ is required, and the versatile $H_3B{\cdot}SMe_2$[14]

(13) Only the clear supernatant liquid was investigated by ^{11}B NMR spectroscopy. The heavier phase, partially solid, may contain the products in a different proportion.

(14) H. C. Brown, "Organic Synthesis via Boranes"; Wiley: New York, 1975.

Table III. Product Distribution As Determined by ^{11}B NMR Spectroscopy[a]

	$\delta(^{11}B)$	$^1J(BH)$, Hz	mol % 0 °C	mol % −78 °C
$LiRBH_3$[d]	−23.3	73	60	68
$LiBH_4$	−41.1	82	30	24
$RBH_2 \cdot SMe_2$[d]	−3.8	10	2	4
$[RBH_2]_2$[d]	23.7	44/130[c]	1	3
$R_3B_2H_3$[d]	37.4	d	2	1
	18.0			
BR_3[d]	85		3	
$LiBR_4$[d]	−15.4		2	

[a] Observed by reacting equimolar quantities of *i*-PrLi and $H_3B \cdot SMe_2$ in hexane and adding THF after reaction to form a clear solution.[16] [b] Triplet of doublet. [c] Broad signals in proton undecoupled spectrum. [d] R = *i*-Pr.

was chosen for that reason. This reagent has the additional advantage that reactions can be performed in nonpolar solvents.[11b]

n-Butyllithium in hexane reacts exothermically with $H_3B \cdot SMe_2$ at ambient temperature, and a precipitate is formed. When THF was added to the suspension, the resulting clear solution contained 44 mol % $LiBH_4$, 41 mol % Li(*n*-Bu)BH_3, and 9 mol % LiB(*n*-Bu)$_4$ as shown by ^{11}B NMR spectroscopy. The yield of $LiRBH_3$ has, therefore, greatly improved as compared with $BH_3 \cdot THF$ as the borane source. Addition of $H_3B \cdot SMe_2$ to a *n*-BuLi solution at −10 °C increased the yield of Li(*n*-Bu)BH_3 to 77%, and still higher yields may be obtained by slowly adding borane–dimethyl sulfide to *n*-BuLi at −20 °C. Under these conditions the base displacement reaction (14) is much

$$n\text{-BuLi} + H_3B \cdot SMe_2 \rightarrow Li(n\text{-Bu})BH_3 + SMe_2 \quad (14)$$

$$Li(n\text{-Bu})BH_3 + H_3B \cdot SMe_2 \rightarrow LiBH_4 + n\text{-BuBH}_2 \cdot SMe_2 \quad (15)$$

faster than the hydride abstraction according to (15). Products containing up to 87% Li(*n*-Bu)BH_3 were observed. However, the solution characteristics of $LiBH_4$ and Li(*n*-Bu)BH_3 in ethers are rather similar. Therefore, no ready separation of the two products was achieved.[15a] This is, to a certain extent, in contrast to previous experience.[15b]

Isopropyllithium produces good yields of Li(*i*-Pr)BH_3 in its low-temperature reaction with $H_3B \cdot SMe_2$. Due to the good solubility of this monoalkylborate and the insolubility of $LiBH_4$ in hexane, ready separation is possible and pure, solid Li(*i*-Pr)BH_3 can be isolated from toluene/hexane solutions. Table III shows product distributions as well as the byproducts.

Even if fairly large errors are associated with the low yield figures of the various boranes that are present as byproducts, they prove that low temperatures provide better reaction conditions than ambient temperature. They also lend credence to the reaction sequences similar to those described by eq 7–13 (with SMe_2 replacing THF), because the postulated borane intermediates were detected in these systems. Since butylboranes are absent in *n*-BuLi/$H_3B \cdot SMe_2$ reactions, this suggests slower reaction rates for bulkier carbanions than for less bulkier carbanions. One might, therefore, expect even larger quantities of boranes to be formed in reactions using the *tert*-butyl anion. Some $LiBH_4$, the only hexane insoluble product, formed in all reactions. Its yield has been determined in some instances and found to comply with the amount of borane products.

Results of the reaction of *t*-BuLi with $H_3B \cdot SMe_2$ in hexane are summarized in Table IV.

Lithium *tert*-butyltrihydroborate has been isolated as a free flowing powder in 56% yield from a low-temperature reaction. A fairly good yield of Li(*t*-Bu)BH_3 is also obtained at room-temperature, but a larger proportion of byproducts is formed. It is not surprising that LiB(*t*-Bu)$_4$ could not be detected, because this borate will not form from *t*-BuLi and *t*-Bu_3B due to severe steric hindrance.[17] For an increase in the yield of the organotrihydroborate, slow addition of $H_3B \cdot SMe_2$ is necessary. There is, obviously, a temperature range in which the reaction takes a different course as indicated by the results obtained at −10 °C. In this instance the formation of byproducts outweighs by far the production of $LiRBH_3$. However, we have not studied this somewhat surprising result any further. The formation of specific organolithium compounds is either facilitated or possible only in the presence of suitable ligands such as DABCO (diaminobicyclo[2.2.2]octane) or TMEDA (*N,N,N′,N′*-tetramethylethylenediamine). This prompted us to study the reactions of *n*-BuLi·DABCO and *n*-BuLi·TMEDA with $H_3B \cdot SMe_2$ as model systems.

n-BuLi·DABCO is rather insoluble in hexane at low temperatures. Therefore, ether was added to provide homogeneous reaction conditions and $H_3B \cdot SMe_2$ was added at −78 °C. The resulting solution, at ambient temperature, showed only two quartets in the ^{11}B NMR spectrum. The quartet at δ −10.8 ($^1J(BH)$ = 99 Hz) is readily assigned to DABCO·$2BH_3$.[18] The quartet centered at δ −16.4 ($^1J(BH)$ = 88 Hz) suggests a species of the type LiR_2NBH_3.[19] Such a compound could result from CN cleavage of DABCO. The two signals have intensity ratios of 7:3. Since neither Li(*n*-Bu)BH_3 nor $LiBH_4$ are formed under these conditions, the principal reaction is described by the base displacement (16). A similar result was obtained in the reaction of *n*-BuLi·TMEDA with $H_3B \cdot SMe_2$.

$$n\text{-BuLi}\cdot\text{DABCO} + 2H_3B \cdot SMe_2 \rightarrow \text{DABCO}\cdot 2BH_3 + n\text{-BuLi} + 2SMe_2 \quad (16)$$

Reactions of Organolithium Compounds with Borane–Trimethylamine. Although $H_3B \cdot SMe_2$ proved to be a better reagent than $H_3B \cdot THF$ for the preparation of lithium monoorganotrihydroborates, hydride abstraction could not be prevented totally, definitely not to an extent that it could be considered negligible. Therefore, we turned our attention to borane–trimethylamine, which is a more stable borane adduct than borane–dimethyl sulfide.[21]

No reaction was noted between *n*-BuLi and $H_3B \cdot NMe_3$ in hexane from −78 °C to ambient temperature. However, 20 h of refluxing resulted in a 60% yield of $LiBH_4$. No reaction was also observed in toluene as a solvent at 20 °C but 30 min at reflux temperature sufficed to produce Li(*n*-Bu)BH_3 in high yield. Table V shows a typical product

(15) (a) Li(*n*-Bu)BH_3 is slightly soluble in CH_2Cl_2 in contrast to $LiBH_4$. However, it will react slowly. According to a qualitative experiment, the mixture of Li(*n*-Bu)BH_3 and $LiBH_4$ may be separated by benzene in which Li(*n*-Bu)BH_3 is appreciably soluble. (b) S. Kim, Y. Ch. Moon, and K. H. Ahn, *J. Org. Chem.*, **47**, 3311 (1982), found that Li(*n*-Bu)BH_3 prepared from *n*-BuLi and $H_3B \cdot SMe_2$ is soluble in hexane–toluene.

(16) Assignments for the isopropylboranes are based on results in the R_3B/BH_3/THF and R_3B/BH_3/THF/SMe_2 systems: R. Contreras and B. Wrackmeyer, *Z. Naturforsch., B: Anorg. Chem., Org. Chem.* **35B**, 1229 (1980).

(17) H. Nöth and T. Taeger, *J. Organomet. Chem.*, **142**, 281 (1977).

(18) A. R. Gatti and T. Wartik, *Inorg. Chem.*, **5**, 2075 (1966).

(19) P. C. Keller, *Inorg. Chem.*, **10**, 2256 (1971).

(20) H. Nöth and D. Sedlak, *Chem. Ber.* in press. Contribution 131 of this series.

(21) Dissociation energies for the coordinate bonds are −32.3 kcal/mol for $H_3B \cdot NMe_3$ and −5.3 kcal/mol for $H_3B \cdot SMe_2$. S. R. Gum, *J. Phys. Chem.*, **69**, 1010 (1965); R. K. Hertz, H. D. Johnson, and S. G. Shore, *Inorg. Chem.*, **12**, 1875 (1973).

Table IV. ^{11}B NMR Analysis of the Products from Equimolar Quantities of t-BuLi and $H_3B{\cdot}SMe_2$ [a]

	$\delta(^{11}B)$	$^1J_{BH}$, Hz	mol % −78 °C [b]	−78 °C [c]	−40 °C [d]	−10 °C	−20 °C
Li(t-Bu)BH_3	−20.1	75	90	79		20	79
t-$BuBH_2{\cdot}SMe_2$	−0.2	106	4	10	30	35	7
t-$BuBH_2$	24.0	44/130	2	11	8	10	7
BR_3 [e]	51.7				50		
R_2BH [f]	47.8	127	4		8		
t-Bu_3B	83.0					35	7
$(BH_2CH_2SMe)_2$	−13.6	105			3		
$(BH_2CH_2SMe)_2$ [g]	−17.2	105			1		

[a] Only the pentane-soluble part was investigated. $LiBH_4$ precipitated from solution. [b] Reaction time 4 h. [c] Reaction time 2.5 h. [d] Solutions added at −40 °C, kept for 15 min, and then quickly warmed to ambient temperature. [e] $B(CH_2SMe)_3$ or t-Bu_2BCH_2SMe. [f] R = t-Bu and/or CH_2SMe. [g] Second isomer.

Table V. Product Distribution Observed for the Reaction of Equimolar Quantities of n-BuLi and $H_3B{\cdot}NMe_3$ in Toluene (30 min, Reflux)

	$\delta(^{11}B)$	^1J(BH), Hz	mol % 30 min	2 days
$LiRBH_3$	−28.1	75	80	64
$H_3B{\cdot}NMe_3$	−7.8	96	10	
$LiPhCH_2BH_3$	−26.1	75	2	6
$LiMe_2NCH_2BH_3$	−32.0	75	4	15
$LiBH_4$	−40.6	82	4	15

[a] R = n-Bu.

distribution of the toluene solution.

Equation 17 represents the main reaction. In addition, n-BuLi deprotonates both toluene and borane–trimethylamine to a small but definite extent. The benzyllithium formed in the former process reacts in analogy to (17), producing lithium benzyltrihydroborate, while the

$$n\text{-BuLi} + H_3B{\cdot}NMe_3 \rightarrow \text{Li}(n\text{-Bu})BH_3 + NMe_3 \quad (17)$$

$$\text{Li}(n\text{-Bu})BH_3 + H_3B{\cdot}NMe_3 \rightarrow LiBH_4 + n\text{-}BuBH_2{\cdot}NMe_3 \quad (18)$$

deprotonation product of $H_3B{\cdot}NMe_3$ rearranges to give lithium [(dimethylamino)methyl]trihydroborate. The formation of $LiBH_4$ can be described by eq 18, which in effect is a hydride abstraction reaction due to dissociation of the borane–amine. This was demonstrated clearly by treating 2 mol of $H_3B{\cdot}NMe_3$ with 1 mol of n-BuLi in hexane/toluene. In addition to the ^{11}B NMR signals reported in Table V, a triplet centered at δ −1.8 (^1J(BH) = 98 Hz) evolved slowly as the reaction proceeded, and the compound n-$BuBH_2{\cdot}NMe_3$ can be assigned to this signal.

After 2 h the intensity of the Li(n-Bu)BH_3 signal attained its maximum. Also, more $LiMe_2NCH_2BH_3$ was formed as compared to the 1:1 reaction. At that time the signal intensities for these two compounds plus that of $LiBH_4$ equaled that of the unreacted $H_3B{\cdot}NMe_3$. This clearly shows that reaction 17 is much faster than reaction 18, and, indeed, practically no n-$BuBH_2{\cdot}NMe_3$ was observed. This suggests, then, that the $LiBH_4$ formed up to this stage is probably due to n-BuLi decomposition, yielding LiH that will react with $H_3B{\cdot}NMe_3$ to give $LiBH_4$.

As the reaction proceeds further, the intensity of the borane–trimethylamine signal decreases; it disappeared after 8 days. On the other hand no n-BuLi was detected after 5 days, when n-$BuBH_2{\cdot}NMe_3$ has formed quantitatively. This supports the conclusions drawn for the relative rates of reactions 17 and 18. Impure Li(n-Bu)BH_3 can be isolated from the reaction mixture since it is readily soluble in toluene while $LiBH_4$ is not. However, the other two lithium salts could not be removed.

The borane–trimethylamine method can also be used to prepare lithium organotrihydroborates complexed with TMEDA; this is important for RLi reagents that can only be prepared as RLi·TMEDA.[22] Since $H_3B{\cdot}NMe_3$ is much more stable than $H_3B{\cdot}SMe_2$, BH_3 transfer to TMEDA is very slow and definitely slower than reaction 19. The TMEDA complexes of $LiPhBH_3$ and $LiPhCH_2BH_3$ were isolated in 35 and 90% yield, respectively. Both compounds crystallize readily from hexane/toluene solutions.

$$\text{RLi}{\cdot}\text{TMEDA} + H_3B{\cdot}NMe_3 \rightarrow \text{TMEDA}{\cdot}LiRBH_3 + NMe_3 \quad (19)$$

Discussion

Lithium organotrihydroborates are easily prepared from RLi and $H_3B{\cdot}SMe_2$ or $H_3B{\cdot}NMe_3$ in a nonpolar solvent. Any $LiBH_4$ formed in a hydride transfer reaction can be separated due to its insolubility in these solvents. The solubility of $LiRBH_3$ compounds increases as the R groups become more bulky. If RLi·TMEDA complexes are used as the alkyl anion source, only $H_3B{\cdot}NMe_3$ provides the proper conditions.

The advantage of the methods described here over those recently reported,[4,5] i.e., hydride addition to $(RBH_2)_2$, hydride transfer from $LiAlH_4$ to $(RBH_2)_2$ in presence of DABCO, or the reaction of $LiAlH(OR)_3$ with $(RBH_2)_2$, is that a large variety of R groups can be bonded to boron in the borates, RBH_3^-. The disadvantage, however, is the limitation to the lithium salts, and it appears that hydride addition to dialkyldiboranes is the preferred method if the borane is readily available by hydroboration of an olefine or alkine. If this is not the case, then the route described in this report seems to be the more versatile one. In this context we have been able to prepare $LiMeSCH_2BH_3$ and $MeSCH_2BH_2{\cdot}NMe_3$ and other materials.[20]

Experimental Section

All experiments were performed in the absence of moisture and oxygen under dry nitrogen or argon. The syringe technique has been used in most cases. All reaction were monitored by using a Bruker WP 200 PFT-NMR spectrometer and a multinuclei probe. ^{11}B chemical shifts refer to $BF_3{\cdot}OEt_2$ as external standard (Me = CH_3, Pr = C_3H_7, Bu = C_4H_9, Ph = C_6H_5).

Organolithium compounds were commercial products (Metallgesellschaft AG) or were prepared by standard methods. $BH_3{\cdot}THF$ was freshly prepared from $NaBH_4$ in diglyme and BF_3, and the diborane released was dissolved in pure THF. $H_3B{\cdot}SMe_2$ was purchased and $H_3B{\cdot}NMe_3$ made from $NaBH_4$ and Me_3NHCl. The purity of the samples was checked by NMR methods. Elemental analyses were obtained in the institute's Analytical Laboratory.

Reactions of RLi with BH_3 in Tetrahydrofuran. Attempts to separate unique products from the solutions by fractional

(22) G. G. Eberhardt and W. A. Butte, *J. Am. Chem. Soc.*, 92, 2928 (1964).

crystallization or precipitation with dioxane yielded no pure products. Table I contains the product distribution as deduced from the signal intensities of the ^{11}B NMR spectra.

(a) MeLi and BH_3/THF. A solution of 14.4 mmol of BH_3 in 7.2 mL of THF was cooled to −70 °C and 14.4 mL of an ethereal solution of MeLi, prepared from Li and MeCl, containing 14.4 mmol of MeLi was added within 20 min while being vigorously stirred. After having warmed the mixture to −20 °C, a sample of the clear solution was analyzed.

(b) Me_3SiCH_2Li and BH_3/THF. A 1.23-g sample of Me_3SiCH_2Cl (10 mmol) dissolved in 5 mL of diethyl ether was added to a stirred suspension of 0.95 g (140 mmol) of granulated Li metal in 20 mL of diethyl ether at 50 °C. While the mixture gradually warmed to −20 °C, the chloride reacted quantitatively within 1 h to form Me_3SiCH_2Li (δ ^1H) −0.8 (9) and −2.06 (2). Insoluble materials (LiCl, excess Li) were removed by filtration at −20 °C; the solution was cooled to −60 °C, and 9.5 mmol of BH_3 dissolved in 4.8 mL of THF was added to the stirred solution. An ^{11}B NMR spectrum was recorded of the resulting solution at room temperature. The solvent then was stripped off and the residue distilled: 300 mg (33%) of $B(CH_2SiMe_3)_3$, bp 50–52 °C (101 torr), was isolated as a colorless liquid:[23] $\delta(^1H)$ in benzene 0.98 (6), 0.12 (27),; $\delta(^{11}B)$ in benzene 78.9 (lit.[24] 78.4).

(c) *n*-BuLi and BH_3/THF. A solution of 16 mmol of BH_3 in 9.7 mL of THF was cooled to −78 °C, and 16 mmol of *n*-BuLi, dissolved in 10 mL of hexane, was added with stirring. The mixture was allowed to warm to −30 °C within 1 h. A sample was taken for NMR analysis. This experiment was repeated by cooling the *n*-BuLi solution (14 mmol in 8.8 mL of hexane) and adding a solution of 14 mmol of BH_3 in 8.5 mL of THF. The NMR results were identical, within the limits of error, for both experiments.

(d) *sec*-BuLi and BH_3/THF. The reaction conditions corresponded to those in (c) with inverse addition: 16.2 mmol of *sec*-BuLi in 19.3 mL of pentane was added to 16.2 mmol of BH_3 in 10 mL of THF.

(e) *t*-BuLi and BH_3/THF. A 14.4-mmol sample of *t*-BuLi in 10 mL of pentane was added to 14.4 mmol of BH_3 in 7.2 mL of THF. NMR samples were taken at −10 °C.

The figures given in the Table I are based on the following assumptions: full separation of the phases; the total concentration of the dissolved products in the two phases are proportional to their volumes. A quick check of the data reveals that these assumptions provide only a crude measure. It turns out that more $LiBH_4$ is indicated than could possibly form on the basis of the data of the alkylhydroborates.

Reactions of *n*-BuLi with $H_3B{\cdot}SMe_2$. Product distribution was checked by ^1H and ^{11}B NMR. (a) A 7.15 mL sample of 1 M *n*-BuLi in *n*-hexane was added over a period of 10 min to 1.00 mL of $H_3B{\cdot}SMe_2$ that was well stirred by a magnetic stirring bar. An insoluble product formed in a mild exothermic reaction. A minimum amount of THF then was added to dissolve the solid. The solution obtained showed the following ^{11}B NMR signals: $\delta(^{11}B)$ −17.6 (s, $LiB(n\text{-}Bu)_4$) −29.2 (q, $J(BH)$ = 75 Hz, $Li(n\text{-}Bu)BH_3$, and −42.1 (quin, $J(BH)$ = 82 Hz, $LiBH_4$) in a 15:41:44 ratio.

(b) A 20-mL sample of a 0.5 M *n*-BuLi solution in *n*-hexane was cooled to −10 °C and 1.40 mL of $H_3B{\cdot}SMe_2$ added with stirring. It took a few minutes until an insoluble product separated. After 20 min, all volatile material was stripped off in vacuo, and the solid residue then was dissolved in THF. The ^{11}B NMR spectrum showed three components at δ −17.6, −29.2, and −41.9 ($LiB(n\text{-}Bu)_4$, $Li(n\text{-}Bu)BH_3$, $LiBH_4$) in a 5:77:18 ratio.

Attempts To Separate Lithium *n*-Butyltrihydroborate. (a) A 100-mL sample of a *n*-BuLi solution in hexane containing 80.5 mmol of *n*-BuLi was cooled to −20 °C, and 11.2 mL of $H_3B{\cdot}SMe_2$ (80.5 mmol) was added to the vigorously stirred solution within 60 min. Two hours later all volatiles were removed in vacuo. A sample of the material left behind was dissolved in THF and showed the presence of $Li(n\text{-}Bu)BH_3$, $Li(n\text{-}Bu)_3BH$, and $LiBH_4$ in a 68:8:24 ratio. This material then was suspended in 50 mL of *n*-hexane, and THF was added to form a solution. Removal of these solvents left an oily material that dissolved in CH_2Cl_2 (20 mL). When pentane was added (20 mL), $LiBH_4$ (THF solvated) separated. The solution then contained 91% $Li(n\text{-}Bu)BH_3$ as judged from its ^{11}B NMR spectrum. Repetition of the procedure gave a slightly purer product.

(b) The same amounts as described in (a) were reacted; however, $H_3B{\cdot}SMe_2$ was added over a period of 4 h. The resulting suspension was stirred overnight. The solid formed was separated by filtration. It consisted of $Li(n\text{-}Bu)BH_3$ (87%) and $LiBH_4$ (13%). The solvent from the filtrate then was removed and the residue treated with a 1:1 mixture of CH_2Cl_2 and pentane. Two phases formed: a clear CH_2Cl_2-rich phase and a turbid pentane phase. The CH_2Cl_2 phase showed ^{11}B NMR signals at δ −28.7 ($Li(n\text{-}Bu)BH_3$), −40.9 ($LiBH_4$), −18.6 ($LiB(n\text{-}Bu)_4$), and 1.1 ($n\text{-}BuBH_2{\cdot}SMe_2$). The insoluble part contained 85% $Li(n\text{-}Bu)BH_3$ and 15% $LiBH_4$. $Li(n\text{-}Bu)BH_3$ seemed to react slowly with CH_2Cl_2.

Lithium Isopropyltrihydroborate. A 40-mL sample of a *n*-hexane solution of *i*-PrLi (11.2 mmol) was cooled to −78 °C, and 1.6 mL of $H_3B{\cdot}SMe_2$ then was added with vigorous stirring. When the mixture was warmed to −68 °C, a solid started separating. It dissolved partially on further warming. The insoluble part then was removed by filtration, washed with hexane, and dried in vacuo; yield 60 mg of $LiBH_4$. Solvents were removed from the filtrate and dissolved in pentane and very little THF. Crystals separated from this solution on cooling to −40 °C. These were filtered; the solution contained 97% $Li(i\text{-}Pr)BH_3$ and 3% $LiBH_4$. The bulk of the solid material was treated with 80 mL of toluene and 80 mL of hexane, with stirring, for 1 day. After having removed the insoluble materials, crystals of $Li(i\text{-}Pr)BH_3$ separated at −20 °C from the clear concentrated solution, yield 210 mg (29%). The crystals became soft at 80 °C, forming a glassy mass: IR (cm^{-1}) selected bands of ν(CH) 2850, 2880, 2930; ν(BH) 2150 2190 (sh); $\delta(^{11}B\{^1H\})$ −24.3 (THF), −22.8 (toluene). Anal. Calcd for $C_3H_{10}BLi$ (63.9): C, 56.42; H, 15.78; B, 16.93; Li, 10.87. Found: C, 55.66; H, 14.72; B, 16.9; Li, 11.0.

Lithium *tert*-Butyltrihydroborate. (a) A 1.00-mL sample of $H_3B{\cdot}SMe_2$ (7.5 mmol) was added dropwise to a stirred solution of 7.5 mmol of *t*-BuLi in 10 mL of *n*-pentane at −40 °C. An oily precipitate formed on slowly warming to −30 °C. It solidified on further stirring and warming to room temperature. A 130-mg sample of $LiBH_4$ was removed from the solution and identified by its ^{11}B NMR spectrum in THF solution ($\delta(^{11}B)$ −41 ($^1J(BH)$ = 82 Hz)).

(b) With use of the same quantities of materials, a suspension of $LiBH_4$ formed readily when $H_3B{\cdot}SMe_2$ was added to *t*-BuLi at −10 °C. The results of the analysis of the ^{11}B NMR spectra are shown in Table IV.

(c) A 1.06-mL sample of $H_3B{\cdot}SMe_2$ (8.0 mmol) was added to 10 mL of a 0.8 M solution of *t*-BuLi at −78 °C. The solution obtained was analyzed by its ^{11}B NMR spectrum at room temperature. Results are shown in Table IV. Results of additional experiments are included in this table.

(d) A 2.15 mL sample of $H_3B{\cdot}SMe_2$ (16.1 mmol) was added over a period of 15 min to a well-stirred solution of 16.1 mmol of *t*-BuLi in 20 mL of *n*-pentane. An insoluble product formed immediately. The clear supernatant liquid showed the presence of $Li(t\text{-}Bu)BH_3$ in the ^{11}B NMR spectrum as well as the boranes shown in Table IV. The solid was filtered and dissolved in THF. This solution then contained 60 mol % of $Li(t\text{-}Bu)BH_3$, 35% $LiBH_4$, and 5% borane species.

(e) A 100-mL sample of a pentane solution containing 80.5 mmol of *t*-BuLi was cooled to −78 °C and 11.0 mL of $H_3B{\cdot}SMe_2$ (81 mmol) was added to the well-stirred solution over a period of 2.5 h. The mixture then was allowed to slowly attain room temperature (~4 h), and 270 mg of pure $LiBH_4$ (16%) was filtered. The solution then was concentrated to about one-third of its original volume. The material that settled on standing for about 4 h from the solution at −30 °C was removed and freed from impurities by washing twice with 5 mL of pentane (−50 °C). After the mixture was dried at 50 °C (10^{-3} torr) for 15 min, 3.52 g (56%) of $Li(t\text{-}Bu)BH_3$ was obtained: mp 207–212 °C; decomp 250 °C; IR 2920 (m), 2880 (st), 2840 (st), 2220 (st), 2150 (st), 1475 (m), 1465 (m), 1450 (m), 1350 (m), 1150 (st), 715 (m), 940 (w), 630, 610 (w). Anal. Calcd for $C_4H_{12}BLi$ (77.9): C, 61.68 H, 15.53 B, 13.88. Found: C, 58.85; H, 14.18; B, 13.9.

Reactions of Borane–Dimethyl Sulfide with the *n*-Butyllithium–Diaminobicyclo[2.2.2]octane Complex. (a) A 1.2-mL sample of $H_3B{\cdot}SMe_2$ (10 mmol) was added to a freshly

(23) D. Seyferth, *J. Am. Chem. Soc.*, 81, 1844 (1959).
(24) H. Nöth and B. Wrackmeyer, *NMR: Basic Princ. Prog.* 14 (1978).

Table VI

	$Me_3N{\cdot}BH_3$	$LiPhCH_2BH_3$	$Li(n\text{-}Bu)BH_3$	$LiMe_2NCH_2BH_3$	$LiBH_4$
$\delta(^{11}B)$	−7.8 (q)	−26.2, −26.1 (q)	−28.1 (q)	−32.0 (q)	40.3, −40.6 (quint)
mol %					
30 min	7	3	80	5	5
2 days		6	64	15	15

Table VII

	$(Me_2NCH_2BH_2)_2$	$Me_3N{\cdot}BH_3$	$Li(n\text{-}Bu)BH_3$	$LiMe_2NCH_2BH_3$	$LiBH_4$
$\delta(^{11}B)$	−1.7	−8.1	−27.7	−32.1	−40.5
mol %					
2 h		50	40	7	3
12 h	20	40	30	6	4
2 days	37	43	10	7	3
5 days	70	25		4	1

prepared solution of n-BuLi·DABCO in 25 mL of n-hexane and 20 mL of diethyl ether at −78 °C. An insoluble, white precipitate formed almost immediately. After being warmed to ambient temperature, the solution showed two ^{11}B NMR signals at δ −10.8 (q, DABCO·BH_3) and at −16.4 (q), possibly a material with an LiR_2NBH_3 structure in the ratios 7:3. No additional precipitate formed on adding $H_3B{\cdot}SMe_2$. When THF was added to the mixture, more DABCO·BH_3 went into solution but no new ^{11}B NMR signal appeared.

(b) With use of the same materials but reacting them at −10 °C led to the following ^{11}B NMR signals: δ −10.7, −16.4, and −29.1 ($^1J(BH)$ = 75 Hz, q), the latter corresponding to $Li(n\text{-}Bu)BH_3$.

(c) A 4.2-mL sample of $H_3B{\cdot}SMe_2$ (31.5 mmol) was added slowly to a stirred solution of 10 mmol of n-BuLi·DABCO in 10 mL of n-hexane and 10 mL of diethyl ether. The ^{11}B NMR spectrum finally showed the presence of DABCO·BH_3 (δ −10.7), $LiBH_4$ (δ −41), and some $LiB(n\text{-}Bu)_4$ (δ −17.5). All $H_3B{\cdot}SMe_2$ had reacted.

Reactions of Borane–Dimethyl Sulfide with *n*-Butyllithium–Tetramethylethylenediamine Complex. Equimolar amounts were reacted, and $H_3B{\cdot}SMe_2$ was added to n-BuLi·$Me_2NCH_2CH_2NMe_2$ in hexane (1.2 M solution). An insoluble product formed. THF was added to produce a clear solution that was then analyzed by ^{11}B NMR spectroscopy.

(a) A 10-mmol sample of the reactants, each at 0 °C: ^{11}B NMR δ −9.1/−10.0 (TMEDA·BH_3 and TMEDA·$2BH_3$), −29.0 ($Li(n\text{-}Bu)BH_3$, −30.9 ($LiMe_2SCH_2BH_3$), −41.4 ($LiBH_4$). TMEDA adduct NMR signal intensities were 90% to those of the total intensity.

(b) A 5-mmol sample of each of n-BuLi·TMEDA, $H_3B{\cdot}SMe_2$, and TMEDA at 0 °C: only TMEDA·BH_3, $\delta(^{11}B)$ −9.0, was detected.

(c) A 5-mmol sample of each of n-BuLi·TMEDA and $H_3B{\cdot}SMe_2$ at 50 °C in 10 mL of diethyl ether: only TMEDA·BH_3, $\delta(^{11}B)$ −9, and TMEDA·$2BH_3$ δ −10.0, were detected.

(d) A 5-mmol sample of n-BuLi·TMEDA and 15 mmol of $H_3B{\cdot}SMe_2$ were reacted at 50 °C. A 10 mL sample of hexane was added. The ^{11}B NMR spectrum showed signals of TMEDA·$2BH_3$ (δ −10.0 (q)), $LiMeSCH_2BH_3$ (δ −31.0 (q), $LiBH_4$ (δ −41.6 (quint)), and an unidentified product at δ −2.5 (br).

(e) A mixture of 5 mmol each of n-BuLi·TMEDA and $H_3B{\cdot}SMe_2$ was kept under reflux for 2.5 h, after 50 mL of toluene had been added. The ^{11}B NMR spectrum now showed the formation of $LiBH_4$ (50%), $Li(n\text{-}Bu)BH_3$ (40%), and $LiMeSCH_2BH_3$ (10%) and no TMEDA·BH_3.

Reactions of Borane–Trimethylamine and *n*-Butyllithium. (a) A mixture of 10 mmol of n-BuLi 16.6 mL of n-hexane and 730 mg of $Me_3N{\cdot}BH_3$ and 10 mL of toluene was heated at reflux for 2 days. A slightly turbid solution had then formed that was analyzed by ^{11}B NMR spectroscopy. The results obtained after 30 min and two days are shown in Table VI. The mixture then was treated with an excess of $Me_3N{\cdot}HCl$ and again analyzed by ^{11}B NMR spectroscopy after no more gas evolved: δ −1.7 (t, $BuBH_2{\cdot}NMe_3$), −6.5 (t, $Me_2NCH_2BH_2{\cdot}NMe_3$), and −7.7 (q, $H_3B{\cdot}NMe_3$).

(b) A 5-mmol sample of n-BuLi in 3.3 mL of n-hexane was added to a solution of 720 mg of $Me_3N{\cdot}BH_3$ (10 mmol) in 10 mL of benzene. This mixture was kept under reflux, and ^{11}B NMR spectra were taken at the intervals indicated (Table VII).

Reaction of Phenyllithium–Tetramethylethylenediamine with Borane–Trimethylamine. A solution containing 16 mmol of PhLi·TMEDA in 10 mL of n-hexane and 10 mL of benzene was heated to reflux. A 1.17-g sample of $Me_3N{\cdot}BH_3$ (16 mmol) then was added and the mixture kept refluxing for 12 h. Crystals separated from the solution within 3 days. They were isolated and washed with cold pentane: yield 1.2 g of $LiPhBH_3{\cdot}TMEDA$ (35%); mp 120 °C dec. Anal. Calcd for $C_{12}H_{24}BLiN_2$ (214.1); C, 67.32; H, 11.30; N, 13.08; B, 5.05. Found: C, 66.03; H, 9.73; N, 12.28; B, 5.0.

Reaction of Isopropyllithium with Borane–Trimethylamine. A 10-mL sample of a 1.12 M solution of i-PrLi in hexane was added to 800 mg (11.2 mmol) of $H_3B{\cdot}NMe_3$ dissolved in 15 mL of toluene. After this mixture was kept 16 h at reflux, the following ^{11}B NMR signals were observed: $\delta(^{11}B)$ −7.8 (br, $Me_3N{\cdot}BH_3$), −23.1 ($LiMe_2CHBH_3$), −26.2 ($LiPhCH_2BH_3$), −32.1 ($LiMe_2NCH_2BH_3$), −40.8 ($LiBH_4$).

Reaction of *tert*-Butyllithium with Borane–Trimethylamine. A mixture of 570 mg of $Me_3N{\cdot}BH_3$ (7.9 mmol), 5.0 mmol of t-BuLi, 5 mL of hexane, and 10 mL of toluene was kept under reflux for 140 min. The ^{11}B NMR spectrum of the solution then showed a signal of $LiMe_2NCH_2BH_3$ (δ −30.8 ($^1J(BH)$ = 76 Hz, q). The insoluble part consisted of $LiBH_4$ (δ −41).

Lithium Benzyltrihydroborate. A 75-mmol sample of n-BuLi in 100 mL of n-hexane was added to a solution of 11.2 mL (75 mmol) of TMEDA in 100 mL of toluene. A deep red solution formed within 30 min. After 5.12 g (70 mmol) of $H_3B{\cdot}NMe_3$ was added, this solution discolored on heating for 1 h while being refluxed. A gas containing trimethylamine evolved quickly during the first stages of the reaction. According to ^{11}B NMR spectra ~90% $LiPhCH_2BH_3$ and 10% $LiBH_4$ had formed. The resulting solution was kept for 3 days at −25 °C. A 14.5-g (90%) sample of crystalline $LiPhCH_2BH_3{\cdot}TMEDA$ separated. Anal. Calcd for $C_{13}H_{26}BLiN_2$ (228.1): C, 68.45; H, 11.49; N, 12.28. Found: C, 67.84; H, 11.32; N, 12.01.

Acknowledgment. A grant of DFG for purchasing the Bruker WP 200 multinuclear NMR spectrometer is gratefully acknowledged as well as the continuous support by Fonds der Chemischen Industrie, BASF-Aktiengesellschaft and Metallgesellschaft AG. We thank Dr. B. Wrackmeyer for helpful discussions relating to NMR spectra and Miss H. Bauer, Mrs. L. Moser, and Mr. K. Schönauer for assistance in recording spectra and carrying out analyses. H.N. wishes to thank the Department of Chemistry, Ohio State University, Columbus, OH, for an invitation to work at this institution, where this manuscript was prepared.

Registry No. $LiMeBH_3$, 52950-75-1; $LiMe_2BH_2$, 84280-31-9; $LiMe_3BH$, 63526-12-5; $LiBMe_4$, 2169-38-2; $Li(n\text{-}Bu)BH_3$, 82111-98-6; $Li(n\text{-}Bu)_2BH_2$, 84280-32-0; $Li(n\text{-}Bu)_3BH$, 67355-72-2; $LiB(n\text{-}Bu)_4$, 15243-31-9; $Li(sec\text{-}Bu)BH_3$, 84280-33-1; $Li(sec\text{-}Bu)_2BH_2$, 84280-34-2; $Li(sec\text{-}Bu)_3BH$, 38721-52-7; $LiMe_3SiCH_2BH_3$, 84280-35-3; $Li(Me_3SiCH_2)_3BH$, 84280-36-4; $Li(t\text{-}Bu)BH_3$, 76826-51-2; $Li(t\text{-}Bu)_2BH_2$, 84280-37-5; $Li(t\text{-}Bu)_3BH$, 63717-92-0; $Li(i\text{-}Pr)BH_3$, 84280-38-6; $(i\text{-}Pr)BH_2{\cdot}SMe_2$, 84280-39-7; $[(i\text{-}Pr)BH_2]_2$, 22784-04-9; $(i\text{-}Pr)_3B_2H_3$, 22784-05-0; $B(i\text{-}Pr)_3$, 1776-66-5; $LiB(i\text{-}Pr)_4$, 84280-40-0; $t\text{-}BuBH_2{\cdot}SMe_2$, 84280-41-1; $t\text{-}BuBH_2$, 43795-48-8; $B(CH_2SMe)_3$, 84280-48-8; $t\text{-}Bu_2BH$, 65568-76-5; $(BH_2CH_2SMe)_2$

(isomer 1), 84280-49-9; $(BH_2CH_2SMe)_2$ (isomer 2), 84280-50-2; $(t\text{-Bu})_2BCH_2SMe$, 84280-51-3; $(MeSCH_2)_2BH$, 84280-52-4; $LiMe_2NCH_2BH_3$, 84280-42-2; TMEDA·$2BH_3$, 5843-32-3; TMEDA-$2BH_3$, 5843-33-4; $Me_3N{\cdot}BH_3$, 75-22-9; $LiPhCH_2BH_3$, 84280-43-3; $t\text{-Bu}_3B$, 1113-42-4; $(Me_2NCH_2BH_2)_2$, 84280-53-5; $LiPhBH_3$·TMEDA, 84280-44-4; $LiPhCH_2BH_3$·TMEDA, 84280-46-6; $H_3B{\cdot}SMe_2$, 13292-87-0; MeLi, 917-54-4; Me_3SiCH_2Li, 1822-00-0; *n*-BuLi, 109-72-8; *sec*-BuLi, 598-30-1; *t*-BuLi, 594-19-4; *i*-PrLi, 1888-75-1; Me_3SiCH_2Cl, 2344-80-1; BH_3, 13283-31-3; $B(CH_2SiMe_3)_3$, 18077-26-4; $LiMeSCH_2BH_3$, 84280-47-7.

Comparative X-ray Crystallographic and Thermodynamic Studies of Substituted Styrene Complexes of Palladium(II) Containing the η^5-Cyclopentadienyl Ligand. Appreciation of Olefin–Palladium(II) π Interaction in the 18-Electron Complex

Kunio Miki, Osamu Shiotani, Yasushi Kai, Nobutami Kasai,* Hideki Kanatani,† and Hideo Kurosawa*†

Department of Applied Chemistry and Department of Petroleum Chemistry, Faculty of Engineering, Osaka University, Yamadaoka, Suita, Osaka 565, Japan

Received November 15, 1982

The molecular structures of the substituted styrene complexes of Pd^{II} with 18-electron configuration $[Pd(\eta^5\text{-}C_5H_5)(PPh_3)(CH_2{=}CHC_6H_4Y\text{-}p)]X$ (**2b**, Y = OMe, X = BF_4, **2c**, Y = H, X = PF_6, **2d**, Y = Cl, X = BF_4) have been determined by means of X-ray diffraction. Crystals of **2b–d** all belong to the monoclinic system. The crystal data are as follows. **2b**: a = 10.538 (1) Å, b = 16.333 (2) Å, c = 9.680 (1) Å, β = 100.06 (1)°, Z = 2, space group $P2_1$. **2c**: a = 15.571 (4) Å, b = 11.187 (2) Å, c = 17.596 (3) Å, β = 107.71(2)°, Z = 4, space group $P2_1/n$. **2d**: a = 10.359 (2) Å, b = 16.474 (3) Å, c = 9.654 (2) Å, β = 100.82 (2)°, Z = 2, space group $P2_1$. The structures of three complexes were solved by the heavy-atom method and refined by the least-squares procedure to R values 0.040, 0.048, and 0.050 for **2b**, **2c**, and **2d**, respectively. In each of **2b–d**, the palladium atom is surrounded by cyclopentadienyl, triphenylphosphine, and olefinic ligands in the cationic complex. The C=C bond is almost perpendicular to the coordination plane defined by the Pd and P atoms and the centers of the Cp and olefin ligands. The bond length between Pd and the terminal olefin carbon is almost substituent independent, while that between Pd and the aryl-substituted olefin carbon becomes shorter with increasing electron-withdrawing ability of Y. The thermodynamic parameters for the equilibrium $pd\text{–}NCR' + CH_2{=}CHC_6H_4Y\text{-}p \rightleftharpoons pd(CH_2{=}CHC_6H_4Y\text{-}p) + R'CN$ where $pd = Pd(\eta^5\text{-}C_5H_5)(PR_3)^+X^-$ (R = Ph, Et, *n*-Bu; X = ClO_4, BF_4; R′ = tolyl) have been determined in dilute solutions. The equilibria showing the smaller $\Delta G°$ values for the more donating styrene complexes are controlled mostly by $\Delta S°$ terms, with $\Delta H°$ being almost substituent independent. The structural and thermodynamic results mentioned above have been discussed in terms of the nature of the olefin–Pd^{II} bonding in the d^8 ML_4(olefin) framework involving more appreciable π back-bonding contribution than previously assumed in square-planar (olefin)Pd^{II} complexes.

Much attention has been focused upon both the reactivity and the nature of the bonding of the (olefin)Pd^{II} complexes.[1,2] The general consensus concerning these subjects seems to be that the Pd^{II} centered in square-planar complexes primarily acts as an electrophile toward the coordinated olefin, thereby rendering this ligand very susceptible to the attack of nucleophiles.[1,2] The electrophilic nature of Pd^{II} toward the olefin may in turn be understood in terms of the Dewar–Chatt–Duncanson scheme as olefin-to-Pd σ donation overwhelming π back-bonding. Perhaps the best supporting evidence for this concept was obtained by the observation[3] of a good correlation between the thermodynamic parameters for equilibrium 1 involving complexes of type 1 and the Hammett σ^+ constants, suggesting the importance of the bonding mode A. The bonding mode of type A was also shown to play a key role in enhancing the nucleophilic attack at the coordinated olefin[1,4] and olefin oligomerization and polymerization with a *cationic* Pd^{II} catalyst.[5]

We have recently isolated some *cationic, 18-electron* complexes of type 2 and examined their stability in solutions by ^1H NMR spectroscopy.[6] It was somewhat surprising to find that, though the more electron-donating styrene complex does exhibit the higher stability as in the case of 1, the Hammett relation for eq 1 involving 2 holds better by using σ rather than σ^+ constants. Further, the

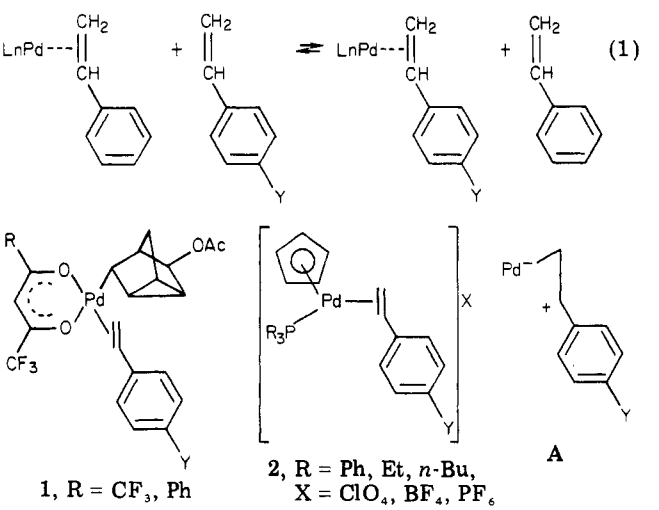

† Department of Petroleum Chemistry.

(1) Eisenstein, O.; Hoffmann, R. *J. Am. Chem. Soc.* 1981, *103*, 4308 and references therein.

(2) Collman, J. P.; Hegedus, L. S. "Principles and Applications of Organotransition Metal Chemistry"; University Science Books: Mill Valley, CA, 1980; pp 603.

0276-7333/83/2302-0585$01.50/0

(isomer 1), 84280-49-9; $(BH_2CH_2SMe)_2$ (isomer 2), 84280-50-2; $(t\text{-Bu})_2BCH_2SMe$, 84280-51-3; $(MeSCH_2)_2BH$, 84280-52-4; $LiMe_2NCH_2BH_3$, 84280-42-2; TMEDA·$2BH_3$, 5843-32-3; TMEDA-$2BH_3$, 5843-33-4; $Me_3N{\cdot}BH_3$, 75-22-9; $LiPhCH_2BH_3$, 84280-43-3; $t\text{-Bu}_3B$, 1113-42-4; $(Me_2NCH_2BH_2)_2$, 84280-53-5; $LiPhBH_3$·TMEDA, 84280-44-4; $LiPhCH_2BH_3$·TMEDA, 84280-46-6; $H_3B{\cdot}SMe_2$, 13292-87-0; MeLi, 917-54-4; Me_3SiCH_2Li, 1822-00-0; *n*-BuLi, 109-72-8; *sec*-BuLi, 598-30-1; *t*-BuLi, 594-19-4; *i*-PrLi, 1888-75-1; Me_3SiCH_2Cl, 2344-80-1; BH_3, 13283-31-3; $B(CH_2SiMe_3)_3$, 18077-26-4; $LiMeSCH_2BH_3$, 84280-47-7.

Comparative X-ray Crystallographic and Thermodynamic Studies of Substituted Styrene Complexes of Palladium(II) Containing the η^5-Cyclopentadienyl Ligand. Appreciation of Olefin–Palladium(II) π Interaction in the 18-Electron Complex

Kunio Miki, Osamu Shiotani, Yasushi Kai, Nobutami Kasai,* Hideki Kanatani,† and Hideo Kurosawa*†

Department of Applied Chemistry and Department of Petroleum Chemistry, Faculty of Engineering, Osaka University, Yamadaoka, Suita, Osaka 565, Japan

Received November 15, 1982

The molecular structures of the substituted styrene complexes of Pd^{II} with 18-electron configuration $[Pd(\eta^5\text{-}C_5H_5)(PPh_3)(CH_2{=}CHC_6H_4Y\text{-}p)]X$ (**2b**, Y = OMe, X = BF_4, **2c**, Y = H, X = PF_6, **2d**, Y = Cl, X = BF_4) have been determined by means of X-ray diffraction. Crystals of **2b–d** all belong to the monoclinic system. The crystal data are as follows. **2b**: a = 10.538 (1) Å, b = 16.333 (2) Å, c = 9.680 (1) Å, β = 100.06 (1)°, Z = 2, space group $P2_1$. **2c**: a = 15.571 (4) Å, b = 11.187 (2) Å, c = 17.596 (3) Å, β = 107.71(2)°, Z = 4, space group $P2_1/n$. **2d**: a = 10.359 (2) Å, b = 16.474 (3) Å, c = 9.654 (2) Å, β = 100.82 (2)°, Z = 2, space group $P2_1$. The structures of three complexes were solved by the heavy-atom method and refined by the least-squares procedure to R values 0.040, 0.048, and 0.050 for **2b**, **2c**, and **2d**, respectively. In each of **2b–d**, the palladium atom is surrounded by cyclopentadienyl, triphenylphosphine, and olefinic ligands in the cationic complex. The C=C bond is almost perpendicular to the coordination plane defined by the Pd and P atoms and the centers of the Cp and olefin ligands. The bond length between Pd and the terminal olefin carbon is almost substituent independent, while that between Pd and the aryl-substituted olefin carbon becomes shorter with increasing electron-withdrawing ability of Y. The thermodynamic parameters for the equilibrium $pd\text{–}NCR' + CH_2{=}CHC_6H_4Y\text{-}p \rightleftharpoons pd(CH_2{=}CHC_6H_4Y\text{-}p) + R'CN$ where $pd = Pd(\eta^5\text{-}C_5H_5)(PR_3)^+X^-$ (R = Ph, Et, *n*-Bu; X = ClO_4, BF_4; R′ = tolyl) have been determined in dilute solutions. The equilibria showing the smaller $\Delta G°$ values for the more donating styrene complexes are controlled mostly by $\Delta S°$ terms, with $\Delta H°$ being almost substituent independent. The structural and thermodynamic results mentioned above have been discussed in terms of the nature of the olefin–Pd^{II} bonding in the d^8 ML_4(olefin) framework involving more appreciable π back-bonding contribution than previously assumed in square-planar (olefin)Pd^{II} complexes.

Much attention has been focused upon both the reactivity and the nature of the bonding of the (olefin)Pd^{II} complexes.[1,2] The general consensus concerning these subjects seems to be that the Pd^{II} centered in square-planar complexes primarily acts as an electrophile toward the coordinated olefin, thereby rendering this ligand very susceptible to the attack of nucleophiles.[1,2] The electrophilic nature of Pd^{II} toward the olefin may in turn be understood in terms of the Dewar–Chatt–Duncanson scheme as olefin-to-Pd σ donation overwhelming π back-bonding. Perhaps the best supporting evidence for this concept was obtained by the observation[3] of a good correlation between the thermodynamic parameters for equilibrium 1 involving complexes of type 1 and the Hammett σ^+ constants, suggesting the importance of the bonding mode A. The bonding mode of type A was also shown to play a key role in enhancing the nucleophilic attack at the coordinated olefin[1,4] and olefin oligomerization and polymerization with a *cationic* Pd^{II} catalyst.[5]

We have recently isolated some *cationic, 18-electron* complexes of type 2 and examined their stability in solutions by ^1H NMR spectroscopy.[6] It was somewhat surprising to find that, though the more electron-donating styrene complex does exhibit the higher stability as in the case of 1, the Hammett relation for eq 1 involving 2 holds better by using σ rather than σ^+ constants. Further, the

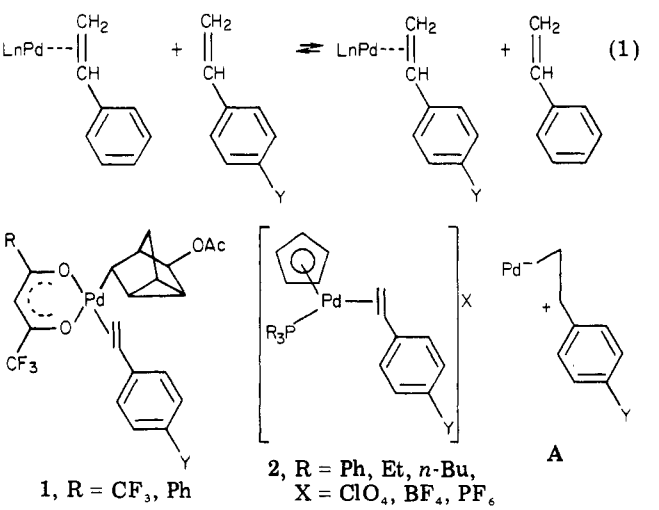

† Department of Petroleum Chemistry.

(1) Eisenstein, O.; Hoffmann, R. *J. Am. Chem. Soc.* 1981, *103*, 4308 and references therein.

(2) Collman, J. P.; Hegedus, L. S. "Principles and Applications of Organotransition Metal Chemistry"; University Science Books: Mill Valley, CA, 1980; pp 603.

0276-7333/83/2302-0585$01.50/0

Table I. Crystal Data for $[Pd(\eta^5\text{-}C_5H_5)(PPh_3)(CH_2{=}CHC_6H_4\text{-}Y\text{-}p)]X$

	2b	2c	2d
Y	OCH_3	H	Cl
X	BF_4	PF_6	BF_4
formula	$C_{32}H_{30}OPPd\cdot BF_4\cdot CH_2Cl_2$	$C_{31}H_{28}PPd\cdot PF_6$	$C_{31}H_{27}ClPPd\cdot BF_4\cdot CH_2Cl_2$
fw	739.7	682.9	744.1
$F(000)$	748	1376	748
cryst system	monoclinic	monoclinic	monoclinic
space group	$P2_1$	$P2_1/n$	$P2_1$
a, Å	10.538 (1)	15.571 (4)	10.359 (2)
b, Å	16.333 (2)	11.187 (2)	16.474 (3)
c, Å	9.680 (1)	17.596 (3)	9.654 (2)
β, deg	100.06 (1)	107.71 (2)	100.82 (2)
U, Å^3	1640.5 (3)	2919.8 (9)	1618.3 (5)
D_{calcd}, g cm^{-3}	1.498	1.553	1.527
D_{measd}, g cm^{-3}	1.49	1.55	1.52
Z	2	4	2
μ(Mo Kα), cm^{-1}	8.18	7.97	9.06

thermodynamic parameters were counteranion dependent. We tentatively ascribed these findings to the occurrence of tight ion-pair formation under the NMR experimental conditions. In order to gain insight into the more intrinsic nature of the olefin–Pd^{II} bonding, we have undertaken an X-ray crystallographic study of **2**.

We reported[7] the X-ray crystal structure analysis of $[Pd(\eta^5\text{-}C_5H_5)(PEt_3)(CH_2{=}CHC_6H_5)]BF_4$ (**2a**) and now extended this to a series of the para-substituted styrene complexes $[Pd(\eta^5\text{-}C_5H_5)(PPh_3)(CH_2{=}CHC_6H_4Y\text{-}p)]X$ (**2b**, Y = OMe, X = BF_4, **2c**, Y = H, X = PF_6, and **2d**, Y = Cl, X = BF_4). We further reexamined the stability of **2** in *dilute solutions* by UV spectroscopy to avoid, as well as possible, complexity arising from the ion-pair formation. Here we describe an intriguing stability trend of **2**, attained through both X-ray structural and thermodynamic studies, that suggests a more important role of the π back-bonding than previously assumed in the usual, four-coordinate square-planar (olefin)Pd^{II} complexes. Such unique nature of the olefin-Pd^{II} bond in the 18-electron complexes not only is of theoretical interest[1,8] but also has bearing on some key steps in synthetic reactions including ligand substitution[9] and olefin insertion/β-hydrogen elimination.[10]

Experimental Section

Materials. A basic method to prepare the styrene complexes of type **2** was described previously.[6] Crystals suitable for X-ray crystallography were grown from CH_2Cl_2–*n*-hexane solutions kept in the refrigerator. Spectroscopic grade of CH_2Cl_2 was used in UV experiments. *o*-Tolunitrile and the styrenes were purified by distillation before use in UV measurement.

Crystallographic Data. Crystals of **2b–d** are all black prisms. Crystal data are summarized in Table I. The accurate unit-cell dimensions were determined by the least-squares fit of 2θ values of 25 strong reflections ($20° < 2\theta < 31°$). Densities of the crystals were measured by the flotation in carbon tetrachloride–*n*-hexane (or chlorobenzene) mixed solution. Crystals of **2b** and **2d**, which belong to a noncentrosymmetric space group, are isomorphous with each other. They were found to contain one CH_2Cl_2 molecule solvated in an asymmetric unit considering from the observed and calculated densities, which were later confirmed by the structures determined. Attempts were made to determine the molecular structure of $[Pd(\eta^5\text{-}C_5H_5)(PPh_3)(CH_2{=}CHC_6H_5)]BF_4$ (**2e**). Crystals of **2e** belong to the triclinic space group $P\bar{1}$ with unit-cell dimensions of a = 21.34 Å, b = 26.09 Å, c = 10.75 Å, α = 99.8, β = 91.7, and γ = 108.6°. The density calculated for Z = 8 gives a plausible value of 1.49 g cm^{-3}, which showed that the asymmetric unit contains four independent molecules in the crystal. Therefore, the structure analysis of **2e** was abandoned.

Collection and Reduction of Intensity Data. Well-shaped crystals with approximate dimensions of 0.30 × 0.35 × 0.40 mm (**2b**), 0.30 × 0.35 × 0.40 mm (**2c**), and 0.25 × 0.40 × 0.40 mm (**2d**) were mounted on a Rigaku automated, four-circle, single-crystal diffractometer. Several strong reflections of each crystal were examined by the ω scan, and each crystal was found to give diffraction profiles good enough for the intensity measurement. Integrated intensities were collected by the θ–2θ scan technique by using graphite-monochromatized Mo Kα radiation (λ = 0.71069 Å). The scan speed was 4° min^{-1} in 2θ, and the scan width was $\Delta 2\theta = (2.0 + 0.70 \tan \theta)°$. The background intensities were measured for 7.5 s at both ends of a scan. The scan was repeated twice in the case of weak reflections ($F < 3\sigma(F)$). Four standard reflections (600, 080, 005, and 04$\bar{4}$ for **2b**, 12,0,0, 080, 0,0,10, and 660 for **2c**, and 080, 005, 04$\bar{4}$, and 33$\bar{3}$ for **2d**) measured at regular intervals to monitor the stability and orientation of the crystals showed no significant decay throughout the data collection. Both hkl and $hk\bar{l}$ reflection data were collected within 2θ up to 54.0° ($(\sin \theta)/\lambda$ = 0.639 Å^{-1}), and $\bar{h}\bar{k}\bar{l}$ and $\bar{h}\bar{k}l$ Bijvoet pair reflections were additionally measured for **2b** and **2d**. Totals of 7188, 6376, and 7071 independent reflections were obtained after the symmetry equivalent reflections (e.g., $0kl$/and $0k\bar{l}$) were averaged for **2b**, **2c**, and **2d**, respectively. The discrepancy factors for symmetry equivalent reflections ($R_{sym} = \sum ||F| - \langle|F|\rangle| / \sum \langle|F|\rangle$, $\langle|F|\rangle$, the average value of two or more equivalent reflections) were 0.003, 0.014, and 0.004 for **2b**, **2c**, and **2d**, respectively. These small R_{sym}'s indicate the high quality of the reflection data in the present analyses. Corrections for Lorentz and polarization effects were applied to the intensity data, while no absorption corrections were carried out in view of the small crystal sizes and absorption coefficients ($(\mu R)_{max}$ = 0.25 (**2b**), 0.25 (**2c**), and 0.28 (**2d**)).

Determination and Refinement of the Structure. The structures of **2c** and **2d** were solved by the conventional heavy-atom method. All the non-hydrogen atoms were reasonably found on the Fourier syntheses that were based on the positions of the Pd atom determined from the Patterson map. In **2d**, one CH_2Cl_2 molecule was found to be solvated in an asymmetric unit. The structure refinements were carried out by the block-diagonal least-squares procedure (HBLS-V[11]), the function minimized being $\sum w(|F_o| - |F_c|)^2$. At the first stage of the refinement of the structure of **2b**, the atomic positions of non-hydrogen atoms in **2d** were used except for the Cl atom in the styrene ligand and the atoms in the BF_4 anion and CH_2Cl_2 molecule. All of these atoms omitted were reasonably found in the subsequent Fourier maps. The locations of anion and solvent molecule were essentially identical with those in **2d**. After anisotropic refinement of the non-hydrogen atoms, all the hydrogen atoms in three complexes were reasonably found in the difference Fourier maps, which were refined isotropically in the subsequent refinement. For the final stage of the refinements of **2b** and **2d**, the Bijvoet pair $|F(hkl)|$ and $|F(\bar{h}\bar{k}\bar{l})|$ reflections were treated as independent data including anomalous dispersion effects. The absolute configuration of the molecule in **2d** was confirmed by the refinement of both models (x, y, z and $\bar{x}, \bar{y}, \bar{z}$), including H atom contribution to convergence. The chosen model had finally an R value of 0.0496, while the enantiomeric structure gave an R of 0.0506. The R factor ratio test[12] applied to these R values showed that the alternative model may be rejected at less than 0.005 significant level. The same procedure as **2d** was applied to the refinement of the structure of **2b**. However, the final R values of the chosen model and its enantiomer were equal to each other, and there are no significant

(3) Ban, E.; Hughes, R. P.; Powell, J. *J. Organomet. Chem.* **1974**, *69*, 455.
(4) Chang, T. C.; Foxman, B. M.; Rosenblum, M.; Stockman, C. *J. Am. Chem. Soc.* **1981**, *103*, 7361.
(5) Sen, A.; Lai, T. W. *Organometallics* **1982**, *1*, 415; *J. Am. Chem. Soc.* **1981**, *103*, 4627.
(6) Kurosawa, H.; Majima, T.; Asada, N. *J. Am. Chem. Soc.* **1980**, *102*, 6996.
(7) Miki, K.; Yama, M.; Kai, Y.; Kasai, N. *J. Organomet. Chem.* **1982**, *239*, 269.
(8) Hartley, F. R. *J. Organomet. Chem.* **1981**, *216*, 277.
(9) Basolo, F.; Pearson, R. G. "Mechanisms of Inorganic Reactions"; Wiley: New York, 1967; pp 371.
(10) Thorn, D. L.; Hoffmann, R. *J. Am. Chem. Soc.* **1978**, *100*, 2079; Ozawa, F.; Ito, T.; Yamamoto, A. *Ibid.* **1980**, *102*, 6457.
(11) Ashida, T. "The Universal Crystallographic Computing System-Osaka", 2nd ed.; Computation Center: Osaka University, 1979; pp 53.
(12) Hamilton, W. C. *Acta Crystallogr.* **1965**, *18*, 502.

Table II. Refinement Details

	2b	2c	2d
no. of reflctns used[a]	6711	5371	6260
no. of parameters refined	517	474	496
weighting parameter[b]			
a[c]	0.0149	0.0657	0.0220
b[c]	0.0004	0.0001	0.0001
final R value[d]	0.040	0.048	0.050
final weighted R value (R_w)[e]	0.047	0.063	0.047

[a] $|F_o| > 3\sigma(|F_o|)$. [b] Weighting scheme used: $w = (\sigma_{cs}^2 + a|F_o| + b|F_o|^2)^{-1}$, where σ_{cs} is the standard deviation obtained from counting statistics. [c] Used in the final refinement. [d] $R = \Sigma||F_o| - |F_c||/\Sigma|F_o|$. [e] $R_w = \{\Sigma w(|F_o| - |F_c|)^2/\Sigma w|F_o|^2\}^{1/2}$.

differences in bond lengths and bond angles of the both refined structures. Therefore, the similar model that had the same configuration as **2d** was adopted as the final model of **2b**. Details of the results on the refinements are summarized in Table II. The atomic scattering factors and anomalous dispersion corrections for non-hydrogen atoms were obtained from ref 13. Scattering factors of hydrogen atoms were taken from those of Stewart et al.[14] Final atomic positional parameters, together with the B_{eq}[15] for non-hydrogen atoms and B values for hydrogen atoms, are listed in Table III. Tables of anisotropic temperature factors for non-hydrogen atoms and observed and calculated structure factors are available in Tables S1 and S2, as supplementary material.

Computation. All the calculations were done on an ACOS 700S computer at Crystallographic Research Center, Institute for Protein Research, Osaka University.

Stability Measurement. The equilibrium constants (K) of eq 2 were determined in CH_2Cl_2 at 0, 15, and 30 °C on a Hitachi Model 200-20 spectrophotometer. The equilibrium mixture was

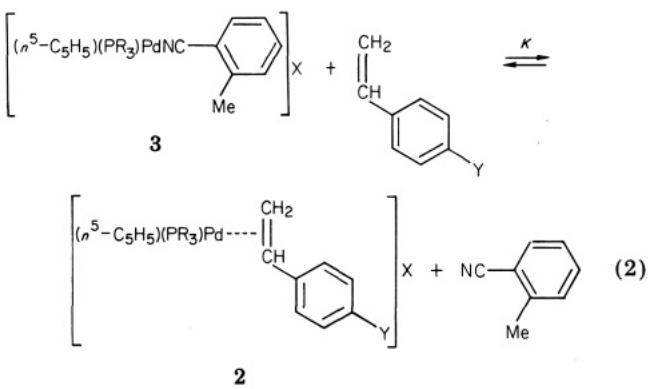

(2)

attained by adding to **2** or **3** ((4∼6) × 10^{-5} M) in CH_2Cl_2 a mixture of the appropriate styrene and *o*-tolunitrile (R′CN) with a known mole ratio, $[R'CN]_0/[\text{styrene}]_0$. Both ligands were used in sufficiently excess amounts with regard to Pd for simplicity of the calculation and avoidance of the decomposition of the complexes during the measurements. In the case of the complexes with R = Et and *n*-Bu where no *o*-tolunitrile complexes could be isolated, the absorbances of the solution containing R′CN and **2** (R = Et, *n*-Bu; Y = H; X = ClO_4)($[R'CN]/[2] \geq 200$) were used as those of **3** in the calculation

$$K = ([R'CN]_0/[\text{styrene}]_0)(\{(\text{Abs}) - (\text{Abs})_3\}/\{(\text{Abs})_2 - (\text{Abs})\})$$

A typical spectral change of the equilibrium mixture in the range of 400–300 nm is shown in Figure 1. The change of the absorbances in the range of 340–315 nm was used in the calculation. Each K value was obtained as an average of three to four measurements employing different $[R'CN]_0/[\text{styrene}]_0$ ratios. Attempts to determine the K values for eq 2 involving the para-nitro and para-dimethylamino substituents were unsuccessful owing to strong absorptions of the free olefin ligands in the range ≤350 nm that prevented reproducible calculations to be obtained. Representative Hammett relations and thermodynamic parameters are shown in Tables IV and V.

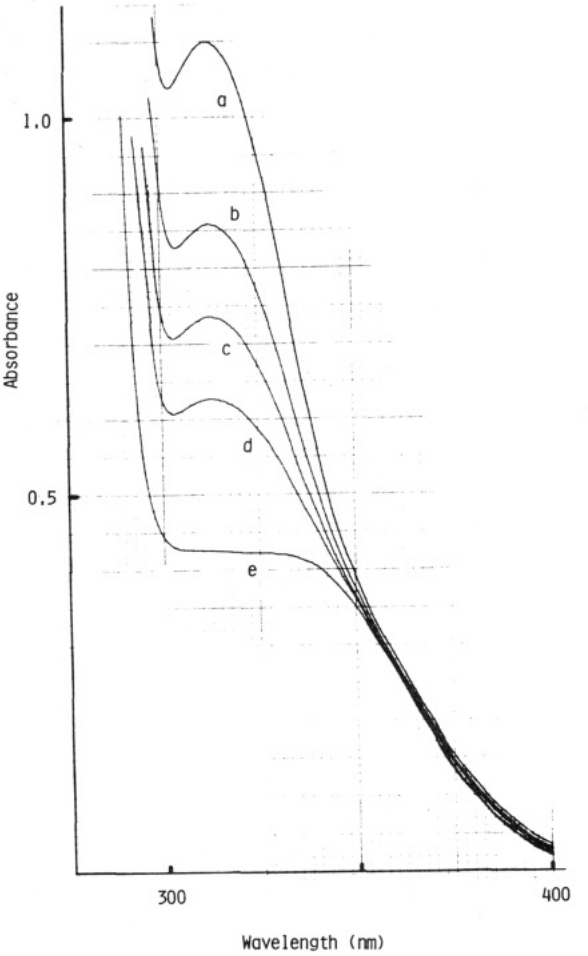

Figure 1. Spectral change corresponding to equilibrium 2 (R = Et, Y = H, X = ClO_4 in CH_2Cl_2 at 15 °C; cell length = 1 cm). To $[Pd(\eta^5\text{-}C_5H_5)(PEt_3)(CH_2{=}CHC_6H_5)]ClO_4$ (6.00 × 10^{-5} mol/L) was added a mixture of styrene/*o*-tolunitrile, [mol/L]/[mol/L]: [4.36 × 10^{-3}]/[0.0] (a); [1.74 × 10^{-2}]/[2.74 × 10^{-3}] (b); [8.72 × 10^{-3}]/[2.74 × 10^{-3}] (c); [4.36 × 10^{-3}]/[2.74 × 10^{-3}] (d); [0.0]/[1.20 × 10^{-2}] (e).

Results and Discussion

Molecular Structure. The molecular structures of **2b–d** are shown in Figure 2. The bond lengths and bond angles are listed in Tables VI and VII, respectively. The structures of three cations are quite similar to each other. In each cationic complex, the Pd atom is coordinated by the cyclopentadienyl (Cp) group, the triphenylphosphine (PPh_3) ligand, and the olefin bond of styrene. A similar coordination geometry around the metal atom has been found in $[Rh(\eta^5\text{-}C_5Me_5)(PPh_3)(\text{ethylene})]$[17] as well as **2a**.[7] The Pd atom, the P atom in the PPh_3 ligand, the center of the Cp group (CCP), and the midpoint of the C(1)=C(2) double bond lie on a plane approximately. The equations of the least-squares planes are listed in Table S3. Figure 3 presents perspective views of the cations in **2b–d** as well as **2a** as viewed along the olefin–metal axis. The atomic numbering scheme of the cation is shown in Figure 4. In **2b–d**, the phenyl groups of the styrene ligands are located

(13) "International Tables for X-ray Crystallography"; Kynoch Press: Birmingham, England, 1974; Vol. IV.
(14) Stewart, R. F.; Davidson, E. R.; Simpson, W. T. *J. Chem. Phys.* **1965**, *42*, 3175.
(15) Hamilton, W. C. *Acta Crystallogr.* **1959**, *12*, 609.
(16) Johnson, C. K. ORTEP-II, Report ORNL-5138; Oak Ridge National Laboratory: TN.
(17) Porzio, W.; Zocchi, M. *J. Am. Chem. Soc.* **1978**, *100*, 2048.

Table III. Final Atomic Parameters along with Their Estimated Standard Deviations in Parentheses[a]

atom	x	y	z	B_{eq}/B	atom	x	y	z	B_{eq}/B
			(a) $[Pd(\eta^5\text{-}C_5H_5)(PPh_3)(CH_2{=}CHC_6H_4OCH_3\text{-}p)]BF_4$ (2b)						
Pd	0.94035 (3)	0.75	0.88380 (3)	3.5	F(1)	0.2945 (5)	0.7979 (3)	0.5863 (6)	10.2
P(1)	0.78509 (10)	0.82057 (7)	0.97217 (10)	3.3	F(2)	0.3119 (5)	0.6618 (3)	0.5790 (5)	9.6
O	0.8847 (4)	0.5316 (3)	0.2881 (4)	6.1	F(3)	0.2670 (4)	0.7302 (3)	0.3829 (4)	8.3
C(1)	0.9822 (5)	0.8375 (3)	0.7275 (6)	4.8	F(4)	0.4617 (3)	0.7460 (5)	0.5108 (5)	10.9
C(2)	0.8776 (5)	0.7942 (4)	0.6606 (5)	4.6	Cl(1S)	0.3565 (5)	0.8968 (3)	0.0873 (4)	17.1
C(3)	0.8776 (5)	0.7268 (3)	0.5634 (4)	4.2	Cl(2S)	0.3224 (4)	0.99477 (17)	0.3235 (3)	12.2
C(4)	0.7636 (5)	0.6858 (4)	0.5073 (5)	5.0	C(S)	0.3697 (13)	0.9011 (7)	0.2576 (10)	11.9
C(5)	0.7614 (5)	0.6213 (4)	0.4163 (6)	5.6	H(1A)	0.981 (5)	0.898 (4)	0.757 (5)	5.5 (12)
C(6)	0.8755 (5)	0.5949 (3)	0.3775 (5)	4.6	H(1B)	1.069 (4)	0.821 (3)	0.715 (5)	3.8 (9)
C(7)	0.9892 (5)	0.6353 (4)	0.4291 (5)	4.6	H(2)	0.810 (5)	0.806 (3)	0.659 (5)	4.4 (10)
C(8)	0.9909 (5)	0.6998 (3)	0.5193 (5)	4.4	H(4)	0.686 (4)	0.707 (3)	0.529 (4)	3.9 (9)
C(9)	0.7704 (8)	0.4889 (6)	0.2305 (9)	9.5	H(5)	0.690 (5)	0.595 (3)	0.382 (5)	4.4 (10)
C(11)	0.9979 (7)	0.6637 (4)	1.0595 (6)	6.6	H(7)	1.060 (5)	0.621 (3)	0.400 (5)	5.0 (11)
C(12)	0.9367 (7)	0.6108 (4)	0.9509 (7)	6.7	H(8)	1.071 (5)	0.728 (3)	0.554 (5)	4.8 (11)
C(13)	1.0055 (7)	0.6138 (4)	0.8486 (7)	6.7	H(9A)	0.722 (5)	0.519 (4)	0.165 (6)	6.5 (13)
C(14)	1.1136 (6)	0.6638 (5)	0.8873 (7)	7.1	H(9B)	0.781 (5)	0.458 (3)	0.174 (6)	5.5 (11)
C(15)	1.1132 (6)	0.6916 (5)	1.0282 (7)	7.3	H(9C)	0.747 (6)	0.472 (4)	0.317 (7)	8.4 (16)
C(21)	0.6596 (4)	0.7484 (4)	1.0011 (4)	3.7	H(11)	0.970 (6)	0.675 (5)	1.142 (7)	8.4 (16)
C(22)	0.6131 (4)	0.7455 (5)	1.1264 (4)	4.6	H(12)	0.850 (5)	0.584 (3)	0.949 (5)	5.1 (11)
C(23)	0.5157 (6)	0.6894 (4)	1.1409 (6)	5.6	H(13)	0.976 (6)	0.590 (4)	0.757 (7)	8.2 (16)
C(24)	0.4670 (5)	0.6388 (4)	1.0321 (7)	6.0	H(14)	1.175 (5)	0.684 (4)	0.831 (5)	5.7 (12)
C(25)	0.5130 (6)	0.6406 (4)	0.9096 (7)	6.1	H(15)	1.169 (6)	0.725 (4)	1.085 (6)	7.1 (14)
C(26)	0.6094 (5)	0.6955 (4)	0.8937 (5)	5.0	H(22)	0.649 (4)	0.777 (3)	1.201 (5)	4.3 (10)
C(31)	0.8349 (5)	0.8744 (3)	1.1377 (5)	3.8	H(23)	0.494 (5)	0.687 (3)	1.231 (5)	4.6 (10)
C(32)	0.9513 (5)	0.8579 (4)	1.2230 (5)	5.1	H(24)	0.392 (4)	0.602 (3)	1.047 (4)	3.2 (8)
C(33)	0.9819 (7)	0.8962 (4)	1.3534 (6)	6.4	H(25)	0.482 (7)	0.607 (4)	0.845 (7)	7.8 (16)
C(34)	0.8980 (8)	0.9485 (4)	1.3976 (5)	6.9	H(26)	0.638 (6)	0.699 (4)	0.807 (5)	6.1 (12)
C(35)	0.7825 (7)	0.9684 (4)	1.3119 (6)	6.1	H(32)	1.014 (5)	0.822 (3)	1.190 (5)	4.6 (10)
C(36)	0.7500 (6)	0.9311 (4)	1.1813 (6)	5.1	H(33)	1.058 (5)	0.880 (4)	1.410 (6)	5.9 (12)
C(41)	0.7073 (4)	0.8993 (3)	0.8532 (4)	3.4	H(34)	0.915 (6)	0.968 (4)	1.488 (6)	6.7 (14)
C(42)	0.5905 (5)	0.8854 (3)	0.7650 (5)	4.2	H(35)	0.720 (7)	1.004 (4)	1.342 (7)	8.5 (16)
C(43)	0.5428 (5)	0.9430 (4)	0.6639 (6)	4.9	H(36)	0.665 (5)	0.943 (3)	1.121 (5)	4.7 (10)
C(44)	0.6059 (6)	1.0153 (4)	0.6517 (6)	5.3	H(42)	0.536 (4)	0.836 (3)	0.774 (5)	4.2 (10)
C(45)	0.7240 (5)	1.0304 (3)	0.7440 (5)	4.3	H(43)	0.454 (6)	0.927 (4)	0.598 (6)	6.8 (14)
C(46)	0.7718 (5)	0.9726 (3)	0.8430 (5)	4.0	H(44)	0.579 (5)	1.054 (4)	0.582 (5)	5.3 (11)
B	0.3373 (6)	0.7355 (5)	0.5154 (7)	5.7	H(45)	0.774 (5)	1.081 (3)	0.739 (5)	4.5 (10)
					H(46)	0.844 (4)	0.979 (3)	0.899 (4)	3.2 (8)
					H(1S)	0.328 (10)	0.866 (7)	0.301 (10)	15.6 (32)
					H(2S)	0.462 (8)	0.904 (6)	0.301 (9)	12.0 (23)
			(b) $[Pd(\eta^5\text{-}C_5H_5)(PPh_3)(CH_2{=}CHC_6H_5)]PF_6$ (2c)						
Pd	0.58112 (2)	0.31990 (3)	0.345776 (18)	3.6	F(1)	0.3197 (4)	0.0432 (7)	0.4308 (5)	14.9
P(1)	0.60003 (7)	0.16556 (10)	0.26704 (6)	3.1	F(2)	0.2196 (5)	0.0123 (5)	0.4838 (3)	12.5
C(1)	0.7069 (4)	0.4140 (6)	0.3562 (3)	4.3	F(3)	0.1334 (5)	0.1462 (9)	0.3991 (6)	19.6
C(2)	0.7265 (3)	0.3394 (4)	0.4202 (3)	3.6	F(4)	0.2366 (5)	0.1700 (4)	0.3430 (3)	10.6
C(3)	0.7329 (3)	0.3733 (4)	0.5034 (3)	3.6	F(5)	0.1912 (6)	−0.0125 (5)	0.3573 (3)	17.8
C(4)	0.7384 (4)	0.2838 (5)	0.5592 (3)	4.5	F(6)	0.2622 (6)	0.1943 (5)	0.4704 (4)	15.2
C(5)	0.7427 (4)	0.3138 (6)	0.6372 (4)	5.6	H(1A)	0.724 (3)	0.392 (5)	0.311 (3)	4.8 (11)
C(6)	0.7428 (4)	0.4309 (7)	0.6596 (3)	5.9	H(1B)	0.694 (3)	0.490 (4)	0.360 (3)	3.7 (9)
C(7)	0.7380 (4)	0.5192 (6)	0.6055 (4)	5.5	H(2)	0.756 (3)	0.267 (4)	0.414 (3)	3.6 (9)
C(8)	0.7327 (4)	0.4920 (5)	0.5271 (3)	4.4	H(4)	0.738 (3)	0.203 (4)	0.542 (3)	3.8 (10)
C(11)	0.4318 (4)	0.3216 (8)	0.3147 (4)	8.3	H(5)	0.747 (4)	0.258 (6)	0.675 (4)	7.1 (15)
C(12)	0.4623 (5)	0.2791 (7)	0.3943 (5)	7.2	H(6)	0.745 (4)	0.447 (5)	0.714 (3)	5.8 (13)
C(13)	0.5087 (4)	0.3668 (8)	0.4399 (4)	7.1	H(7)	0.736 (4)	0.601 (5)	0.619 (3)	4.9 (11)
C(14)	0.5076 (5)	0.4655 (7)	0.3912 (5)	7.1	H(8)	0.733 (3)	0.556 (4)	0.489 (3)	4.4 (10)
C(15)	0.4555 (5)	0.4423 (8)	0.3151 (4)	7.7	H(11)	0.404 (5)	0.280 (7)	0.273 (4)	9.6 (19)
C(21)	0.5448 (3)	0.0320 (4)	0.2872 (3)	4.0	H(12)	0.458 (4)	0.205 (5)	0.411 (3)	6.2 (13)
C(22)	0.4864 (4)	−0.0340 (5)	0.2264 (4)	5.3	H(13)	0.534 (4)	0.361 (6)	0.496 (4)	7.1 (15)
C(23)	0.4436 (4)	−0.134[illegible] (6)	0.2464 (5)	7.2	H(14)	0.533 (5)	0.541 (6)	0.404 (4)	9.3 (19)
C(24)	0.4591 (5)	−0.1683 (6)	0.3219 (6)	8.0	H(15)	0.444 (5)	0.498 (7)	0.270 (4)	10.2 (20)
C(25)	0.5167 (6)	−0.1041 (7)	0.3831 (5)	8.5	H(22)	0.481 (3)	−0.009 (4)	0.172 (3)	4.3 (10)
C(26)	0.5596 (5)	−0.0020 (6)	0.3665 (4)	6.2	H(23)	0.411 (4)	−0.177 (5)	0.205 (4)	7.1 (15)
C(31)	0.5570 (3)	0.1900 (4)	0.1602 (3)	3.7	H(24)	0.432 (5)	−0.243 (6)	0.333 (4)	8.8 (17)
C(32)	0.4934 (3)	0.2764 (5)	0.1280 (3)	4.1	H(25)	0.527 (5)	−0.126 (7)	0.441 (4)	9.8 (19)
C(33)	0.4610 (4)	0.2936 (5)	0.0464 (3)	5.0	H(26)	0.594 (4)	0.054 (5)	0.409 (3)	6.1 (13)
C(34)	0.4929 (4)	0.2247 (7)	−0.0034 (4)	6.1	H(32)	0.478 (4)	0.320 (4)	0.159 (3)	5.2 (12)
C(35)	0.5552 (5)	0.1382 (7)	0.0274 (4)	6.5	H(33)	0.421 (4)	0.352 (5)	0.027 (3)	5.4 (12)
C(36)	0.5876 (4)	0.1186 (6)	0.1086 (3)	5.3	H(34)	0.471 (4)	0.237 (6)	−0.062 (4)	7.4 (15)
C(41)	0.7178 (3)	0.1274 (4)	0.2839 (3)	3.6	H(35)	0.575 (4)	0.093 (5)	−0.004 (4)	6.5 (14)
C(42)	0.7608 (4)	0.0405 (5)	0.3379 (3)	4.8	H(36)	0.626 (4)	0.055 (5)	0.129 (3)	5.5 (12)
C(43)	0.8522 (4)	0.0218 (7)	0.3557 (4)	6.9	H(42)	0.730 (3)	−0.000 (5)	0.363 (3)	4.7 (11)
C(44)	0.9019 (4)	0.887 (8)	0.3199 (5)	8.2	H(43)	0.877 (4)	−0.033 (5)	0.392 (3)	6.3 (13)
C(45)	0.8611 (4)	0.1764 (6)	0.2659 (5)	7.3	H(44)	0.962 (4)	0.073 (5)	0.335 (4)	6.4 (14)
C(46)	0.7690 (4)	0.1973 (5)	0.2477 (4)	5.1	H(45)	0.889 (4)	0.217 (6)	0.242 (4)	8.0 (16)
P(2)	0.22498 (10)	0.09229 (14)	0.41317 (9)	5.3	H(46)	0.739 (4)	0.255 (5)	0.209 (3)	5.8 (12)

Table III (*Continued*)

(c) $[Pd(\eta^5\text{-}C_5H_5)(PPh_3)(CH_2{=}CHC_6H_4Cl\text{-}p)]BF_4$ (2d)

Pd	0.93728 (4)	0.75	0.89122 (4)	3.2	F(1)	0.2831 (5)	0.7921 (4)	0.5859 (7)	10.6
Cl(1)	0.8223 (3)	0.51742 (13)	0.2764 (3)	7.7	F(2)	0.3061 (8)	0.6620 (4)	0.5599 (7)	13.0
P(1)	0.77824 (13)	0.82142 (9)	0.97504 (13)	3.2	F(3)	0.2430 (5)	0.7334 (4)	0.3743 (5)	9.0

atom	x	y	z	B_{eq}/B	atom	x	y	z	B_{eq}/B
C(1)	0.9947 (7)	0.8345 (4)	0.7389 (7)	4.8	F(4)	0.4455 (4)	0.7472 (7)	0.4891 (7)	14.1
C(2)	0.8821 (6)	0.7985 (4)	0.6718 (6)	4.1	Cl(1S)	0.3241 (4)	0.99317 (18)	0.3078 (3)	11.5
C(3)	0.8701 (5)	0.7313 (3)	0.5724 (5)	3.6	Cl(2S)	0.3215 (5)	0.9064 (3)	0.0473 (4)	15.3
C(4)	0.7456 (6)	0.6977 (4)	0.5231 (6)	4.5	C(S)	0.3437 (15)	0.9042 (7)	0.2238 (14)	13.0
C(5)	0.7307 (7)	0.6324 (5)	0.4318 (7)	5.2	H(1A)	0.989 (7)	0.881 (5)	0.779 (7)	7.9 (18)
C(6)	0.8411 (7)	0.6001 (4)	0.3896 (6)	4.7	H(1B)	1.072 (5)	0.818 (4)	0.712 (6)	4.7 (12)
C(7)	0.9627 (6)	0.6335 (4)	0.4350 (6)	4.6	H(2)	0.824 (4)	0.824 (3)	0.673 (5)	2.5 (9)
C(8)	0.9760 (6)	0.6983 (4)	0.5237 (6)	4.2	H(4)	0.667 (5)	0.726 (3)	0.557 (5)	3.5 (11)
C(11)	0.9931 (8)	0.6653 (4)	1.0701 (7)	6.1	H(5)	0.654 (6)	0.609 (4)	0.408 (6)	6.0 (15)
C(12)	0.9252 (8)	0.6120 (4)	0.9600 (8)	5.7	H(7)	1.023 (4)	0.612 (3)	0.403 (4)	1.4 (8)
C(13)	0.9957 (8)	0.6115 (4)	0.8571 (7)	5.9	H(8)	1.049 (5)	0.720 (3)	0.543 (5)	4.1 (12)
C(14)	1.1107 (7)	0.6614 (5)	0.8991 (8)	6.3	H(11)	0.961 (6)	0.677 (4)	1.147 (6)	6.3 (15)
C(15)	1.1103 (7)	0.6884 (5)	1.0345 (8)	6.4	H(12)	0.839 (6)	0.591 (4)	0.967 (6)	6.0 (15)
C(21)	0.6501 (4)	0.7516 (5)	1.0008 (5)	3.6	H(13)	0.986 (6)	0.593 (4)	0.772 (6)	6.0 (15)
C(22)	0.5996 (5)	0.7478 (7)	1.1240 (5)	4.6	H(14)	1.161 (6)	0.667 (5)	0.835 (7)	7.2 (17)
C(23)	0.5033 (6)	0.6907 (5)	1.1380 (7)	5.3	H(15)	1.167 (6)	0.721 (3)	1.081 (6)	5.6 (15)
C(24)	0.4557 (6)	0.6397 (5)	1.0302 (8)	5.7	H(22)	0.631 (5)	0.777 (3)	1.188 (6)	4.7 (13)
C(25)	0.5057 (8)	0.6427 (5)	0.9094 (8)	6.4	H(23)	0.473 (6)	0.688 (4)	1.232 (6)	5.3 (13)
C(26)	0.6022 (6)	0.6976 (4)	0.8931 (7)	5.0	H(24)	0.367 (5)	0.592 (3)	1.050 (5)	3.8 (11)
C(31)	0.8282 (6)	0.8747 (4)	1.1410 (5)	3.6	H(25)	0.475 (7)	0.619 (4)	0.865 (7)	7.4 (17)
C(32)	0.9469 (6)	0.8580 (4)	1.2303 (6)	4.4	H(26)	0.631 (5)	0.696 (3)	0.811 (5)	2.9 (10)
C(33)	0.9764 (7)	0.8962 (5)	1.3614 (7)	5.5	H(32)	1.013 (5)	0.816 (3)	1.201 (5)	3.1 (10)
C(34)	0.8930 (8)	0.9502 (4)	1.4018 (6)	5.8	H(33)	1.054 (7)	0.880 (5)	1.403 (8)	8.3 (19)
C(35)	0.7757 (8)	0.9679 (5)	1.3137 (7)	6.2	H(34)	0.909 (6)	0.969 (4)	1.505 (7)	6.7 (16)
C(36)	0.7431 (7)	0.9321 (4)	1.1841 (7)	5.1	H(35)	0.730 (6)	1.001 (4)	1.339 (7)	6.5 (16)
C(41)	0.7015 (5)	0.8994 (3)	0.8548 (5)	3.2	H(36)	0.670 (5)	0.947 (4)	1.131 (6)	4.2 (12)
C(42)	0.5789 (6)	0.8883 (4)	0.7682 (6)	4.0	H(42)	0.527 (5)	0.839 (3)	0.769 (5)	3.2 (10)
C(43)	0.5329 (6)	0.9456 (5)	0.6644 (7)	5.4	H(43)	0.455 (7)	0.938 (5)	0.624 (7)	7.8 (18)
C(44)	0.6019 (6)	1.0135 (4)	0.6466 (7)	4.9	H(44)	0.574 (5)	1.055 (3)	0.574 (5)	3.6 (11)
C(45)	0.7239 (6)	1.0257 (4)	0.7361 (7)	4.1	H(45)	0.768 (4)	1.067 (3)	0.730 (4)	1.6 (8)
C(46)	0.7724 (5)	0.9698 (4)	0.8392 (6)	3.7	H(46)	0.846 (5)	0.970 (3)	0.893 (5)	3.1 (10)
B	0.3233 (7)	0.7369 (7)	0.5032 (9)	5.8	H(1S)	0.410 (10)	0.896 (7)	0.249 (11)	14.9 (33)
					H(2S)	0.303 (8)	0.883 (5)	0.256 (8)	9.4 (21)

[a] Positional parameters in fraction of cell edges and thermal parameters (B_{eq} for non-hydrogen atoms and B for hydrogen atoms) in the form of $\exp\{-B((\sin\theta)/\lambda)^2\}$, where B_{eq} is the equivalent isotropic temperature factor calculated from the corresponding anisotropic factors.[15]

Table IV. Equilibrium Constants (K) and Hammett Correlations[a] for Equilibrium 2 at 15 °C

R	X	Y	K	$-\rho$ (r)	$-\rho^+$ (r)
Ph	ClO_4	Cl	0.048 ± 0.002	1.94 (0.9995)	0.97 (0.920)
		H	0.13 ± 0.01		
		Me	0.27 ± 0.03		
		OMe	0.45 ± 0.04		
	BF_4	Cl	0.050 ± 0.002	1.83 (0.999)	0.89 (0.891)
		H	0.14 ± 0.01		
		Me	0.28 ± 0.03		
		OMe	0.40 ± 0.04		
Et	ClO_4	Cl	0.095 ± 0.009	2.01 (0.996)	1.02 (0.931)
		H	0.27 ± 0.02		
		Me	0.52 ± 0.04		
		OMe	1.01 ± 0.06		
n-Bu	ClO_4	Cl	0.092 ± 0.008	1.91 (0.995)	0.96 (0.919)
		H	0.27 ± 0.02		
		Me	0.47 ± 0.05		
		OMe	0.88 ± 0.08		

[a] $\log K = \rho\sigma + C$ or $\rho^+\sigma^+ + C'$.

at the Cp side, while at the PEt_3 side in **2a**.[7] This is due to the difference of the steric hindrance between the PPh_3 and PEt_3 ligands. The C(1)=C(2) olefin bonds are almost perpendicular to the coordination plane of Pd in agreement with the theoretical prediction (see later). However, there are slight twists of the C=C bond about the olefin–Pd bond. The angles between the C(1)=C(2) bond and the P–Pd–CCP plane are 83.0, 89.9, and 78.1° for **2b**, **2c**, and **2d**, respectively (cf. 77.3° for **2a**[7]). In the previous paper, we suggested that the twist of the C=C bond has probably resulted from intramolecular contacts between the styrene and the other ligands in **2a**. Also in the present complexes, the styrene ligands contact with both the Cp and PPh_3 ligands: C(1)···C(14) = 3.408 (8), 3.391 (9), and 3.358 (10) Å, C(1)···C(46) = 3.449 (7), 3.403 (8), and 3.471 (8) Å, C(2)···C(41) = 3.288 (6), 3.347 (6), and 3.260 (7) Å, C(3)···C(13) = 3.397 (8), 3.327 (9), and 3.435 (9) Å, C(8)···C(13) = 3.462 (9), 3.637 (10), and 3.493 (9) Å for **2b**, **2c**, and **2d**, respectively. The slight differences of the twist angles in **2b**, **2c**, and **2d** are probably caused by both these intra-

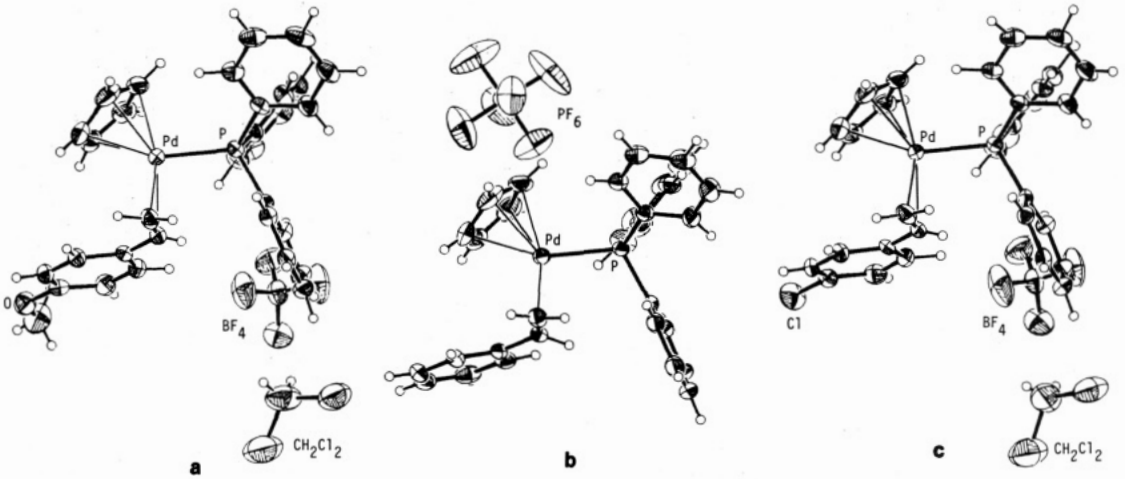

Figure 2. The molecular structure of **2b**, **2c**, and **2d** (ORTEP drawing[16]). Non-hydrogen atoms are represented by thermal ellipsoids at 30% probability levels, whereas temperature factors of hydrogens are arbitrarily reduced for clarity: (a) **2b**; (b) **2c**; (c) **2d**.

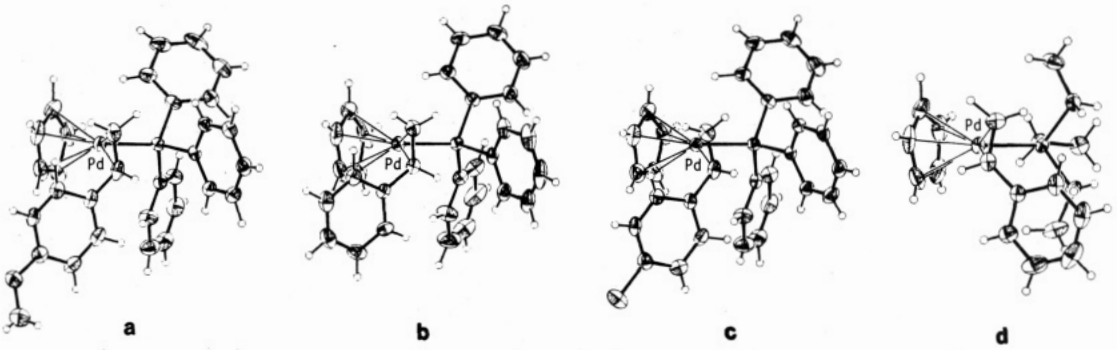

Figure 3. Perspective views of the cations viewed along the olefin–metal axis. Representations of atoms are same as those in the Figure 2 (ORTEP drawing[16]): (a) **2b**; (b) **2c**; (c) **2d**; (d) **2a** ($[Pd(\eta^5\text{-}C_5H_5)(PEt_3)(CH_2{=}CHC_6H_5)]$ cation).[7]

Table V. Thermodynamic Data for Equilibrium 2

R	X	Y	$\Delta G°$(288 K), KJ/mol	$-\Delta H°$, KJ/mol	$-\Delta S°$(288 K), J/(mol deg)
Ph	ClO_4	Cl	7.3 ± 0.1	9.3 ± 0.9	58 ± 4
		H	4.9 ± 0.2	9.9 ± 1.0	51 ± 4
		Me	3.1 ± 0.3	10.4 ± 1.0	47 ± 5
		OMe	1.9 ± 0.2	11.0 ± 1.0	45 ± 4
	BF_4	Cl	7.2 ± 0.1	8.9 ± 0.9	56 ± 4
		H	4.7 ± 0.2	9.5 ± 0.9	49 ± 4
		Me	3.0 ± 0.3	10.2 ± 1.0	46 ± 5
		OMe	2.2 ± 0.3	11.1 ± 1.0	46 ± 5
Et	ClO_4	Cl	5.6 ± 0.3	12.7 ± 1.3	63 ± 6
		H	3.1 ± 0.2	13.7 ± 1.3	58 ± 6
		Me	1.6 ± 0.2	13.8 ± 1.4	53 ± 6
		OMe	0.0 ± 0.2	13.3 ± 1.3	46 ± 6
n-Bu	ClO_4	Cl	5.7 ± 0.2	12.9 ± 1.3	65 ± 6
		H	3.1 ± 0.2	13.5 ± 1.3	58 ± 6
		Me	1.8 ± 0.3	12.6 ± 1.3	50 ± 6
		OMe	0.3 ± 0.2	12.6 ± 1.3	45 ± 6

molecular contacts and the intermolecular contacts in crystal structures.

Olefin–Palladium Bonding. The Pd–C(1) distances in **2b**, **2c**, and **2d** are significantly shorter than the Pd–C(2) ones, as in the other styrene complexes of Pd and Pt[7,18-20] [M–C(1) = 2.14–2.19, M–C(2) = 2.20–2.26 Å]. Such asymmetrical coordination of two carbon atoms in asymmetrically substituted olefins to the metal atom has been

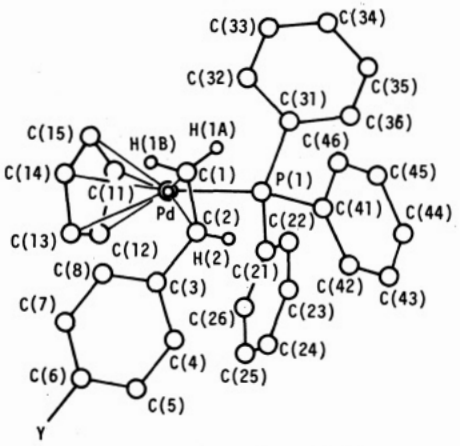

Figure 4. Numbering systems of non-hydrogen atoms in the cation. For numberings of hydrogen atoms, the same numbers as the carbon atoms are used. Y is O–C(9), H(6), and Cl for **2b**, **2c**, and **2d**, respectively.

pointed out and discussed in terms of the nature of the olefin–metal bond.[19,21] Useful informations for the nature of the olefin–Pd bond may be obtained from comparison of Pd–C(olefin) distances in the substituted styrene complexes, particularly those in **2b** and **2d** that are isomorphous with each other as mentioned before. In **2b–d**, there is no significant difference in the Pd–C(1) distance, while the Pd–C(2) distance tends to shorten with increase of the electron-withdrawing ability of Y; the difference of the

(18) Ball, R. G.; Payne, N. C. *Inorg. Chem.* **1976**, *15*, 2494.
(19) Nyburg, S. C.; Simpson, K.; Wong-Ng, W. *J. Chem. Soc., Dalton Trans.* **1976**, 1865.
(20) van der Poel, H.; van Koten, G.; Kokkes, M.; Stam, C. H. *Inorg. Chem.* **1981**, *20*, 2941.
(21) Albright, T. A.; Hoffmann, R.; Thibeault, J. C.; Thorn, D. L. *J. Am. Chem. Soc.* **1979**, *101*, 3801.

Table VI. Selected Bond Lengths (Å) along with Their Estimated Standard Deviations in Parentheses

	2b	2c	2d
Pd-C(1)	2.182 (5)	2.182 (5)	2.187 (6)
Pd-C(2)	2.264 (5)	2.255 (5)	2.235 (6)
Pd-CET[a]	2.115	2.112	2.104
Pd-C(11)	2.210 (7)	2.221 (9)	2.211 (8)
Pd-C(12)	2.367 (7)	2.306 (8)	2.378 (8)
Pd-C(13)	2.370 (7)	2.329 (8)	2.399 (8)
Pd-C(14)	2.301 (7)	2.271 (7)	2.305 (7)
Pd-C(15)	2.300 (7)	2.313 (8)	2.286 (8)
Pd-C(Cp)[b] [av]	2.310	2.288	2.316
Pd-CCP[c]	1.983	1.964	1.988
Pd-P(1)	2.286 (1)	2.288 (1)	2.292 (1)
C(1)-C(2)	1.373 (7)	1.361 (7)	1.360 (9)
C(2)-C(3)	1.448 (7)	1.485 (6)	1.456 (7)
C(3)-C(4)	1.400 (7)	1.386 (7)	1.402 (8)
C(4)-C(5)	1.371 (8)	1.395 (8)	1.381 (9)
C(5)-C(6)	1.389 (8)	1.368 (9)	1.389 (9)
C(6)-C(7)	1.383 (7)	1.357 (9)	1.369 (9)
C(7)-C(8)	1.366 (7)	1.389 (8)	1.360 (8)
C(8)-C(3)	1.407 (6)	1.392 (7)	1.383 (7)
C(6)-O	1.362 (6)		
O-C(9)	1.419 (9)		
C(6)-Cl			1.735 (7)
C(11)-C(12)	1.425 (10)	1.418 (11)	1.454 (11)
C(12)-C(13)	1.327 (10)	1.332 (11)	1.339 (11)
C(13)-C(14)	1.399 (10)	1.396 (11)	1.441 (11)
C(14)-C(15)	1.437 (10)	1.363 (11)	1.382 (11)
C(15)-C(11)	1.380 (10)	1.399 (12)	1.377 (11)
C(Cp)-C(Cp)[b] [av]	1.394	1.382	1.399
P(1)-C(21)	1.830 (6)	1.812 (5)	1.808 (8)
C(21)-C(22)	1.386 (9)	1.387 (8)	1.388 (13)
C(22)-C(23)	1.401 (9)	1.405 (10)	1.396 (12)
C(23)-C(24)	1.366 (8)	1.331 (12)	1.356 (10)
C(24)-C(25)	1.358 (9)	1.377 (13)	1.363 (10)
C(25)-C(26)	1.383 (8)	1.398 (11)	1.378 (10)
C(26)-C(21)	1.384 (8)	1.396 (8)	1.388 (10)
P(1)-C(31)	1.823 (5)	1.815 (5)	1.815 (6)
C(31)-C(32)	1.380 (7)	1.376 (7)	1.391 (8)
C(32)-C(33)	1.396 (8)	1.383 (7)	1.395 (9)
C(33)-C(34)	1.351 (10)	1.368 (9)	1.348 (10)
C(34)-C(35)	1.387 (10)	1.360 (10)	1.377 (11)
C(35)-C(36)	1.392 (9)	1.381 (9)	1.367 (10)
C(36)-C(31)	1.403 (7)	1.396 (7)	1.408 (9)
P(1)-C(41)	1.822 (4)	1.818 (4)	1.812 (5)
C(41)-C(42)	1.388 (6)	1.381 (7)	1.395 (7)
C(42)-C(43)	1.387 (7)	1.378 (9)	1.394 (9)
C(43)-C(44)	1.370 (8)	1.361 (10)	1.357 (9)
C(44)-C(45)	1.420 (7)	1.378 (11)	1.405 (9)
C(45)-C(46)	1.377 (6)	1.391 (10)	1.379 (8)
C(46)-C(41)	1.389 (6)	1.401 (7)	1.397 (7)
B-F(1)	1.349 (9)		1.327 (12)
B-F(2)	1.399 (9)		1.376 (13)
B-F(3)	1.368 (8)		1.361 (12)
B-F(4)	1.331 (10)		1.309 (15)
P(2)-F(1)		1.514 (8)	
P(2)-F(2)		1.554 (7)	
P(2)-F(3)		1.498 (10)	
P(2)-F(4)		1.566 (7)	
P(2)-F(5)		1.517 (9)	
P(2)-F(6)		1.516 (9)	
Cl(1S)-C(S)	1.632 (14)		1.706 (15)
Cl(2S)-C(S)	1.762 (13)		1.676 (16)
C(1)-H(1A)	1.03 (5)	0.94 (5)	0.86 (7)
C(1)-H(1B)	0.98 (5)	0.88 (5)	0.93 (6)
C(2)-H(2)	0.74 (5)	0.96 (5)	0.73 (5)

[a] CET is the midpoint of the olefinic C(1)=C(2) bond in styrene. [b] C(Cp) is the carbon of the cyclopentadienyl ring. [c] CCP is the center of the cyclopentadienyl ring.

Pd–C(2) distances in **2b** and **2d** is 0.029 (8) Å. The former trend is somewhat surprising in view of the fact that in the square-planar complexes, *trans*-$PtCl_2$(Me-pyridine)-(CH_2=CHC_6H_4Y-*p*)[19] the Pt–C(1) distance in the more donating styrene (Y = NMe_2) complex is shorter than that in the less donating styrene (Y = H) complex by 0.043 (21) Å, and the Pt–C(2) distance in the former is somewhat longer than that in the latter by 0.026 (19) Å. This observation was a part of the bases for the significant contribution of form A.[19] By contrast, the present trend can be understood if the π back-bonding plays some role in the olefin–Pd bonding of **2** (see later).

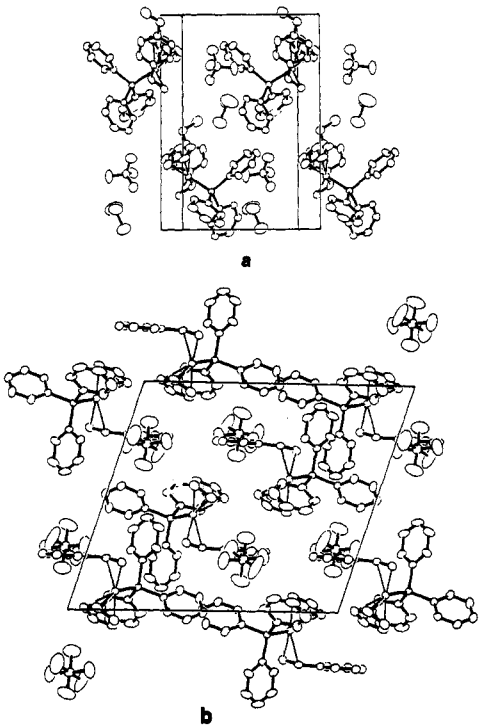

Figure 5. Crystal structures viewed along the c* axis for **2b** and along the *b* axis for **2c** (ORTEP drawings[16]). Atoms are represented by 30% probability ellipsoids. Hydrogen atoms are omitted for clarity: (a) **2b**; (b) **2c**.

Another point of interest lies in the fact that the Pd–C(2) distance of **2c** is longer than that of **2a**[7] by 0.021 (7) Å though the Pd–C(1) distances are much the same in **2c** and **2a** [Pd–C(1) = 2.176 (6) Å]. On the other hand, the Pd–C(Cp) distances in **2c** are almost the same as or rather a little shorter than those in **2a** (see below). This would be understood if the olefin–Pd bond, but not the Cp–Pd bond, in **2a** effectively accepted, through π interaction, the more electron density donated by PEt_3 as compared to PPh_3.

Cyclopentadienyl Ligand. The complexes **2b** and **2d** exhibit the marked asymmetric coordination of and the electron localization around the Cp ring, as in the other (cyclopentadienyl)transition-metal complexes[22] including those that should be symmetric in nature (e.g., M(η^5-C_5H_5)$(CO)_3$, M = Re, Mn).[22c,d] In the present case examination of intra- and intermolecular contacts to the Cp carbons did not reveal any correlation with the observed asymmetry, and we cannot present any reasonable explanation for it. The Pd–C(Cp) distances of **2a** and **2c** show somewhat narrower variations, and those of the latter are almost the same as or slightly shorter than those of the former (2.251–2.353 Å, average 2.292 Å).

Crystal Structure. The crystal structures of **2b** and **2c** are presented in Figure 5. All the intermolecular atomic contacts are considered to be normal van der Waals distances, the shortest contact between non-hydrogen

(22) (a) Bennett, M. J.; Churchill, M. R.; Gerloch, M.; Mason, R. *Nature (London)* **1964**, *201*, 1318. (b) Byers, L. R.; Dahl, L. F. *Inorg. Chem.* **1980**, *19*, 892. (c) Fitzpatrick, P. J.; Page, Y. L.; Butler, I. S. *Acta Crystallogr., Sect. B* **1981**, *B37*, 1052. (d) Fitzpatrick, P. J.; Page, Y. L.; Sedman, J.; Butler, I. S. *Inorg. Chem.* **1981**, *20*, 2852.

Table VII. Selected Bond Angles (deg) along with Their Estimated Standard Deviations in Parentheses

	2b	2c	2d		2b	2c	2d
P(1)-Pd-CET[a]	97.84	98.18	98.81	C(21)-C(22)-C(23)	119.1 (6)	118.9 (6)	120.3 (9)
P(1)-Pd-CCP[a]	129.29	130.58	128.99	C(22)-C(23)-C(24)	120.1 (6)	121.4 (8)	120.5 (8)
CET[a]-Pd-CCP[a]	132.30	131.13	131.77	C(23)-C(24)-C(25)	121.1 (6)	120.7 (9)	119.4 (7)
C(1)-Pd-C(2)	35.91 (18)	35.68 (17)	35.8 (3)	C(24)-C(25)-C(26)	119.5 (6)	120.1 (8)	121.5 (7)
Pd-C(1)-C(2)	75.3 (3)	75.1 (3)	74.1 (4)	C(25)-C(26)-C(21)	120.8 (6)	119.2 (7)	120.0 (7)
Pd-C(1)-H(1A)	115 (3)	106 (3)	102 (5)	P(1)-C(31)-C(32)	121.4 (4)	121.6 (4)	121.6 (5)
Pd-C(1)-H(1B)	102 (3)	105 (3)	111 (4)	P(1)-C(31)-C(36)	118.8 (4)	119.7 (4)	119.7 (5)
H(1A)-C(1)-H(1B)	111 (4)	116 (5)	122 (6)	C(36)-C(31)-C(32)	119.7 (5)	118.7 (5)	118.6 (6)
C(2)-C(1)-H(1A)	126 (3)	119 (3)	118 (5)	C(31)-C(32)-C(33)	119.7 (5)	120.9 (5)	119.4 (6)
C(2)-C(1)-H(1B)	119 (3)	122 (3)	116 (4)	C(32)-C(33)-C(34)	120.6 (7)	119.8 (6)	121.2 (7)
Pd-C(2)-C(1)	68.8 (3)	69.2 (3)	70.2 (4)	C(33)-C(34)-C(35)	120.9 (7)	120.0 (7)	120.0 (8)
Pd-C(2)-C(3)	110.1 (4)	110.6 (3)	109.1 (4)	C(34)-C(35)-C(36)	119.5 (7)	121.1 (7)	120.8 (8)
Pd-C(2)-H(2)	103 (4)	106 (3)	104 (4)	C(35)-C(36)-C(31)	119.6 (6)	119.5 (6)	120.0 (7)
C(1)-C(2)-C(3)	127.4 (5)	126.2 (5)	127.3 (6)	P(1)-C(41)-C(42)	121.8 (4)	122.1 (4)	122.1 (4)
C(1)-C(2)-H(2)	124 (4)	115 (3)	112 (4)	P(1)-C(41)-C(46)	118.8 (3)	118.7 (4)	118.8 (4)
C(3)-C(2)-H(2)	108 (4)	116 (3)	118 (4)	C(46)-C(41)-C(42)	119.3 (4)	118.9 (5)	118.8 (5)
C(2)-C(3)-C(4)	121.2 (5)	119.0 (5)	118.9 (5)	C(41)-C(42)-C(43)	119.8 (5)	120.9 (6)	119.5 (6)
C(2)-C(3)-C(8)	122.1 (5)	122.2 (5)	123.2 (5)	C(42)-C(43)-C(44)	121.6 (5)	120.3 (7)	122.1 (7)
C(4)-C(3)-C(8)	116.7 (5)	118.8 (5)	117.9 (5)	C(43)-C(44)-C(45)	118.7 (5)	120.2 (8)	118.3 (6)
C(3)-C(4)-C(5)	122.2 (6)	119.8 (5)	120.6 (6)	C(44)-C(45)-C(46)	119.6 (5)	120.3 (7)	120.8 (6)
C(4)-C(5)-C(6)	119.6 (6)	120.6 (6)	119.1 (6)	C(45)-C(46)-C(41)	121.1 (4)	119.4 (6)	120.3 (5)
C(5)-C(6)-C(7)	119.4 (5)	120.0 (7)	120.8 (6)	F(1)-B-F(2)	108.6 (6)		107.2 (9)
C(6)-C(7)-C(8)	120.8 (5)	120.7 (6)	119.6 (6)	F(1)-B-F(3)	110.6 (6)		111.8 (9)
C(7)-C(8)-C(3)	121.2 (5)	120.1 (5)	122.0 (6)	F(1)-B-F(4)	109.8 (7)		113.1 (10)
C(5)-C(6)-O	124.7 (5)			F(2)-B-F(3)	104.1 (6)		102.9 (9)
C(7)-C(6)-O	116.0 (5)			F(2)-B-F(4)	113.0 (7)		111.0 (10)
C(6)-O-C(9)	118.2 (5)			F(3)-B-F(4)	110.6 (7)		110.3 (10)
C(5)-C(6)-Cl			118.9 (5)	F(1)-P(2)-F(3)		176.8 (5)	
C(7)-C(6)-Cl			120.3 (5)	F(2)-P(2)-F(4)		176.4 (4)	
C(15)-C(11)-C(12)	109.9 (7)	108.0 (8)	108.2 (7)	F(5)-P(2)-F(6)		177.7 (6)	
C(11)-C(12)-C(13)	107.0 (7)	107.8 (8)	106.9 (7)	F(1)-P(2)-F(2)		85.1 (4)	
C(12)-C(13)-C(14)	110.3 (7)	108.1 (8)	109.0 (7)	F(1)-P(2)-F(4)		91.4 (4)	
C(13)-C(14)-C(15)	107.5 (6)	110.1 (7)	107.5 (7)	F(1)-P(2)-F(5)		88.7 (5)	
C(14)-C(15)-C(11)	104.7 (6)	105.5 (7)	107.9 (7)	F(1)-P(2)-F(6)		89.2 (5)	
Pd-P(1)-C(21)	108.42 (19)	110.33 (16)	108.5 (3)	F(2)-P(2)-F(3)		94.8 (5)	
Pd-P(1)-C(31)	117.19 (15)	116.02 (15)	117.1 (2)	F(2)-P(2)-F(5)		88.9 (5)	
Pd-P(1)-C(41)	113.06 (13)	112.80 (15)	113.3 (2)	F(2)-P(2)-F(6)		90.3 (5)	
C(21)-P(1)-C(31)	106.3 (3)	106.2 (3)	106.3 (4)	F(3)-P(2)-F(4)		88.8 (5)	
C(21)-P(1)-C(41)	107.1 (3)	106.9 (3)	107.1 (4)	F(3)-P(2)-F(5)		94.5 (6)	
C(31)-P(1)-C(41)	104.1 (2)	104.0 (2)	104.0 (3)	F(3)-P(2)-F(6)		87.7 (6)	
P(1)-C(21)-C(22)	122.1 (5)	121.8 (4)	123.4 (7)	F(4)-P(2)-F(5)		91.1 (5)	
P(1)-C(21)-C(26)	118.6 (5)	118.4 (5)	118.3 (6)	F(4)-P(2)-F(6)		89.6 (5)	
C(26)-C(21)-C(22)	119.3 (6)	119.8 (5)	118.3 (8)	Cl(1S)-C(S)-Cl(2S)	115.1 (8)		117.3 (9)

[a] Abbreviations: see the footnote to the Table VI.

atoms being 3.388 (7) Å (C(8)(x, y, z)···F(2)(1 + x, y, z)) for **2b**, 3.114 (9) Å (C(42)(x, y, z)···F(2)(1 − $\bar{x}$, $\bar{y}$, 1 − $\bar{z}$)) for **2c**, and 3.392 (10) Å (C(15)(x,y,z)···F(3)(1 + x, y, 1 + z)) for **2d**, respectively.

Relative Stability in Dilute Solutions. Conductivity measurement in CH_2Cl_2 suggested that 1:1 ion pair formation constants for **2** (R = n-Bu, X = ClO_4 and BF_4) lie in the range of 10^4–4×10^3 L/equiv.[6] On the basis of these values more than 80% of the complexes are calculated to exist as free ions under the UV experimental conditions. In accord with this assumption the thermodynamic parameters for eq 2 involving **2** (R = Ph) were found to be almost counteranion independent, unlike the corresponding parameters determined in the concentrated solution (5×10^{-2} M) by ^{1}H NMR spectra.[6] Under the latter condition the amount of the complexes existing as free ions would be very small.

Of particular note in Table V is that the change of $\Delta G°$ as a function of Y is primarily controlled by the change of $\Delta S°$, with $\Delta H°$ for **2** (R = Et, n-Bu) being almost independent of Y. In addition, competition between the nitrile and the styrene ligands in coordinating with palladium (eq 2) is also entropy controlled. The negative values of $\Delta S°$ for eq 2 would partly be a reflection of the smaller degree of solvent orientation in the vicinity of the palladium atom of the nitrile complex than that of **2**. The reduced solvent orientation in the former could be attributed to the reduced effective nuclear charge on the palladium arising from the more effective delocalization of the positive charge over the coordinated ligands and the much smaller contribution of the π back-bonding effect. Similarly, the change of $\Delta S°$ as a function of Y may be ascribed to the more positive charge residing on the palladium of the more electron-withdrawing styrene complexes as a result of the decreasing σ donation and increasing π back-donation effects (see later).

The range of the variation of $\Delta H°$ for **2** (R = Ph) is well within the experimental error. However, its trend, if assumed to be real and compared with that for **2** (R = Et, n-Bu), suggests a slightly more electrophilic nature of the $(\eta^5\text{-}C_5H_5)(PPh_3)Pd^+$ moiety than the $(\eta^5\text{-}C_5H_5)(PR_3)Pd^+$ (R = Et, n-Bu) ones. In any case, by far the smaller sensitivity of $\Delta H°$ of **2** to the change of Y than that of **1** (e.g., $\Delta H°_{Y=H} - \Delta H°_{Y=OMe} = 5.2$ KJ/mol)[3] is remarkable. Of further remark is that the Hammett relation for eq 2 holds better with σ than σ^+ constants (Table IV). These results are now understandable[23] in terms of the difference in the intrinsic nature of the olefin–Pd bond in **1** and **2**.

The Nature of the Olefin–Palladium Bond. The most significant difference in the electronic effects of **1** and

(23) In the absence of knowledge about structures of ion pairs or ion aggregates, it is difficult to rationalize the observed trend in $\Delta H°$ and $\Delta S°$ of **2** in the concentrated solutions.

2 on the olefin–Pd bond is clearly the number of the valence shell electrons or, in other words, the effective coordination number. Thus, **2** may be regarded as an analogue of ML_4(olefin) complexes, for a small distortion of the ML_4 fragment and substitution of the Cp group for three L's cis to each other lead to a rough representation of the $M(\eta^5\text{-}C_5H_5)L$ fragment. The configuration of **2** determined crystallographically is essentially the one predicted by the MO consideration[8,21] of d^8 ML_4(olefin) complexes. That is, the olefin π^* interacts well with the filled metal orbital (b_2) in configuration B rather than in

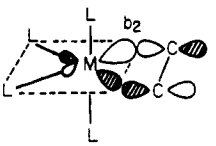

B

the one in which the olefin has rotated about the olefin–M axis by 90°. Moreover, the b_2 orbital used in B is more favorably situated in its energy and shape in overlapping with the olefin π^* than the metal orbitals used in the π interaction in the square-planar olefin complexes.

We propose that it is the enhanced role of the π backbonding in the 18-electron complexes as shown above that is responsible for the different trends in the thermodynamic parameters of **2** than those of **1**. In **1** the substituent effect was suggested to be transferred to the interaction center predominantly through the form A. On the other hand, in **2** an increase in the π interaction energy in the more electron-withdrawing styrene complex must have compensated for a decrease in the σ interaction energy to some extent. Also, if the π interaction were not important in **2**, the Pd–C(1) length of the more electron-withdrawing styrene complex would have become longer than that of the more donating styrene complex to an experimentally appreciable extent, as was the case in the square-planar complexes *trans*-$PtCl_2$(Me-pyridine)($CH_2{=}CHC_6H_4Y$-*p*) (Y = NMe_2, H).[19] 9 The observed difference in the Pd–C(olefin) lengths of **2a** and **2c** is also consistent with the palladium atom in the former complex bearing the more donating phosphine acting as a better π base.

Finally, however, it should be stressed that the almost constant $\Delta H°$ values in **2** do not necessarily imply that the π interaction makes almost the same contribution as the σ interaction does, for the observed $\Delta H°$ values are well expected to include in addition to the contributions from the intrinsic olefin–Pd bond strength those from the solvation effects. It seems rather unreasonable to believe that the π interaction is as important as the σ interaction, particularly in the cationic Pd^{II} complexes. The C(1)–C(2) lengths observed in **2a–d** are well within the range of the carbon–carbon double bond. Also, the barrier to the rotation of ethylene in $[Pd(\eta^5\text{-}C_5H_5)(PPh_3)(C_2H_4)]ClO_4$ is small[6] and is estimated to be less than 35 KJ/mol at −90 °C on the assumption that the chemical shift difference in the nonequivalent ethylene proton resonances is almost the same as that of $[Pt(\eta^5\text{-}C_5H_5)(PPh_3)(C_2H_4)]ClO_4$.[6] In conclusion, the π interaction energy in the olefin–Pd^{II} bond may not be very large in nature, as has been pointed out previously,[1] but the relative contribution of this interaction with regard to that of the σ interaction can be increased in the 18-electron complexes to such a point as to influence the structural and thermodynamic parameters to an experimentally observable extent.

Registry No. **2** (R = Ph, X = BF_4, Y = OMe), 84432-87-1; **2** (R = Ph, X = PF_6, Y = H), 84432-88-2; **2** (R = Ph, X = BF_4, Y = Cl), 84432-89-3; **2** (R = Ph, X = ClO_4, Y = Cl), 75346-33-7; **2** (R = Ph, X = ClO_4, Y = H), 75346-35-9; **2** (R = Ph, X = ClO_4, Y = Me), 75346-37-1; **2** (R = Ph, X = ClO_4, Y = OMe), 75346-39-3; **2** (R = Ph, X = BF_4, X = Me), 84432-90-6; **2** (R = Et, X = ClO_4, Y = Cl), 84432-92-8; **2** (R = Et, X = ClO_4, Y = H), 75345-58-3; **2** (R = Et, X = ClO_4, Y = Me), 84432-94-0; **2** (R = Et, X = ClO_4, Y = OMe), 84454-18-2; **2** (R = Bu, X = ClO_4, Y = Cl), 75346-43-9; **2** (R = Bu, X = ClO_4, Y = H), 75346-45-1; **2** (R = Bu, X = ClO_4, Y = Me), 75346-47-3; **2** (R = Bu, X = ClO_4, Y = OMe), 75346-49-5; **2** (R = Ph, X = BF_4, Y = H), 84432-97-3; **3** (R = Ph), 75346-64-4; **3** (R = Et), 84432-95-1; **3** (R = Bu), 84432-96-2; 2-methylbenzonitrile, 529-19-1; 4-chlorostyrene, 1073-67-2; styrene, 100-42-5; 4-methylstyrene, 622-97-9; 4-methoxystyrene, 637-69-4.

Supplementary Material Available: A table of anisotropic temperature factors (Table S1), a listing of structure factors (Table S2), and least-squares planes and atomic deviations from the plane (Table S3) for **2b–d** (51 pages). Ordering information is given on any current masthead page.

A New Nickel Complex for the Oligomerization of Ethylene

Marcell Peuckert† and Wilhelm Keim*

Institut für Technische Chemie und Petrolchemie, Rheinisch-Westfälische Technische Hochschule Aachen, Worringer Weg 1, D-5100 Aachen, West Germany

Received October 20, 1982

We report the synthesis of $(\eta^3\text{-}C_8H_{13})((C_6H_5)_2PCH_2COO)Ni$ (1), which proved to be an excellent one-component model catalyst for the oligomerization of ethylene as practiced in Shell's higher olefin process (SHOP). In toluene solution this complex exists in two isomeric forms, the C_8H_{13} ligand being 60% 4-enyl and 40% η^3-allyl. Under reaction conditions (75 °C, 10–80 bar, ethylene in toluene) 1 catalyzed the highly selective oligomerization of ethylene to linear (99+%), α olefins (93–99%) at activities of 0.6 mol of ethylene/mol of Ni/s. The chain growth factor K ranges from 0.67 to 0.77 depending on reaction conditions. Kinetic activation parameters and reaction constants could be determined (E_a = 71 kJ mol^{-1}; $S^{\ddagger}$ = −49 J mol^{-1} K^{-1}; $k_{\text{insert.}/348K}$ = 0.81 s^{-1}).

I. Introduction

The industrial manufacture of α olefins in the C_8–C_{20} range is of substantial technical interest to provide olefins for detergents, plasticizers, lubricants, oil additives, and a variety of fine chemicals. Recently, Shell developped a new ethylene oligomerization process, SHOP, which was discovered by W.K. and which is practiced worldwide in various plants.[1] This process is characterized by a remarkable selectivity. Chelating ligands are responsible for the high selectivity, which is needed to combine oligomerization and metathesis in the process scheme.[2]

The majority of papers dealing with homogeneous transition-metal catalysts relate to monodentate ligands, primarily tertiary phosphines. The effect of chelates has found only scattered interest. This is surprising, when considering the impact chelating ligands play in nature.

In our search to understand the reaction mechanism of ethylene oligomerization, we prepared the complex $(\eta^3\text{-}C_8H_{13})((C_6H_5)_2PCH_2COO)Ni$ (1) that contains a P,O chelate. Compound 1 showed high activity and selectivity in the SHOP reaction.

In this paper we give an account of the preparation of 1 and its catalytic performance.

II. Experimental Section

All experiments were carried out in an argon atmosphere and with dry solvents.[3]

Preparation of $(\eta^3\text{-}C_8H_{13})((C_6H_5)_2PCH_2COO)Ni$ (1). A 18-mmol sample of $(COD)_2Ni$[4] (COD = cyclooctadiene) and 14 mmol of $(C_6H_5)_2PCH_2COOH$[5] are dissolved in 100 mL of toluene. After 1-h reaction at room temperature, the solvent is distilled off at 10^{-2} torr. GC analysis shows that the distillate contains about 8 mmol of cyclooctadiene isomers. The dry residue is dissolved in a mixture of 100 mL of toluene and 100 mL of n-hexene. Unreacted $(COD)_2Ni$ precipitates at −30 °C and is filtered off. To the clear solution are successively added 50 mL of n-hexane and 100 mL of n-octane. After several days burgundy red crystals of 1 are formed. Recrystallization from a mixture of toluene, hexane, and octane yields 6.3 mmol of $(\eta^3\text{-}C_8H_{13})((C_6H_5)_2PCH_2COO)Ni$ (1) in large tetragonal crystals ($a = b$ = 2.51 nm, c = 2.79 nm), mp 214–216 °C. Elemental analysis and chemical decomposition of 1 by added triphenylphosphine proved that the compound contains 1 mol of C_8H_{13} per mol and about 20% toluene and octane as crystal liquid solvent and free 1 could not be obtained. Spectroscopic characterization included MS, IR and ^{1}H, ^{13}C, and ^{31}P NMR: MS (70 eV, chemical ionization with isobutene, 210 °C), m/e 243 (phosphinoacetic acid), 109 (C_8H_{13}); IR (KBr, cm^{-1}) ν(C–H) 3050, 2920, 2860, 2810, ν(C=O) 1580, ν(C–O) 1375, ν(C–C(arom)) 1480, 1430, ν(P–C(arom)) 1100, 1085, ν(P–C(aliph)) 735; ^{31}P NMR (109.32 MHz, in C_6D_6, external standard 85% H_3PO_4) one signal at −2.6 ppm vs. −15.4 ppm for pure $(C_6H_5)_2PCH_2COOH$; ^{1}H and ^{13}C NMR spectral data are shown in Table I (1 was recrystallized from toluene-d_8). ESCA, K edge X-ray absorption spectra,[6] and X-ray structure analysis are to be published in a later paper.

Scheme I

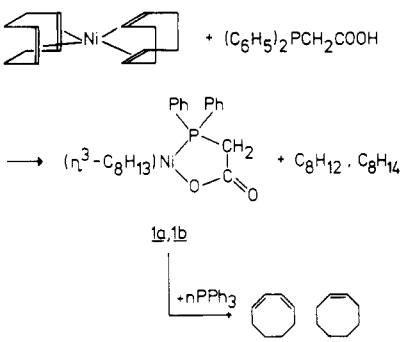

The discontinuous kinetic experiments were carried out by using 75-mL, V4A, stainless-steel batch autoclaves equipped with magnetic stirrers. Under an argon blanket they were charged with a toluene solution of 1, toluene, n-heptane as the GC standard, and ethylene, adding up to a total of 40 mL (at 25 °C). After a fast heatup to the desired temperature the pressure drop due to the catalytic reaction could be followed by means of a manometer. Through independent determination of the P–T function of various toluene/ethylene mixtures the measured P–T curves, as shown in Figure 1, could be calibrated as concentration over time, which finally yield absolute rates of reaction and turnover numbers N. The oligomer products were analyzed after a total reaction time of 35 min by capillary gas chromatography (Carlo Erba 2200; silicon OV 101, 60 m × 0.25 mm i.d. WGA Duesseldorf; temperature progression 6 min, isothermal at 30 °C, 8°/min heatup, isothermal at 230 °C).

III. Results and Discussion

A. The Catalyst. When bis(cyclooctadiene)nickel was reacted with (diphenylphosphino)acetic acid, complex 1

† Institut für Grenzflächenforschung und Vakuumphysik, Kernforschungsanlage Jülich, D-5170 Jülich, West Germany.

(1) (a) Keim, W., et al. (Shell Dev.) U.S. Patents 3 635 937, 3 647 914, 3 686 159, 3 644 563, 3 647 914, 1972. (b) *Eur. Chem. News* Apr 5, **1982**, 26; Jan 26, **1981**, 27; Jul 6, **1981**, 23; Feb 11, **1980**, 27.
(2) Freitas, E. R.; Gum, C. R. *Chem. Eng. Prog.* **1979**, *75*(1), 73–76.
(3) Peuckert, M. Thesis Rheinisch-Westfälische Technische Hochschule Aachen, Aachen, West Germany, 1980.
(4) Schunn, R. A. *Inorg. Synth.* **1974**, *15*, 5–9.
(5) (a) Issleib, K.; Thomas, G. *Chem. Ber.* **1960**, *93*, 803–808. (b) Hewertson, W.; Watson, H. R. *J. Chem. Soc.* **1962**, 1490–1494.
(6) Peuckert, M.; Weber, R. S.; Storp, S.; Keim, W., accepted for publication in *J. Mol. Catal.*

0276-7333/83/2302-0594$01.50/0

Table I. ^{1}H NMR and ^{13}C NMR Spectral Data of $(\eta^3\text{-}C_8H_{13})((C_6H_5)_2PCH_2COO)Ni$ (1)[a]

^{1}H NMR[b]	C_6H_5P o-H	C_6H_5P m,p-H	CH=CH	H_a	H_b	C-CH$_2$-C	P-CH$_2$-COO	Ni-C-CH
δ[c]	7.77 m	7.10 m	5.80 m	4.5 d	3.67 t	2.68 m[d] 2.4 m 1.6 m	1.37 s	0.17 m −0.45 d
integration	4	6	1.3	0.55	1.1	8.7	2	0.7 0.7

^{13}C NMR[b]	COO	C_4	C_2	C_1	C_3	C_a	C_b	C_c	CH
δ	178	137.6	132.4	128	125.4	112	88	79	40-14

[a] Complex 1 recrystallized from toluene-d_8. [b] Solvent C_6D_6, external standard Me_4Si. [c] Multiplicity, s = singlet, d = doublet, t = triplet, m = multiplet. [d] Only main signals are listed, between 2.9 and 1.0 many methylene signals.

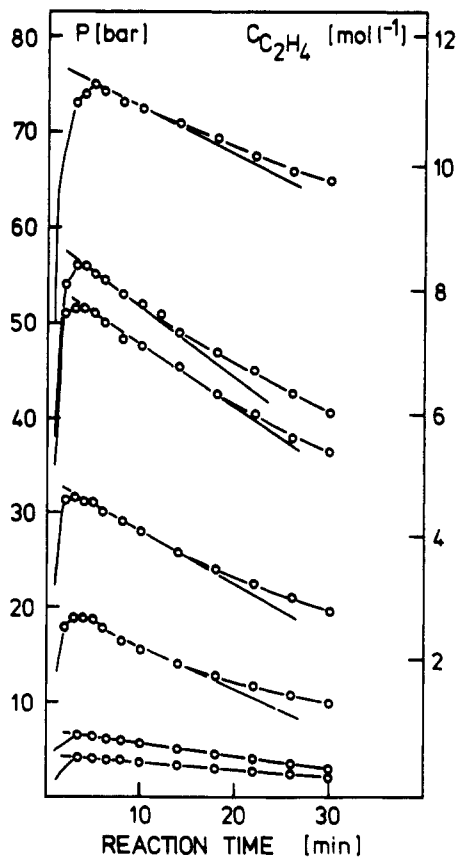

Figure 1. Pressure–time curves for the oligomerization of ethylene with catalyst 1 in toluene at 75 °C (Table II, experiments 1–7).

was obtained as shown in Scheme I. One cyclooctadiene ligand in $(COD)_2Ni$ is displaced by the $(C_6H_5)_2PCH_2COO^-$ moiety as a mixture of 1,3-, 1,4-, and 1,5-cyclooctadiene, bicyclo[3.3.0]oct-2-ene, and cyclooctene. The remaining C_8H_{13} group in 1 is formed via addition of the acidic hydrogen of Ph_2PCH_2COOH to the second 1,5-cyclooctadiene ring.

Though 1 is easily recrystallized from toluene/alkane mixtures and one always measures identical spectra of the substrate (see Experimental Section), the ^{1}H NMR spectrum (as well as the ^{13}C NMR) at first sight is somewhat puzzling (Table I). The relative intensities of aromatic to nonaromatic signals are 10:15 as expected. The two acetato methylene protons at 1.37 ppm are easily identified, but integration of the remaining signals leads to constant and reproducible but noninteger relations. These findings are interpreted as an equilibrium between the two isomeric forms 4-enyl **1a** and η^3-allyl **1b** at a ratio of 3:2.[7-9]

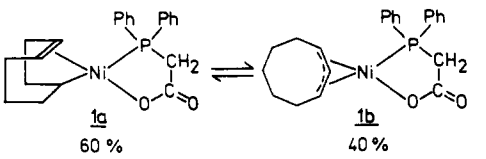

Characteristic for the 4-enyl isomer are the two signals about 0 ppm and the olefin signal at 5.80 ppm. Typical allyl signals (integration 1:2) appear at 4.5 and 3.67 ppm.[10,11] Since the 4-enyl to π-allyl ratio was foound to stay constant through repeated recrystallization procedures of 1, the question arises, whether in the solid state both isomers exist or only **1a** exists that then quickly equilibrates in solution. This point—though not bearing much importance for the catalysis—will be clarified by X-ray structure analysis.

The facile transformation of the 4-enyl structure **1a** into the π-allyl form **1b** is quite noteworthy and is in sharp contrast to the generally observed stability of Ni and Co complexes with O,O chelate ligands.[12] On the other hand, almost complete 4-enyl-to-η^3-allyl isomerization has been reported for the reaction of $(C_8H_{13})Ni(acac)$ with more basic σ donor ligands as for example C_2H_5SH and $P(O\text{-}C_6H_5)_3$.[13] This illustrates the different behavior of O,O and O,P chelate complexes.

B. Catalytic Performance. In conformity with widespread usage, complex 1 so far has been referred to as the "catalyst". From a kinetic point of view this is not quite correct, as the term "catalyst" should rather be ascribed to the "active species".

(7) Fischer, E. O.; Werner, H. *Z. Chem.* **1962**, *2*, 174–178.
(8) Wilke, G. et al. *Angew. Chem.* **1966**, *78*, 157–172.
(9) Clarke, H. L. *J. Organomet. Chem.* **1974**, *80*, 155–173.
(10) (a) Mann, B. E.; Shaw, B. L.; Shaw, G. *J. Chem. Soc. A* **1979**, 3536–3543. (b) Mann, B. E.; Pietropaolo, R.; Shaw, B. L. *J. Chem. Soc., Dalton Trans.* **1973**, 2390–2393. (c) Mann, B. E. *Adv. Organomet. Chem.* **1974**, *12*, 135–213.
(11) Barnett, K. W. *J. Organomet. Chem.* **1970**, *21*, 477–485.
(12) Keim, W.; Hoffmann, B.; Lodewick, R.; Peuckert, M.; Schmitt, G.; Fleischhauer, J.; Meier, U. *J. Mol. Catal.* **1979**, *6*, 79–97.
(13) Jolly, P. W.; Wilke, G. "The Organic Chemistry of Nickel", Academic Press: New York, 1974; Vol. 1.

Table II. Results of Batch Oligomerization of Ethylene with Catalyst 1[a]

expt	T, °C	$c_{C_2H_4}$, mol L^{-1}	$10^{-3}c_{cat.}$, mol L^{-1}	conversn, %	N, s^{-1}	linear, %	$\bar{\alpha}$ portion in C_4-C_{24}, %	β C_{10}-C_{20}
1	75	0.38	2.3	53	0.14	99+	99+	0.39
2	75	0.83	2.53	59	0.23	99+	99+	0.30
3	75	2.41	2.34	50	0.47	99+	99	0.29
4	75	4.72	2.47	41	0.57	99+	97	0.29
5	75	7.00	2.70	32	0.62	99+	98	0.30
6	75	8.95	3.39	30	0.57	99+	95	0.34
7	75	11.22	2.64	15	0.48	99+	96	0.50
8	75	4.58	0.99	24	0.71	99+	98	0.24
9	75	4.22	5.00	65	0.53	99+	93	0.37
10	60	4.83	2.27	9	0.17	99+	99+	0.16
11	85	4.95	2.29	62	1.12	99+	99+	0.10
12	95	4.75	2.32	69	1.83	99+	99+	0.10
13[b]	75	5.01	1.93	25	0.65	99+	99	0.27

[a] Solvent toluene; capillary GC analysis after 35-min total reaction time. [b] Addition of 1.67 mol L^{-1} 1-hexene.

Scheme II

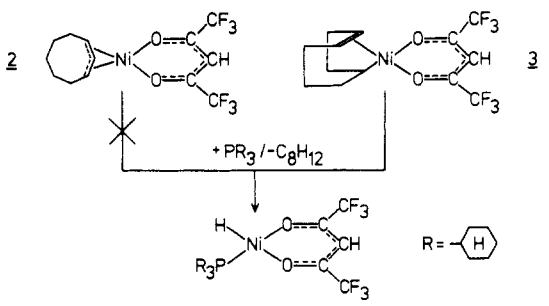

After ethylene in slight stoichiometric excess was added to a solution of **1a**/**1b** at 75 °C, 20% bicyclo[3.3.0]oct-2-ene (via intramolecular insertion of the 4-enyl), 7% 1,5-cyclooctadiene, 34% 1,4-cyclooctadiene, 8% 1,3-cyclooctadiene, and 31% cyclooctene were detected by GC analysis. One is tempted to assume that the 61% of bicyclo[3.3.0]oct-2-ene, and 1,5- and 1,4-cyclooctadiene stem from **1a**, whereas the 39% of 1,3-cyclooctadiene and cyclooctene originate from **1b**. Relevant to this displacement is a recent finding in our laboratory.[14] We could isolate the isomeric complexes **2** and **3** (Scheme II). No equilibrium such as **1a** ⇄ **1b** could be observed for **2** and **3**. Most remarkably, **3** is an excellent catalyst for the oligomerization of 1-butene. Complex **2** is practically inactive. This can be understood when considering the ease of nickel hydride formation from **2** and **3** via elimination of C_8H_{12} (Scheme II). Upon reaction of **3** with tricyclohexylphosphine, a nickel hydride complex could be isolated.[15] Identical experiments with **2** failed.

All attempts to convert **1** to a Ni–H complex by adding R_3P were not successful. However, the quantitative displacement of the second C_8 ring occurred.

The isolation of a nickel hydride complex would have been of interest in view of mechanistic consideration shown in Figure 4. A widely accepted mechanism for olefine oligomerizations invokes metal hydrides as active species,[16–18] thus isolation of a Ni–H complex could have been further support for a hydride mechanism. During the startup reaction of **1** with ethylene, a set of three high-field

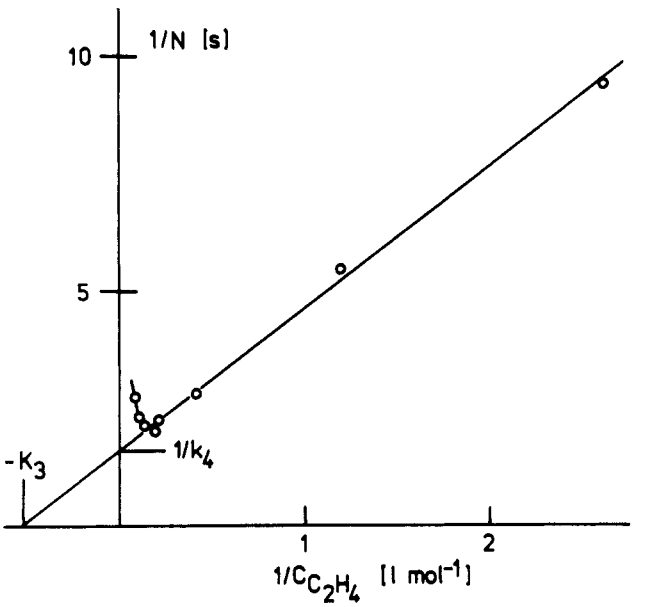

Figure 2. Lineweaver–Burk diagram for experiments 1–7 (Table II): reciprocal turnover numbers vs. $1/[C_2H_4]$.

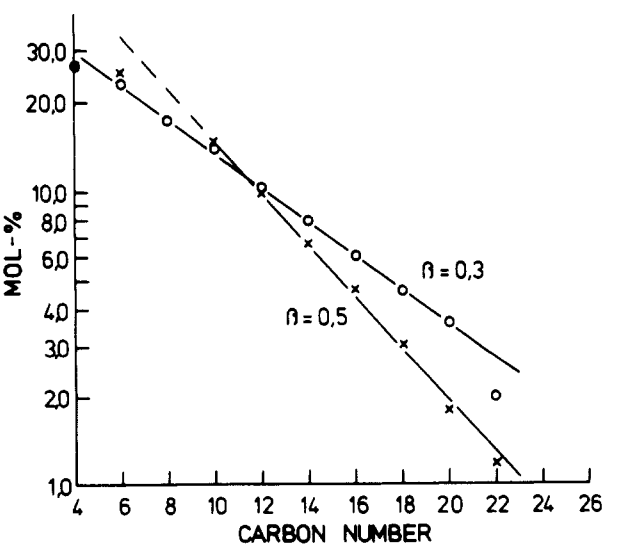

Figure 3. Schulz–Flory type oligomer distribution (Table II, experiments 2 and 7). The β values 0.3 and 0.5 correspond with K factors of 0.77 and 0.67, respectively.

^{1}H NMR signals (0.7, 0.15, and −0.5 ppm) evolved, which is characteristic of a nickel–alkyl group. Initial nickel–hydride formation as the activation step followed by re-

(14) Kraus, G. Thesis Rheinisch-Westfälische Technische Hochschule Aachen, Aachen, West Germany, 1982.
(15) Despeyroux, B.; Lodewick, R.; Keim, W. *Compend. Erdöl Kohle Erdgas Petrochem.* **1981**, *Bd. 80/81*, 123–125.
(16) Langer, A. W. *J. Macromol. Sci. Chem.* **1970**, *A4*, 775–787.
(17) (a) Henrici-Olivé, G.; Olivé, S. *Adv. Polym. Sci.* **1974**, *15*, 1–30. (b) *Top. Curr. Chem.* **1976**, *67*, 107–127.
(18) Henrici-Olivé, G.; Olivé, S. "Monographs in Modern Chemistry", Verlag Chemie: Weinheim, 1977; Vol. 9.

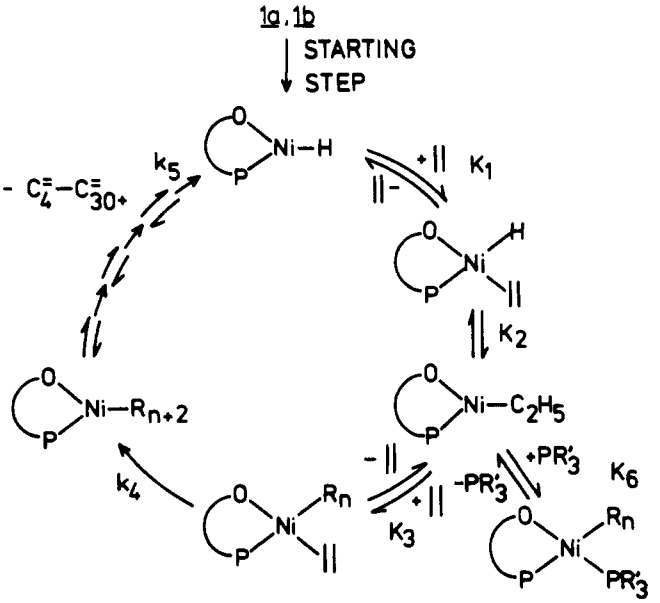

Figure 4. Simplified mechanism proposed for ethylene oligomerization with nickel O,P chelate complexes like 1 and the SHOP catalyst.

action with ethylene to form a nickel alkyl—as shown in Figure 4—can be supposed.

In Figure 1 and Table II the results of the oligomerization experiments are summarized. After the autoclaves are charged at room temperature and immersed into a heat bath, thermal equilibrium is reached within 3–5 min, upon which the catalytic reaction commences immediately as recorded by the pressure drop. At 25 °C 1 shows no activity. From the initial rates specific turnover numbers N (mol of ethylene per mol of Ni per s) are calculated. The rate is first-order in catalyst concentration (experiments 4, 8, and 9). Plotting $1/N$ over reciprocal ethylene concentration results in a straight line (Figure 2); only at very high concentrations of C_2H_4 is a deviation observed, probably due to a solvent effect of the substrate itself. This so-called Lineweaver–Burk diagram is in good agreement with the proposed Michaelis–Menten-type mechanism (Figure 4): association constant $K_3 = 0.52$ L mol^{-1} and $k_4 = 0.81$ s^{-1} being the rate constant of the rate-determining step in the rate law for the oligomerization.

$$r_{olig} = [\mathrm{Ni}^*]\,\frac{k_4K_3[C_2H_4]}{1 + K_3[C_2H_4]}$$

$$[\mathrm{Ni}^*] = \text{catalyst concentration}$$

Activation energy and entropy were determined (experiments 4 and 9–12) as $E_a = 71$ kJ mol^{-1} and $S^{\ddagger} = -49$ mol^{-1} K^{-1}.

So far we have just focused on the activity of 1. The selectivity is also listed in Table II. The oligomers are practically 100% linear and the α olefin content ranges from 93% to 99+%. This underlines the remarkable selectivity of 1 for ethylene only. To investigate the possibility of cooligomerization, we added 1-hexene and propylene (experiment 13). No branched or odd carbon number products could be found.

The chain length distribution is of the Schulz–Flory-type and can best be described by the β value (Figure 3).[19,20] That is the ratio between the rate r_{elim} of the chain growth terminating step and the rate r_{olig} of the propagation step. This is exemplified in Figure 4 by step 4 and step 5.

$$\beta = \frac{r_{elim}}{r_{olig}} = \frac{k_5(1 + K_3[C_2H_4])}{k_4K_3[C_2H_4]} \approx \frac{1}{TP}$$

Since the β values are determined only at the end of each run at high conversion, the steady-state condition is not strictly obeyed and a numerical analysis of our experiments seems difficult. Another molar growth factor often used to characterize the product composition is defined as

$$K = \frac{\text{mol fraction } C_{n+2}\text{-alkene}}{\text{mol fraction } C_n\text{-alkene}} = (1 + \beta)^{-1}$$

For an average $\beta = 0.3$ the K factor equals 0.77.[2]

Whereas the influence of the substrate concentration on the chain length is rather weak, there is a pronounced increase of the β value caused by addition of phosphine to the reaction mixture. Our proposed mechanism (Figure 4) therefore has to be completed by the equilibrium K_6, and β is then given by

$$\beta = \frac{k_5(1 + K_6[PR_3] + K_3[C_2H_4])}{k_4K_3[C_2H_4]}$$

Acknowledgment. We thank Deutsche Forschungsgemeinschaft for supporting this work. We are grateful to Mrs. M. Sistig and Dr. W. Meltzow for assistance with the spectroscopic and analytical work.

Registry No. **1a**, 84108-24-7; **1b**, 84099-45-6; $(C_6H_5)_2PCH_2COOH$, 3064-56-0; ethylene, 74-85-1; bis(1,5-cyclooctadiene)nickel, 1295-35-8.

(19) (a) Schultz, G. V. *Z. Phys. Chem., Abt. B* **1935**, *30*, 379–398. (b) *Ibid.* **1939**, *43*, 25–46.
(20) Flory, P. J. *J. Am. Chem. Soc.* **1940**, *62*, 1561–1565.

Nickel-Catalyzed Synthesis of Arylacetic Esters from Arylzinc Chlorides and Ethyl Bromoacetate

T. Klingstedt and T. Frejd*

Organic Chemistry 1, Chemical Center, The University of Lund, S-220 07 Lund, Sweden

Received September 1, 1982

Arylacetic ethyl esters are prepared from arylzinc chlorides and ethyl bromoacetates with a catalytic amount of bis(acetylacetonato)nickel(II)–phosphine complex.

Introduction

Aromatic acetic acids and esters are an important class of compounds both per se[1] and for further transformations. Recently, two transition-metal-mediated syntheses of arylacetic esters were reported (eq 1 and 2), that can be formally described as a combination of a positive aryl species with a negative carbalkoxymethylene species. The

$$\mathrm{Ar(hal)} + \mathrm{LiCH_2COO}\text{-}t\text{-Bu} \xrightarrow{\text{"Ni"}} \mathrm{ArCH_2COO}\text{-}t\text{-Bu}\ (\mathrm{Ar^+} + {}^-\mathrm{CH_2COOR}) \quad (1)^2$$

$$\mathrm{Ar(hal)} + \mathrm{ZnBrCH_2COOEt} \xrightarrow{\text{"Ni"}} \mathrm{ArCH_2COOEt}\ (\mathrm{Ar^+} + {}^-\mathrm{CH_2COOR}) \quad (2)^3$$

$$\mathrm{ArZnCl} + \mathrm{BrCH_2COOEt} \xrightarrow{\text{"Ni"}} \mathrm{ArCH_2COOEt}\ (\mathrm{Ar^-} + {}^+\mathrm{CH_2COOR}) \quad (3)$$

reaction in eq 1 was catalyzed by nickel(II) bromide reduced by butyllithium but gave useful yields only with a stoichiometric amount of the nickel species.[2] The Reformatsky-type coupling (eq 2) was catalytic in tetrakis(triphenylphosphine)nickel(0) but required HMPA as cosolvent for best results.[3] Moreover, the nickel(0) catalyst had to be preformed since the Reformatsky reagent is not able to reduce Ni(II) to Ni(0). The relatively high reaction temperature (45 °C) and long reaction time (3 h) make this reaction less attractive for the synthesis of substances such as allyl ethers that are sensitive to transition-metal catalysts.

We now wish to report a third mild and simple alternative of arylacetic ester synthesis, in which an arylzinc halide is coupled with ethyl bromoacetate by the aid of a catalytic amount of bis(acetylacetonato)nickel(II)–phosphine complex. This reaction can be formalized as a combination of a negative aryl species and a positive carbethoxymethylene species (eq 3).

Results and Discussion

The arylacetic esters were prepared by adding ethyl bromoacetate to a catalytic amount of the appropriate phosphine and $Ni(acac)_2$ followed by the arylzinc chloride.[4] The results are shown in Table I. The only byproducts of importance were the homocoupled biaryls (13–15 %), which to a small extent were present in the arylzinc halide preparations.[5] Thus, the major part, about 10% GC yield, must have been formed in the presence of the catalyst. At higher reaction temperatures, the amount of biaryls increased. The byproducts were easily removed by flash chromatography.[6]

Table I. Yields of Reaction Products in the Reaction between Arylzinc Chlorides and Ethyl Bromoacetate Catalyzed by $Ni(acac)_2$ Phosphine Complex

entry	ArZnCl, Ar =	% yield of $ArCH_2COOEt$ (isolated/GC)[a]
1	C_6H_5	59/77[b]
2	o-$CH_3C_6H_4$	60/66[b]
3	o-$OCH_3C_6H_4$	53/76[b]
4	2-furyl	38/54[c]
5	2-thienyl	45/63[c]
6	2-selenienyl	55/60[c]
7	3-pyridyl	*b*

[a] The yields refer to the charged amount of ethyl bromoacetate. [b] 0.01 equiv of triphenylphosphine and 0.01 equiv of $Ni(acac)_2$ were used as catalyst at −5 °C. [c] 0.05 equiv of cyclohexyldiphenylphosphine and 0.05 equiv of $Ni(acac)_2$ were used as catalyst at +20 °C.

Since it has been demonstrated that the catalytic species for other nickel(0)-catalyzed carbon–carbon bond formations does contain phosphine ligands associated with the nickel atom,[7] we repeated the coupling reaction with several different ligands. Ligands[8] with large cone angles ($P(o\text{-tol})_3$, $P(c\text{-Hx})_3$) or small cone angles (PEt_3) and ligands with electron-withdrawing substituents ($P(OEt)_3$) gave low yields of 2-thienylacetic ester (<20%). The bidentate ligands[8] dppp and dppb were reasonably efficient (40–50%), while dppe gave an inferior yield (~10%). It should be noted that Kumada et al.[7] have reported the latter ligand to be quite efficient for the coupling of butylmagnesium bromide with chlorobenzene. Another point of interest is that Rathke et al.[2] reported no reaction at all when phosphine ligands were present in the coupling of lithium ester enolates with vinyl halides in the presence of nickel chloride. In our coupling reactions we observe the reverse, i.e., negligible coupling without ligands.

In an attempt to minimize the formation of the homocoupled product (biaryls), we used diphenylzinc as a precursor for phenylzinc chloride. Unexpectedly, the yield of phenylacetic ester was only 5%, together with 5% of

(1) E.g., as nonsteroidal antiinflammatory agents: (a) Dunn, J. P.; Muchowski, J. M.; Nelson, P. H., *J. Med. Chem.* **1981**, *24*, 1097. (b) Brancaccio, G.; Larizza, A.; Lettieri, G., *Ibid.* **1981**, *24*, 998. (c) Tamura, Y.; Yoshimoto, Y.; Tada, S.; Kunimoto, K.; Matsumara, S.; Murayama, M.; Shibata, Y.; Enomoto, H., *Ibid.* **1981**, *24*, 1006; **1981**, *24*, 43. (d) Lambelin, G.; Roba, J.; Gillet, C.; Buu-Hoi, N. P. *Arzneim.-Forsch.* **1970**, *20*, 610.

(2) Millard, A. B.; Rathke, M. W. *J. Am. Chem. Soc.* **1977**, *99*, 4833.

(3) Fauvarque, J. F.; Jutand, A. *J. Organomet. Chem.* **1979**, *177*, 273; **1977**, *132*, C17; **1981**, *209*, 109.

(4) These general reaction conditions were first described by: Negishi, E.; King, A. O.; Okukado, N. *J. Org. Chem.* **1977**, *42*, 1821, for biaryl formation and are related to those of: Tamao, K.; Sumitani, K.; Kumada, M. *J. Am. Chem. Soc.* **1972**, *94*, 4374, and Corriu, R. J. P.; Masse, J. P. *J. Chem. Soc., Chem. Commun.* **1972**, 144, for the Kharasch reaction.

(5) A similar homocoupling has recently been described by: Kobayashi, M.; Negishi, E. *J. Org. Chem.* **1980**, *45*, 5223. Negishi, E.; Valente, L. F.; Kobayashi, M. *J. Am. Chem. Soc.* **1980**, *102*, 3298.

(6) Still, W. C.; Kahn, M.; Mitra, A. *J. Org. Chem.* **1978**, *43*, 2923.

(7) Tamao, K.; Sumitani, K.; Kiso, Y.; Zembayashi, M.; Fujioka, A.; Kodama, S.; Nakajima, I.; Minato, A.; Kumada, M. *Bull. Chem. Soc. Jpn.* **1976**, *49*, 1958.

(8) Abbreviations: o-tol = o-tolyl, c-Hx = cyclohexyl, dppp = bis(diphenylphosphino)propane, dppb = bis(diphenylphosphino)butane, dppe = bis(diphenylphosphino)ethane.

0276-7333/83/2302-0598$01.50/0

biphenyl, in the nickel-catalyzed coupling reaction using this phenylzinc chloride preparation. However, the addition of 1 equiv of lithium chloride (LiCl) to the coupling mixture increased the yield of ethyl phenylacetate to 60%, while still only 5% of biphenyl was formed. When lithium chloride was replaced by magnesium bromide ($MgBr_2$), only 30% of the phenylacetic ester and 25% of the biphenyl were formed. When 1 equiv of lithium chloride and 1 equiv of magnesium bromide were used together, the yields were 18% and 36%, respectively. Thus, the reaction is quite dependent on which salt is present.

The failure of coupling in the pyridine case (entry 7) to give the corresponding acetic ester is most certainly due to strong complexation of the pyridine nitrogen with zinc chloride and with 3-pyridylzinc chloride, should it be formed.[9] Thus, 3-pyridyllithium together with zinc chloride formed a gumlike precipitate in THF, which could be redissolved upon addition of *N,N,N′,N′*-tetramethylethylenediamine. None the less, no 3-pyridylacetic ester was formed upon attempted coupling. Another point of interest in this context is that 2,2′-bipyridyl used as a ligand for the Ni(O) complex essentially prevented the formation of the arylacetic ester. Thus, the pyridine nucleus seems incompatible with this reaction even though it has been shown that other halopyridines can be coupled with alkyl Grignard reagents in the presence of bis(phosphino)nickel dichloride complexes.[10]

In order to test the coupling reaction on a more complex case, we prepared the ethyl ester of the antiinflammatory substance **1** (Alclofenac),[1d] which was obtained in 55% yield (65% GC yield) from allyl 4-bromo-2-chlorophenyl ether. The ligand of choice in this case proved to be cyclohexyldiphenylphosphine (0.05 equiv).

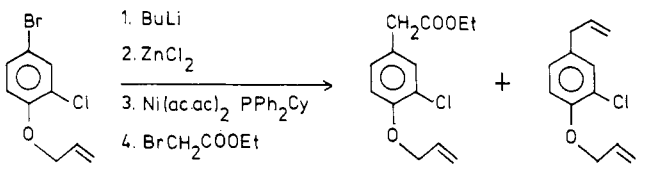

1 **2**

The butyl bromide formed in the halogen–metal exchange did not interfere with the coupling reaction. This makes the reaction more useful, since in many cases it is difficult or impossible to form the aryllithium derivative directly from the aryl halide and lithium metal.

In short, the following general characteristic features of the reaction were observed: (1) no coupling occurred without the presence of the catalyst, not even with ethyl iodoacetate; (2) no coupling occurred if only $Ni(acac)_2$ was used without ligands; (3) the best ligands generally were triphenylphosphine and cyclohexyldiphenylphosphine; (4) the presence of lithium chloride seemed essential for good results, while magnesium bromide had a negative effect by increasing the amount of homocoupling of the aromatic and decreasing the heterocoupled product; (5) the yield of arylacetic ester increased when the arylzinc chloride was used in excess over the bromo ester; (6) when the amount of the bromo ester was increased but the arylzinc chloride was kept at 1 equiv, the yield of heterocoupled product increased only marginally; (7) too little and too much of the ligand gave inferior yields (the best yields were obtained with a ligand to metal ratio of 1:1); (8) finally, the use of bis(acetylacetonato)palladium(II) instead of the corresponding nickel salt gave no arylacetic esters. Only homocoupled biaryls were found by GC analysis. This is somewhat surprising, since palladium salts are well-known catalysts, sometimes even better than nickel salts, in similar reactions,[11] and this discrepancy must await further investigations.

Experimental Section

GC yields were determined on a Perkin-Elmer 900 gas chromatograph (3% OV 101 on 80–100 mesh Varaport 30, length 3.0 m, i.d. 2.0 mm, stainless steel) and refer to the charged amount of ethyl bromoacetate in all cases. Heptadecane was used as an internal standard.

Ether and THF freshly distilled over sodium wire and benzophenone were used as solvents. All reactions with organometallic reagents were performed under nitrogen in vessels, oven dried at 110 °C, flushed with nitrogen, and sealed with rubber septa. All transfer of sensitive reagents and solvents was performed by using the syringe technique. Dry zinc chloride was prepared according to ref 12.

A. Ethyl Esters of Phenyl-, *o*-Tolyl-, and *o*-Anisylacetic Acid. A predried, 100-mL, round-bottomed reaction flask containing a magnetic stirring bar was charged with bis(acetylacetonato)nickel(II) (30.2 mg, 0.118 mmol) and triphenylphosphine (30.9 mg, 0.118 mmol), swept with nitrogen, and sealed with a rubber septum. The flask was cooled to −5 °C, and 5.0 mL of THF was added, after which ethyl bromoacetate (1.97 g, 11.8 mmol) dissolved in 10 mL of THF was introduced. To this mixture was added dropwise (very slowly) the appropriate arylzinc chloride[13] solution (23.6 mmol, 2.0 equiv). After the solution was stirred for 20 min at −5 °C, 15 mL of aqueous saturated ammonium chloride was introduced. The ethereal phase was separated, washed with water, dried ($MgSO_4$), and evaporated to give a crude product, which was purified by column chromatography (silica gel, mesh size 230–400, Merck, petroleum ether (60–71)/ethyl acetate (95/5)). The yields are presented in Table I, and all compounds had physical data in agreement with those reported in the literature.[14]

B. Ethyl esters of 2-furyl-, 2-thienyl-, and 2-selenienylacetic acid were prepared as in A, except that 0.05 equiv of the catalyst was used at +20 °C.

C. Ethyl (4-(allyloxy)-3-chlorophenyl)acetate[1d] was prepared from the arylzinc chloride derived from allyl 4-bromo-2-chlorophenyl ether[15] (5.84 g, 23.6 mmol), ethyl bromoacetate (1.96 g, 11.8 mmol), and bis(acetylacetonato)nickel(II) (151 mg, 0.590 mmol) as B, except that cyclohexyldiphenylphosphine (158 mg, 0.590 mmol) was used as a ligand. The crude product was flash chromatographed on silica gel with petroleum ether (60–71 °C)/ethyl acetate (85/15) as eluent to give the pure title compound (1.58 g, 53%, GC yield 65%). GC–MS analysis of the crude ethereal extract indicated the presence of a side product (17%), which is tentatively assigned to be allyl 4-allyl-2-chlorophenyl ether (**2**). The yields of **1** and **2** varied considerably depending on the reaction conditions. When triphenylphosphine was used as a ligand, the yields of **1** and **2** were 51% and 38%, respectively. With only 1 equiv of the allyl 4-bromo-2-chlorophenyl ether as starting material for the arylzinc chloride reagent, the yields of **1** and **2** decreased to 42% and less than 5%, respectively.

Salt Effects. To a solution of diphenylzinc (2.2 g, 10 mmol) in 60 mL of ether was added dry zinc chloride (1.3 g, 9.8 mmol)

(9) "Houben-Weyl, Methoden der Organischen Chemie", Georg Thieme Verlag: Stuttgart 1973; 13/2, pp 666.
(10) Kumada, M.; Tamao, K.; Sumitani, K., *Org. Synth.* **1978**, *58*, 127, Piccolo, O.; Marinengo, T. *Synth. Commun.* **1981**, *11*, 497.
(11) Minato, A.; Tamao, K.; Hayashi, T.; Suzuki, K.; Kumada, M. *Tetrahedron Lett.* **1981**, 5319.
(12) Pray, A. R. *Inorg. Synth.* **1957**, *5*, 154.
(13) The arylzinc chloride solutions were prepared via zinc chloride treatment of the aryllithium derivatives. Phenyl-, *o*-tolyl-, and *o*-anisyllithium were prepared from the corresponding aryl bromides and lithium metal: Gilman, H. *Org. React.* **1954**, *8*, 286, or preferably with butyllithium. 2-Furyl-, 2-thienyl-, and 2-selenienyllithium were prepared from the parent heterocycles and butyllithium. 3-Pyridyllithium in THF was prepared from 3-bromopyridine and ethyllithium in ether followed by removal of the solvent and ethyl bromide (formed in the reaction) at reduced pressure at 40 °C. The residue was then dissolved in THF.
(14) References to ^1H NMR data and refractive indices of the arylacetic esters (supplementary material, Table II).
(15) Piers, E.; Brown, R. K. *Can. J. Chem.* **1963**, *41*, 2917.

in 60 mL of ether, and the reaction mixture was stirred at room temperature for 15 min.[16] The reaction mixture was concentrated to 10 mL by distillation under nitrogen, whereupon 30 mL of THF was added to the suspension. This phenylzinc chloride solution was added in four equal portions (1 equiv in each) as described above to four different flasks, each containing bis(acetylacetonato)nickel(II) (13 mg, 0.050 mmol), triphenylphosphine (13 mg, 0.050 mmol), ethyl bromoacetate (0.83 g, 5.0 mmol), internal standard (heptadecane, 120 mg, 0.500 mmol), and metal salt in 5 mL of THF, differing only in the metal salt. Thus, flask a contained no salt, flask b dry lithium chloride[17] (212 mg, 5.00 mmol), flask c magnesium bromide prepared from magnesium and dibromo ethane[18] (920 mg, 5.00 mmol), and flask d a 1:1 mixture of lithium chloride and magnesium bromide (212 and 920 mg, respectively). The ethereal extracts were analyzed by GC and found to contain ethyl phenylacetate and biphenyl, respectively, in the proportions: (a) 5%, 5%; (b) 60%, 5%; (c) 30%, 25%, and (d) 18%, 36%.

Acknowledgment. Financial support from the Swedish Natural Science Research Council (T.F.) and a scholarship from Stiftelsen Bengt Lundqvists Minne (T.K.) are gratefully acknowledged.

Supplementary Material Available: Table II, ^{1}H NMR data and refractive indices of the ethyl arylacetates (1 page). Ordering information is given on any current masthead page.

(16) Sheverdina, N. I.; Abramova, L. V. *Proc. Acad. Sci. USSR (Engl. Transl.)* **1959**, *124*, 65.
(17) Simmons, J. P.; Sreimuth, H.; Russell, H. *J. Am. Chem. Soc.* **1936**, *58*, 1692.
(18) Seyferth, D. *Inorg. Chem.* **1962**, *1*, 227.

Crystal and Molecular Structure of the Dimeric 1:1 Adduct of Dimethyltin(IV) Dichloride with 2,6-Dimethylpyridine (2,6-Lutidine) *N*-Oxide at 138 K

S.-W. Ng, C. L. Barnes, D. van der Helm, and J. J. Zuckerman*

Department of Chemistry, University of Oklahoma, Norman, Oklahoma 73019

Received October 26, 1982

Dimethyltin(IV) dichloride–2,6-dimethylpyridine *N*-oxide, $C_{18}H_{30}Cl_4N_2O_2Sn_2$, forms colorless crystals, mp 147 °C, in the monoclinic space group $C2/c$ with a = 15.581 (4) Å, b = 12.781 (4) Å, c = 13.098 (4) Å, and β = 102.26 (3)°, V = 2549 Å^3, Z = 4, and ρ_{calcd} = 1.787 g cm^{-3}. The structure was determined by direct methods from 1880 reflections measured at 138 ± 2 K on an Enraf-Nonius CAD/4 diffractometer using monochromatized Mo Kα radiation and refined to a final R value of 0.0364 for the 1820 reflections included in the least-squares sums. The dimeric molecule contains six-coordinated, octahedral tin with the oxygen atom of the ligand and one chlorine atom in a trans position making an O–Sn–Cl angle of 177.44 (7)Å. The tin atom lies 0.03 Å above the plane formed by the two trans methyl groups [C(1) and C(2)] and the chlorine atoms [Cl(2) and Cl(1′)] toward the oxygen atom to which it makes a bond of 2.289 (2) Å. The angle made by the methyl groups is 145.3 (2)°. The angle formed by the Sn–O–N system and the pyridine *N*-oxide ring is 87.17 (6)°. One of the ligand methyl groups makes a short, nonbonded contact to one of the tin methyl groups. The center of the planar Sn_2Cl_2 ring of the dimer is located on a crystallographic center of symmetry. The geometry of the octahedron at each tin atom is best described as trans, trans, trans.

Diorganotin(IV) dihalides, and more particularly dimethyltin(IV) dichloride, form the well-known 1:2 adducts with Lewis bases.[1] However, with certain pointed ligands in which the donor atom carries only one attachment (unbranched) in a >C=O,[2-4] >C=S,[3] >S=O,[5,6] ≥N→O,[6,7] or ≥P=O[8] system,[9] 1:1 adducts with dimethyltin(IV) dichloride are also known. The detailed molecular structure data are largely lacking,[12] but the formation of the 1:1 systems is curious since the pointed ligands should be less, not more sterically demanding and allow the syntheses of the complexes to proceed to the 1:2 formulations without difficulty. It must be remembered that dimethyltin(IV) dichloride itself forms an associated solid through double, unsymmetrical chlorine–tin bridges,[13] and chlorine bridging may help complete the tin coordination sphere in these

(1) Petrosyan, V. S.; Yashina, N. S.; Reutov, O. A. *Adv. Organomet. Chem.* **1976**, *14*, 63.
(2) Matsubayashi, G.-E.; Tanaka, T.; Okawara, R. *J. Inorg. Nucl. Chem.* **1968**, *30*, 1831.
(3) Matsubayashi, G.-E.; Hiroshima, M.; Tanaka, T. *J. Inorg. Nucl. Chem.* **1971**, *33*, 3787.
(4) Srivastava, T. N.; Bajpai, B.; Srivastava, P. C. *Ind. J. Chem.* **1978**, *16A*, 164.
(5) Kitching, W.; Moore, C. J.; Doddrell, D. *Aust. J. Chem.* **1969**, *22*, 1149.
(6) Liengme, B. V.; Randall, R. S.; Sams, J. R. *Can. J. Chem.* **1972**, *50*, 3212.
(7) Kitching, W.; Kumar Das, V. G. *Aust. J. Chem.* **1968**, *21*, 2401.
(8) Burger, K.; Vertes, A.; Tzschach, A.; Mech, H. *Radiochem. Radioanal. Lett.* **1970**, *5*, 335.

(9) In the 1:1 *N,N*-dimethylthionicotinamide complexes with dimethyltin(IV) dichloride the coordination from infrared evidence is through the nitrogen on the pyridine ring,[3] and a 1:1 complex of 3,5-dimethylpyrazole is also known.[10] A 1:1 complex with dimethyl selenoxide could not be isolated,[11] and another with (dimethylamino)nitrosobenzene has been claimed, but its characterization is not described.[3]
(10) Ettorre, R.; Plazzogna, G. *Inorg. Chim. Acta* **1975**, *15*, 21.
(11) Tanaka, T.; Kamitani, T. *Inorg. Chim. Acta* **1968**, *2*, 175.
(12) Zubieta, J. A.; Zuckerman, J. J. *Prog. Inorg. Chem.* **1978**, *24*, 251.
(13) Davies, A. G.; Milledge, H. J.; Puxley, D. C.; Smith, P. J. *J. Chem. Soc., Dalton Trans.* **1977**, 1090.

0276-7333/83/2302-0600$01.50/0

in 60 mL of ether, and the reaction mixture was stirred at room temperature for 15 min.[16] The reaction mixture was concentrated to 10 mL by distillation under nitrogen, whereupon 30 mL of THF was added to the suspension. This phenylzinc chloride solution was added in four equal portions (1 equiv in each) as described above to four different flasks, each containing bis(acetylacetonato)nickel(II) (13 mg, 0.050 mmol), triphenylphosphine (13 mg, 0.050 mmol), ethyl bromoacetate (0.83 g, 5.0 mmol), internal standard (heptadecane, 120 mg, 0.500 mmol), and metal salt in 5 mL of THF, differing only in the metal salt. Thus, flask a contained no salt, flask b dry lithium chloride[17] (212 mg, 5.00 mmol), flask c magnesium bromide prepared from magnesium and dibromo ethane[18] (920 mg, 5.00 mmol), and flask d a 1:1 mixture of lithium chloride and magnesium bromide (212 and 920 mg, respectively). The ethereal extracts were analyzed by GC and found to contain ethyl phenylacetate and biphenyl, respectively, in the proportions: (a) 5%, 5%; (b) 60%, 5%; (c) 30%, 25%, and (d) 18%, 36%.

Acknowledgment. Financial support from the Swedish Natural Science Research Council (T.F.) and a scholarship from Stiftelsen Bengt Lundqvists Minne (T.K.) are gratefully acknowledged.

Supplementary Material Available: Table II, ^{1}H NMR data and refractive indices of the ethyl arylacetates (1 page). Ordering information is given on any current masthead page.

(16) Sheverdina, N. I.; Abramova, L. V. *Proc. Acad. Sci. USSR (Engl. Transl.)* **1959**, *124*, 65.
(17) Simmons, J. P.; Sreimuth, H.; Russell, H. *J. Am. Chem. Soc.* **1936**, *58*, 1692.
(18) Seyferth, D. *Inorg. Chem.* **1962**, *1*, 227.

Crystal and Molecular Structure of the Dimeric 1:1 Adduct of Dimethyltin(IV) Dichloride with 2,6-Dimethylpyridine (2,6-Lutidine) *N*-Oxide at 138 K

S.-W. Ng, C. L. Barnes, D. van der Helm, and J. J. Zuckerman*

Department of Chemistry, University of Oklahoma, Norman, Oklahoma 73019

Received October 26, 1982

Dimethyltin(IV) dichloride–2,6-dimethylpyridine *N*-oxide, $C_{18}H_{30}Cl_4N_2O_2Sn_2$, forms colorless crystals, mp 147 °C, in the monoclinic space group $C2/c$ with a = 15.581 (4) Å, b = 12.781 (4) Å, c = 13.098 (4) Å, and β = 102.26 (3)°, V = 2549 Å^3, Z = 4, and ρ_{calcd} = 1.787 g cm^{-3}. The structure was determined by direct methods from 1880 reflections measured at 138 ± 2 K on an Enraf-Nonius CAD/4 diffractometer using monochromatized Mo Kα radiation and refined to a final R value of 0.0364 for the 1820 reflections included in the least-squares sums. The dimeric molecule contains six-coordinated, octahedral tin with the oxygen atom of the ligand and one chlorine atom in a trans position making an O–Sn–Cl angle of 177.44 (7)Å. The tin atom lies 0.03 Å above the plane formed by the two trans methyl groups [C(1) and C(2)] and the chlorine atoms [Cl(2) and Cl(1′)] toward the oxygen atom to which it makes a bond of 2.289 (2) Å. The angle made by the methyl groups is 145.3 (2)°. The angle formed by the Sn–O–N system and the pyridine *N*-oxide ring is 87.17 (6)°. One of the ligand methyl groups makes a short, nonbonded contact to one of the tin methyl groups. The center of the planar Sn_2Cl_2 ring of the dimer is located on a crystallographic center of symmetry. The geometry of the octahedron at each tin atom is best described as trans, trans, trans.

Diorganotin(IV) dihalides, and more particularly dimethyltin(IV) dichloride, form the well-known 1:2 adducts with Lewis bases.[1] However, with certain pointed ligands in which the donor atom carries only one attachment (unbranched) in a >C=O,[2-4] >C=S,[3] >S=O,[5,6] ≥N→O,[6,7] or ≥P=O[8] system,[9] 1:1 adducts with dimethyltin(IV) dichloride are also known. The detailed molecular structure data are largely lacking,[12] but the formation of the 1:1 systems is curious since the pointed ligands should be less, not more sterically demanding and allow the syntheses of the complexes to proceed to the 1:2 formulations without difficulty. It must be remembered that dimethyltin(IV) dichloride itself forms an associated solid through double, unsymmetrical chlorine–tin bridges,[13] and chlorine bridging may help complete the tin coordination sphere in these

(1) Petrosyan, V. S.; Yashina, N. S.; Reutov, O. A. *Adv. Organomet. Chem.* **1976**, *14*, 63.
(2) Matsubayashi, G.-E.; Tanaka, T.; Okawara, R. *J. Inorg. Nucl. Chem.* **1968**, *30*, 1831.
(3) Matsubayashi, G.-E.; Hiroshima, M.; Tanaka, T. *J. Inorg. Nucl. Chem.* **1971**, *33*, 3787.
(4) Srivastava, T. N.; Bajpai, B.; Srivastava, P. C. *Ind. J. Chem.* **1978**, *16A*, 164.
(5) Kitching, W.; Moore, C. J.; Doddrell, D. *Aust. J. Chem.* **1969**, *22*, 1149.
(6) Liengme, B. V.; Randall, R. S.; Sams, J. R. *Can. J. Chem.* **1972**, *50*, 3212.
(7) Kitching, W.; Kumar Das, V. G. *Aust. J. Chem.* **1968**, *21*, 2401.
(8) Burger, K.; Vertes, A.; Tzschach, A.; Mech, H. *Radiochem. Radioanal. Lett.* **1970**, *5*, 335.

(9) In the 1:1 *N,N*-dimethylthionicotinamide complexes with dimethyltin(IV) dichloride the coordination from infrared evidence is through the nitrogen on the pyridine ring,[3] and a 1:1 complex of 3,5-dimethylpyrazole is also known.[10] A 1:1 complex with dimethyl selenoxide could not be isolated,[11] and another with (dimethylamino)nitrosobenzene has been claimed, but its characterization is not described.[3]
(10) Ettorre, R.; Plazzogna, G. *Inorg. Chim. Acta* **1975**, *15*, 21.
(11) Tanaka, T.; Kamitani, T. *Inorg. Chim. Acta* **1968**, *2*, 175.
(12) Zubieta, J. A.; Zuckerman, J. J. *Prog. Inorg. Chem.* **1978**, *24*, 251.
(13) Davies, A. G.; Milledge, H. J.; Puxley, D. C.; Smith, P. J. *J. Chem. Soc., Dalton Trans.* **1977**, 1090.

0276-7333/83/2302-0600$01.50/0

systems. Disregarding ancient claims, examples of these 1:1 adducts number fewer than 30 species and include as ligands several dialkyl sulfoxides,[5,6] DMF,[2,6] hexamethylphosphoramide,[8] *N,N*-dimethylpicolinamide, -nicotinamide, and -isonicotinamide and their thio derivatives,[3] salicylaldehyde,[14] diphenylcyclopropenone,[15,16] and variously substituted pyridine *N*-oxides.[6,7,17] In certain cases both 1:1 and 1:2 complexes of dimethyltin(IV) dichloride with the same ligand have been isolated, for example, with methyl benzyl sulfoxide,[6] tetramethylurea,[4] 3,5-dimethylpyrazole,[10] and *N,N*-dimethylnicotinamide, -isonicotinamide, and -thionicotinamide,[3] and pyridine *N*-oxide.[6,19,20] The basicity of the donor atom, the acidity of the tin atom, steric effects originating on the tin or donor moieties, and the creation of strong dipoles or ionic charges in the resulting adducts must play a role in the choice of the structure of the product.[24] Suprisingly, neither the stoichiometry of the reactants nor the reaction conditions appear to exert much influence.

Until recently only one published structure report was available for a 1:1 adduct of a diorganotin(IV) dihalide, that of the dimethyltin(IV) dichloride complex of salicylaldehyde,[26] a potentially chelating donor. However, the phenolic OH group of this ligand intramolecularly hydrogen bonds to the adjacent aldehydic oxygen held at the ortho position rather than chelate the tin atom. The aldehydic oxygen is attached to the tin atom through an angle of 174.7° with one of the tin–chlorine vectors and 79.9° with the other. The methyl–tin–methyl angle is opened to 131.4°. The phenolic oxygen makes a short intermolecular contact to the tin atom of an adjacent molecule in the cell of 3.36 Å and at an angle of 163.1° to one of the chlorine–tin vectors and 68.4° to the other.[27] The structure is described, however, as a trigonal bipyramid with the two methyl groups and one chlorine atom equatorial with the aldehydic oxygen of the ligand and the second chlorine atom axial.[26]

The 1:1 adduct of dimethyltin(IV) dichloride with diphenylcyclopropenone, whose structure we have recently solved,[28] can also be described as a trigonal bipyramid with axial ligand and chlorine attachments, but here again, there is a short intermolecular contact, this time with the axial chlorine atom of an adjacent molecule of 3.561 Å. This attachment is made along an equatorial chlorine–tin vector at an angle of 166.1°.[28]

Table I. Crystal Data for Dimethyltin(IV) Dichloride–2,6-Dimethylpyridine *N*-Oxide

formula	$C_{18}H_{30}Cl_4N_2O_2Sn_2$
fw	685.66
a, Å	15.581 (4)
b, Å	12.781 (4)
c, Å	13.098 (4)
β,[a] deg	102.26 (3)
V, Å^3	2549
space group[b]	$C2/c$
Z	4
$F(000)$	1344
ρ_{calcd}, g cm^{-3}	1.787
μ, cm^{-1}	22.16
dimens of data crystal, mm	0.15 × 0.40 × 0.45

[a] From ±2θ values of 48 reflections with the use of Mo Kα_1 radiation (λ = 0.709 26 Å). [b] Based upon systematic absences hkl, $h + k = 2n + 1$, and $h0l$, $l = 2n + 1$.

Data from tin-119m Mössbauer quadrupole splittings (QS) can potentially throw light upon the question of which is the correct coordination number of the tin atom in the 1:1 complexes. In general QS values for diorganotin(IV) systems increase with increasing carbon–tin–carbon angle.[29] For octahedral systems of the formula $R_2SnX_nL_{4-n}$, a treatment can be applied on the basis of a point-charge model in which the QS values can be used to predict these angles at tin,[30] and excellent results have been obtained for the dimethyl-[30,31] and diphenyltin(IV)[30,32] derivatives where structural data are available.[12] An analogous additivity model for five-coordinated diorganotin compounds has also been proposed. According to the latter treatment, a system of the type $(CH_3)_2SnX_{3-n}L_n$ should exhibit a QS of 3.00[33]–3.25[16] mm s^{-1}. The QS of the 1:1 complex of dimethyltin(IV) dichloride with salicylaldehyde is 3.33[14,26] and of diphenylcyclopropenone 3.52 mm s^{-1}.[16] Using these values in the treatment mentioned above for six-coordination yields predictions of methyl–tin–methyl angles of 137.2° and 143.1°, respectively, vs. 131.4°[27] and 142.2°[28] actually found.

However, in this treatment the magnitude of the QS is assumed to arise only as a result of the nature of the two organic attachments and the angle they make with the tin atom. Neither the nature of the ligands nor their number are assumed to make any difference to the electric field gradient at tin. Hence, the magnitude of the QS in this treatment cannot be used to distinguish between five- and six-coordination, since it is assumed that, for example, trans O_h and axial trigonal-bipyramidal geometries (180°) would give rise to the same values, as would cis O_h and axial and equatorial trigonal-bipyramidal geometries (90°). It is also true, however, that while the *trans*-R_2SnL_4 geometry is ubiquitous for six-coordinated complexes, the analogous axial R_2SnL_3 is rare for the five-coordinated complexes that prefer the equally ubiquitous axially most-electronegative geometry with equatorial organic groups. Thus angles C–Sn–C above 120° (QS ≥ 2.5 mm s^{-1}) are likely to correspond to six-coordination, as do those

(14) Ali, K. M.; Cunningham, D.; Frazer, M. J.; Donaldson, J. D.; Senior, B. J. *J. Chem. Soc. A* **1969**, 2836.
(15) Kumar Das, V. G.; Ng, S.-W. *Malays. J. Sci.* **1978**, *5B*, 143.
(16) Kumar Das, V. G.; Ng, S.-W.; Smith, P. J.; Hill, R. *J. Chem. Soc., Dalton Trans.* **1981**, 552.
(17) Arsine oxides[18] also yield 1:1 complexes with other dialkyl- and diphenyltin(IV) dichlorides.
(18) Mullins, F. P. *Can. J. Chem.* **1971**, *49*, 2719.
(19) Kumar Das, V. G.; Kitching, W. *J. Organomet. Chem.* **1968**, *13*, 523.
(20) Both 1:1 and 1:2 adducts of pyridine *N*-oxide with tin(II) chloride have been reported,[21] but attempts to prepare the 1:2 adduct a decade later failed, as did attempts to form 1:2 adducts with 2-, 3- and 4-picoline and 2,6-lutidine *N*-oxides.[22] However, one group did manage to repeat the syntheses in order to record the Mössbauer spectra.[23]
(21) Morrison, J. S.; Haendler, H. M. *J. Inrog. Nucl. Chem.* **1967**, *29*, 393.
(22) Kauffman, J. W.; Moor, D. H.; Williams, R. J. *J. Inorg. Nucl. Chem.* **1977**, *39*, 1165.
(23) Donaldson, J. D.; Nicholson, D. G. *J. Chem. Soc. A* **1970**, 145.
(24) The stability constants of the tin(II) chloride–pyridine *N*-oxide complexes in acetonitrile are as follows: pyridine *N*-oxide (22), 2-picoline *N*-oxide (51), and 3- (243), 4- (78), and 2,6-lutidine (28). Thus the powerful inductive enhancement effect of the methyl group at the meta position is mediated by steric effects at the ortho position where the stability constant is halved by the substitution of the second ortho methyl group.[25]
(25) Scott, P. T.; Kauffman, J. W.; Rogers, J. W.; Williams, R. J. *J. Inorg. Nucl. Chem.* **1977**, *39*, 2253.
(26) Cunningham, D.; Douek, I.; Frazer, M. J.; McPartlin, M. *J. Organomet. Chem.* **1975**, *90*, C23.
(27) McPartlin, M., private communication, 1981.
(28) Ng, S.-W.; Barnes, C. L.; Hossain, M. B.; van der Helm, D.; Zuckerman, J. J. *J. Am. Chem. Soc.*, **1982**, *104*, 5359.
(29) Zuckerman, J. *J. Adv. Organomet. Chem.* **1970**, *9*, 21.
(30) Sham, T. K.; Bancroft, G. M. *Inorg. Chem.* **1975**, *14*, 2281.
(31) Molloy, K. C.; Hossain, M. B.; van der Helm, D.; Zuckerman, J. J.; Mullins, F. P. *Inorg. Chem.* **1981**, *20*, 2172.
(32) Lefferts, J. L.; Molloy, K. C.; Zuckerman, J. J.; Haiduc, I.; Curtui, M.; Guta, C.; Ruse, D. *Inorg. Chem.* **1980**, *19*, 2861.
(33) Bancroft, G. M.; Kumar Das, V. G.; Sham, T. K.; Clark, M. G. *J. Chem. Soc., Dalton Trans.* **1976**, 643.

Table II. Data Collection Parameters for Dimethyltin(IV) Dichloride–2,6-Dimethylpyridine *N*-Oxide

diffractometer	Enraf-Nonius CAD/4
radiation	Mo $K\bar{\alpha}$ (λ = 0.710 69 Å)
temp, K	138 ± 2
scan technique	θ–2θ
2θ limit, deg	$0 < 2\theta < 47$
max scan time, s	60
scan angle, deg	0.9 + 0.2 tan θ
aperture width, mm	3.5 + 0.86 tan θ
aperture height, mm	6
aperture distance, mm	173
intensity monitors	3
max fluctuation	<3.0%
orientatn monitors[a]	3
no. of unique data	1880
no. of observed data[b]	1820
correctns	Lorentz–polarization

[a] New orientation matrix if angular change >0.1 measured after each 150 reflections. Orientation matrix based upon 24 reflections. [b] $I > 2\sigma(I)$.

in the 1:1 adducts of dimethyltin(IV) dichloride with salicylaldehyde[14,26,27] and diphenylcyclopropenone.[16,28]

The 1:1 complex of dimethyltin(IV) dichloride with pyridine *N*-oxide is said to adopt a trigonal-bipyramidal structure in which the ligand binds equatorially with the two methyl groups on the basis of infrared and Raman evidence.[6] However, the QS value is 3.97 mm s^{-1} [6] for a predicted angle of 162.0° using the point–charge model. The 1:2 complex exhibits a QS of 4.02 mm s^{-1},[6] and the structure shows the tin atom located on a crystallographic center of symmetry to give the ∠C–Sn–C = 180°.[34] The availability of this structure report prompted us to extend our structural studies of the potentially six-coordinated diorganotin(IV) dihalides to the pyridine *N*-oxide series. We chose the sterically crowded 2,6-dimethylpyridine (2,6-lutidine) *N*-oxide ligand to test the effect of the possibly severe nonbonded repulsions arising from the 2,6 substituents on the formation of a genuinely five-coordinated 1:1 adduct.

Experimental Section

Synthesis of 2,6-Dimethylpyridine *N*-Oxide–Dimethyltin(IV) Dichloride. Dimethyltin(IV) dichloride was a gift from M&T Chemicals. 2,6-Dimethylpyridine *N*-oxide (Aldrich Chemicals) was used without further purification. Concentration of a chloroform solution of dimethyltin(IV) dichloride (2.20 g, 10.0 mmol) and 2,6-dimethylpyridine *N*-oxide (1.23 g, 10.0 mmol) gave a cream-colored solid that was recrystallized twice from chloroform to yield a white product. Single crystals of the adduct which melt sharply at 147 °C were obtained by slow evaporation of a chloroform solution of the adduct. Dimethyltin(IV) dichloride–2,6-dimethylpyridine *N*-oxide is stable in air. Its tin-119 NMR chemical shift is −13.24 ppm relative to tetramethyltin.

Crystal Data. Data were obtained on an Enraf-Nonius CAD/4 automatic counter diffractometer at 138 ± 2 K controlled by a PDP-8/e computer and fitted with a low-temperature apparatus. Crystal data are listed in Table I.

Details of our experimental apparatus and methods of data reduction have been outlined previously.[35] Specific parameters relating to the collection of this data set are listed in Table II. The structure factors for each reflection were assigned weights on the basis of counting statistics.[35] No absorption correction was applied. The minimum and maximum transmission factors are 0.37 and 0.72, respectively.

Structure and Refinement. Systematic absences gave two possible space groups *Cc* and *C*2/*c*. The position of the tin atom was found on solving the Patterson map. The averaged, normalized structure factor, *E*, suggested that the space group could be noncentrosymmetric. The structure factors calculated assuming a noncentrosymmetric space group gave an *R* factor ($R = \sum||kF_o| - |F_c||/\sum|kF_o|$) of 0.489 after two cycles of refinement. A difference Fourier map was then calculated. From the difference map, all the non-hydrogen atoms were located. Two molecules per asymmetric unit were found, and they were observed to be related by a two fold axis of rotation. The atoms were then refined using the SHELX program[36] in the *C*2/*c* space group isotropically. When the R factor was a minimum, a difference map was calculated from which the hydrogen positions were located. The hydrogens were then refined isotropically, whereas the other atoms were refined anisotropically to a final *R* value of 0.0364.

The scattering factors used were for neutral atoms and were taken from ref 37 (Sn, Cl, O, and C).

Table III. Atomic Coordinates for Dimethyltin(IV) Dichloride–2,6-Dimethylpyridine *N*-Oxide[a]

atom	*x*/*a*	*y*/*b*	*z*/*c*
Sn	667.3 (2)	1539.1 (2)	632.6 (2)
Cl(1)	−916.5 (6)	949.1 (8)	173.0 (8)
Cl(2)	191.6 (6)	3237.5 (8)	1065.9 (8)
O	2080 (2)	2147 (2)	1061 (2)
N	2702 (2)	1719 (2)	1825 (3)
C(1)	976 (3)	584 (4)	1975 (4)
C(2)	792 (4)	1726 (4)	−932 (3)
C(3)	3190 (2)	910 (3)	1575 (3)
C(4)	3815 (3)	478 (3)	2352 (4)
C(5)	3970 (3)	863 (3)	3354 (4)
C(6)	3473 (3)	1707 (3)	3577 (4)
C(7)	2828 (3)	2136 (3)	2796 (3)
C(8)	2279 (3)	3036 (4)	2969 (4)
C(9)	3012 (3)	552 (3)	459 (3)

[a] Estimated standard deviations are in parentheses.

Table IV. Intramolecular Distances (Å) in Dimethyltin(IV) Dichloride–2,6-Dimethylpyridine *N*-Oxide[a]

Sn–Cl(1)	2.528 (1)	C(5)–C(6)	1.394 (6)
Sn–Cl(2)	2.400 (1)	C(6)–C(7)	1.387 (6)
Sn–C(1)	2.110 (4)	C(7)–N	1.354 (5)
Sn–C(2)	2.113 (4)	C(7)–C(8)	1.479 (6)
Sn–O	2.289 (2)	C(3)–C(9)	1.499 (6)
O–N	1.352 (4)	Sn–Cl(1′)[b]	3.399 (1)
N–C(3)	1.365 (5)	Sn–Sn′	4.5918 (4)
C(3)–C(4)	1.367 (5)	Cl(1)–Cl(1′)	3.8468 (13)
C(4)–C(5)	1.374 (6)		

[a] Estimated standard deviations are in parentheses. [b] Cl(1′) is the bridging atom.

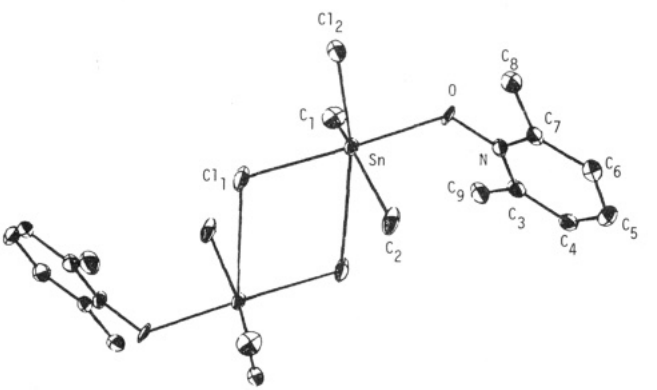

Figure 1. The dimethyltin(IV) dichloride–2,6-dimethylpyridine *N*-oxide dimer showing the atomic numbering.

(34) Blom, E. A.; Penfold, B. R.; Robinson, W. T. *J. Chem. Soc. A* **1969**, 913.
(35) Ealick, S. E.; van der Helm, D.; Weinheimer, A. J. *Acta Crystallogr., Sect. B* **1975**, *B31*, 1618.
(36) Sheldrick, G. M. SHELX-76, University Chemical Laboratory, Cambridge, England, 1976.
(37) "International Tables for X-ray Crystallography"; Kynoch Press: Birmingham, England, 1974; Vol. IV, p 72.

Table V. Intramolecular Angles (deg) in Dimethyltin(IV) Dichloride–2,6-Dimethylpyridine *N*-Oxide[a]

Cl(1)-Sn-Cl(2)	89.50 (3)	C(1)-Sn-C(2)	145.3 (2)	C(5)-C(6)-C(7)	120.0 (4)
Cl(1)-Sn-O	177.44 (7)	O-Sn-C(1)	87.4 (1)	C(6)-C(7)-N	118.4 (3)
Cl(1)-Sn-C(1)	93.7 (1)	O-Sn-C(2)	85.3 (2)	Cl(1′)-Sn-Cl(1)	79.46 (3)
Cl(1)-Sn-C(2)	95.1 (1)	Sn-O-N	123.0 (2)	Cl(1′)-Sn-Cl(2)	168.79 (3)
Cl(2)-Sn-O	87.95 (7)	C(3)-N-C(7)	123.2 (3)	Cl(1′)-Sn-C(1)	72.3 (1)
Cl(2)-Sn-C(1)	110.7 (1)	N-C(3)-C(4)	118.2 (3)	Cl(1′)-Sn-C(2)	76.4 (1)
Cl(2)-Sn-C(2)	102.9 (1)	C(3)-C(4)-C(5)	121.3 (4)	Cl(1′)-Sn-O	103.09 (7)
		C(4)-C(5)-C(6)	119.0 (4)		

[a] Estimated standard deviations are in parentheses.

Table VI. Least-Squares Planes in Dimethyltin(IV) Dichloride–2,6-Dimethylpyridine *N*-Oxide

	orthonormal equation $M_1x + M_2y + M_3z + d = 0$						
planes through atoms	M_1	M_2	M_3	d	plane P	dihedral angle between [P,P′]	rms
Cl(2), C(1), C(2), Cl(1)′	−0.9791	−0.2031	−0.0047	1.3720	1[a]		0.2472
Sn(1), Cl(1), Sn(1)′, Cl(1)′	−0.0722	0.3283	−0.9418	0	2	89.51 [1,2]	0
O, N, C(3), C(4), C(5), C(6), C(7)	0.6719	0.6393	−0.3740	−3.6183	3	−38.19 [1,3]	0.0064
						59.10 [2,3]	
Sn, O, N	0.2579	−0.0248	−0.7370	1.4150	4[b]	87.17 [3,4]	0
Sn, O, C(1)	0.2904	−0.7291	−0.6197	1.5159	5[b]	9.20 [4,5]	0

[a] The tin atom is 0.0252 (3) Å from this plane in the direction of the Sn–O vector. [b] The Sn–C(1) and O–N vectors make an angle of 9.20° when viewed along the Sn–O axis.

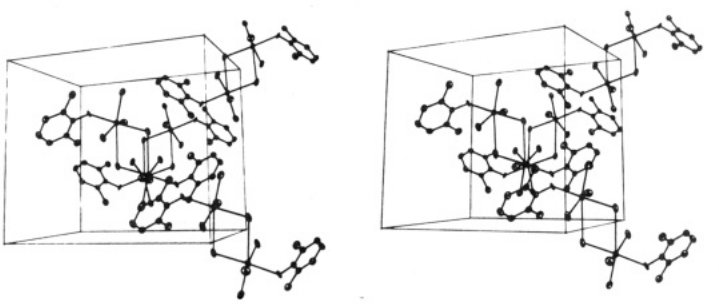

Figure 2. A stereoview of the unit-cell contents of the dimethyltin(IV) dichloride–2,6-dimethylpyridine *N*-oxide dimer.

Final atomic parameters are given in Table III and final intramolecular distances and angles in Tables IV and V, respectively. Least-squares planes are given in Table VI.

The asymmetric unit showing the atomic numbering is depicted in Figure 1. Hydrogen atoms are numbered with respect to the carbon atom to which they are attached (all hydrogens are C–H), e.g., H(C1). Where methyl carbons hold more than one hydrogen atom, these are labeled, e.g., as H(C1)A, H(C1)B, and H(C1)C. A stereoview of the unit cell contents is shown in Figure 2. Figure 3 is a view of the monomer unit down the trans chlorine(1)–tin–oxygen vector.

Results

For the adduct the NMR tin–proton coupling constant $|^2J(^{119}Sn–C–^1H)| = 80.4$ Hz as measured in deuteriochloroform. The corresponding value in the related 1:1 adduct with 2,4,6-trimethylpyridine *N*-oxide is reported as 80 Hz.[7]

The ν_{asym} and $\nu_{sym}(Sn–CH_3)$ modes appear in the infrared spectrum at 564 (m) and 518 (m) cm^{-1} and in the Raman at 572 (w) and 514 (s) cm^{-1}, respectively. In addition, bands at 538 (w) and 525 (m) cm^{-1} appear in the infrared and Raman spectra, respectively. The corresponding ν-($Sn–CH_3$) bands for the 1:1 adduct with pyridine *N*-oxide are reported at 570 and 508 cm^{-1} in the infrared and at 566 and 506 cm^{-1} in the Raman, respectively.[6] These bands are found at 566 and 512 cm^{-1} in the infrared of the 1:1 adduct with 2,4,6-trimethylpyridine *N*-oxide.[7] In the ν-(N–O) region, bands are seen at 1212, 1197, and 1172 cm^{-1} compared with the 1246-cm^{-1} band in the free ligand.[38]

(38) Shindo, H. *Chem. Pharm. Bull.* **1956**, *4*, 460.

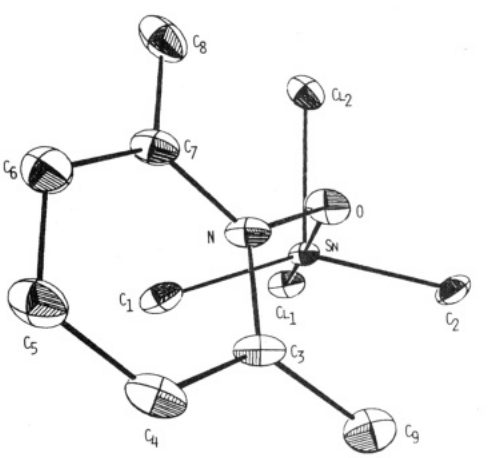

Figure 3. The monomer unit viewed down the trans chlorine(1)–tin–oxygen vector. The bridging chlorine atom [Cl(1′) is found trans to chlorine(2).

The corresponding 1:1 complex with tin(II) chloride has ν(N–O) = 1181 cm^{-1} ($\Delta\nu$ = 65 cm^{-1}).[22] The more strongly Lewis acidic tin(IV) derivative should exhibit a larger ν-(N–O) shift, and hence we can assign the ν(N–O) mode in our adduct at 1172 cm^{-1} ($\Delta\nu$ = 74 cm^{-1}) on this basis.

The Mössbauer spectrum is a well-separated doublet with isomer shift (IS) of 1.44 ± 0.03, quadrupole splitting (QS) of 3.80 ± 0.06 [ρ=QS/IS=2.64], and Γ_1 = 1.38 and Γ_2 = 1.32 ± 0.03 mm s^{-1}. For the corresponding 1:1 pyridine *N*-oxide adduct, IS = 1.33 and QS = 3.97 mm s^{-1} [ρ = 2.98].[6]

Description and Discussion of the Structure. From Figure 1 it is seen that the 1:1 nature of the title complex arises because the sixth coordination position at tin is taken up by a chloride donor atom from a second molecule to form an unsymmetrical, double-bridged Sn_2Cl_2 ring system whose dimensions include a short [Sn–Cl(1) = 2.528(1) Å] and a long [Sn–Cl(1′) = 3.399 (1) Å] tin–chlorine distance. One chlorine atom in each molecule is terminal at [Sn–Cl(2) = 2.400 (1) Å]. The resulting geometry about the tin atom is thus distorted octahedral with trans-dimethyl dimethyl groups [∠C(1)–Sn–C(2) = 145.3 (2)°]. The bridging chlorine from the second molecule approaches along the Sn–Cl(2) vector to create a *trans*-dichlorotin system [∠Cl(1′)–Sn–Cl(2) = 168.79 (3)°]. The chlorine atom trans to the *N*-oxide ligand [∠O–Sn–Cl(1) = 177.44 (7)°] forms the bridge. The planar Sn_2Cl_2 ring is located on a crystallographic center of symmetry as seen in the unit-cell diagram shown in Figure 2. This dimerization went undetected in the tin-119m Mössbauer spectroscopic study of the related pyridine *N*-oxide complex, where the IS (1.33) and QS (3.97) are not very different from the 1:2 complex (1.35 and 4.02 mm s^{-1}, respectively).[6] Other 1:1 complexes are also reported to exhibit large QS's[6,8,15,16] and are probably six-coordinated in the solid through chlorine bridging. The ability to complete the coordination sphere through oligomerization or polymeric association may lie at the root of why 1:1 complexes form at all and may explain why they are found almost exclusively[9] with pointed >C=O, >C=S, >S=O, >N→O, or >P=O ligands.

Dimethyltin(IV) dichloride itself forms an associated solid in which the distortion from tetrahedral geometry is very severe. The molecular units align themselves so that double chlorine bridges can form to give Sn_2Cl_2 planes with tin–chlorine distances of 2.40 and 3.54 Å and methyl groups projecting above and below (∠C–Sn–C = 123.5°).[13] A similar arrangement is adopted by the two central, six-coordinated diphenyltin(IV) dichloride molecules in that tetrameric chain structure[39] which contains tin–chlorine distances of 2.357 and 3.77 Å but rather closed carbon–tin–carbon angles of 125.5°.[40] A more symmetrical polymer of this type is formed by the difluoride analogue,[41,42] and trimethyltin(IV) chloride also crystallizes as an infinite, chlorine-bridged polymer.[43] A different arrangement in which both chlorine atoms from one molecule chelate the same tin atom of a neighboring molecule is found in the bis(chloromethyl)tin(IV) dichloride structure. The tin–chlorine distances here are 2.37 and 3.71 Å, and the carbon–tin–carbon angle is opened to 135°.[39] In our structure there is no possibility for further association unless higher than six coordination is utilized, and the bridging mode chosen to form the dimer most strongly resembles that found in dimethyltin(IV) dichloride itself, except that the dimethyltin angle is more open [123.5°[13] vs. 145.3 (2)°]. Comparison data for dimethyltin(IV) dichloride and its two pyridine *N*-oxide complexes are displayed in Table VII.

Close reexamination of the structural data for the related 1:1 complex of salicylaldehyde[26,27] reveals that the short contact between the phenolic oxygen of one molecule and the tin atom of the next (3.36 Å) is directed along an Sn–Cl vector.[27] This is suggestive of an octahedral geometry at the tin atom with one intramolecular trans Cl–Sn–O system formed with the donor aldehydic oxygen and a second trans Cl–Sn–O formed intermolecularly with the phenolic oxygen atom of an adjacent molecule. This phenol group also engages in internal hydrogen bonding with the ortho aldehyde, consistent with infrared evidence. The dimethyltin angle is opened to 131.4° to complete the distorted trans, trans, trans arrangement.

Table VII. Comparison Data for Dimethyltin(IV) Dichloride and Its Pyridine *N*-Oxide Complexes

	$(CH_3)_2SnCl_2 \cdot n$pyNO		
	$n = 1^a$	$n = 2^b$	$n = 0^c$
d(Sn–Cl), Å	2.400 (1), 2.528 (1)	2.584	2.41, 3.54
d(Sn–O), Å	2.289 (2)	2.251	
d(Sn–C), Å	2.112 (4), 2.110 (4)	2.225	2.21
d(O–N), Å	1.352 (4)	1.37	
$d(N-C)_{av}$, Å	1.364 (5)	1.35	
∠C–Sn–C, deg	145.3 (2)	180	123.5
∠Cl–Sn–Cl, deg	89.50 (3)	180	93.0
∠Cl–Sn–O, deg	85.3 (2), 177.44 (7)	89.5, 90.5	
∠C–Sn–O, deg	87.4 (1), 85.3 (2)	95.6, 84.4	
∠Sn–O–N, deg	123.0 (2)	117	
∠Cl–Sn–C, deg	93.7 $(1)_{ax}$, 95.1 $(1)_{ax}$, 102.9 $(1)_{eq}$, 110.7 $(2)_{eq}$	89.5, 90.5	109.0
∠O–Sn–O, deg		180	
∠pyNO ring and Sn–O–N plane, deg	87.17 (6)°	83	

[a] This work. Estimated deviations are in parentheses. [b] Reference 34. [c] Reference 13.

In the 1:1 complex with diphenylcyclopropenone, the dimethyltin angle is opened even farther to 142.2°, and the nearest nonbonded chlorine is found at 3.561 Å in a position suggestive of coordination.[28]

Observation of both ν_{asym} and ν_{sym}(Sn–C) modes in the infrared and Raman spectra corroborates the nonlinear dimethyltin system found, and the application of a treatment based upon a point-charge model[30] links the observed Mössbauer QS value to a predicted carbon–tin–carbon angle in octahedral complexes. The results of the calculation, which is based upon the assumption that the partial QS of the chlorine and ligand groups are negligible, are listed in Table VIII. Data for the 1:1 complex of pyridine *N*-oxide[6] are included on the assumption that this complex will also be found to be dimeric in the solid.

Thus the most direct comparison with the structure of the title compound is with the octahedral 1:2 complex of dimethyltin(IV) dichloride with the unsubstituted pyridine *N*-oxide[34] and with its five-coordinated, 1:1 complex with triphenyltin(IV) nitrate that has been solved in both its mono-[44] and triclinic modifications,[45] but there are available published reports of the structures of a wide variety of transition metal complexes of pyridine *N*-oxide[46–49] which encompass copper(II),[50–66] zinc(II),[62,64,67]

(39) Bokii, N. G.; Struchkov, Yu. T.; Prok'iev, A. K. *J. Struct. Chem.* (*Engl. Transl.*) **1972**, *13*, 619.
(40) Greene, P. T.; Bryan, R. F. *J. Chem. Soc. A* **1971**, 2549.
(41) Rush, J. J.; Hamilton, W. C. *Inorg. Chem.* **1966**, *5*, 995.
(42) Schlemper, E. O.; Hamilton, W. C. *Inorg. Chem.* **1966**, *5*, 2238.
(43) Lefferts, J. L.; Molloy, K. C.; Hossain, M. B.; van der Helm, D.; Zuckerman, J. J. *Inorg. Chim. Acta* **1979**, *36*, L409; *J. Organomet. Chem.*, **1982**, *240*, 349.
(44) Pelizzi, C.; Pelizzi, G.; Tarasconi, P. *J. Organomet. Chem.* **1977**, *124*, 151.
(45) Pelizzi, G. *Inorg. Chim. Acta* **1977**, *24*, L31.
(46) Katritzky, A. R.; Lagowski, J. M. "Chemistry of the Heterocyclic *N*-Oxides"; Academic Press: New York, 1971.
(47) Orchin, M.; Schmidt, P. J. *Coord. Chem. Rev.* **1968**, *3*, 345.
(48) Garvey, R. G.; Nelson, J. H.; Ragsdale, R. O. *Coord. Chem. Rev.* **1968**, *3*, 375.
(49) Karayannis, N. M.; Pytlewski, L. L.; Mikulski, C. M. *Coord. Chem. Rev.* **1973**, *11*, 93.

Table VIII. Comparison Data and Predicted Methyl-Tin-Methyl Angles from Mössbauer Quadrupole Splittings (QS) for Dimethyltin(IV) Derivatives

compd	QS, mm s^{-1}	d(Sn-C), Å	∠C-Sn-C, deg found	∠C-Sn-C, deg predicted[a]	ref
$(CH_3)_2SnCl_2$	3.55[b]-3.60[c]	2.16 2.21	123.5		13
1:2 pyNO	4.02[c]	2.225	180.0		34
1:1 pyNO	3.97			162.0	
1:1 2,6-lut-NO	3.80 ± 0.06	2.110 (4) 2.112 (4)	145.3 (2)	153.0	*d*
1:1 salicylaldehyde	3.33	2.098 2.107	131.4	137.2	*e*
1:1 diphenylcyclopropenone	3.52	2.111 2.116	142.2	143.1	*f*

[a] On the basis of a six-coordinated, octahedral model. [b] Reference 13. [c] Reference 6. [d] This work. Estimated standard deviations are in parentheses. [e] Reference 27. [f] Reference 28.

nickel(II),[68-70] cobalt(II),[63,70-72] iron(II),[63] platinum(II),[73] and mercury(II)[74,75] in three-,[74] four-,[50,51,53-55,58,59,65,67,73] five-,[52,56,59-61,65,71] and six-coordination[57,62-64,68,69,72,75] in neutral[50-52,55-61,65,66,70,71] and cationic[53,54,57,62-65,69-72,75] species. We are aware of data for some 30 transition-metal complexes, and these are listed in Table IX. The structures of the parent pyridine *N*-oxide ligand are known in the solid[76] as well as the gas phase (electron diffraction),[77] along with those of the solid 4-nitro-,[78] 4,4-*trans*-azo-[79] and *N*-oxyphenazine[80] derivatives. In addition, the structures of the hydrochloride,[81] the hydrogen-bonded semiperchlorate,[82] and trichloroacetic acid[83] complexes are known. These data are listed in Table X. There are structures which utilize 2-[52,68] and 4-[58,64] methyl (picoline), 4-phenyl,[59] 2,6-dimethyl (lutidine),[55,65] 4-nitro,[57] 3-[65] and 4-[66,67] carboxylate, 4-methoxy,[73] and 3,5-dibromo[74] substituents on the pyridine *N*-oxide ligands. Thus sufficient structural data are available at this time for meaningful comparison and to resolve such questions as (i) does the ligand N–O distance lengthen on coordination to an acceptor atom, (ii) does electron releasing methyl 2 or 2,6 substitution in picoline and lutidine ligands weaken the coordinative interaction, and (iii) what is the nature of the bond between the oxygen atom and the acceptor in pyridine *N*-oxide complexes?

The electronic situation in the pyridine *N*-oxide ligand can be represented as

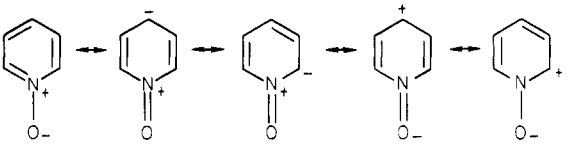

I II III

which are said to have equal weights.[46] Canonical forms II should be favored by electron-withdrawing groups, and the shorter N–O distance (1.260 Å) in the 4-nitro derivative[78] is usually attributed to the enhanced double-bond character of the N–O bond in this compound.[84] Electron-releasing substituents such as methyl should, on the other hand, favor forms I and III, which should be better donor ligands. Coordination should lengthen the N–O distance, but the evidence, taking the X-ray structure of pyridine *N*-oxide as the basis, is very mixed. This arises in part from the fact that the pyridine *N*-oxide crystal itself contains two independent molecules whose N–O distances (1.33 and 1.37 Å) differ by 0.04 Å[76] and encompass a large

(50) Schäfer, H. L.; Morrow, J. C.; Smith, H. M. *J. Chem. Phys.* **1965**, *42*, 504.
(51) Sager, R. S.; Williams, R. J.; Watson, W. H. *Inorg. Chem.* **1967**, *6*, 951.
(52) Sager, R. S.; Watson, W. H. *Inorg. Chem.* **1968**, *7*, 2035.
(53) Lee, J. D.; Brown, D. S.; Melsom, B. G. A. *Acta Crystallogr., Sect. B* **1969**, *B25*, 1378.
(54) Lee, J. D.; Brown, D. S.; Melsom, B. G. A. *Acta Crystallogr., Sect. B* **1969**, *B25*, 1595.
(55) Sager, R. S.; Watson, W. H. *Inorg. Chem.* **1969**, *8*, 308.
(56) Ščavničar, S.; Matkovič, B. *Acta Crystallogr., Sect. B* **1969**, *B25*, 2046.
(57) Williams, R. J.; Cromer, D. T.; Watson, W. H. *Acta Crystallogr., Sect. B* **1971**, B27, 1619.
(58) Johnson, D. R.; Watson, W. H. *Inorg. Chem.* **1971**, *10*, 1068.
(59) Watson, W. H.; Johnson, D. R. *J. Coord. Chem.*, **1971**, *1*, 145.
(60) Mighell, A. D.; Reimann, C. W.; Santoro, A. *Acta Crystallogr., Sect. B* **1972**, *B28*, 126.
(61) Whinnery, J. E.; Watson, W. H. *J. Coord. Chem.* **1972**, *1*, 207.
(62) O'Connor, C. J.; Sinn, E.; Carlin, R. L. *Inorg. Chem.* **1977**, *16*, 3314.
(63) Taylor, D. *Aust. J. Chem.* **1978**, *31*, 713.
(64) Wood, J. S.; Day, R. O.; Keijzers, C. P.; deBoer, E.; Yildirim, A. E.; Klaassen, A. A. K. *Inorg. Chem.* **1981**, *20*, 1982.
(65) Knuuttila, H. *Inorg. Chim. Acta* **1981**, *50*, 221.
(66) Knuuttila, P. *Inorg. Chim. Acta* **1982**, *51*, 201.
(67) Sager, R. S.; Watson, W. H. *Inorg. Chem.* **1968**, *7*, 1358.
(68) Horrocks, W. deW., Jr.; Templeton, D. H.; Zalkin, A. *Inorg. Chem.* **1968**, *7*, 1552.
(69) van Ingen Schenau, A. D.; Verschoor, G. C.; Romers, C. *Acta Crystallogr., Sect. B* **1974**, *B30*, 1686.
(70) Knuuttila, P. *Inorg. Chim. Acta* **1981**, *50*, 141.
(71) Coyle, B. A.; Ibers, J. A. *Inorg. Chem.* **1970**, *9*, 767.
(72) Bergendahl, T. J.; Wood, J. S. *Inorg. Chem.* **1975**, *14*, 338.
(73) Hamilton, R. S.; Corey, E. R., unpublished work cited in ref 47. Hamilton, R. S. *Diss. Abstr.* **1968**, *29B*, 1595.
(74) Genet, F.; Leguen, J.-C. *Acta Crystallogr., Sect. B* **1969**, *B25*, 2029.
(75) Kepert, D. L.; Taylor, D.; White, A. H. *J. Chem. Soc., Dalton Trans.* **1973**, 670.
(76) Ülkü, D.; Huddle, B. P.; Morrow, J. C. *Acta Crystallogr., Sect. B* **1971**, *B27*, 432.
(77) Chiang, J. F. *J. Chem. Phys.* **1974**, *61*, 1280.
(78) Eichhorn, E. L. *Acta Crystallogr.* **1956**, *9*, 787.
(79) Eichhorn, E. L. *Acta Crystallogr.* **1959**, *12*, 746.
(80) Curti, R.; Riganti, V.; Locchi, S. *Acta Crystallogr.* **1961**, *14*, 133.
(81) Tsoucaris, G. *Acta Crystallogr.* **1961**, *14*, 914.
(82) Jaskólski, M.; Gdaniec, M.; Kosturkiewicz, Z.; Szafran, M. *Pol. J. Chem.* **1978**, *52*, 2399; *Chem. Abstr.* **1980**, *92*, 5983g.
(83) Golič, L.; Hadži, D.; Lazarini, F. *J. Chem. Soc., Chem. Commun.* **1971**, 860.
(84) However, a more recent structure determination of (4-nitropyridine *N*-oxide)$_2$CuCl$_2$·2H$_2$O reveals a situation in which the ligand is only loosely coordinated to the copper(II) center [*d*(Cu–O) = 2.635 Å].[57] The N–O distance in this ligand molecule, which is hydrogen-bonded to the water molecules, is 1.325 Å rather than the 1.260 Å reported for the 4-nitro derivative itself.[75]

Table IX. The Pyridine *N*-Oxide Ligand in Metal Complexes[a]

complex	CN and geom	d(N–O), Å	d(M–O), Å	∠M–O–N, deg	d(C–N)$_{av}$, Å	pyNO plane orientatn	ref
[μ-pyNOCuCl$_2$]$_2$	4 T_d	1.24	1.99		1.35		50
			2.10				
	4 sq pl[b]	1.346	1.979	123.5	1.341	70.0	51
			2.036	127.8			
Niacac$_2$(pyNO)$_2$-*cis*	6 O_h	1.321	2.088	119.2	1.339	48.4	66
		1.337	2.105	122.4		67.5	
(2-CH$_3$pyNO)$_2$Cu$_3$Cl$_6$·2H$_2$O	5 sq py	1.36	1.98	121.6	1.36	88.8	52
			2.01	127.1			
[2,6-(CH$_3$)$_2$pyNO]$_2$ZnCl$_2$	4 T_d	1.38	2.01	118.6	1.39		65
3,5-Br$_2$pyNOHgCl$_2$	3 "T" shaped	1.27	2.51	125.7	1.37		71
[(pyNO)$_4$Cu]$^{2+}$(ClO$_4^-$)$_2$	4 T_d	1.33	1.92	116.7	1.34	88.7	53
		1.34	1.93	118.7		79.1	
[(pyNO)$_4$Cu]$^{2+}$(BF$_4^-$)$_2$	4 sq pl	1.31	1.93	116.7	1.34	89.9	54
		1.36	1.91	118.6		78.9	
[(2,6-(CH$_3$)$_2$pyNO]$_2$CuCl$_2$	4 T_d to cis sq pl	1.31	1.97	118.6	1.38		55
		1.36	1.93	121.6			
(4-NO$_2$py)$_2$CuCl·2H$_2$O[c]	6 O_h	1.325	2.635	109.9	1.354		57
[(pyNO)$_2$Cu]$^{2+}$(NO$_3^-$)$_2$	5 distorted tetra py	1.362	1.968	118.6	1.346	64.0	56
		1.361	1.951	119.4			
[(2-CH$_3$pyNO)$_5$Co]$^{2+}$(ClO$_4^-$)$_2$	5 tbp	1.275 (av)	2.098$_{ax}$ (av)	124.2 (av) (120–134)		41–84	68
			1.975$_{eq}$ (av)				
[μ-(pyNO)$_2$CuBr$_2$]$_2$	5 sq py	1.345, 1.347 (terminal)	1.944, 1.949 (terminal)	119.7, 119.5 (terminal)	1.342 (terminal), 1.341 (bridging)		60
		1.365, 1.366 (bridging)	2.162, 1.975, 2.240, 1.976 (bridging)	121.2, 123.6, 125.3, 121.3 (bridging)			
4-CH$_3$pyNOPt(CO)Cl$_2$	4 sq pl	1.35	1.99	120.0	1.35	87.5	70
(4-CH$_3$pyNO)$_2$CuCl$_2$ (green modification)	4 T_d	1.34	1.949	122.0	1.34	93.9	58
[μ-pyNOCuBr$_2$]$_2$	5 sq py	1.381	1.965	125.9	1.355	83.0	61
			1.994	123.8			
[μ-4-PhpyNOCuCl$_2$]$_2$	4 sq pl	1.371	1.978	123.0	1.343	85.1	59
			1.986				
[μ-4-PhpyNOCuCl$_2$·2H$_2$O]$_2$	5 sq py	1.347	1.980	124.5	1.330	79.7	59
			2.040				
(pyNO)$_6$Hg^{2+}(ClO$_4^-$)$_2$	6 O_h	1.32	2.35	114.3	1.36	72.9	72
[(pyNO)$_6$Ni]$^{2+}$(BF$_4^-$)$_2$	6 O_h	1.332	2.060	119.0	1.41	71.4	67
[(pyNO)$_6$Co]$^{2+}$(ClO$_4^-$)$_2$	6 O_h	1.334	2.088	119.5	1.337	72.2	69
[(pyNO)$_6$Cu]$^{2+}$(ClO$_4^-$)$_2$	6 O_h	1.324	2.086	118.7	1.340		62
[(pyNO)$_6$Cu]$^{2+}$(BF$_4^-$)$_2$	6 O_h	1.333	2.088	118.75	1.335		62
[(pyNO)$_6$Zn]$^{2+}$(ClO$_4^-$)$_2$	6 O_6	1.330	2.102	119.25	1.341		62
[(pyNO)$_6$Zn]$^{2+}$(BF$_4^-$)$_2$	6 O_h	1.326	2.102	119.2	1.341		62
[(pyNO)$_6$Cu]$^{2+}$(ClO$_4^-$)$_2$	6 O_h	1.332	2.076	119.1	1.333	72.8	63
[(pyNO)$_6$Co]$^{2+}$(ClO$_4^-$)$_2$	6 O_h	1.331	2.090	119.3	1.341	72.7	63
[(pyNO)$_6$Fe]$^{2+}$(ClO$_4^-$)$_2$	6 O_h	1.331	2.112	119.7	1.338	71.8	63
[(4-CH$_3$pyNO)$_6$Cu]$^{2+}$(ClO$_4^-$)$_2$	6 O_h	1.326	1.965	120.2	1.350		64
		1.312	2.008	119.4			
		1.326	2.385	116.1			
[(4-CH$_3$pyNO)$_6$Zn]$^{2+}$(ClO$_4^-$)$_3$	6 O_h	1.352	2.068	119.0	1.358		64
		1.309	2.113	119.5			
		1.344	2.160	116.5			

$[(3\text{-}O_2CpyNO)_4Cu_3(OH)_2 \cdot 2H_2O]_n$	4 sq pl 5 sq py	1.327	2.426	1.336		65
$[Co(H_2O)_6]^{2+}[4\text{-}O_2CpyNO]_2$	*d*	1.324	*d*	1.343	*d*	70
$[Ni(H_2O)_6]^{2+}[4\text{-}O_2CpyNO]_2$	*d*	1.319	*d*	1.350	*d*	70
$[(4\text{-}O_2CpyNO)Cu]_4SO_4(OH)_2 \cdot H_2O$	*d*	1.30	*d*	1.37	*d*	66
$(C_6H_5)_3SnNO_3 \cdot pyNO$						
monoclinic	5 tbp	1.34	2.227	120.4	1.34	78.9	44
triclinic	5 tbp		2.299 2.238				45
$(CH_3)_2SnCl_2 \cdot 2pyNO$	6 O_h	1.37	2.251	117.0	1.36	83	34
$[(CH_3)_2SnCl_2 \cdot 2,6\text{-}(CH_3)_2pyNO]_2$	6 O_h	1.352 (4)	2.289 (2)	123.0 (2)	1.359 (5)	87.17 (6)	*d*

[a] The complexes are listed in the chronological order of the study being submitted for publication, with the transition-metal derivatives first. [b] Reinterpreted as five-coordinate with square-pyrimidal geometry at copper [Sager, F. S.; Williams, R. J.; Watson, W. H. *Inorg. Chem.* **1969**, *8*, 694]. [c] The 4-NO_2pyNO ligand is held predominantly by hydrogen bonding. [d] The pyNO ligand is not bonded to M. [e] This work. Estimated standard deviations are in parentheses.

Table X. Structural Data for Pyridine *N*-Oxide

	d(N–O), Å	*d*(C–N), Å	ref
4-NO_2pyNO	1.260	1.382 1.384	75
4,4-*trans*-azo-pyNO	1.283	1.351 1.364	76
N-oxyphenazine	1.24	1.35	77
pyNO·HCl	1.37	1.31 1.36	78
pyNO (X-ray)	1.33 1.37	1.34 1.34	73
pyNO (gas-phase electron diffraction)	1.290	1.384	74
pyNO trichloroacetic acid	1.39		80
pyNO semiperchlorate	1.34	1.38	79

part of the range represented by the known data for the complexes.[47–49] In the simplest systems, the formation of the hydrochloride[81] and the strong hydrogen bond to trichloroacetic acid[83] produce N–O distances of 1.37 and 1.39 Å, respectively. The *d*(N–O) data for the transition-metal complexes range from 1.26 Å, for one of the 2-picoline ligands in $[(2\text{-}CH_3pyNO)_5Co]^{2+}(ClO_4^-)_2$[71] to 1.362 Å for one of the pyNO ligands in $[(pyNO)_2Cu]^{2+}(NO_3^-)_2$.[56] Another particularly short N–O distance is reported for the mercury(II) complex, 3,5-Br_2pyNO·$HgCl_2$ (1.27 Å)[74] in which the ligand carries two electron-withdrawing substituents which apparently enhance the contribution of canonical forms II. However, in the comparison among the three related copper(II) chloride complexes $(4\text{-}CH_3pyNO)_2CuCl_2$,[58] $[(2,6\text{-}(CH_3)_2pyNO]_2CuCl_2$,[55] and $(4\text{-}NO_2pyNO)_2CuCl_2 \cdot 2H_2O$,[57] the last of which is six-coordinated and octahedral, while the first two are four-coordinated and tetrahedral, the N–O distances are 1.34,[58] 1.31 and 1.36 (average 1.34 Å),[55] and 1.325 Å,[57] respectively. Thus the electron-releasing and -withdrawing substituents do not seem to register any measurable effect on *d*(N–O) in complexed pyridine *N*-oxides.

We can conclude that where data are available for comparison, there is no systematic change to the expected longer N–O distances on coordination of the pyridine *N*-oxide ligands to acceptors, nor do the data support a convincing shortening or lengthening of *d*(N–O) on substitution by electron-withdrawing and -releasing ligands on the pyridine ring in complexes. The observed changes in the frequencies of bands assigned to ν(N–O) must arise from other origins such as the orientation of the pyridine ring in the molecule,[34] or the assigned bands must be highly coupled to other modes.[85]

In most examples the pyridine *N*-oxide ligand coordinates with metal atoms so as to make an angle M–O–N of roughly 120°, suggesting sp^2 hybridization at the oxygen atom (two lone pairs plus the N–O bond pair) with the third lone pair in a pure p orbital available for π interaction with the aromatic system of the pyridine ring as in canonical forms II. If this π interaction were important, then the planes of the M–O–N and pyridine rings should be coincident, but this is not the case for the complexes listed in Table IX nor for pyridine *N*-oxide hydrochloride[81] nor for the structure of the title compound where it is 87.17 (6)°. Thus a description based upon a distortion from sp^3 hybridization at oxygen (canonical forms I and III) would appear to be more valid, with minimum contribution from form II and angular coordination to acceptor atoms. Forcing the M–O–N and pyridine ring planes into coin-

(85) Mirone, P. *Atti Accad. Naz. Lincei, Cl. Sci. Fis., Mat. Nat., Rend.* **1963**, *35*, 530; *Chem. Abstr.* **1964**, *61*, 7843b.

cidence would maximize the steric interference of the aromatic ring with the other ligands on the metal atom, which is probably why it is not chosen. Delocalization of the second lone pair at oxygen into the aromatic ring (an alternative way to achieve canonical forms II) is probably not favored because of the somewhat disadvantageous geometry of this orbital, its high s character and the low energy of the oxygen orbitals. Lack of contribution from canonical forms II probably lies at the root of the absence of N–O bond lengthening on coordination to metal atoms, since changes in this distance from forms I and III would be expected to be minimal. Overlap of the second lone pair orbital with the acceptor orbital of the metal atom is probably somewhat poor energetically since a plus charge on the nitrogen (in canonical form I) would reduce electron flow from oxygen. Both lone pairs of electrons on oxygen are utilized in coordination in the dimeric copper(II) halide complexes $[\mu\text{-pyNOCuCl}_2]_2$,[50,51] $[\mu\text{-pyNO(pyNO)CuBr}_2]_2$,[60] $[\mu\text{-4-phenyl-pyNOCuCl}_2]_2$,[59] $[\mu\text{-4-phenyl-pyNOCuCl}_2\cdot 2H_2O]_2$,[59] and $(\mu\text{-2-CH}_3\text{pyNO})_2Cu_3Cl_6\cdot 2H_2O$[52] in which bridging oxygen atoms from the pyNO ligands are found. The μ-N–O distances are 1.24[50] or 1.346,[51] 1.366 (average of two dimer molecules),[60] 1.371,[59] 1.347,[59] and 1.36 Å,[52] respectively. A particularly interesting comparison is available for $[(\mu\text{-pyNO})_2CuBr_2]_2$ in which both terminal and bridging ligands are found at 1.346 and 1.366 Å, respectively,[60] which gives rise to the observation of two infrared ν(N–O) stretching frequencies.[86] The orientation of the bridging pyridine rings in the two dimers is virtually the same, but the angle about the Cu–O bond is ca. 60° different for the terminal ligands in the two dimers. Unfortunately, the angles between the planes made by the Cu–O–N bonds and the pyridine rings are not listed.

Against this background the structural data for the title complex can be better understood. It is seldom that data for two such closely related materials as the 1:2 and 1:1 pyridine *N*-oxide complexes of dimethyltin(IV) dichloride are available,[12] and the structure of the parent dimethyltin(IV) dichloride which is somewhat associated in the solid state to a very distorted octahedral geometry about the central tin atom[13] is also known. In the comparison of the data in Table VII it is seen that the bonds that the tin atom forms to the chlorine atoms and methyl groups are longer in the more regular coordination sphere of the six-coordinated, 1:2 complex in which the tin atom occupies a crystallographic center of symmetry giving rise to a perfect trans, trans, trans octahedron. However, the distance to the oxygen atom of the ligand in the title complex is longer. Thus, the expected enhancement of donor bond strength by the electron-releasing methyl groups may, in this case, as with the analogous complexes with tin(II) chloride,[24,25] be offset by steric interference of these 2,6 substituents with the tin attachments, giving a net weakening of the tin–ligand bond.

The octahedral geometry about the tin atoms in the dimer is rather irregular. While the trans bonds holding the ligand are almost linear [∠C(1)–Sn–O = 177.4 (1)°], the dimethyltin system is quite bent [∠C(1)–Sn–C(2) = 145.3 (2)°]. In the 1:1 complex with salicylaldehyde[26] in which contact with a nonbonded phenolic oxygen atom of an adjacent molecule[27] raises the coordination number at the tin atom to six, the dimethyltin system makes an angle of 131.4°. In the associated structures of dimethyltin(IV) dichloride itself, this angle is 123.5°.[13] In the six-coordinated 1:1 complex with diphenylcyclopropenone, this angle is 142.2°.[28]

(86) Muto, Y.; Jonassen, H. B. *Bull. Chem. Soc. Jpn.* **1966**, *39*, 58.

Pairs of $(CH_3)_2SnCl_3^-$ anions also form dimeric units through axial chlorine bridging to tin at *d*(Sn···Cl) = 3.486 Å in the quinolinium salt.[87] The unfavorable electrostatic situation must be balanced by a countervailing gain in overall stability of the crystal.

Viewing the molecule down the trans oxygen–tin–chlorine(1) vector as in Figure 3, the O–N bond is seen to lie within 9.20° of eclipsing the tin–carbon(1) bond, between it and the second [C(2)] methyltin bond. The pyridine ring bends away from the plane formed by the two methyl groups [C(1) and C(2)] and the chlorine [Cl(2)] and bridging chlorine [Cl(1′)] atoms, with the Sn–O–N angle = 123.0 (2)°. If the plane of the pyridine ring were coincident with the plane formed by the Sn–O–N system, then the nonbonded distance to the methyl substituent on the pyridine ring (C(1)···C(8)) would be quite close. To alleviate this situation, the pyridine ring is rotated to bring the side of the ring holding the C(9) methyl substituent to a position between the two methyltin groups so that the two planes intersect at 87.17 (6)°. The shortest nonbonded contact distances adopted are thus C(1)···C(8) = 3.819 and C(2)···C(9) = 3.858 Å. This conformation apparently minimizes the potentially severe nonbonded interactions within the 1:1 complex. From inspection of the unit-cell diagram for the corresponding 1:2 complex,[34] it appears that the two trans-pyridine *N*-oxide ligands also take positions that nearly eclipse the tin–methyl vectors.

The central Sn_2Cl_2 ring is flat since the two halves of the asymmetric unit are related by an inversion point at the center of the ring. The interior angles and distances are ∠Sn–Cl(1)–Sn′ = 100.54 (3) and ∠Cl(1)–Sn–Cl(1′) = 79.46 (3)°, and *d*(Sn···Sn′) = 4.5918 (4) and *d*[Cl(1)···Cl(1′)] = 3.8468 (13) Å. The tin atom lies 0.03 Å above the plane formed by the two trans methyl groups [C(1) and C(2)] and the chlorine atoms [Cl(2) and Cl(1′)] toward the oxygen atom.

In the dimer, the bridging chlorine Cl(1′) makes a short intradimer contact with a hydrogen on the tin methyl and with another hydrogen on the pyridine methyl [*d*(Cl(1′)–H(C2)C = 2.78; *d*(Cl(1′)–H(C9)C = 2.71 Å]. The nonbridging chlorine Cl(2) makes a short contact with a hydrogen on the methyl group of the ligand [*d*(Cl(2)–H(C8)B) = 2.99 Å]. The dimeric units are densely packed in the lattice. There are short interdimer contacts at Cl(1)–H(C6), Cl(1)–H(C8)A, and Cl(2)–H(C6) [2.91, 2.88, and 2.96 Å, respectively].

The question of 1:1 adducts of dimethyltin(IV) dichloride forming six-coordinated solids has been discussed by us in a preliminary communication.[88]

Acknowledgment. Our work is supported by the Office of Naval Research and the National Science Foundation through Grant No. CHE-78-26548 (J.J.Z.) and the National Cancer Institute, DHEW, through Grant No. CA-17562 (D.v.d.H.). We thank the University of Oklahoma for providing computer time.

Registry No. dimethyltin(IV) dichloride–2,6-dimethylpyridine *N*-oxide dimer, 84195-00-6.

Supplementary Material Available: A listing of observed and calculated structure factors and tables of anisotropic temperature factors and hydrogen parameters and distances (11 pages). Ordering information is given on any current masthead page.

(87) Buttenshaw, J.; Duchêne, M.; Webster, M. *J. Chem. Soc., Dalton Trans.* **1975**, 2230.

(88) Ng, S.-W.; Zuckerman, J. J. *J. Chem. Soc., Chem. Commun.* **1982**, 475.

Metal dimers as catalysts. 5. Catalytic synthesis of [(.eta.6-arene)Cr(CO)2(CNR)] and the crystal and molecular structure of [(.eta.6-C6H5CO2Me)Cr(CO)2(CNCMe3)]

Gillian W. Harris, Michel O. Albers, Jan C. A. Boeyens, and Neil J. Coville

Organometallics, **1983**, 2 (5), 609-614• DOI: 10.1021/om00077a007 • Publication Date (Web): 01 May 2002

Metal Dimers as Catalysts. 5.[1] Catalytic Synthesis of $[(\eta^6\text{-Arene})Cr(CO)_2(CNR)]$ and the Crystal and Molecular Structure of $[(\eta^6\text{-}C_6H_5CO_2Me)Cr(CO)_2(CN\text{-}t\text{-}Bu)]$

Gillian W. Harris, Michel O. Albers, Jan C. A. Boeyens, and Neil J. Coville*

Department of Chemistry, University of the Witwatersrand, Johannesburg, Republic of South Africa

Received September 8, 1982

The reaction between $[(\eta^6\text{-arene})Cr(CO)_3]$ and isocyanides, RNC, is catalyzed by $[(\eta^5\text{-}C_5R'_5)Fe(CO)_2]_2$/PdO mixtures (R′ = H, Me) in refluxing heptane and yields $[(\eta^6\text{-arene})Cr(CO)_2(CNR)]$ (η^6-arene = $C_6H_5CO_2Me$, C_6H_6, and C_6H_5Me and R = *t*-Bu and 2,6-$Me_2C_6H_3$; η^6-arene = C_6H_5Cl and $C_6H_3Me_3$ and R = *t*-Bu) in moderate yield (50–90%). The crystal and molecular structure of $[(\eta^6\text{-}C_6H_5CO_2Me)Cr(CO)_2(CN\text{-}t\text{-}Bu)]$ is reported. Crystal data are as follows: space group $P\bar{1}$, a = 12.812 (6) Å, b = 9.314 (5) Å, c = 6.087 (3) Å, α = 97.28 (3)°, β = 87.94 (3)°, γ = 106.02 (3)°, V = 774.47 Å^3; Z = 2. Least-squares refinement on 2115 unique reflections yielded R = 0.042. The $Cr(CO)_2(CNR)$ tripod is staggered with respect to the C atoms of the arene ring while the RNC and CO_2Me groups show near parallel alignment. The C–N–C angle of the *t*-BuNC ligand is nonlinear [166.8 (4)°] and can account for the anomalous IR (ν(NC) region) spectra observed.

Introduction

The recently reported "solvent-assisted" reaction between $[Cr(CO)_6]$ and arenes provides a facile high yield synthetic route to $[(\eta^6\text{-arene})Cr(CO)_3]$ complexes,[2] and further progress in the investigation of the chemical[3] and catalytic properties[4] of these tricarbonyl complexes is thus assured. A noticeable feature of the chemistry of the $[(\eta^6\text{-arene})Cr(CO)_3]$ complexes is however, their thermal stability toward CO substitution, and the CO ligands have been reported to be displaced *only* by photochemical procedures.[2] Under typical thermal reaction conditions that induce Cr–CO bond cleavage, displacement of the arene ring from the Cr–$(CO)_3$ moiety by a ligand, L, becomes a competing process[5] leading to reactant decomposition or formation of $[Cr(CO)_{6-n}L_n]$ (n = 2, 3) complexes.

Our previous success in catalyzing the CO substitution reactions of numerous metal carbonyl (e.g., $[Fe(CO)_5]$[6]) and substituted metal carbonyl complexes (e.g., $[Fe(CO)_4$(olefin)][7]) suggested to us that a catalytic approach to the problem of substituting CO in $[(\eta^6\text{-arene})Cr(CO)_3]$ complexes should be possible. In theory, a suitable catalyst should not only lower the activation barrier for a general substitution reaction, but further, the catalyst should lower the energy barrier for the reaction Cr–CO + L → Cr–L + CO relative to the energy barrier for the reaction Cr–(arene) + L → Cr–L + arene.

This publication describes our successful results[8] using the catalyst mixture $[(\eta^5\text{-}C_5R'_5)Fe(CO)_2]_2$/PdO (R′ = H, Me) for the thermal replacement of CO in $[(\eta^6\text{-arene})Cr(CO)_3]$, specificially for the model reaction $[(\eta^6\text{-arene})Cr(CO)_3]$ + RNC → $[(\eta^6\text{-arene})Cr(CO)_2(CNR)]$ + CO (RNC = isocyanide). Previous synthetic routes to the above types of complexes via direct[9] or indirect[10] photochemical procedures have established that isocyanide derivatives are amenable to characterization and study.

Unexpectedly, infrared studies conducted on our isocyanide complexes have established that the new products exist in different conformational geometries, both in the solid state and in solution. An X-ray crystal structure determination of $[(\eta^6\text{-}C_6H_5CO_2Me)Cr(CO)_2(CN\text{-}t\text{-}Bu)]$ was carried out to elucidate this result. Our data on the structure determination is also included in this publication.

Experimental Section

The $[(\eta^6\text{-arene})Cr(CO)_3]$ complexes were either prepared by literature procedures[2] or purchased from Strem Chemicals. $[(\eta^5\text{-}C_5R'_5)Fe(CO)_2]_2$ (R′ = H, Me) was prepared by modification of the literature procedure.[1,11] $C_5H_5CO_2Me$ was synthesized from $ClCO_2Me$.[12] *t*-BuNC and 2,6-$Me_2C_6H_3NC$ were purchased from Fluka AG and PdO was purchased from Johnson Matthey Chemicals, Ltd. Heptane was distilled from CaH_2 under nitrogen prior to use. Column chromatography on silica (Merck 60F) was typically performed on 2 cm × 40 cm columns with degassed solvents under argon.

Infrared spectra were recorded on a Pye-Unicam SP300 spectrophotometer, NMR spectra on a Bruker WP80 FTNMR spectrometer and mass spectra on a Varian MAT CH5 spectrometer operating at 70 eV. Melting points were recorded on a Kofler micro hot-stage apparatus and are uncorrected. Microanalyses were performed by the Microanalytical Laboratories, CSIR, Pretoria.

The Catalyzed Synthesis of $[(\eta^6\text{-Arene})Cr(CO)_2(CN\text{-}t\text{-}Bu)]$ (Arene = $C_6H_3Me_3$, C_6H_5Me, C_6H_6, C_6H_5Cl, $C_6H_5CO_2Me$). $[(\eta^6\text{-Arene})Cr(CO)_3]$ (2.0 mmol), *t*-BuNC (5.0 mmol), $[(\eta^5\text{-}C_5H_5)Fe(CO)_2]_2$ (0.1 mmol), and PdO (0.03 mmol) were combined with freshly distilled heptane (10 mL) in a two-necked round-bottomed reaction flask. The reaction mixture was heated under reflux (oil bath preset at 120 °C) and the progress of the reaction monitored by TLC (silica gel, mobile phase, hexane or hexane/diethyl ether, 9:1) or IR spectroscopy. On completion of the reaction (or until no further changes were apparent), ca. 5–10 g of silica gel was added to the reaction mixture, and the solvent was removed in vacuo. Nitrogen or argon was admitted to the flask and column chromatography (carried out under a blanket of nitrogen with degassed solvents—silica gel, hexane, or hexane/diethyl ether mixtures) gave the required product as a yellow

(1) Part 4: Coville, N. J.; Albers, M. O.; Singleton, E. *J. Chem. Soc., Dalton Trans.* **1982**, 1389.
(2) Mahaffy, C. A. L.; Pauson, P. L. *Inorg. Synth.* **1979**, *19*, 154.
(3) Sneeden, R. P. A. "Organochromium Compounds"; Academic Press: New York, 1975.
(4) Dabard, R.; Jaouen, G.; Simonneaux, G. *J. Organomet. Chem.* **1980** *184*, 91.
(5) Adedeji, F. A.; Brown, D. L. S.; Connor, J. A.; Leung, M. L.; Paz-Andrade, I.; Skinner, H. A. *J. Organomet. Chem.* **1975**, *97*, 221.
(6) Albers, M. O.; Coville, N. J.; Ashworth, T. V.; Singleton, E.; Swanepoel, H. E. *J. Chem. Soc., Chem. Commun.* **1980**, 489. Albers, M. O.; Coville, N. J.; Singleton, E. *J. Chem. Soc., Dalton Trans.* **1982**, 1069.
(7) Albers, M. O.; Coville, N. J.; tenDoeschate, P.; Singleton, E. *S. Afr. J. Chem.* **1981**, *34*, 81.
(8) Albers, M. O.; Coville, N. J.; Singleton, E. *J. Organomet. Chem.* **1982**, *234*, C13.
(9) Strohmeier, W.; Hellmann, H. *Chem. Ber.* **1964**, *97*, 1877.
(10) Le Maux, P.; Simmoneaux, G.; Jaouen, G. *J. Organomet. Chem.* **1981**, *217*, 61.
(11) King, R. B. "Organometallic Synthesis"; Academic Press: New York, 1965; Vol. I.
(12) Peters, D. *J. Chem. Soc.* **1959**, 1757.

0276-7333/83/2302-0609$01.50/0

Table I. Analytical Data for the New (η^6-Arene)Cr(CO)$_2$(CNR) Complexes

	color	mp,[a] °C	elemental anal.,[b] % C	H	N
[(η^6-$C_6H_3Me_3$)Cr(CO)$_2$(CN-*t*-Bu)]	yellow	102–103	61.5 (61.7)	6.72 (6.75)	4.52 (4.50)
[(η^6-C_6H_5Me)Cr(CO)$_2$(CN-*t*-Bu)]	yellow	77–78	59.5 (59.4)	5.82 (6.01)	4.92 (4.94)
[(η^6-C_6H_5Cl)Cr(CO)$_2$(CN-*t*-Bu)]	yellow	86–88	51.4 (51.4)	4.68 (4.61)	4.63 (4.61)
[(η^6-$C_6H_5CO_2Me$)Cr(CO)$_2$(CN-*t*-Bu)]	red	84–85	54.8 (55.0)	5.19 (5.20)	4.35 (4.28)
[(η^6-C_6H_5Me)Cr(CO)$_2$($CNC_6H_3Me_2$-2,6)]	orange	99–100	66.1 (65.2)	5.26 (5.17)	5.10 (4.23)
[(η^6-$C_6H_5CO_2Me$)Cr(CO)$_2$($CNC_6H_3Me_2$-2,6)]	red	73	60.4 (60.8)	4.58 (4.57)	3.80 (3.73)

[a] Uncorrected. [b] Found, calculated in parentheses.

or orange crystalline material (Table I). Yields were generally found to be >60%.

The Catalyzed Synthesis of [(η^6-Arene)Cr(CO)$_2$($CNC_6H_3Me_2$-2,6)] (Arene = C_6H_5Me, C_6H_6, $C_6H_5CO_2Me$). [(η^6-Arene)Cr(CO)$_3$] (1.0 mmol), 2,6-$Me_2C_6H_3NC$ (1.3 mmol), [(η^5-C_5Me_5)Fe(CO)$_2$]$_2$ (0.05 mmol), and PdO (0.02 mmol) were combined in freshly distilled heptane (15 mL), the sample was heated at reflux, and the reaction was monitored as described above. At the end of the reaction (or after 18 h), the reaction mixture was allowed to cool and the product was purified as above to yield the isocyanide derivatives (Table I) and Cr(CO)$_{6-n}$(CNR)$_n$ (n = 3, 4; R = 2,6-$Me_2C_6H_3$) derivatives (see text).

Preparation of [($C_5H_4CO_2Me$)Fe(CO)$_2$]$_2$. A mixture of [Fe(CO)$_5$] (8 mL, 0.06 mol), octane (100 mL) and $C_5H_5CO_2Me$ (3 g, 0.024 mol) was degassed and the reaction mixture refluxed under argon (120 °C) for 24 h. The mixture was cooled in ice, prior to filtering, and yielded 1.7 g (32%) of deep purple product: IR (CH_2Cl_2) 2012 (s), 1974 (m), 1790 (s), 1720 (m) cm^{-1}; ^{1}H NMR (C_6D_6) δ 3.60 (s, $C_5H_4CO_2$*Me*), 4.35 and 4.90 (m, C_5*H*$_4CO_2$Me). Anal. Calcd for $C_9H_7O_4Fe$: C, 46.00; H, 3.00. Found: C, 46.38; H, 2.94).

Reaction of [($C_5H_4CO_2Me$)Fe(CO)$_2$]$_2$ with *t*-BuNC (1:1 Ratio). [($C_5H_4CO_2Me$)Fe(CO)$_2$]$_2$ (0.47 g, 1.00 mmol) was dissolved in benzene (20 mL), and to this was added *t*-BuNC (130 μL, 1.2 mmol). The solution was then brought to reflux (80 °C). The reaction was monitored by TLC (mobile phase, benzene–ether (20%)) and indicated the formation of three products, with R_f values of 0.34, 0.60, and 0.75 (trace). The products were separated by column chromatography (eluant, benzene–ether (20%)), and purified by filtration and recrystallization from benzene–hexane. The lower brown band (R_f 0.60) yielded the monosubstituted maroon complex [($C_5H_4CO_2Me$)$_2$Fe$_2$(CO)$_3$(CN-*t*-Bu)] (70%): mp 70–71 °C; IR (CH_2Cl_2) 2136 (m), 1964 (m), 1760 (s), 1713 (m) cm^{-1}; ^{1}H NMR (C_6D_6) δ 0.79 (s, (CH_3)$_3$CNC), 3.70 (s, $C_5H_4CO_2$*Me*), 4.46, and 5.04 (m, C_5*H*$_4CO_2$Me). Anal. Calcd for $C_{22}H_{23}NO_7Fe_2$: C, 50.32; H, 4.41; N, 2.67. Found: C, 50.41; H, 4.55; N, 2.60. The upper green band (R_f 0.37) gave di substituted [($C_5H_4CO_2Me$)Fe(CO)(*t*-BuNC)]$_2$ (<10%), as a bottle-green solid: IR (CH_2Cl_2) 2120 (m), 2000 (w), 1754 (s), 1720 (m) cm^{-1}; ^{1}H NMR (C_6D_6) δ 0.94 (s, (Me_3)$_3$CNC), 3.80 (s, $C_5H_4CO_2$*Me*), 4.41, and 5.10 (m, C_5*H*$_4CO_2$Me). Anal. Calcd for $C_{13}H_{16}NO_3Fe$: C, 53.82; H, 5.56; N, 4.83. Found: C, 54.90; H, 5.84; N, 4.36. The trace product (R_f 0.75) was present in insufficient amount to be isolated.

Reaction of [($C_5H_4CO_2Me$)Fe(CO)$_2$]$_2$ with *t*-BuNC (1:2 Ratio). [($C_5H_4CO_2Me$)Fe(CO)$_2$]$_2$ (0.47 g, 1.00 mmol) was dissolved in benzene (20 mL), and to this was added *t*-BuNC (112 μL, 1.00 mmol). The solution was then brought to reflux (80 °C). The reaction was monitored by infrared spectroscopy. The formation of the monosubstituted [($C_5H_4CO_2Me$)$_2$Fe$_2$(CO)$_3$(CN-*t*-Bu)] was judged to be complete after 15 min. Further *t*-BuNC (150 μL, 1.33 mmol) was added. The progress of the reaction was monitored by TLC (as above). The reaction was allowed to proceed for 4 h, but complete conversion to the disubstituted product had not occurred in this time. The reaction was stopped and the solvent removed in vacuo. The products were separated by column chromatography and purified by recrystallization (as above). The lower brown band (R_f 0.60) yielded maroon [($C_5H_4CO_2Me$)$_2$Fe$_2$(CO)$_3$(CN-*t*-Bu)] (<5%). The green band (R_f 0.41) gave 0.28 g (50%) of green [($C_5H_4CO_2Me$)Fe(CO)(CN-*t*-Bu)]$_2$. The trace product (R_f 0.75) was not collected.

Crystal and Molecular Structure of [($C_6H_5CO_2Me$)Cr(CO)$_2$(CN-*t*-Bu^t)]. The complex was prepared as described above. Red crystals were obtained by slow recrystallization from dichloromethane–hexane under nitrogen at 15 °C. Despite the crystalline appearance in ordinary light, examination under polarized light characterized most of the material as polycrystalline. Suitable single-crystal fragments of diffraction quality could be cut from the large specimens. Preliminary investigation was done by standard Weissenberg and precession photography. Refined cell constants were obtained during data collection on a Philips PW1100 four-circle diffractometer using monochromated Mo Kα radiation ($\bar{\lambda}$ = 0.7107 Å) at room temperature (20 °C). No corrections for adsorption were made. Crystal data and details of the structure analysis are summarized in Table II.

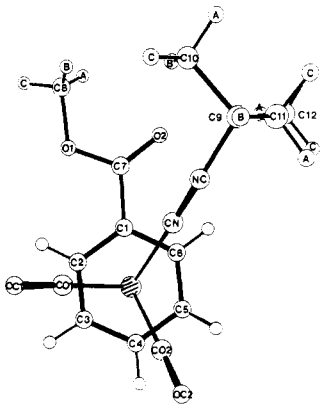

Figure 1. An ORTEP drawing of [(η^6-C_6H_5COOMe)Cr(CO)$_2$(CN-*t*-Bu)] showing 50% electron density probability ellipsoids.

Structure Solution and Refinement. Structure analysis and refinements were carried out by using the program SHELX.[13a] Initial coordinates for the chromium atom were derived from a Patterson synthesis and difference Fourier syntheses yielded positions, first for all 21 non-hydrogen atoms and after least-squares refinement of these, also for the 17 hydrogen atoms. Positional parameters for all atoms and anisotropic temperature factors for non-hydrogen atoms were refined by full-matrix least-squares analyses. Least-squares refinement was considered complete when all parameter shifts were less than 0.5σ. At this stage, the conventional R = 0.0418. Unit weights were used, and scattering factors for Cr° were taken from ref 13b. Anomalous dispersion corrections[13c] for chromium were made. Fractional atomic coordinates (Table III), interatomic distances (Table IV), and bond angles (Table V) have been listed. Structure factor tables and anisotropic thermal parameters have been deposited as supplementary material. An ORTEP[14] drawing of the molecule is shown in Figure 1.

Results and Discussion

The reaction between [(η^6-$C_6H_5CO_2Me$)Cr(CO)$_3$] and *t*-BuNC under argon in refluxing degassed heptane and in the presence of catalytic amounts of [(η^5-C_5H_5)Fe-

(13) (a) Sheldrick, G. M. In "Computing in Crystallography"; Shenk, H., Olthof-Hazekamp, R., van Koningsveld, H., Bassi, G. C., Eds.; Delft University Press: Delft, Holland, 1978. (b) "International Tables for X-ray Crystallography"; Ibers, J. A., Hamilton, W. C., Eds.; Kynoch Press: Birmingham, England, 1974; Vol. IV. (c) Cromer, D. T.; Liberman, D. *J. Chem. Phys.* **1970** *53*, 1891.

(14) Johnson, C. K. ORTEP, Report ORNL-3794, Oak Ridge National Laboratory, TN, 1965.

Table III. Fractional Atomic Coordinates and Their Estimated Standard Deviations for [(η^6-$C_6H_5CO_2Me$)Cr(CO)$_2$(CN-*t*-Bu)]

atom	*x*	*y*	*z*
Cr	0.36681 (4)	0.20010 (6)	0.46788 (8)
C1	0.2524 (3)	0.1541 (5)	0.2213 (6)
C2	0.2814 (4)	0.0211 (5)	0.2408 (6)
C3	0.3914 (4)	0.0227 (6)	0.2384 (7)
C4	0.4723 (4)	0.1571 (6)	0.2202 (7)
C5	0.4434 (4)	0.2885 (6)	0.1933 (7)
C6	0.3354 (4)	0.2873 (6)	0.1949 (6)
C7	0.1381 (4)	0.1619 (5)	0.2306 (6)
C8	−0.0456 (4)	0.0259 (7)	0.2639 (9)
C9	0.1778 (3)	0.5196 (5)	0.7383 (6)
C10	0.0615 (6)	0.4223 (7)	0.7541 (9)
C11	0.1906 (5)	0.6188 (7)	0.5746 (8)
C12	0.2156 (4)	0.6098 (6)	0.9378 (7)
CN	0.2926 (3)	0.3380 (5)	0.6081 (6)
NC	0.2451 (3)	0.4180 (4)	0.6863 (6)
CO1	0.3224 (3)	0.0703 (4)	0.6535 (5)
CO2	0.4873 (3)	0.2861 (4)	0.6244 (5)
OC1	0.2965 (2)	−0.0132 (3)	0.7704 (4)
OC2	0.5619 (2)	0.3369 (3)	0.7267 (4)
O1	0.0678 (3)	0.0274 (4)	0.2513 (5)
O2	0.1105 (3)	0.2741 (4)	0.2218 (5)
H2	0.224 (3)	−0.066 (4)	0.270 (5)
H3	0.408 (3)	−0.071 (4)	0.265 (5)
H4	0.549 (3)	0.157 (4)	0.224 (5)
H5	0.500 (3)	0.383 (4)	0.174 (5)
H6	0.315 (3)	0.376 (4)	0.175 (5)
H8A	−0.065 (3)	0.066 (4)	0.154 (6)
H8B	−0.059 (3)	0.071 (4)	0.385 (6)
H8C	−0.087 (3)	−0.085 (4)	0.225 (5)
H10A	0.019 (3)	0.495 (4)	0.777 (5)
H10B	0.040 (3)	0.372 (4)	0.627 (6)
H10C	0.054 (4)	0.358 (4)	0.876 (5)
H11A	0.144 (3)	0.686 (4)	0.599 (5)
H11B	0.164 (3)	0.557 (4)	0.451 (6)
H11C	0.263 (3)	0.676 (4)	0.563 (5)
H12A	0.205 (3)	0.544 (4)	1.046 (6)
H12B	0.177 (3)	0.685 (4)	0.959 (6)
H12C	0.289 (3)	0.663 (4)	0.936 (6)

Table IV. Interatomic Distances (Å) with Esds for [(η^6-$C_6H_5CO_2Me$)Cr(CO)$_2$(CN-*t*-Bu)]

Cr-C1	2.190 (4)	C5-C6	1.381 (7)
Cr-C2	2.198 (4)	C6-C1	1.420 (6)
Cr-C3	2.207 (5)	C1-C7	1.486 (7)
Cr-C4	2.190 (5)	C7-O1	1.346 (5)
Cr-C5	2.224 (5)	C7-O2	1.201 (6)
Cr-C6	2.212 (5)	C8-O1	1.448 (6)
Cr-CO1	1.827 (4)	CN-NC	1.155 (6)
Cr-CO2	1.838 (3)	C9-NC	1.451 (6)
Cr-CN	1.940 (5)	C9-C10	1.524 (6)
C1-C2	1.410 (7)	C9-C11	1.512 (8)
C2-C3	1.405 (8)	C9-C12	1.523 (6)
C3-C4	1.404 (7)	CO1-OC1	1.159 (5)
C4-C5	1.407 (9)	CO2-OC2	1.157 (4)

(CO)$_2$]$_2$/PdO rapidly and reproducibly leads to the required product [(η^6-$C_6H_5CO_2Me$)Cr(CO)$_2$(CN-*t*-Bu)] (88% yield, 10 min). Under analogous reaction conditions, but in nondegassed heptane, a slow reaction was observed (45% yield, 12 h). Partial solvent degassing led to intermediate nonreproducible reaction times and product yields. In the absence of catalyst or in the presence of either [(η^5-C_5H_5)Fe(CO)$_2$]$_2$ or PdO separately <5% product formation was observed by IR spectroscopy even after long reaction times (6 h).

The catalyzed reaction can readily be extended to other [(η^6-arene)Cr(CO)$_3$] complexes (Table I). As expected,[9] the reaction time was found to increase for arenes with electron-releasing groups [e.g., η^6-C_6H_5Me (45 min), η^6-$C_6H_3Me_3$ (5 h)]. This trend is in keeping with the increased metal–CO bond strength reflected, for instance, in the ν(CO) stretching frequency of the starting materials, (e.g., [(η^6-$C_6H_5CO_2Me$)Cr(CO)$_3$] at 1990 and 1924 cm^{-1} and [(η^6-$C_6H_3Me_3$)Cr(CO)$_3$] at 1974 and 1904 cm^{-1}).

Table V. Interatomic Angles (deg) with Esds for [(η^6-$C_6H_5CO_2Me$)Cr(CO)$_2$(CN-*t*-Bu)]

C6-Cr-C1	37.6 (1)	CN-Cr-C4	147.1 (2)
C6-Cr-C2	67.2 (2)	CN-Cr-C5	110.2 (2)
C6-Cr-C3	78.7 (2)	CN-Cr-C6	86.5 (2)
C6-Cr-C4	66.5 (2)	CN-Cr-CO1	90.7 (2)
C6-Cr-C5	36.3 (2)	CN-Cr-CO2	90.2 (2)
OC1-CO1-Cr	178.3 (3)	C6-C1-C2	119.2 (4)
OC2-CO2-Cr	177.9 (3)	C7-C1-C6	118.1 (4)
C8-O1-O7	115.3 (4)	C3-C2-C1	119.8 (4)
NC-CN-Cr	177.3 (4)	C4-C3-C2	120.0 (5)
CN-NC-C9	166.8 (4)	C5-C4-C3	120.1 (5)
C2-Cr-C1	37.5 (2)	C6-C5-C4	119.9 (4)
C3-Cr-C1	67.3 (2)	C7-C1-C2	122.7 (4)
C3-Cr-C2	37.2 (2)	O1-C7-C1	112.0 (4)
C4-Cr-C1	79.8 (2)	O2-C7-C1	124.6 (4)
C4-Cr-C2	67.4 (2)	O2-C7-O1	123.4 (4)
C4-Cr-C3	37.2 (2)	C11-C9-C10	111.9 (5)
C5-Cr-C1	67.0 (2)	C12-C9-C10	110.1 (4)
C5-Cr-C2	79.1 (2)	C12-C9-C11	112.2 (4)
C5-Cr-C3	66.7 (2)	NC-C9-C10	106.9 (4)
C5-Cr-C4	37.2 (2)	NC-C9-C11	107.1 (4)
CO1-Cr-C1	112.7 (1)	NC-C9-C12	108.4 (4)
CO1-Cr-C2	89.0 (2)	Cr-C1-C2	71.6 (2)
CO1-Cr-C3	93.4 (2)	Cr-C1-C6	72.0 (2)
CO1-Cr-C4	122.1 (2)	Cr-C1-C7	127.3 (3)
CO1-Cr-C5	159.0 (2)	Cr-C2-C1	70.9 (2)
CO1-Cr-C6	150.1 (1)	Cr-C2-C3	71.7 (3)
CO2-Cr-C2	149.1 (2)	Cr-C3-C2	71.1 (3)
CO2-Cr-C4	89.7 (2)	Cr-C3-C4	70.7 (3)
CO2-Cr-C5	95.2 (2)	Cr-C4-C3	72.0 (3)
CO2-Cr-C6	123.6 (2)	Cr-C4-C5	72.7 (3)
CO2-Cr-CO1	86.2 (2)	Cr-C5-C4	70.1 (3)
CN-Cr-C1	90.3 (2)	Cr-C5-C6	71.4 (3)
CN-Cr-C2	120.4 (2)	Cr-C6-C1	70.3 (3)
CN-Cr-C3	157.0 (2)	Cr-C6-C5	72.3 (3)

The reaction between [(η^6-arene)Cr(CO)$_3$] and an aryl isocyanide (2,6-$Me_2C_6H_3NC$) was also investigated in the presence of catalysts. The most efficient catalyst for this reaction was found to be [(η^5-C_5Me_5)Fe(CO)$_2$]$_2$/PdO mixtures (vide infra). Reaction times were slower than reactions with *t*-BuNC but were again dependent on the functionalized coordinated arene (e.g., [(η^6-$C_6H_5CO_2Me$)-Cr(CO)$_2$(CNC_6H_3Me-2,6)] (70% yield, 6 h) vs. [(η^6-C_6H_5Me)Cr(CO)$_2$(CN$C_6H_3Me_2$-2,6)] (50% yield, 18 h) under comparable reaction conditions.) A feature of the reaction between [(η^6-$C_6H_5CO_2Me$)Cr(CO)$_3$] and 2,6-$Me_2C_6H_3NC$ was the formation of products resulting from cleavage of the (η^6-arene)–Cr bond. Thus, $C_6H_5CO_2Me$ together with [Cr(CO)$_{6-n}$(CN$C_6H_3Me_2$-2,6)$_n$] (n = 3, 4) were also isolated (total yield ~5%) from the reaction mixture by column chromatography. The latter complexes were characterized by independent synthesis from [Cr(CO)$_6$] and 2,6-$Me_2C_6H_3NC$ in the presence of PdO as catalyst.[15] The tetrasubstituted derivative is unexpected and could arise from two potential pathways (a) displacement of the arene ligand to give [Cr(CO)$_3$(CNR)$_3$] followed by catalytic displacement of CO to give [Cr(CO)$_2$(CNR)$_4$][15] or (b) formation of [(η^6-arene)Cr(CO)$_2$(CNR)] followed by displacement of the arene ring by RNC.

A blank reaction carried out in the absence of catalyst indicated that ~5% [(η^6-$C_6H_5CO_2Me$)Cr(CO)$_2$-(CN$C_6H_3Me_2$-2,6)] as well as ~15% ring cleavage products had formed in 6 h as detected by IR spectroscopy. This suggests that the major, if not exclusive pathway to formation of the [Cr(CO)$_{6-n}$(CNR)$_n$] (n = 3, 4) derivatives is via a thermal *noncatalytic* route. Further, the reaction

(15) Coville, N. J.; Albers, M. O. *Inorg. Chim. Acta Lett.* **1982**, *65*, L7.

Table VI. Spectroscopic Data for the New $[(\eta^6\text{-Arene})Cr(CO)_2(CNR)]$ Complexes

	IR,[a] cm^{-1}		NMR,[b] δ	
	ν(NC)	ν(CO)	RNC(Me)	arene
$[(\eta^6\text{-}C_6H_3Me_3)Cr(CO)_2(CN\text{-}t\text{-}Bu)]$	2023, 1998	1908, 1868	1.39	2.12 ($C_6H_3\mathit{Me}_3$), 4.54 ($C_6\mathit{H}_3Me_3$)
$[(\eta^6\text{-}C_6H_5Me)Cr(CO)_2(CN\text{-}t\text{-}Bu)]$	2038, 2002	1921, 1883	1.39	2.09 ($C_6H_5\mathit{Me}$), 4.99 (C_6H_5Me)
$[(\eta^6\text{-}C_6H_6)Cr(CO)_2(CN\text{-}t\text{-}Bu)]$	2046, 2028	1942, 1894	1.38	5.43 ($C_6\mathit{H}_6$)
$[(\eta^6\text{-}C_6H_5Cl)Cr(CO)_2(CN\text{-}t\text{-}Bu)]$	2095, 2060	1933, 1893	1.42	5.01, 5.05 ($C_6\mathit{H}_5Cl$)
$[(\eta^6\text{-}C_6H_5CO_2Me)Cr(CO)_2(CN\text{-}t\text{-}Bu)]$[c]	2102, 2060	1937, 1894	1.40	3.83 ($C_6H_5CO_2\mathit{Me}$), 4.99-5.78[d] ($C_6\mathit{H}_5CO_2Me$)
$[(\eta^6\text{-}C_6H_5Me)Cr(CO)_2(CNC_6H_3Me_2\text{-}2,6)]$	2050, 2010	1916, 1888	2.17[e]	2.38 ($C_6H_5\mathit{Me}$), 4.97 ($C_6\mathit{H}_5Me$)
$[(\eta^6\text{-}C_6H_6)Cr(CO)_2(CNC_6H_3Me_2\text{-}2,6)]$	2040, 1992	1916, 1874	2.37[f]	5.12 ($C_6\mathit{H}_6$)
$[(\eta^6\text{-}C_6H_5CO_2Me)Cr(CO)_2(CNC_6H_3Me_2\text{-}2,6)]$[g,h]	2060	1938, 1902	2.37[i]	3.81 ($C_6H_5CO_2\mathit{Me}$), 5.02-5.98[d] ($C_6\mathit{H}_5CO_2Me$)

[a] Recorded in hexane. [b] Recorded in $CDCl_3$ relative to Me_4Si. [c] ν(COOMe) = 1720 cm^{-1}. [d] Multiplet. [e] Ph, δ 6.83. [f] Ph, δ 7.00. [g] ν(COOMe) 1725 cm^{-1}. [h] IR (KBr) ν(NC) 2070, ν(CO) 1904, 1855, 1840. [i] Ph, δ 6.63.

between $[(\eta^6\text{-}C_6H_5CO_2Me)Cr(CO)_2(CNC_6H_3Me_2\text{-}2,6)]$ and 2,6-$Me_2C_6H_3NC$ in both the absence (no reaction) and presence of catalyst (<1% ring cleavage) under similar reaction conditions rules out the possibility that the ring cleavage derivatives are formed in secondary reactions via decomposition of the product. The significant feature of the above experiments is the finding that catalytic cleavage of an (η^6-arene)–Cr bond does not take place under our reaction conditons.

Although $[(\eta^5\text{-}C_5H_5)Fe(CO)_2]_2$ is added as a catalyst to the reaction solutions containing $[(\eta^6\text{-arene})Cr(CO)_3]$ and *t*-BuNC, the catalyst is modified by substitution under the reaction conditions. Thus, the catalyst is rapidly converted to $[(\eta^5\text{-}C_5H_5)_2Fe_2(CO)_3(CN\text{-}t\text{-}Bu)]$[16] (quantitative) and then more slowly to $[(\eta^5\text{-}C_5H_5)Fe(CO)(CN\text{-}t\text{-}Bu)]_2$[17] (low yield) in refluxing heptane. The modification of the catalyst can be readily detected by IR spectroscopy during the reaction. Further, PdO is a poor catalyst for the reaction $[(\eta^5\text{-}C_5H_5)Fe(CO)_2]_2 + RNC \rightarrow [(\eta^5\text{-}C_5H_5)_2Fe_2(CO)_{4-n}(CNR)_n] + nCO$ (n = 1, 2)[18] and thus is not responsible for the substitution reaction observed.

Addition of aryl isocyanides to $[(\eta^5\text{-}C_5H_5)Fe(CO)_2]_2$ on the other hand rapidly leads to the synthesis of $[(\eta^5\text{-}C_5H_5)Fe(CNR)_2]_2$ under our reaction conditions.[1] Thus, addition of either $[(\eta^5\text{-}C_5H_5)Fe(CO)_2]_2$ or $[(\eta^5\text{-}C_5H_5)Fe(CNC_6H_3Me_2\text{-}2,6)_2]_2$ (independently synthesized) to $[(\eta^6\text{-}C_6H_5CO_2Me)Cr(CO)_3]$, resulted in the same rate of formation of $[(\eta^6\text{-}C_6H_5CO_2Me)Cr(CO)_2(CNC_6H_3Me_2\text{-}2,6)]$, as determined by IR spectroscopy (ca. 15% product was observed for both reactions after 8 h). Initially, we had anticipated that $[(\eta^5\text{-}C_5H_5)Fe(CNC_6H_3Me_2\text{-}2,6)_2]_2$ would be an excellent catalyst for our reactions since previous studies on catalyzed CO substitution reactions have shown that increased isocyanide (CN-*t*-Bu) substitution of the iron dimer leads to enhanced catalytic activity.[18,19] However, other factors (e.g., the possible geometric and/or steric role of bridging vs. terminal isocyanide substitution on the catalyst[16]) must also be important, as only moderate catalysis was observed for the tetrasubstituted iron dimer.

Further confirmation that modification of the catalyst via increased RNC substitution does not necessarily lead to increased reaction rates is shown by our attempt to use $[(\eta^5\text{-}C_5H_4CO_2Me)Fe(CO)_2]_2$ (and PdO) as a catalyst for the reaction between $[(\eta^6\text{-arene})Cr(CO)_3]$ and RNC. IR data indicated that although *initially* substitution was more rapid than with the $[(\eta^5\text{-}C_5H_5)Fe(CO)_2]_2$/PdO catalyst, the reactions rates soon inverted and after ~3 h the reaction with $[(\eta^5\text{-}C_5H_4CO_2Me)Fe(CO)_2]_2$ as catalyst ceased. These data can be explained in terms of the increased ability of the $[(\eta^5\text{-}C_5H_4CO_2Me)Fe(CO)_2]_2$ complex to undergo CO substitution since electron-withdrawing groups on the ring enhance the substitution reaction. Consistent with this proposal is the data given below.

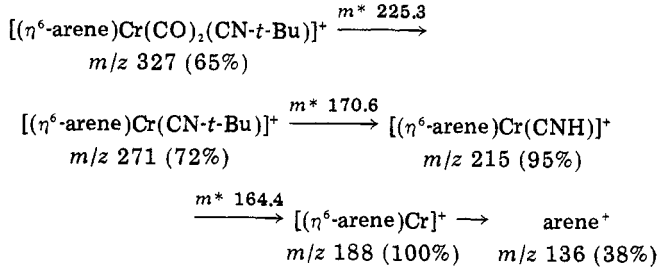

Figure 2. Fragmentation pattern for $[(\eta^6\text{-arene})Cr(CO)_2(CN\text{-}t\text{-}Bu)]$. Fragments and intensity data refer to the samples with η^6-arene = $\eta^6\text{-}C_6H_5CO_2Me$. The spectrum was recorded at 48 °C and all fragments with m/z <110 are not reported.

In a blank experiment, a 1:2 reaction between $[(\eta^5\text{-}C_5H_4CO_2Me)Fe(CO)_2]_2$ and *t*-BuNC, in refluxing benzene, rapidly (<15 min) gave $[(\eta^5\text{-}C_5H_4CO_2Me)Fe_2(CO)_3(CN\text{-}t\text{-}Bu)]$ and more slowly $[(\eta^5\text{-}C_5H_4CO_2Me)Fe(CO)(CN\text{-}t\text{-}Bu)]_2$ (50% isolated yield, 4 h). (These new complexes have been completely characterized, and the pertinent analytical and spectral data are reported in the Experimental Section.) By contrast, the reactions between $[(\eta^5\text{-}C_5H_5)Fe(CO)_2]_2$ and *t*-BuNC, under identical reaction conditions, give only $[(\eta^5\text{-}C_5H_5)_2Fe_2(CO)_3(CN\text{-}t\text{-}Bu)]$, in near quantitative yield, and trace amounts (<2%) of $[(\eta^5\text{-}C_5H_5)Fe(CO)_2(CN\text{-}t\text{-}Bu)]_2$.[16] Under our reaction conditions (i.e., large excess of RNC), it can be anticipated that multiple CO substitution of $[(\eta^5\text{-}C_5H_4CO_2Me)Fe(CO)_2]_2$ by RNC eventually occurs, presumably leading to catalyst deactivation.

To avoid this phenomena, we thus investigated the use of $[(\eta^5\text{-}C_5Me_5)Fe(CO)_2]_2$ as a catalyst for reactions involving 2,6-$Me_2C_6H_3NC$. This dimer is inert to CO substitution and a $[(\eta^5\text{-}C_5Me_5)Fe(CO)_2]$/PdO mixture was found to be a convenient, although not highly active, catalyst for the substitution of $[(\eta^6\text{-arene})Cr(CO)_3]$ by 2,6-$Me_2C_6H_3NC$ (see Experimental Section). Further, it was possible to isolate the unsubstituted dimer catalyst at the end of the reaction, thus confirming our hypothesis.

We have made no attempt to explore the mechanism by which this catalyst mixture induces chemical reactivity in these reactions. Attempts to obtain mechanistic information are, however, in progress on related simpler systems and will be reported later.

Product Characterization. The isocyanide complexes were readily characterized by NMR spectroscopy, mass

(16) Bellerby, J.; Boylan, M. J.; Ennis, M.; Manning, A. R. *J. Chem. Soc., Dalton Trans.* **1978**, 1185.
(17) Howell, J. A. S.; Mathur, P. *J. Organomet. Chem.* **1979**, *174*, 335.
(18) Coville, N. J.; Albers, M. O.; Ashworth, T. V.; Singleton, E. *J. Chem. Soc., Chem. Commun.* **1981**, 408.
(19) Coville, N. J.; Albers, M. O.; Singleton, E. *J. Chem. Soc., Dalton Trans.*, submitted for publication.

Table VII. IR Spectral Study of [(η^6-$C_6H_5CO_2Me$)Cr(CO)$_2$(CN-*t*-Bu)] in Different Solvents[a]

solvent	ν(CO), cm^{-1}	ν(NC), cm^{-1} A	ν(NC), cm^{-1} B	intensity ratio (A/B)[b]
chloroform	1924 vs, 1872 s, 1708 m	2112 ms	2074 sh	2.5
dichloromethane	1920 vs, 1868 s, 1710 m	2100 ms	2060 sh	2.3
toluene	1922 vs, 1865 s, 1700 m	2106 m	2070 sh	1.9
tetrahydrofuran	1924 vs, 1879 s, 1718 m	2104 m	2076 sh	1.5
benzene	1960 vs, 1880 s, 1697 m	2100 m	2076 sh	1.9
n-hexene	1940 vs, 1898 s, 1720 m	2100 mw	2070 w	1.1
carbon tetrachloride	1930 vs, 1884 s, 1699 m	2112 m	2070 ms	0.8

[a] IR (KBr) spectrum recorded on the polycrystalline material: ν(NC) 2090, 2060 (sh), ν(CO) 1908, 1856, ν(COOMe) 1700 cm^{-1}. [b] Determined from peak areas (±15%).

Table VIII. Least-Squares Plane in [(η^6-$C_6H_5CO_2Me$)Cr(CO)$_2$(CN-*t*-Bu)][a]

atom	dev, Å	atom	dev, Å
C1	0.015 (7)	C6	−0.007 (3)
C2	−0.005 (2)	C7	0.079 (1)
C3	−0.013 (7)	C8	0.138 (1)
C4	0.021 (5)	O1	0.062 (2)
C5	−0.010 (9)	O2	0.145 (7)

[a] Equation of plane: $0.0478x + 1.1172y + 6.5972z = 1.6293$.

spectrometry and elemental analyses. The ^{1}H NMR data gave the expected resonances (number, position) (Table VI) while the mass spectra gave fragments consistent with the structural formulation proposed. A typical example is shown in Figure 2, which indicates the fragmentation pattern (together with peak intensities and metastable peaks) for the mass spectrum of [(η^6-$C_6H_5CO_2Me$)Cr(CO)$_2$(CN-*t*-Bu)].

The IR data, however, showed anomalous behavior. Whereas two ν(CO) and one ν(NC) stretching frequencies are predicted, two ν(CO) and *two* ν(NC) absorptions were usually observed in both solution and the solid state (polycrystalline material). We have estimated the relative intensity of the two bands of the complex in a variety of solvents (Table VII). The data indicate the intensity of the lower frequency absorption band decreases with increasing solvent polarity, suggesting the existence of two conformers, with different dipole moments. This effect is not due to interaction of the RNC group with the arene-ring substituent, since [(η^6-C_6H_6)Cr(CO)$_2$(CN-*t*-Bu)] also has two ν(NC) stretching frequencies. Further, unless there is fortuitous overlap of two sets of CO stretching frequencies, the two different conformers must have the CO ligands in very similar environments. To determine the nature of the different conformers, we decided to carry out a crystal structure determination on one of the derivatives, [(η^6-$C_6H_5CO_2Me$)Cr(CO)$_2$(CN-*t*-Bu)].

Crystal Structure. The molecular structure is shown in Figure 1. In general bond lengths (Table IV) and bond angles (Table V) are in agreement with previous structure determinations of complexes of the type [(η^6-$C_6H_5CO_2Me$)Cr(CO)$_2$L] (L = CO,[20,21] CS,[22] CSe,[23] P(C_6H_5)$_3$,[24] CNCOC_6H_5,[25] PF_3[26]). The distance from the Cr atom to the mean plane of the arene ring (1.697 (1) Å) is normal and lies between the values found for [(η^6-$C_6H_5CO_2Me$)Cr(CO)$_3$] (1.714 (1) Å)[21] and [(η^6-$C_6H_5CO_2Me$)Cr(CO)$_2$(PPh$_3$)] (1.695 (1) Å).[24] A least-squares plane drawn through the six carbon atoms of the arene ring (Table VIII) indicates the arene ring is puckered with C1 and C4 bending toward the Cr atom. The CO_2Me group also bends toward the Cr(CO)$_2$(CNR) side of the ring. Both of these effects have been commented on previously,[26] and our study again indicates the generality of this phenomena.

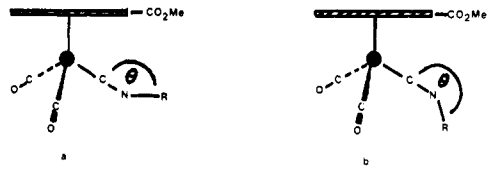

Figure 3. Side view of two conformers of [(η^6-$C_6H_5CO_2Me$)Cr(CO)$_2$(CNR)]: a corresponds to the conformer observed in the crystal structure when R = *t*-Bu [θ = 166.8 (4)°].

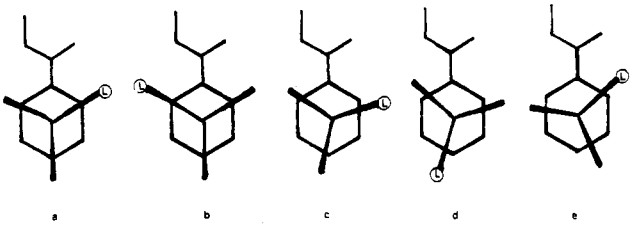

Figure 4. Projection of [(η^6-$C_6H_5CO_2Me$)Cr(CO)$_2$L] as viewed along the (η^6-arene)–Cr bond axis (a, L = CO, CS, CSe; b, L = P(C_6H_5)$_3$; c, L = PF_3; d, L = C_6H_5CONC; e, L = *t*-BuNC).

There are, however, two significant features relating to the geometry that require comment. The first relates to the CNC angle of 166.8 (4) Å. Although the nonlinear bond is not unusual and has been observed in the related [(η^6-$C_6H_5CO_2Me$)Cr(CO)$_2$(CNCOC_6H_5)] complex [168 (1)°],[25] it does allow for rationalization of the anomalous IR spectral data. This nonlinear bond allows for the possibility of different conformers, with different dipole moments, two of which are shown in Figure 3. This phenomenon, although not described previously for the RNC ligand[9] (no ν(NC) band was observed for ligands of the type C_6H_5CONC[10]), has been reported for the related acyl ligand in complexes of the type [(η^5-C_5H_5)Pt(Me)$_2$COR][27] and [(η^5-C_5H_5)Fe(CO)$_2$COR].[28]

The second feature relates to the alignment of the RNC ligand relative to the CO_2Me group. Whereas the comlex [(η^6-$C_6H_5CO_2Me$)Cr(CO)$_2$L] (L = CO, CS, CSe, and P-

(20) Saillard, J. Y.; Grandjean, D. *Acta Crystallogr., Sect. B* **1976**, *B32*, 2285.
(21) Carter, O. L., McPhail, A. T.; Sim, A. G. *J. Chem. Soc. A* **1967**, 1619.
(22) Saillard, J. Y.; Le Borgne, G.; Grandjean, D. *J. Organomet. Chem.* **1975**, *94*, 409.
(23) Saillard, J. Y.; Grandjean, D. *Acta Crystallogr., Sect. B* **1978**, *B34*, 3772.
(24) Andrianov, V. G.; Struchkov, T.; Baranetzkaya, N. K.; Setkina, V. R.; Kursanov, D. N. *J. Organomet. Chem.* **1975**, *101*, 209.
(25) Le Maux, P.; Simmoneaux, G.; Jaouen, G.; Ouahab, L.; Batail, P. *J. Am. Chem. Soc.* **1978**, *100*, 4312.
(26) Saillard, J. Y.; Grandjean, D.; LeBeuze, A.; Simonneaux, G. *J. Organomet. Chem.* **1981**, *204*, 197.
(27) Shaver, A. *Can. J. Chem.*, **1978**, *56*, 2281.
(28) Cotton, F. A.; Frenz, B. A.; Shaver, A. *Inorg. Chim. Acta* **1973**, *7*, 161.

$(C_6H_5)_3$) has structure **4a** or **4b** (Figure 4) (i.e., L ortho to the CO_2Me group and eclipsed with respect to the ring C atoms) when L = *t*-BuNC, the structure observed is **4e**. In this structure, the $Cr(CO)_3$ tripod is staggered with respect to the arene C atoms and further, the isocyanide ligand has moved *toward* the CO_2Me group. (The angle between Cr–CN and Cr–C1 projected on the plane of the arene ring is 37.7°.) This is to be contrasted with the complex with L = PF_3 (**4c**)[26] in which the PF_3 ligand has moved *away* from the CO_2Me group (∠C1–Cr–CN = 77.6°). On electronic grounds, an eclipsed structure would have been predicted, but theoretical calculations have indicated that the energy barrier between the eclipsed and staggered conformations will be small.[29] Steric factors are unlikely to be responsible for this phenomena as the $P(C_6H_5)_3$ ligands adopts an eclipsed geometry (**4b**)[24] and the steric bulk of the *t*-BuNC is expected to be smaller than the $P(C_6H_5)_3$ ligand.[30] Although a possible interaction between O2 and a H atom on the RNC ligand might account for the molecular geometry observed (e.g., H10C–O2 = 2.75 Å), the result could also be the result of intermolecular bonding forces (e.g., H11B–O2 = 2.81 Å).

It is interesting to note that in the crystal structure determination of one other [(η^6-arene)$Cr(CO)_2$(CNR)] derivative reported,[25] the complex has a completely different orientation of the $Cr(CO)_2L$ tripod relative to the arene ring (Figure 4d). Here again, the tripod is staggered (relative to the ring), but more significantly, the RNC and CO_2Me groups are antiparallel. Although these effects might be a consequence of purely packing considerations in the crystal, it is thought that underlying energy considerations will provide a rationalization for this data. Further crystal structure determinations on related isocyanide complexes are thus in progress.

Acknowledgment. Financial support from the University and the CSIR are acknowledged. N.J.C. wishes to acknowledge and thank Professor E. L. Muetterties and the University of California for all hospitality and courtesy extended during the writing of this paper while on sabbatic leave from the University of the Witswatersrand, Johannesburg, South Africa. We would also like to thank J. Albain for collecting the X-ray data.

Registry No. (η^6-$C_6H_3Me_3$)$Cr(CO)_2$(CN-*t*-Bu), 83111-31-3; (η^6-C_6H_5Me)$Cr(CO)_2$(CN-*t*-Bu), 83111-30-2; (η^6-C_6H_5Cl)$Cr(CO)_2$(CN-*t*-Bu), 83111-27-7; (η^6-$C_6H_5CO_2Me$)$Cr(CO)_2$(CN-*t*-Bu), 83111-28-8; (η^6-C_6H_5Me)$Cr(CO)_2$($CNC_6H_3Me_2$-2,6), 84393-99-7; (η^6-$C_6H_5CO_2Me$)$Cr(CO)_2$($CNC_6H_3Me_2$-2,6), 84394-00-3; (η^6-C_6H_6)$Cr(CO)_2$(CN-*t*-Bu), 83111-29-9; (η^6-C_6H_6)$Cr(CO)_2$($CNC_6H_3Me_2$-2,6), 84394-01-4; (η^6-$C_6H_5CO_2Me$)$Cr(CO)_3$, 12125-87-0; (η^6-C_6H_6)$Cr(CO)_3$, 12082-08-5; (η^6-C_6H_5Me)$Cr(CO)_3$, 12083-24-8; (η^6-C_6H_5Cl)$Cr(CO)_3$, 12082-03-0; (η^6-$C_6H_3Me_3$)$Cr(CO)_3$, 12129-67-8; Bu-*t*-NC, 7188-38-7; 2,6-$Me_2C_6H_3NC$, 2769-71-3; [(η^5-C_5H_5)$Fe(CO)_2]_2$, 12154-95-9; PdO, 1314-08-5; [(η^5-C_5Me_5)$Fe(CO)_2]_2$, 35344-11-7; [($C_5H_4CO_2Me$)$Fe(CO)_2]_2$, 84394-02-5; $Fe(CO)_5$, 13463-40-6; $C_5H_5CO_2Me$, 45657-86-1; ($C_5H_4CO_2Me$)$_2Fe_2(CO)_3$(CN-*t*-Bu), 84394-03-6; [($C_5H_4CO_2Me$)Fe(CO)(Bu-*t*-NC)$]_2$, 84394-04-7.

Supplementary Material Available: Table II, crystal data and details of structure analysis, and tables of anisotropic thermal parameters for non-hydrogen atoms, structures factors, deviations greater than 2σ and bond distances and angles involving the hydrogen atom (13 pages). Ordering information is given on any current masthead page.

(29) Albright, T. A.; Hofmann, P.; Hoffmann, R. *J. Am. Chem. Soc.* **1977**, *99*, 7546 and reference cited therein.
(30) Yamamoto, Y.; Aoki, K.; Yamazaki, H. *Inorg. Chem.* **1979**, *18*, 1681.

Olefin Complexes of Nickel(0). 4. Equilibria in Solutions Containing P(O-*o*-tolyl)$_3$ and Cyanoolefins†

Chadwick A. Tolman

Central Research Department, Experimental Station, E. I. du Pont de Nemours and Company, Wilmington, Delaware 19898

Received October 25, 1982

^{31}P and ^1H NMR and IR spectroscopy and spectrophotometry are used to demonstrate the presence of both olefin and nitrile complexes in solutions containing cyanoolefins, P(O-*o*-tol)$_3$ (tol = tolyl), and nickel(0). Coordination of the olefinic double bond is favored by a terminal location and by conjugation with the nitrile group. Coordination of the nitrile nitrogen is favored by conjugation and by increased concentrations of free P(O-*o*-tol)$_3$. A number of equilibrium constants and electronic spectra in benzene at 25 °C are reported and discussed in terms of the structures of the cyanoolefins.

Introduction

In earlier papers,[1,2] we have discussed the solution species and equilibria present in solutions containing zero-valent nickel, tri-*o*-tolyl phosphite (hereafter abbreviated L), and olefins. The major reactions found are represented by eq 1–3. In the presence of nitriles, NiL_3

$$NiL_3 + Ol \overset{K_1}{\rightleftharpoons} (Ol)NiL_2 + L \quad (1)$$

$$(Ol)NiL_2 + Ol \overset{K_2}{\rightleftharpoons} (Ol)_2NiL_2 \quad (2)$$

$$NiL_3 + L \overset{K_4}{\rightleftharpoons} NiL_4 \quad (3)$$

also reacts according to eq 4. The equilibrium constant K_N is ~200 M^{-1} at 25 °C for aceto-, propio-, or valeronitrile.[3]

$$NiL_3 + RCN \overset{K_N}{\rightleftharpoons} (RCN)NiL_3 \quad (4)$$

In this paper, we describe the behavior of solutions containing Ni(0), P(O-*o*-tol)$_3$ (tol = tolyl), and cyanoolefins, which contain both nitrile and olefin functions in the same

† Contribution No. 3144

(1) Gosser, L. W.; Tolman, C. A. *Inorg. Chem.* **1970**, *9*, 2350.
(2) (a) Seidel, W. C.; Tolman, C. A. *Inorg. Chem.* **1970**, *9*, 2354. (b) Tolman, C. A.; Seidel, W. C. *J. Am. Chem. Soc.* **1974**, *96*, 2774. (c) Tolman, C. A. *Ibid.* **1974**, *96*, 2780.
(3) Tolman, C. A. *Inorg. Chem.* **1971**, *10*, 1540.

0276-7333/83/2302-0614$01.50/0

$(C_6H_5)_3$) has structure **4a** or **4b** (Figure 4) (i.e., L ortho to the CO_2Me group and eclipsed with respect to the ring C atoms) when L = *t*-BuNC, the structure observed is **4e**. In this structure, the $Cr(CO)_3$ tripod is staggered with respect to the arene C atoms and further, the isocyanide ligand has moved *toward* the CO_2Me group. (The angle between Cr–CN and Cr–C1 projected on the plane of the arene ring is 37.7°.) This is to be contrasted with the complex with L = PF_3 (**4c**)[26] in which the PF_3 ligand has moved *away* from the CO_2Me group (∠C1–Cr–CN = 77.6°). On electronic grounds, an eclipsed structure would have been predicted, but theoretical calculations have indicated that the energy barrier between the eclipsed and staggered conformations will be small.[29] Steric factors are unlikely to be responsible for this phenomena as the $P(C_6H_5)_3$ ligands adopts an eclipsed geometry (**4b**)[24] and the steric bulk of the *t*-BuNC is expected to be smaller than the $P(C_6H_5)_3$ ligand.[30] Although a possible interaction between O2 and a H atom on the RNC ligand might account for the molecular geometry observed (e.g., H10C–O2 = 2.75 Å), the result could also be the result of intermolecular bonding forces (e.g., H11B–O2 = 2.81 Å).

It is interesting to note that in the crystal structure determination of one other $[(\eta^6\text{-arene})Cr(CO)_2(CNR)]$ derivative reported,[25] the complex has a completely different orientation of the $Cr(CO)_2L$ tripod relative to the arene ring (Figure 4d). Here again, the tripod is staggered (relative to the ring), but more significantly, the RNC and CO_2Me groups are antiparallel. Although these effects might be a consequence of purely packing considerations in the crystal, it is thought that underlying energy considerations will provide a rationalization for this data. Further crystal structure determinations on related isocyanide complexes are thus in progress.

Acknowledgment. Financial support from the University and the CSIR are acknowledged. N.J.C. wishes to acknowledge and thank Professor E. L. Muetterties and the University of California for all hospitality and courtesy extended during the writing of this paper while on sabbatic leave from the University of the Witswatersrand, Johannesburg, South Africa. We would also like to thank J. Albain for collecting the X-ray data.

Registry No. $(\eta^6\text{-}C_6H_3Me_3)Cr(CO)_2(CN\text{-}t\text{-}Bu)$, 83111-31-3; $(\eta^6\text{-}C_6H_5Me)Cr(CO)_2(CN\text{-}t\text{-}Bu)$, 83111-30-2; $(\eta^6\text{-}C_6H_5Cl)Cr(CO)_2(CN\text{-}t\text{-}Bu)$, 83111-27-7; $(\eta^6\text{-}C_6H_5CO_2Me)Cr(CO)_2(CN\text{-}t\text{-}Bu)$, 83111-28-8; $(\eta^6\text{-}C_6H_5Me)Cr(CO)_2(CNC_6H_3Me_2\text{-}2,6)$, 84393-99-7; $(\eta^6\text{-}C_6H_5CO_2Me)Cr(CO)_2(CNC_6H_3Me_2\text{-}2,6)$, 84394-00-3; $(\eta^6\text{-}C_6H_6)Cr(CO)_2(CN\text{-}t\text{-}Bu)$, 83111-29-9; $(\eta^6\text{-}C_6H_6)Cr(CO)_2(CNC_6H_3Me_2\text{-}2,6)$, 84394-01-4; $(\eta^6\text{-}C_6H_5CO_2Me)Cr(CO)_3$, 12125-87-0; $(\eta^6\text{-}C_6H_6)Cr(CO)_3$, 12082-08-5; $(\eta^6\text{-}C_6H_5Me)Cr(CO)_3$, 12083-24-8; $(\eta^6\text{-}C_6H_5Cl)Cr(CO)_3$, 12082-03-0; $(\eta^6\text{-}C_6H_3Me_3)Cr(CO)_3$, 12129-67-8; Bu-*t*-NC, 7188-38-7; $2,6\text{-}Me_2C_6H_3NC$, 2769-71-3; $[(\eta^5\text{-}C_5H_5)Fe(CO)_2]_2$, 12154-95-9; PdO, 1314-08-5; $[(\eta^5\text{-}C_5Me_5)Fe(CO)_2]_2$, 35344-11-7; $[(C_5H_4CO_2Me)Fe(CO)_2]_2$, 84394-02-5; $Fe(CO)_5$, 13463-40-6; $C_5H_5CO_2Me$, 45657-86-1; $(C_5H_4CO_2Me)_2Fe_2(CO)_3(CN\text{-}t\text{-}Bu)$, 84394-03-6; $[(C_5H_4CO_2Me)Fe(CO)(Bu\text{-}t\text{-}NC)]_2$, 84394-04-7.

Supplementary Material Available: Table II, crystal data and details of structure analysis, and tables of anisotropic thermal parameters for non-hydrogen atoms, structures factors, deviations greater than 2σ and bond distances and angles involving the hydrogen atom (13 pages). Ordering information is given on any current masthead page.

(29) Albright, T. A.; Hofmann, P.; Hoffmann, R. *J. Am. Chem. Soc.* **1977**, *99*, 7546 and reference cited therein.
(30) Yamamoto, Y.; Aoki, K.; Yamazaki, H. *Inorg. Chem.* **1979**, *18*, 1681.

Olefin Complexes of Nickel(0). 4. Equilibria in Solutions Containing P(O-*o*-tolyl)$_3$ and Cyanoolefins†

Chadwick A. Tolman

Central Research Department, Experimental Station, E. I. du Pont de Nemours and Company, Wilmington, Delaware 19898

Received October 25, 1982

^{31}P and ^1H NMR and IR spectroscopy and spectrophotometry are used to demonstrate the presence of both olefin and nitrile complexes in solutions containing cyanoolefins, P(O-*o*-tol)$_3$ (tol = tolyl), and nickel(0). Coordination of the olefinic double bond is favored by a terminal location and by conjugation with the nitrile group. Coordination of the nitrile nitrogen is favored by conjugation and by increased concentrations of free P(O-*o*-tol)$_3$. A number of equilibrium constants and electronic spectra in benzene at 25 °C are reported and discussed in terms of the structures of the cyanoolefins.

Introduction

In earlier papers,[1,2] we have discussed the solution species and equilibria present in solutions containing zero-valent nickel, tri-*o*-tolyl phosphite (hereafter abbreviated L), and olefins. The major reactions found are represented by eq 1–3. In the presence of nitriles, NiL_3

$$NiL_3 + Ol \overset{K_1}{\rightleftharpoons} (Ol)NiL_2 + L \quad (1)$$

$$(Ol)NiL_2 + Ol \overset{K_2}{\rightleftharpoons} (Ol)_2NiL_2 \quad (2)$$

$$NiL_3 + L \overset{K_4}{\rightleftharpoons} NiL_4 \quad (3)$$

also reacts according to eq 4. The equilibrium constant K_N is ~200 M^{-1} at 25 °C for aceto-, propio-, or valeronitrile.[3]

$$NiL_3 + RCN \overset{K_N}{\rightleftharpoons} (RCN)NiL_3 \quad (4)$$

In this paper, we describe the behavior of solutions containing Ni(0), P(O-*o*-tol)$_3$ (tol = tolyl), and cyanoolefins, which contain both nitrile and olefin functions in the same

† Contribution No. 3144

(1) Gosser, L. W.; Tolman, C. A. *Inorg. Chem.* **1970**, *9*, 2350.
(2) (a) Seidel, W. C.; Tolman, C. A. *Inorg. Chem.* **1970**, *9*, 2354. (b) Tolman, C. A.; Seidel, W. C. *J. Am. Chem. Soc.* **1974**, *96*, 2774. (c) Tolman, C. A. *Ibid.* **1974**, *96*, 2780.
(3) Tolman, C. A. *Inorg. Chem.* **1971**, *10*, 1540.

0276-7333/83/2302-0614$01.50/0

molecule. ^{31}P and ^{1}H NMR and infrared spectroscopy, and spectrophotometry are used to establish the presence of both olefin and nitrile complexes in solution and to determine a number of equilibrium constants for reactions 1, 2, and 4.

This work was carried out as part of a systematic study of the mechanism of homogeneous catalytic olefin hydrocyanation by zero-valent nickel catalysts. The reaction of HCN with NiL_3 and NiL_4 complexes was described earlier.[4] Detailed studies of cyanoolefin equilibria were carried out in the $P(O\text{-}o\text{-tol})_3$ system because it is one of the most active hydrocyanation systems known.[5]

Experimental Section

Preparations of $Ni[P(O\text{-}o\text{-tol})_3]_3$[1,6] and (styrene)$Ni[P(O\text{-}o\text{-tol})_3]_2$[2b] are described elsewhere. Cyanoolefins 2-methyl-3-butenenitrile (2M3BN), 4-pentenenitrile (4PN), *trans*-3-pentenenitrile (T3PN), *cis*- and *trans*-2-pentenenitrile (C2PN and T2PN), and *cis*- and *trans*-2-methyl-2-butenenitrile (C2M2BN and T2M2BN) were prepared by the Ni(0)-catalyzed addition of HCN to butadiene[7] and were purified by preparative gas chromatography. 5-Hexenenitrile (5HN) was prepared by Dr. F. Weigert by the thermal reaction of acrylonitrile and propylene.[8] 3-Butenenitrile (3BN) and acrylonitrile (ACN) were purchased commercially and freshly distilled before use. The purities of the cyanoolefins were checked by gas chromatography and proton NMR spectroscopy. Reagent grade nitriles were purchased and used without further purification.

Spectroscopic experiments were carried out as described earlier.[2a] Infrared spectra were not calibrated, and the reported frequencies may be uncertain to ±5 cm^{-1}. Spectrophotometric measurements were made on benzene solutions, usually at 25 °C. Reported wavelengths are believed accurate to ±3 nm and extinction coefficients to ±10%. All solutions were prepared and handled under a N_2 atmosphere.

Cyanoolefin complexes were generated in solution by the addition of cyanoolefin to solutions of $Ni[P(O\text{-}o\text{-tol})_3]_3$ or (styrene)$Ni[P(O\text{-}o\text{-tol})_3]_2$. Dilute solutions of cyanoolefin (≤0.05 M) for spectrophotometric experiments were usually obtained by adding 1 M cyanoolefin by Hamilton syringe to a known volume of nickel complex in a serum-capped optical cell under conditions where the dilution of nickel was no greater than 5%. More concentrated cyanoolefin solutions were made up in 2-cm^3 volumetric flasks.

Addition of cyanoolefins to solutions of the nickel complexes NiL_3 and (styrene)NiL_2 caused immediate color changes, indicating very fast reactions. In the case of the allylic cyanides (3BN, 3PN, and 2M3BN), subsequent slow reactions occurred over a period of several hours, with concomitant changes in electronic spectra. Spectra of these solutions were, therefore, run as quickly as possible on freshly prepared solutions.

Results

The nature of the species present in moderately concentrated solutions of NiL_3 and cyanoolefins is probably best shown by ^{31}P NMR spectroscopy. Data on solutions of 0.07 M nickel complex and 0.14 M nitrile or cyanoolefin in toluene at 26 °C are given in Table I. The solutions containing nitrile show a sharp (~5-Hz width at half-height) resonance at ~−131 ppm (85% H_3PO_4), assignable to phosphorus nuclei in (RCN)NiL_3 complexes.[3] All solutions containing the cyanoolefins, except that of acrylonitrile, show this same characteristic resonance. Some, notably those with a terminal carbon–carbon double bond and *trans*-2-pentenenitrile, which contains a conjugated double bond, show an additional broad (~40-Hz width at half-height) resonance at ~−137 ppm, attributed to phosphorus nuclei in (olefin)NiL_2 and free L in rapid exchange.[9] There was no ^{31}P NMR evidence for NiL_4 (−129.3 ppm) in any of these solutions. When the temperature of the solutions was lowered to 0 °C or below, the resonance due to (Ol)NiL_2 and L in rapid exchange disappeared, and only the resonance of (RCN)NiL_3 at ~131 ppm was observed. Thus, nitrile-bonded species are favored over olefin-bonded species as the temperature is lowered. This behavior is consistent with earlier thermodynamic data, which indicate that reaction 1 with 1-hexene is nearly thermoneutral[2c] while reaction 4 with acetonitrile is exothermic to the extent of 9 kcal/mol.[3]

Table I. ^{31}P NMR Chemical Shifts[a] for Solutions[b] of Nitriles or Cyanoolefins with $Ni[P(O\text{-}o\text{-tolyl})_3]_3$

nitrile or cyanoolefin[d]	(RCN)NiL_3	(Ol)NiL_2[c]
acetonitrile	−131.0	
valeronitrile	−130.7	
adiponitrile	−130.7	
C_6H_5CN	−131.2	
$p\text{-}FC_6H_4CN$	−131.3	
acrylonitrile		−136.6
3BN	−130.0	−137.7
2M3BN	−130.2	−137.0
4 PN	−130.4	−137.3
T2 PN	−131.2	−136.3
T3 PN	−130.8	
C2M2BN	−130.9	

[a] With respect to 85% H_3PO_4. Measured at 36.43 MHz. [b] About 0.07 M $Ni[P(O\text{-}o\text{-tolyl})_3]_3$ and 0.14 M nitrile or cyanoolefin in toluene at 26 °C. [c] These broad resonances represent (Ol)NiL_2 and L in rapid exchange: $\delta_{av} = {}^2/_3\delta[(Ol)NiL_2] + {}^1/_3\delta[L]$. [d] Abbreviations used: 3BN, 3-butyronitrile ($CH_2{=}CHCH_2CN$); 2M3BN, 2-methyl-3-butyronitrile ($CH_2{=}CHCH(CH_3)CN$); T2PN, *trans*-2-pentenenitrile (*trans*-$CH_3CH_2CH{=}CHCN$), etc.

The ^{31}P NMR studies show that formation of olefin complexes by cyanoolefins is favored by the presence of a terminal C=C and by conjugation of the double bond with the nitrile. Acrylonitrile has both these features, and no (RCN)NiL_3 was observed in the ^{31}P spectrum. The presence of *two* alkyl groups on the double bond of C2M2BN overcomes the favorable effect of nitrile conjugation, and no olefin complex was observed.

The presence of substantial concentrations of (RCN)NiL_3 complexes in moderately concentrated solutions of cyanoolefins (other than ACN) and NiL_3 was also shown by proton NMR. Spectra of the cyanoolefins themselves at 100 MHz were sharp and showed well-resolved spin–spin coupling. The vinylic protons appeared in the region of τ 4.4–5.4. Solutions containing NiL_3 and excess cyanoolefin gave spectra in which the vinylic protons were only slightly shifted (0.2 ppm or less), and the resonances were broadened as the results of rapid exchange. Typical spectra with 4PN are shown in Figure 1. Small shifts of vinylic protons in cyanoolefin complexes are indicative of nitrile bonding.[10]

In the olefin-bonded complexes $(C_2H_4)NiL_2$, (ACN)NiL_2, (styrene)NiL_2, and (maleic anhydride)NiL_2, the mean chemical shifts of the vinylic protons are upfield by 1.5–3.6

(4) Druliner, J. D.; English, A. D.; Jesson, J. P.; Meakin, P.; Tolman, C. A. *J. Am. Chem. Soc.* **1976**, *98*, 2156.
(5) King, C. M.; Seidel, W. C.; Tolman, C. A. US Patent 3 798 256, Mar 1974.
(6) Tolman, C. A.; Seidel, W. C.; Gosser, L. W. *Organometallics*, submitted for publication.
(7) Tolman, C. A.; Seidel, W. C.; Druliner, J. C., et al., to be submitted for publication.
(8) Albisetti, C. J.; Fisher, N. G.; Hogsed, M. J.; Joyce, R. M. *J. Am. Chem. Soc.* **1956**, *78*, 2637.
(9) Pure (ACN)NiL_2 and L in separate solutions show single sharp resonances at −139.4[2a] and −130.0[1], respectively. The calculated chemical shift for (ACN)NiL_2 and L in rapid exchange is ${}^2/_3(-139.4) + {}^1/_3(-130.0) = -136.3$.
(10) Ross, B. L.; Grasselli, J. G.; Ritchey, M. W.; Kaesz, H. D. *Inorg. Chem.* **1963**, *2*, 1023.

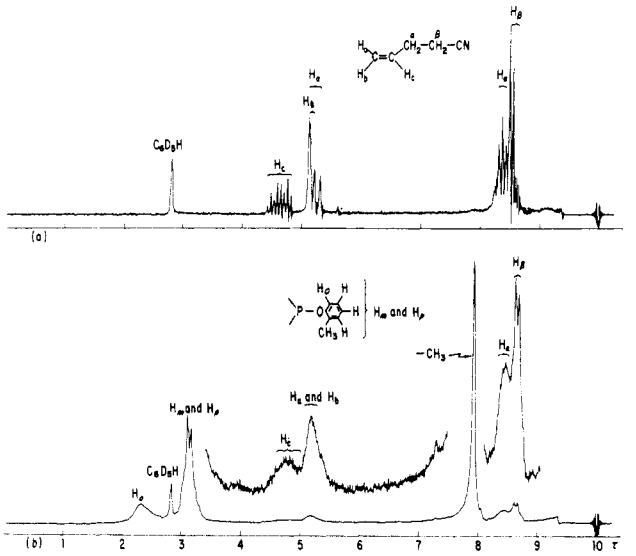

Figure 1. Proton NMR spectra at 100 MHz in C_6D_6 at ambient temperature: (a) 0.3 M 4-pentenenitrile; (b) 0.15 M Ni[P(O-*o*-tolyl)$_3$]$_3$ and 0.3 M 4-pentenenitrile.

ppm from their positions in the free olefins.[2a,b]

The predominance of nitrile complexes in the proton NMR spectra is also indicated by the positions of the ligand protons. The three resonances at τ 2.30, 3.12, and 7.93 in Figure 1b assigned to ortho H, unresolved meta and para H's, and ligand CH_3 are very close to those found for the complex $(CH_3CN)NiL_3$: τ 2.28, 3.16, and 7.93.[3] $(Ol)NiL_2$ complexes are expected to give ligand resonances at about 2.60, 3.10, and 7.88, while resonances of NiL_4 would appear at τ 2.26, 3.24, and 8.04.[1]

An infrared spectrum of a solution of ~0.1 M NiL_3 and ~0.1 M 3BN in CH_2Cl_2 showed two bands in the CN stretching region at about 2260 and 2250 cm^{-1} and a band in the C=C stretching region at 1650 cm^{-1}. This indicates that both free and coordinated nitriles were present in solution and that some of the C=C bonds were not coordinated. After addition of acrylonitrile, there was only one band near 2250 cm^{-1} due to uncoordinated 3BN, and the intensity of the 1650-cm^{-1} band was slightly enhanced. New bands assigned to ν_{CN} of free ACN and ACN in olefin-bonded $(ACN)NiL_2$[2b] appeared at about 2235 and 2200 cm^{-1}. The spectral changes can be accounted for by reactions 5 and 6, in which 3BN is nitrile bonded in (3BN)NiL_3 and olefin bonded in $(3BN)NiL_2$.

$$(3BN)NiL_3 + ACN \rightarrow (ACN)NiL_2 + L + 3BN \quad (5)$$

$$(3BN)NiL_2 + ACN \rightarrow (ACN)NiL_2 + 3BN \quad (6)$$

Spectrophotometric studies in benzene at 25 °C confirmed the presence of both olefin and nitrile complexes in solutions of cyanoolefins, nickel(0), and P(O-*o*-tol)$_3$ and permitted accurate determination of a number of equilibrium constants.

The complex nature of the equilibria in solution is illustrated by Figures 2 and 3, which show the effects on the electronic spectra when increasing concentrations of 5-hexenenitrile are added to solutions of NiL_3 that differ in concentration by a factor of about 10. In 0.3 M 5HN, the more dilute 2.04×10^{-3} M nickel solution (Figure 2) shows a distinct absorption maximum at 349 nm and shoulder with inflection at 386 nm. The apparent extinction coefficients of these features are 4.0×10^3 and 2.8×10^3 cm^{-1} M^{-1}. The spectrum is very similar to that of (1-hexene)NiL_2 [λ_{max} 354 nm (ϵ 4.2×10^3); λ_{sh} 392 nm (ϵ 3.0×10^3)][2c] and indicates substantial conversion of the NiL_3 to the olefin complex (5HN)NiL_2. The more concentrated

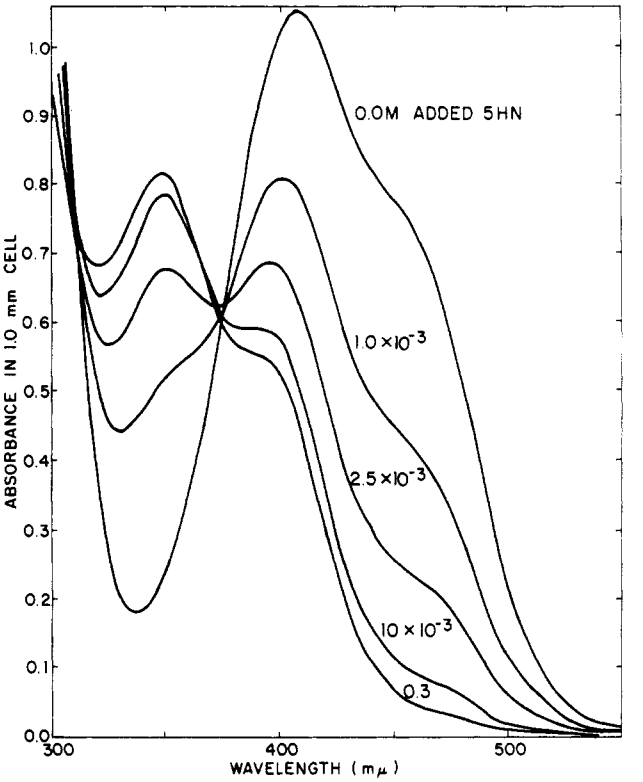

Figure 2. Electronic spectra of solutions of 2.04×10^{-3} M Ni[P(O-*o*-tolyl)$_3$]$_3$ with increasing concentrations of added 5-hexenenitrile in benzene at 25 °C.

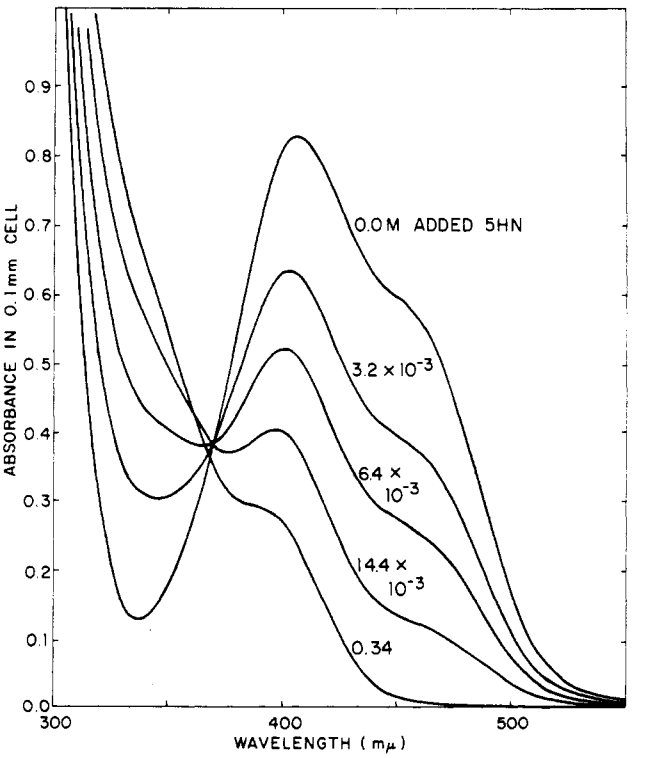

Figure 3. Electronic spectra of solutions of 1.86×10^{-2} M Ni[P(O-*o*-tolyl)$_3$]$_3$ with increasing concentrations of added 5-hexenenitrile in benzene at 25 °C.

1.86×10^{-2} M nickel solution (Figure 3) does not show a maximum near 350 nm in ~0.3 M 5 HN. There is a shoulder at 386 nm but the apparent extinction coefficient is only 1.6×10^3.

The different behavior of the spectra in Figures 2 and 3 can be explained in terms of the different relative con-

Table II. Calculation of K_8 for the Reaction of 5-Hexenenitrile with 1.03×10^{-3} M (Styrene)Ni[P(O-o-tolyl)$_3$]$_2$ [a]

soln no.	$[5HN]_{total}$ [b]	$10^3[S]$ [f]	$A(314)$ [c]	10^3-$[(S)NiL_2]$ [d]	10^3-$[(5HN)NiL_2]$ [e]	K_8 [h]
1	0.00	5.00	1.085	1.03	0.00	
2	0.01	5.27	0.865	0.765	0.265	0.19
3	0.025	5.48	0.685	0.55	0.48	0.20
4	0.05	5.66	0.53	0.365	0.665	0.21
5	0.10	5.84	0.38	0.185	0.845	0.27
6	0.10	0.98	0.265	0.048	0.98	0.20
	∞	1.03	(0.225) [g]	0.00	1.03	
						0.22 ± 0.03

[a] In benzene at 25 °C. All solutions except no. 6 contain 0.005 M added styrene. [b] Total concentration of 5-hexenenitrile. $[5HN] \cong [5HN]_{total}$. [c] Absorbance at 314 nm in 1.0-mm cell. [d] $[(S)NiL_2] = 1.03 \times 10^{-3}\ [A(314) - A_\infty]/[1.085 - A_\infty]$. [e] $[(5HN)NiL_2] = 1.03 \times 10^{-3} - [(S)NiL_2]$. [f] Concentration of free styrene in solution. $[S] = [S]_{added} + [(5HN)NiL_2]$. [g] A_∞, determined by successive approximation to make K_8(calcd) for solution no. 6 equal to the mean K_8. [h] $K_8 = [(5HN)NiL_2][S]/[(S)NiL_2][5HN]$.

centrations of nitrile and olefin complexes in the two solutions. The ratio $[(RCN)NiL_3]/[(Ol)NiL_2]$ can be obtained by subtracting eq 1 from eq 4. The mass action expression is

$$[(RCN)NiL_3]/[(Ol)NiL_2] = K_N[L]/K_1 \quad (7)$$

The terms [RCN] and [Ol] are approximately equal for a large excess of cyanoolefin and cancel out. The greater proportion of nitrile complex in Figure 3 is a consequence of a higher free L concentration generated by reaction 1.

One approach to determining K_1 would be to use still more dilute nickel solutions in order to minimize the ratio $[(RCN)NiL_3]/[(Ol)NiL_2]$. An alternative approach that we have used is to determine K_1 values for the cyanoolefins indirectly, by determining the equilibrium constant for reaction 8. The equilibrium constant for reaction 9 is

$$\text{cyanoolefin} + \text{(styrene)NiL}_2 \rightleftharpoons \text{(cyanoolefin)NiL}_2 + \text{styrene} \quad (8)$$

known to be 10 ± 1.[2a] The desired K_1 is given by the

$$\text{styrene} + \text{NiL}_3 \rightleftharpoons \text{(styrene)NiL}_2 + \text{L} \quad (9)$$

product K_8K_9. The styrene complex is convenient to use because it can be prepared analytically pure[2b] and has a rather different electronic spectrum from those of other $(Ol)NiL_2$ complexes. A series of spectra with (styrene)-NiL_2, styrene and increasing concentrations of 5HN are shown in Figure 4. From spectrum 6, which is essentially that of olefin-bonded $(5HN)NiL_2$, we can determine λ_{max} 351 nm (ϵ 4.3×10^3) and λ_{sh} 386 nm (ϵ 3.1×10^3). The determination of K_8 is illustrated in Table II.

Using the value of $K_1 = 10K_8 = 2.2$ and assuming the value of $K_N \approx 200\ M^{-1}$ found for alkanenitriles,[3] the ratio K_N/K_1 is about 100. Equation 7 can then be solved by making the approximation that $[L] = [(Ol)NiL_2]$.[11] We calculate that 83% of the nickel is $(Ol)NiL_2$ for initially 2.04×10^{-3} M NiL_3 while only 49% is $(Ol)NiL_2$ for initially 1.86×10^{-2} M NiL_3; the remaining nickel in both solutions is mostly the nitrile complex $(5HN)NiL_3$ in ~0.3 M cyanoolefin. The calculated apparent extinction coefficients at 386 nm of 2.7×10^3 and 1.6×10^3 are in excellent agreement with the values obtained from Figures 2 and 3.

The 3-pentenenitriles have neither a terminal C=C nor a conjugated CN. Their reduced tendency to form olefin complexes is indicated by the ^{31}P NMR experiments (Table I). Figure 5 shows electronic spectra obtained with 2.04×10^{-3} M NiL_3 and increasing concentrations of *trans*-3-pentenenitrile. The spectra up to 0.1 M T3PN look very similar to those obtained on adding alkanenitriles to NiL_3, which showed an isosbestic point at 356 nm.[3] The increased absorbance in the range 350–400 nm at higher cyanoolefin concentrations is attributed to formation of the bis(olefin) complex $(T3PN)_2NiL_2$, since this behavior was not observed at high concentrations of alkanenitriles. A value for K_N can be determined from Figure 5 once K_1 is known. The reaction with $(styrene)NiL_2$ gave $K_1 = (1.7 \pm 0.5) \times 10^{-2}$ for T3PN. The determination of K_N is shown in Table III. It was necessary to consider both the olefin complex $(PN)NiL_2$ and the nitrile complex $(PN)NiL_3$. The

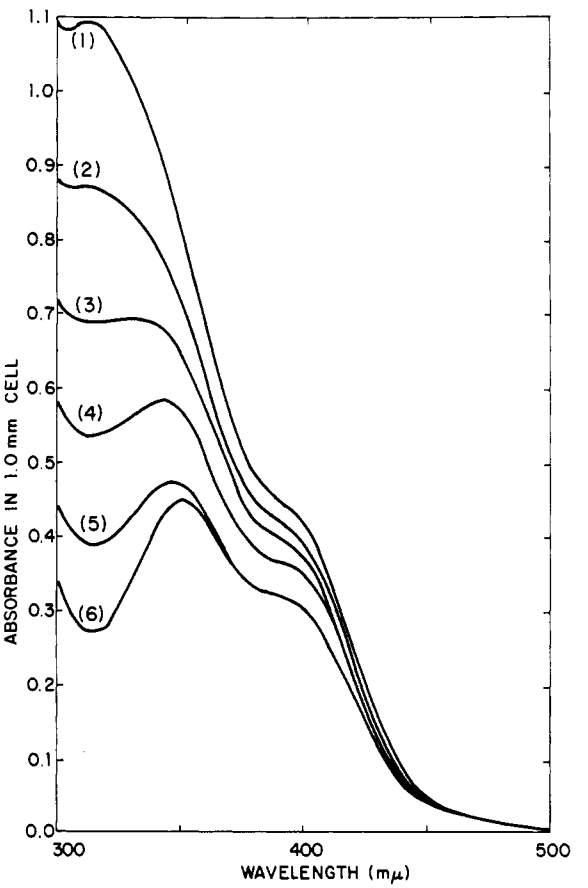

Figure 4. Electronic spectra of solutions of 1.03×10^{-3} M (styrene)Ni[P(O-o-tolyl)$_3$]$_2$. Concentrations (M) of 5HN were as follows: (1) 0.00; (2) 0.01; (3) 0.025; (4) 0.05; (5 and 6) 0.10. Solutions 1–5 had 0.005 M added styrene solution, and solution 6 had none added.

(11) Actually [L] is slightly less than $[(Ol)NiL_2]$ because some of the ligand freed in reaction 1 can react with NiL_3 to give NiL_4 in reaction 3. The concentrations of NiL_3 and NiL_4 in these solutions with excess cyanoolefin and no added L are so vanishingly small, however, that they can be safely neglected.

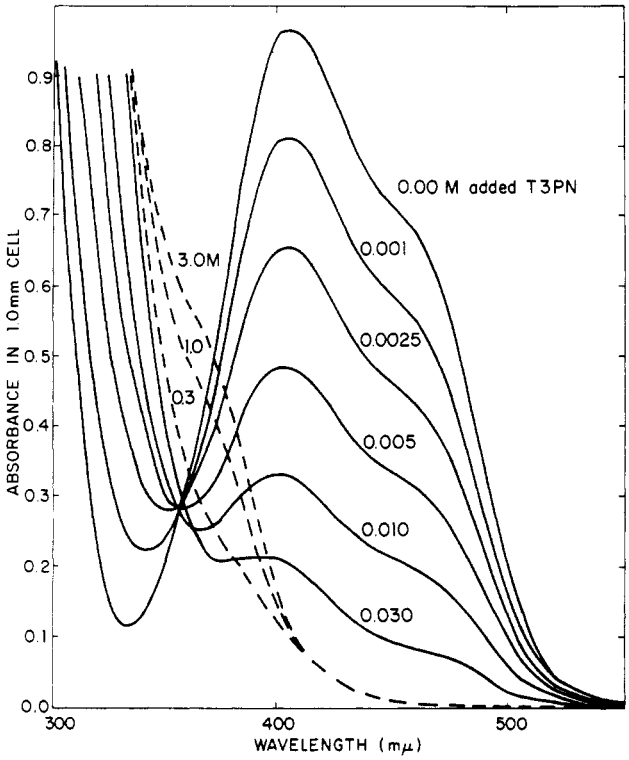

Figure 5. Electronic spectra of solutions of 2.04×10^{-3} M Ni[P(O-*o*-tolyl)$_3$]$_3$ with increasing concentrations of *trans*-3-pentenenitrile.

fraction of PN-bonded nickel present as olefin complex was calculated by quadratic equation and equilibrium 10. It

$$(PN)NiL_3 \xrightleftharpoons{K_1/K_N} (PN)NiL_2 + L \qquad (10)$$

was necessary to assume a value of K_1/K_N at this point. The first value assumed (10^{-4} M) gave a mean K_N of 190 ± 15 M^{-1} in the last column of Table III. Since K_1 was known from the (styrene)NiL_2 reaction to be (1.7 ± 0.5) × 10^{-2}, the value of K_1/K_N was good enough to require no further iteration.

Though K_2 cannot be accurately determined from these data, a value of $K_2 \approx 0.2$ M^{-1} can be estimated, assuming that ~50% of the nickel is present as bis(olefin) complex in 1 M T3PN. Equilibrium constants K_2 of about this magnitude were found earlier for 1-hexene and *trans*-2-hexene.[2c]

The 2-pentenenitriles are internal olefins with a conjugated nitrile. Spectra of solutions of 2×10^{-3} M NiL_3 and increasing concentrations of 2PN's below 0.1 M gave spectrophotometric titrations with sharp end points at a cyanoolefin:nickel ratio of 1:1. Spectra in 0.1 M 2PN showed shoulders at 330 and 370 nm, indicating the presence of the olefin complexes (2PN)NiL_2. At C2PN concentrations higher than ~0.1 M further spectral changes occurred; the shoulders became less distinct and their absorbance fell. An absorbance matrix analysis[12] indicated the presence of two predominant chromophores below 0.1 M C2PN [NiL_3 and (Ol)NiL_2] and two others at C2PN concentrations of 0.1–3.0 M [(Ol)NiL_2 and (Ol)$_2NiL_2$]. Since the spectra of NiL_3 and NiL_3 with 10^{-3} M C2PN added crossed at 388 nm, this was taken to be the isosbestic point of NiL_3 and the olefin complex (C2PN)NiL_2. A plot of $[\Delta A(388)]^{-1}$ against $[C2PN]^{-1}$ for [C2PN] ≥ 0.1 M gave a straight line whose slope gave K_2 = 2 M^{-1}.

(12) Coleman, J. S.; Varga, L. P.; Mastin, S. A. *Inorg. Chem.* **1970**, *9*, 1015.

Table III. Calculation of K_N for the Reaction of *trans*-3-Pentenenitrile with 2.04×10^{-3} M Ni[P(O-*o*-tolyl)$_3$]$_3$ [a]

soln no.	$10^3[PN]_{total}$ [b]	$10^3[PN]$ [h]	$A(450)$ [c]	$10^3[NiL_3]$ [d]	$10^3[Ni(PN)]$ [e]	$10^3[(PN)NiL_2]$ [f]	$10^3[(PN)NiL_3]$ [g]	K_N, [i] M^{-1}
1	0.0	0.00	0.73	2.04	0.00	0.00	0.00	
2	1.0	0.66	0.61	1.70	0.34	0.14	0.20	180
3	2.5	1.80	0.48	1.34	0.70	0.22	0.48	200
4	5.0	3.94	0.35	0.98	1.06	0.28	0.78	200
5	10.0	8.6	0.22	0.62	1.42	0.33	1.09	205
6	30.0	28.2	0.10	0.28	1.76	0.38	1.38	175
7	100.0	98	0.03	0.084	1.956	0.395	1.56	190
	∞	∞	(0.00)	0.00	2.04	0.40	1.64	
								190 ± 15

[a] In benzene at 25 °C. [b] Total concentration of *trans*-3-pentenenitrile. [c] Absorbance at 450 nm in 1.0-mm cell. [d] $[NiL_3] = 2.04 \times 10^{-3}\ A(450)/0.73$. [e] Ni(PN) represents nickel in any way coordinated to pentenenitrile. $[Ni(PN)] = 2.04 \times 10^{-3} - [NiL_3]$. [f] (PN)$NiL_2$ represents the olefin-bonded complex. [(PN)NiL_2] was calculated by quadratic equation from [Ni(PN)] with $K_1/K_N = 10^{-4}$ M. $[(PN)NiL_2] = 0.5\{-K_1/K_N + [(K_1/K_N)^2 + 4[Ni(PN)](K_1/K_N)]^{1/2}\}$. [g] (PN)$NiL_3$ represents the nitrile-bonded complex. $[(PN)NiL_3] = [Ni(PN)] - [(PN)NiL_2]$. [h] $[PN] = [PN]_{total} - [Ni(PN)]$. [i] $K_N = [(PN)NiL_3]/[NiL_3][PN]$.

Table IV. Calculation of K_N for the Reaction of *cis*-2-Pentenenitrile with 2.05×10^{-3} M $Ni[P(O\text{-}o\text{-tolyl})_3]_3$ and 0.1 M $P(O\text{-}o\text{-tolyl})_3$[a]

soln no.	$10^3[PN]_{total}$	$10^3[PN]$[e]	$A(360)$[b]	$10^3[Ni(PN)]$[c]	$10^3[Ni(L)]$[d]	K',[g] M^{-1}
1	0.0	0.00	0.10	0.00	2.05	
2	1.0	0.815	0.16	0.185	1.865	120
3	2.0	1.56	0.24	0.435	1.615	170
4	4.0	3.19	0.36	0.81	1.24	200
5	8.0	6.80	0.485	1.20	0.85	210
6	24.0	22.4	0.63	1.645	0.405	180
	∞	∞	(0.76)[f]	2.05	0.00	
						180 ± 25

[a] In benzene at 25 °C. [b] Absorbance at 360 nm in 1.0-mm cell. [c] $[Ni(PN)] = 2.05 \times 10^{-3}\ [A(360) - 0.10]/[A_\infty - 0.10] = [(PN)NiL_3] + [(PN)NiL_2]$. [d] $[Ni(L)] = 2.05 \times 10^{-3} - [Ni(PN)] = [NiL_3] + [NiL_4]$. [e] $[PN] = [PN]_{total} - [Ni(PN)]$. [f] Determined by successive approximation to make K' (calcd) for solution no. 6 equal to the mean K'. [g] $K' = [Ni(PN)]/[Ni(L)][PN]$; $K' = \{[(PN)NiL_3]/[NiL_3][PN]\}\{[Ni(PN)]/[(PN)NiL_3]\}\{[NiL_3]/[Ni(L)]\}$; $K' = K_N\{1 + K_1/K_N[L]\}\{1 + K_a[L]\}^{-1}$.

Table V. Equilibrium Constants[a] for Reactions of Cyanoolefins with $Ni[P(O\text{-}o\text{-tolyl})_3]_3$ and Electronic Spectra[b] of (Olefin)NiL_2

cyanoolefin	K_1	K_2, M^{-1}	λ_{max}	$10^3\text{-}\epsilon_{max}$	ϵ_{sh}	$10^3\text{-}\epsilon_{sh}$	K_N, M^{-1}	λ_{max}	$10^3\text{-}\epsilon_{max}$
ACN[g]	$(4 \pm 2) \times 10^4$	0.9 ± 0.3	326	4.6	362	3.7	*e*	367[d]	*e*
C2PN	17 ± 2	2 ± 1	330[c]	4.3	370	3.1	435 ± 50	~375[d]	~5.2
T2PN	17 ± 1.5	*e*	330[c]	4.6	370	3.4	*e*		*e*
3BN	10 ± 1	0.1 ± 0.04	346	4.6	381	3.4	*e*		
2M3BN	6.0 ± 0.3	~0	347	4.2	380	3.0	*e*		
4PN	3.6 ± 0.3	0.2 ± 0.1	349	4.4	385	3.1	*e*		
5HN	2.2 ± 0.3	0.3 ± 0.1	351	4.3	386	3.1	*e*		
T3PN	$(1.7 \pm 0.5) \times 10^{-2}$	~0.2					190 ± 15		
T2M2BN	$\sim 10^{-2}$	*e*					480 ± 50	372	~4.7
benzonitrile[h]							1000 ± 400	396	5.8
acetonitrile[h]							230 ± 20	*f*	

[a] All data are in benzene at 25 °C. [b] Wavelengths are in nm. Extinction coefficients have units of $cm^{-1}\ M^{-1}$. [c] Appearing only as a shoulder. [d] Observed in the presence of added L. [e] Not determined. [f] (Alkane nitrile)NiL_3 complexes show a band as a slight shoulder ~300 nm ($\epsilon \sim 14 \times 10^3$) but no longer wavelength bands. [g] Data on olefin complexes from ref 4. [h] Data on nitrile complexes from ref 5.

Values of K_1 for *cis*- and *trans*-2-pentenenitriles were determined by the reaction with (styrene)NiL_2 and found to be the same (~17) within experimental error.

The value of K_N for *cis*-2-pentenenitrile was determined by adding C2PN to solutions containing NiL_3 and added L. The added phosphite ligand suppressed reaction 10 and favored nitrile complex formation. Figure 6 shows spectra obtained with increasing concentrations of C2PN in a solution containing 2.05×10^{-3} M NiL_3 and 0.1 M L. The first spectrum without added PN shows reduced absorbance beyond ca. 330 nm compared to Figure 2 as a consequence of the reaction of L with NiL_3 by eq 3. The spectra show a well-defined isosbestic point at 420 nm in spite of the fact that there are four chromophoric species at appreciable concentrations at intermediate concentrations of cyanoolefin: NiL_3, NiL_4, $(PN)NiL_2$, and $(PN)NiL_3$. The two independent concentration variables may be taken as [Ni(L)], the concentration of nickel bound to ligand only, and [Ni(PN)], the concentration of nickel bound to penetenenitrile. The ratios of $[NiL_3]$ to $[NiL_4]$ and of $[(PN)NiL_3]$ to $[(PN)NiL_2]$ are fixed by [L][13] and equilibria 3 and 10. Table IV shows how K_N was calculated by using Figure 6 and previously determined values of K_1 and K_a.[14] From the last equation in footnote *g* of Table IV we find $K_N = (1 + K_a[L])K' - K_1/[L]$ or $K_N = 460\ M^{-1}$. A similar experiment with 0.2 M added L gave $K_N = 410\ M^{-1}$, in satisfactory agreement. For C2PN, we take the value of K_N to be $435 \pm 50\ M^{-1}$. Thus, in the experiment of Figure 6, 31% of Ni(L) was NiL_3 and 72% of Ni(PN) was the nitrile complex $(PN)NiL_3$.

(13) Phosphite ligand was present in such large excess that its concentration stayed effectively constant.

(14) Interpolation of data[1] at 10 and 30 °C gives $K_a = 25\ M^{-1}$ at 25 °C.

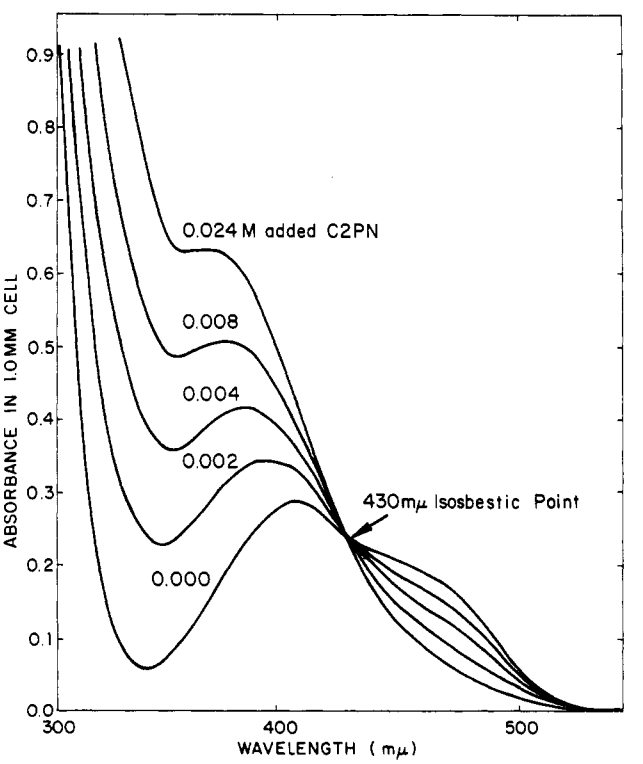

Figure 6. Electronic spectra of solutions of 2.05×10^{-3} M $Ni[P(O\text{-}o\text{-tolyl})_3]_3$, 0.1 M added $P(O\text{-}o\text{-tolyl})_3$, and increasing concentrations of *cis*-2-pentenenitrile.

The final spectrum in Figure 6 shows a slight maximum at ~375 nm. This electronic band appears to be characteristic of (cyanoolefin)NiL_3 complexes in which the CN

group of the N-bonded nitrile is conjugated to an olefinic double bond. From the known concentrations and electronic spectra of the various species in solution, we can estimate ϵ_{375} for C2PN at 5.2×10^3 cm^{-1} M^{-1}. A similar band was observed in the reaction of NiL_3 with T2M2BN, where $(Ol)NiL_2$ complex formation was much less favorable.

A value of K_1 for T2M2BN could not be accurately determined because styrene could not be completely displaced in reaction 8 even with a large excess of the cyanoolefin. K_1 could be estimated at $\sim 10^{-2}$, but the limiting spectrum of the olefin complex could not be obtained.

Acrylonitrile is unique among the cyanoolefins studied because it has both a terminal C=C and a conjugated CN group. Both factors are expected to favor coordination as an olefin. A solution prepared by adding ACN to NiL_3 in a 1:1 ratio has an electronic spectrum identical with that of the isolated $(ACN)NiL_2$ complex, whose NMR spectra in solution[2b] and X-ray crystal structure in the solid state[15] show it to be an olefin complex. If, however, acrylonitrile is added to a solution of NiL_3[16] containing 1 M added L at 25 °C, the spectrum of the olefin complex [λ_{max} 326 nm (ϵ 4.6×10^3), λ_{sh} 362 nm (ϵ 3.7×10^3)][3] is not obtained. Instead, there is a new maximum at 367 nm. Since this electronic band is not seen except in solutions containing ACN and high concentrations of added ligand, it is attributed to a complex with the composition $(ACN)NiL_3$. The observation of similar bands for the $(nitrile)NiL_3$ complexes of the conjugated cyanoolefins C2PN and T2M2BN indicates that the acrylonitrile in the complex is coordinated as a nitrile.

When the solution containing ACN and 1 M added L was heated, the absorbance maximum at 367 nm disappeared. At 70 °C, there was only a shoulder at 349 nm. Apparently, equilibrium 10 between nitrile and olefin-bonded forms shifts to the right on raising the temperature. We were unable to determine the concentrations of the various species in solution from the spectra. The spectrum of a solution rapidly cooled to 25 °C appeared similar to that at 70 °C. Only on standing did the maximum reappear, indicating a surprisingly slow reversal of reaction 10.

Attempts to establish the existence of a $(nitrile)NiL_3$ complex with ACN by ^{31}P NMR spectroscopy were unsuccessful. The solubility of $(ACN)NiL_2$ was too low in very high concentrations of added L to obtain a ^{31}P spectrum.

Equilibrium constants and electronic spectral data for all of the cyanoolefins investigated are summarized in Table V.

Discussion

Solutions containing zero-valent nickel, L = $P(O\text{-}o\text{-}tol)_3$, and cyanoolefins generally contain a complex mixture of species and are described by equilibria 1–4. For the most part, the reactions are readily reversible and rapid, often on an NMR time scale. The distribution of Ni(0) among the various solution species will depend on the particular cyanoolefin, its concentration, and the concentrations of nickel and added L, as well as on temperature and solvent. Formation of $(Ol)NiL_2$ complexes is favored for cyanoolefins with a terminal olefinic double bond and by conjugation of the double bond with the nitrile. $(Nitrile)NiL_3$ complexes are favored for conjugated cyanoolefins, by adding L and by lowering the temperature. Decreased solvent polarity has been found to stabilize nitrile complexes[3] but is expected to have little effect on formation constants of olefin complexes. Bis(olefin) complexes may become important for high cyanoolefin concentrations of $\sim$1 M or greater.

The concentrations of all the Ni(0) species in solution can be readily calculated by using the equilibrium constants K_1, K_2, K_N, and K_a. The material balance for nickel gives (11). From the mass action expressions of reactions

$$[Ni]_{total} = [NiL_3] + [NiL_4] + [(Ol)NiL_2] + [(Ol)_2NiL_2] + [(RCN)NiL_3] \quad (11)$$

$$[Ni]_{total} = [NiL_3]\{1 + K_a[L] + K_1[Ol] \times [L]^{-1} + K_1K_2[Ol]^2[L]^{-1} + K_N[RCN]\} \quad (12)$$

1–4 we obtain eq 12. From (12), we can obtain the fraction of Ni(0) represented by each of the Ni-containing species

$$f(NiL_3) = \{\ \}^{-1}$$

$$f(NiL_4) = K_a[L]\{\ \}^{-1}$$

$$f[(Ol)NiL_2] = K_1[Ol][L]^{-1}\{\ \}^{-1}$$

$$f[(Ol)_2NiL_2] = K_1K_2[Ol]^2[L]^{-1}\{\ \}^{-1}$$

$$f[(RCN)NiL_3] = K_N[RCN]\{\ \}^{-1}$$

where { } represents expression enclosed by braces in eq 12. The ratio of concentrations of any two species is simply obtained by dividing two fractions; in this case, the complex expression in braces drops out. The ratio $f[(RCN)NiL_3]:f[(Ol)NiL_2]$ is the same as given by eq 7.

Equation 12 can be used, for example, to calculate the percentages of species in a solution of 1.86×10^{-2} M NiL_3 to which is added 0.34 M 5HN (corresponding to the final spectrum in Figure 3). We taken $K_a = 25^{-1}$, $K_1 = 2.2$, $K_2 = 0.3$ M^{-1} (Table V), and $K_N = 200$ M^{-1}. We assume a value of [L] between 0 and [Ni] total and then calculate [L] by using

$$[L]_{calcd} = [(Ol)NiL_2] + [(Ol)_2NiL_2] - [NiL_4]$$

After a few successive approximations, the solution converges to $[L] = 1.00 \times 10^{-2}$ M with the nickel distributed as follows: 0.7% NiL_3, 0.2% NiL_4, 49.3% $(Ol)NiL_2$, 5.0% $(Ol)_2NiL_2$, and 44.8% $(RCN)NiL_3$. A similar procedure with 2.04×10^{-3} M NiL_3 to which 0.3 M 5HN is added (the final spectrum in Figure 2) gives $[L] = 1.80 \times 10^{-3}$ M with the nickel distribution: 0.2% NiL_3, 0.0% NiL_4, 83.0% $(Ol)NiL_2$, 5.0% $(Ol)_2NiL_2$, and 12.0% $(RCN)NiL_3$. The larger percentage of $(Ol)NiL_2$ in the final spectrum of Figure 2 as compared to Figure 3 is evident in the absorption band at 350 nm.

Several features of the data in Table V are noteworthy. Values of K_1 for *cis*- and *trans*-2-pentenenitrile are essentially identical. A similar insensitivity to cis–trans isomerization in our system is shown by the olefins *cis*- and *trans*-2-hexene, which both show $K_1 = 2.5 \times 10^{-3}$ within experimental error.[2c] Methyl substitution not on the double bond has a small but measurable effect, reducing K_1 from 10 for 3BN to 6 to 2M3BN. Direct alkyl substitution on the double bond has a much larger effect, reducing K_1 by about 2×10^3 on going from acrylonitrile to T2PN and again going from T2PN to T2M2BN.

One interesting effect is the way K_1 falls with increasing n for the σ,ω-cyanoolefins $CH_2{=}CH(CH_2)_nCN$.

n	K_1	n	K_1
0	4×10^4	3	2.2
1	10	∞	0.5
2	3.6		

The value of K_1 for infinite separation of olefin and CN

(15) Guggenberger, L. J. *Inorg. Chem.* **1973**, *12*, 499.
(16) Under these conditions most of the nickel is present as NiL_4 before the addition of cyanoolefin.[1]

groups is taken to be that of 1-hexene.[2c] The very large drop in K_1 on increasing n from 0 to 1 is attributed to blocking resonance interaction between the olefin and cyano groups. The smaller subsequent effect of increasing chain length is attributable to a diminishing inductive effect. Surprisingly, the CN group still has a pronounced effect on K_1 even when separated from the double bond by three methylene units. That this effect is electronic can be seen by the steady increase in λ_{max} and λ_{sh} of the (Ol)NiL_2 complexes with increasing n in Table V. Values for 1-hexene are 354 and 392 nm.

The nitrile complex formation constant K_N = 190 for the nonconjugated cyanoolefin 3PN is essentially the same as that found for the alkanenitriles[3] suggesting that the isolated C=C has little effect on nitrile coordination. The conjugated cyanoolefins C2PN and T2M2BN, however, show larger values of $K_N \approx 450$. The larger K_N is attributed to electron delocalization effects. This conclusion is supported by the shift in the longest wavelength electronic transition from ~300 nm in the (RCN)NiL_3 complexes with alkanenitrile to ~370 nm with conjugated cyanoolefins. Benzonitrile, which has a larger delocalized π system, shows a further shift of λ_{max} to 396 nm and an increase in K_N to $\sim 10^3$.[3]

The ^{31}P NMR chemical shifts of the (RCN)NiL_3 complexes (Table I) are found in a narrow and characteristic range; there is, however, a tendency for the conjugated nitrile complexes to give resonances at slightly lower fields.

Cyanoolefins represent a type of ambidentate ligand that can bond in more than one way. Numerous complexes of acrylonitrile have been described, some of which are olefin and some nitrile bonded.[17] For example, acrylonitrile has been shown to be nitrile bonded in $(ACN)W(CO)_5$ and olefin bonded in $(ACN)_3W(CO)_3$. To our knowledge, however, our work on cyanoolefins is the first to show the presence of both olefin and nitrile complexes in equilibrium in solution and to determine equilibrium constants which provide a complete description of the system.

Acknowledgment. I am indebted to Drs. F. J. Weigert and C. M. King for samples of cyanoolefins and to Mrs. Adah B. Richmond for chromatographic separations. Thanks are also owed to Dr. P. Meakin for assistance with the ^{31}P spectra and Mr. D. W. Reutter for the spectrophotometric work. Helpful discussions with Dr. W. C. Seidel are gratefully acknowledged.

Registry No. NiL_3, 28829-00-7; $BNiL_2$ (B = styrene), 41685-58-9; $BNiL_3$ (B = acetonitrile), 33270-65-4; $BNiL_3$ (B = valeronitrile), 33270-67-6; $BNiL_3$ (B = adiponitrile), 41686-93-5; $(C_6H_5CN)NiL_3$, 33270-68-7; $(p\text{-}FC_6H_4CN)NiL_3$, 41686-99-1; $(ACN)NiL_2$, 31666-48-5; $(3BN)NiL_3$, 84521-37-9; $(3BN)NiL_2$, 84521-38-0; $(2M3BN)NiL_3$, 41686-95-7; $(2M3BN)NiL_2$, 84521-39-1; $(4PN)NiL_3$, 41852-92-0; $(4PN)NiL_2$, 84521-40-4; $(T2PN)NiL_3$, 84620-19-9; $(T2PN)NiL_2$, 84521-41-5; $(T3PN)NiL_3$, 84581-09-9; $(C2M2BN)NiL_3$, 84521-42-6; $[(5HN)NiL_2]$, 84521-43-7; $[(T3PN)NiL_2]$, 84521-44-8; $[(C2PN)NiL_3]$, 84620-20-2; $[(C2PN)NiL_2]$, 84581-10-2; C_6H_5CN, 100-47-0; $P\text{-}FC_6H_4CN$, 1194-02-1; ACN, 107-13-1; 3BN, 109-75-1; 2M3BN, 16529-56-9; 4PN, 592-51-8; T2PN, 26294-98-4; T3PN, 16529-66-1; C2M2BN, 20068-02-4; 5HN, 5048-19-1; C2PN, 25899-50-7; acetonitrile, 75-05-8; valeronitrile, 110-59-8; adiponitrile, 111-69-3.

(17) Jones, R. *Chem. Rev.* **1968**, *68*, 785.

Metalation-Resistant Ligands: Some Properties of Dibenzocyclooctatetraene Complexes of Molybdenum, Rhodium, and Iridium

Douglas R. Anton and Robert H. Crabtree*

Sterling Chemistry Laboratory, Yale University, New Haven, Connecticut 06511

Received September 22, 1982

The chelating diolefinic ligand dibenzo[*a*,*e*]cyclooctatetraene (dct) displaces 1,5-cyclooctadiene (cod) from $[Ir(cod)Cl]_2$ to give $[Ir(dct)Cl]_2$. This reacts with $AgBF_4$ and PPh_3 to give $[Ir(dct)L_2]BF_4$. The addition of H_2 at −80 °C gives *cis*-$[IrH_2(dct)L_2]BF_4$, which is stable at 20 °C in CH_2Cl_2 but rearranges with methanol catalysis at −30 °C to *cis,trans*-$[IrH_2(dct)L_2]BF_4$. This appears to be the first case of such a catalyzed rearrangement and takes place by a deprotonation/reprotonation sequence. The intermediate $[IrH(dct)L_2]$ can be obtained from the cis,trans dihydride and *t*-BuOK. Where L_2 is 1,3-bis(diphenylphosphino)propane (dpp), a cis dihydride is obtained at −80 °C, which rearranges with methanol catalysis to a new trans isomer. The analogous rhodium complex $[Rh(dct)L_2]PF_6$ (L = PPh_3) does not react with H_2, but $[RhH_2(dct)L_2]PF_6$, the first rhodium dihydride olefin complex, can be obtained from dct and $[RhH_2(Me_2CO)_2L_2]PF_6$. The strongly electrophilic character imparted to its complexes by the dct ligand is discussed with reference to the IR of $(dct)Mo(CO)_4$ which suggests that dct is substantially more electron-withdrawing than cod. A Tolman-type electronic parameter for both monodentate and chelating ligands is proposed. The substitution of dct for cod makes the complex *cis,trans*-$[IrH_2(diene)(PPh_3)_2]BF_4$ more acidic by at least 8 pK units.

Introduction

Over the last few years, we have been trying to develop transition-metal complexes as homogeneous systems for the selective activation of CH bonds, especially of alkanes.[1] We expected intramolecular cyclometalation[2] of ligand CH bonds to occur to the exclusion of intermolecular alkane activation. For this reason, in 1977 we set about the construction of metalation resistant ligands (see below). In 1979, we were surprised to find that alkane activation could occur[3] even in systems that can cyclometalate. More

(1) Parshall, G. W. *Acc. Chem. Res.* **1975**, *8*, 113.

(2) Bruce, M. I. *Angew. Chem., Int. Ed. Engl.* **1977**, *89*, 75. K. Omae, I. *Coord. Chem. Rev.* **1980**, *32*, 235.

0276-7333/83/2302-0621$01.50/0

groups is taken to be that of 1-hexene.[2c] The very large drop in K_1 on increasing n from 0 to 1 is attributed to blocking resonance interaction between the olefin and cyano groups. The smaller subsequent effect of increasing chain length is attributable to a diminishing inductive effect. Surprisingly, the CN group still has a pronounced effect on K_1 even when separated from the double bond by three methylene units. That this effect is electronic can be seen by the steady increase in λ_{max} and λ_{sh} of the (Ol)NiL_2 complexes with increasing n in Table V. Values for 1-hexene are 354 and 392 nm.

The nitrile complex formation constant K_N = 190 for the nonconjugated cyanoolefin 3PN is essentially the same as that found for the alkanenitriles[3] suggesting that the isolated C=C has little effect on nitrile coordination. The conjugated cyanoolefins C2PN and T2M2BN, however, show larger values of $K_N \approx 450$. The larger K_N is attributed to electron delocalization effects. This conclusion is supported by the shift in the longest wavelength electronic transition from ~300 nm in the (RCN)NiL_3 complexes with alkanenitrile to ~370 nm with conjugated cyanoolefins. Benzonitrile, which has a larger delocalized π system, shows a further shift of λ_{max} to 396 nm and an increase in K_N to $\sim 10^3$.[3]

The ^{31}P NMR chemical shifts of the (RCN)NiL_3 complexes (Table I) are found in a narrow and characteristic range; there is, however, a tendency for the conjugated nitrile complexes to give resonances at slightly lower fields.

Cyanoolefins represent a type of ambidentate ligand that can bond in more than one way. Numerous complexes of acrylonitrile have been described, some of which are olefin and some nitrile bonded.[17] For example, acrylonitrile has been shown to be nitrile bonded in $(ACN)W(CO)_5$ and olefin bonded in $(ACN)_3W(CO)_3$. To our knowledge, however, our work on cyanoolefins is the first to show the presence of both olefin and nitrile complexes in equilibrium in solution and to determine equilibrium constants which provide a complete description of the system.

Acknowledgment. I am indebted to Drs. F. J. Weigert and C. M. King for samples of cyanoolefins and to Mrs. Adah B. Richmond for chromatographic separations. Thanks are also owed to Dr. P. Meakin for assistance with the ^{31}P spectra and Mr. D. W. Reutter for the spectrophotometric work. Helpful discussions with Dr. W. C. Seidel are gratefully acknowledged.

Registry No. NiL_3, 28829-00-7; $BNiL_2$ (B = styrene), 41685-58-9; $BNiL_3$ (B = acetonitrile), 33270-65-4; $BNiL_3$ (B = valeronitrile), 33270-67-6; $BNiL_3$ (B = adiponitrile), 41686-93-5; $(C_6H_5CN)NiL_3$, 33270-68-7; $(p\text{-}FC_6H_4CN)NiL_3$, 41686-99-1; $(ACN)NiL_2$, 31666-48-5; $(3BN)NiL_3$, 84521-37-9; $(3BN)NiL_2$, 84521-38-0; $(2M3BN)NiL_3$, 41686-95-7; $(2M3BN)NiL_2$, 84521-39-1; $(4PN)NiL_3$, 41852-92-0; $(4PN)NiL_2$, 84521-40-4; $(T2PN)NiL_3$, 84620-19-9; $(T2PN)NiL_2$, 84521-41-5; $(T3PN)NiL_3$, 84581-09-9; $(C2M2BN)NiL_3$, 84521-42-6; $[(5HN)NiL_2]$, 84521-43-7; $[(T3PN)NiL_2]$, 84521-44-8; $[(C2PN)NiL_3]$, 84620-20-2; $[(C2PN)NiL_2]$, 84581-10-2; C_6H_5CN, 100-47-0; $P\text{-}FC_6H_4CN$, 1194-02-1; ACN, 107-13-1; 3BN, 109-75-1; 2M3BN, 16529-56-9; 4PN, 592-51-8; T2PN, 26294-98-4; T3PN, 16529-66-1; C2M2BN, 20068-02-4; 5HN, 5048-19-1; C2PN, 25899-50-7; acetonitrile, 75-05-8; valeronitrile, 110-59-8; adiponitrile, 111-69-3.

(17) Jones, R. *Chem. Rev.* **1968**, *68*, 785.

Metalation-Resistant Ligands: Some Properties of Dibenzocyclooctatetraene Complexes of Molybdenum, Rhodium, and Iridium

Douglas R. Anton and Robert H. Crabtree*

Sterling Chemistry Laboratory, Yale University, New Haven, Connecticut 06511

Received September 22, 1982

The chelating diolefinic ligand dibenzo[*a*,*e*]cyclooctatetraene (dct) displaces 1,5-cyclooctadiene (cod) from $[Ir(cod)Cl]_2$ to give $[Ir(dct)Cl]_2$. This reacts with $AgBF_4$ and PPh_3 to give $[Ir(dct)L_2]BF_4$. The addition of H_2 at −80 °C gives *cis*-$[IrH_2(dct)L_2]BF_4$, which is stable at 20 °C in CH_2Cl_2 but rearranges with methanol catalysis at −30 °C to *cis,trans*-$[IrH_2(dct)L_2]BF_4$. This appears to be the first case of such a catalyzed rearrangement and takes place by a deprotonation/reprotonation sequence. The intermediate $[IrH(dct)L_2]$ can be obtained from the cis,trans dihydride and *t*-BuOK. Where L_2 is 1,3-bis(diphenylphosphino)propane (dpp), a cis dihydride is obtained at −80 °C, which rearranges with methanol catalysis to a new trans isomer. The analogous rhodium complex $[Rh(dct)L_2]PF_6$ (L = PPh_3) does not react with H_2, but $[RhH_2(dct)L_2]PF_6$, the first rhodium dihydride olefin complex, can be obtained from dct and $[RhH_2(Me_2CO)_2L_2]PF_6$. The strongly electrophilic character imparted to its complexes by the dct ligand is discussed with reference to the IR of $(dct)Mo(CO)_4$ which suggests that dct is substantially more electron-withdrawing than cod. A Tolman-type electronic parameter for both monodentate and chelating ligands is proposed. The substitution of dct for cod makes the complex *cis,trans*-$[IrH_2(diene)(PPh_3)_2]BF_4$ more acidic by at least 8 pK units.

Introduction

Over the last few years, we have been trying to develop transition-metal complexes as homogeneous systems for the selective activation of CH bonds, especially of alkanes.[1] We expected intramolecular cyclometalation[2] of ligand CH bonds to occur to the exclusion of intermolecular alkane activation. For this reason, in 1977 we set about the construction of metalation resistant ligands (see below). In 1979, we were surprised to find that alkane activation could occur[3] even in systems that can cyclometalate. More

(1) Parshall, G. W. *Acc. Chem. Res.* **1975**, *8*, 113.

(2) Bruce, M. I. *Angew. Chem., Int. Ed. Engl.* **1977**, *89*, 75. K. Omae, I. *Coord. Chem. Rev.* **1980**, *32*, 235.

0276-7333/83/2302-0621$01.50/0

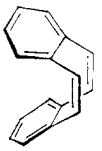

Figure 1. The conformation of free dct.

recently, other such systems have been found.[4] Clearly cyclometalation may be reversible in these systems and merely compete with alkane activation. It seems probable that more efficient activation could result if ligands resistant to cyclometalation could be used. In this paper we return to the question of metalation-resistant ligands, because we think that progress in this area may lead to significant advances in alkane activation.

Ligands tend to cyclometalate more readily in bulky systems where a stable ring can be formed. For phosphorus ligands the tendency to cyclometalate increases as $PMe_3 < PPh_3 < P(OPh)_3$.[2] A general method we are attempting to use to prevent cyclometalation is the construction of a ligand having a conformation that prevents the formation of a internally cyclometalated product.

In this paper we report some of the chemistry of dibenzocyclooctatetraene (1, dct), a tub-shaped molecule (Figure 1), which we hoped would be metalation-resistant by virtue of its lack of allylic hydrogens.

We first looked at the donor/acceptor properties of dct by IR spectroscopy of the tetracarbonyl molybdenum derivatives. We then examined some iridium and rhodium complexes of dct, the corresponding 1,5-cyclooctadiene (cod) chemistry of which we had already studied:[5] striking differences were observed.

Results and Discussion

Dibenzocyclooctatetraene (1) has been obtained by several routes[6,7] and has been shown to bind to transition metals.[7] The synthesis we have used[7] gives ca. 25% yield of dct from $\alpha,\alpha,\alpha',\alpha'$-tetrabromo-*o*-xylene, but it is inconvenient involving a $Ni(CO)_4$-mediated coupling and a pyrolysis. Dct is also commercially available. X-ray crystallography shows that dct adopts in the tub conformation[8] (Figure 1). This must also be the conformation in which dct binds to a metal. Force-field calculations[9] suggest that free cod adopts the twist-boat conformation, with the chair being only slightly (1.3 kcal/mol) higher. The C_{2v} boat, like that for dct, is less stable, probably due to eclipsing interactions in the allylic CH_2 groups.

For these reasons alone, dct might be expected to be a much better ligand than cod. Another contributing factor is the aryl substituent on the C=C bond. An arene ring is electron withdrawing in the σ framework and electron donating in the π framework. In dct, the aryl rings are twisted relative to the C=C bond in such a way as to decouple the π effect, leaving only the σ effect. The increase in electron-acceptor behavior on going from cod and dct is therefore expected to be substantial. We wished to form some idea of the magnitude of this effect.

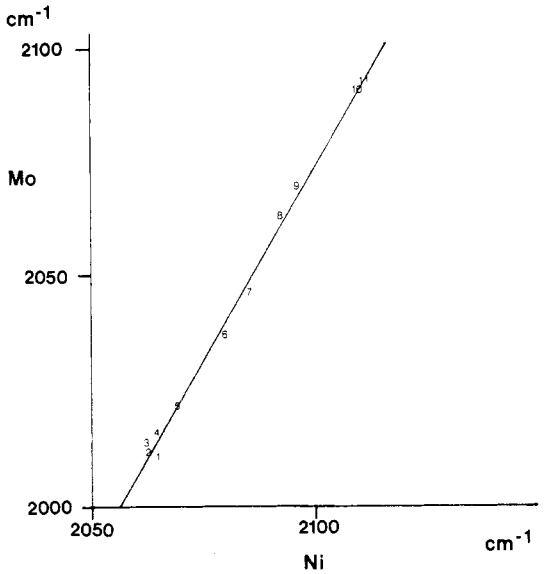

Figure 2. The electronic parameter ν_{Mo} plotted against Tolman's parameter ν_{Ni}. Identifying labels are as follows: 1, PMe_2Ph; 2, PEt_2Ph; 3, PEt_3; 4, PMe_3; 5, PPh_3; 6, $P(OMe)_3$; 7, $P(OPh)_3$; 8, $PCl_2(OEt)$; 9, PCl_3; 10, PF_3; 11, $P(CF_3)F_2$.

Tolman[10] has compared the electronic effects of various monodentate ligands by using the A_1 ν(CO) vibration of $LNi(CO)_3$. Chelating ligands cannot be studied with $LNi(CO)_3$, so we searched for a more suitable system. *cis*-$Mo(CO)_4L_2$ seems to fit the requirements. These are easily made, air-stable complexes, and both chelating and monodentate ligands can be studied.[11,12] Literature data are available for many derivatives of this type.[12] Further advantages of the Mo system are the greater convenience and much lower toxicity of $Mo(CO)_6$ relative to $Ni(CO)_4$ and the wider range of ligands L that bind, including N, O, and S donor ligands. The halide ions can also be used in this system. We adopted the same criterion as Tolman, using the highest frequency (A_1) vibration for comparison. The normal mode associated with this vibration mainly involves the pair of trans CO groups, but the bands are always strong enough to be easily observed and assigned.

In Figure 2, the molybdenum and nickel parameters are compared for 11 phosphorus ligands of various types for which data are available. The correlation coefficient is 0.996, showing that the parameters are very close agreement in measuring the same property of the ligands, presumably their overall donor power. The slope of the graph (1.69) shows that the molybdenum parameter has the advantage of being more sensitive. This is probably due to the presence of two L ligands in the Mo case (0.5 L/CO) compared to one L in the Ni case (0.33 L/CO). For convenience, the equation connecting the Tolman parameter ν_{Ni} with the present parameter ν_{Mo} is given below (eq 1).

$$\nu_{Ni} = 0.593\nu_{Mo} + 871 \quad (1)$$

We have made $(cod)Mo(CO)_4$ and $(dct)Mo(CO)_4$ by literature methods[11] and have measured their IR spectra in pentane solution. Comparing these with other values

(3) Crabtree, R. H.; Mellea, M. F.; Mihelcic, J. M.; Quirk, J. M. *J. Am. Chem. Soc.* **1982**, *104*, 107; **1979**, *101*, 7738.
(4) Baudry, D.; Ephritikine, M.; Felkin, H. *J. Chem. Soc., Chem. Commun.* **1980**, 1243. Green, M. A.; Rybak, W. K.; Huffman, J. C.; Ziolkowski, J. J. *J. Organomet. Chem.* **1981**, *218*, C39 Janowicz, A. H.; Bergman, R. G. *J. Am. Chem. Soc.* **1982**, *104*, 352. Hoyano, J. K.; Graham, W. A. G. *Ibid.* **1982**, 104.
(5) Crabtree, R. H.; Felkin, H.; Fillebeen-Khan, T.; Morris, G. E. *J. Organomet. Chem.* **1979**, *168*, 183.
(6) Fieser, L. F.; Pechet, M. M. *J. Am. Chem. Soc.* **1946**, *68*, 2577. Cope, A. C.; Fenton, S. W. *Ibid.* **1951**, *73*, 1668. Griffin, C. E.; Peters, J. A. *J. Org. Chem.* **1963**, *28*, 1715.
(7) Arram, M.; Dinu, D.; Mateescu, G.; Neritzescu, C. D. *Ber. Dtsch. Chem. Ges.* **1960**, *93*, 1189.
(8) Irngartiner, H.; Reibel, W. R. K. *Acta Crystallogr., Sect. B* **1981**, *B37*, 1724.
(9) Allinger, N. L.; Sprague, J. T. *Tetrahedron* **1975**, 21.
(10) Tolman, C. A. *J. Am. Chem. Soc.* **1970**, *92*, 2953.
(11) Muller, J.; Goser, D.; Elian, M. *Angew. Chem., Int. Ed. Engl.* **1969**, *8*, 374.
(12) Chatt, J; Watson, H. R. *J. Chem. Soc.* **1961**, 4980. Delbeke, F. T.; Claeys E. G.; van der Kelan, G. P.; Eeckhant, Z. *J. Organomet. Chem.* **1970**, *25*, 213, 219.

Scheme I. Some Reactions of the Iridium Complexes[a]

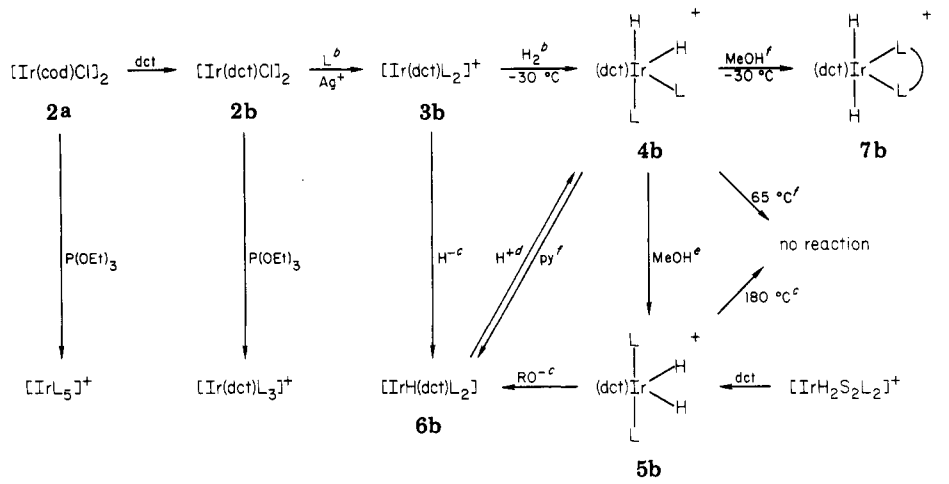

[a] cod = 1,5-cyclooctadiene; dct = dibenzocyclooctatetrene; S = Me_2CO; py = pyridine. [b] L = PPh_3, $PMePh_2$, 0.5dpe, or 0.5dpp. [c] L = PPh_3. [d] L = PPh_3 or 0.5dpp. [e] L = PPh_3 or $PMePh_2$. [f] L = 0.5dpp.

found for *cis*-$[L_2Mo(CO)_4]$ complexes in the literature gives the following order of donor strength: PCl_3 (2072) < dct (2052) < $P(OPh)_3$ (2046) < cod (2038) < $P(OMe)_3$ (2037) < PPh_3 (2022).

This strong electron-acceptor character of dct relative to cod probably helps increase the strength of the metal–olefin bonding and accounts, together with the factors mentioned above, for the exceptionally strong bonding we observed between dct and rhodium and iridium (see below).

We wished to see whether the electron-withdrawing properties of dct would enhance the electrophilic character we have found for a variety of cod complexes of rhodium and iridium[13] and were therefore interested in the synthesis of $[Ir(dct)Cl]_2$.

1 (dct) reacts smoothly with $[Ir(cod)Cl]_2$ (**2a**) in CH_2Cl_2 to give a bright yellow solution and microcrystalline precipitate of the corresponding $[Ir(dct)Cl]_2$ (**2b**).[14] Additional **2b** was precipitated with hexane. In contrast with the cod analogue, **2b** is air stable both in the solid and in solution. The ^1H NMR and IR spectra are consistent with the proposal that dct binds as a chelating diolefin like cod. In particular, the ν(C=C) vibration at 1646 cm^{-1} in the IR spectrum of dct is shifted to 1603 cm^{-1} on coordination, and δ(CH) vinyl is shifted from δ 6.8 to δ 5.33, as expected[15] for this structure. Other cases are known in which dct binds in an η^4 fashion,[7] but η^6 binding to the aromatic ring has been reported only for the $Cr(CO)_3$ group.[11]

The product is relatively insoluble, in contrast to **2a**, and recrystallization is therefore difficult. We find, however, that **2b** dissolves in CH_2Cl_2 in the presence of C_2H_4, presumably to form $(dct)IrCl(C_2H_4)_x$ (x = 1 or 2). Ethylene is readily lost over several hours or more rapidly on purging with N_2, and pure **2b** crystallizes from the solution.

As expected **2b** reacts with PPh_3 and $AgBF_4$ in CH_2Cl_2 to give $[(dct)IrL_2]BF_4$ (**3b**) (L = PPh_3) after removal of the AgCl formed. The complex can be isolated with hexanes to give a CH_2Cl_2 solvate or can be recrystallized from CH_2Cl_2/MeOH to give the mixed MeOH/CH_2Cl_2 solvate. The ^1H NMR spectrum supports the formulation. The phenylene ring protons absorb at δ 6.8 and 7.0, as expected for uncoordinated groups, and the cod vinyl protons at δ 4.7. In the case of **3b**·CH_2Cl_2·MeOH, free MeOH at δ 3.3 can also be seen. In each case free CH_2Cl_2 at δ 5.3 is seen. At −80 °C **3b**·CH_2Cl_2 adds H_2 to give the expected *cis*-$[(dct)IrH_2L_2]BF_4$, which is the only product that can be detected by ^1H NMR spectroscopy (eq 2 and Scheme I).

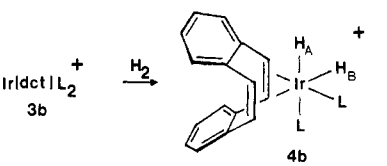

[2]

H_A appears as a doublet of doublets at δ −7.5 and H_B as a triplet at δ −12.75. While H_B appears in almost exactly the same place (δ −12.63) in the cod analogue[5] **4a**, H_A is shifted 2.2-ppm downfield (**4a**, δ −9.7; **4b**, δ −7.52).

The solution of **4b** can be warmed to room temperature without either loss of the H_2 or transfer to and hydrogenation of the olefin ligand; **4a** does both above −20 °C. At 80 °C H_2 is lost, but dct hydrogenation still does not occur. Indeed we have found no conditions under which dct can be hydrogenated homogeneously. This presumably arises from the strength of the dct–metal bond and the rigidity of dct itself. Models show that one C=C group of coordinated dct cannot insert into an M–H bond without the second C=C group becoming detached. This effect means that dct is a permanently bound ligand like PPh_3 not subject to hydrogenation rather than a ligand such as cod, which can be hydrogenated.

In contrast to the behavior found for **3b**·CH_2Cl_2, a sample of the dihydride **4b** formed at −80 °C from **3b**·CH_2Cl_2·MeOH, rearranged on warming to −30 °C. The product was *cis,trans*-$[Ir(dct)H_2L_2]BF_4$, **5b**, as shown by ^1H NMR spectroscopy. A triplet at δ −12.6 is assigned to the IrH groups and a triplet at δ 5.2 to the dct vinyls. By ^{13}C NMR spectroscopy the vinyl carbon appears as a singlet at 89.8 ppm, showing[16] the dct is cis to the L groups and confirming the cis,trans structure. Both the cis (**4a**) and cis,trans (**5a**) isomers are known in the case of cod, but they do not interconvert under any conditions we have studied. We inferred that the rearrangement was catalyzed by MeOH in the dct case and confirmed this by adding MeOH (1 equiv/Ir) to a sample of **4b** at 0 °C formed from

(13) Crabtree, R. H.; Felkin, H.; Khan, T.; Morris, G. E. *J. Organomet. Chem.* **1978**, *144*, C15.

(14) Compounds are numbered **a** for cod derivatives and **b** for dct derivatives.

(15) Chatt, J.; Venanzi, L. M. *J. Chem. Soc.* **1957**, 4735. Giordano, G.; Crabtree, R. H. *Inorg. Synth.* **1979**, *19*, 218.

(16) Crabtree, R. H.; Morris, G. E. *J. Organomet. Chem.* **1977**, *135*, 395.

Table I. ^{1}H NMR Data for the New Complexes[a]

complex	aryl	vinyl	hydride	other resonances
$[Ir(dct)Cl]_2$	6.9, c	5.33, s		
$[Ir(dct)(PPh_3)_2]BF_4$	7.0, c	4.7, br		
	6.8, c			
cis-$[IrH_2(dct)(PPh_3)_2]BF_4$ [b]	6.7, c	4.4, t (8)	−7.5, dd (19, 83)	
		5.2, t (7)	−12.75, t (15)	
		5.4, c		
		5.8, d (8)		
cis,trans-$[IrH_2(dct)(PPh_3)_2]BF_4$	6.7, c	5.2, t (3)	−12.5, t (14)	
	6.3, c			
$[IrH(dct)(PPh_3)_2]$	6.6, c	4.65, d (12)	−13.7, t (21)	
$[Ir(dct)(dpe)]PF_6$	7.5, br	5.4, s		2.5, c, CH_2
	6.9, br			
cis-$[IrH_2(dct)(dpe)]PF_6$ [b]	7.4, br	6.1, br	−7.5, dd (16, 85)	3.1, br, CH_2
	7.1, br	5.2, br	−13.5, t (16)	
		4.7, br		
$[Ir(dct)(dpp)]PF_6$	7.7, br	5.2, s		3.1, br, CH_2
	7.2, br			2.4, br, CH_2
	7.1, br			
cis-$[IrH_2(dct)(dpp)]PF_6$ [b]	7.7, br	6.3, br		3.3, br, CH_2
	7.1, br	6.0, br		2.9, br, CH_2
	6.8, br	5.0, br		1.4, br, CH_2
	6.6, br	4.8, br		
trans-$[IrH_2(dct)(dpp)]PF_6$	7.4, br	4.3, br	−5.9, t (17)	3.4, br, CH_2
	6.8, br			1.4, br, CH_2
$[Ir(dct)(PMePh_2)_2]PF_6$	7.3, c	5.1, t (3)		2.3, t (4), Me
	6.8, c			
	6.6, c			
trans-$[IrH_2dct(PMePh_2)_2]PF_6$	6.8, c	5.1, t (14)	−13.2, t (15)	2.3, t (14), Me
$[Ir(dct)(P\{OEt\}_3)_3]PF_6$	6.8, s	4.6, q (1)		4.1, c, CH_2
				1.3, t, Me
$[Rh(dct)Cl]_2$	6.9, br	5.0, d (2)		
$[Rh(dct)(PPh_3)_2]PF_6$	7.1, c	5.1, br		
	6.8, c			
cis,trans-$[RhH_2(dct)(PPh_3)_2]PF_6$ [b]	7.1, c	5.3, br		−12, c
	6.7, c			

[a] Spectra recorded at 25 °C in $CDCl_3$ (except where noted) and reported as position (δ, relative to internal Me_4Si), multiplicity (coupling constant in hertz): c, complex; br, broad; d, doublet. [b] At −80 °C in CD_2Cl_2.

3b·CH_2Cl_2. Rearrangement was effectively instantaneous at room temperature. Even atmospheric moisture was capable of promoting the rearrangement.

The mechanism of this rearrangement is most probably a deprotonation/reprotonation sequence. Addition of MeOD leads to **5b**-d_2 in which the H ligands have been completely exchanged. Exchange does not occur below the rearrangement temperature, however.

The postulated monohydride intermediate $[IrH(dct)L_2]$ (**6b**) can be made by the acton of *t*-BuOK on *cis,trans*-$[IrH_2(dct)L_2]$ (**5b**) or less conveniently by reaction $LiBEt_3H$ on $[Ir(dct)L_2]BF_4$. The product is a colorless microcrystalline solid and, like the cod analogue **6a**, is fluxional in solution on the ^{1}H NMR time scale (see Table I). Protonation (CF_3CO_2H, −80 °C) gave a solution in which only the cis dihydride **4b** could be observed (NMR). This implies that multiple deprotonation/reprotonation steps are required to convert **4b** to **5b**, since one cycle would largely reform the cis isomer **4b**. An alternative possibility is that **5b** is only formed by protonation of **6b** above −30 °C. The most reasonable[17] structure for the monohydride is shown in Figure 3. Of the three possible positions at which protonation can take place (marked with arrows) two lead to the cis and one to the *cis,trans* isomers. Possibly the approach of the acid is kinetically determined by the steric bulk of L, or there may be a preference to attack trans to L the ligand of lowest trans effect.

This appears to be the first case of a metal hydride rearrangement going to a deprotonation/reprotonation equilibrium and shows the influence that weak bases such as water or methanol can have on reactions of metal hydrides.

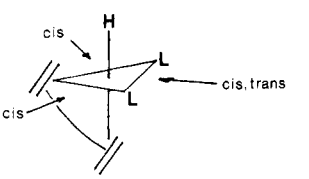

Figure 3. Protonation of $IrH(dct)L_2$ to give *cis*- or *cis,trans*-$[IrH_2(dct)L_2]^+$.

We have pointed out[18a] that cod complexes such as **2a** are electrophilic or Lewis acid in their properties. Hydrogen addition tends to be reductive in this series, so that the hydrogen ligands of the adducts **4a** and **5a** tend to take on δ+ character. The additional electron-acceptor character of dct, compared to cod, enhances the electrophilic character of **3b** compared to **3a** to such a point that the dihydride **4b** distinctly acidic and can even partially protonate methanol. Since the cis dihydride **4b** converts to the cis,trans complex **5b** by deprotonation/reprotonation, **5b** must be the least acidic of the two. **5b** does not exchange with MeOD.[18b] In CD_2Cl_2 **5b** can be deprotonated by pyridine (2 molar equiv) but not by aniline (2 molar equiv), suggesting that pK_a[19] of the metal hydride is ca. 11. The cod analogue **5a** cannot be deprotonated even by NEt_3, suggesting it has a pK_a above 19.

(17) Churchill, M. R.; Bezman, S. A. *Inorg. Chem.* **1972**, *11*, 2243.

(18) (a) Crabtree, R. H.; Hlatky, G. G. *Inorg. Chem.* **1980**, *19*, 571. Crabtree, R. H.; Quirk, J. M. *J. Organomet. Chem.* **1980**, *199*, 99. (b) This implies that both hydrides in **4b** must be MeOD exchangeable, since **5b**-d_2 is obtained above −30 °C.

(19) Based on pK_b values of the amines in CH_3CN (Jordan, R. F.; Norton, J. R. *J. Am. Chem. Soc.* **1982**, *104*, 1255).

cis,trans-$[IrH_2(dct)L_2]BF_4$ (**5b**) was also formed from $[IrH_2(Me_2CO)_2L_2]BF_4$ and dct in CH_2Cl_2, just as **5a** is obtained with cod.[5] While the cod analogue **5a** loses H_2 above 80 °C on heating, **5b** is stable at least to 180 °C in air or on reflux in $CHCl_3$ for at least 1 h. This degree of stability in a dihydrido olefin complex is striking and a further example of the electrophilic character of the metal. On classical ideas, electron-withdrawing substituents should destabilize an oxidative addition product; here, the electron-withdrawing dct stabilizes **4**, because the metal becomes more negative on H_2 addition. In short, the addition is reductive not oxidative as we have found in several related cases[18] (see below). No dct hydrogenation was observed in this system. In a future paper[20] we will discuss the use of dct as a selective hydrogenation-resistant poison for homogeneous catalysts in a test for the homogeneity of catalyst systems.

Complexes of Other Phosphine Ligands. Other complexes of type **3b** were also obtained as hexafluorophosphate[21] salts by the same method as mentioned above where L = $PMePh_2$, 0.5dpe, and 0.5dpp (dpe = 1,2-bis(diphenylphosphino)ethane; dpp = 1,3-bis(diphenylphosphino)propane). In the synthesis of $[Ir(cod)(dpe)]PF_6$, cod is relatively easily displaced and some $[Ir(dpe)_2]PF_6$ is formed unless care is taken. Dpe showed no tendency to displace the more strongly bound dct. The $PMePh_2$ case was very similar to that of PPh_3, in that only the cis,trans dihydride of type **5b** is observed in moist CH_2Cl_2 on passing H_2 at room temperature.

One unusual feature of $[Ir(dct)(PMePh_2)_2]PF_6$ was the ^1H NMR resonance of the PMe group. This showed full virtual coupling as would be expected for a trans complex. Occasionally virtual coupling of an intermediate type is observed for cis phosphines, as in $[Ir(cod)(PMePh_2)_2]PF_6$, but to our knowledge this is the first case where full virtual coupling has been observed.

The analogous complexes with the chelating phosphines behaved differently. **3b** (L = 0.5dpe) reacts with H_2 to give the cis adduct **4b**. No cis,trans complex of type **5b** is possible in this case nor is H_2 lost even on refluxing in $CHCl_3$ (65 °C) for 0.5 h. Nor does hydrogenation occur even though the stereochemistry enforces a coplanar M(C=C)H arrangement, the one most favorably to hydrogenation.[5]

In this case both the starting complex and the cis dihydride adduct are stable enough for ^{13}C NMR study. Two features of interest emerge. First, the addition of H_2 produces a large upfield shift of the C vinyl resonances in the C=C group of the dct ligand that is trans to the phosphine. We have interpreted such shifts in the cod analogues as suggesting that the addition of H_2 reduces the metal, rather than oxidizing it, as is commonly the case.[22] The shift here, 9.7 ppm, is over twice the shift in the corresponding cod series,[18] consistent with the greater electron-withdrawing character of dct compared with cod. These shifts must be affected to some degree by the change from four- to six-coordination of the attached metal ion, over and above the changes in electron density we are trying to estimate. In the case of dct, we can also study the corresponding quaternary carbons of the dct ligand. These should be much less affected by such extraneous factors. They too, are shifted upfield, in this case by 7.9 ppm. This also suggests that the H_2 addition indeed has reductive character and tends to confirm our interpretation.[18] In CD_2Cl_2, the dihydride can be deprotonated by pyridine (2 M equiv) but not by aniline, suggesting it has a pK_a of about 11.

The dpp case is different again. Here the cis dihydride is formed at −80 °C as shown by ^1H NMR spectroscopy (Table I), but on warming a complete and irreversible rearrangement takes place at 15 °C, or at 0 °C with $CF_3CO_2^-$ catalysis, to give a complex having a triplet hydride resonance at δ −5.63. The most reasonable structure for this complex is *trans*-$[IrH_2(dct)L_2]PF_6$ (**7b**) with mutually trans hydrides (Scheme I). An isomer of $[IrH_2(nbd)(PPh_3)_2]$ (nbd = norbornadiene) has been assigned the same configuration by Howarth et al.[23] The IrH resonance in this complex appears at δ −7.7, comparable with the value for **7b**. This assignment is confirmed for **7b** by the position of the ν(Ir–H) vibration in the IR spectrum at 1871 cm^{-1}. As Chatt[24] showed, this vibration is sensitive to the trans ligand. A band above 2000 cm^{-1} is expected and observed for all isomers except **7**, for which a much lower frequency is expected in view of the mutually trans hydride arrangement. The apparent trans addition of H_2 to $[Ir(dct)(dpp)]PF_6$ above 15 °C is therefore due to a cis addition followed by rearrangement.

It is not clear why a trans isomer is never observed for dpe unless **6b**, the monohydride intermediate, has an axial H, an axial–equatorial dpe, and a diequatorial dct, in which case only the cis isomer could reform on reprotonation.

Finally, we wished to see how strongly dct was bound by comparing the reactivity of $[Ir(diene)Cl]_2$ (**2**) with $P(OEt)_3$. At 80 °C, the cod complex **2a** quickly loses cod and $[Ir\{P(OEt)_3\}_5]^+$ is formed.[25] In contrast, **2b** can be refluxed in EtOH with $P(OEt)_3$ for 12 h without any loss of dct, $[Ir(dct)\{P(OEt)_3\}_3]^+$ being isolated in essentially quantitative yield. Some of these complexes (e.g., L_2 = dpe and L = $PMePh_2$) are very oxygen sensitive, apparently giving O_2 adducts. We are currently investigating these in more detail.

Rhodium Complexes. Cod reacts with $[RhH_2(EtOH)_2L_2]^+$ (L = PPh_3) to give only $[Rh(cod)L_2]^+$ and no trace of dihydrido olefin complex of type **4** or **5** even at low temperature.[26]

We find that dct (1 equiv/Rh) reacts with the rhodium solvent complex at −80 °C in CD_2Cl_2 to give *cis,trans*-$[RhH_2(dct)L_2]^+$. This is the first example of a dihydrido olefin complex of rhodium. The ^1H NMR spectrum is very similar to that of the iridium analogue **5b**, showing an RhH resonance at δ −12.0, a CH (vinyl) resonance at δ 5.3, as well as free EtOH (see Table I). On warming above −20 °C the hydride resonances decrease in intensity and the resonances of $[Rh(dct)L_2]^+$ smoothly replace those of the dihydrido olefin complex. This loss of H_2 seems to be irreversible, and we were unable to find any conditions under which H_2 would add to $[Rh(dct)L_2]^+$. The dihydride is therefore thermodynamically unstable with respect to $[Rh(dct)L_2]^+$, in sharp contrast to the corresponding Ir case, confirming the stronger binding of H_2 to Ir over Rh.

Conclusion

We have shown that dct is different from cod in several respects: (1) it is substantially more electron withdrawing; (2) it is hydrogenation resistant; and (3) it is more tightly

(20) Anton, D. R.; Crabtree, R. H. *Organometallics*, in press.
(21) PF_6 and BF_4 salts had very similar properties. We report the one most convenient to prepare.
(22) Vaska, L.; Werneke, M. F. *Trans. N.Y. Acad. Sci.* **1971**, *33*, 70. Chatt, J.; Butter, S. A. *Chem. Commun.* **1967**, 501.
(23) Howarth, O. W.; McAteer, C. H.; Moore, P.; Morris, G. E. *J. Chem. Soc., Chem. Commun.* **1982**, 745.
(24) Chatt, J.; Coffey, R. S.; Shaw, B. L. *J. Chem. Soc.* **1965**, 7391.
(25) Haines, L. M.; Singleton, E. *J. Chem. Soc., Dalton Trans.* **1972**, 1891.
(26) Crabtree, R. H.; Demou, P. C.; Eden, D.; Mihelcic, J. M.; Parnell, C.; Quirk, J. M.; Morris, G. E. *J. Am. Chem. Soc.* **1982**, *104*, 6994.

bound. In future papers we will discuss the related properties of metalation resistance and resistance to nucleophilic attack.

The extra electrophilic character conferred on the metal by dct compared to cod is enough to make the metal hydrides sufficiently acidic to partially protonate methanol, leading to a new deprotonation/reprotonation mechanism for metal "hydride" rearrangements. The change in pK_a of the metal hydrides induced by a substitution of dct for cod is at least 8 units.

Experimental Section

NMR spectra were recorded on Brucker HX-270 and JEOL FX-90Q instruments and IR spectra on a Nicolet-7199 instrument. Standard Schlenk tube inert-atmosphere techniques were used. Dct,[7] (dct)Mo(CO)$_4$,[11] (cod)Mo(CO)$_4$,[11] and [IrCl(cod)]$_2$[27] were prepared by literature methods. Dct is also commercially available (ICN, K&K Labs).

Dichlorobis(η^4-dibenzo[*a*,*e*]cyclooctatetraene)diiridium(I). To [Ir(cod)Cl]$_2$ (820 mg) in CH_2Cl_2 (20 mL) was added dct (500 mg) in CH_2Cl_2 (20 mL) over 30 min. The solution was reduced to 10 mL in vacuo, and hexanes (25 mL) were added. The yellow product was filtered; yield 130 mg (65%). This was sufficiently pure for use in the preparations described below, but analytically pure material was only obtained after recrystallization as follows. A suspension of crude [Ir(dct)Cl]$_2$ (200 mg) in CH_2Cl_2 (20 mL) containing dct (20 mg) was prepared. Ethylene was passed until the complex dissolved and the excess C_2H_4 removed by passing N_2 briefly. Hexane (20 mL) was added carefully so that it formed a second layer above the CH_2Cl_2. After 20 h, pure microcrystalline [Ir(dct)Cl]$_2$ was formed: yield 130 mg (65%); IR (cm^{-1}, CH_2Cl_2 solution) 1603 (m), 1582 (m), 1490 (s), 1098 (m), 1002 (m), 831 (m). Anal. Calcd for $C_{16}H_{12}IrCl$: C, 44.49; H, 2.80. Found: C, 44.31; H, 2.84.

(Dibenzo[*a*,*e*]cyclooctatetraene)bis(triphenylphosphine)iridium(I) Fluoroborate. To a solution of [Ir(dct)Cl]$_2$ (100 mg, 0.22 mmol) and PPh_3 (120 mg, 0.44 mmol) in CH_2Cl_2 (20 mL) was added $AgBF_4$ (45 mg, 0.22 mmol). After 10 min of stirring, the resulting AgCl is filtered off, and the volume of the solution reduced to 15 mL. Hexanes and diethyl ether (3:1, 15 mL) were added to form a second layer. Red crystals of the product were deposited (1 day), filtered, and washed with Et_2O: yield 169 mg (76%); IR ($CDCl_3$, cm^{-1}) 3063 (m), 1597 (m), 1484 (s), 1434 (s), 1265, 1061 (vs); ^{13}C NMR ($CDCl_3$, reported as position δ from internal Me_4Si (multiplicity, coupling constant (Hz), assignment) 142.4 (complex, aryl), 85.9 (t, $^2J_{PC}$ = 5, vinyl). Anal. Calcd for $C_{52}H_{42}IrP_2BF_4 \cdot CH_2Cl_2$: C, 58.25; H, 4.06. Found: C, 58.09; H, 4.22.

The methylene chloride–methanol solvate was prepared by dissolving the crude complex (100 mg) in CH_2Cl_2/MeOH (4:1, 10 mL) and adding a second layer of hexanes. Red crystals of the product were formed in 1 day. Anal. Calcd for $C_{52}H_{42}IrP_2BF_4 \cdot MeOH \cdot CH_2Cl_2$: C, 57.65; H, 4.30. Found: C, 57.70; H, 4.19.

The $PMePh_2$ analogue was prepared in the same way in comparable yield.

***cis*-Dihydrido(dibenzo[*a*,*e*]cyclooctatetraene)bis(triphenylphosphine)iridium(III) Tetrafluoroborate.** [Ir(dct)(PPh$_3$)$_2$]BF_4 (100 mg) in CH_2Cl_2 (10 mL) at −80 °C was treated with H_2 (1 atm) until the red color was discharged. Et_2O (25 mL) was added at −80 °C, and white microcrystals were deposited, filtered cold, and dried: the ^1H NMR was recorded at −80 °C (Table I); IR (Nujol mull, cm^{-1}) 2181 (w), 2140 (w), 1054 (s), 752 (m), 695 (s). The complex had limited thermal stability and tended to rearrange to the cis,trans isomer in the presence even of weak bases.

***cis,trans*-Dihydrido(dibenzo[*a*,*e*]cyclooctatetraene)bis(triphenylphosphine)iridium(III) Tetrafluoroborate.** To *cis,trans*-[IrH$_2$(Me$_2$CO)$_2$(PPh$_3$)$_2$]BF_4 (250 mg) in CH_2Cl_2 (5 mL) was added dct (56 mg). After the solution was stirred for 30 min, Et_2O–hexane (1:1, 15 mL) was added as an upper layer. The crude product precipitated and was recrystallized by CH_2Cl_2/Et_2O–hexane bilayer diffusion, filtered, washed (Et_2O), and dried: yield 170 mg (65%) of colorless crystals; ^{13}C NMR ($CDCl_3$) δ 141.4 (c, Ar), 89.8 (s, vinyl); IR (CD_2Cl_2, cm^{-1}) 2182 (m), 1605 (m), 1481 (m), 1060 (vs), 1000 (m), 866 (m) 826 (m).

Observation of the H_2 Adducts. [Ir(dct)L$_2$]BF_4 (50 mg) was dissolved in CD_2Cl_2 in an NMR tube and cooled to −80 °C. H_2 was passed until the color of the solution was bleached. The ^1H NMR spectrum showed the resonances in Table I. On warming rearrangement occurred (L = PPh_3, $PMePh_2$, and 0.5dpp), and a second set of resonances were observed (see Table I). In the case L$_2$ = dpe the ^{13}C NMR spectrum of the dihydride adduct was also observed: vinyl dct carbons at δ 134.8, 134.6, 134.3, and 134.1 (s); quaternary dct carbons at δ 91.5 (s), 84.6 (d, J = 2), 79.4 (dt, J = 2 and 30, integration for two carbons).

Hydrido(dibenzo[*a*,*e*]cyclooctatetraene)bis(triphenylphosphine)iridium(I). Method A. To [Ir(dct)(PPh$_3$)$_2$]BF_4 (50 mg 0.05 mmol) in CH_2Cl_2/THF (3:5, 8 mL) at 0 °C was added LiBHEt$_3$ (0.1 mL of 1 M THF solution) slowly. The solution was stirred for 15 min, and the solvents were removed. The oily residue was dissolved in CH_2Cl_2 (5 mL) and filtered. MeOH/H_2O (2:1, 5 mL) was added as an upper layer. Off-white crystals were deposited, washed with cold MeOH, and dried: yield 15 mg (30%); IR (CH_2Cl_2, cm^{-1}) 2132 (m), 1603 (m), 1481 (s), 870 (m), 821 (m).

Method B. To *cis,trans*-[IrH$_2$(dct)(PPh$_3$)$_2$]BF_4 (50 mg, 0.05 mmol) in CH_2Cl_2 (5 mL) was added potassium *tert*-butoxide (8 mg). After 10 min of stirring, MeOH/H_2O (2:1, 10 mL) was added as an upper layer. Off-white crystals were deposited as in method A: yield 35 mg (70%). We prefer method B.

(Dibenzo[*a*,*e*]cyclooctatetraene)(1,2-bis(diphenylphosphino)ethane)iridium(I) Hexafluorophosphate. To [Ir(dct)Cl]$_2$ (100 mg, 0.23 mmol) and dpe (92 mg, 0.23 mmol) in CH_2Cl_2 (15 mL) was added [Et$_3$O]PF_6 (75 mg, 0.3 mmol). To the resulting red solution was added a layer of hexane (30 mL). Red crystals were formed, filtered, washed with hexane, and dried: yield 180 mg (84%); ^{13}C NMR δ 142.3 (s, quaternary dct carbons), 89.1 (t, J = 5, dct vinyls). Anal. Calcd for $C_{42}H_{36}IrP_3F_6$: C, 53.67; H, 3.86. Found: C, 53.62; H, 4.02.

(Dibenzo[*a*,*e*]cyclooctatetraene)(1,3-bis(diphenylphosphino)propane)iridium(I) Hexafluorophosphate. To [Ir(dct)Cl]$_2$ (100 mg, 0.23 mmol) and dpp (95 mg, 0.23 mmol) in CH_2Cl_2 (10 mL) was added $AgPF_6$ (58 mg, 0.23 mmol). After being stirred for 1 min, the red solution was filtered through Celite. The Celite was washed with CH_2Cl_2 (3 mL) and the combined filtrate reduced to 4 mL in vacuo. Et_2O/hexanes (1:1, 10 mL) was added as an upper layer, and the resulting red crystals were filtered, washed (hexane), and dried; yield 155 mg (71%).

(Dibenzo[*a*,*e*]cyclooctatetraene)tris(triethyl phosphite)iridium(I) Hexafluorophosphate. To [Ir(dct)Cl]$_2$ (50 mg) in EtOH (10 mL) was added P(OEt)$_3$ (0.25 mL) and the solution refluxed for 12 h. To the cooled solution was added saturated aqueous KPF_6 (1 mL), and the solvents were removed in vacuo. The CH_2Cl_2 (10 mL) extract was filtered and reduced to 3 mL in vacuo. Hexane (10 mL) was added, and the resulting white crystals were filtered, washed (hexane), and dried; yield 90 mg (75%). Anal. Calcd for $C_{34}H_{57}O_9P_4F_6Ir$: C, 39.27; H, 5.53. Found: C, 39.50; H, 5.60.

Chloro(dibenzo[*a*,*e*]cyclooctatetraene)rhodium(I). [Rh(cod)Cl]$_2$ (122 mg) in CH_2Cl_2 (5 mL) was treated with dct (100 mg) in CH_2Cl_2 (3 mL). Yellow crystals were deposited over several minutes. A layer of hexane (5 mL) was added to complete the precipitation. The resulting yellow crystals were filtered, washed (hexane), and dried; yield 100 mg (60%). This complex cannot be recrystallized, and it was used directly for subsequent preparations.

(Dibenzo[*a*,*e*]cyclooctatraene)bis(triphenylphosphine)rhodium(I) Hexafluorophosphate. To [Rh(dct)Cl]$_2$ (100 mg) and PPh_3 (153 mg) in CH_2Cl_2 (10 mL) was added $AgPF_6$ (74 mg). After 10 min of stirring the solution was filtered and the filtrate treated with hexane (20 mL) to give orange microcrystals, which were filtered, washed (hexane), and dried: yield 215 mg (76%). Anal. Calcd for $C_{52}H_{42}RhP_3F_6 \cdot CH_2Cl_2$: C, 59.96; H, 4.17. Found: C, 59.99; H, 4.32.

Acknowledgment. We thank the NSF for funding, Professor J. Norton for helpful discussions, and Ms.

(27) Norton, J. *Acc. Chem. Res.* **1979**, *13*, 139.
(28) Crabtree, R. H.; Quirk, J. M.; Felkin, H.; Fillebeen-Khan, T. *Synth. React. Inorg. Met.-Org. Chem.* **1982**, *12*, 407.

Michelle Mellea for experimental assistance, and R.H.C. thanks the A. P. Sloan and the Henry and Camille Dreyfus Foundations for fellowships.

Registry No. 2a, 12112-67-3; **2b**, 84500-08-3; **3b** (L = PPh_3) BF_4, 84500-10-7; **3b** (L_2 = dpe) PF_6, 84500-15-2; **3b** (L_2 = dpp) PF_6, 84500-19-6; **3b** (L = $PMePh_2$)PF_6, 84500-23-2; **4b** (L = PPh_3) BF_4, 84500-12-9; **4b** (L_2 = dpe) PF_6, 84500-17-4; **4b** (L_2 = dpp) PF_6, 84581-01-1; **5b** (L = PPh_3) BF_4, 84580-15-4; **6b** (L = PPh_3), 84500-13-0; **7b** (L_2 = dpp) PF_6, 84500-21-0; **7b** (L = $PMePh_2$) PF_6, 84500-25-4; $[Ir(dct)(P\{OEt\}_3)_3]PF_6$, 84500-27-6; $[Rh(dct)Cl]_2$, 84500-28-7; $[Rh(dct)(PPh_3)_2]PF_6$, 84500-30-1; *cis,trans*-$[RhH_2(dct)(PPh_3)_2]PF_6$, 84500-32-3; *cis,trans*-$[IrH_2(Me_2CO)_2(PPh_3)_2]BF_4$, 82582-67-0; $[Rh(Cod)Cl]_2$, 12092-47-6.

X-ray Crystal Structure of the Mononuclear Tris(trimethyl phosphite)(maleic anhydride)cobalt(0) Complex

K. A. Woode†

Department of Chemistry, University of Virginia, Charlottesville, Virginia 22901

J. C. J. Bart,* M. Calcaterra, and G. Agnès

Istituto di Ricerche "G. Donegani" S.p.A., 28100 Novara, Italy

Received July 20, 1982

The crystal structure of a new mononuclear cobalt(0) complex with trimethyl phosphite and maleic anhydride (MA) ligands has been determined from X-ray diffractometer data. The crystals are monoclinic of space group $P2_1/c$ with $Z = 4$ in a unit cell of dimensions a = 9.517 (4) Å, b = 15.432 (14) Å, c = 16.915 (8) Å, and β = 113.17 (6)°. The structure was solved by direct and Fourier methods and refined by full-matrix least-squares techniques to R = 0.063 for 2726 independent reflections. The metal is linked to three P atoms of the trimethyl phosphite groups and to the CH=CH moiety of MA. The molecular structure of C_1 symmetry contains a pseudotetrahedrally coordinated Co atom with bond distances Co–P(mean) = 2.172 (2) Å, Co–C(olefinic)(mean) = 2.033 (7) Å, and Co–X = 1.898 Å and bond angles P–Co–P(mean) = 99.4 (4)° and P–Co–X 117.4° (X is the midpoint of the olefinic bond). The parameters and bonding of the (trimethyl phosphite)cobalt part of the complex are standard with a mean P–O distance of 1.594 (6) Å and indicates a certain degree of π bonding. The mean O–C bond length is 1.443 (12) Å; Co–P–O angles average to 117.1 (2)° and O–P–O to 100.6 (5)°. The bond lengths in the MA ring (with C_s symmetry) indicate strong π-electron delocalization, in accordance with the large decrease in ν(C=O) from 1780 and 1850 cm^{-1} in free MA to 1722 and 1787 cm^{-1} in the complex.

Introduction

Cobalt(0) complexes are catalytically active in hydrogenation, carbonylation, and oligo- and polymerization reactions. As part of the studies on the reactivity and structure of mononuclear d^9 metal complexes,[1–4] the intermediate I has been isolated and characterized.

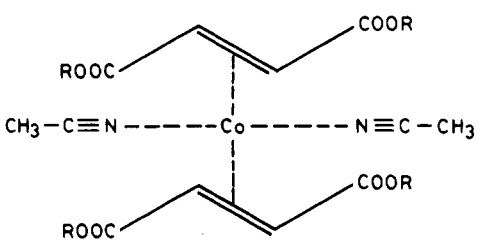

I

Various mono- and polynuclear complexes are easily formed by partial or total displacement in I,[5] as shown in Figure 1. Of particular interest is the synthetic route to compounds II and III, as cobalt complexes with phosphitic ligands are known to be extremely active and selective hydrogenation catalysts.[6–8] In the presence of unsaturated ligands, these complexes allow for electron delocalization that may lead to interesting properties in terms of activity and selectivity. The elucidation of the structures of such complexes is therefore useful not only in establishing the nature of the coordination around cobalt(0) but also in gaining a better insight into the role of the metal in catalysis. Since only rather few examples of mononuclear d^9 complexes of cobalt have been prepared[4,9–13] and in view of the paucity of molecular structural data,[4,12] an X-ray study of tris(trimethyl phosphite)(maleic anhydride)cobalt(0) (COCA) was undertaken.

Experimental Section

Preparation. COCA was prepared by the total ligand displacement reaction involving addition of 5.0 g (40 mmol) of trimethyl phosphite and 1.0 g (10 mmol) of maleic anhydride to 4.85 g (10 mmol) of a toluene solution (50 mL) of bis(ethyl fumarate)bis(acetonitrile)cobalt(0) under continuous stirring until complete dissolution of the anhydride:

$$Co(CH_3CN)_2L_2 + 3P(OCH_3)_3 + MA \rightarrow [P(OCH_3)_3]_3CoMA + 2L + 2CH_3CN$$

L = ethyl fumarate; MA = maleic anhydride

† Visiting Scientist at Istituto di Ricerche "G. Donegani".

(1) Agnès, G.; Chiusoli, C. P.; Cometti, G. *Chem. Commun.*, **1968**, 1515.
(2) Agnès, G.; Cometti, G. *Organomet. Chem. Synth.* **1970/1972**, *1*, 185.
(3) Agnès, G.; Santini, C., unpublished results.
(4) Agnès, G.; Bassi, I. W.; Benedicenti, C.; Intrito, R.; Calcaterra, M.; Santini, C. *J. Organomet. Chem.* **1977**, *129*, 401.
(5) Agnès, G.; Bart, J. C. J.; Santini, C.; Woode, K. A. *J. Am. Chem. Soc.* **1982**, *104*, 5254.
(6) Rakowski, M. C.; Muetterties, E. L. *J. Am. Chem. Soc.* **1977**, *99*, 739.
(7) Hirsekorn, F. J.; Rakowski, M. C.; Muetterties, E. L. *J. Am. Chem. Soc.* **1975**, *97*, 237.
(8) Gosser, L. W. *Inorg. Chem.* **1976**, *15*, 1348.
(9) Klein, H. F. *Angew. Chem., Int. Ed. Engl.* **1971**, *10*, 343.
(10) Chatt, J.; Hart, F. A.; Rosevear, D. T. *J. Chem. Soc.* **1961**, 5504.
(11) Kruck, T.; Lang, W. *Z. Anorg. Allg. Chem.* **1966**, *343*, 181.
(12) Ward, D. L.; Caughlan, C. N.; Voecks, G. E.; Jennings, P. W. *Acta Cyrstallogr., Sect. B* **1972**, *B28*, 1949.
(13) Klein, H. F. *Angew. Chem., Int. Ed. Engl.* **1980**, *19*, 362.

0276-7333/83/2302-0627$01.50/0

X-ray crystal structure of the mononuclear tris(trimethyl phosphite)(maleic anhydride)cobalt(0) complex

K. A. Woode, J. C. J. Bart, M. Calcaterra, and G. Agnes

Organometallics, **1983**, 2 (5), 627-633• DOI: 10.1021/om00077a010 • Publication Date (Web): 01 May 2002

Michelle Mellea for experimental assistance, and R.H.C. thanks the A. P. Sloan and the Henry and Camille Dreyfus Foundations for fellowships.

Registry No. 2a, 12112-67-3; **2b**, 84500-08-3; **3b** (L = PPh_3) BF_4, 84500-10-7; **3b** (L_2 = dpe) PF_6, 84500-15-2; **3b** (L_2 = dpp) PF_6, 84500-19-6; **3b** (L = $PMePh_2$)PF_6, 84500-23-2; **4b** (L = PPh_3) BF_4, 84500-12-9; **4b** (L_2 = dpe) PF_6, 84500-17-4; **4b** (L_2 = dpp) PF_6, 84581-01-1; **5b** (L = PPh_3) BF_4, 84580-15-4; **6b** (L = PPh_3), 84500-13-0; **7b** (L_2 = dpp) PF_6, 84500-21-0; **7b** (L = $PMePh_2$) PF_6, 84500-25-4; $[Ir(dct)(P\{OEt\}_3)_3]PF_6$, 84500-27-6; $[Rh(dct)Cl]_2$, 84500-28-7; $[Rh(dct)(PPh_3)_2]PF_6$, 84500-30-1; *cis,trans*-$[RhH_2(dct)(PPh_3)_2]PF_6$, 84500-32-3; *cis,trans*-$[IrH_2(Me_2CO)_2(PPh_3)_2]BF_4$, 82582-67-0; $[Rh(Cod)Cl]_2$, 12092-47-6.

X-ray Crystal Structure of the Mononuclear Tris(trimethyl phosphite)(maleic anhydride)cobalt(0) Complex

K. A. Woode†

Department of Chemistry, University of Virginia, Charlottesville, Virginia 22901

J. C. J. Bart,* M. Calcaterra, and G. Agnès

Istituto di Ricerche "G. Donegani" S.p.A., 28100 Novara, Italy

Received July 20, 1982

The crystal structure of a new mononuclear cobalt(0) complex with trimethyl phosphite and maleic anhydride (MA) ligands has been determined from X-ray diffractometer data. The crystals are monoclinic of space group $P2_1/c$ with $Z = 4$ in a unit cell of dimensions a = 9.517 (4) Å, b = 15.432 (14) Å, c = 16.915 (8) Å, and β = 113.17 (6)°. The structure was solved by direct and Fourier methods and refined by full-matrix least-squares techniques to R = 0.063 for 2726 independent reflections. The metal is linked to three P atoms of the trimethyl phosphite groups and to the CH=CH moiety of MA. The molecular structure of C_1 symmetry contains a pseudotetrahedrally coordinated Co atom with bond distances Co–P(mean) = 2.172 (2) Å, Co–C(olefinic)(mean) = 2.033 (7) Å, and Co–X = 1.898 Å and bond angles P–Co–P(mean) = 99.4 (4)° and P–Co–X 117.4° (X is the midpoint of the olefinic bond). The parameters and bonding of the (trimethyl phosphite)cobalt part of the complex are standard with a mean P–O distance of 1.594 (6) Å and indicates a certain degree of π bonding. The mean O–C bond length is 1.443 (12) Å; Co–P–O angles average to 117.1 (2)° and O–P–O to 100.6 (5)°. The bond lengths in the MA ring (with C_s symmetry) indicate strong π-electron delocalization, in accordance with the large decrease in ν(C=O) from 1780 and 1850 cm^{-1} in free MA to 1722 and 1787 cm^{-1} in the complex.

Introduction

Cobalt(0) complexes are catalytically active in hydrogenation, carbonylation, and oligo- and polymerization reactions. As part of the studies on the reactivity and structure of mononuclear d^9 metal complexes,[1-4] the intermediate I has been isolated and characterized.

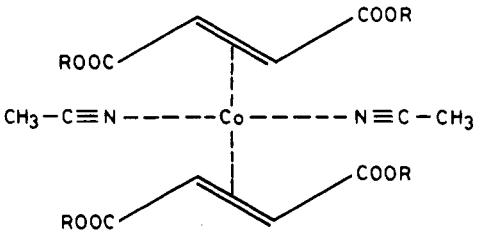

I

Various mono- and polynuclear complexes are easily formed by partial or total displacement in I,[5] as shown in Figure 1. Of particular interest is the synthetic route to compounds II and III, as cobalt complexes with phosphitic ligands are known to be extremely active and selective hydrogenation catalysts.[6-8] In the presence of unsaturated ligands, these complexes allow for electron delocalization that may lead to interesting properties in terms of activity and selectivity. The elucidation of the structures of such complexes is therefore useful not only in establishing the nature of the coordination around cobalt(0) but also in gaining a better insight into the role of the metal in catalysis. Since only rather few examples of mononuclear d^9 complexes of cobalt have been prepared[4,9-13] and in view of the paucity of molecular structural data,[4,12] an X-ray study of tris(trimethyl phosphite)(maleic anhydride)cobalt(0) (COCA) was undertaken.

Experimental Section

Preparation. COCA was prepared by the total ligand displacement reaction involving addition of 5.0 g (40 mmol) of trimethyl phosphite and 1.0 g (10 mmol) of maleic anhydride to 4.85 g (10 mmol) of a toluene solution (50 mL) of bis(ethyl fumarate)bis(acetonitrile)cobalt(0) under continuous stirring until complete dissolution of the anhydride:

$$Co(CH_3CN)_2L_2 + 3P(OCH_3)_3 + MA \rightarrow [P(OCH_3)_3]_3CoMA + 2L + 2CH_3CN$$

L = ethyl fumarate; MA = maleic anhydride

† Visiting Scientist at Istituto di Ricerche "G. Donegani".

(1) Agnès, G.; Chiusoli, C. P.; Cometti, G. *Chem. Commun.*, **1968**, 1515.
(2) Agnès, G.; Cometti, G. *Organomet. Chem. Synth.* **1970/1972**, *1*, 185.
(3) Agnès, G.; Santini, C., unpublished results.
(4) Agnès, G.; Bassi, I. W.; Benedicenti, C.; Intrito, R.; Calcaterra, M.; Santini, C. *J. Organomet. Chem.* **1977**, *129*, 401.
(5) Agnès, G.; Bart, J. C. J.; Santini, C.; Woode, K. A. *J. Am. Chem. Soc.* **1982**, *104*, 5254.
(6) Rakowski, M. C.; Muetterties, E. L. *J. Am. Chem. Soc.* **1977**, *99*, 739.
(7) Hirsekorn, F. J.; Rakowski, M. C.; Muetterties, E. L. *J. Am. Chem. Soc.* **1975**, *97*, 237.
(8) Gosser, L. W. *Inorg. Chem.* **1976**, *15*, 1348.
(9) Klein, H. F. *Angew. Chem., Int. Ed. Engl.* **1971**, *10*, 343.
(10) Chatt, J.; Hart, F. A.; Rosevear, D. T. *J. Chem. Soc.* **1961**, 5504.
(11) Kruck, T.; Lang, W. *Z. Anorg. Allg. Chem.* **1966**, *343*, 181.
(12) Ward, D. L.; Caughlan, C. N.; Voecks, G. E.; Jennings, P. W. *Acta Cyrstallogr., Sect. B* **1972**, *B28*, 1949.
(13) Klein, H. F. *Angew. Chem., Int. Ed. Engl.* **1980**, *19*, 362.

0276-7333/83/2302-0627$01.50/0

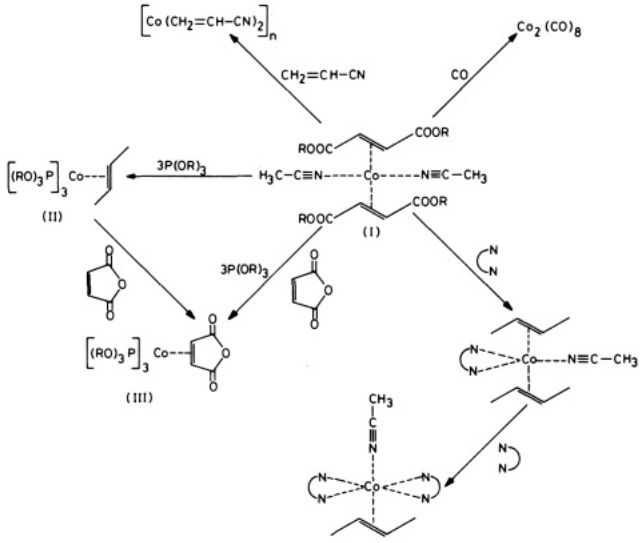

Figure 1. Various mono- and polynuclear complexes formed by partial or total displacement in I: N N, 1,10-phenanthroline; ⟍⟋, dialkylfumarate; R = CH_3, C_2H_5, $CH(CH_3)_2$.

After removal of the solvent under vacuum and repeated washing of the residue with *n*-hexane, 5.0 g of a dark red solid was obtained. The complex is air sensitive, and all manipulations were carried out in inert atmosphere; solvents were outgassed before use. The complex was recrystallized from toluene as dark red prisms in almost quantitative yield (mp 134–135 °C). Microanalytical data and cryoscopic determinations of the molecular weight in benzene are consistent with the above-mentioned mononuclear nature of the molecules. Considerable NMR line broadening shows that COCA is paramagnetic. The EPR spectrum of the powdered sample of COCA (at 298 K) shows a broad signal centered at $g_{iso} \approx 2.10$ due to the d^9 system with $s = {}^1/_2$.

X-ray analysis: $C_{13}H_{29}CoO_{12}P_3$: $M_r = 529.22$; monoclinic; $a = 9.517$ (4) Å, $b = 15.432$ (14) Å, $c = 16.915$ (8) Å, $\beta = 113.17$ (6)°; $V = 2283.9$ Å^3; $D_{calcd} = 1.54$ g·cm^{-1}; $Z = 4$; space group $P2_1/c$ (No. 14) from systematic absences (0*k*0) for *k* odd and (*h*0*l*) for *l* odd; $F(000) = 1100$.

Dark red crystals of COCA were examined in nitrogen-filled Lindemann glass capillary tubes. Accurate cell dimensions and an orientation matrix were determined by a least-squares fit of χ, ϕ, ω, and 2θ values of 12 independent reflections using a Picker FACS-1 four-circle diffractometer. Intensity data were collected with a parallelepiped crystal (0.4 × 0.4 × 0.7 mm) mounted with *b* along the ϕ axes of the diffractometer using Zr-filtered Mo Kα radiation, a 2θ scan rate of 1° min^{-1}, and scan range of 2.0–2.5° (for K($\alpha_1 - \alpha_2$) separation). Background counts of 10 s were measured at each end of every 2θ scan. Three standard reflections were monitored after every 50 reflections for scaling purposes; their intensities were constant throughout. Of the 4018 independent reflections measured (up to $2\theta = 50°$) 2726 were judged to be observed with $I \geq 2.5\sigma$ ($\sigma = [N_s + (t_s/t_b)^2 N_b]^{1/2}$, where N_s is the total peak count during the time of scanning, t_s, and t_b is the time spent in measuring the N_b background counts). An arbitrary intensity of 0.5 of the observable limit was assigned to each of the nonsignificant reflections. Intensities were corrected for Lorentz and polarization effects but not for absorption (μ(Mo Kα) = 10.65 cm^{-1}).

The structure was solved by direct methods (MULTAN[14]). The *E* map computed for the phase solution with the highest combined figure of merit gave the positions of the cobalt atom and most of the non-hydrogen atoms. The positions of the remaining atoms were obtained from a subsequent ΔF synthesis. Fully anisotropic refinement of all the non-hydrogen atoms gave an *R* factor of 0.074. H atoms were introduced in fixed positions, on stereochemical grounds (C–H = 1.0 Å) and in agreement with a ΔF synthesis. The *B* value of each H atom was set at 5.0 Å^2. Refinement converged to $R = 0.063$ for the 2726 observed reflections. The final shifts of the atomic parameters were negligible and all well below the corresponding σ. The final ΔF synthesis was also featureless.

Positional and thermal parameters of the non-hydrogen atoms were refined with the least-squares program of Immirzi.[15] Atomic scattering factors were calculated according to ref 16 and 17.

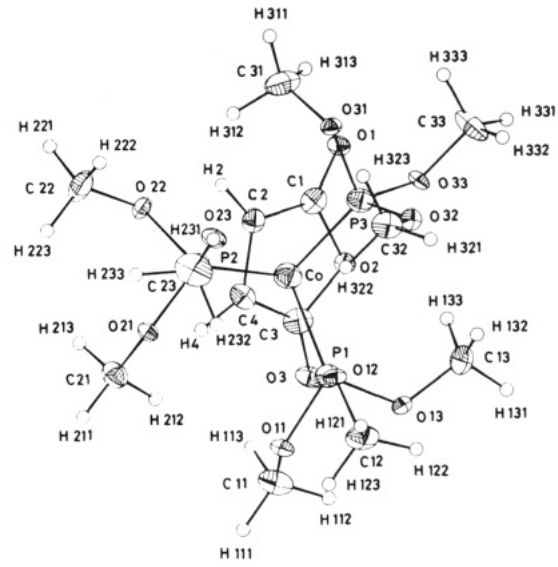

Figure 2. View of tris(trimethyl phosphite)(maleic anhydride)cobalt(0) indicating the atom labeling scheme and 30% probability thermal vibration ellipsoids.

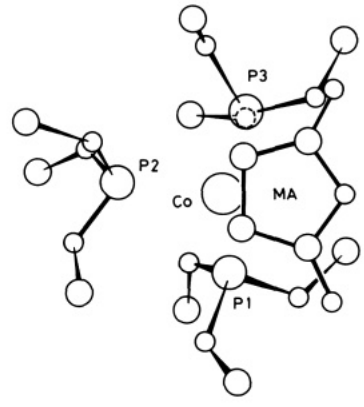

Figure 3. Molecular structure of tris(trimethyl phosphite)(maleic anhydride)cobalt(0) viewed onto the anhydride ligand plane. Principle distances to this plane: P(1), 3.12 Å; P(2), 1.84 Å; P(3), 3.15 Å; Co, 1.88 Å.

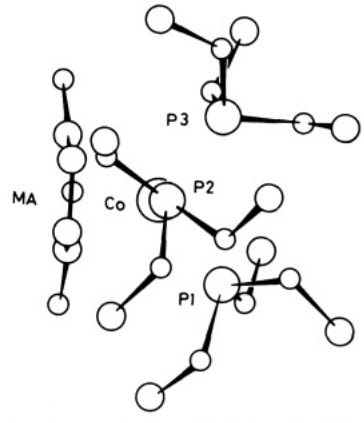

Figure 4. Molecular structure of tris(trimethyl phosphite)(maleic anhydride)cobalt(0) viewed onto the C(2)C(4)P(1)P(3) plane.

(14) Germain, G.; Main, P.; Woolfson, M. M. *Acta Crystallogr., Sect. A* **1971**, *A27*, 368.

(15) Immirzi, A. *Ric. Sci.* **1967**, *37*, 743.

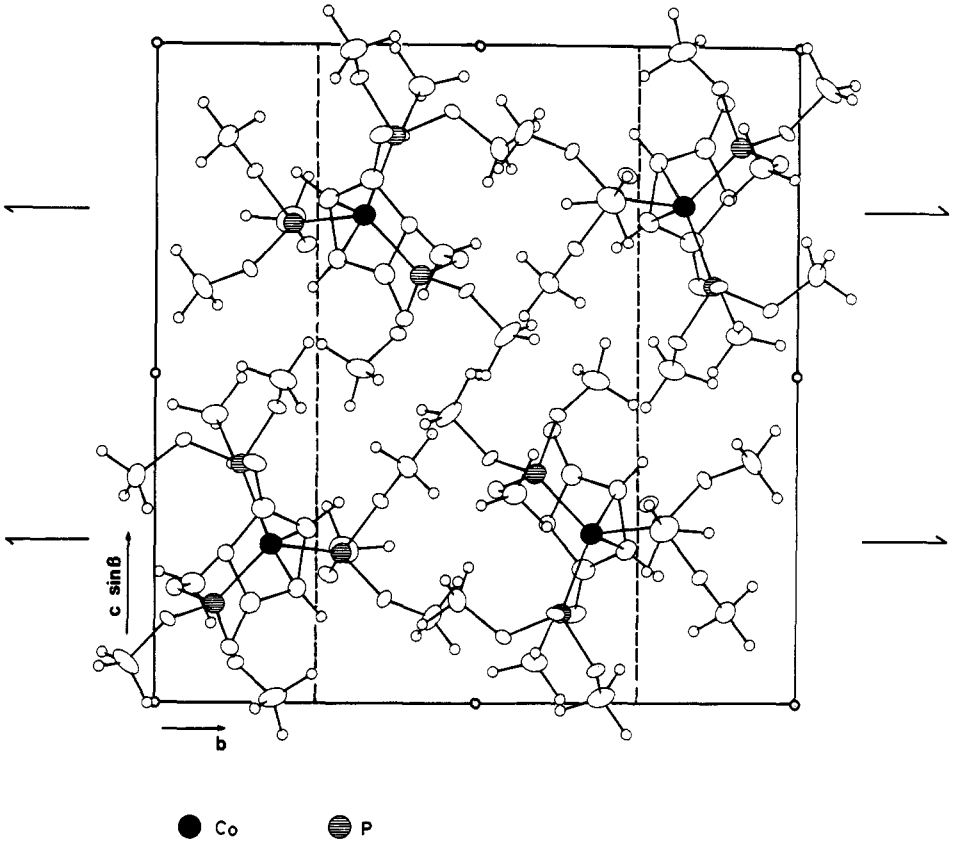

Figure 5. Packing arrangement of the tris(trimethyl phosphite)(maleic anhydride)cobalt(0) molecules viewed down the *a* axis.

Cruickshank's[18] weighting scheme, $1/w = A + B|F_o| + C|F_o|^2$, was used, where $A = 2F_o(\text{min})$, $B = 1.0$, and $C = 2/F_o(\text{max})$. The final coordinates are listed in Table I and the bond lengths and angles in Table II. Figures 2–4 show views of COCA, together with the labeling scheme and the thermal vibration ellipsoids of the non-hydrogen atoms.[19] The packing of the structure components in the unit cell is shown in Figure 5.

Results and Discussion

The crystal structure of COCA consists in the packing of discrete mononuclear molecules separated by van der Waals forces (Figure 5). The cobalt metal is linked to the three phosphorus atoms of the trimethyl phosphite groups and the $CH_2{=}CH_2$ moiety of the maleic anhydride unit (Figure 2).

The molecular structure (C_1 symmetry) consists of a pseudotetrahedrally coordinated Co atom, assuming one coordination site for the olefinic ligand, with the olefin plane nearly perpendicular to C(2), C(4), P(1), and P(3) (Figure 4). The mean Co–P bond length of 2.172 (2) Å (range 2.153–2.198 Å) agrees with that of the mononuclear hydridodinitrogentris(triphenylphosphine)cobalt(I) complex (2.167 Å)[20] and is at the lower bound of the usual Co–P range (2.05–2.55 Å), denoting strong π bonding. The fact that the Co–P bond is significantly (about 0.1 Å) shorter than the analogous metal–phosphine bond is rationalized either by π-bonding capability of the phosphite ligand being greater than that of phosphine ligands[21] or by the minor steric requirements as compared to phosphines.[22] The mean Co–C(olefinic) distance of 2.033 (7) Å (Co–X of 1.898 Å; X is the midpoint of the olefinic bond) is close to the values of 2.060 (9) and 2.084 (4) Å of bis(ethyl fumarate)bis(acetonitrile)cobalt(0)[4] and *trans*-bis(μ-carbonyl)bis(π-2,3-*cis*-dimethylbutadiene)carbonylcobalt,[23] respectively, and within the usual range of 1.90–2.10 Å for π bonding.

The mean bond angles P–Co–P and P–Co–X are 99.4 (4) and 117.4°, respectively. Nearly tetrahedral symmetry is known for some cobalt(0) complexes such as dicarbonylnitrosyl(triphenylphosphine)cobalt(0)[12] in which the metal forms σ bonds. In this case the Co–P distance is significantly larger (2.224 (1) Å) than in COCA (2.172 (2) Å), where the metal forms one π and three σ bonds. Angular distortions around cobalt depend on the π-accepting abilities of the ligand and the nonbonded repulsions. The latter are smaller for the nonbulky $P(OCH_3)_3$. Typical short values are P(2)···C(2) = 3.30 Å, P(2)···C(4) = 3.34 Å, P(3)···C(1) = 3.46 Å, O(22)···H(312) = 2.49 Å, and H(212)···H(113) = 2.53 Å.

Viewing down the maleic anhydride (MA) plane (Figure 3), the coordination of COCA may also be described as a deformed tetragonal pyramid with an apical trimetyl phosphite ligand and the Co atom 0.37 Å out of the basal plane. This formal description requires a difference in apical and basal Co–P bonds, contrary to the observations. A difficulty with a model involving a "metallacyclopropene" unit

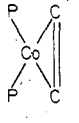

is also the ambiguity of oxidation states arising from the

(16) Vand, A.; Eiland, P. E.; Pepinsky, R. *Acta Crystallogr.* **1957**, *10*, 303.
(17) Moore, F. H. *Acta Crystallogr.* **1963**, *16*, 1169.
(18) Cruickshank, D. W. J.; Pilling, D. E.; Bujosa, A.; Lovell, F. M.; Truter, M. R. "Computing Methods and the Phase Problem in X-ray Crystal Analysis"; Pergamon Press: Oxford, 1961; p 32.
(19) Johnson, C. K. ORTEP, Report ORNL-3794; Oak Ridge National Laboratory: Oak Ridge, TN, 1970.
(20) Davis, B. R.; Payne, N. C.; Ibers, J. A. *Inorg. Chem.* **1969**, *8*, 2719.
(21) Verkade, J. G. *Coord. Chem. Rev.* **1972**, *9*, 1.
(22) Kirchner, R. M.; Ibers, J. A.; *Inorg. Chem.* **1974**, *13*, 1667.
(23) Stephens, F. S. *J. Chem. Soc. A* **1970**, 2745.

Table I. Final Fractional Coordinates with Estimated Standard Deviations in Parentheses

atom	x	y	z
Co	0.12407 (9)	0.82079 (6)	0.75886 (5)
P(1)	0.11812 (20)	0.86814 (12)	0.63783 (11)
P(2)	0.27838 (19)	0.71077 (12)	0.77202 (11)
P(3)	0.28434 (19)	0.90865 (12)	0.84979 (11)
O(11)	0.0384 (6)	0.8120 (4)	0.5509 (3)
O(12)	0.2821 (6)	0.8762 (4)	0.6364 (3)
O(13)	0.0326 (7)	0.9572 (4)	0.6012 (3)
O(21)	0.2658 (5)	0.6506 (3)	0.6928 (3)
O(22)	0.2707 (7)	0.6439 (3)	0.8424 (4)
O(23)	0.4565 (6)	0.7312 (4)	0.8051 (4)
O(31)	0.4059 (6)	0.8743 (4)	0.9397 (3)
O(32)	0.3970 (6)	0.9702 (4)	0.8257 (4)
O(33)	0.1887 (5)	0.9804 (3)	0.8735 (3)
C(11)	−0.1210 (11)	0.8034 (7)	0.5095 (6)
C(12)	0.3107 (11)	0.9088 (7)	0.5630 (6)
C(13)	0.0477 (12)	1.0302 (6)	0.6562 (6)
C(21)	0.1214 (9)	0.6098 (6)	0.6406 (5)
C(22)	0.3730 (13)	0.5704 (6)	0.8694 (7)
C(23)	0.5590 (10)	0.7067 (8)	0.7669 (7)
C(31)	0.3666 (13)	0.8158 (8)	0.9924 (6)
C(32)	0.5345 (9)	0.9412 (6)	0.8190 (6)
C(33)	0.2584 (11)	1.0446 (7)	0.9389 (7)
O(1)	−0.0543 (7)	0.8836 (4)	0.9166 (4)
O(2)	−0.1766 (6)	0.8901 (4)	0.7737 (3)
O(3)	−0.3001 (6)	0.8471 (5)	0.6365 (4)
C(1)	−0.0684 (8)	0.8524 (5)	0.8493 (5)
C(2)	0.0002 (8)	0.7794 (5)	0.8263 (5)
C(3)	−0.1964 (8)	0.8324 (6)	0.7045 (5)
C(4)	−0.0820 (8)	0.7656 (5)	0.7346 (5)
H(111)	−0.149	0.764	0.453
H(112)	−0.172	0.867	0.490
H(113)	−0.166	0.775	0.552
H(121)	0.431	0.907	0.577
H(122)	0.268	0.974	0.548
H(123)	0.251	0.868	0.507
H(131)	−0.019	1.084	0.620
H(132)	0.167	1.049	0.687
H(133)	0.008	1.013	0.706
H(211)	0.135	0.571	0.590
H(212)	0.035	0.659	0.611
H(213)	0.084	0.568	0.680
H(221)	0.353	0.533	0.918
H(222)	0.493	0.593	0.897
H(223)	0.361	0.529	0.815
H(231)	0.672	0.731	0.804
H(232)	0.520	0.734	0.702
H(233)	0.562	0.637	0.762
H(311)	0.465	0.801	1.050
H(312)	0.323	0.756	0.957
H(313)	0.278	0.844	1.010
H(321)	0.591	0.994	0.802
H(322)	0.507	0.891	0.769
H(323)	0.611	0.913	0.879
H(331)	0.176	1.087	0.946
H(332)	0.342	1.082	0.925
H(333)	0.320	1.011	1.001
H(2)	0.097	0.742	0.870
H(4)	−0.064	0.715	0.695

convention of regarding σ-bonded alkyl groups as carbanions in assigning formal oxidation states. According to this convention, COCA is to be regarded as a Co(II) complex, contrary to XPS results which indicate that assignment of a Co(0) oxidation state is more appropriate.

The geometry of trimethyl phosphite ligands is heavily restricted by the metal binding site and conformations with methyl groups oriented toward the top of the phosphorus pyramid are excluded.[24] The asymmetric ligands of COCA exhibit two different "two down and one up" arrangements, which are some of the five distinct conformations usually observed in the solid state. In both cases the point symmetry is C_1 instead of C_3, C_s, or the experimentally unobserved C_{3v}. While the conformation of the P(2) ligand is one of the eight most stable forms in the free state, the conformation of the P(1) and P(3) phosphites is energetically unfavorable in the isolated molecule. Minor differences in the conformations around P(1) and P(3) are probably on account of packing requirements.

The mean distances of the P and Co atoms to the phosphite oxygen planes are 0.725 Å (range 0.715–0.735 Å) and 2.880 Å (range 2.865–2.895 Å), respectively. The metal is displaced "off-center" by 0.34 Å on the average in the direction of those carbon atoms (C(12), C(22), and C(33)) that are most out of the oxygen plane (1.44 Å on average). With the trivalent phosphorus coordination being pseudotetrahedral, the Co–P–O and O–P–O angles are related, and as usual the mean Co–P–O angle is larger (117.1°) and the O–P–O angle (100.6°) smaller than 109.5 Å. The latter is in good agreement with the standard value (101.4°).[24]

Although complexation determines the conformation of the $P(OCH_3)_3$ ligands (defines the torsional angles), average bond lengths and angles in the phosphitic ligands in COCA are not significantly different from those observed in other trimethyl phosphites and also are close to the related orthophosphate esters, gaseous $P(OEt)_3$, and strain-free P_4O_6, with the crystal structure of $P(OCH_3)_3$ being unknown (Table III). Yet, MNDO calculations[24] indicate that complexation affects these parameters slightly, leading to some C–O lengthening.

The P–O bonds of the phosphite ligands (1.595 Å) exhibit double-bond character and are shorter than the P–C bonds in triphenylphosphorous (1.828 Å)[28] and dicarbonylnitrosyl(triphenylphosphine)cobalt(0) (1.821 Å)[12] by an amount that cannot be accounted for only by the difference in covalent radii of O (0.66 Å) and C (0.77 Å) atoms. Therefore, the P–O lengths fall short of the theoretical single-bond value of 1.73 Å.[29] On the basis of the relation between bond order and P(V)–O bond lengths,[30] applicable for P(III) compounds after a slight correction (about 0.05 Å), a π-bond order of about 0.4 is derived for the P–O bonds of COCA.

The mean O–C bond length of 1.443 (12) Å and P–O–C angle of 122.9 (4)° in COCA are in good agreement with the usual values of 1.440 Å and 124.0° in $P(OCH_3)_3$ complexes.[24] As in $Ru(CO)_4[P(OCH_3)_3]$[31] and other crystal structures with disordered $P(OCH_3)_3$ groups,[22,32-35] the analysis of COCA suffered because of some disorder in the $O-CH_3$ arms of the phosphite ligands, as reflected in the relatively high-temperature factors for the carbon atoms of the ligands (see supplementary material).

Crystallographic evidence for strong cobalt–maleic anhydride interaction in COCA is given by a considerable conformational change of the MA ring compared to the

(24) Bart, J. C. J.; Favini, G.; Todeschini, R., submitted for publication in *Phosphorus Sulfur*.
(25) Corbridge, D. E. C. "The Structural Chemistry of Phosphorus"; Elsevier: Amsterdam, 1974; p 264.
(26) Cruickshank, D. W. J. *Acta Crystallogr.* **1964**, *17*, 675.
(27) Reference 25; p 201.
(28) Daly, J. J. *J. Chem. Soc.* **1964**, 3799.
(29) Pauling, L. "The Nature of the Chemical Bond"; Cornell University Press: Ithaca, NY, 1960; p 321.
(30) Cruickshank, D. W. J. *J. Chem. Soc.* **1961**, 5486.
(31) Cobbledick, R. E.; Einstein, F. W. B.; Pomeroy, R. K.; Spetch, E. R. *J. Organomet. Chem.* **1980**, *195*, 77.
(32) Drew, M. G. B.; Wilkins, J. D. *J. Chem. Soc. Dalton Trans.* **1975**, 1984.
(33) Love, R. A.; Chin, H. B.; Koetzle, T. F.; Kirtley, S. W.; Whittlesey, B. R.; Bau, R. *J. Am. Chem. Soc.* **1976**, *98*, 4491.
(34) Teller, R. G.; Wilson, R. D.; McMullan, R. K.; Koetzle, T. F.; Bau, R. *J. Am. Chem. Soc.* **1978**, *100*, 3071.
(35) Cann, K.; Riley, P. E.; Davis, R. E.; Pettit, R. *Inorg. Chem.* **1978**, *17*, 1421.

Table II. Bond Distances (Å) and Angles (deg) with Esd's in Parentheses

Bond Distances

Co-P(1)	2.153 (2)	P(1)-O(11)	1.616 (6)	O(11)-C(11)	1.405 (14)
Co-P(2)	2.198 (2)	P(1)-O(12)	1.575 (6)	O(12)-C(12)	1.461 (11)
Co-P(3)	2.164 (2)	P(1)-O(13)	1.593 (7)	O(13)-C(13)	1.432 (10)
Co-P[a]	2.172 (2)	P(2)-O(21)	1.596 (5)	O(21)-C(21)	1.452 (12)
		P(2)-O(22)	1.598 (7)	O(22)-C(22)	1.447 (14)
Co-C(2)	2.039 (7)	P(2)-O(23)	1.594 (7)	O(23)-C(23)	1.417 (10)
Co-C(4)	2.027 (8)	P(3)-O(31)	1.596 (8)	O(31)-C(31)	1.419 (13)
Co-C[a]	2.033 (7)	P(3)-O(32)	1.601 (6)	O(32)-C(32)	1.429 (10)
Co-X[b]	1.898	P(3)-O(33)	1.582 (5)	O(33)-C(33)	1.437 (12)
		P-O[a]	1.594 (6)	O-C[a]	1.443 (12)
C(2)=C(4)	1.451 (14)				
O(2)-C(1)	1.413 (13)	C(1)-C(2)	1.431 (10)	O(1)=C(1)	1.193 (10)
O(2)-C(3)	1.423 (14)	C(3)-C(4)	1.439 (13)	O(3)=C(3)	1.207 (14)
O-C[a]	1.418 (14)	C-C[a]	1.435 (13)	O=C[a]	1.200 (12)
		Co···H(2)	2.337 (1)		
		Co···H(4)	2.347 (1)		

Bond Angles

Co-P(1)-O(11)	120.7 (2)	P(1)-Co-C(2)	146.5 (4)	P(1)-O(11)-C(11)	122.1 (5)
Co-P(1)-O(12)	112.7 (2)	P(1)-Co-C(4)	106.8 (2)	P(1)-O(12)-C(12)	123.9 (4)
Co-P(1)-O(13)	118.7 (3)	P(2)-Co-C(2)	102.2 (1)	P(1)-O(13)-C(13)	121.4 (4)
Co-P(2)-O(21)	122.6 (2)	P(2)-Co-C(4)	104.5 (2)	P(2)-O(21)-C(21)	120.2 (4)
Co-P(2)-O(22)	110.5 (2)	P(3)-Co-C(2)	101.5 (1)	P(2)-O(22)-C(22)	121.3 (5)
Co-P(2)-O(23)	117.3 (2)	P(3)-Co-C(4)	139.7 (3)	P(2)-O(23)-C(23)	127.9 (4)
Co-P(3)-O(31)	120.9 (3)			P(3)-O(31)-C(31)	122.6 (5)
Co-P(3)-O(32)	123.1 (2)	O(11)-P(1)-O(12)	98.1 (2)	P(3)-O(32)-C(32)	124.1 (4)
Co-P(3)-O(33)	107.7 (2)	O(11)-P(1)-O(13)	97.0 (2)	P(3)-O(33)-C(33)	122.7 (4)
Co-P-O[a]	117.1 (2)	O(12)-P(1)-O(13)	106.4 (2)	P-O-C[a]	122.9 (4)
		O(21)-P(2)-O(22)	103.8 (2)		
Co-C(2)-C(1)	109.3 (3)	O(21)-P(2)-O(23)	97.2 (2)	O(1)=C(1)-O(2)	117.7 (3)
Co-C(4)-C(2)	69.6 (4)	O(22)-P(2)-O(23)	102.7 (2)	O(3)=C(3)-O(2)	117.5 (4)
Co-C(2)-C(4)	68.6 (4)	O(31)-P(3)-O(32)	97.6 (2)	O=C-O[a]	117.6 (4)
Co-C(4)-C(3)	107.9 (4)	O(31)-P(3)-O(33)	105.3 (2)		
		O(32)-P(3)-O(33)	99.1 (2)	O(1)=C(1)-C(2)	133.2 (4)
P(1)-Co-P(2)	97.1 (4)	O-P-O[a]	100.6 (2)	O(3)=C(3)-C(4)	133.8 (5)
P(1)-Co-P(3)	102.1 (4)			O=C-C[a]	133.5 (5)
P(2)-Co-P(3)	98.9 (4)	C(1)-C(2)=C(4)	107.1 (3)		
P-Co-P[a]	99.4 (4)	C(3)-C(4)=C(2)	106.7 (4)	O(2)-C(1)-C(2)	109.0 (4)
		C-C=C[a]	106.9 (4)	O(2)-C(3)-C(4)	108.7 (3)
P(1)-Co-X[b]	126.9			O-C-C[a]	108.9 (4)
P(2)-Co-X	104.3	C(1)-O(2)-C(3)	107.5 (4)		
P(3)-Co-X	120.9				
P-Co-X[a]	117.4				

[a] This is the mean distance or mean angle. [b] X is the midpoint of C=C.

Table III. Geometry around Phosphorous

compound	⟨P-O⟩, Å	⟨O-C⟩, Å	⟨O-P-O⟩, deg	⟨P-O-C⟩, deg	ref
$[CHC(O)]_2OCo[P(OCH_3)_3]_3$	1.595	1.443	100.6	122.9	this work
$P(OC_2H_5)_3$	1.600	1.42	96	120	25
$P(OCH_3)_3$ complexes	1.583	1.440	101.4	124.0	24
P_4O_6	1.638		100		26
substituted phosphates	1.590	1.44	100	116	27

free anhydride,[36] electron delocalization in the ligand and the Co–C(olefin) distance of 2.033 Å. (The distance of cobalt to the maleic anhydride plane is 1.88 Å). The MA ring symmetry changes from C_{2v} in the free anhydride to an idealized C_s configuration in COCA. The deformation results from the two carbonyl groups bending out of the mean plane of the ring away from the metal atom by an average of 0.2 Å (see Figure 4 and Table IV). Similar distortions have previously been observed, *e.g.*, in cyclopentadienyl(duroquinone)cobalt dihydrate.[37] Free MA is only slightly nonplanar with the ring oxygen atom 0.03 Å out of the plane of the other atoms.[36]

In the absence of any significant differences between the chemically equivalent bond data in free MA[36] and in various compounds containing maleic anhydride such as COCA, tricarbonyl(2,3-bis(diphenylphosphino)maleic anhydride)cobalt (COCAMB),[38] tricarbonyl(2,3-bis(diphenylphosphino)maleic anhydride)iron (FECAMB),[38] diiodo(2,3-bis(diphenylphosphino)maleic anhydride)nickel(II) 1,2-dichloroethane solvate (NICAMB),[39] 2,3-bis(diphenylstibino)maleic anhydride (STIMA),[40] and various diadducts,[41-50] we shall discuss the dimensions of MA in

(36) Marsh, R. E.; Ubell, E.; Wilcox, H. E.; *Acta Crystallogr.* **1962**, *15*, 35.
(37) Utchman, V. A.; Dahl, L. F. *J. Organomet. Chem.* **1972**, *40*, 403.
(38) Fenske, D. *Chem. Ber.* **1979**, *112*, 363.
(39) Becher, H. J.; Bensmann, W.; Fenske, D. *Chem. Ber.* **1977**, *110*, 315.
(40) Fenske, D.; Teichert, H.; Prokscha, H.; Renz, W.; Becher, H. J. *J. Monatsh, Chem.* **1980**, *111*, 177.
(41) Filippini, G.; Gramaccioli, C. M.; Rovere, C. Simonetta, M. *Acta Crystallogr., Sect. B.* **1972**, *B28*, 2869.
(42) Destro, R.; Filippini, G.; Gramaccioli, C. M.; Simonetta, M. *Acta Crystallogr., Sect. B* **1971**, *B27*, 2023.
(43) Craig, R. E. R.; Craig, A. C.; Larsen, R. D.; Caughlan, C. N. *J. Org. Chem.* **1977**, *42*, 3188.
(44) Caglioti, L.; Foresti, E.; Riva di Sanseverino, L. *Tetrahedron Lett.* **1970**, *16*, 1347.

Table IV. Planarity of Groups of Atoms in the Structure[a]

Plane 1			
$0.806x + 0.566y - 0.173z - 0.131 = 0$			
O(2)	0.057 (6)	C(1)	−0.050 (8)
C(2)	0.024 (8)	C(3)	−0.042 (9)
C(4)	0.011 (8)		
Not Defining the Plane			
Co	1.879 (1)	O(1)	−0.211 (7)
O(3)	−0.162 (7)	P(1)	3.221 (2)
P(2)	1.996 (2)	P(3)	3.144 (2)
Plane 2			
$0.980x + 0.182y - 0.085z + 1.470 = 0$			
P(1)	0.000 (2)	P(2)	0.000 (2)
P(3)	0.000 (2)		
Not Defining the Plane			
Co	−1.027 (1)	C(2)	−2.827 (8)
C(4)	−2.913 (8)		

Dihedral Angles between Planes: Plane 1-Plane 2 = 24.9°

[a] Equations of the least-squares planes are expressed in a^*bc orthogonal space as $Px + Qy + Rz - S = 0$. The distances of the atoms from the planes are in Å.

these compounds in terms of the average of the observed values (Table V). The C=C distance in COCA (1.451 Å) is significantly larger than that of 1.303 Å in MA,[36] 1.325–1.386 Å in several metal complexes, and 1.33 Å in ethylene,[51] which is usually chosen as the normal C=C bond, and indicates a weakening of the double bond. Yet, the bond is considerably stronger than the observed single bonds in several diadducts (Table V). The mean C–C bond distance in COCA is among the shortest and is significantly less than the value of 1.470 Å in free MA,[36] indicating a considerable degree of π-double-bond character. Further evidence for the greater double-bond character of the C(1)–C(2) and C(3)–C(4) bonds in COCA compared to free MA[36] is given by the external bond angles at C(1) and C(3): the O=C—O angles are 16° smaller than the O=C—C angles as compared to 11° in free MA. The mean C–O bond length within the ring of COCA (1.418 Å) is longer than in MA (1.388 Å) and is an extreme value. The mean C=O bond (1.200 Å) is slightly longer than in the free ligand (1.189 Å). The changes in the bond angles are less pronounced than in case of the diadducts. The variations in the dimensions of the ring of COCA as compared to MA and the other complexes indicate strong electron delocalization which is achieved even though cobalt is located sideways with respect to the ligand (Figure 3) and is not at all involved in any short contacts to the C=O part. The out-of-plane tipping of the carbonyl oxygen atoms (Figure

Table V. Comparison of Mean Bond Distances (Å) and Angles (deg) in Maleic Anhydride and Its Adducts

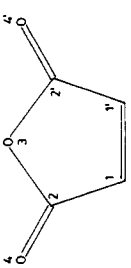

compd[a]	11′	12	24	23	1′12	124	324	123	232′	ref
MA	1.303 (5)	1.470 (5)	1.189 (5)	1.388 (5)	108.5 (10)	131.6 (10)	120.7 (10)	107.7 (10)	107.5 (10)	36
COCA	1.451 (14)	1.435 (11)	1.200 (12)	1.418 (11)	106.9 (4)	133.5 (5)	117.6 (4)	108.9 (4)	107.5 (4)	this work
FECAMB	1.325 (4)	1.497 (5)	1.185 (5)	1.395 (5)						38
NICAMB	1.33 (1)	1.50 (1)	1.17 (1)	1.40 (1)						39
STIMA	1.338 (8)	1.504 (8)	1.185 (8)	1.402 (8)	108.2 (...)	131.8 (...)	120.9 (...)	107.3 (...)	108.9 (...)	40
COCAMB	1.386 (5)	1.435 (5)	1.209 (5)	1.417 (5)						38
diadducts	1.528 (6)	1.502 (6)	1.193 (6)	1.385 (6)	104.3 (6)	129.9 (6)	119.6 (6)	110.4 (6)	110.3 (6)	41–50

[a] Abbreviations: MA, maleic anhydride; COCA, tris(trimethyl phosphite)(maleic anhydride)cobalt(0); FECAMB, tricarbonyl(2,3-bis(diphenylphosphino)maleic anhydride)iron; NICAMB, diiodo(2,3-bis(diphenylphosphino)maleic anhydride)nickel(II) 1,2-dichloroethane solvate; STIMA, bis(diphenylstibino)maleic anhydride; COCAMB, tricarbonyl(2,3-bis(diphenylphosphino)maleic anhydride)cobalt.

(45) Craig, R. E. R.; Craig, A. C.; Larsen, R. D.; Caughlan, C. N. *J. Org. Chem.* **1976**, *41*, 2129.
(46) Baggio, S.; Barriola, A.; de Perazzo, P. K. *J. Chem. Soc., Perkin Trans. 2* **1972**, 934.
(47) Cameron, A. F.; Ferguson, G. *J. Chem. Soc. B* **1970**, 943.
(48) Destro, R.; Filippini, G.; Gramaccioli, C. M.; Simonetta, M. *Acta Crystallogr., Sect. B* **1969**, *B25*, 2465.
(49) Filippini, G.; Induni, G.; Simonetta, M. *Acta Crystallogr. Sect. B* **1973**, *B29*, 2471.
(50) Murray-Rust, P.; Murray-Rust, J. *Acta Crystallogr., Sect. B* **1977**, *B33*, 3929.
(51) Bartell, L. S.; Bonham, R. A. *J. Chem. Phys.* **1957**, *27*, 1414.
(52) Otsuka, S.; Yoshida, T.; Tatsuno, Y. *J. Am. Chem. Soc.* **1971**, *93*, 6462.
(53) Tolman, C. A.; Seidel, W. C. *J. Am. Chem. Soc.* **1974**, *96*, 2774.
(54) Yamamoto, T.; Yamamoto, A.; Ikeda, S. *J. Am. Chem. Soc.* **1971**, *93*, 3350.
(55) Weiss, E.; Stark, K.; Lancaster, J. E.; Murdoch, H. D. *Helv. Chim. Acta* **1963**, *46*, 288.
(56) Weiss, E.; Stark, K. *Z. Naturforsch., Sect. B: Anorg. Chem., Org. Chem., Biochem., Biophys. Biol.* **1965**, *20B*, 490.
(57) Cenini, S.; Ugo, R.; Monica, G. L. *J. Chem. Soc. A* **1971**, 409.

Table VI. C=O Stretching Frequencies in Maleic Anhydride and Its Metal Complexes[a]

compd	ν(C=O), cm^{-1}	ref
MA	1850, 1780 (Nujol mull)	this work
(MA)Co(P(OCH$_3$)$_3$)	1787, 1722 (Nujol mull)	this work
(MA)Pd(*t*-BuNC)$_2$	1805, 1732 (Nujol mull)	52
(MA)Ni(*t*-BuNC)$_2$	1799, 1730 (Nujol mull)	52
(MA)Ni[P(O-*o*-tolyl)$_3$]$_2$	1805, 1733 (CH$_2$Cl$_2$)	53
MA	1845, 1777 (CH$_2$Cl$_2$)	53
(MA)$_2$Ni(bpy)	1815, 1730 (KBr)	54
(MA)Fe(CO)$_4$	1824, 1746 (KBr)	55
(MA)$_2$Ni	1810, 1730 (KBr)	56
(MA)Pt[PPh$_3$]$_2$	1800, 1725 (CHCl$_2$)	57
MA	1850, 1770 (CHCl$_3$)	57

[a] Abbreviation: MA, maleic anhydride. The table indicates that the frequency in an olefin-bonded MA complex is lower than in free MA and decreases as the back-donation from the metal increases.

4) is likely to be the result of an effect that is essentially electronic in origin. The extensive degree of electron delocalization, which causes the major bond length variations, probably leads to this distortion.

Stabilization of the complex is accomplished in part by an electron transfer from the metal to give aromatic character. The bonding between cobalt and maleic anhydride arises primarily from interactions between the highest occupied molecular orbital (HOMO) of the olefin and the lowest unoccupied molecular orbital (LUMO) of Co[P(OCH$_3$)$_3$]$_3$ and between the HOMO of the Co[P(OCH$_3$)$_3$]$_3$ and π^* LUMO of maleic anhydride. The former interaction can be considered as the donation of olefin π electrons to the metal and the latter as the back-donation from a d orbital of the metal to the olefin π^* orbital. The effect is confirmed indirectly by the relatively small decrease of the C=O stretching frequencies from 1780 and 1850 cm^{-1} in free MA to 1722 and 1787 cm^{-1} in COCA. Similar features of lower C=O stretching frequencies in complexes compared to free MA have been observed before (see Table VI). There exists an approximate linear relationship between ν(C=O) and the electron affinity of the unsaturated ligand.[58,59] Infrared spectral evidence thus confirms that the C=O groups are not directly involved in π coordination in COCA as otherwise the shifts in ν(C=O) would be much higher.[60,61] This is also in accordance with the greater mean distance of Co–C(O) of 2.838 Å as compared to Co–X of 1.898 Å (X is midpoint of C=C). This differs greatly from cyclopentadienyl(duroquinone)cobalt dihydrate,[37] where the metal is symmetrically located with respect to the ligand and interacts with the π orbitals of the carbonyl groups. In this compound Co–X and Co–C(O) bond distances are 1.984 and 2.370 Å; the carbonyl bond is stretched to 1.282 Å.

The bonding properties of many previously synthesized MA complexes (see Table VI) are probably similar to those observed in COCA. In the complexes of Pd(0)[52] and Pt(0)[57] we notice ν(C=O) shifts of ca. 50 cm^{-1} as compared to about 60 cm^{-1} in COCA. It is then reasonable to suppose that the carbonyl group is again only indirectly involved in bonding to these metals.

Cenini et al.[57] have suggested that the reduction of ν(C=O) of olefins with conjugated carbonyl groups provides a measure of metal–olefin π bonding. The electronic effect of the C=O substituents of the metal–olefin geometry is consistent with the σ–π formalism[62,63] for metal–olefin bonding. In this interpretation, the C=O group lowers the olefin π^* orbital energy promoting dπ–π^* donation from the cobalt atom. Increased population of the π^* olefin orbital decreases the C=C bond order and usually leads to a shift of about 150 cm^{-1} to 1450–1500 cm^{-1} of the infrared band related to the double bond. This band was not clearly identified in COCA (assignment was difficult due to the presence of other bands). However, the change in the double bond character in the olefin is expressed indirectly by the shift of the ν(C=O) bands, as occurs also in other complexes such as MAFe(CO)$_4$[55] and [Pt(PPh$_3$)$_2$MA].[57]

Electron-withdrawing olefins such as MA (with an high Alfrey-Price *e* value[64]) give complexes with correspondingly higher frequencies of the charge-transfer bands, and hence the lowering of the d orbital energy levels is indicated. In case of MA, back-donation causes considerable charge transfer accompanied by oxidation of cobalt and the resulting complex becomes paramagnetic. Therefore, we consider cobalt in COCA to be only formally zero valent. Electron-withdrawing substituents such as C=O on the olefin stabilize the π bond formed by the latter with the zero-valent metal.

A survey of the short intermolecular contacts in the structure (Co···H(2) = 2.337 (1) Å and Co···H(4) = 2.347 (1) Å) indicates that they conform to normal Van der Waals interactions.

Registry No. I (R = Et), 63372-41-8; III, 82555-94-0.

Supplementary Material Available: A table of anisotropic thermal parameters and a listing of structure factor amplitudes (18 pages). Ordering information is given on any current masthead page.

(58) Scott, R. N.; Shriver, D. F.; Vaska, L. *J. Am. Chem. Soc.* **1968**, *90*, 1079.
(59) Baddley, W. H. *J. Am. Chem. Soc.* **1968**, *90*, 3705.
(60) Fritz, H. P.; Schrauzer, G. N. *Chem. Ber.* **1961**, *94*, 650.
(61) King, R. B.; Fronzaglia, A. *Inorg. Chem.* **1966**, *5*, 1837.
(62) Dewar, M. J. S. *Bull. Soc. Chim. Fr.* **1951**, *18*, C79.
(63) Chatt, J.; Duncanson, L. A. *J. Chem. Soc.* **1953**, 2939.
(64) Brandrup, J.; Immergut, E. H. "Polymer Handbook"; Interscience: New York, 1966; Vol. II, p 341.

Addition compounds of alkali-metal hydrides. 23. Preparation of potassium triisopropoxyborohydride in improved purity

Herbert C. Brown, Behrooz Nazer, and James A. Sikorski

Organometallics, **1983**, 2 (5), 634-637• DOI: 10.1021/om00077a011 • Publication Date (Web): 01 May 2002

Addition Compounds of Alkali-Metal Hydrides. 23. Preparation of Potassium Triisopropoxyborohydride in Improved Purity

Herbert C. Brown,* Behrooz Nazer,[1a] and James A. Sikorski[1b]

Richard B. Wetherill Laboratory, Purdue University, West Lafayette, Indiana 47907

Received August 4, 1982

Commercial potassium triisopropoxyborohydride, $K(i\text{-PrO})_3BH$, or the usual material prepared at 25 °C from potassium hydride and triisopropoxyborane in tetrahydrofuran contains a significant impurity, detectable in the ^{11}B NMR spectrum. This impurity, probably potassium tetraisopropoxyborohydride, significantly decreases the yield when the reagent is used to hydride thexylmonoalkylchloroboranes, $ThxBR_1Cl$, for the synthesis of "mixed" thexyldialkylboranes. This impurity can be removed by refluxing a THF solution of the impure potassium triisopropoxyborohydride over potassium hydride. Alternatively, the reaction of triisopropoxyborane with excess KH in refluxing THF gives a product essentially free of the impurity. Storage of the solution KIPBH over a small excess of potassium hydride (~10%) maintains the product essentially free of the impurity. Use of this material permits the preparation of essentially quantitative yields of the desired "mixed" thexyldialkylboranes, $ThxBR_1R_2$, via the hydridation of the intermediate $ThxBR_1Cl$ in the presence of a second olefin.

Early attempts to prepare the lithium and sodium triisopropoxyborohydride proved difficult.[2] The rate of reaction of triisopropoxyborane with lithium hydride and sodium hydride was very slow so that reaction could be achieved only at elevated temperatures (eq 1). In those pre-NMR days we could not be confident of the homogeneity of the product produced under such vigorous conditions.

$$(i\text{-PrO})_3B + NaH \xrightarrow[1\ h]{150\ °C,\ DG} Na(i\text{-PrO})_3BH \quad (1)$$

The discovery by C. A. Brown that potassium hydride, KH, is far more reactive than lithium hydride or sodium hydride,[3,4] reacting readily at room temperature with such hindered Lewis acids of boron as tri-*sec*-butylborane[4a] and triisopropoxyborane,[4b,c] made these borohydrides readily available (eq 2 and 3). K-*sec*-Bu_3BH, like its lithium

$$KH + sec\text{-}Bu_3B \xrightarrow[25\ °C]{THF} K\text{-}sec\text{-}Bu_3BH \quad (2)$$

$$KH + (i\text{-PrO})_3B \xrightarrow[25\ °C]{THF} K(i\text{-PrO})_3BH \quad (3)$$

derivatives,[5] proved to be a highly stereoselective reducing agent.[4a] Somewhat surprisingly, $K(i\text{-PrO})_3BH$ proved to be a very gentle reducing agent.[4c]

The characteristics of $K(i\text{-PrO})_3BH$ appeared to make it the ideal reagent for our new synthesis of mixed thexyldialkylboranes[6] (eq 4 and 5). The reaction worked satisfactorily. However, the yields were in the range of only 59–75%. Moreover, they appeared to vary somewhat with the sample of KIPBH used.[7] ^{11}B NMR examination of commercial KIPBH solution in THF showed two peaks, one at δ 6.1 and one at δ 2.7 (Figure 1). The relative areas of the two peaks varied from sample to sample from 90:10

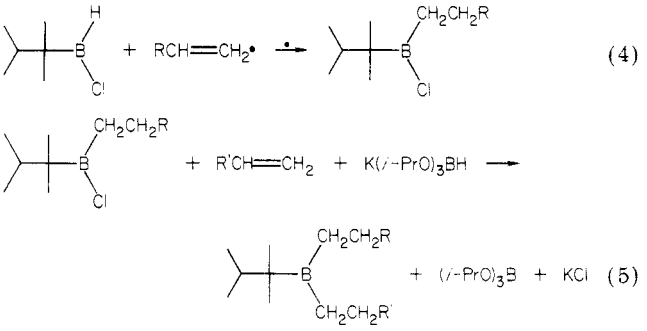

to 65:35, respectively.[8] Moreover, the yields of the products in the thexyldialkylborane synthesis varied roughly inversely with the magnitude of the minor peak.

Investigation revealed that this minor peak was present not only in the commercial products but also in material prepared by the literature procedure.[4b,c] Accordingly, we undertook a study to establish the nature of this impurity and to see if we could devise a means either of removing it from the commercial product or of synthesizing the reagent free of the impurity.

Results and Discussion

It appeared clear that the major peak at δ 6.1 (d, J_{B-H} = 117 Hz) must be due to $K(i\text{-PrO})_3BH$. The question remaining was the source of the minor peak at δ 2.7 (s). We suspected that this peak might be due to the presence of a tetraalkoxyborohydride, $K(RO)_4B$. Indeed, the controlled addition of acetone resulted in a decrease in the major peak at δ 6.1 and a sharp increase in the minor peak (eq 6). Addition of 1 equiv of acetone resulted in the complete disappearance of the peak at δ 6.1 and its replacement by an equivalent large peak at δ 2.7.

$$(CH_3)_2CO + K(i\text{-PrO})_3BH \rightarrow K(i\text{-PrO})_4B \quad (6)$$

Similarly, addition of pure potassium tetraisopropoxyborate, readily prepared from the combination of equivalent quantities of potassium isopropoxide and triisopropoxyborane (eq 7) to the KIPBH sample, resulted in a sharp increase only in the minor peak.

$$i\text{-PrOK} + (i\text{-PrO})_3B \xrightarrow{THF} K(i\text{-PrO})_4B \quad (7)$$

(1) (a) Postdoctoral research associate on Grant ARO-DAAG-29-79-C-0027 supported by the U.S. Army Research Office. (b) Graduate research assistant on temporary academic leave from Monsanto Agricultural Products Co.

(2) Brown, H. C.; Mead, E. J.; Shoaf, C. J. *J. Am. Chem. Soc.* **1956**, *78*, 3616.

(3) Brown, C. A. *J. Chem. Soc., Chem. Commun.* **1974**, 680.

(4) (a) Brown, C. A. *J. Am. Chem. Soc.* **1973**, *95*, 4100. (b) Brown, C. A. *J. Org. Chem.* **1974**, *39*, 3913. (c) Brown, C. A.; Krishnamurthy, S.; Kim, S. C. *J. Chem. Soc., Chem. Commun.* **1973**, 391.

(5) Brown, H. C.; Krishnamurthy, S. *J. Am. Chem. Soc.* **1972**, *94*, 7159.

(6) Kulkarni, S. U.; Lee, H. D.; Brown, H. C. *J. Org. Chem.* **1980**, *45*, 4542.

(7) Sikorski, J. A.; Brown, H. C., unpublished results.

(8) Since concentrations of $K(i\text{-PrO})_3BH$ and $K(i\text{-PrO})_4B$ are not directly related to the observed areas of ^{11}B NMR spectra, we shall use only ares in discussing the relative magnitudes of these two peaks.

0276-7333/83/2302-0634$01.50/0

Table I. Preparation of $K(i\text{-PrO})_3BH$ Using Different $KH:(i\text{-PrO})_3B$ Ratios[a]

expt no.	$KH:(i\text{-PrO})_3B$	solvent	results
1	1;1:1.0[b]	THF	formation of 15-20% of the minor component
2	1.3:1.0[b]	THF	formation of 10-15% of the minor component
3	1.5:1.0	THF	formation of 10-12% of the minor component
4	2.0:1.0	THF	formation of 8-10% of the minor component
5	2.0:1.0	Et_2O	formation of 4-5% of the minor component
6	2.0:1.0	glyme	formation of 8-10% of the minor component
7	10.0:1.0	THF	formation of 2% of the minor component

[a] All preparations were done at room temperature. [b] Using 10% and 30% excess potassium hydride, a third peak at δ -11.3 (q, J_{B-H} = 87.4) was observed. The peak is assigned to a $K\text{-}i\text{-PrOBH}_3$ moiety.

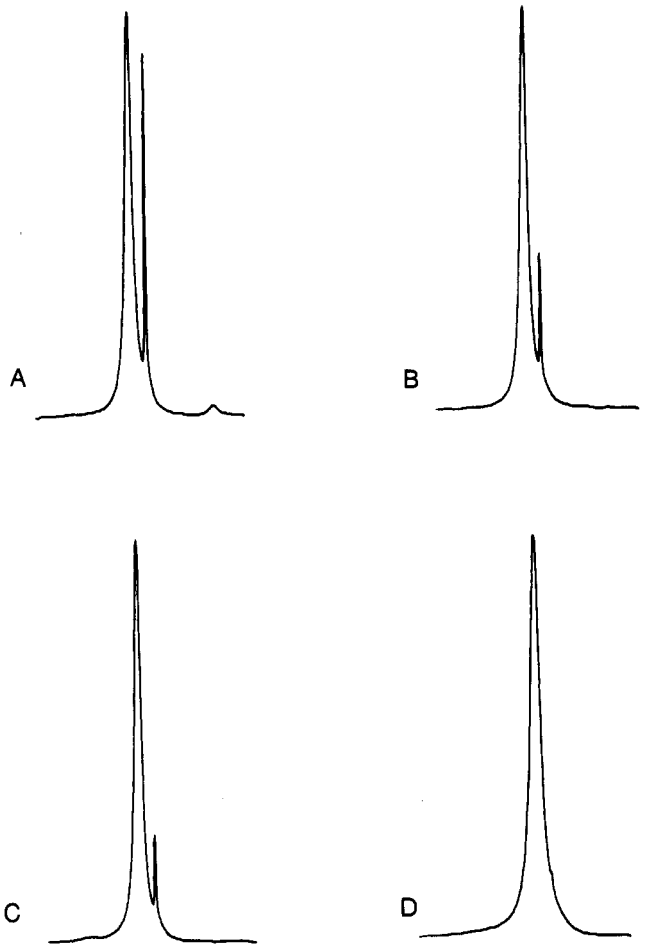

Figure 1. ^1H-Decoupled ^{11}B NMR spectra of $K(i\text{-PrO})_3BH$ reagents: (A) commercial reagent; (B) reagent prepared at 25 °C; (C) reagent prepared at 0 °C; (D) reagent refluxed over excess KH, ≥99% pure.

Addition of *n*-butyraldehyde to the KIPBH sample had the same effect. Consequently, while we can be confident that the peak at δ 2.7 is attributable to a tetraalkoxyborohydride, we cannot assign the peak to $(i\text{-PrO})_4B^-$ rather than to $n\text{-BuO}(i\text{-PrO})_3B^-$ or some other tetraalkoxyborohydride.

A 1 M solution of commercial KIPBH was analyzed for potassium (by titration as potassium hydroxide), isopropoxide (by GLC analysis as isopropyl alcohol), boron (by titration as boric acid in the presence of mannitol), and hydride (by measurement of hydrogen gas evolved). The composition agreed with the theoretical: $K_{1.00}(i\text{-PrO})_{3.00}B_{1.00}H_{1.00}$. Consequently, the minor peak cannot be due to the presence of an alkoxide impurity in the potassium hydride or an alcohol impurity in triisopropoxyborane used for the preparation.

A sample of KIPBH, prepared by the published procedure,[4b,c] was subjected to the same analysis. The ^{11}B NMR spectrum showed the same two peaks (Figure 1) with the area of the minor peak at δ 2.7 being in the neighborhood of 8–10% that of the major peak at δ 6.1. Here also, an almost theoretical analysis of 1.00:3.00:1.00:1.00 was obtained for the four components. Formation of *n*-butoxy through cleavage of the THF solvent was ruled out since GC analysis of the hydrolyzed product revealed no 1-butanol present in the 2-propanol.

Preparation of KIPBH in monoglyme or diethyl ether yielded a solution that exhibited the same minor component in the ^{11}B NMR spectrum.

Analysis of potassium hydride samples did not reveal the presence of any organic impurity that might affect the preparation of the reagent. The commercial sample of $(i\text{-PrO})_3B$ contained ca. 0.5% free 2-propanol. Distillation from a small amount of potassium metal gave a pure sample of the ester, free of alcohol. Yet the product of this ester $(i\text{-PrO})_3B$ and potassium hydride revealed the same minor peak.

We were therefore forced to the conclusion that the minor peak must arise not from any impurity in the solvent, inert atmosphere, or reactants. It must arise from a disproportionation of the product itself (eq 8). However,

$$2K(i\text{-PrO})_3BH \rightleftarrows K(i\text{-PrO})_2BH_2 + K(i\text{-PrO})_4B \quad (8)$$

this conclusion left us with two puzzles. Why did different samples or reagent solution exhibit considerably different magnitude of the minor peak? Why did we not see a third peak, for $K(i\text{-PrO})_2BH_2$, in the ^{11}B NMR spectrum?

Careful ^{11}B NMR reexamination of commercial KIPBH samples did reveal three peaks: a major peak at δ 6.1 (d, J_{BH} = 117 Hz), assigned to $(i\text{-PrO})_3BH^-$, a minor peak at δ 2.7 (s), assigned to $(i\text{-PrO})_4B^-$, and a new, very small peak at δ -11.3 (q, J_{BH} = 87.4). Since this peak is a quartet, it is attributed to the species $i\text{-PrOBH}_3^-$. Apparently, the equilibria in the spectrum are more complex than that shown in eq 8, involving also the formation of potassium monoisopropoxyborohydride (eq 9).

$$2K(i\text{-PrO})_2BH_2 \rightleftarrows K\text{-}i\text{-PrOBH}_3 + K(i\text{-PrO})_3BH \quad (9)$$

There are two possible explanations for our failure to detect a fourth peak, a triplet, assignable to $K(i\text{-PrO})_2BH_2$. One is that the equilibrium favors the other three components, so that the concentration of $K(i\text{-PrO})_2BH_2$ is too low to detect under these conditions. The second is that the exchange rate of $K(i\text{-PrO})_2BH_2$ is such that it causes the peak to disappear into the background.[9]

We attempted to prepare an authentic sample of $K(i\text{-PrO})_2BH_2$ by treating diisopropoxyborane with potassium hydride at 0 °C (eq 10). However, the reaction product

$$KH + (i\text{-PrO})_2BH \xrightarrow[\text{THF}]{0\ °C} K(i\text{-PrO})_2BH_2 \quad (10)$$

was a mixture of $(i\text{-PrO})_3B$, $K(i\text{-PrO})_4B$, $K(i\text{-PrO})_3BH$, and

(9) Brown, C. A.; Krishnamurthy, S. *J. Organomet. Chem.* 1978, *156*, 111.

K(i-PrOBH$_3$), with no K(i-PrO)$_2$BH$_2$ detectable. Either the formation of this mixture confirms the suggested instability of K(i-PrO)$_2$BH$_2$ or it is an artifact of the synthesis as observed previously for the reactions of RLi and R'$_2$BH.[10]

Potassium tetraisopropoxyborohydride, K(i-PrO)$_4$B, differs from its sodium analogue,[11] Na(i-PrO)$_4$B, in being very soluble in a variety of solvents, such as THF, Et$_2$O, monoglyme, and even pentane. Attempts to concentrate these solutions to precipitate selectively either K(i-PrO)$_4$B or K(i-PrO)$_3$BH failed.

We next explored the preparation of KIPBH at room temperature by using different ratios of KH and (i-PrO)$_3$B. Here we achieved our first success. A large ratio of KH to (i-PrO)$_3$B produced a relatively pure sample of KIPBH. For example, a tenfold excess of KH results in the formation of KIPBH with approximately 2% (by area) of the minor component. Unfortunately, the need for this large excess of KH made this solution to the problem impractical. These results are summarized in Table I.

We tested the preparation of KIPBH at 0 °C. This provided a material that contained only 4–6% of the minor peak. Storage at 0 °C also decreased the rate of growth of this minor peak.

Finally, we observed an unexpectedly phenomenon, which ultimately provided a solution to the problem. When being refluxed a solution of K(i-PrO)$_4$B in THF slowly liberated (i-PrO)$_3$B (eq 11). When such a solution

$$\mathrm{K}(i\text{-PrO})_4\mathrm{B} \xrightarrow[\mathrm{THF}]{\Delta} i\text{-PrOK} + (i\text{-PrO})_3\mathrm{B} \qquad (11)$$

was refluxed for a considerable time (18 h) and then cooled to room temperature, the ^{11}B NMR spectrum revealed the presence of a peak at δ 17 [(i-PrO)$_3$B] and one at δ 2.7 [K(i-PrO)$_4$B]. The continued growth of (i-PrO)$_3$B in the solution and its failure to recombine with i-PrOK on cooling is a puzzle. It must mean that there is a slow reaction that converts the i-PrOK to a form in which it does not react with (i-PrO)$_3$B. Yet the solution remains clear. Possibly the i-PrOK reacts slowly with the Pyrex glass to be converted into a soluble silicate ester.

In any event, this experiment suggested the possibility of removing the K(i-PrO)$_4$B impurity from the reagent by refluxing it for 24 h over free KH. Indeed, this treatment reduced the minor component in the commercial product to a negligible amount (<1% by area). Presumably, the impurity of K(i-PrO)$_4$B slowly dissociates to triisopropoxyborane, (i-PrO)$_3$B (eq 11), and the liberated ester reacts with the KH present (eq 3).

Alternatively, it proved possible to prepare pure KIPBH by adding (i-PrO)$_3$B to a modest excess of KH in THF, either at room temperature or in refluxing THF, followed by heating the reaction mixture under reflux for 24 h. Again ^{11}B NMR examination of the clear solution revealed essentially pure KIPBH (≥99%) with less than 1% (by area) of the impurity. The process evidently also removes the other minor components K(i-PrO)$_2$BH$_2$ and K-i-PrOBH$_3$.

The KIPBH prepared under these conditions exhibited an additional stability toward the undesirable disproportionation if the material were stored over 10% excess KH. Under these conditions, no disproportionation of the KIPBH reagent has been observed after 8 months at room temperature. This excess KH is not soluble in the solution, and it readily settles to the bottom of the storage flask.

(10) Hubbard, J. L.; Kramer, G. W. *J. Organomet. Chem.* **1978**, *156*, 81.

(11) Brown, H. C.; Mead, E. *J. Am. Chem. Soc.* **1956**, *78*, 3614.

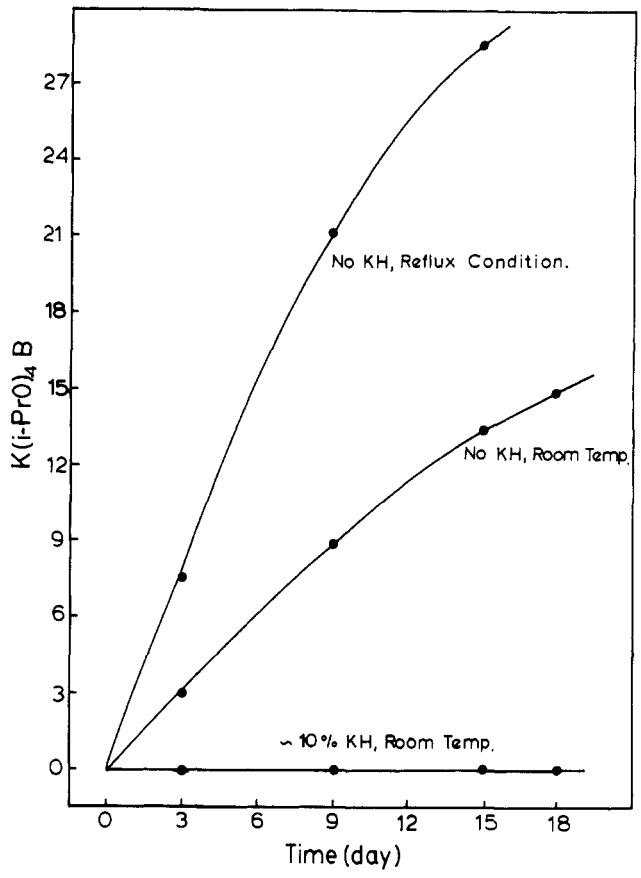

Figure 2. Stability of potassium triisopropoxyborohydride in tetrahydrofuran.

Consequently, the clear solution of the reagent is readily removed, free of the KH. The clear solution, KIPBH, separated from excess KH, does undergo a slow disproportionation (Figure 2). Alternatively, potassium tetraisopropoxyborohydride, K(i-PrO)$_4$B, was added to the pure KIPBH reagent. This KIPBH with added impurity can be regenerated easily by refluxing over a moderate excess KH for 24 h.

We then tested this improved reagent for the hydridation of thexyl-n-octylchloroborane and conversion into thexyl-n-octyl-n-decylborane, followed by carbonylation to the corresponding ketone (eq 12–14). It is clear from these results that our original problem has been solved. It is now possible to prepare and utilize potassium triisopropoxyborohydride in purities approaching 100%.

Conclusion

Potassium triisopropoxyborohydride, K(i-PrO)$_3$BH, can now be prepared in essentially pure form, ≥99%, by adding the ester, triisopropoxyborane, to excess potassium hydride in THF, refluxing the mixture for 24 h, and then storing the product over a small quantity of potassium hydride (~10%). Under these conditions, no disproportionation was observed after 6 months at room temperature. This reagent exhibited excellent behavior in the hybridation of thexylmonoalkylchloroborane in the synthetic route to "mixed" thexyldialkylboranes, providing essentially quantitative yields of the intermediate boranes and the ketones into which these intermediates can be transformed.

Experimental Section

Materials. Tetrahydrofuran was dried over a 4-Å molecular sieve and distilled from a sodium benzophenone ketyl prior to use. Potassium hydride was purchased from Alfa and was freed from the mineral oil according to the published procedure.[3,4] Triisopropoxyborane was either purchased from Aldrich or pre-

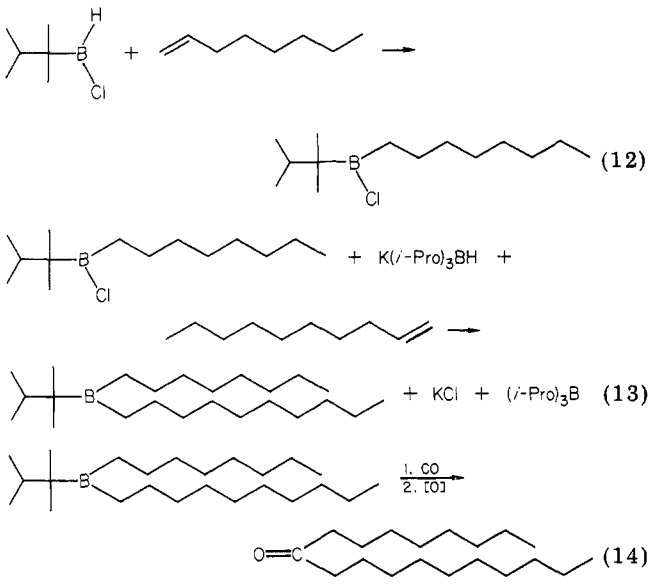

100% GC yield, 94% isolated

pared from 2-propanol and the methyl sulfide–borane complex.[12] Triisopropoxyborane was distilled from a small piece of potassium metal prior to use. All glassware was dried thoroughly in a drying oven and cooled under a dry stream of nitrogen.

Spectra. Spectra were obtained under an inert atmosphere by using apparatus and techniques described elsewhere.[13] ^{11}B NMR spectra were recorded on a Varian FT-80A spectrometer equipped with a broad-band probe and a Hewlett-Packard 3335A frequency synthesizer. All ^{11}B NMR chemical shifts are reported relative to $BF_3 \cdot OEt_2$ (δ 0), with chemical shifts downfield from $BF_3 \cdot OEt_2$ assigned as positive.

Potassium Triisopropoxyborohydride, K(*i*-PrO)$_3$BH, in THF (Room Temperature).[4b] An oven-dried, 100-mL, round-bottom flask with side arm and an adaptor was attached to a mercury bubbler. The flask was charged with 2 g of KH (50.0 mmol) as an oil dispersion; the mineral oil was removed with pentane. The KH was suspended in 30.0 mL of THF, and 5.8 mL (25 mmol) of freshly distilled triisopropoxyborane was added. After the mixture was stirred for 2 h at room temperature, the formation of borohydride was completed. [The ^{11}B NMR spectrum did not show any signal corresponding to (*i*-PrO)$_3$B at δ 17.] The clear solution was analyzed for potassium (as potassium hydroxide), isopropoxide (as isopropyl alcohol), boron (as boric acid), and hydride (as hydrogen gas liberated upon hydrolysis).[13]

Potassium Triisopropoxyborohydride, K(*i*-PrO)$_3$BH, in Monoglyme and Diethyl Ether. The usual procedure[4b] was followed, except two other solvents, monoglyme or diethyl ether, were used in place of THF.

Potassium Triisopropoxyborohydride, K(*i*-PrO)$_3$BH, in THF (at 0 °C). A clean, dry, tared 1-l, round-bottom flask equipped with a nitrogen inlet and magnetic stirring bar was charged with 50 g of potassium hydride (1.25 mol) as an oil dispersion via double-ended needle. The system was maintained under nitrogen. The suspension was allowed to settle, and then the excess mineral oil was decanted off through a double-ended needle. The remaining material was then washed several times with 250-mL portions of dry pentane under nitrogen. The remaining cake of potassium hydride was then dried in vacuo to give a light brown powder, 45.3 g (1.12 mol). This powder was slurried in 500 mL of THF at 0 °C. Then 250 mL of a 3.0 M solution of triisopropyl borate (0.75 mol) in THF was added dropwise over a 1-h period. When the addition was complete, the resulting mixture was stirred at 0 °C for 20 h. At this time the ^{11}B NMR spectrum of the supernatant solution showed that all of the (*i*-PrO)$_3$B, δ 17.0, had even consumed with the concomitant formation of KIPBH (δ 6.1 (d, J_{B-H} = 117 Hz) along with 4–6% of K(*i*-PrO)$_4$B. The supernatant solution was then removed under nitrogen with a double-ended needle and was stored at 0 °C. Standardization for active hydride[13] indicated that the solution was 0.90 M.

Potassium Triisopropoxyborohydride Using Different KH:(*i*-PrO)$_3$B Ratios. The usual procedure[4b] was followed, except that different KH:(*i*-PrO)$_3$B ratios were examined. The results are summarized in Table I.

Potassium Tetraisopropoxyborohydride, K(*i*-PrO)$_4$B. An oven-dried, 100-mL, round-bottom flask was charged with 10 mL of a 3.1 M potassium isopropoxide in THF. To this was added 7.15 mL (31.0 mmol) of triisopropoxyborane in 20 mL of THF at room temperature. The ^{11}B NMR spectrum of the solution showed a single peak at δ 2.7 assigned to the (*i*-PrO)$_4$B$^-$ species. The potassium tetraisopropoxyborohydride was analyzed[13] for its potassium, isopropoxide, and boron contents. A ratio of 1.00:4.00:1.00 for K:*i*-PrO:B, within the experimental error, was observed. The solvent THF was pumped out under reduced pressure. The resulting solid K(*i*-PrO)$_4$B was soluble in monoglyme, diethyl ether, and pentane.

Preparation of Potassium Triisopropoxyborohydride under Reflux Conditions in THF. An oven-dried, 2-L, round-bottom flask with side arm, condenser tube, and an adaptor was attached to a mercury bubbler. The flask was flushed with dry nitrogen and maintained under a static pressure of nitrogen. To this flask was added 50.0 g of KH (1.25 mol) as an oil dispersion with the aid of a double-ended needle. The mineral oil was removed with THF (3 × 50 mL). To this pure KH was added ca. 500 mL of freshly distilled THF. The suspended KH was kept at room temperature by using a water bath. A total of 164.4 g (201.7 mL, 0.87 mol) of distilled triisopropoxyborane was added to the KH suspension via a double-ended needle while the mixture was stirred. After ca. 4 h, the formation of KIPBH was completed. The ^{11}B NMR spectrum showed the formation of 10–15% of the minor compound K(*i*-PrO)$_4$B. To purify the reagent, the THF solution of KIPBH was brought to gentle reflux over the excess KH. The ^{11}B NMR spectrum of the mixture after 24 h showed the formation of a ≥99% pure triisopropoxyborohydride (Figure 1). An aliquot of the above KIPBH solution was quenched with water, and its potassium and boron contents were measured as potassium hydroxide and boric acid.[13] Hydride measurement was done by calculating the number of moles of hydrogen gas evolved after the reagent was quenched with a mixture of THF, glycerine, and 2 N HCl. A 1.200 M concentration of boron and hydride contents was observed. Potassium content was measured as 1.205 M. Hence, a 1.00:1.00:1.00 ratio of K:B:H was established.

Stability of 99% Pure KIPBH. The above KIPBH with purity of ≥99% was tested under different conditions. A sample was separated from KH and was kept in a storage bottle under Argon atmosphere. The ^{11}B NMR spectra of the sample during a time interval (ca. 6 months) were examined. An increase of ca. 25–30% of the minor peak was observed (Figure 2). In another sample of KIPBH, maintained over 10% KH, no disproportionation was detectable after 6 months. Alternatively, the 99% pure reagent can be kept over the unused portion of potassium hydride. The reagent exhibited a much faster rate of disproportionation when refluxed without the presence of extra KH (Figure 2).

Addition of K(*i*-PrO)$_4$ to the 99% Pure KIPBH. A 10.0-mL sample of a 1.0 M potassium tetraisopropoxyborohydride [K(*i*-PrO)$_4$B] was added to a 50.0-mL sample of 1.0 M 99% KIPBH. An immediate increase in the minor compound at δ 2.7 was observed. The solution was transferred to a 4.1 g of KH (102 mmol), freed from the mineral oil, and it was refluxed for 24 h. After this period, the ^{11}B NMR of the clear solution showed a complete recovery of the KIPBH reagent.

Acknowledgment. We thank Dr. C. A. Brown for helpful discussions during this study and gratefully acknowledge the financial assistance from the U.S. Army Research Office (No. ARO-DAAG-29-79-C-0027).

Registry No. K(*i*-PrO)$_3$BH, 42278-67-1; KH, 7693-26-7; K(*i*-PrO)$_4$B, 84581-08-8; triisopropoxyborane, 5419-55-6; THF, 109-99-9; thexylchloroborane, 75030-54-5; 1-octene, 111-66-0; thexyl-*n*-octylchloroborane, 75052-81-2; 1-decene, 872-05-9; thexyl-*n*-octyl-*n*-decylborane, 84521-30-2; 9-nonadecanone, 75030-48-7.

(12) Brown, C. A.; Krishnamurthy, S. *J. Org. Chem.* **1978**, *43*, 2731.
(13) Brown, H. C.; Kramer, G. W.; Levy, A. B.; Midland, M. M. "Organic Syntheses via Boranes"; Wiley-Interscience: New York, 1975.

Synthesis and Reactivity of Cyclohexenylmanganese Tricarbonyl, a Complex Containing a Two-Electron, Three-Center Mn···H···C Interaction

M. Brookhart,* W. Lamanna, and Allan R. Pinhas

Department of Chemistry, University of North Carolina, Chapel Hill, North Carolina 27514

Received October 4, 1982

The cation (benzene)$Mn(CO)_3^+$ undergoes stepwise, vicinal addition of 2 equiv of hydride in an exo fashion to yield a unique transition-metal anion, (1,3-cyclohexadiene)$Mn(CO)_3^-$. The diene anion is highly reactive. Exposure to oxygen results in oxidation of the metal and liberation of free 1,3-cyclohexadiene. Protonation yields an unusual, bridged (cyclohexenyl)$Mn(CO)_3$ species possessing an aliphatic, endo C–H bond that is activated via coordination to manganese. The three-center Mn···H···C interaction in this complex renders the bridging hydrogen acidic and permits facile removal by base to regenerate the diene anion. Alkylation with MeI or $MeOSO_2CF_3$ results in methyl addition to the endo side of the ring and coordination of a second endo C–H bond. A second deprotonation/alkylation sequence can be achieved to give ring-dialkylated cyclohexenyl products. The coordinated C–H bond of the bridged cyclohexenyl species is replaced by external ligands L (L = CO, $P(OMe)_3$) to give (cyclohexenyl)$Mn(CO)_3L$ adducts. Hydride addition to the π-allyl unit of the tetracarbonyl species results in reduction of the polyolefin to cyclohexene. Thermolysis of the phosphite adduct causes loss of CO and formation of the bridged complex (cyclohexenyl)$Mn(CO)_2P(OMe)_3$. The parent complex $C_6H_9Mn(CO)_3$ reacts with diazomethane in an unexpected fashion providing an alternate and complimentary method of ring methylation. Reactions with activated olefins appear to proceed via a free radical mechanism resulting in transfer of H_2 across the double bond.

Introduction

Transition-metal-assisted reactions of arenes with nucleophiles have received particular attention as a unique and potentially useful method of arene reduction and/or functionalization. Nucleophilic addition to transition-metal arene complexes typically yields the corresponding exo-substituted cyclohexadienyl complexes:

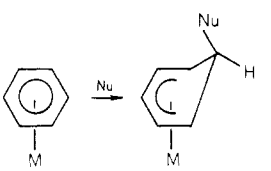

The arene complexes $(C_6H_6)Fe(C_5H_5)^+$,[1] $C_6H_6Mn(CO)_3^+$,[1] and $C_6H_6Cr(CO)_3$[2] and their ring-substituted derivatives are among the most thoroughly studied in this regard. In each case, the exo-substituted cyclohexadienyl complexes can be converted back to the corresponding substituted arenes in either complexed or uncomplexed form. In the iron system, oxidation with *N*-bromosuccinimide results in endo hydrogen abstraction and formation of the substituted arene complex;[3] however, competing abstraction of the added exo Nu is often a problem.[4] A similar conversion is possible in the manganese systems via thermal isomerization of the exo-substituted cyclohexadienyl complex followed by abstraction of the resulting 6-exo hydrogen using the trityl cation.[5] Alternatively, direct oxidation of the 6-exo-substituted complex with cerium(IV)/sulfuric acid results in conversion all the way to the free substituted arene.[6] Mild oxidation of the anionic cyclohexadienylchromium complexes with iodine also gives the free substituted arene via endo hydrogen removal and cleavage from the metal.[2b] This latter reaction has been used extensively by Semmelhack to perform net nucleophilic aromatic substitutions in the chromium system.

In a few rare cases, activation of an arene ligand toward addition of 2 equiv of nucleophile and formation of a diene complex has been demonstrated. Wilkinson[7] has shown that hydride reduction of the dication $(C_6H_6)_2Ru^{2+}$ leads to mixtures of (benzene)(1,3-cyclohexadiene)ruthenium and dicyclohexadienylruthenium. It is not clear, in this case, whether the diene complex arises from initial addition of 2 equiv of hydride to a single ring or thermal isomerization of the dicyclohexadienyl complex. Vollhardt[8] has reported double nucleophilic addition to the (benzene)-cyclopentadienylcobalt(2+) dication upon treatment with methoxide or cyclopentadienide. Nucleophilic addition occurs vicinally and stereospecifically exo on the arene ring. Liberation of the diene by oxidative demetalation could not be achieved. Most recently Maitlis has observed double hydride addition to the benzene rings in the complexes $(C_5(CH_3)_5)MC_6H_6^+$ (M = Ir, Rh) and $(C_6(CH_3)_6)$-$RuC_6H_6^{2+}$ using $NaAlH_2(OCH_2CH_2OCH_3)_2$.[9]

The direct conversions of arenes to 1,3-cyclohexadienes (substituted or unsubstituted) via transition-metal-mediated double nucleophilic additions are particularly interesting from a synthetic standpoint in that they represent a possibly versatile complement to the Birch reduction. Although the current reports clearly indicate that such additions are possible, examples are limited and the chemistry of the resulting diene adducts has been virtually unexplored.

(1) Green, M. L. H.; Davies, S. G.; Mingos, D. M. P. *Tetrahedron* **1978**, *34*, 3047 and references therein.
(2) (a) Semmelhack, M. F.; Hall, H. T.; Farina, R.; Yoshifuji, M.; Clark, G.; Bargar, T.; Hirotsu, K.; Clardy, J. *J. Am. Chem. Soc.* **1979**, *101*, 3535. (b) Semmelhack, M. F.; Hall, H. T.; Yoshituji, M.; Clark, G. *Ibid.* **1975**, *97*, 1247. (c) A substituted cyclohexadiene can be obtained by the single reduction/protonation sequence on an arene chromium tricarbonyl complex: Semmelhack, M. F.; Harrison, J. J.; Thebtaranoth, Y. *J. Org. Chem.* **1979**, *44*, 3275.
(3) Khand, I. V.; Pauson, P. L.; Watts, W. E. *J. Chem. Soc. C* **1969**, 2024.
(4) Nesmeyanov, A. N.; Vol'Kenau, N. A.; Shilovtseva, L. S.; Petrakova, V. A. *J. Organomet. Chem.* **1975**, *85*, 365.
(5) Pauson, P. L.; Munro, G. A. M. *Z. Anorg. Allg. Chem.* **1979**, *458*, 211.
(6) (a) Walker, P. J. C.; Mawby, R. J. *J. Chem. Soc., Chem. Commun.* **1972**, 330. (b) Mawby, A.; Walker, P. J. C.; Mawby, R. J. *J. Organomet. Chem.* **1973**, *55*, C39.
(7) Jones, D.; Pratt, L.; Wilkinson, G. *J. Chem. Soc.* **1962**, 4458.
(8) Lai, Y.-H.; Tam. W.; Vollhardt, K. P. C. *J. Organomet. Chem.* **1981**, *216*, 97.
(9) Grundy, S. L.; Maitlis, P. M. *J. Chem. Soc., Chem. Commun.* **1982**, 379.

0276-7333/83/2302-0638$01.50/0

The results described in this manuscript demonstrate that 2 equiv of hydride can be added to the cationic arene complex (benzene)$Mn(CO)_3^+$ to effect reduction to the (1,3-cyclohexadiene)manganese tricarbonyl anion in high yields. The reduction proceeds in a stepwise fashion through a neutral cyclohexadienylmanganese tricarbonyl intermediate and represents the first example of double nucleophilic addition to a *monocationic* arene complex. The (1,3-cyclohexadiene)manganese tricarbonyl anion is the first anionic diene complex to be characterized. Although thermally quite stable, this species is highly reactive and undergoes a series of unique and interesting conversions. Exposure to oxygen results in oxidation of the metal and liberation of free 1,3-cyclohexadiene. Protonation yields an unusual bridged cyclohexenyl species possessing an aliphatic endo C-H bond that is activated via coordination to manganese. The three-center, two-electron Mn···H···C interaction in this complex renders the bridging hydrogen acidic and permits facile removal by base to regenerate the diene anion. Alkylation of the diene anion results in electrophilic addition to the endo side of the ring and coordination (and activation) of a second endo C–H bond to give monoalkylated cyclohexenyl derivatives. A second deprotonation/alkylation sequence can also be achieved to give ring-dialkylated cyclohexenyl products. In addition, the coordinated C–H bond of the bridged cyclohexenyl species is easily displaced by external ligands L to give (cyclohexenyl)$Mn(CO)_3L$ species. Hydride addition to the π-allyl unit of this species results in further reduction of the polyolefin to cyclohexene. Overall, the reactions reported herein enable a series of potentially useful, manganese-mediated transformations for the selective reduction of benzene to 1,3-cyclohexadiene, cyclohexene, and stereoselectively functionalized derivatives. The net electrophilic substitution reactions of the coordinated C–H bond of the bridged cyclohexenyl species are particularly interesting in that they provide a unique and selective method for the functionalization of aliphatic carbon centers and the formation of carbon–carbon bonds. The chemistry provides valuable insight into the nature of the Mn···H···C interaction in these complexes and suggests in a general way how this new mode of C–H bond activation may be of value in transition-metal-mediated organic syntheses.

A preliminary account of part of this work has appeared[10] as well as a detailed spectroscopic and X-ray structural analysis[11] of the (6-*endo*-methylcyclohexenyl)manganese tricarbonyl complex containing a three-center, two-electron Mn···H···C bond. Pauson has recently reported similar reductions of (arene)manganese tricarbonyl cations using lithium aluminum hydride.[12]

Results and Discussion

Hydride Reduction of (Benzene)manganese Tricarbonyl Hexafluorophosphate. Generation of (Cyclohexadiene)manganese Tricarbonyl Anion and Cyclohexenylmanganese Tricarbonyl. Excess lithium triethylborohydride or potassium triisopropoxyborohydride react in a stepwise fashion with (benzene)manganese tricarbonyl hexafluorophosphate, 1, in tetrahydrofuran (THF) to transfer 2 equiv of hydride. The product (1,3-cyclohexadiene)manganese tricarbonyl anion, 2, resulting from double vicinal addition of hydride to the benzene ligand is generated in good yields (>61%), based on the yield of 4 upon quenching with H_2O (see below). In the

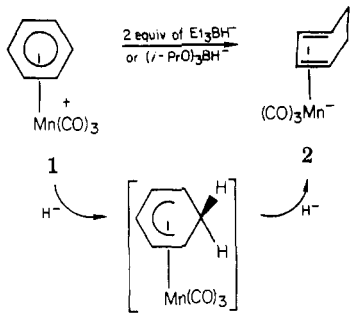

presence of 2.5 equiv of hydride the $LiBEt_3H$ reduction is complete in ca. 30 min, whereas the $KB(i\text{-}PrO)_3H$ reduction requires at least 15 h. The same anion can be produced quantitatively by similar hydride reduction of cyclohexadienylmanganese tricarbonyl, 3, which has been identified by IR (ν_{CO} (in THF) 2017 (s) and 1929 (s, br) cm^{-1}) as the intermediate in the former reactions. The potassium salt of anion 2 exhibits strong IR bands at 1930, 1840, and 1789 cm^{-1} in THF. The IR spectrum of the lithium salt in the metal carbonyl region is more complex, exhibiting bands at 1929 (s), 1896 (s), 1853 (s), 1831 (s), 1811 (s), and 1758 (s) cm^{-1}. This is presumably due to ion-pairing effects with the more highly coordinating lithium cation. The diene anion is stable for days under a nitrogen atmosphere in THF solution; however, exposure to air results in immediate decomposition. No attempt was made to isolate anion 2 in solid form, although NMR studies of the anion have been carried out (see below). Treatment of THF solutions of 2 with water results in rapid protonation and quantitative conversion to the unusual cyclohexenylmanganese tricarbonyl complex 4, possessing an endo C–H bond coordinated to manganese. The Mn···H···C interaction in 4 is best described as a two-electron, three-center bonding arrangement in which the σ electrons of the carbon–hydrogen bond are shared by the nominally 16-electron metal center. If one considers the π-allyl unit as a bidentate ligand, then the structure of 4 is roughly octahedral with the bridging hydrogen occupying the coordination site approximately trans to one carbonyl and cis to the two remaining carbonyls.[11] Although structures of this type are uncommon, a small number of transition-metal complexes possessing coordinated C–H bonds have been reported,[13] the closest analogues being cationic (π-allyl)iron species (below) generated upon protonation of the neutral (diene)FeL_3 complexes.[13,14]

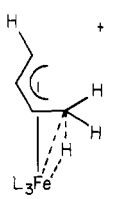

Unlike the thermally unstable iron complexes, bridged structure 4 is stable to temperatures greater than 120 °C. Complete details of the spectroscopic characterization,

(10) Lamanna, W.; Brookhart, M. *J. Am. Chem. Soc.* **1981**, *103*, 989.
(11) Brookhart, M.; Lamanna, W.; Humphrey, M. B. *J. Am. Chem. Soc.* **1982**, *104*, 2117.
(12) Bladon, P.; Munro, G. A. M.; Pauson, P. L.; Mahaffy, C. A. L. *J. Organomet. Chem.* **1981**, *221*, 79.
(13) (a) Brookhart, M.; Whitesides, T. H.; Crockett, J. M. *Inorg. Chem.* **1976**, *15*, 1550. (b) Brookhart, M.; Harris, D. L. *Ibid.* **1974**, *13*, 1540.
(14) (a) Brown, R. K.; Williams, J. M.; Schultz, A. J.; Stucky, G. D.; Ittel, S. D.; Harlow, R. L. *J. Am. Chem. Soc.* **1980**, *102*, 981. (b) Williams, J. M.; Brown, R. K.; Schultz, A. J.; Stucky, G. D.; Ittel, S. D. *Ibid.* **1978**, *100*, 7407. (c) Ittel, S. D.; Van-Carledge, F. A.; Tolman, C. A.; Jesson, J. P. *Ibid.* **1978**, *100*, 1317. (d) Ittel, S. D.; Van-Catledge, F. A.; Jesson, J. P. *Ibid.* **1979**, *101*, 6905.

structure and dynamic behavior of 4 have been previously reported.[11] To aid in understanding the chemistry presented later, it should be noted here that complex 4 exhibits two fluxional isomerization processes detectable by ^{1}H NMR spectroscopy: (1) a low-energy process ($\Delta G^{\ddagger}$ = 8.3 kcal/mol) proceeding through the 16-electron π-allyl species 5 and (2) a higher energy process ($\Delta G^{\ddagger}$ = 15.4 kcal/mol) proceeding through the diene hydride species 6. The low-energy isomerization is fast on an NMR time

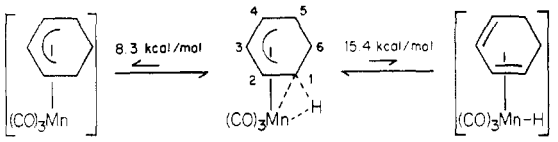

5 4 6

scale at −10 °C and results in rapid exchange of $H_{1\text{-endo}}$ with $H_{5\text{-endo}}$, $H_{1\text{-exo}}$, with $H_{5\text{-exo}}$, and H_2 with H_4. The second isomerization is observed at higher temperature (10–120 °C) and, coupled with the first process, scrambles the six olefinic exo hydrogens (H_2, H_3, H_4, $H_{1\text{-exo}}$, $H_{5\text{-exo}}$, $H_{6\text{-exo}}$) and, separately, the three endo hydrogens ($H_{1\text{-endo}}$, $H_{5\text{-endo}}$, $H_{6\text{-endo}}$).

Stereochemistry of Hydride Reduction and Protonation. The stereochemistry of both the hydride reduction of 1 and the protonation of anion 2 has been probed by using ^{2}H NMR spectroscopy. Treatment of 1 with 5 equiv of triethyl borodeuteride followed by quenching of the diene anion with H_2O yields dideuterated 4. Examination of the ^{2}H NMR of this species at −10 °C (low energy scrambling process is rapid) reveals ^{2}H signals *corresponding only to exo sites*. In particular, no signal is noted at ca. −5.8 ppm where the average D_{1N}, D_{5N} peak would appear. Thus, in both steps of the sequential reduction, 1 to 3 to 2, deuteride is added stereospecifically exo.[15]

To probe the stereochemistry of protonation, anion 2 was generated from 4 by using KH in THF (see below) and then quenched with 99.96% D_2O. Examination of the ^{2}H spectrum at −10 °C showed signals only at δ 0.83 (D_{6N}) and −4.63 (D_{1N}, D_{5N} average) consistent with exclusive endo attack of D^+ on 2. Displacement of the average $^2H_{1N}$, $^2H_{5N}$ signal to a *lower* field position (δ −4.6) relative to the ^{1}H signal of the all protio analogue (δ −5.8) is complementary to the upfield displacement of the ^{1}H signal in the same complex (δ −7.0);[11] the ^{2}H shift indicates a substantial isotope effect of the equilibrium shown below in which the species with H in the bridging position is favored.

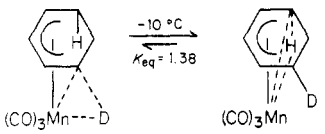

Spectral Characterization and Reactions of the Diene Anion 2. An important consequence of the coordination of the C–H bond in 4 to manganese is that the bridged hydrogen is activated and rendered acidic. Schrock[16] has observed similar enhanced acidity of the

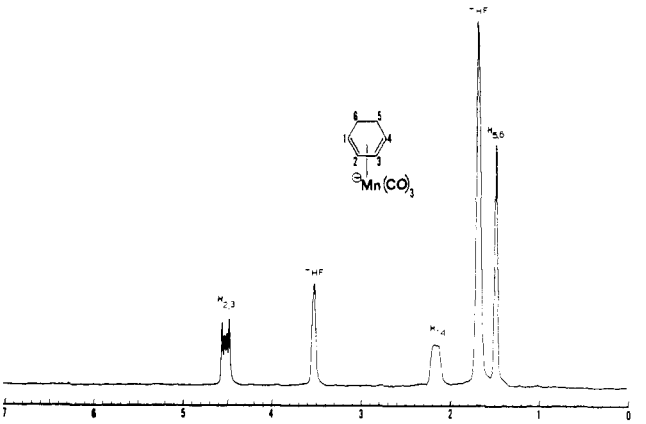

Figure 1. Room temperature ^{1}H NMR spectrum of 2. Shifts are parts per million relative to residual THF-d_8.

Scheme I

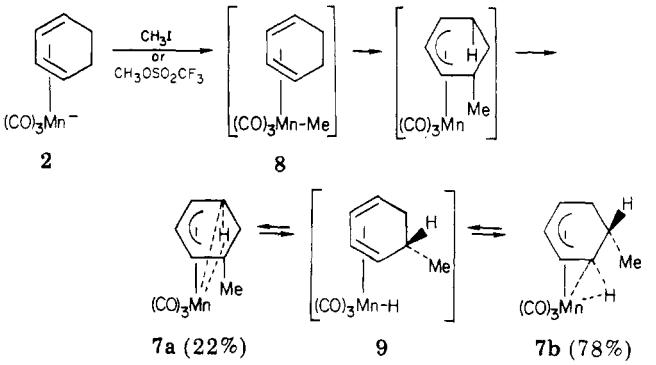

2 8

7a (22%) 9 7b (78%)

bridging hydrogen in electron-deficient tantalum carbene complexes that exhibit substantial M···H···C interactions.[17] Thus, treatment of 4 with a variety of bases (i.e., KH, NaH, *n*-BuLi) in THF results in deprotonation and regeneration of anion 2 as demonstrated by IR spectra of the resulting solutions. The reaction using NaH is slow at 25 °C, proceeding to ca. 80% completion in 18 h. In contrast, *n*-BuLi and KH react rapidly (<5 min at 25 °C), the latter resulting in vigorous hydrogen evolution. The KH reaction proceeds quantitatively producing a pale yellow, homogeneous solution of the diene anion and is the method of choice for NMR spectral characterization and examination of further reactions of 2.

Spectral Characterization. ^{1}H NMR characterization of 2 was possible by treatment of cyclohexenylmanganese tricarbonyl, 4, with KH in THF-d_8. The ^{1}H NMR spectrum of 2, prepared in this manner, is shown in Figure 1 and is identical in band patterns and similar in chemical shifts to the spectrum of (1,3-cyclohexadiene)iron carbonyl.[18a] Most characteristic of the symmetrical 1,3-diene structure is the AA′XX′ splitting pattern exhibited by the two sets of olefinic resonances corresponding to H_2, H_3 (δ 4.4) and H_1, H_4 (δ 2.2). As in the isoelectronic (1,3-cyclohexadiene)iron complex, the two pairs of exo and endo aliphatic hydrogens appear as a single broad four-proton resonance (1.5 ppm).

Methylation of 2. Treatment of the diene anion complex 2 (generated from 4 with KH in THF) with methyl iodide or methyl trifluoromethanesulfonate gave two endo ring-methylated isomers, **7a** and **7b**, as a crystalline orange

(15) Recently, Sweigert has observed exclusive endo addition of hydride to cationic $[(C_6H_6R)Mn(CO)_2NO]$ species, R = Me and Ph. See: Chung, Y. K.; Choi, H. S.; Sweigert, D. A. *J. Am. Chem. Soc.* **1982**, *104*, 4245.

(16) (a) Schrock, R. R. *Acc. Chem. Res.* **1979**, *12*, 98. (b) Schultz, A. J.; Williams, J. M.; Schrock, R. R.; Rupprecht, G. A.; Fellman, J. D. *J. Am. Soc.* **1979**, *101*, 1593. (c) Schultz, A. J.; Brown, R. K.; Williams, J. M.; Schrock, R. R. *Ibid.* **1981**, *103*, 169. (d) Schrock, R. R.; Fellman, J. D.; Messerle, G. A.; Rupprecht, G. A. *Ibid.* **1980**, *102*, 6236. (d) Schrock, R. R.; Stucky, G.; Jennische, P.; Messerle, G. A. *Ibid.* **1980**, *102*, 6744.

(17) Goddard, R. J.; Hoffman, R.; Jemmis, E. D. *J. Am. Chem. Soc.* **1980**, *102*, 7667.

(18) (a) King, R. B., "Organometallic Synthesis"; King, R. B., Eisch, J. J., Eds.; Academic Press: New York, 1965; Vol. 1, p 130. (b) Ibid., p 174.

solid. The two isomers are present in a 22:78 ratio, respectively (in solution at ca. 30 °C), and presumably result from endo ring methylation followed by coordination of a *second* endo C–H bond as shown in Scheme I. Complex **7a** must be the first formed isomer and is thought to arise from initial formation of **8** (or a methyl-bridged species) followed by methyl migration to the endo side of the ring. Isomer **7b** is believed to arise by isomerization of **7a** through diene hydride intermediate **9**. Indeed, variable-temperature ^{1}H NMR studies have demonstrated that the observed isomer ratio **7a**:**7b** is under thermodynamic control as a result of rapid equilibration between these isomers in solution.

The ^{1}H NMR data for **7a,b** at ca. −10 °C are tabulated in Table I. The two isomers are easily distinguished. In the major isomer **7b**, there are two endo hydrogens capable of bridging to manganese and at −10 °C, in analogy with the unsubstituted system,[11] these are rapidly exchanging on an NMR time scale resulting in a single two-proton resonance at −6.5 ppm. This low-energy exchange process is blocked in isomer **7a** by the 5-endo methyl group. Thus, at −10 °C a high-field resonance is observed at −13.7 ppm corresponding to the one endo hydrogen bridged to manganese. Heating a mixture of **7a** and **7b** causes the two isomers to rapidly interconvert via intermediate **9** resulting in coalescence of the $H_{1\text{-endo}}$, $H_{5\text{-endo}}$ resonance (−6.5 ppm) of the major isomer with the $H_{1\text{-endo}}$ (−13.7 ppm) and $H_{6\text{-endo}}$ (ca. 0.2 ppm) resonances of the minor isomer giving an average resonance at −6.4 ppm at 120 °C. An X-ray crystallographic analysis of **7b** has confirmed the proposed structure of this isomer.[11]

Perhaps the most surprising aspect of the mechanism in Scheme I is the proposed metal-to-ring migration of the methyl group upon methylation of diene anion **2**, formally an insertion of an olefin into a metal–alkyl bond. The only well-documented example of a metal-to-ring alkyl migration of this type is Green's observation of transfer of the ethyl group of $Cp_2Mo(Et)Cl$ to the endo side of one of the cyclopentadienyl rings upon treatment with phosphines.[19]

The conversion of **2** to **7** is interesting in that, following methyl migration to the ring, a second endo C–H bond is activated through coordination to manganese. Thus, quantitative deprotonation of **7a,b** by KH can be achieved, giving the monomethylated cyclohexadiene anion **10**. The IR spectrum of **10** in the carbonyl stretching region (ν_{CO} 1930 (s), 1838 (s), and 1789 (s) cm^{-1}) is nearly identical with that of the parent anion **2**. Again, generation of the anion in THF-d_8 allowed verification of the structure of **10** by ^{1}H NMR spectroscopy; ^{1}H shifts and coupling constants are summarized in the Experimental Section.

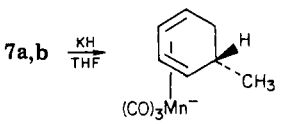

10

The ultimate conversion of **2** to **10** formally represents an electrophilic substitution of an endo hydrogen of cyclohexadiene mediated by manganese activation.

Dimethylation. Methylation of (5-*endo*-Methylcyclohexadiene)manganese Tricarbonyl Anion, 10. Monomethylated anion **10** is also highly nucleophilic and reacts rapidly with methyl iodide in THF. As shown below, addition of the methyl group from the endo side to either end of the bound diene unit in **10** is expected to yield two possible products. Methyl addition to C_4 followed by coordination (and activation) of a *third* endo C–H bond gives **11**. Addition to C_1 gives the 16-electron complex **12** that possesses no potentially bridging endo C–H bonds. The reaction was performed under a carbon monoxide atmosphere in order to facilitate trapping of coordinatively unsaturated **12** as the π-allyl tetracarbonyl adduct **13**.

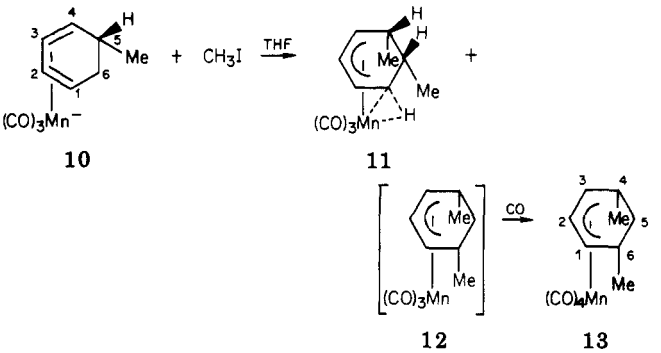

Isolation of the crude product of this reaction followed by column chromatography on neutral alumina allowed separation of orange and yellow bands. The orange oil isolated from the first band (0.1 g, 20% yield) exhibited IR bands in the carbonyl region at 2056 (s), 1986 (m), and 1963 (very s) cm^{-1} and ^{1}H NMR resonances as summarized in Table II. On the basis of comparison with the IR and ^{1}H NMR spectra of (cyclohexenyl)$Mn(CO)_4$ (see below), this product was assigned the symmetrical, π-allyl tetracarbonyl structure **13**. The yellow oil (0.1 g, 20% yield) isolated from the second band exhibited strong carbonyl stretching bands at 2020, 1948, and 1941 cm^{-1} as expected for the bridged tricarbonyl complex **11**. ^{1}H NMR analysis allowed verification of this structure. The ^{1}H chemical shift and coupling constant data for **11** are tabulated Table I. Peak assignments and coupling constants were obtained through a series of ^{1}H decoupling experiments. At −10 °C, decoupling was accompanied by spin-saturation transfer (SST)[20] between exchanging nuclei as a result of fluxional isomerization of **11** via symmetrical diene hydride **14**. As

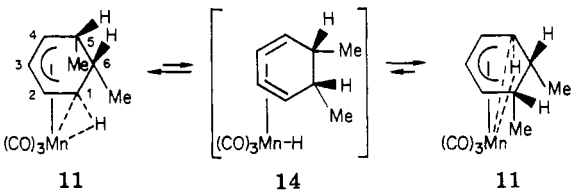

predicted by this mechanism, the following pairs of nuclei are observed to exchange: [$(CH_3)_{5\text{-endo}}$, $(CH_3)_{6\text{-endo}}$], [H_2, H_3], [$H_{1\text{-exo}}$, H_4], [$H_{5\text{-exo}}$, $H_{6\text{-exo}}$]. Only the bridging hydrogen $H_{1\text{-endo}}$ remains unique in this isomerization scheme, which accounts for the absence of SST upon irradiation of this nucleus. These SST results completely confirm the peak assignments. Although no quantitative rate studies were carried out, the conditions for SST and the observed intensity reductions are quite similar to those for the parent system and suggest the rate of isomerization via diene hydride **14** is similar to the corresponding process in the unsubstituted system.

Additional major resonances observed in the spectrum of the yellow oil have been assigned to the (1-methyl-substituted cyclohexadienyl)-, (2-methyl-substituted cyclohexadienyl)-, and (6-*endo*-methyl-substituted cyclohexadienyl)manganese tricarbonyl complexes, respectively.

(19) Green, M. L. H.; Benfield, F. W. S. *J. Chem. Soc., Dalton Trans.* **1974**, 1324.

(20) See ref 11 for a brief discussion of spin-saturation-transfer and appropriate references.

Table I. NMR Data for Bridged (Cyclohexenyl)Mn(CO)$_2$L Complexes[a,b]

Compound	Nucleus	3	2	4	1N	5N	1X	5X	6N	6X	Others
4 (L=CO)[c,d]	^{1}H	5.1 (t, 6 Hz)	4.6 (m)		-5.7 (br)		1.7 (m)		1.0 (m)	0.6 (m)	
7a (L=CO)[e]	^{1}H	f	4.5 (m)	3.3 (m)	-13.7 (br)	--	1.6 (m)	0.4 (m)	f	f	$(CH_3)_{5\text{-endo}}$ 0.6 (d, 7 Hz)
7b (L=CO)[e]	^{1}H	4.5 (t, 6 Hz)	4.0 (m)		-6.5 (m)		0.9 (m)		--	f	$(CH_3)_{6\text{-endo}}$ 0.1 (coupling obscured by overlapping pecks)
11 (L=CO)[d]	^{1}H	5.4 (m)	5.1 (m)	3.8 (ddd, 1,6, 6.6 Hz)	-13.0 (ddd, 16.5 9, 5 Hz)	--	1.0 (dd, 7, 16.5 Hz)	2.2 (m)	--	1.2 (m)	$(CH_3)_{5\text{-endo}}$ 0.8 (d, 8 Hz) $(CH_3)_{6\text{-endo}}$ 0.7 (d, 6.6 Hz)
19 (L=P(OMe)$_3$)[e]	^{1}H	4.8 (br s)	4.2 (br s)		-4.9, -5.9, -6.7 (3 isomers)		1.2 (br s)		0.6 (br s)	0.3 (br s)	P(OMe)$_3$ 3.4(br)
19 (L=P(OMe)$_3$)[e]	^{13}C	92.2	67.5		20.11				18.0		P(OMe)$_3$ 51.6

[a] All NMR spectra are reported between 0 and 30 °C and are referenced to the residual ^{1}H and ^{13}C signal in the deuterated solvent. Thus, in complexes 4, 7b, and 19 the low-temperature scrambling process is rapid; the high-temperature process is slow on the NMR time scale. [b] For the NMR spectrum of 22, see the following paper. [c] Complete ^{1}H and ^{13}C analysis previously reported. [d] Solvent = CD_2Cl_2. [e] Solvent = toluene-d_8. [f] Missing resonances could not be assigned due to spectral complexity.

Table II. NMR Data for (Cyclohexenyl)Mn(CO)$_3$L Complexes[a]

Compound	Nucleus	2	1	3	4X	6X	4N	6N	5X	5N	Other
13 (L=CO)[b]	^{1}H	4.5 (5, 7H)	3.5 (d, 7 Hz)		2.0 (q, 7 Hz)		--		0.9 (m)	0.9 (m)	$(CH_3)_{4\text{-endo},6\text{-endo}}$ 0.8 (d, 7 Hz)
15 (L=P(OMe)$_3$)[b]	^{1}H	5.0 (m)	4.3 (m)	4.0 (m)	2.4 (m)	2.4 (m)	--	2.3 (m)	1.3 (m)	--	$(CH_3)_{4\text{-endo},5\text{-endo}}$ 1.4 (d, 6 Hz), second peak obscured; P(OMe)$_3$ 3.3 (d, 11 Hz)
16 L=P(OMe)$_3$[b]	^{1}H	4.8 (dt, 6,12 Hz)	3.7 (m)		2.4 (m)		--		1.2 (m)	1.2 (m)	$(CH_3)_{4\text{-endo},5\text{-endo}}$ 1.1(d, 6 Hz); P(OMe)$_3$ 3.2 (d, 11 Hz)
17 (L=CO)[b]	^{1}H	4.6 (t, 6.5 Hz)	3.8 (t, 6.5 Hz)		1.9 (m)		1.9 (m)		1.0 (m)	1.0 (m)	
18 (L=P(OMe)$_3$)[c]	^{1}H	4.8 (dt, 11,6 Hz)	3.9 (m)		2.2 (m)		2.2 (m)		1.2 (m)	1.2 (m)	P(OMe)$_3$ 3.2 (d, 11 Hz)
18 (L=P(OMe)$_3$)[c]	^{13}C	91.3	61.4		28.9				20.4		(P(OMe)$_3$ 51.9

[a] All NMR spectra were obtained at room temperature and are referenced to the residual ^{1}H and ^{13}C signal(s) in the deuterated solvent. [b] Solvent = benzene-d_6. [c] Solvent = toluene-d_8.

The first two assignments are based on comparisons with the known ^{1}H NMR spectra of the 1- and 2-methyl isomers.[5,21] The 6-endo-methyl isomer has not been previously prepared; however, resonances observed at δ 5.9 (t, J = 6 Hz, H_3), 2.4 (q, J = 6.5Hz, $H_{6\text{-exo}}$), and 1.4 (d, 6.5 Hz, 6-endo-Me) are totally consistent with this structure. The three cyclohexadienyl isomers are present in an approximate ratio of 2:3:1, respectively, and account for ca. 60% of the product isolated as a yellow oil. Attempts to separate these from **11** by recrystallization from petroleum ether were unsuccessful. The cyclohexadienyl complexes exhibit IR bands in the carbonyl region that are identical with those of **11**, thus accounting for their lack of detection by IR spectroscopy. The formation of the cyclohexadienyl complexes can be explained by invoking an alternate, competing reaction pathway in which the diene anion reacts as a hydride donor with methyl iodide. Similar reactivity has been observed upon reaction of (cyclohexadiene)manganese tricarbonyl anion, **2**, with trimethylsilyl chloride.[22] The absence of cyclohexadienyl products upon similar reaction of **2** with CH_3I is probably best explained in terms of the decreased steric requirements for endo methyl addition in this system.

If the reaction of methyl iodide with the 5-*endo*-methyl diene anion **10** is carried out in the absence of CO, the yield of tetracarbonyl **13** drops substantially (to ca. 10%) and considerable decomposition is evident. The formation of **13** likely arises from trapping of **12** by CO formed by self-decomposition. Such reactions have precedence in the formation of (π-allyl)iron tetracarbonyl cations from 16-electron π-allyl tricarbonyl cations.[23] No evidence was obtained for interaction of the electron-deficient manganese center in **12** with either of the two endo methyl groups.

When trimethyl phosphite is used as the trapping ligand in the methylation reaction, in addition to the cyclohexadienyl products two isomeric (*endo*-dimethylcyclohexenyl)(trimethyl phosphite)manganese tricarbonyl complexes **15** and **16** are isolated together in a ca. 1:8 ratio (ca. 30% overall yield). The complex **15** arises from reaction

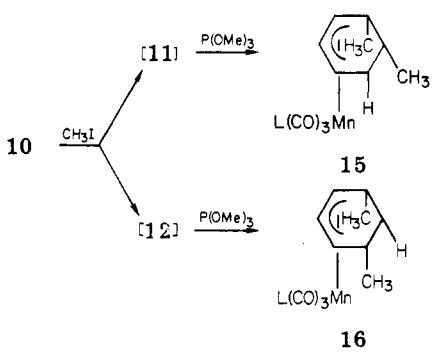

of $P(OMe)_3$ with bridged species **11** (analogous reactions are described below) while **16** arises from trapping of **12** analogous to the formation of **13**. The ^{1}H NMR spectra of **15** and **16** are summarized in Table II. These species could not be separated from one another by chromatography.

Oxidative Cleavage Reactions. Generation of Free Cyclohexadienes. A result that bears directly on the potential synthetic utility of this system is the rapid oxidative cleavage of the diene from the diene anion complexes **2** and **10**. Exposure of a THF solution of **2**, prepared from **4** plus KH, to 1 atm of oxygen causes immediate precipitation of a brown solid and quantitative formation of free 1,3-cyclohexadiene. Further reaction with tetracyanoethylene (TCNE) results in quantitative trapping of the 1,3-cyclohexadiene as the Diels–Alder adduct.

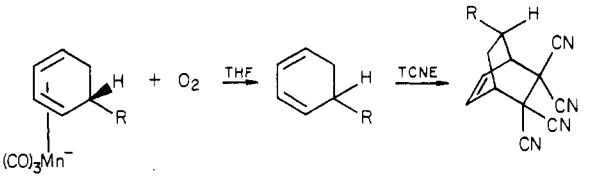

2, R = H
10, R = CH_3

Similar reactivity is observed for the monomethylated diene anion **10** generated from **7a,b**. In each case the isolated Diels–Alder adducts have been characterized by ^{1}H NMR spectroscopy (see Experimental Section). For 5-methylcyclohexadiene, generated from **10**, two Diels–Alder adducts are possible (exo- and endo-Me); however, ^{1}H NMR analysis indicates that only one isomer is present. The isomer that results from attack of TCNE trans to methyl on the least hindered side of the diene (shown above) is presumed to be the product isolated.

Reactions of Cyclohexenylmanganese Tricarbonyl, 4, with Lewis Base Type Ligands. In contrast to the deprotonation reactions observed upon treatment of **12** with strong bases such as KH, reaction of the bridged cyclohexenyl complex with Lewis bases (L) that can act as powerful ligands results in simple replacement of the coordinated C–H bond as shown below. This reaction, which has parallels with the behavior of the protonated (diene)FeL_3 species,[14d] has been observed for L = CO and $P(OMe)_3$. The reaction with CO at 1 atm in petroleum

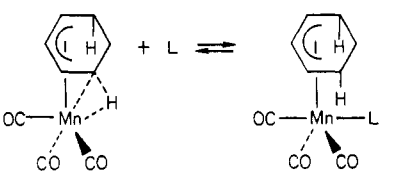

4 **17**, L = CO
18, L = $P(OMe)_3$

ether proceeds to only 50% completion (based on relative intensities of IR bands in the carbonyl region[24]) to give the symmetrical π-allyl tetracarbonyl adduct **17** (ν_{CO} 2055 (s), 1987 (s), 1970 (s) and 1959 (s) cm^{-1}). The reaction is readily reversible; thus, flushing a solution of **17** with N_2 for ca. 5 min results in quantitative regeneration of **4**. A ^{1}H NMR sample of **17** was prepared by saturating a benzene-d_6 solution of **4** with CO at 25 °C and then sealing under 1 atm of CO pressure. The ^{1}H NMR spectrum of the resulting mixture indicated ca. 30% conversion of **4** to the tetracarbonyl complex **17**. The use of a subtraction routine to eliminate resonances arising from **4** gave a clean spectrum that is completely consistent with the proposed symmetrical π-allyl structure **17**. Chemical shifts, coupling constants, and peak assignments for this complex are tabulated in Table II.

Complex **4** reacts with trimethyl phosphite in a similar fashion, but the reaction is quantitative. Thus, treatment of **4** with 1 equiv of $P(OMe)_3$ in 2,2,4-trimethylpentane results in rapid and complete conversion to the π-allyl tricarbonyl monophosphite complex **18** (ν_{CO} 1912 (s), 1942

(21) Lukacs, A.; Brookhart, M. *Organometallics*, following article in this issue.
(22) Lukacs, A.; Brookhart, M., unpublished results.
(23) (a) Gibson, D. H.; Vonnahme, R. L. *J. Am. Chem. Soc.* **1972**, *94*, 5090. (b) Whitesides, T. H.; Arhart, R. W. *Inorg. Chem.* **1975**, *14*, 209.

(24) Relative intensities of IR bands are uncorrected for differences in ϵ, the molar extinction coefficients.

(s), and 2003 (s) cm^{-1}). The same reaction performed in toluene-d_8 allowed characterization of **18** by NMR spectroscopy. The ^1H and ^{13}C NMR spectra are tabulated in Table II. Comparison of the ^1H NMR spectrum of **18** with that of the tetracarbonyl complex **17** reveals distinct similarities in chemical shifts as well as in band patterns. The major distinguishing features in the spectrum of **18** are the methyl doublet due to the metal-bound $P(OMe)_3$ ligand ($^3J_{^1H-^{31}P}$ = 11 Hz) and the appearance of the central allylic ^1H resonance (H_2) as a doublet of triplets due to phosphorus coupling ($^3J_{^1H-^{31}P}$ = 11 Hz). The coupled ^{13}C NMR spectrum of **18** provided $^{13}C-^1H$ coupling constants and aided in the assignment of ^{13}C resonances in the broad-band-decoupled spectrum. The equivalence of the C_1, C_3 and C_4, C_6 pairs of ring carbons in the ^{13}C NMR spectra (broad-band decoupled and gated decoupled) is consistent with pseudooctahedral structure of **18** that possesses a plane of symmetry through C_2, C_5 and Mn. The phosphite ligand presumably occupies the ligand site vacated by the previously coordinated C–H bond, thus situating it immediately beneath the C_5 ring carbon.

Thermolysis of the π-allyl complex **18** in situ results in loss of CO and formation of the C–H-bridged dicarbonyl monophosphite complex **19** analogous in structure to **4**.

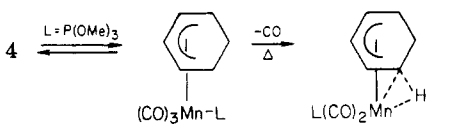

18 **19**, L = $P(OMe)_3$

The phosphite complex **19** is isolated as an orange crystalline solid (85% yield based on **4**) following heating for 1 h at 98 °C in 2,2,4-trimethylpentane and exhibits IR bands in the carbonyl region at 1888 (s) and 1954 (s) cm^{-1}. Heating for longer periods in the presence of excess $P(OMe)_3$ results in further reaction and conversion to *mer*-$(P(OMe)_3)_3(CO)_2Mn-H$. The latter product presumably arises from displacement of the diene ligand in **20** by $P(OMe)_3$ as shown. The phosphite complex **19** undergoes

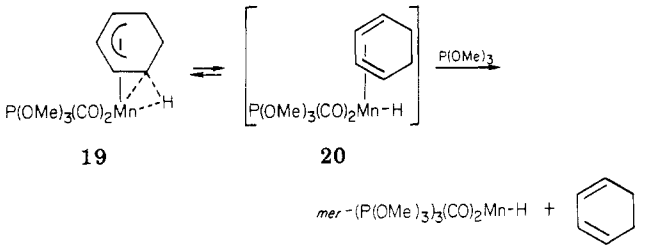

19 **20**

three distinct isomerization processes similar to those observed in the bridged tricarbonyl complex **4**. As in **4**, the isomerizations result in dynamic NMR behavior; however, in the case of **19** the resulting spectra are complicated by the presence of three discrete C–H-bridged isomers **19a,b,c** in which the ligand L is either cis or trans to the bridging hydrogen. Whereas the isomerizations of **4** are all degenerate in nature, this is not the case with **19**.

The low-temperature exchange process interconverts **19a** with **19a′**, a degenerate isomerization, and results in an averaged signal at δ −5.9 as in **4**. The same low-temperature process interconverts isomers **19b** and **19c**, a nondegenerate isomerization. Since **19b** and **19c** are not present in equal population, the high-field averaged signal is split into two peaks centered at approximately −5.8 ppm. Mutual exchange of the three ancillary ligands (two CO's and one $P(OMe)_3$) at somewhat higher temperatures interconverts all three isomers. All isomers are present in significant amounts, and the ^1H and ^{13}C spectral data for

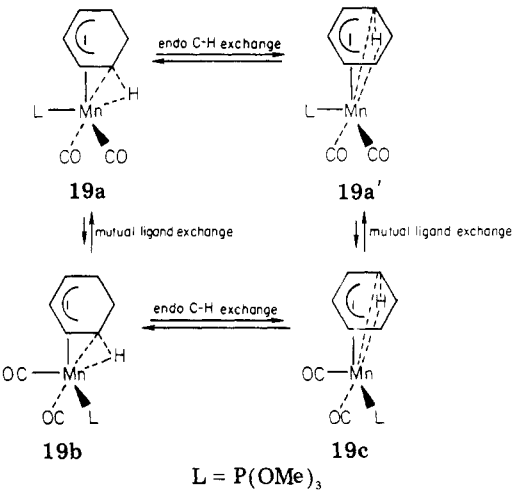

the mixture at 25 °C are summarized in Table I. A detailed analysis of the complex NMR behavior of these species will be published separately.

Hydride Addition to Cyclohexenylmanganese Tetracarbonyl. It is clear that the reactions of cyclohexadienylmanganese tricarbonyl, **3**, with nucleophilic hydride reagents closely parallels the extensively studied reactions of the analogous cationic cyclohexadienyliron complexes,[25] enabling high-yield reduction to the diene anion **2**. Similar hydride addition to the (cyclohexenyl)-$Mn(CO)_4$, **17**, complex was expected to result in further reduction of the polyolefin ligand to give initially the (cyclohexene)manganese tetracarbonyl anion **21**. There exist numerous examples of such nucleophilic additions (exo to metal) to π-allyl species[1] including some isoelectronic iron complexes.[25a,26]

A preliminary investigation of this reaction has been undertaken. As already described, complex **17** is generated through reaction of **4** with CO and exists as an equilibrium mixture with **4** at 1 atm of CO pressure. Reaction of this mixture with $LiBEt_3H$ under 1 atm of CO in THF solvent was expected to yield either the desired (cyclohexene)-manganese tetracarbonyl anion **21** (or secondary decomposition products) or diene anion, **2** (via deprotonation of **4**). Addition of hydride at −78 °C followed by warming

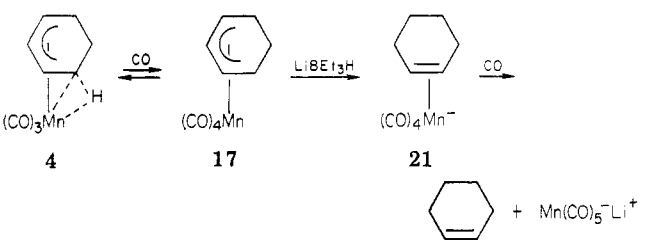

4 **17** **21**

to 25 °C and IR analysis of the resulting solution indicated the presence of manganese pentacarbonyl anion (ν_{CO} 1896 (s) and 1862 (s) cm^{-1}; structural assignment based on an IR spectrum of the same anion generated by reduction of $Mn_2(CO)_{10}$ with $LiBEt_3H$[31] showed $Mn(CO)_5^-$ Li^+ to be the only organometallic product. It is likely that the pentacarbonyl anion arises from preferential hydride addition to **17** followed by dissociation of the bulky cyclohexene ligand from anion **21** and trapping of $Mn(CO)_4^-$ by CO.

(25) (a) For a summary, see: Birch, A. J.; Jenkins, I. D. "Transition Metal Organometallics in Organic Synthesis"; Alper, H., Ed.; Academic Press: New York, 1976; Vol. 1, p 1. (b) For specific synthetic applications, see: Ireland, R. E.; Brown, G. G., Stanford, R. H.; McKenzie, T. C. *J. Org. Chem.* **1974**, *39*, 51. Pearson, A. J. *Acc. Chem. Res.* **1980**, *13*, 463.

(26) Whitesides, T. H.; Arhart, R. W.; Slaven, R. W. *J. Am. Chem. Soc.* **1973**, *95*, 5792.

The production of uncomplexed cyclohexene as a result of this net substitution reaction was confirmed by preparative gas chromatographic analysis of the distilled reaction mixture and positive identification of the alkene by ^1H NMR spectroscopy. The yield of free cyclohexene based on **4** was 76%. Thus, the addition of hydride to **17** represents the final step in the ultimate conversion of benzene to cyclohexene via activation through manganese complexation. Unlike the oxidative diene cleavage reactions, the displacement of cyclohexene from **21** by CO should permit simple recovery of the manganese carbonyl, an advantage in terms of potential synthetic applications.

The Reaction of 4 with Diazomethane. It is well-established that transition-metal hydrides that are moderately acidic can react with diazomethane to give the metal alkyl. Particularly relevant to the present systems is the observation that $(CO)_5Mn-H$ reacts with diazomethane to give $(CO)_5Mn-CH_3$.[27] In view of the acidic nature of the bridging hydrogen in **4**, we felt that reaction with diazomethane may provide an alternative entry into the endo methylated species **7a** and **7b**.

When **4** is treated with a 30-fold excess of diazomethane in methylene chloride, a monomethylated bridged species is observed, but surprisingly *not* the endo methyl isomers **7a** and **7b**. Rather, a complex mixture of exo methyl isomers **22** with the methyl group in the exo or olefinic

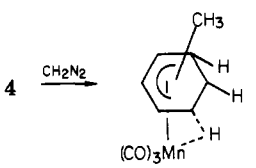

22

positions is obtained (70% yield). All six possible isomers are present in unequal distribution and all are in equilibrium via the dynamic processes previously delineated. A complete characterization of **22** is described in the subsequent paper.[21]

Although the mechanism of this reaction is uncertain, it seems likely that the nucleophilic CH_2N_2 attacks the π-allyl system in an exo fashion to yield an adduct similar to **23** (alternatively, this species may be written as a π-allyl

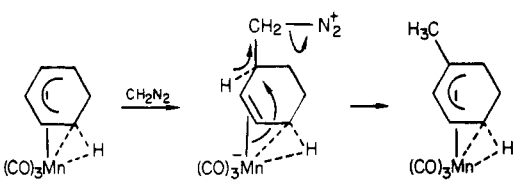

23 **22a**

equilibration with all other exo or olefinic isomers

hydride). Upon loss of N_2 and hydride migration to the developing carbonium ion, the 4-methyl species **22a** is generated which then isomerizes, rapidly scrambling the methyl group among the six exo and olefinic positions. The attack of diazomethane as a nucleophile followed by loss of N_2 with hydride migration has parallels in the mechanism of the reaction of CH_2N_2 with aldehydes to yield methyl ketones.[28]

Three modes of reaction of the bridged species with bases have now been observed: deprotonation of the acidic bridged hydrogen to yield the diene anion (KH, butyllithium), replacement of the coordinated C–H bond (CO, $P(OMe)_3$), and nucleophilic attack on the π-allyl moiety (CH_2N_2).

Reaction of 4 with 1,1-Diphenylethylene. Treatment of **4** with 5 equiv of 1,1-diphenylethylene in THF at 110 °C results in quantitative formation of cyclohexadienylmanganese tricarbonyl, **3**, and 1,1-diphenylethane. In

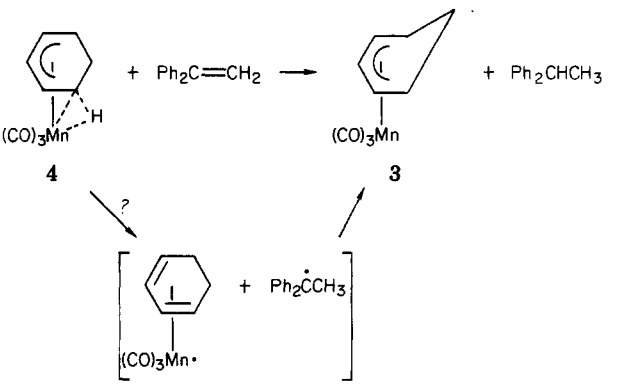

4 **3**

24

analogy with the reactions of $(CO)_5MnH$ with α-methylstyrene,[29] the probable first step in the reaction is the transfer of a hydrogen atom from the bridged site to the alkene to generate the radical pair Ph_2CCH_3 and C_6H_8-$Mn(CO)_3$, **24**. Abstraction of a hydrogen atom by Ph_2CCH_3 from **24** yields the final products. There is evidence neither for formation of an endo $Ph_2(CH_3)C$-substituted bridged species from coupling of Ph_2CCH_3 and **24** nor for dimerization of **24** to the binuclear diene complex $[(C_6H_8)(CO)_3Mn]_2$ analogous to $Mn_2(CO)_{10}$ obtained from the reaction of $(CO)_5MnH$ with α-methylstyrene.[29] Reactions with other alkenes are currently being examined. Preliminary evidence indicates that butadiene reacts with **4** in a similar manner as 1,1-diphenylethylene.

Summary

The chemistry reported here illustrates two unique aspects of transition-metal activation of hydrocarbon ligands. First, the activation of arenes toward addition of 2 equiv of nucleophile to yield coordinated dienes has been demonstrated in the conversion of cationic (benzene)manganese tricarbonyl, **1**, to the anionic 1,3-cyclohexadiene complex **2**. Second, although coordination of C–H bonds to transition metals has been previously observed in a limited number of systems,[13] the transformations of the bridged cyclohexenylmanganese tricarbonyl complex, **4**, represent the first clear illustration that such metal C–H interactions can be used to advantage for carrying out a variety of transformations, especially electrophilic substitutions at the bridged carbon. This chemistry lends valuable insight into the nature of the Mn···H···C interaction and suggests in a general way how metal activated C–H bonds may be utilized to achieve functionalization at saturated carbon centers.

The model reactions performed in this study clearly demonstrate the important role manganese activation can play in promoting the selective and high yield conversion of benzene to 1,3-cyclohexadienes (unsubstituted and substituted derivatives) and cyclohexene. On the basis of these initial studies, extension of this chemistry in a broad fashion is expected to provide useful synthetic methods

(27) (a) Hierber, W.; Wagner, G. *Justus Liebigs. Ann. Chem.* **1958**, *618*, 24; *Z. Naturforsch., B: Anorg. Chem., Org. Chem., Biochem., Biophys., Biol.* **1957**, *B12*, 478; **1958**, *B13*, 339. (b) Herrmann, W. A. *Angew. Chem., Int. Ed. Engl.* **1978**, *17*, 800.

(28) Gutsche, C. D. *Org. Reac.*, **1954**, *8*, 364.

(29) Sweany, R. L.; Halpern, J. *J. Am. Chem. Soc.* **1977**, *99*, 8335.

for the conversion of arenes to reduced and highly functionalized derivatives. The use of nucleophiles other than hydride to generate exo-substituted cyclohexadienyl complexes and the availability of numerous potential electrophiles for reaction with the diene anion and nucleophiles for reaction with the cyclohexenyl complexes should permit versatile ring substitution with control of stereochemistry. Numerous manganese tricarbonyl complexes of substituted arenes are available and will permit further ring functionalization. Work is currently in progress on these extensions. In the folowing paper we report results which indicate that a variety of alkyl-substituted arene complexes may be similarly reduced with borohydride reagents.[21]

Experimental Section

All reactions and manipulations of manganese carbonyl compounds and other air-sensitive materials were conducted under a dry, oxygen-free, nitrogen atmosphere. The nitrogen gas was purified by passage through columns of concentrated sulfuric acid, potassium hydroxide pellets, and BASF catalyst R3-11 (maintained at ca. 110 °C). Benzene and tetrahydrofuran (THF) were freshly distilled under a nitrogen atmosphere from $LiAlH_4$. Other reagent grade solvents were simply degassed by flushing with nitrogen for ca. 15 min and used without further purification unless otherwise stated. Other reagents were used without further purification unless otherwise noted. Manganese pentacarbonyl bromide was prepared from dimanganese decacarbonyl (Strem or Pressure Chemicals) according to the procedure of King.[18b]

^1H NMR spectra were recorded at 100 MHz by using a Varian XL-100 FT NMR spectrometer or at 250 MHz by using a Bruker WM250 FT NMR spectrometer. ^{13}C NMR spectra were recorded at 62.9 MHz by using the Bruker instrument. In all cases, residual solvent resonances were used as internal standards for the reporting of chemical shifts. Deuterated NMR solvents were dried over molecular sieves (4 Å) and stored under nitrogen in ampules equipped with Teflon stopcocks. Infrared spectra of manganese carbonyl compounds were recorded on a Beckman spectrophotometer (IR 4250), and frequencies (cm^{-1}) were assigned relative to a polystyrene standard. Only bands in the carbonyl stretching region (ca. 1500–2300 cm^{-1}) are reported.

Column packings for column chromatography consisted of neutral or basic alumina (Al_2O_3; 70/290 mesh).

All melting points are uncorrected and were determined in unsealed capillaries by using a simple oil bath and thermometer setup.

Preparation of (Benzene)manganese Tricarbonyl Hexafluorophosphate, 1. The hexafluorophosphate salt of (benzene)manganese tricarbonyl, 1, was prepared by using a modification of procedures described by previous workers.[30] Manganese pentacarbonyl bromide (4.12 g, 0.015 mol) and aluminum chloride (4.47 g, 0.034 mol) were refluxed in 30 mL of anhydrous benzene overnight under a nitrogen atmosphere. Initially, carbon monoxide was evolved followed by separation of a brownish bottom layer and a yellow upper layer. After the mixture was cooled in an ice bath, 40 mL of ice water was carefully added in portions and the mixture stirred vigorously resulting in formation of a yellow aqueous layer. The mixture was shaken with 60 mL of toluene and the lower aqueous layer separated, filtered through cotton, and collected. The aqueous fraction was in turn shaken with 50 mL of petroleum ether, separated, and then treated dropwise with a threefold excess of aqueous 4.5 M hexafluorophosphoric acid. The resulting pale yellow precipitate was filtered by suction and washed with water. This yellow solid was then dissolved in acetone, and the resulting solution was filtered through Celite and evaporated to give a yellow-orange crystalline solid, 4.18 g (77% yield). The material isolated was identified as the (benzene)manganese tricarbonyl salt on the basis of infrared and ^1H NMR spectra: IR ν_{CO} (in acetone) 2080 (s), 2020 (s) cm^{-1}; ^1H NMR (in acetone-d_6) δ 6.4 (s).

Preparation of Cyclohexadienylmanganese Tricarbonyl, 3. Cyclohexadienylmanganese tricarbonyl, 3, was prepared by the reaction of (benzene)manganese tricarbonyl hexafluorophosphate, 1, with lithium aluminum hydride ($LiAlH_4$) in diethyl ether. The procedure used was a modification of previously reported procedures[30] and involves longer reaction times and gives somewhat improved yields.

A stirred suspension of 1 (3.25 g, 0.008 97 mol) in anhydrous diethyl ether (100 mL) at 25 °C was treated wtih $LiAlH_4$ (0.56 g, 0.015 mol) in small portions. The solid slowly dissolved forming a yellow solution. After 3.5 h distilled water (20 mL) was added dropwise to destroy the excess hydride. More ether was added, and the layers were separated. The aqueous layer was extracted with two 20-mL portions of ether, and the ether fractions were combined, dried over anhydrous sodium sulfate, filtered through Celite, and evaporated (30 °C (25 mm)) to give a yellow oil. This material was chromatographed on a short column of neutral alumina (activity II) with pentane as eluent. The yellow band that eluted first was collected and the solution evaporated (30 °C (25 mm)) to a crystalline yellow solid. Further purification by recrystallization from pentane at −78 °C, vacuum sublimation at 0.012 mm and 45 °C, and recrystallization again from pentane at −78 °C gave bright yellow crystals (1.06 g, 54% yield based on $C_6H_6Mn(CO)_3PF_6$) identified as 3 on the basis of infrared and ^1H NMR spectra: IR ν_{CO} (in petroleum ether) 2020 (s), 1945 (s), 1927 (s) cm^{-1}; (in THF) 2017 (s), 1929 (s, br) cm^{-1}; ^1H NMR (in $CDCl_3$) δ 2.0 (d, J = 12 Hz, $H_{6\text{-exo}}$), 2.6 (m, $H_{6\text{-endo}}$), 2.9 (t, J = 6 Hz, H_1, H_5), 4.8 (t, J = 6 Hz, H_2, H_4), 5.8 (t, J = 6 Hz, H_3).

Preparation of Cyclohexenylmanganese Tricarbonyl, 4. Method A. Reduction of (Benzene)manganese Tricarbonyl Cation with $LiBEt_3H$. This procedure has been reported in a previous publication.[11]

Method B. Reduction of (Benzene)manganese Tricarbonyl Cation with $KB(i\text{-}OPr)_3H$. (Benzene)manganese tricarbonyl hexafluorophosphate, 1 (24.38 g, 0.0673 mol, was suspended in 250 mL of THF and 168 mL of $KB(i\text{-}OPr)_3H$ (1 M in THF, 2.5 equiv) was slowly added with stirring at 25 °C. Infrared spectra of 1-mL aliquots removed from the reaction mixture at periodic intervals showed that hydride addition proceeds in a stepwise fashion through a neutral cyclohexadienylmanganese tricarbonyl intermediate (ν_{CO} 2017 (s), 1929 (s, br) cm^{-1}). Upon quantitative formation of the (1,3-cyclohexadiene)manganese tricarbonyl anion, 2 (ca. 16 h based on infrared spectra; ν_{CO} 1930 (s), 1840 (s), 1789 (s) cm^{-1}), 50 mL of degassed, distilled water was added (dropwise initially). Sodium chloride was then added until the layers separated. The organic layer was removed and dried with magnesium sulfate, and the solvent was evaporated. The remaining dark oil was extracted with 100 mL of petroleum ether, and the resulting solution was then dried, filtered, and evaporated to give a red oil. This material was purified by dissolving in a minimum amount of petroleum ether, cooling to −78 °C, and decanting off the solvent. The product, which melted at 0 °C, was dried under vacuum to give 9.11 g of 4 (61.5% yield).

Method C. Reduction of Cyclohexadienylmanganese Tricarbonyl. The procedure used to prepare 4 from cyclohexadienylmanganese tricarbonyl, 3, was identical with that described in methods A or B above. A complete characterization of 4 by variable-temperature ^1H and ^{13}C NMR spectroscopy is included in a previous publication:[11] IR ν_{CO} (in pentane) 2020 (s), 1945 (s), 1937 (s) cm^{-1}. Anal. Calcd: C, 49.11; H, 4.12; Mn, 24.96. Found: C, 48.80; H, 4.31; Mn, 25.21.

Deprotonation of 4 and IR Characterization of the (1,3-Cyclohexadiene)manganese Tricarbonyl Anion, 2. Method A. Using n-BuLi. Cyclohexenylmanganese tricarbonyl (80 mg, 0.36 mmol) was dissolved in 50 mL of anhydrous THF, and 0.34 mL of 1.6 M n-BuLi (1.5 equiv) was added with stirring. The solution underwent an immediate color change from yellow to orange. After ca. 20 min at 25 °C an IR spectrum was obtained that indicated complete conversion to 2: IR ν_{CO} (in THF) 1929 (s), 1853 (s), 1831 (s), 1811 (s), 1758 (s) cm^{-1}.

Method B. Using NaH. A large excess of NaH was suspended in 25 mL of anhydrous THF, and ca. 50 mg of 4 was added with stirring. No reaction was observed initially; however, after 18 h at 25 °C IR analysis of the mixture indicated ca. 80% conversion to anion 2: IR ν_{CO} (in THF) 1930 (s), 1843 (s, br), 1786 (s, br) cm^{-1}.

(30) Pauson, P. L.; Seagal, J. A. *J. Chem. Soc., Dalton Trans.* **1975**, 1677, 1683.

Method C. Using KH. Potassium hydride (30 mg, 0.75 mmol) was washed with petroleum ether and then suspended in 25 mL of anhydrous THF, and 50 mg of 4 was added with stirring. Vigorous hydrogen evolution was observed, and the color of the solution immediately faded to pale yellow. Slow hydrogen evolution continued for ca. 30 min; however, IR analysis of the reaction mixture after 20 min at 25 °C indicated complete conversion of 4 to the anion 2: IR ν_{CO} (in THF) 1930 (s), 1840 (s, br), 1789 (s, br) cm^{-1}.

Preparation of ^1H NMR Samples of Diene Anions 2 and 10. (1,3-Cyclohexadiene)manganese Tricarbonyl Anion, 2. A solution of cyclohexenylmanganese tricarbonyl, 4 (49.3 mg, 0.224 mmol), in 3 mL of THF-d_8 was prepared and transferred via syringe to a Schlenk tube containing 24 mg (0.61 mmol) of dry KH. The mixture was stirred at 25 °C causing vigorous hydrogen evolution and formation of a pale yellow solution. After ca. 20 min the excess KH was allowed to settle and the solution was transferred through a stainless-steel cannula to a 5-mm NMR tube equipped with a ground-glass joint and a Schlenk adapter. The NMR sample was degassed on a high vacuum (0.005 mm) manifold by a number of freeze–pump–thaw cycles and then sealed in vacuo. Samples prepared in this manner were stable for weeks in the refrigerator. The ^1H NMR spectrum shown in Figure 1 was recorded at room temperature.

(5-*endo*-Methyl-1,3-cyclohexadiene)manganese Tricarbonyl Anion, 10. Samples of 10 were prepared for ^1H NMR analysis by using the same procedure described for 2 by the reaction of 70 mg of (5-*endo*-methylcyclohexenyl)- and (6-*endo*-methylcyclohexenyl)manganese tricarbonyl (mixture of isomers 7a and 7b) with excess KH: ^1H NMR (THF-d_8) δ 4.6 (m, H_3), 4.5 (m, H_2), 2.2 (m, H_1), 2.1 (m, H_4), 1.9 (ddd, J = 13.0, 3.2, 8.0 Hz, $H_{6\text{-exo}}$), 1.6 (m, $H_{5\text{-exo}}$), 1.0 (ddd, J = 13.0, 2.7, 4.8 Hz, $H_{6\text{-endo}}$), 0.7 (d, J = 7.4 Hz, $(CH_3)_{5\text{-endo}}$).

Preparation of (5-*endo*-Methylcyclohexenyl)- and (6-*endo*-Methylcyclohexenyl)manganese Tricarbonyl, 7a,b. Potassium hydride (12.5 g) was suspended in 250 mL of anhydrous THF, and 3.84 g of cyclohexenylmanganese tricarbonyl, 4, was added with stirring at room temperature. Hydrogen evolution and disappearance of the yellow color attributed to 4 was rapid, giving a pale yellow solution of the diene anion 2 (confirmed by IR spectroscopy). After ca. 30 min the anion solution was filtered through glass wool/Celite to remove excess KH. The filtrate was slowly added with stirring to a flask containing 21.7 mL of CH_3I (ca. 20-fold excess) causing immediate formation of a white precipitate (KI) and an orange solution. The KI was removed by filtration through glass wool/Celite, and the filtrate was evaporated (25 °C (25 mm)) to an orange oil. The oil was extracted with a minimum amount of petroleum ether, filtered through Celite to remove residual KI, and evaporated again to an orange oil. Remaining traces of solvent were removed under high vacuum (0.005 mm), giving 3.51 g of pure monomethylated product 7 (86% yield based on 12) as an orange oil. Dissolution of the oil in a minimum amount of petroleum ether and cooling to −78 °C resulted in precipitation of 7a,b which was isolated as a crystalline orange solid (mp 40–42 °C). In solution this material exists as a 22:78 mixture of the 5-*endo*-methyl and 6-*endo*-methyl isomers that are in rapid equilibrium as demonstrated by their temperature-dependent ^1H NMR spectra. The infrared spectrum of this mixture in the carbonyl stretching region was identical with that of the parent complex: IR ν_{CO} (in petroleum ether) 2020 (s), 1945 (s), 1937 (s) cm^{-1}.

Reaction of (5-*endo*-Methyl-1,3-cyclohexadiene)manganese Tricarbonyl Anion, 10, with Methyl Iodide under a CO Atmosphere. A large excess of potassium hydride was suspended in 20 mL of anhydrous THF and 0.488 g of (5-*endo*-methylcyclohexenyl)- and (6-*endo*-methylcyclohexenyl)manganese tricarbonyl, 7a,b, was added in portions with stirring at room temperature. Infrared analysis of the reaction solution following cessation of hydrogen evolution (ca. 30 min) indicated quantitative conversion to diene anion 10 (ν_{CO} 1930 (s), 1838 (s), 1789 (s) cm^{-1}). The anion solution was filtered through glass wool/Celite to remove excess KH, and the filtrate was slowly added with stirring to a flask containing 5.2 mL of CH_3I under ca. 1 atm of CO (slight positive pressure of CO maintained by oil bubbler). Addition resulted in immediate formation of a white precipitate (KI) and an orange solution. The KI was removed by filtration through glass wool/Celite, and the filtrate was evaporated (25 °C (20 mm)) to an orange oil. The oil was extracted with a minimum amount of petroleum ether (bp 30–65 °C), filtered through Celite, and evaporated again to an orange oil. Remaining traces of solvent were removed under high vacuum (0.005 mm), giving 0.249 g of crude product. Infrared analysis of this material indicated that a mixture of carbonyl-containing compounds were present. Column chromatography on neutral, activity II alumina using petroleum ether as eluent allowed separation of an orange (eluted first) and a yellow band (eluted second). These were collected separately and the petroleum ether solvent evaporated (25 °C (20 mm)). The orange oil isolated from the first band (ca. 0.1 g, 20% yield) was identified as (4,6-*endo*-dimethylcyclohexenyl)manganese tetracarbonyl, 13, based on its ^1H NMR (Table II) and IR spectra (ν_{CO} (in petroleum ether) 2056 (s), 1986 (m), 1963 (very s) cm^{-1}). The ^1H NMR spectrum of the yellow oil isolated from the second band (ca. 0.1 g, 20% yield) indicated that a mixture of products was present. The bridge (5,6-*endo*-dimethylcyclohexenyl)manganese tricarbonyl complex, 11, accounts for ca. 40% of the total mixture and was thoroughly characterized by a series of ^1H decoupling and SST experiments (see Results and Discussion). The remainder of this material (60%) is comprised of the monomethylated cyclohexadienyl isomers (2:3:1 ratio), which were identified in the Results and Discussion. Attempts to separate 11 from the cyclohexadienyl species by recrystallization from a minimum amount of petroleum ether were unsuccessful. An IR spectrum of the yellow oil exhibited strong carbonyl bands at 2020, 1948, and 1941 cm^{-1} (in petroleum ether).

Reaction of (5-*endo*-Methyl-1,3-cyclohexadiene)manganese Tricarbonyl Anion, 10, with Methyl Iodide under a N_2 Atmosphere. To a suspension of 0.66 (mmol) of KH in 100 mL of THF was added 0.67 g (2.66 mmol) of (5-*endo*-methylcyclohexenyl)- and (6-*endo*-methylcyclohexenyl)manganese tricarbonyl, 7. This reaction was monitored as above and then filtered into a flask containing 3 mL of CH_3I under an atmosphere of nitrogen. The solution turned dark brown almost immediately. As reported above, this solution was filtered, extracted wtih petroleum ether, filtered again, evaporated, and chromatographed. The product was found to consist of 10% yield (4,6-*endo*-dimethylcyclohexenyl)manganese tricarbonyl, 7% yield (5,6-dimethylcyclohexenyl)manganese tricarbonyl, and 5% yield of a mixture of (methylcyclohexadienyl)manganese tricarbonyl isomers.

Reaction of (5-*endo*-Methyl-1,3-cyclohexadiene)manganese Tricarbonyl Anion, 10, with Methyl Iodide and Trimethyl Phosphite. To a suspension of 0.30 g (7.5 mmol) of KH in 20 mL of THF was added 0.16 g (0.68 mmol) of (5-*endo*-methylcyclohexenyl)- and (6-*endo*-methylcyclohexenyl)manganese tricarbonyl, 7. This reaction was monitored as above and then filtered into a flask containing 0.6 mL of methyl iodide and 0.6 mL of trimethyl phosphite under an atmosphere of nitrogen. As above this solution was filtered, extracted, and filtered again, and the solvent was removed. The resulting material was chromatographed on alumina using a 50/50 mixture of petroleum ether and methylene chloride. Only one band was obtained in 30% yield. This proved to be an 8:1 mixture of the two possible (*endo*-dimethylcyclohexenyl)manganese tricarbonyl monophosphite complexes.

Oxidation of Diene Anions 2 and 10 and Trapping of Free Diene with TCNE. (1,3-Cyclohexadiene)manganese Tricarbonyl Anion, 2. Potassium hydride (0.75 g) was suspended in 50 mL of anhydrous THF, and 1.027 g of cyclohexenylmanganese tricarbonyl, 4, was added with stirring at room temperature. After ca. 30 min, the resulting anion solution was filtered through glass wool/Celite to remove excess KH, and the filtrate was transferred to a dry two-necked, round-bottomed Schlenk flask. The filtered THF solution was cooled to 0 °C and flushed with oxygen for ca. 5 min, causing immediate precipitation of a brown solid. The flask was charged with ca. 1 atm of O_2 (slight positive pressure), and the THF solution was stirred at 0 °C for an additional 25 min. The reaction mixture was again filtered through glass wool/Celite, and the filtrate was added to a stirring solution of 1.14 g of TCNE in 20 mL of THF at 0 °C. Following addition, the reaction mixture was allowed to warm to room temperature, and stirring was continued for an additional 20 min. Evaporation of solvent and further drying of the light green solid residue under high vacuum (0.005 mm) gave 1.60 g of the

Diels–Alder adduct plus excess TCNE (quantitative yield based on 4). Purification of the solid by transfer to a sintered-glass filter and washing with nine 15-mL portions of 50:50 petroleum ether/toluene followed by three 15-mL portions of petroleum ether gave 0.771 g (79% yield) of pure Diels–Alder adduct gave being dried in vacuo (0.005 mm). Characterization as the Diels–Alder adduct was based on the ^{1}H NMR spectrum of this material that was identical with the ^{1}H NMR spectrum of the same adduct prepared from an authentic sample of 1,3-cyclohexadiene plus TCNE in a control experiment performed under the same reaction conditions: ^{1}H NMR (acetone-d_6) δ 6.8 (m, H_2, H_3), 3.9 (m, H_1, H_4), 2.2 and 1.7 (m, $H_{7\text{-exo}}$, $H_{8\text{-exo}}$ and $H_{7\text{-endo}}$, $H_{8\text{-endo}}$).

(5-*endo*-Methyl-1,3-cyclohexadiene)manganese Tricarbonyl Anion, 10. Diene anion 10 was generated by the reaction of 7a,b (0.271 g) with excess KH. Oxidation with oxygen and trapping of 5-methyl-1,3-cyclohexadiene with 0.344 g of TCNE was performed by using the same procedure described for anion 4. The crude Diels–Alder adduct was isolated in quantitative yield (based on 7a,b). Washing with 50:50 petroleum ether/toluene gave 0.227 g (88.2% yield) of the pure adduct that was characterized as the 5-methyl isomer by ^{1}H NMR spectroscopy: ^{1}H NMR (acetone-d_6) δ 6.9 and 6.7 (m, H_2 and H_3), 3.9 (m, H_4), 3.7 (d, J = 6.3 Hz, H_1), 2.4 (m, H_7, H_8), 1.2 (m, H_8), 1.0 (d, J = 5.4 Hz, $(CH_3)_7$).

Generation and IR Characterization of (Cyclohexenyl)-Mn(CO)$_3$L Adducts. (Cyclohexenyl)Mn(CO)$_4$, 17. A solution of ca. 100 mg of cyclohexenylmanganese tricarbonyl, 4, in 10 mL of petroleum ether was prepared and flushed with CO for 10 min at room temperature. Infrared analysis of the reaction solution indicated ca. 50% conversion (based on relative intensities of IR bands in CO region)[24] to cyclohexenylmanganese tetracarbonyl, 17 (ν_{CO} 2055 (s), 1987 (s), 1970 (s), 1959 (s) cm^{-1}). Stirring of the reaction solution under ca. 1 atm of CO for an additional 21 h at room temperature resulted in no change in the relative ratios of 4 and 17. Flushing this solution with nitrogen for 10 min at 50 °C resulted in complete conversion back to the original bridged tricarbonyl complex 4.

(Cyclohexenyl)Mn(CO)$_3$P(OMe)$_3$, 18. A solution of 0.145 g of 4 in 100 mL of 2,2,4-trimethylpentane was prepared, and 0.082 g of trimethyl phosphite (1 equiv) was added at room temperature with stirring. The original yellow color attributed to 4 immediately faded to light yellow. Infrared analysis of the reaction mixture after 10 min indicated quantitative conversion to the (cyclohexenyl)Mn(CO)$_3$P(OMe)$_3$ adduct, 18 (ν_{CO} 1912 (s), 1942 (s), 2003 (s) cm^{-1}).

Preparation of ^{1}H NMR Sample of (Cyclohexenyl)Mn-(CO)$_4$, 17. A solution of cyclohexenylmanganese tricarbonyl, 4 (30 mg), in 0.5 mL of benzene-d_6 was prepared in a 5-mm tube equipped with a female ground-glass joint and a Schlenk adapter. The solution was flushed with CO for ca. 3 min at room temperature. After an additional 10 min under 1 atm of CO and while a slight positive CO pressure (from an oil blubber) was maintained, the NMR sample was sealed. The ^{1}H NMR spectrum of this sample was recorded at room temperature and exhibited a complex series of resonances attributable to a 70:30 mixture of 4 and 17, respectively. Elimination of the resonances arising from 4 was possible by recording a second ^{1}H NMR spectrum of 4 in benzene-d_6 in the absence of CO and subtracting this spectrum from the first using a DIFFSPEC subtraction program supplied by Varian Instrument Division. The resulting difference spectrum exhibited resonances arising only from 17 and allowed positive identification of this species (chemical shifts, coupling constants, and peak assignments are summarized in Table II).

Preparation of NMR Sample of (Cyclohexenyl)Mn-(CO)$_3$P(OMe)$_3$, 18. To a 5-mm NMR tube equipped with a female ground-glass joint and a Schlenk adapter was added 0.069 g of 4 (0.313 mmol), 0.039 g of trimethyl phosphite (0.313 mmol), and ca. 0.5 mL of toluene-d_8. The sample was degassed by a number of freeze–pump–thaw cycles and sealed in vacuo (0.005 mm). The ^{1}H and ^{13}C NMR spectra of this sample allowed unambiguous characterization of the (cyclohexenyl)Mn(CO)$_3$P-(OMe)$_3$ adduct, 17, which is formed quantitatively. (See Table II for ^{1}H NMR data).

Preparation of (Cyclohexenyl)Mn(CO)$_2$P(OMe)$_3$, 19. A solution of cyclohexenylmanganese tricarbonyl, 4 (0.47 g, 2.114 mmol), in 100 mL of 2,2,4-trimethylpentane was treated with 0.273 g of trimethyl phosphite (2.14 mmol) with stirring at room temperature. The resulting tricarbonyl monophosphite adduct 18 was heated to reflux (98–99 °C) for 1 h. The infrared spectrum of the reaction solution after being cooled to room temperature exhibited major bands at 1888 and 1954 cm^{-1} (minor bands (ca. 10%) assigned to $C_6H_9Mn(CO)_3$, 4, and $C_6H_9Mn(CO)_3P(OMe)_3$, 18, were also observed). Evaporation of solvent (30 °C (20 mm)) gave an orange oil that was redissolved in a minimum amount of petroleum ether (bp 30–65 °C) and chromatographed on a column of neutral, activity I alumina using petroleum ether as eluent. Two yellow bands were observed, and these were collected separately. The yellow oil isolated from the first minor fraction was identified as $C_6H_9Mn(CO)_3$, 4, by its infrared spectrum. Evaporation of solvent from the second major fraction gave an orange oil (0.593 g, 85% yield) that crystallized upon standing. Characterization of this material as the C–H-bridged dicarbonyl monophosphite complex 19 (all three possible isomers) was based on (1) its variable-temperature ^{1}H and ^{13}C NMR spectra (see Table I), (2) its IR spectrum in the carbonyl region, and (3) elemental analysis. Further purification was possible by crystallization from a minimum amount of petroleum ether at −20 °C: IR ν_{CO} (in 2,2,4-trimethylpentane) 1888 (s), 1954 (s) cm^{-1}. Anal. Calcd: C, 41.79; H, 5.74; P, 9.80; Mn, 17.38. Found: C, 41.62, H, 5.67; P, 9.69; Mn, 17.13.

Thermolysis of 18 for longer periods in the presence of excess trimethyl phosphite resulted in further reaction and isolation of a clear oily solid (yield undetermined) following column chromatography. This material was identified as *mer*-(P(OMe)$_3$)$_3$-(CO)$_2$Mn–H by its ^{1}H NMR and IR spectra: IR ν_{CO} (in 2,2,4-trimethylpentane) 1895 (s), 1954 (s) cm^{-1}; ^{1}H NMR (in CD_2Cl_2) δ 3.60 (m, P(OCH$_3$)$_3$), −8.55 (dt, J = 50, 65, Hz, Mn–H).

Reaction of (Cyclohexenyl)Mn(CO)$_4$, 17, with LiBEt$_3$H. A solution of cyclohexenylmanganese tricarbonyl, 4 (0.557 g, 2.53 mmol), in 20 mL of anhydrous THF was prepared and cooled to −78 °C. The solution was flushed with CO for ca. 10 min to establish equilibrium between 4 and the tetracarbonyl 17 (confirmed by IR spectroscopy). While a CO atmosphere (ca. 1 atm of CO pressure was provided by an expanded balloon) was maintained, 3.29 mL of LiBEt$_3$H (1 M in THF; 1.3 equiv) was added dropwise with stirring causing an immediate color change to deep red. Following addition, the solution was allowed to stir an additional 10 min at −78 °C before slowly warming to room temperature. Stirring was continued under CO for another 2 h at room temperature to ensure complete reaction. An infrared spectrum of the reaction solution after this period exhibited major bands in the carbonyl region at 1896 (s) and 1862 (s) cm^{-1} assigned to the pentacarbonyl anion, (CO)$_5$Mn$^-$Li$^+$, by comparison with the IR spectrum of the same anion generated by reduction of $Mn_2(CO)_{10}$ with LiBEt$_3$H.[31] Minor carbonyl bands (ca. 10%) attributed to unreacted $C_6H_9Mn(CO)_4$, 19, and $C_6H_9Mn(CO)_3$, 4, were also observed. The reaction mixture was vacuum distilled (30–70 °C (20 mm)) to remove nonvolatiles and the distillate analyzed for the presence of cyclohexene by gas chromatography following addition of 0.360 g (2.53 mmol) decane as internal standard. (Hewlett-Packard Research Chromatograph series 5750B equipped with a flame ionization detector and a 12 ft × $^1/_8$ in. stainless-steel column packed with 25% QF-1 on Chromosorb W (80/100 mesh).) Cyclohexene was identified as a significant component of this solution by comparison of retention times with a cyclohexene in THF standard. Similar comparisons with a 1,3-cyclohexadiene in THF standard indicated that none of this material was present. Quantitative measurement of cyclohexene and decane relative peak areas (corrected for differences in detector response) indicated that cyclohexene is produced in 76% yield (based on $C_6H_9Mn(CO)_3$, 4) from this reaction. Collection of the supposed cyclohexene fractions following repeated injections on a preparative scale chromatographic unit (Varian Aerograph Model 90-P equipped with a thermal conductivity detector and a 14 ft × $^1/_4$ in. stainless-steel column packed with 25% QF-1 Chromosorb W (60/80 mesh)) and analysis of these by ^{1}H NMR allowed positive identification of cyclohexene (δ (in $CDCl_3$) 5.6 (t, 2 H), 2.0 (m, 4 H), 1.6 (m, 4 H); structural as-

(31) Gladysz, J. A.; Williams, G. M.; Tam, W.; Johnson, D. L.; Parker, D. W.; Selover, J. C. *Inorg. Chem.*, **1979**, *18*, 553.

signment based on comparison with ^{1}H NMR spectrum of authentic cyclohexene sample).

Reaction of 4 with Diazomethane. To an Erlenmeyer flask containing 3.35 g (32 mmol) of *N*-methyl-*N*-nitrosourea in 60 mL of methylene chloride at 0 °C was added 60 mL of a 10% KOH solution. The reaction which ensues produces 32 mmol of diazomethane dissolved in the methylene chloride layer. This layer was added over a 1-h period to a second flask containing 0.24 g (1.09 mmol) of cyclohexenylmanganese tricarbonyl, **4**, in 60 mL of methylene chloride at 0 °C. The flask was allowed to warm slowly to room temperature while the mixture was stirred overnight.

The solvent and excess diazomethane were removed under aspirator vacuum, and the solid residue was extracted with petroleum ether. The yellow solution was filtered through Celite, concentrated, and chromatographed on a short alumina column, with petroleum ether as eluent, to give 0.18 g (0.77 mmoles, 70% yield) of a mixture of (methylcyclohexenyl)manganese tricarbonyl complexes, **22**. Six isomers were observed by NMR in which the methyl group occupied either an exo or olefinic site on the cyclohexenyl ring. No endo methyl isomers were identified.

Reaction of 4 with 1,1-Diphenylethylene. To a stainless-steel bomb was added 0.30 g (1.36 mmol) of cyclohexenylmanganese tricarbonyl, **4**, 1.2 mL (1.22 g, 6.8 mmol) of 1,1-diphenylethylene, and 7 mL of tetrahydrofuran. The bomb was sealed and heated to 110 °C for 3 days. The bomb was then allowed to cool, and its contents were transferred to a round-bottom flask under nitrogen. The solvent was removed under vacuum to give 1.24 g (82% recovery) of product, which proved to be exclusively unreacted diphenylethylene, diphenylethane, and cyclohexadienylmanganese tricarbonyl, **3**.

Acknowledgment is made to the donors of the Petroleum Research Fund, administered by the American Chemical Society, and to the National Institutes of Health (Grant 1 R01 GM2393801) for the support of this research.

Registry No. **1**, 38834-51-4; **2**, 76830-94-9; **3**, 12108-14-4; **4**, 76830-97-2; **7a**, 76830-98-3; **7b**, 76830-99-4; **10**, 76831-00-0; **11**, 84810-74-2; **12**, 84810-75-3; **13**, 84810-76-4; **14**, 84810-77-5; **15**, 84810-78-6; **16**, 84810-79-7; **17**, 76831-01-1; **18**, 84810-80-0; **19**, 84810-81-1; **21**, 84810-82-2; **22** (isomer 1), 84823-04-1; **22** (isomer 2), 84773-78-4; **22** (isomer 3), 84712-01-6; **22** (isomer 4), 84712-00-5; *mer*-$(P(OMe)_3)_3(CO)_2MnH$, 84847-66-5.

Preparation of Alkyl-Substituted Derivatives of Cyclohexenylmanganese Tricarbonyl via Reduction of Methylated Arene Complexes. Characterization of and Substituent Site Preference Determination for Interconverting Cyclohexenyl Isomers Containing a Two-Electron, Three-Center Mn•••H•••C Interaction

M. Brookhart* and Alexander Lukacs

Department of Chemistry, University of North Carolina, Chapel Hill, North Carolina 27514

Received October 4, 1982

Treatment of the cations (toluene)$Mn(CO)_3^+$, (*o*-xylene)$Mn(CO)_3^+$, (*p*-xylene)$Mn(CO)_3^+$, and (mesitylene)$Mn(CO)_3^+$ with triisopropoxyborohydride results in vicinal addition of 2 equiv of hydride to yield methylated tricarbonyl anions. Analogous to (1,3-cyclohexadiene)$Mn(CO)_3^-$, protonation of these methyl-substituted 1,3-cyclohexadiene anions yields bridged (cyclohexenyl)$Mn(CO)_3$ species, each possessing an aliphatic, endo C–H bond that is activated via coordination to manganese. Several isomers are observed for each system, differing only in methyl substitution at the available ring sites. The structures and thermodynamic ratios of isomers have been determined through ^{1}H and ^{13}C NMR analysis including variable-temperature NMR and spin saturation transfer experiments. Decided preference for vinylic substitution by methyl is demonstrated. Results indicate that attack by hydride at the endo face of the dienyl ligand cannot be ruled out for the mesitylene complex, since both the *endo,exo,exo*- and the *exo,exo,exo*-trimethyl-substituted cyclohexenyl systems are generated from the reduction of and subsequent protonation of the mesitylene cation.

Introduction

The double nucleophilic reduction of coordinated arenes to coordinated cyclohexadienes represents a unique and potentially useful method for arene reduction and functionalization. Such double nucleophilic addition has been achieved for certain highly activated arene complexes.[1-3] In the preceding paper we have described the reduction of monocationic (benzene)manganese tricarbonyl to (1,3-cyclohexadiene)manganese tricarbonyl anion in good yield. This conversion can be effected with either triisopropoxyborohydride or triethyl borohydride.[4,5] Pauson has noted similar reductions of certain substituted systems using lithium aluminum hydride.[6,7] We have developed

(1) Jones, D.; Pratt, L.; Wilkinson, G. *J. Chem. Soc.* **1962**, 4458.
(2) Lai, Y.-H.; Tam, W.; Vollhardt, K. P. C. *J. Organomet. Chem.* **1981**, *216*, 97.
(3) Grundy, S. L.; Maitlis, P. M. *J. Chem. Soc., Chem. Commun.* **1982**, 379.
(4) Lamanna, W.; Brookhart, M. *J. Am. Chem. Soc.* **1981**, *103*, 989.
(5) Brookhart, M.; Lamanna, W.; Humphrey, M. B. *J. Am. Chem. Soc.* **1982**, *104*, 2117.
(6) Bladon, P.; Munro, G. A. M., Pauson, P. L.; Mahaffy, C. A. L. *J. Organomet. Chem.* **1981**, *221*, 79.

0276-7333/83/2302-0649$01.50/0

signment based on comparison with ^{1}H NMR spectrum of authentic cyclohexene sample).

Reaction of 4 with Diazomethane. To an Erlenmeyer flask containing 3.35 g (32 mmol) of *N*-methyl-*N*-nitrosourea in 60 mL of methylene chloride at 0 °C was added 60 mL of a 10% KOH solution. The reaction which ensues produces 32 mmol of diazomethane dissolved in the methylene chloride layer. This layer was added over a 1-h period to a second flask containing 0.24 g (1.09 mmol) of cyclohexenylmanganese tricarbonyl, **4**, in 60 mL of methylene chloride at 0 °C. The flask was allowed to warm slowly to room temperature while the mixture was stirred overnight.

The solvent and excess diazomethane were removed under aspirator vacuum, and the solid residue was extracted with petroleum ether. The yellow solution was filtered through Celite, concentrated, and chromatographed on a short alumina column, with petroleum ether as eluent, to give 0.18 g (0.77 mmoles, 70% yield) of a mixture of (methylcyclohexenyl)manganese tricarbonyl complexes, **22**. Six isomers were observed by NMR in which the methyl group occupied either an exo or olefinic site on the cyclohexenyl ring. No endo methyl isomers were identified.

Reaction of 4 with 1,1-Diphenylethylene. To a stainless-steel bomb was added 0.30 g (1.36 mmol) of cyclohexenylmanganese tricarbonyl, **4**, 1.2 mL (1.22 g, 6.8 mmol) of 1,1-diphenylethylene, and 7 mL of tetrahydrofuran. The bomb was sealed and heated to 110 °C for 3 days. The bomb was then allowed to cool, and its contents were transferred to a round-bottom flask under nitrogen. The solvent was removed under vacuum to give 1.24 g (82% recovery) of product, which proved to be exclusively unreacted diphenylethylene, diphenylethane, and cyclohexadienylmanganese tricarbonyl, **3**.

Acknowledgment is made to the donors of the Petroleum Research Fund, administered by the American Chemical Society, and to the National Institutes of Health (Grant 1 R01 GM2393801) for the support of this research.

Registry No. **1**, 38834-51-4; **2**, 76830-94-9; **3**, 12108-14-4; **4**, 76830-97-2; **7a**, 76830-98-3; **7b**, 76830-99-4; **10**, 76831-00-0; **11**, 84810-74-2; **12**, 84810-75-3; **13**, 84810-76-4; **14**, 84810-77-5; **15**, 84810-78-6; **16**, 84810-79-7; **17**, 76831-01-1; **18**, 84810-80-0; **19**, 84810-81-1; **21**, 84810-82-2; **22** (isomer 1), 84823-04-1; **22** (isomer 2), 84773-78-4; **22** (isomer 3), 84712-01-6; **22** (isomer 4), 84712-00-5; *mer*-$(P(OMe)_3)_3(CO)_2MnH$, 84847-66-5.

Preparation of Alkyl-Substituted Derivatives of Cyclohexenylmanganese Tricarbonyl via Reduction of Methylated Arene Complexes. Characterization of and Substituent Site Preference Determination for Interconverting Cyclohexenyl Isomers Containing a Two-Electron, Three-Center Mn•••H•••C Interaction

M. Brookhart* and Alexander Lukacs

Department of Chemistry, University of North Carolina, Chapel Hill, North Carolina 27514

Received October 4, 1982

Treatment of the cations (toluene)$Mn(CO)_3^+$, (*o*-xylene)$Mn(CO)_3^+$, (*p*-xylene)$Mn(CO)_3^+$, and (mesitylene)$Mn(CO)_3^+$ with triisopropoxyborohydride results in vicinal addition of 2 equiv of hydride to yield methylated tricarbonyl anions. Analogous to (1,3-cyclohexadiene)$Mn(CO)_3^-$, protonation of these methyl-substituted 1,3-cyclohexadiene anions yields bridged (cyclohexenyl)$Mn(CO)_3$ species, each possessing an aliphatic, endo C–H bond that is activated via coordination to manganese. Several isomers are observed for each system, differing only in methyl substitution at the available ring sites. The structures and thermodynamic ratios of isomers have been determined through ^{1}H and ^{13}C NMR analysis including variable-temperature NMR and spin saturation transfer experiments. Decided preference for vinylic substitution by methyl is demonstrated. Results indicate that attack by hydride at the endo face of the dienyl ligand cannot be ruled out for the mesitylene complex, since both the *endo,exo,exo*- and the *exo,exo,exo*-trimethyl-substituted cyclohexenyl systems are generated from the reduction of and subsequent protonation of the mesitylene cation.

Introduction

The double nucleophilic reduction of coordinated arenes to coordinated cyclohexadienes represents a unique and potentially useful method for arene reduction and functionalization. Such double nucleophilic addition has been achieved for certain highly activated arene complexes.[1-3] In the preceding paper we have described the reduction of monocationic (benzene)manganese tricarbonyl to (1,3-cyclohexadiene)manganese tricarbonyl anion in good yield. This conversion can be effected with either triisopropoxyborohydride or triethyl borohydride.[4,5] Pauson has noted similar reductions of certain substituted systems using lithium aluminum hydride.[6,7] We have developed

(1) Jones, D.; Pratt, L.; Wilkinson, G. *J. Chem. Soc.* **1962**, 4458.
(2) Lai, Y.-H.; Tam, W.; Vollhardt, K. P. C. *J. Organomet. Chem.* **1981**, *216*, 97.
(3) Grundy, S. L.; Maitlis, P. M. *J. Chem. Soc., Chem. Commun.* **1982**, 379.
(4) Lamanna, W.; Brookhart, M. *J. Am. Chem. Soc.* **1981**, *103*, 989.
(5) Brookhart, M.; Lamanna, W.; Humphrey, M. B. *J. Am. Chem. Soc.* **1982**, *104*, 2117.
(6) Bladon, P.; Munro, G. A. M., Pauson, P. L.; Mahaffy, C. A. L. *J. Organomet. Chem.* **1981**, *221*, 79.

0276-7333/83/2302-0649$01.50/0

Scheme I

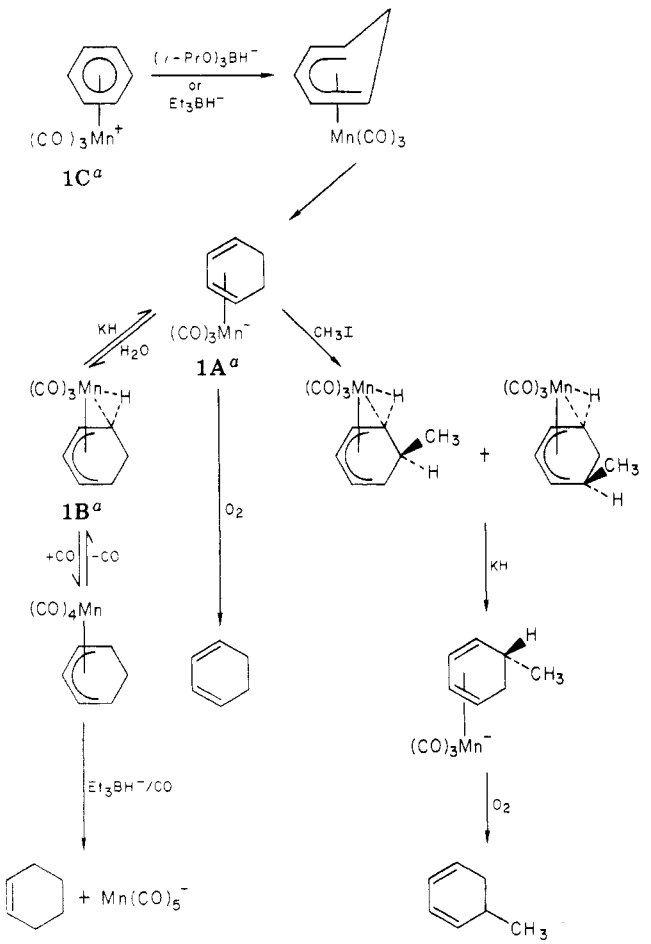

[a] Abbreviations: C = cation; A = anion; B = bridged.

the reaction sequence shown in Scheme I for the unsubstituted system. The potential synthetic utility of this sequence is threefold: (1) the reduction to the diene anion occurs in good yields and the free diene can be readily recovered by oxidation of **1A**,[4,8] (2) electrophilic substitution of the diene anion **1A** can be achieved and results in substitution at a saturated carbon,[4,5,8] and (3) the diene anion can be readily converted to the π-allyl tetracarbonyl complex and subsequently to cyclohexene.[4,8]

The unique Mn···H···C bridged complex **1B** is thermally stable (>120 °C), only mildly air sensitive, and readily prepared by reduction of **1C** followed by aqueous workup. The complex appears to be the synthetically most convenient source for both the diene anion **1A** (via treatment with KH) and the cyclohexenylmanganese tetracarbonyl complex (via treatment with CO). The dynamics and structure of this species have been previously reported.[4,5]

In light of the potential application of these reaction sequences to the reduction of substituted arenes, we wish to report here the hydride reduction and conversion of a series of alkyl-substituted (arene)manganese tricarbonyl cations to their corresponding bridged complexes. Those systems studied include the bridged compounds dervied from the toluene, *o*-xylene, *p*-xylene, and mesitylene cations. This work establishes (1) the feasibility of the reduction of alkyl-substituted arene systems, (2) the site and stereochemistry of hydride additions to these substituted systems, and (3) the equilibrium distributions and general substituent site preferences in the isomeric fluxional hydrogen-bridged systems.

Results and Discussion

The triisopropoxyborohydride reduction of a series of alkyl-substituted (arene)manganese tricarbonyl cations **2C–5C** to their corresponding (cyclohexadiene)manganese tricarbonyl anions is described below. Isolation of the reduction products was normally achieved by converting the initially formed diene anions **2A–5A** to the alkyl derivatives of the bridged species **2B–5B**, which can exist as complex mixtures of interconverting isomers.

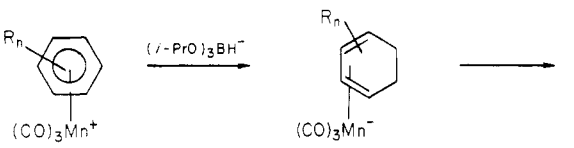

C A

complex	R_n	complex	R_n
1C	H	1A	H
2C	CH_3	2A	CH_3
3C	1,2-dimethyl	3A	1,2-dimethyl
4C	1,4-dimethyl	4A	1,4-dimethyl
5C	1,3,5-trimethyl	5A	1,3,5-trimethyl

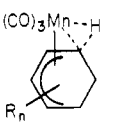

B

complex	R_n
1B	H
2B	CH_3
3B	1,2-dimethyl
4B	1,4-dimethyl
5B	1,3,5-trimethyl

The key to analysis of these isomeric compositions lies in unraveling the quite complex dynamic ^{1}H NMR spectra of these systems. The parent complex **1B** exhibits two dynamic averaging processes as detected by ^{1}H NMR spectroscopy: (a) a low-temperature site exchange (eq 1)

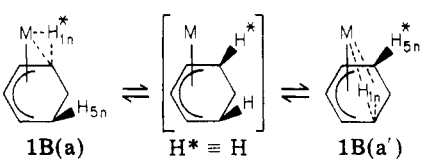

1B(a) H* ≡ H 1B(a′) (1)

that interconverts two enantiomers in a degenerate equilibrium via a π-allyl species (this process occurs with $\Delta G^{\ddagger}$ = 8.5 kcal/mol and is "rapid" on the NMR time scale above ca −20 °C); (b) a high-temperature proton scrambling (eq 2) proceeding through a diene hydride that when

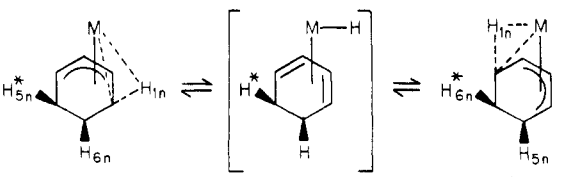

1B(a) H* ≡ H 1B(a′) (2)

coupled with (a) averages all three "endo" sites and, separately, all six "exo" sites[9] (this process occurs with $\Delta G^{\ddagger}$

(7) Recently, Sweigart prepared the neutral methyl and phenyl substituted (1,3-cyclohexadiene)Mn(CO)$_2$(NO) complexes via the addition of a single equivalent of nucleophile to (benzene)manganese tricarbonyl cation, followed by reactivation of the cyclohexadienyl ring using $NOPF_6$ and subsequent reduction using $NaBH_4$: Chung, Y. K.; Choi, H. S.; Sweigart, D. A. *J. Am. Chem. Soc.* **1982** *104*, 4245.

(8) Brookhart, M.; Lamanna, W.; Pinhas, A. R. *Organometallics*, preceding article in this issue.

= 15.8 kcal/mol and induces initial line broadening around 25 °C). Spin saturation transfer experiments also establish this exchange process at 40 °C.[10]

Conveniently, in the temperature range −10 to +25 °C process a is "rapid" and process b "slow" on the NMR time scale and ^{1}H NMR spectra are moderately narrow. Thus, for example, H_{1n} and H_{5n} exhibit a single, narrow, two-proton resonance at δ −5.7, the average of the shifts in the static spectrum (−100 °C) occurring at δ −12.8 for the bridged site H_{1n} and δ 1.4 for the nonbridged site H_{5n}. As shall be evident below, the most informative ^{1}H NMR data for each isomeric system comes from examination of the high field region of the spectrum (0 to −15 ppm) in the −10 to 25 °C temperature range.

Before a detailed analysis of the substituted systems is advanced, two general cases will be examined. First, consider the case in which a substituent, G, occupies a site such that the low-energy process is degenerate. For illustration, we use a three-substituted system. In this case

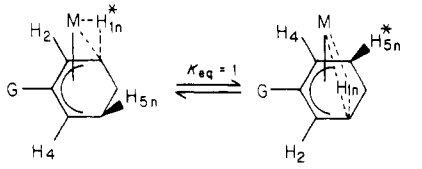

enantiomer G_3 enantiomer G_3'

H_{1n} and H_{5n} undergo a degenerate site exchange, resulting in coincident averaged signals for H* and H located at δ −6.0. Just as in the unsubstituted case, a narrow, two-proton signal is observed. Second, consider a case where the substituent is placed at a site (e.g., the two-substituted complex) where the equilibrium is not degenerate. In this

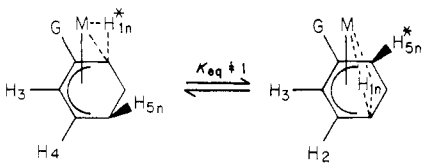

isomer G_2 isomer G_4

case H_{1n} does *not* undergo a degenerate site exchange with H_{5n}. The chemical shift of H* will be the population weighted average of its shift in G_2 (ca. δ −13) and G_4 (ca. δ 1), whereas the shift of H will be the weighted average of its shift in G_2 (ca. δ 1) and G_4 (ca. δ −13). Consequently, two one-proton resonances of equal intensity are observed split symmetrically about δ −6.0. That signal of the pair which is farthest upfield can be assigned to the hydrogen occupying the bridged site in the preferred isomer. In addition, since the magnitude of the chemical shift differences between these two signals is related directly to the equilibrium imbalance between the isomeric forms, it can be used to estimate K_{eq}. A decision as to which of the two possible structures in each pair represents the major isomer can be made by examining other features of the

(9) The fluxional processes described above result in the scrambling of those hydrogens labeled H_x into the exo methylene sites of the complex. A similar analysis applies for the H_n hydrogens, which scramble through the three endo methylene sites.

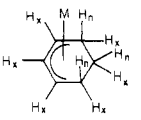

(10) See ref 5 for a brief discussion of spin saturation transfer and appropriate references.

Scheme II

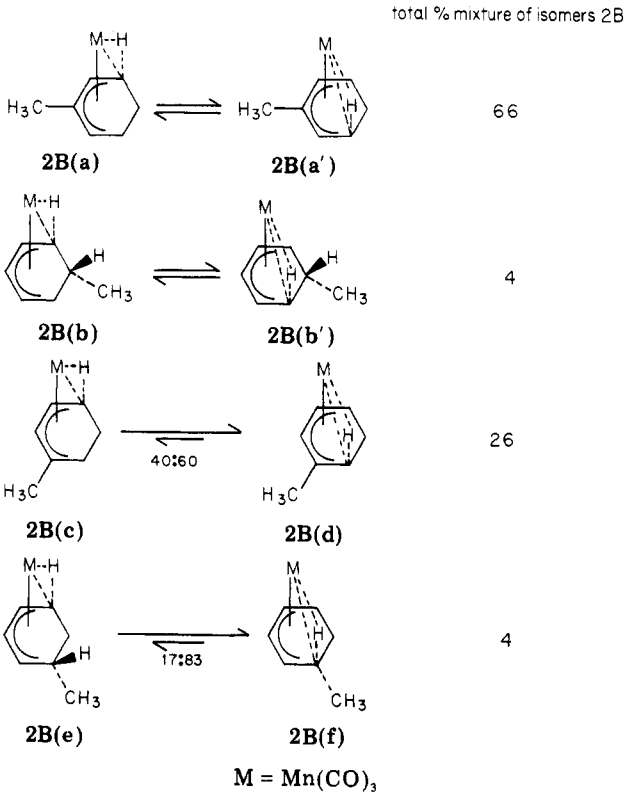

NMR spectrum and by use of the spin-saturation transfer technique (see below).

A detailed analysis of the monomethyl system **2B** is given below followed by an abbreviated summary of results using the same techniques of spectral analysis for **3B**, **4B**, and **5B**.

Reduction of the (Toluene)manganese Tricarbonyl Cation. Treatment of (toluene)manganese tricarbonyl hexafluorophosphate, **2C**, in THF with 1.0 equiv of potassium triisopropoxyborohydride generates the isomeric (1-methylcyclohexadienyl)- and (2-methylcyclohexadienyl)manganese tricarbonyl complexes, **6** and **7**.

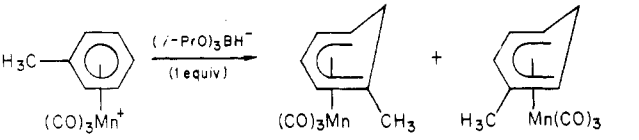

2C **6** **7**

40:60

These isomers are isolated in a 40:60 ratio similar to the isomer ratio obtained by Pauson after thermal rearrangement of the 6-*exo*-methyl complex.[11] If 3.5 equiv of triisopropoxyborohydride are instead used, and the reaction is let proceed for 16 h at reflux, quantitative conversion to the isomeric diene anions **2A** is observed.[12] Protonation of anions **2A** with water followed by separation of the organic layer and solvent removal gives a 79% yield of the isomeric (methylcyclohexenyl)manganese tricarbonyl complexes, **2B**, as a yellow oil. By comparison to an authentic sample,[8] the ^{1}H NMR spectrum reveals that < 2% of the material contains the methyl group in

(11) Munro, G. A. M.; Pauson, P. L. *Z. Anorg. Allg. Chem.* **1979**, *458*, 211.

(12) Experiments are currently underway to determine the exact isomeric composition of the substituted 1-3 cyclohexadiene anions generated via this reduction technique. See ref 8 for details concerning oxidation of the diene anion and Diels–Alder trapping techniques.

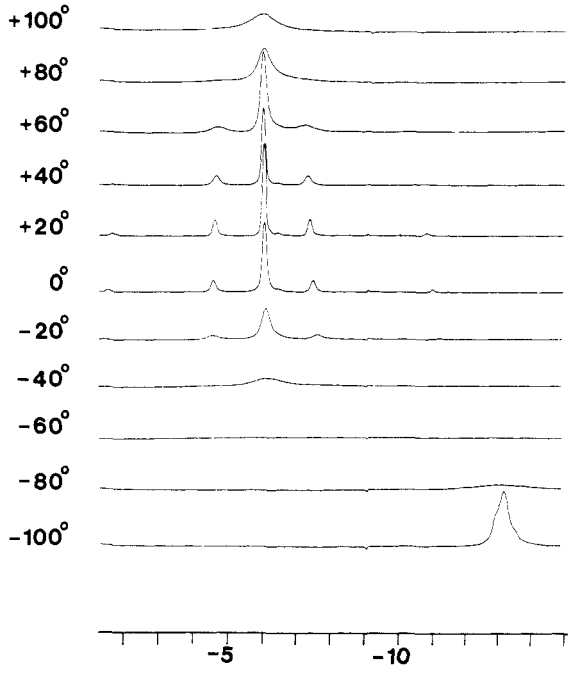

Figure 1. 250-MHz, variable-temperature ^{1}H NMR spectra of (methylcyclohexenyl)manganese tricarbonyl, **2B**, from −100 to +100 °C in $C_6D_5CD_3$ solvent. Only that portion of the spectrum from −2 to −15 ppm is shown.

any endo position; all species contain the methyl group at one of the vinylic or exo methylene sites (the "exo pool"). Indeed, ^{1}H and ^{13}C NMR analysis reveals that all such possible isomers are present in the equilibrium mixture. The distribution at 20 °C is listed below. For clarity, the isomers are shown as pairs that are rapidly interconverting via the low-energy process in Scheme II (the first two equilibria shown are degenerate and interconvert enantiomers).

^{1}H NMR Analysis. The high field (δ 0 to −15) region of the ^{1}H NMR spectrum of isomers **2B** at 20 °C shows six signals at δ −1.5, −4.4, −6.0, −6.2, −7.5, and −10.8 with intensity ratios of 2:13:66:4:13:2 (see Figure 1).[13] The two bands at δ −6.0 and −6.2 clearly reflect the averaged resonances of H_{1n} and H_{5n} in each of the degenerate equilibria (see Scheme II). The two pairs of equal-intensity signals [(δ −1.5, −10.8) and (δ −4.4, −7.5)] each symmetrically displaced about δ −6.0 can be assigned to H_{1n} and H_{5n} of the two nondegenerate equilibrating pairs.

Of the two degenerate systems, the major one (66%) with a two-proton resonance at δ −6.0 is readily assigned to the 3-methyl-substituted isomers **2B(a)** and **2B(a′)**. The major methyl resonance in the spectrum (δ 1.6) is a singlet, indicating vinylic substitution, while the low-field region (δ 3.0–6.0) shows only *one* major resonance at δ 4.0, due to the two-proton-averaged signal for H_2 and H_4. This signal splits into two bands at δ 3.3 and 4.4 at −100 °C in the static spectrum. At −100 °C all resonances for the major (3-substituted) isomer can be observed and assigned (see Table I). The −95 °C ^{13}C spectrum totally supports this assignment (see below). The minor degenerate isomer is then the 6-exo-substituted system **2B(b)** and **2B(b′)**.

The major (26%) nondegenerate pair can be assigned to the 2- and 4-methyl-substituted isomers **2B(c)** and **2B(d)**. Only *two* low-field π-allyl resonances of appropriate

(13) Pauson has prepared the methylcyclohexenyl complex via $LiAlH_4$ reduction of (6-*exo*-methylcyclohexadienyl)manganese tricarbonyl. He reports one upfield band at δ −5.75 ($C_6D_5CD_3$) in the room-temperature ^{1}H NMR spectrum (poorly resolved). He assigns this isomer structure **2B(b)**. See ref 6 for details.

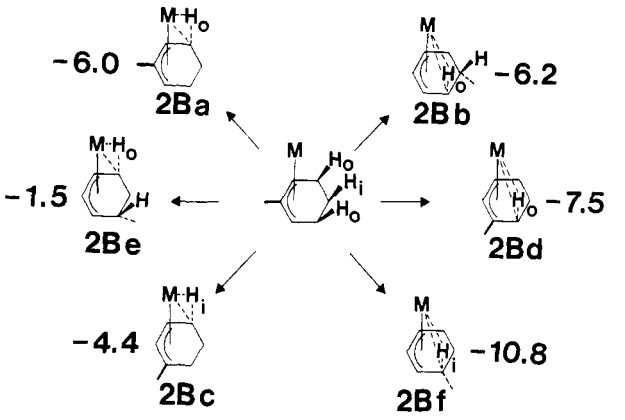

Figure 2. Endo hydrogen scrambling as effected through the two dynamic processes for (methylcyclohexenyl)manganese tricarbonyl, **2B**. H_i populates the bridged site in isomers **2B(c)** and **2B(f)** to the exclusion of either H_o hydrogen. Chemical shift assignments are noted adjacent to each structure.

intensity for this pair are observed. The lowest field signal, δ 4.5, is a doublet (J = 10 Hz), indicating vicinal methyl substitution and can unequivocally be assigned to the central allyl proton of the pair. The remaining allyl resonance appears at δ 3.8. The second most intense methyl resonance in the spectrum (δ 1.8) is a *singlet*, again indicating vinyl methyl substitution. ^{13}C data again corroborate this assignment. The remaining isomeric pair **2B(e)** and **2B(f)** thus gives rise to the signals at δ −1.5 and −10.8 (4% total).

With the assumption that all bridging hydrogen signals and H_{5n} resonances occur at ca. δ −13.0 and ca. δ +1.0 respectively, then isomer ratios of 40:60 and 17:83 can be estimated for the nondegenerate pairs, based on the chemical shift differences observed for each pair of symmetrically disposed signals (see below). However, signal assignment to the major isomer in each pair cannot be made on the basis of the chemical shift data alone. In order to determine which of the two possible structures represents the major isomer in each isomeric pair, a series of spin saturation transfer experiments were performed.

If the three endo hydrogens for the monomethyl system are labeled as below in Figure 2 and all possible permutations derived from the two averaging processes are considered, there emerge two distinct sets of protons H_o and H_i, which do not exchange with each other. Operation of the scrambling processes allows the H_o protons to enter the bridging positions in four of the six distinct isomers. On the other hand, H_i remains unique, entering the bridged site in isomers **2B(c)** and **2B(f)** only and to the exclusion of either H_o proton. Thus, saturation at 40 °C of the upfield signal representing H_i in **2B(c)** should lead to a decrease in intensity of the upfield signal due to isomer **2B(f)** *only*.[14] The remaining four high-field signals (due to the H_o set) should be connected in similar fashion, with irradiation of any *one* resulting in a decrease in intensity of the remaining *three*. This is confirmed experimentally and provides the remaining structural assignments. Irradiation of the band at δ −10.8 results in a substantial (ca. 75%) and completely selective decrease in the signal at δ −4.4 (See Figure 3). Since each of these signals represents one structure in each of two separate equilibrating pairs, the crossover provides for unambiguous structural assignment. Expectedly, irradiation at δ −6.0 leads to a

(14) At 40 °C both fluxional processes are well established; however, signals are still moderately narrow, conveniently allowing application of the spin saturation transfer technique. At higher temperatures significant broadening occurs.

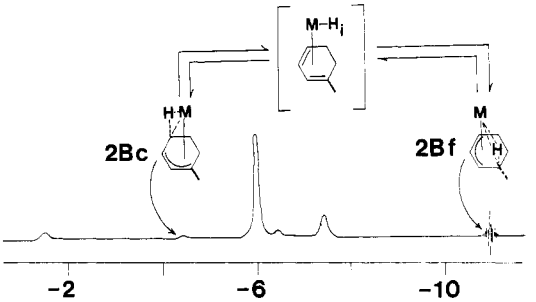

Figure 3. +40 °C, ^{1}H spin saturation transfer experiment for (methylcyclohexenyl)manganese tricarbonyl, **2B**. Since H$_i$ exclusively populates the bridged site in isomers **2B(c)** and **2B(f)**, which interconvert via the high-temperature process, irradiation at either band serves to provide the necessary crossover to assign these structures. Spectrum obtained in $C_6D_5CD_3$; only that portion of the spectrum from −1 to −12 ppm is shown.

decrease in intensity of the three resonances at δ −1.5, −6.2, and −7.5 and thereby links these four isomers. The shift assignments are therefore those shown in Figure 2, and the calculated isomer ratios are ca. 60:40 for **2B(d)**/**2B(c)** and ca. 83:17 for **2B(f)**/**2B(e)**.

^{13}C NMR Analysis. The ^{13}C spectrum of **2B** at −95 °C represents the static mixture of all isomers and shows only one predominant isomer (>75%), assigned to the 3-methyl-substituted system. The fact that the fraction of this isomer at −100 °C is substantially increased over its fraction at 25 °C, and the fact that none of the remaining isomers exceed 10–15% allows unambiguous identification. The assignment of its structure is straightforward, and ^{13}C NMR shifts, $J_{^{13}C-^1H}$ coupling constants, and assignments are summarized in Table II. These shifts and coupling constants are consistent with those observed for the unsubstituted system **1B**. This analysis is further verified by the observation of pairwise averaging of the shifts δ 71.3 with δ 69.2 and δ 26.2 with δ 12.3 as the temperature is raised to −20 °C and the degenerate averaging process becomes rapid. Although it is difficult to assign all of the ^{13}C resonances of the remaining minor isomers present, the low-field region of the coupled spectrum does clearly reveal a set of three allyl resonances that can be assigned to the next most abundant isomer **2B(d)**: δ 63.0 (d, J = 153 Hz), 92.8 (d, J = 170 Hz), and 89.4 (s).

Dynamic Processes. Due to the complexity of the system, no attempt was made to analyze in detail the dynamic ^{1}H NMR spectra and obtain rate constants for interconversion of the various isomers. However, the *general* dynamic behavior of the methyl-substituted system is quite similar to the parent complex.[5] As the temperature is lowered, all the high-field bands broaden, and at −100 °C one broad high-field band at δ −13.2 can be observed (see Figure 1). Several shoulders on this band indicate the presence of minor isomers. All other bands between δ −0.5 and δ −12.5 have vanished. Line-shape analysis of the variable-temperature ^{1}H NMR spectra indicate the rate constant for interconversion of the 3-methyl-substituted enantiomers can be estimated as 600 s^{-1} at −85 °C (ΔG^* = 8.3 kcal/mol), a value quite similar to the parent system. The high-temperature ^{1}H NMR spectrum shows broadening and merging of all the high-field bands to a broad band at δ −6.0 at +100 °C. Rates of broadening are similar to **1B**. The spin saturation transfer experiments (see above) also suggest quite comparable exchange rates for the substituted isomers relative to **1B** for the high-energy exchange process (ΔG^* = ca. 16.0 kcal/mol).

Reduction of (*o*-Xylene)manganese Tricarbonyl Cation. Analogous to the toluene cation, (*o*-xylene)manganese tricarbonyl perchlorate **3C**, when treated with 1.0 equiv of potassium triisopropoxyborohydride results in two isomeric cyclohexadienyl complexes **8** and **9**. If 3.5 equiv of triisopropoxyborohydride are instead used and the reaction is let proceed 27 h in refluxing THF, conversion to the isomeric diene anions **3A** is observed.[12] Protonation of anions **3A** with water followed by the same workup used for the monomethyl system gives a 64% yield of two isomeric bridged complexes **3B**, as a yellow solid (Scheme III). Again, no exo reduction at any methyl-substituted carbon is observed, thereby relegating both methyl substituents to the "exo pool". Structural assignments were confirmed through the use of ^{1}H and ^{13}C NMR spectral analysis. In the upfield region of the room-temperature ^{1}H NMR spectrum of **3B** one pair of equal intensity bands at δ −2.6 and −8.8 is present, thereby confirming the product indeed exists as a mixture of two nondegenerate isomers. The only two methyl resonances present δ 1.9 and 1.6 are both singlets, confirming vinylic substitution for both methyl groups. The one-proton singlet observed at δ 3.6 is the only signal in the δ 3 through 6 region of the spectrum and is assigned to the lone vinylic proton. The fact that only two isomers exist for the system makes the remainder of the spectrum remarkably clear. Unambiguous assignment could be made for the remaining bands through spin saturation transfer techniques similar to those used for the parent system **1B**.[5] Additionally, assignment of the major isomer to structure **3B(a)** proceeds from an analysis similar to that used for the monomethyl system.

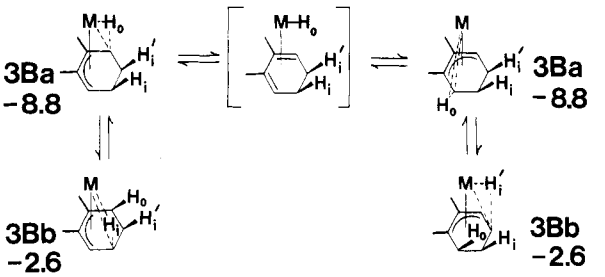

Figure 4. Endo hydrogen scrambling for (dimethylcyclohexenyl)manganese tricarbonyl, **3B**. Whereas H$_o$ uniquely populates the bridged site in isomers **3B(a)**, the two H$_i$ hydrogens alternately populate the bridged site and the 6-endo site in isomer **3B(b)**. Although high-temperature scrambling from isomer **3B(b)** is possible, **3B(a)** and **3B(b)** are the only two isomers observed. Chemical shift assignments are noted adjacent to each structure.

Scheme III

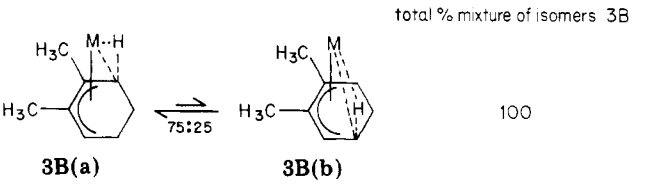

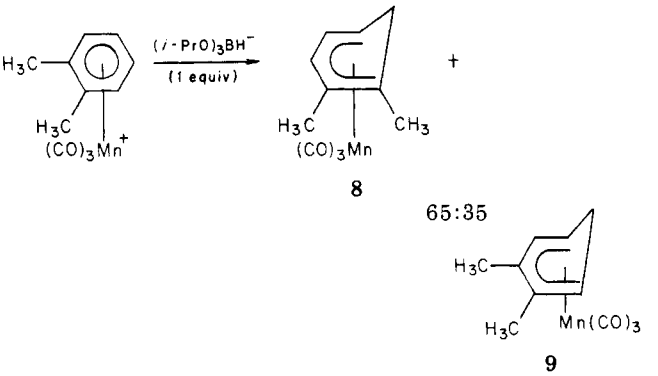

Scheme IV

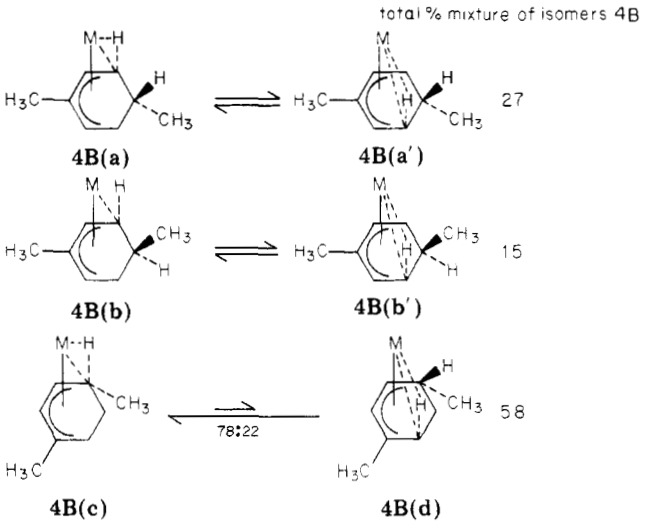

High-temperature scrambling from isomer **3B(b)** results in an isomer that is present in apparently only very small concentration, since it is not observed in the spectrum. As a result, this process is inconsequential to the analysis. On the other hand, high-temperature scrambling from isomer **3B(a)** regenerates the identical structure and, similar to the monomethyl case, divides the three endo hydrogens into two distinct sets that do not exchange with each other (see Figure 4). H_o, the bridging proton in isomer **3B(a)**, remains unique and populates the bridging site in **3B(a)** [H_{5n} in **3B(b)** through the low-energy process] solely and to the exclusion of either H_i proton. On the other hand, the two H_i protons are observed to undergo site exchange between their bridging site in isomer **3B(b)** [H_{5n} in **3B(a)** through the low-energy process] and the H_{6n} site in both isomers. As a result, irradiation at that upfield signal due to H_o should have no effect on the rest of the spectrum, whereas irradiation at that upfield signal populated by the H_i set should result in a decrease in intensity of that signal due to H_{6n}. Indeed, irradiation at δ −2.6 resulted in a near quantitative and selective decrease in the signal at δ 0.5. Irradiation of the band at δ −8.8, however, had no observable effect of the spectrum. Structural assignments could thus be made unambiguously as indicated in Figure 4, the major isomer (δ −8.8) being assigned structure **3B(a)**.

Reduction of (*p*-Xylene)manganese Tricarbonyl Cation. Addition of 1 equiv of potassium triisopropoxyborohydride to a suspension of (*p*-xylene)manganese tricarbonyl perchlorate in THF led to the isolation of (1,4-dimethylcyclohexadienyl)manganese tricarbonyl, **10**, to the exclusion of all other isomers. Generation of the anions

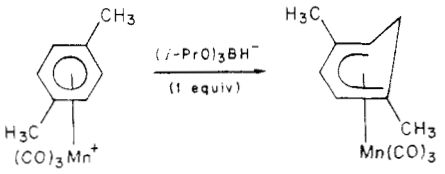

4A was accomplished by the addition of 3.5 equiv of triisopropoxyborohydride to a suspension of **4C** in THF.[12] Conversion was effected after 22 h at reflux. Subsequent protonation with water led to the isolation of the bridged complexes **4B** in 70% yield as a yellow-orange oil (see Scheme IV). In contrast to the previous two systems, reduction of (*p*-xylene)manganese tricarbonyl cation did yield some *endo*-methyl-substituted product. Isomers

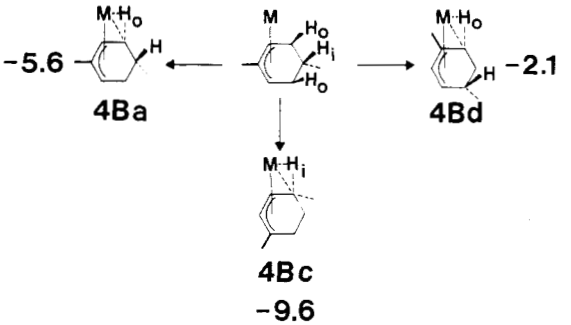

Figure 5. Endo hydrogen scrambling for the exo,exo-substituted isomers of (dimethylcyclohexenyl)manganese tricarbonyl, **4B**. Since H_2 uniquely populates the bridged site in **4B(c)**, spin saturation transfer experiments serve to distinguish this isomer from **4B(d)**, which interconverts with **4B(a)** through the high-energy dynamic process. Chemical shift assignments are noted adjacent to each structure.

4B(b) and **4B(b')** obviously arise from exo reduction at a methyl-substituted center. ^{1}H and ^{13}C NMR spectral analysis was again used to verify the structures of the product mixture. Four upfield bands are noted in the +25 °C spectrum of the bridged complexes **4B**. Two degenerate isomers appear at δ −5.6 and −6.2, with one nondegenerate pair displaying bands at δ −2.1 and −9.6. Although the remainder of the ^{1}H NMR spectrum is ill-resolved due to the number of isomers present, a series of spin saturation transfer experiments suffices to fully characterize the system.

Structural assignments for the system can be made by noting that in the exo,exo-substituted isomers the three endo protons are again divided into two distinct sets with regard to the averaging processes (Figure 5). In this case H_i populates the bridging site in **4B(c)** exclusively. Since the high-energy process as applied to **4B(c)** regenerates the identical isomer, irradiation at 40 °C of that band due to H_i should not affect the spectrum. On the other hand, since the two H_o protons alternately occupy the bridging sites in the isomers **4B(a)** [**4B(a')**] and **4B(d)**, irradiation at that signal due to the nondegenerate isomer **4B(d)** should bring about a marked decrease in signal intensity for that signal due to the degenerate system **4B(a)** and **4B(a')**. This experiment thus not only serves as a means of differentiating between the *nondegenerate* structures **4B(c)** vs. **4B(d)** but also as a way to determine which of the two signals in the δ −6 region of the spectrum represents the exo/exo-substituted isomer **4B(a)** vs. the endo/exo degenerate system **4B(b)**. Indeed, irradiation of the signal at δ −2.1 resulted in a large decrease in intensity for the band located at δ −5.6. Irradiation at δ −9.6 had no effect on the spectrum. Structural assignments could thus be made as indicated in Figure 5, the signal at δ −6.2 being assigned to the degenerate endo/exo system **4B(b)**. Although detailed features of the ^{1}H NMR spectra for this system were obscured, low-temperature ^{13}C spectral data bear out these assignments. Two singlets at δ 108.3 and 107.8 in the coupled ^{13}C spectrum indicate methyl substitution at C_3 for two isomers. These must necessarily be the degenerate systems **4B(a)** and **4B(b)**. A third singlet at δ 82.1 indicates vinylic substitution at either C_2 or C_4 for the third isomer. This band is assigned to the nondegenerate system **4B(c)** and **4B(d)**. The remaining six signals in the region 70–110 ppm are all doublets. Exact assignments are given in Table II.

Reduction of (Mesitylene)manganese Tricarbonyl Cation. the addition of only 1 equiv of hydride to (mesitylene)manganese tricarbonyl cation occurs quite readily (ca. 20 min). Isolation of the product in this case reveals

Scheme V

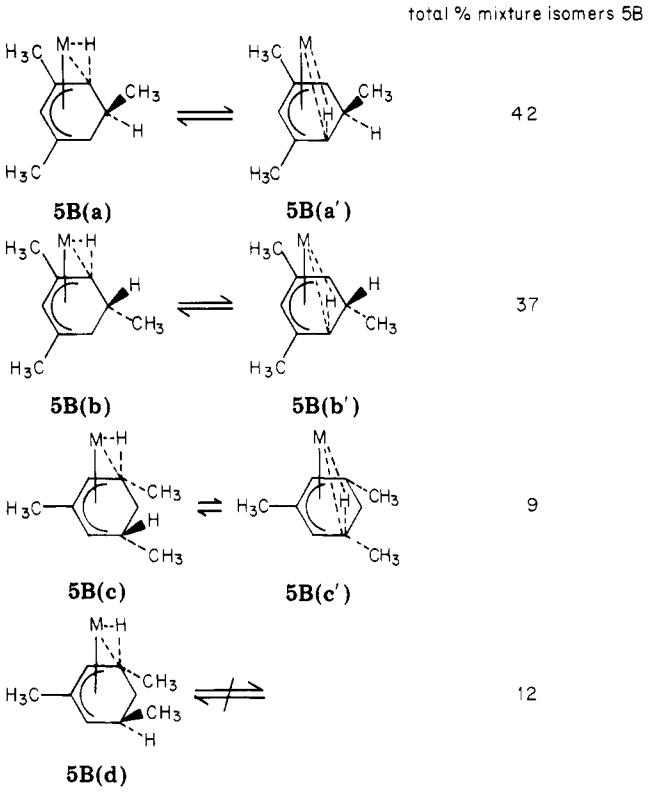

the 1,3,5-trimethylcyclohexadienyl complex **11** to be the kinetically favored product (88%) over the 2,4,6-*exo*-trimethylcyclohexadienyl isomer **12** (12%).[15] Double re-

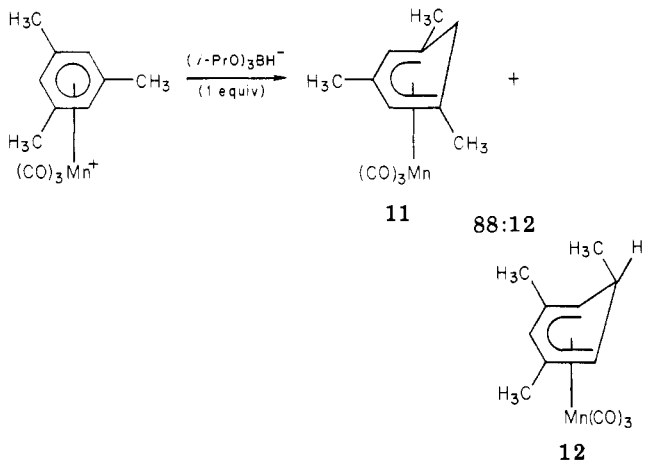

duction of (mesitylene)manganese tricarbonyl hexafluorophosphate using potassium triisopropoxyborohydride, however, proceeded quite slowly compared to the other systems studied. Whereas the mono- and disubstituted systems could be converted to their corresponding anions in less than 30 h, ca. 90% conversion of (mesitylene)manganese tricarbonyl cation to the isomeric anions **5A** could be attained only after 5 days in refluxing THF by using 5 equiv of triisopropoxyborohydride.[12] Protonation and standard workup gave a 57% yield of the isomeric bridged complexes **5B** as a yellow-orange oil. Analysis of the mono- and dimethyl-substituted systems indicated that reduction at methyl-substituted carbons was disfavored. With the assumption that reduction to diene anion

Scheme VI

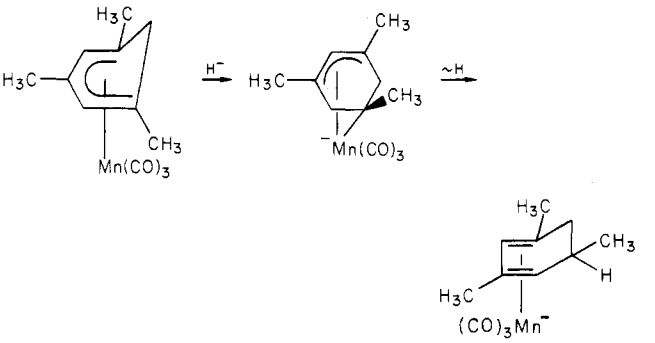

occurs (1) exclusively at the exo face of the coordinated ring and (2) at the terminal carbons of the dienyl ligand, reduction of a mixture of **11** and **12** would be expected to occur quite slowly, but result in a large preponderance of *endo,exo,exo*-trimethyl-substituted complex relative to *exo,exo,exo*-trimethyl-substituted complex. Clearly, reduction of both **11** and **12** does occur, since protonation of the anions generated from **5C**, followed by standard workup led to both *endo,exo,exo*-trimethyl-substituted bridged complexes as well as *exo,exo,exo*-trimethyl-substituted complexes (see Scheme V).

Surprisingly, however, 46% of the total product mixture consisted of *exo,exo,exo*-trimethyl-substituted isomers **5B(b)** and **5B(c)**. With the assumption that hydride attack occurs from the exo face and at the terminal carbons of the dienyl ligand exclusively, a maximum of 12% exo,exo,exo-substituted isomers is expected, all arising from reduction of **12**. At first, enrichment of isomer **12** at the expense of **11** under the reaction conditions used for generation of the anions **5A** was thought to account for the discrepancy. Indeed, analysis of the residue of unreacted cyclohexadienyl complex in the spectrum of the bridged isomers **5B** indicated isomers **11** and **12** were present as a ca. 50:50 mixture. However, attempted thermal isomerization of an 88:12 mixture of cyclohexadienyl isomers **11** to **12** under the reaction conditions used to generate **5A** resulted in isolation of these isomers in the original 88:12 ratio. These data are consistent with a kinetically favored reduction of isomer **11** over isomer **12**.

The large proportion of exo,exo,exo-bridged isomers present in the product mixture indicates that formally **11** is being reduced at the terminal carbons from both the exo and the endo face. This may occur by direct endo attack at the terminal carbons C_1 and C_5. Previous work, however, indicates that normally endo reduction is substantially disfavored over exo reduction, as noted for the unsubstituted system.[8] An alternate mechanism can be envisioned which accomplishes net endo reduction at a methylated carbon but yet involves exo hydride attack. If exo attack occurs at the unsubstituted C_2 or C_4 positions of **11** and is followed by endo hydrogen migration (as outlined in Scheme VI) the *exo,exo,exo*-trimethyl-substituted system results. This mechanism is not without precedent;[16,17] however, further investigation is required to distinguish between these two pathways for achieving net endo reduction.

Structural assignments were again made from ^{1}H and ^{13}C NMR analysis. Four upfield signals, δ −5.4, −5.8, −6.0,

(15) Pauson similarly found the 1,3,5-trimethyl-substituted complex to be the favored isomer when LAH is used to accomplish the reduction rather than potassium triisopropoxyborohydride. Munro, G. A. M.; Pauson, P. L. *Isr. J. Chem.* **1977**, *15*, 258.

(16) Burrows, A. L.; Johnson, B. F. G.; Lewis, J.; Parker, D. G. *J. Organomet. Chem.* **1980**, *194*, C11–C13.

(17) Although reduction at C_2 is rare for cyclohexadienyl complexes, it is not at all uncommon for cycloheptadienyl ligands to be reduced in this manner. For a review of nucleophilic addition to transition-metal complexes see: Pauson, P. L. *J. Organomet. Chem.* **1980**, *200*, 207.

and −13.4, are observed in the room-temperature ^{1}H NMR spectrum for the bridged isomers **5B**. One of the expected isomers **5B(d)** represents a static structure with respect to the low-temperature averaging process. Its bridging proton would thus be expected to display a chemical shift very close to δ −13. That band located at δ −13.4 was thus immediately assigned structure **5B(d)**. The three other upfield bands noted all occur at approximately δ −6, thereby indicating the remaining isomers consist of degenerate systems with respect to the low-temperature process. This is consistent with the expected structures. Since the *endo,exo,exo*-methyl-substituted isomer **5B(d)** is linked to the similarly *endo,exo,exo*-methyl-substituted system **5B(a)** and **5B(a′)** through the high-energy process, irradiation at δ −13.4 was expected to pinpoint the upfield signal representing the degenerate **5B(a)** system. Indeed, irradiation of the band at δ −13.4 brought about a marked decrease in the intensity of the signal located at δ −6.0, which was then assigned the degenerate structures **5B(a)** and **5B(a′)**. Structural assignment for the degenerate systems **5B(b)** and **5B(c)** was made on the basis of low-temperature ^{13}C spectral data. Two large doublets at δ 94.4 and 96.2 and two small singlets at δ 106.2 and 107.5 in the coupled spectrum indicated the major two isomers in the mixture **5B(a)** and **5B(b)** were each substituted at both ends of the allyl unit. Thus, it could be concluded that the **5B(b)** and **5B(b′)** system was favored over the **5B(c)** and **5B(c′)** system. Reference to the ^{1}H NMR spectrum for the mixture indicated the major *exo,exo,exo*-methyl-substituted isomer was represented by the band at δ −5.8 rather than the band at δ −5.4. Isomers **5B(b)** and **5B(b′)** were consequently assigned the signal at δ −5.8, while the signal at δ −5.4 was assigned to isomers **5B(c)** and **5B(c′)**.[18]

Summary

Several points have been demonstrated from the work done in this study. First, it has been shown that (monoalkylarene)-, (dialkylarene)-, and (trialkylarene)manganese tricarbonyl cations can be doubly reduced in good yields to their corresponding diene anions. These can be further converted, through protonation with water, to methylated cyclohexenyl complexes of the sort reported previously, each containing an aliphatic endo C–H bond that is activated by coordination to manganese. Second, in those fluxional cyclohexenyl species where the methyl substituent(s) is part of the "exo pool" specific-site preferences are observed. In general, those isomers with methyl substituents at vinylic positions are substantially more stable than those isomers with methyl at any saturated or bridged site. Among the vinyl positions, methyl substituents prefer the internal position (C_3) to substitution at either C_2 or C_4, but the bias is not strong. The 17:83 ratio of **2B(f)** to **2B(e)** illustrates that methyl substitution at the bridged carbon results in greater stability of the complex than substitution at a saturated site. This may be a consequence of the postulated partial double-bond character between C_1 and C_2 and the resultant rehybridization of C_1 from sp^3 toward sp^2. Thirdly, it has been demonstrated that reduction at terminally methyl-substituted dienyl ligands is slower than that observed for cyclohexadienyl complexes in which one of the terminal ends of the dienyl ligand is unsubstituted. Methyl substitution at the 6-exo-position of a cyclohexadienyl complex, however, appears to significantly retard reduction, even if both ends of the dienyl ligand are unsubstituted.

Previous studies have demonstrated that high-yield conversion of benzene to 1,3-cyclohexadiene and cyclohexene through cyclohexenylmanganese tricarbonyl is indeed feasible.[8] The ease of reduction of alkylated arenes and the specific-site preferences observed suggest that these reaction sequences can be used to carry out stepwise reduction of substituted arenes to cyclohexadienes and cyclohexenes with substantial regioselectivity. These studies are in progress with the alkylarenes reported here and other substituted arene complexes.

Experimental Section

General Data. All reactions were performed under a dry, oxygen-free nitrogen atmosphere. Tetrahydrofuran solvent was freshly distilled from $LiAlH_4$ under a nitrogen atmosphere; other solvents were simply degassed unless otherwise noted. Manganese pentacarbonyl bromide was prepared from dimanganese decacarbonyl (Strem or Pressure Chemicals) according to the procedure of King.[19]

^{1}H NMR spectra were recorded at 100 MHz by using a Varian XL-100 FT NMR spectrometer or at 250 MHz by using a Bruker WM250 FT NMR spectrometer. ^{13}C NMR spectra were recorded at 62.9 MHz by using the Bruker instrument. In all cases residual solvent resonances were used as internal standards for the reporting of chemical shifts. Probe temperatures were calibrated by measurement of peak separations in standard methanol or ethylene glycol samples. NMR samples were degassed by several freeze–pump–thaw cycles, and NMR sample tubes were sealed under vacuum (~0.01 mm). Deuterated NMR solvents were dried over molecular sieves (4 Å) and stored under nitrogen in ampules equipped with Teflon stopcocks.

Infrared spectra were recorded on a Beckman spectrophotometer (IR 4250) and frequencies (cm^{-1}) were assigned relative to a polystyrene standard. Only bands in the carbonyl stretching region (ca. 1500–2300 cm^{-1}) are reported.

Column packings for column chromatography consisted of neutral or basic alumina (Al_2O_3: 70/290 mesh).

(Toluene)manganese Tricarbonyl Hexafluorophosphate, 2C. The hexafluorophosphate salt of (toluene)manganese tricarbonyl was prepared by using a modification of procedures described previously.[20,21] Manganese pentacarbonyl bromide (10.0 g, 0.0364 mol) and anhydrous, technical grade aluminum chloride (12.0 g, 0.090 mol) were heated at 100 °C in 60 mL of anhydrous toluene overnight. Initially, carbon monoxide was evolved with resultant formation of a deep red solution. After the mixture was cooled to 0 °C, 100 mL of ice water were added dropwise with stirring, resulting in formation of a yellow aqueous layer. The aqueous layer was separated, washed with 100 mL of pentane, and then treated dropwise with 14 mL of 65% aqueous hexafluorophosphoric acid while being stirred vigorously at 0 °C. The resulting pale yellow precipitate was washed with small portions of methanol and water by using a medium frit as filter. The product was taken up into 100 mL of acetone and filtered again through a medium frit filter. The acetone solvent was evaporated and the product dried in vacuo (0.01 mm) to give 9.84 g (71.8% based on $Mn(CO)_5Br$) of (toluene)manganese tricarbonyl hexafluorophosphate as a yellow solid: IR ν_{CO} ($(CH_3)_2CO$) 2066, 2016 cm^{-1}; ^{1}H NMR ($(CD_3)_2CO$) δ 6.93 (apparent t, 2), 6.65 (apparent d, 3), 2.61 (s, 3, CH_3).

(*o*-Xylene)manganese Tricarbonyl Perchlorate, 3C. Due to the unsuitability of the aluminum chloride method for the preparation of (*o*-xylene)manganese tricarbonyl cation (isomerization occurs at the temperatures required) this complex was

(18) Pauson has prepared the trimethylcyclohexenyl complex via $LiAlH_4$ reduction of (1,3,5-trimethylcyclohexadienyl)manganese tricarbonyl. He observed one major upfield resonance at δ −6.02 that he assigns to structure **5B(b)**. This is in agreement with our results in that we also assign the major exo,exo,exo isomer structure **5B(b)** to a signal observed at δ −5.80. Pauson suggests the presence of isomer **5B(c)** due to a second but much weaker high field signal he observes at δ −7.20 ($C_6D_5CD_3$ at −20 °C). We have assigned this structure to a signal located at δ −5.4 (C_6D_6at +20 °C). See ref 6 for details.

(19) King, R. B. "Organometallic Synthesis"; King, R. B., Eisch, J. J., Ed.; Academic Press: New York, 1965; Vol. 1, p 130.

(20) Winkhaus, G.; Pratt, L.; Wilkinson, G. *J. Chem. Soc.* **1961**, 3807.

(21) Pauson, P. L.; Segal, J. A. *J. Chem. Soc. Dalton Trans.* **1975**, 1677.

prepared by arene–ligand exchange from $Mn(CO)_5OClO_3$ by using a modification of the method reported by Pauson.[22] $AgClO_4$ (7.21 g, 0.0348 mol) was added to a solution of $Mn(CO)_5Br$ (5.72 g, 0.0208 mol) in 1-L of methylene chloride. The reaction mixture was stirred for 3 h at room temperature with the exclusion of light, at which time quantitative conversion to the coordinated perchlorate was observed (ν_{CO} (CH_2Cl_2) 2168, 2085, 2034 cm^{-1}).[23,24] The white AgBr precipitate was then filtered from the solution by using a fritted Schlenk filter and the yellow filtrate added to 15 mL of *o*-xylene. This solution was refluxed under nitrogen with the exclusion of light for 3 days. The volume of solvent was then reduced to 200 mL, and 800 mL of petroleum ether was added. The resulting yellow precipitate was filtered from solution and washed with petroleum ether several times before drying in vacuo (0.01 mm) to yield 6.10 g (85% based on $Mn(CO)_5Br$) of (*o*-xylene)manganese tricarbonyl perchlorate as a yellow solid: IR ν_{CO} ($(CH_3)_2CO$) 2080, 2020 cm^{-1}; ^{1}H NMR ($(CD_3)_2CO$) δ 6.47 (br, 4), 2.50 (br, 6, CH_3).

(*p*-Xylene)manganese Tricarbonyl Perchlorate, 4C. This complex was prepared in analogous fashion to (*o*-xylene)manganese tricarbonyl perchlorate with the following exceptions: 4.5 g of $Mn(CO)_5Br$ was used in the reaction. Accompanying reagents were scaled down accordingly. The reaction yielded 4.8 g (85% based on $Mn(CO)_5Br$ of (*p*-xylene)manganese tricarbonyl perchlorate as a pale yellow solid: IR ν_{CO} ($(CH_3)_2CO$) 2081, 2020 cm^{-1}; ^{1}H NMR ($(CD_3)_2CO$) δ 6.69 (br, 4), 2.49 (br, 6, CH_3).

(Mesitylene)manganese Tricarbonyl Hexafluorophosphate, 5C. This compound was prepared in analogous fashion to (toluene)manganese tricarbonyl hexafluorophosphate with the following exceptions: 5.0 g of $Mn(CO)_5Br$ was used to prepare the cation. Accompanying reagents were scaled down accordingly. The reaction was run at 110 °C, resulting in 6.1 g (83% based on $Mn(CO)_5Br$) of (mesitylene)manganese tricarbonyl hexafluorophosphate as a yellow solid: IR ν_{CO} ($(CH_3)_2CO$) 2068, 2018 cm^{-1}; ^{1}H NMR ($(CD_3)_2CO$) δ 6.35 (s, 3), 2.57 (s, 9, CH_3).

(1-Methylcyclohexadienyl)- and (2-Methylcyclohexadienyl)manganese Tricarbonyl, 6 and 7. In a modification of procedures used by previous workers,[20,21] a stirred suspension of (toluene)manganese tricarbonyl hexafluorophosphate (1.5 g, 0.004 mol) in tetrahydrofuran (30 mL, freshly distilled) was treated at room temperature with a 1 M solution of potassium triisopropoxyborohydride in THF (4.4 mL, 0.0044 mol). After 20 min, 30 mL of NaCl brine was added dropwise at 0 °C to destroy any excess hydride. The organic layer was dried with anhydrous sodium sulfate and the solvent evaporated. The crude product was taken up into 60 mL of petroleum ether and dried further with anhydrous sodium sulfate. The product was purified by evaporation of the solvent and subsequent chromatography on a short column of neutral alumina (activity II) using petroleum ether as the eluent. The yellow band that eluted first was collected and the solvent evaporated, (25 °C (25 mm)) to give a yellow solid. Subsequent recrystallization from pentane at −78 °C yielded intensely yellow crystals (0.60 g, 65% based on $C_6H_5(CH_3)Mn(CO)_3PF_6$) of the desired product. ^{1}H NMR analysis indicated a 40:60 mixture of **6** to **7** resulted from the preparation: IR ν_{CO} (THF) 2004, 1928 cm^{-1}; ^{1}H NMR (C_6D_6) δ 5.13 (m, H_3 (**6** and **7**)), 4.13 (m, H_4 (**6**) and H_4 (**7**)), 3.99 (d, H_2 (**6**)), 2.35 (m, H_1 (**7**) and H_5 (**6** and **7**)), 2.15 (d, $H_{6\text{-endo}}$ (**6** and **7**)), 1.77 (dd, $H_{6\text{-exo}}$ (**6** and **7**)), 1.41 (s, CH_3 (**7**)), 1.20 (s, CH_3 (**6**)).

(1,2-Dimethylcyclohexadienyl)- and (2,3-Dimethylcyclohexadienyl)manganese Tricarbonyl, 8 and 9. These compounds were prepared in similar fashion to (1-methylcyclohexadienyl)- and (2-methylcyclohexadienyl)manganese tricarbonyl with the following exceptions: 1.0 g of (*o*-xylene)manganese tricarbonyl perchlorate was used in place of the toluene cation, and all reagents were scaled down accordingly. The product was in the form of yellow crystals (0.44 g, 62% based on *o*-$C_6H_4(CH_3)_2Mn(CO)_3ClO_4$), the structure of which was confirmed by ^{1}H NMR analysis. Spectral analysis indicated a 65:35 mixture of **8** to **9**: IR ν_{CO} (THF) 2002, 1925 cm^{-1}; ^{1}H NMR (C_6D_6) δ 4.98 (d, H_3 (**8**)), 4.23 (apparent t, H_4 (**8**) and H_4 (**9**)), 2.26 (m, H_1 (**9**) and H_5 (**8** and **9**)), 2.15 (d, $H_{6\text{-endo}}$ (**8** and **9**)), 1.79 (dd, $H_{6\text{-exo}}$ (**8** and **9**)), 1.99 (s, CH_3 (**9**)), 1.41 (s, CH_3 (**9**)), 1.39) (s, CH_3 (**8**)), 1.19 (s, CH_3 (**8**)).

Table I. ^{1}H NMR Data for Various Methyl-Substituted Isomers of Cyclohexenylmanganese Tricarbonyl[a]

+25°C, C_6D_6, M = $Mn(CO)_3$	H_{1n}	H_{5n}	H_2	H_4	H_3	H_{1x}	H_{5x}	H_{6n}	H_{6x}	Me	Me
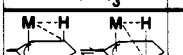	-6.0 br,2H		4.0 s,2H		–	1.0 d,2H		0.3 m	0.0 m	–	1.6 s
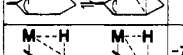	-7.5 br	-4.4 br	–	3.8 m	4.5 m	(a)				1.8 s	–
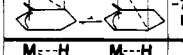	-8.8 br	-2.6 br	–	3.6 s	–	0.8 d	1.3 m	0.5 m	0.1 m	1.9 s	1.6 s
	-9.6 br	-2.1 br									
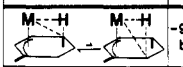	-5.6 br,2H										
	-6.2 br,2H										
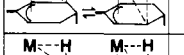	-6.0 br,2H										
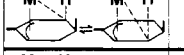	-5.8 br,2H										
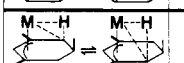	-5.4 br,2H										
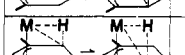	-13.4 br	–									

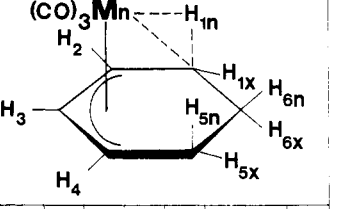

−100°C, $C_6D_5CD_3$	H_{1n}	H_{5n}	H_2	H_{1x}	H_4	H_{5x}	H_{6n}	H_{6x}	Me
	-13.2	1.0	4.4 & 3.3		1.5 & 0.3		0.3	-0.1	1.6

[a] Shifts are in ppm relative to residual C_6D_6. Signals obscured by peaks due to the major isomer are represented by (a).

(1,4-Dimethylcyclohexadienyl)manganese Tricarbonyl, 10. This compound was prepared in similar fashion to (1-methylcyclohexadienyl)- and (2-methylcyclohexadienyl)manganese tricarbonyl with the following exceptions: 1.0 g of *p*-xylene-manganese tricarbonyl perchlorate was used in place of the toluene cation, and all reagents were scaled down accordingly. The product was in the form of yellow crystals (0.52 g, 72% based on *p*-$C_6H_4(CH_3)_2Mn(CO)_3ClO_4$), the structure of which was confirmed as the 1,4-dimethylcyclohexadienyl isomer by ^{1}H NMR analysis: IR ν_{CO} (THF) 2001, 1928 cm^{-1}; ^{1}H NMR (C_6D_6) δ 4.96 (d, 1, H_3), 3.92 (d, 1, H_2), 2.30 (br s, 1, H_5), 2.16 (d, 1, $H_{6\text{-endo}}$), 1.37 (s, 3, CH_3), 1.17 (s, 3, CH_3), $H_{6\text{-exo}}$ obscured.

(1,3,5-*exo*-Trimethylcyclohexadienyl)- and (2,4,6-*exo*-Trimethylcyclohexadienyl)manganese tricarbonyl, 11 and 12. These compounds were prepared in similar fashion to (1-methylcyclohexadienyl)- and (2-methylcyclohexadienyl)manganese tricarbonyl with the following exceptions: 1.0 g of (mesitylene)manganese tricarbonyl hexafluorophosphate was used in place of the toluene cation, and all reagents were scaled down accordingly. The product was in the form of yellow crystals (0.35 g, 54% based on $C_6H_3(CH_3)_3Mn(CO)_3PF_6$), the structure of which was confirmed as an 88:12 mixture of **11** to **12** by ^{1}H NMR analysis IR ν_{CO} (THF) 2004, 1923 cm^{-1}; ^{1}H NMR (C_6D_6) δ 4.90 (s, H_3 (**12**)), 4.12 (s, H_2 and H_4 (**11**)), 2.64 (d, H_1 and H_5 (**12**)), 2.15 (d, $H_{6\text{-endo}}$ (**11** and **12**)), 1.89 (d, $H_{6\text{-exo}}$ (**11** and **12**)), 2.04 (s, CH_3 (**11**)), 1.43 (s, CH_3 (**12**)), 1.27 (s, CH_3 (**11**)), 0.12 (d, CH_3 (**12**)).

Reduction of (Toluene)Mn(CO)$_3^+$ to (Methylcyclohexenyl)manganese Tricarbonyl, 2B(a–f). In a method similar to that used to prepare the parent complex **1B**,[5] (toluene)manganese tricarbonyl hexafluorophosphate (10.9 g, 0.028 mol) was suspended in 200 mL of tetrahydrofuran and 98.0 mL of potassium triisopropoxyborohydride (1 M in THF) was added dropwise with stirring. After the mixture was refluxed for 16 h, IR analysis indicated complete conversion to the isomerric diene anions **2A** (ν_{CO} (THF) 1925, 1831, 1782 cm^{-1}). [IR monitoring during the

(22) Bhasin, K. K.; Balkeen, W. G.; Pauson, P. L. *J. Organomet. Chem.* **1981**, *204*, C25–C26.
(23) Wimmer, F. L.; Snow, M. R. *Aust. J. Chem.* **1978**, *31*, 267.
(24) Usón, R.; Riera, V.; Gimeno, J.; Laguna, M.; Gamasa, M. P. *J. Chem. Soc., Dalton Trans.* **1979**, 996.

Table II. ^{13}C NMR Data for Various Methyl-Substituted Isomers of Cyclohexenylmanganese Tricarbonyl[a]

−95°C CD_2Cl_2 M = $Mn(CO)_3$	C_1	C_2	C_3	C_4	C_5	C_6	Me	Me
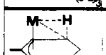	12.3 dd,148, 86 Hz	71.3 d,183 Hz	107.8 s	69.2 d,156 Hz	26.2 t,128 Hz	16.3 t,133 Hz	22.3 q,126 Hz	–
	18.4 (b)	89.4 s	92.8 d,170 Hz	63.0 d,153 Hz	25.2 (b)	14.4 (b)	23.9 (b)	–
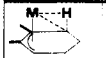	17.4 dd,150, 84 Hz	86.8 s	105.0 s	65.9 d,154 Hz	27.1 t,129 Hz	16.2 t,133 Hz	19.3 q,127 Hz	20.4 q,127 Hz
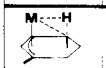	(a)	73.1 d,178 Hz	93.1 d,164 Hz	82.1 s				
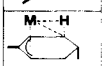		68.1 d,182 Hz	108.3 s	65.7 d,154 Hz				
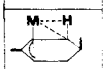		71.2 d,181 Hz	107.8 s	67.2 d,153 Hz				
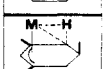		77.9 s	94.4 d,164 Hz	76.3 s				
		77.2 s	96.2 d,168 Hz	75.7 s				
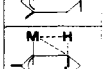		(75–78)	107.5 s	(75–78)				
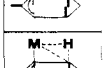		(75–78)	106.2 s	(75–78)				

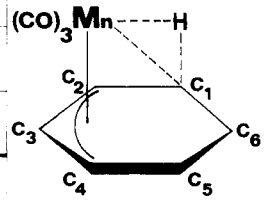

−20°C CD_2Cl_2	C_1 & C_5	C_2 & C_4	C_3	C_6	Me
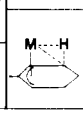	19.8	70.5	108.6	17.2	22.7

[a] Shifts are in ppm relative to residual CD_2Cl_2. Signals Obscured due to the large number of isomers present in the equilibrium mixture are represented by (a). Coupling constants for those signals obscured by peaks due to the major isomer are represented by (b).

course of the reaction indicated stepwise reduction to **2A** through the neutral methylcyclohexadienyl complex.] The solution was then cooled to 0 °C, and 300 mL of degassed NaCl brine was added slowly with constant stirring. The organic layer was dried over anhydrous sodium sulfate, filtered, and evaported (25 °C (20 mm)) to a red oil. The oil was chromatographed on a column of basic alumina (activity II) by using petroleum ether as the eluent. The first band eluting (yellow) was collected and stripped of solvent to yield a yellow-orange oil. The product was further dried in vacuo (0.01 mm) to give 5.2 g (79% based on $C_6H_5(CH_3)Mn(CO)_3PF_6$) of the isomeric bridged complexes as a yellow oil: IR ν_{CO} (pentane) 2016, 1942, 1934 cm^{-1}; see Tables I and II for ^1H NMR and ^{13}C NMR spectroscopic data.

Reduction of (*o*-Xylene)Mn(CO)$_3^+$ to Dimethylcyclohexenylmanganese Tricarbonyl, 3B(a,b). (Dimethylcyclohexenyl)manganese tricarbonyl isomers **3B(a,b)** were prepared from (*o*-xylene)manganese tricarbonyl perchlorate by the identical method used for the preparation of the monomethyl complexes with the following exceptions: 5.0 g of *o*-xylenemanganese tricarbonyl perchlorate was used instead of the toluene cation, and all other reagents were scaled down accordingly. Conversion to the isomeric anions **3A** was observed after 27 h at reflux (ν_{CO} (THF) 1922, 1830, 1782 cm^{-1}). The yellow-orange oil obtained from the workup was recrystallized from a minimum amount of petroleum ether at −78 °C to yield 2.3 g (64% based on *o*-$C_6H_4(CH_3)_2Mn(CO)_3ClO_4$) of the bridged complexes as a yellow solid: IR ν_{CO} (pentane) 2018, 1935 (br) cm^{-1}; see Tables I and II for ^1H NMR and ^{13}C NMR spectroscopic data. Anal. Calcd for $C_{11}H_{13}MnO_3$: C, 53.23; H, 5.28; Mn, 22.14. Found: C, 53.37; H, 5.29; Mn, 21.96.

Reduction of (*p*-Xylene)Mn(CO)$_3^+$ to (Dimethylcyclohexenyl)manganese Tricarbonyl, 4B(a–d). (Dimethylcyclohexenyl)manganese tricarbonyl isomers **4B(a–d)** were prepared from (*p*-xylene)manganese tricarbonyl perchlorate by the identical method used for the preparation of the monomethyl complex with the following exceptions: 5.0 g of (*p*-xylene)manganese tricarbonyl perchlorate was used instead of the toluene cation, and all other reagents were scaled down accordingly. Conversion to the isomeric anions **4A** was observed after 22 h at reflux (ν_{CO} (THF) 1921, 1830, 1782 cm^{-1}). Workup yielded 2.5 g (70% based on *p*-$C_6H_4(CH_3)_2Mn(CO)_3ClO_4$) of the bridged complexes as a yellow oil: IR ν_{CO} pentane) 2017, 1936 (br) cm^{-1}, see Tables I and II for ^1H NMR and ^{13}C spectroscopic data. Exact mass calcd for $C_{11}H_{13}MnO_3$: 248.0261. Found: 248.0245.

Reduction of (Mesitylene)Mn(CO)$_3^+$ to (Trimethylcyclohexenyl)manganese Tricarbonyl, 5B(a–d). (Trimethylcyclohexenyl)manganese tricarbonyl was prepared from (mesitylene)manganese tricarbonyl hexafluorophosphate by the identical method used for the preparation of the monomethyl complex with the following exceptions: 3.0 g of (mesitylene)manganese tricarbonyl hexafluorophosphate was used instead of the toluene cation, and 4.5 equivs of potassium triisopropoxyborohydride (1 M in THF) was added to generate the anions **5A** in lieu of the usual 3.5 equiv. All other reagents were scaled down accordingly. Approximately 90% conversion to the isomeric anions **5A** was observed after refluxing the mixture for 5 days (ν_{CO} (THF) 1920, 1828, 1783 cm^{-1}). Workup yielded 1.1 g (57% based on $C_6H_3(CH_3)_3Mn(CO)_3PF_6$) of the bridged complexes as a yellow oil: IR ν_{CO} pentane) 2014, 1936, 1930 cm^{-1}; see Tables I and II for ^1H NMR and ^{13}C NMR spectroscopic data. Exact mass calcd for $C_{12}H_{15}MnO_3$: 262.0418. Found: 262.0401.

Acknowledgment is made to the National Institutes of Health (Grant 1 R01 GM2893801) for support of this research.

Registry No. **2B(a)**, 84712-00-5; **2B(b)**, 84773-78-4; **2B(c)**, 84712-01-6; **2B(e)**, 84823-04-1; **2C**, 38834-51-4; **3B(a)**, 84712-02-7; **3C**, 84711-95-5; **4B(a)**, 84731-10-2; **4B(b)**, 84798-61-8; **4B(c)**, 84712-03-8; **4C**, 84711-96-6; **5B(a)**, 84712-04-9; **5B(b)**, 84773-79-5; **5B(c)**, 84731-11-3; **5B(d)**, 84798-62-9; **5C**, 35399-67-8; **6**, 34830-40-5; **7**, 59592-96-0; **8**, 84711-97-7; **9**, 84711-98-8; **10**, 84711-99-9; **11**, 12307-62-9; $Mn(CO)_5OClO_3$, 66034-78-4; $Mn(CO)_5Br$, 14516-54-2; $AgClO_4$, 7783-93-9; $AlCl_3$, 7446-70-0; K[(*i*-PrO)$_3$BH], 42278-67-1.

Radical Pathways in Substitutions of $(\eta^5\text{-}C_5H_5)Fe(CO)_2(\eta^1\text{-}C_5H_5)$ and Related Reactions

Benedict D. Fabian[1a] and Jay A. Labinger*[1b]

Department of Chemistry, University of Notre Dame, Notre Dame, Indiana 46556

Received October 13, 1982

The η^1-cyclopentadienyl complex $(\eta\text{-}C_5H_5)Fe(CO)_2(\eta^1\text{-}C_5H_5)$ (1) undergoes unexpectedly facile CO substitution by phosphorus ligands. Evidence is presented that this involves a radical chain mechanism, wherein $(\eta\text{-}C_5H_5)Fe(CO)_2$ is generated and undergoes rapid substitution, followed by transfer of C_5H_5 from 1 to $(\eta\text{-}C_5H_5)Fe(CO)L$. The resulting $(\eta\text{-}C_5H_5)Fe(CO)L(\eta^1\text{-}C_5H_5)$ was isolated only for L = $P(OPh)_3$ or $P(O\text{-}i\text{-}Pr)_3$. For L = $P(OR)_3$ (R = Me or Et) an Arbuzov-like rearrangement leads to $(\eta\text{-}C_5H_5)Fe(CO)(P(OR)_3)(PO(OR)_2)$, while for L = PR_3 a redox reaction with chlorinated solvent gives $[(\eta\text{-}C_5H_5)Fe(CO)(PR_3)_2]^+Cl^-$. With L = PMe_3, $[(\eta\text{-}C_5H_5)Fe(CO)(PMe_3)_2]^+(C_5H_5)^-$ was obtained. The η^1-allyl analogue undergoes the same rapid radical-chain substitution mechanism but none of the subsequent reactions found for 1.

Introduction

The intervention of odd-electron intermediates in transformations that stoichiometrically appear to satisfy the 16–18-electron rule has been observed with increasing frequency in organotransition-metal chemistry in recent years. Some examples include oxidative addition of alkyl halides[2] and substitution reactions of hydridometal carbonyls,[3] among others.[4] In many of these cases, products that are expected from a straightforward nonradical pathway are actually produced by a radical chain mechanism. Frequently the first indication that the reaction is *not* straightforward comes from reactivity much higher than predicted for the nonradical path (hydridometal carbonyls undergoing substitution much faster than corresponding alkyls, ethyl halides oxidatively adding faster than methyl, etc.).

We initially set out to synthesize complexes of type $CpFe(CO)L(\eta^1\text{-}Cp)$ (throughout Cp = C_5H_5; η^5 unless specified otherwise) for the purpose (among others) of examining the fluxional process.[5] The parent compound $CpFe(CO)_2(\eta^1\text{-}Cp)$ (1) was first reported over 25 years ago,[6] but no substituted derivatives had previously been synthesized. At first sight, direct replacement of CO by L does not appear to be a very promising route: such substitution in $CpFe(CO)_2Me$ requires elevated temperatures or photolysis, conditions under which 1 readily decarbonylates to give ferrocene. Nonetheless, we found that 1 does react readily with phosphine and phosphite ligands at room temperature, although simple substitution is by no means always observed. We describe here our studies on these reactions, and present evidence that here as elsewhere the unusually high reactivity is the result of operation of a radical chain pathway. Preliminary accounts of parts of this work have appeared.[7,8]

(1) (a) Parker Division, 32100 Stephenson Highway, Madison Heights, MI 48071. (b) Address correspondence at Atlantic Richfield Co., Los Angeles, CA 90071.

(2) Labinger, J. A.; Osborn, J. A. *Inorg. Chem.* **1980**, *19*, 3230–3236. Labinger, J. A.; Osborn, J. A.; Coville, N. J. *Ibid.* **1980**, *19*, 3236–3243.

(3) Byers, B. H.; Brown, T. L. *J. Am. Chem. Soc.* **1977**, *99*, 2528–2532. Hoffman, N. W.; Brown, T. L. *Inorg. Chem.* **1978**, *17*, 613–617 and references therein.

(4) An excellent monograph on organometallic mechanisms emphasizes the role of radical pathways throughout: Kochi, J. K. "Organometallic Mechanisms and Catalysis"; Academic Press: New York, 1978.

(5) Fabian, B. D.; Labinger, J. A. *J. Organomet. Chem.* **1981**, *204*, 387–392.

(6) Piper, T. S.; Wilkinson, G. *J. Inorg. Nucl. Chem.* **1956**, *3*, 104–124.

(7) Labinger, J. A. *J. Organomet. Chem.* **1977**, *136*, C31–C36.

(8) Fabian, B. D.; Labinger, J. A. *J. Am. Chem. Soc.* **1979**, *101*, 2239–2240.

Results and Discussion

Reactions of Phosphites with 1. Our initial observation was that 1 reacts rapidly (minutes at room temperature) with excess $P(OMe)_3$, to give $CpFe(CO)(P(OMe)_3)(PO(OMe)_2)$ (**2a**) in good yield.[7] This is a striking contrast with the behavior of $CpFe(CO)_2Me$, which is essentially unreactive to all phosphorus ligands at room temperature. Two questions must be asked: what is the reason for the enhanced reactivity and how does the formation of a phosphonate ligand in **2a** occur ?

Taking the latter first, formation of **2a** is accompanied by an equimolar amount of methylcyclopentadiene; this is a net Arbuzov-like rearrangement, then, with the cyclopentadienyl group acting as nucleophile. One route by which this could take place is displacement of Cp^- (eq 1);

$$1 + P(OMe)_3 \longrightarrow [CpFe(CO)_2(P(OMe)_3)]^+Cp^- \longrightarrow \underset{\mathbf{3a}}{CpFe(CO)_2(PO(OMe)_2)} + MeCp \xrightarrow{P(OMe)_3} \mathbf{2a} + CO \qquad (1)$$

the high reactivity of 1 relative to $CpFe(CO)_2Me$ would reflect the ability of Cp^- to act as leaving group. Indeed, **2a** is formed by this route (with Cl^- as leaving group and nucleophile) in the reaction of $CpFe(CO)_2Cl$ with $P(OMe)_3$.[9] However, the latter reaction also yields substantial amounts of the dicarbonyl **3a**. No **3a** is observed in the reaction of 1, even when less than an equivalent of $P(OMe)_3$ is used, implying that the substitution product **4a** is an intermediate, as in eq 2. According to eq 2, 4

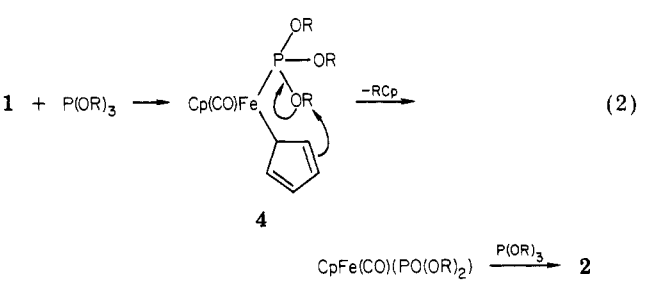

(2)

should be isolable if R is not susceptible to nucleophilic attack. This is the case: whereas for R = Me or Et, phosphonate complexes **2** are the only products observed, for R = i-Pr or Ph the substituted η^1-Cp complexes **4c** and **4d** were obtained. The fluxional behavior of **4d**[7] and its η^1-MeCp analogue[5] have been described.

The above equation still leaves the enhanced reactivity of 1 to be explained. Three interpretations that do not involve any radical path seem at least somewhat plausible.

0276-7333/83/2302-0659$01.50/0

(i) Interaction between the free C=C π orbitals and the Fe-centered orbitals in **1** could render it electronically significantly different from $CpFe(CO)_2Me$, conferring greater reactivity (e.g., by a substantially weakened Fe–CO bond). While we *have* seen evidence for some interaction of this sort in photoelectron spectra of these compounds,[10] the close similarity of spectral parameters such as ν_{CO} between **1** and other $CpFe(CO)_2R$ indicates that this effect cannot be very large. (ii) Substitution could proceed dissociatively via a stabilized intermediate **5** (eq 3), making

$$\underset{}{1} \overset{-CO}{\rightleftharpoons} \underset{\mathbf{5}}{CpFe(CO)(\eta^3\text{-}Cp)} \xrightarrow{L} \underset{\mathbf{4}}{CpFe(CO)L(\eta^1\text{-}Cp)} \quad (3)$$

it more favorable. A related η^3-Cp complex is in fact known.[11] Arguing against this is the fact that η^1-allyl complex **6** exhibits reactivity patterns quite similar to those of **1** (see below). The analogous mechanism (eq 4) would

$$\underset{\mathbf{6}}{CpFe(CO)_2(\eta^1\text{-allyl})} \xrightarrow{-CO} \underset{\mathbf{7}}{CpFe(CO)(\eta^3\text{-allyl})} \xrightarrow{L} \text{no reaction} \quad (4)$$

involve η^3-allyl **7** as intermediate; but **7** is completely stable to ligands L under these reaction conditions. Furthermore, it seems more likely that if **5** were formed, it would proceed with extreme facility to ferrocene; but no ferrocene is detected in reactions of **1** with $P(OMe)_3$ or $P(OEt)_3$. (iii) Migration of Cp to CO might be invoked, but there is no obvious reason why this should be more facile than migration of Me; indeed, no example of migration of η^1-Cp has been reported. None of these nonradical mechanisms accounts comfortably for the unusual reactivity of **1** toward substitution.

Evidence for a Radical Pathway. Photochemical studies indicate that the 17-electron intermediate $CpFe(CO)_2$ (**8**) is involved in substitution of **1**. The reaction of **1** with $P(OPh)_3$ in the dark leads only slowly to **4d**: rates are somewhat variable, but periods of 4–8 h for 50% reaction are typical. If the reaction mixture is irradiated with near-UV light, there is rapid *initial* conversion to **4d** (ca. 5% in 5 min), but thereafter only conversion to ferrocene is observed. However, if the reaction mixture also contains a small amount of dimer $(CpFe(CO)_2)_2$ (**9**), irradiation brings about rapid and continuing formation of **4d** (ca. 25% in 5 min; further irradiation gives more **4d** but also begins to convert **4d** to ferrocene; the maximum conversion to **4d** obtainable is about 50%). This behavior is strongly reminiscent of that of hydridometal carbonyls[3] and suggests an analogous mechanism for substitution of **1** (eq 5–8). In the absence of irradiation, this chain mechanism

$$\underset{\mathbf{1}}{CpFe(CO)_2(\eta^1\text{-}Cp)} + Q\cdot \rightarrow QCp + \underset{\mathbf{8}}{CpFe(CO)_2\cdot} \quad (5)$$

$$\underset{\mathbf{9}}{(CpFe(CO)_2)_2} \overset{h\nu}{\rightleftharpoons} \underset{\mathbf{8}}{2CpFe(CO)_2\cdot} \quad (6)$$

$$8 + L \xrightarrow{fast} CpFe(CO)L\cdot + CO \quad (7)$$

$$CpFe(CO)L\cdot + 1 \rightarrow \underset{\mathbf{4}}{CpFe(CO)L(\eta^1\text{-}Cp)} + 8 \quad (8)$$

would be initiated by adventitious impurities Q· (eq 5), accounting for the variability of observed reaction rates. Alternatively, the key species **8** is produced by photocleavage of dimer **9**, a well-established method of producing such 17-electron fragments;[12] this provides a much more efficient source of initiator. Substitution of CO in 17-electron intermediates (eq 7) has been shown to be facile, although there is still some question as to whether these are associative or dissociative reactions.[13,14]

The crucial step which distinguishes reactions of **1** from other alkyl complexes is the transfer of Cp between metal centers (eq 8). If this is viewed as a homolytic displacement reaction, it is readily understandable why this should not be an efficient process for a saturated alkyl group as in $CpFe(CO)_2Me$: homolytic displacements on saturated alkyls are generally unfavorable. However, **1** can undergo displacement by an addition-elimination sequence shown in eq 9. A similar sequence should be available for an

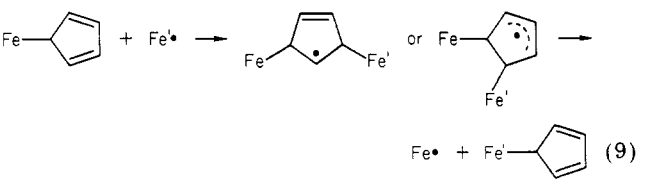

(9)

η^1-allyl complex,[15] and indeed, as noted earlier, **6** exhibits reactivity patterns very similar to those of **1**: slow reactions with ligands L in the dark, conversion primarily to the CO-loss product **7** on irradiation with L but no **9**, and rapid formation of $CpFe(CO)L(\eta^1\text{-allyl})$ (**10**) on irradiation with both L and **9** present. Other metal allyls such as $CpM(CO)_3(\eta^1\text{-allyl})$ (M = Mo, W) and $Mn(CO)_5(\eta^1\text{-allyl})$ show the same general behavior. No rearrangement such as was found for **1** is observed in reactions of these allyls with $P(OMe)_3$; only the simple substitution products are obtained.

Evidence for Transfer of Alkyl Groups between Metal Centers. While the preceding section provides strong support for the involvement of **8** as intermediate in substitution of **1**, the alkyl-transfer step remains to be established. This was achieved by means of crossover experiments. In the first, a benzene solution of equimolar **1** and $((MeCp)Fe(CO)_2)_2$ (**9′**) was irradiated; in the absence of any Cp exchange, the only result should be the conversion of **1** to ferrocene, while **9′** would remain unchanged. After 1 h ca. 75% of **1** had been consumed, and chromatography of the reaction mixture gave three bands. NMR analysis showed that these consisted respectively of ferrocene and methylferrocene, **1** and $(MeCp)Fe(CO)_2(\eta^1\text{-}Cp)$ (**1′**), and **9** and **9′** ($(MeCp)CpFe_2(CO)_4$ is presumably also present but would not be distinguished by NMR spectroscopy). This result requires transfer of Cp groups between metal centers, as in Scheme I.

(9) Haines, R. J.; Du Preez, A. L.; Marais, I. L. *J. Organomet. Chem.* **1971**, *28*, 405–413.
(10) Fabian, B. D.; Fehlner, T. P.; Hwang, L. S.; Labinger, J. A. *J. Organomet. Chem.* **1980**, *191*, 409–413.
(11) Huttner, G.; Brintzinger, H. H.; Bell, L. G.; Freidrich, P.; Bejenke, V.; Neugebauer, D. *J. Organomet. Chem.* **1978**, *145*, 329–333.
(12) Wrighton, M. *Chem. Rev.* **1974**, *74*, 401–430 and references cited therein.
(13) Kidd, D. R.; Brown, T. L. *J. Am. Chem. Soc.* **1978**, *100*, 4095–4103.
(14) Fox, A.; Malito, J.; Poe, A. *J. Chem. Soc., Chem. Commun.* **1981**, 1052–1053.
(15) It has been reported that homolytic displacement on allylcobalt(III) complexes by the $Cl_3C\cdot$ radical proceeds readily under ambient conditions,[16] whereas the same reaction of benzylcobalt(III) requires irradiation and/or heating.[17]
(16) Gupta, B. D.; Funabiki, T.; Johnson, M. D. *J. Am. Chem. Soc.* **1976**, *98*, 6697–6698.
(17) Funabiki, T.; Gupta, B. D.; Johnson, M. D. *J. Chem. Soc., Chem. Commun.* **1977**, 653–654.

Scheme I

$$9' \underset{}{\overset{h\nu}{\rightleftharpoons}} 2\,8' \quad (10)$$

$$8' + 1 \rightleftarrows 1' + 8 \quad (11)$$

$$8 + 8' \underset{h\nu}{\rightleftharpoons} (MeCp)CpFe_2(CO)_4 \quad (12)$$

$$2\,8 \underset{h\nu}{\rightleftharpoons} 9 \quad (13)$$

$$1 \xrightarrow{h\nu} Cp_2Fe + 2CO \quad (14)$$

$$1' \xrightarrow{h\nu} (MeCp)CpFe + 2CO \quad (15)$$

A conceptually straightforward method of demonstrating that this exchange takes place under actual substitution conditions would be to react a ligand such as $P(OPh)_3$ (which gives simple substitution) with a mixture of $(MeCp)Fe(CO)_2(\eta^1\text{-Cp})$ and $CpFe(CO)_2(\eta^1\text{-MeCp})$. With exchange, the products should include, inter alia, the dimethyl species $(MeCp)Fe(CO)L(\eta^1\text{-MeCp})$, whose presence should be demonstrable by mass spectroscopy. Unfortunately, Cp exchange occurs in the mass spectrometer in studies of these species: the mass spectrum for **1'** shows fragment peaks for ferrocene and dimethylferrocene as well as for the expected methylferrocene, rendering any such experiment equivocal.

As an alternative, a benzene solution of equimolar **1'** and **6** was treated with $P(OMe)_3$. With the assumption that reaction rates for substitution of **1** and **6** are comparable, if alkyl groups (Cp and allyl) are transferred between metal centers, two sets of products will be formed: **2a** and methyl-substituted $(MeCp)Fe(CO)(P(OMe)_3)(PO(OMe)_2)$ (**2a'**) and $CpFe(CO)(P(OMe)_3)(\eta^1\text{-allyl})$ (**10a**) and $(MeCp)Fe(CO)(P(OMe)_3)(\eta^1\text{-allyl})$ (**10a'**). This experiment is facilitated by the fact that **2** is much less soluble in hexane than **10**. When the reaction mixture was concentrated and extracted with hexane, the insoluble fraction was shown by NMR spectroscopy to contain approximately equimolar **2a** and **2a'**, while the soluble fraction consisted of **10a** and **10a'**. Thus *both* Cp and allyl groups do undergo exchange between metal centers during substitution.

The addition-elimination mechanism for alkyl transfer requires that the carbon atom bonded to metal change during substitution. This cannot be tested for η^1-Cp complexes, as they are fluxional, but it should be subject to verification for η^1-allyls. In fact, $CpFe(CO)_2(\eta^1\text{-}CH_2CH{=}CD_2)$ has been reported to equilibrate under mild conditions with isomeric $CpFe(CO)_2(\eta^1\text{-}CD_2CH{=}CH_2)$.[18] It is tempting to ascribe this to homolytic displacement involving small amounts of **8** (eq 16). More recently

$$Cp(CO)_2FeCH_2CH{=}CD_2 + \underset{8}{Cp(CO)_2Fe\cdot} \rightarrow Cp(CO)_2FeCD_2CH{=}CH_2 + 8 \quad (16)$$

Rosenblum et al. used a crossover experiment to demonstrate that an isomerization of type $CpFe(CO)L(\eta^1\text{-}CHRCH{=}CH_2) \rightarrow CpFe(CO)L(\eta^1\text{-}CH_2CH{=}CHR)$ occurs concurrently with exchange of allyl groups between metal centers.[19]

Dimer Substitution as a Possible Alternate Mechanism. Flash photolysis studies by Meyer et al. suggest that substitution of **9** by PPh_3 does not proceed through **8**. Two transient intermediates are observed in flash photolysis, assigned as **8** and $Cp_2Fe_2(CO)_3$; but only the latter reacts with PPh_3.[20] This indicates an alternate mechanistic possibility, shown in Scheme II, for substitutions of **1** (at least under conditions of photolysis with **9** present; it is unlikely that dimer substitution is involved in the slower thermal reactions). This mechanism would be significantly different from that previously discussed (it still involves radical intermediates but is not a chain reaction). It thus seemed worthwhile to test whether this sequence is responsible for the photoactivated reactivity.

Scheme II

$$9 + L \xrightarrow{h\nu} \underset{11}{Cp_2Fe_2(CO)_3L} \quad (17)$$

$$11 \xrightarrow{h\nu} CpFe(CO)_2\cdot + CpFe(CO)L\cdot \quad (18)$$

$$CpFe(CO)L\cdot + 1 \rightarrow 4 + 8 \quad (8)$$

$$2\,8 \rightarrow 9 \quad (13)$$

Formation of **4** from **1** and **11** is indeed possible, as demonstrated by photolyzing a mixture of **1** and $Cp_2Fe_2(CO)_3(P(OPh)_3)$ (**11d**). After 90 min about 40% conversion of **1** to **4d** had occurred (along with some decarbonylation to ferrocene). However, when a solution of equimolar **1** and **9** containing excess $P(OPh)_3$ was irradiated for 15 min, 50% of **1** was converted to **4d**, while only 15% of **9** was converted to **11d**. Since the combination of **9** plus free ligand effects substitution of **1** much more efficiently than does **11d** and since substitution of **1** is faster than substitution of **9** to give **11d**, it is not possible that **11d** is a major intermediate in the formation of **4d**, and this route cannot be important compared to the previous one involving substitution of **8**.

While at first sight this conclusion appears at variance with the finding that PPh_3 does not react with **8** in the flash photolysis studies, we find that PPh_3 (in contrast to sterically less demanding ligands) does *not* react with either **1** or **6** under our reaction conditions. This suggests that PPh_3 substitutes **8** too slowly to keep the radical chain path going; any **8** produced by initiation steps simply undergoes virtual exchange of alkyl group and, eventually, destructive termination. Similarly, in photolysis of **9**, any **8** produced would recombine to **9** faster than being substituted; formation of $Cp_2Fe_2(CO)_3(PPh_3)$ would occur by direct substitution of the intact dimer **9**.[21] It would be of considerable interest to repeat the flash photolysis studies with a less bulky ligand than PPh_3, since the chain mechanism that operates here suggests that substitution of **8** by such a ligand should be observable.

It is notable that no disubstituted dimer, $(CpFe(CO)L)_2$, was detected in any of these reactions. If substituted radicals $CpFe(CO)L\cdot$ are present as proposed, they do not dimerize, presumably again for steric reasons. No such disubstituted dimer (where L is a phosphorus ligand) has previously been fully characterized, although formation and partial characterization of $[CpFe(CO)(P(OMe)_3)]_2$ has been reported.[21,22] Under conditions where the latter forms, bulkier $P(O\text{-}i\text{-}Pr)_3$ gives only monosubstitution.[21] We find that by using a still *less* bulky ligand, the cage phosphite $P(OCH_2)_3CEt$, it is possible to isolate $(CpFe(CO)L)_2$ (see Experimental Section for details).

Reactions of Phosphines with 1. The reactions of **1** with phosphine ligands lead to entirely different products

(18) Merour, J. Y.; Cadiot, P. *C. R. Hebd. Acad. Sci., Ser. C.* **1970**, *270*, 83–85.
(19) Rosenblum, M.; Waterman, P. *J. Organomet. Chem.* **1981**, *206*, 197–209.
(20) Caspar, J. V.; Meyer, T. J. *J. Am. Chem. Soc.* **1980**, *102*, 7795–7797.
(21) Tyler, D. R.; Schmidt, M. A.; Gray, H. B. *J. Am. Chem. Soc.* **1979**, *101*, 2753–2755.
(22) Haines, R. J.; Du Preez, A. L. *Inorg. Chem.* **1969**, *8*, 1459–1464.

Scheme III

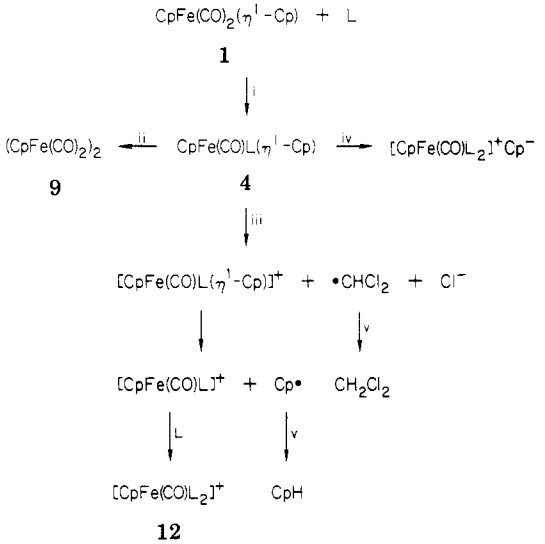

i, several-step chain mechanism; ii, non-halogenated solvent (L = $PMePh_2$); iii, acetone-chloroform mixture; iv, L = PMe_3; v, hydrogen abstraction from L

from those observed with phosphites. 1 reacts rapidly with $PMePh_2$ in acetone, but the major identifiable product 9 contains no ligand. Most of the starting complex is transformed into an organic-insoluble, acid-soluble, NMR-silent material that has not been fully characterized but is probably an Fe salt of some type.[7] A much cleaner reaction can be observed in mixed acetone-chloroform solution (reaction proceeds only very slowly in pure chloroform). The major product is an ionic compound, $[CpFe(CO)(PMePh_2)_2]^+Cl^-$ (12); small amounts of ferrocene and 9 are also formed. No reaction between 1 and PPh_3 is observed under these conditions.

In contrast to $PMePh_2$, PMe_3 reacts rapidly with 1 in benzene, giving evolution of gas and formation of a yellow precipitate. The latter is highly air-sensitive, unlike most of the compounds dealt with here which generally react only slowly with air. It is insoluble in polar solvents such as THF or acetonitrile but dissolves readily in $CHCl_3$ to give a red solution, which contains the $[CpFe(CO)(PMe_3)_2]^+$ ion. Addition of water to the yellow solid liberates free cyclopentadiene. The yellow precipitate is thus identified as $[CpFe(CO)(PMe_3)_2]^+Cp^-$; thus Cp is behaving as a leaving group in this reaction. Displacement of a coordinated Cp group by neutral ligands has been observed before, primarily in reactions of Cp_2Ni.[23] Direct displacement of Cp by PMe_3 in 1 cannot be occurring, however, because the product would be $[CpFe(CO)_2(PMe_3)]^+Cp^-$; instead, Cp^- loss must follow substitution of PMe_3 for CO.

It is tempting to assign an analogous reaction to account for the behavior of 1 with $PMePh_2$ in acetone/chloroform. In this medium, Cp^- would abstract a proton to give CpH, while the Cl^- observed in the final product requires $CHCl_3$ to be converted to Cl^- plus products derived from CCl_2. The NMR spectrum of the reaction mixture shows that CpH is indeed produced. However, when the reaction is carried out in deuterated solvent, no deuterium is incorporated into the cyclopentadiene. Furthermore, 1 equiv of CH_2Cl_2 is produced from acetone (or acetone-d_6)/$CHCl_3$; if $CDCl_3$ is used, the product is $CHDCl_2$; and if acetone-

Scheme IV

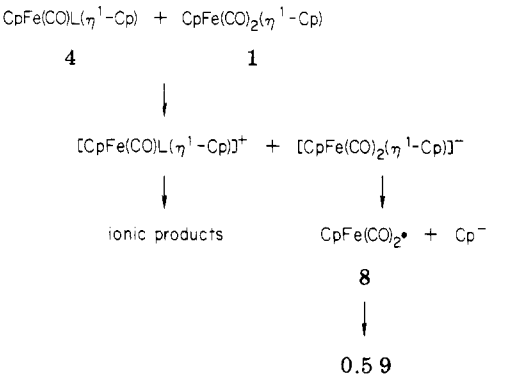

/CCl_4 is employed as solvent, the reaction proceeds just as readily, giving $CHCl_3$ along with CpH and 12. These observations argue for H (and Cl) transfer occurring via radical, not ionic processes; since solvent is apparently not the source of hydrogen, excess phosphine ligand must be. There are previous reports of H· being abstracted from ligand in preference to solvent in related systems.[24]

A mechanism that accounts for all these observations is shown in Scheme III. The first step for *all* ligands is the formation of substitution product 4, following the radical chain mechanism discussed previously. From here the reaction may proceed in any of several different ways. If L is a phosphite, 4 is either stable or rearranges by the Arbuzov-like path found for $P(OMe)_3$. If L is a phosphine, 4 is never stable. In inert solvents (L = $PMePh_2$) it decomposes to give 9 and ionic products, possibly by a redox mechanism[25] such as that shown in Scheme IV. The fact that the overall disappearance of 1 is much faster in acetone than in benzene or chloroform can be understood as well: the redox decomposition, which should be faster in a more polar solvent, will be accompanied by generation of radical species that can in turn function as initiators in the chain process leading to 4. (It may be noted that the reaction of 1 with $P(OMe)_3$ or $P(OEt)_3$ is *much* faster than with $P(O\text{-}i\text{-}Pr)_3$ or $P(OPh)_3$; perhaps the rearrangement of 4 to 2, observed only for the first two, is also accompanied by generation of small amounts of initiating species.) In the mixed solvent acetone/chloroform, a redox reaction with solvent becomes rapid; this generates the several radical species that eventually lead to the observed products 12, CpH, and CH_2Cl_2. When L = PMe_3, the ligand is sufficiently small and/or electron donating to bring about a direct internal redox reaction, leading to the ionic product even in benzene solution.

The fact that 4 is stable for phosphites but not for phosphines coupled with the fact that substitution products of 6, $CpFe(CO)L(\eta^1\text{-allyl})$, are stable for phosphines as well as phosphites suggests that it is excessive electron density that is responsible for the instability of $CpFe(CO)(PR_3)(\eta^1\text{-Cp})$. We have previously shown by photoelectron spectroscopy and electrochemical data that 1 is significantly more electron rich than 6,[10] presumably the result of some interaction between the olefinic π orbitals and metal-centered orbitals. Apparently the combination of this effect and a strongly electron-donating phosphine ligand results in a species that is sufficiently strongly reducing to transfer an electron, either to another organo-

(23) Barefield, E. K.; Krost, D. A.; Edwards, D. S.; Van Derveer, D. G.; Trytko, R. L.; O'Rear, S. P. *J. Am. Chem. Soc.* **1981**, *103*, 6219–6222 and references cited therein.

(24) Howell, J. A. S.; Rowan, A. J. *J. Chem. Soc., Dalton Trans.* **1980**, 1845–1851. Howell, J. A. S.; Rowan, A. J.; Snell, M. S. *Ibid.* **1981**, 325–327.

(25) We have previously observed that addition of reducing agents such as MeLi to 1 leads to formation of 9 and LiCp: Labinger, J. A. *J. Organomet. Chem.* **1980**, *187*, 287–296.

Scheme V

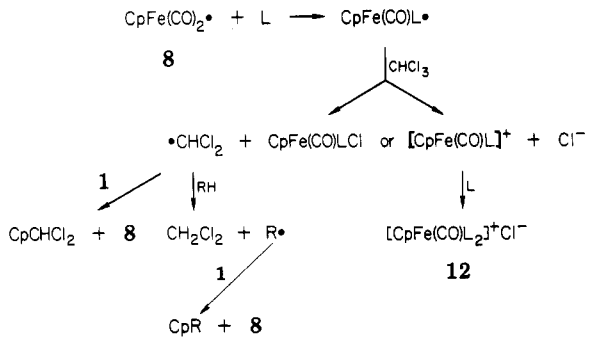

metallic molecule or to a halocarbon solvent, or (in the case of PMe_3) to displace Cp^-. It would be of interest to examine intermediate ligands $PR_2(OR')$ or $PR(OR')_2$ (where R′ is Ph or some other group not susceptible to Arbuzov rearrangement) to ascertain the limits of stability of **4**.

An alternate mechanism for participation of halocarbon in reactions of **1** with phosphines should be briefly considered: one could envision $CHCl_3$ acting to interrupt the chain mechanism that leads to **4**, diverting to ionic products instead. However, as shown in Scheme V, to carry on the chain mechanism, substituted cyclopentadienes would have to be formed, rather than CpH; no such species were observed.[26] Furthermore, such a route might be expected to give neutral chloride complexes such as CpFe(CO)LCl, as in the typical behavior of 17-electron fragments with halocarbons.[12] On both these grounds, it appears that Scheme III is more consistent with experimental observations.

Conclusions

The unusual reactivities delineated here arise from several properties of the η^1-Cp ligand (and, to a lesser extent, the η^1-allyl). First and foremost is the ability of the free C=C double bonds to undergo attack in a homolytic substitution step and thus make a radical chain process possible. This is well illustrated here by contrasting the reactivity of $CpFe(CO)_2Me$ to that of **1** and **6** in substitution reactions. Secondly, the ability of the C=C bonds to act as nucleophiles (in **1**, but not in **6**) leads to the Arbuzov rearrangements observed in reactions of $P(OR)_3$ (R = Me or Et); finally, the interaction of the C=C electron density with metal orbitals causes complexes $CpFe(CO)(PR_3)(\eta^1\text{-Cp})$ to undergo facile redox reactions, preventing their isolation.

Experimental Section

General Data. All reactions and manipulations were carried out under argon atmosphere using standard Schlenk techniques or in a nitrogen-filled Vacuum Atmospheres Co. glovebox. Reaction solvents were distilled from sodium benzophenone ketyl under argon; chromatography solvents were degassed before use. NMR spectra were recorded on Varian A-60A, EM-390, and XL-100 instruments; infrared spectra on Perkin-Elmer 137-A and 727-B instruments; mass spectra on AEI MS-902 and Du Pont DP-1 GC/MS instruments. Elemental analyses were performed by Midwest Microlab (Indianapolis, IN) and Galbraith Labs (Knoxville, TN).

Complexes $(CpFe(CO)_2)_2$ (**9**),[27] $CpFe(CO)_2I$,[27] $CpFe(CO)_2(\eta^1\text{-Cp})$ (**1**),[6] $Na[CpFe(CO)_2]$,[28] and $CpFe(CO)_2(\eta^1\text{-allyl})$ (**6**)[29] were prepared by literature methods, as were the MeCp analogues. Ligands and other reagents were, except where otherwise noted, obtained commercially and used without further purifications.

Reactions of 1 with Phosphite Ligands. The preparation of $CpFe(CO)(P(OMe)_3)(PO(OMe)_2)$ (**2a**) and $CpFe(CO)(P(OPh)_3)(\eta^1\text{-Cp})$ (**4d**) have already been reported.[7] The reaction of **1** with $P(OEt)_3$ proceeds rapidly in benzene to give $CpFe(CO)(P(OEt)_3)(PO(OEt)_2)$ (**2b**), which was characterized by NMR spectroscopy only: δ 4.60 (t, J_{PH} = 1.0 Hz, Cp), 4.0 (m, OCH_2CH_3), 1.2 (m, OCH_2CH_3). $CpFe(CO)(P(O\text{-}i\text{-}Pr)_3)(\eta^1\text{-Cp})$ (**4c**) was prepared by irradiating **1** with excess $P(O\text{-}i\text{-}Pr)_3$ and a trace of **9** in benzene; repeated chromatography separated **4c** from all other organometallics, but complete removal of unreacted ligand could not be achieved: ^1H NMR (C_6D_6) δ 6.29 (br s, η^1-Cp), 4.5 (m, $OCH(CH_3)_2$), 3.75 (s, η^5-Cp), 1.1 (m, $OCH(CH_3)_2$).

Effect of Irradiation on Reaction. The following describes a typical experiment: four thin-walled Pyrex NMR tubes were closed by serum caps, degassed by using a syringe needle attached to the Schlenk line, and then loaded by syringe with 0.5 mL of a solution of **1** (0.12 M in benzene) plus 0.2 mL of $P(OPh)_3$. One tube was wrapped in foil and allowed to react in the dark; a second was irradiated in a Rayonet photochemical reactor using long UV light ($\lambda_{max} \approx 3500$ Å). The third and fourth tubes contained, in addition, a few milligrams of galvinoxyl and of **9**, respectively; these were irradiated along with the second tube. Progress of the reactions was followed by recording the ^1H NMR spectrum: the η^5-Cp region, in particular, exhibits distinct peaks for the various components present (**1**, **4d**, **9**, and ferrocene). Results of this and similar studies are described in the Results and Discussion.

$CpFe(CO)(P(OMe)_3)(\eta^1\text{-allyl})$ (10a). A mixture of 0.4 mL of $P(OMe)_3$ with a benzene solution of **6** (5 mL, 0.44 M) was allowed to stand for 2 h. Volatiles were pumped off, and the residue was extracted with hexane. The extract was concentrated and then distilled at low pressure to give a viscous, yellow-red oil, which was redistilled: ^1H NMR (C_6H_6) δ 4.9 (m, $CH{=}CH_2$ (the remaining vinylic proton signal was obscured by solvent peak)), 4.24 (s, Cp), 3.24 (d, J_{PH} = 11.5 Hz, $P(OCH_3)_3$), 2.0 (m, $FeCH_2$); IR (neat) ν_{CO} 1910 cm^{-1}. Anal. Calcd for $C_{12}H_{19}FeO_4P$: C, 45.89; H, 6.10. Found: C, 44.89; H, 6.22.

Irradiation of a solution of **6**, $P(OMe)_3$, and a trace of **9** gave the above product rapidly. Similar behavior was observed with $P(OPh)_3$, but the product could not be isolated by either vacuum distillation or chromatography—it was not sufficiently volatile for the former, and the latter led to decomposition. Decomposition on attempted chromatography was, surprisingly, a common problem among these substituted η^1-allyl systems.

$CpFe(CO)(PMe_2Ph)(\eta^1\text{-allyl})$ (10f). A 2-mL sample of a benzene solution of **6** (0.7 M) and 0.4 mL of PMe_2Ph were mixed and irradiated for 1 h in the presence of a trace of **9**. A 0.1-mL sample of MeI was added to quaternize unreacted ligand; after 10 min the reaction mixture was concentrated and extracted with hexane. The extracts were treated with activated charcoal, filtered, and pumped to dryness to give a red oil: ^1H NMR (C_6D_6) δ 7.3 (m, Ph), 6.3 (m, $CH_2CH{=}CH_2$), 4.8 (m, $CH_2CH{=}CH_2$), 4.01 (d, J_{PH} = 1 Hz, Cp), 1.7 (m, $FeCH_2CH{=}CH_2$), 1.23 (d), 1.18 (d, J_{PH} = 8 Hz (the two methyl groups are rendered nonequivalent by the chiral center at Fe), PMe_2Ph); IR (neat) ν_{CO} 1921 cm^{-1}. Anal. Calcd for $C_{17}H_{21}FeOP$: C, 62.22; H, 6.45. Found: 62.07; H, 6.38.

Attempted chromatography of the above reaction mixture on alumina gave a major green band, which was eluted with toluene; its NMR spectrum corresponds to substituted dimer[22] $Cp_2Fe_2(CO)_3(PMe_2Ph)$ (**11f**): δ 4.52 (s, Cp), 4.05 (d, J_{PH} = 1.6 Hz, Cp), 0.99 (d, J_{PH} = 9 Hz, PMe_2Ph).

The analogous reaction with $PMePh_2$ exhibited similar behavior, but the product **10g** was not isolated in pure form: NMR (C_6H_6) δ 4.7 (m, $CH{=}CH_2$), 4.13 (d, J_{PH} = 1.5 Hz, Cp), 2.0 (m, $FeCH_2$), 1.60 (d, J_{PH} = 8 Hz, $PMePh_2$ (remaining signals hidden by solvent peak)).

A mixture of **6** with PPh_3 showed no reaction after several days in the dark; on irradiation with **9** as above, only slow formation of **7** and small amounts of $Cp_2Fe_2(CO)_3(PPh_3)$ was observed.

$CpFe(CO)(PMe_3)(\eta^1\text{-allyl})$ (10e). A reaction mixture of 2 mL of **6** (0.6 M) in benzene, 1.5 mL of PMe_3 (10.8 M), and a trace

(26) For example, nickelocene reacts with CCl_4 to give $CpCCl_3$: Moberg, C.; Nilsson, M. *J. Organomet. Chem.* **1973**, *49*, 243–248.
(27) King, R. B.; Stone, F. G. A. *Inorg. Synth.* **1963**, *7*, 110–112.
(28) Reger, D. L.; Fauth, D. J.; Dukes, M. D. *Synth. React. Inorg. Met.-Org. Chem.* **1977**, *7*, 151–155.
(29) Magatti, C. V.; Giering, W. P. *J. Organomet. Chem.* **1974**, *73*, 85–92.

of **9** was irradiated for 1 h, concentrated to dryness, and extracted with hexane; the extracts were pumped down and vacuum distilled (bath temperature 65 °C) to give a yellow-red oil: NMR (C_6D_6) 6.2 (m, $CH_2CH{=}CH_2$), 4.7 (m, $CH_2CH{=}CH_2$), 4.05 (d, J_{PH} = 1.5 Hz, Cp), 1.6 (m, $FeCH_2$), 0.90 (d, J_{PH} = 9 Hz, PMe_3); IR (neat) ν_{CO} 1950 cm^{-1}. Anal. Calcd for $C_{12}H_{19}FeOP$: C, 54.14; H, 7.14. Found: C, 53.35; H, 6.30.

Crossover Experiments. A solution of 0.8 mmol each of **1** and **9′** in 4 mL of benzene was irradiated for 1 h. The solution was concentrated and chromatographed on alumina, using petroleum ether/toluene to elute. Three successive orange to red-orange bands were collected, corresponding respectively to ferrocene, **1**, and **9** (neglecting substitution on rings). The NMR spectrum of each fraction showed the presence of η^5-MeCp groups (multiplet around δ 4; singlet around δ 1.4); integration demonstrated that each fraction contained approximately equal amounts of η^5-Cp and η^5-MeCp complex.

A solution of 2 mmol of **1′**, 3 mmol of **6**, and 0.6 mL of $P(OMe)_3$ in 10 mL of benzene was allowed to react in the dark for 20 min. The mixture was concentrated and extracted with hexane; the residue and extract were shown by NMR to contain, respectively, phosphinate product **2a** and substituted allyl **10a**. As in the preceding paragraph, both fractions contained both η^5-Cp and η^5-MeCp groups (δ 4.5 (m) and 1.8 (s) for **2a′**; δ 4.2 (m) and 1.8 (s) for **10a′**).

Effect of Substituted Dimer. $Cp_2Fe_2(CO)_3(P(OPh)_3)$ (**11d**) was prepared by the literature route.[22] A solution of 0.5 mmol of **1** and 0.5 mmol of **11d** in benzene was irradiated for 90 min. The NMR spectrum of the resulting reaction mixture indicated the following composition: 0.23 mmol of **1**, 0.33 mmol of **11d**, 0.17 mmol of **9**, 0.1 mmol of ferrocene, and 0.17 mmol of **4d**. A similar mixture stored for 20 h in the dark showed only 5% formation of **4d**.

A solution of 0.5 mmol of **1**, 0.5 mmol of **9**, and 0.14 mL of $P(OPh)_3$ in benzene was irradiated for 15 min. NMR showed that 0.25 mmol of **4d**, and only 0.08 mmol of **11d** had been produced.

$Cp_2Fe_2(CO)_3(P(OCH_2)_3CEt)$ and $Cp_2Fe_2(CO)_2(P(OCH_2)_3CEt)_2$. A solution of 0.36 g of **9** and 0.5 g of $P(OCH_2)_3CEt$ in benzene was refluxed for 17 h. Filtration of the cooled reaction mixture gave a green solid that was recrystallized from $CHCl_3$/benzene and identified as the disubstituted dimer $Cp_2Fe_2(CO)_2(P(OCH_2)_3CEt)_2$: NMR ($CDCl_3$) δ 4.45 (d, J_{PH} = 0.4 Hz, Cp), 3.95 (d, J_{PH} = 1.5 Hz, $P(OCH_2)_3$), 1.0 (m, Et (the latter signal was distorted by the large Me_4Si lock signal)); IR (Nujol) ν_{CO} 1710 cm^{-1} (bridging). Anal. Calcd for $C_{24}H_{32}Fe_2O_8P_2$: C, 46.30; H, 5.14. Found: C, 46.33; H, 5.18.

The filtrate was concentrated and the red solid recrystallized from benzene/hexane and found to be monosubstituted $Cp_2Fe_2(CO)_3(P(OCH_2)_3CEt)$: NMR ($CDCl_3$) δ 4.70 (s, Cp (unsubstituted Fe)), 4.59 (br s, Cp (substituted Fe)), 3.96 (d, J_{PH} = 2 Hz, $P(OCH_2)_3$); IR (Nujol) ν_{CO} 1930 (terminal), 1740 cm^{-1} (bridging). Anal. Calcd for $C_{19}H_{21}Fe_2O_6P$: C, 46.76; H, 4.34. Found: C, 47.01; H, 4.67.

Reaction of 1 with $PMePh_2$. A solution of 1 mmol of **1** in 0.4 mL of $CHCl_3$ plus 1.6 mL of acetone was treated with 0.3 mL of $PMePh_2$. After 1 h, all volatiles were flash-distilled at room temperature into a liquid N_2-cooled flask. The NMR of the volatiles showed the presence of CH_2Cl_2 (δ 5.28) and CpH (δ 6.45, 2.88); the latter was confirmed by adding 0.1 g of maleic anhydride to the solution and allowing it to stand for 1 week; the NMR showed the presence of the Diels–Alder adduct (by comparison to an authentic sample).

The residue was washed with hexane, dried, and identified spectroscopically as $[CpFe(CO)(PMePh_2)_2]^+Cl^-$ (**12**): NMR δ 7.8, 7.5, 7.1 (Ph), 5.15, (br s, Cp), 1.73 (apparent t, J_{PH} = 4 Hz, $PMePh_2$); IR (Nujol) ν_{CO} 1940 cm^{-1}. Metathesis with $NaBF_4$ in ethanol gave a crystalline sample of the BF_4 salt. Anal. Calcd for $C_{32}H_{31}BF_4FeOP_2$: C, 60.41; H, 4.91. Found: C, 59.31; H, 5.61.

Reaction of 1 with PMe_3. A solution of 1 mmol of **1** and 2.4 mmol of PMe_3 in 7 mL of benzene was stirred at room temperature for 15 min. Gas evolution and deposition of a voluminous yellow precipitate were observed. The precipitate was washed with hexane and found to be insoluble in THF, DME, or MeCN; it dissolved in $CHCl_3$ to give a *red* solution, whose NMR spectrum (δ 5.0 (br s, Cp), 1.6 (br apparent t, J = 4 Hz, PMe_3)) suggests the presence of $[CpFe(CO)(PMe_3)_2]^+$. Addition of water to a benzene suspension of the yellow solid liberated CpH, as shown by the NMR of the separated benzene layer. The yellow precipitate is thus formulated as $[CpFe(CO)(PMe_3)_2]^+Cp^-$: IR (Nujol) ν_{CO} 1940 cm^{-1}. Anal. Calcd for $C_{17}H_{28}FeOP_2$: C, 55.76; H, 7.71. Found: C, 54.73; H, 7.61.

Reaction of 1 with PPh_3. Solutions of **1** with excess PPh_3 in chloroform/acetone, or in benzene (on irradiation with **9** present), showed no reaction other than formation of ferrocene in the later case.

Acknowledgment. We thank the donors of the Petroleum Research Fund, administered by the American Chemical Society, and the National Science Foundation, Grants CHE 77-01585 and CHE 80-06518, for support of this work.

Registry No. **1**, 12247-96-0; **1′**, 84848-88-4; **2b**, 77307-41-6; **4c**, 84848-89-5; **6**, 38960-10-0; **9**, 12154-95-9; **9′**, 84799-37-1; **10a**, 75094-20-1; **10e**, 84848-90-8; **10f**, 84848-91-9; **10g**, 84848-92-0; **11d**, 37131-60-5; **12**·Cl^-, 70526-84-0; **12**·BF_4^-, 84863-59-2; $P(OEt)_3$, 122-52-1; $P(O\text{-}i\text{-}Pr)_3$, 116-17-6; $P(OMe)_3$, 121-45-9; PMe_2Ph, 672-66-2; $PMePh_2$, 1486-28-8; PPh_3, 603-35-0; PMe_3, 594-09-2; $P(OCH_2)_3CEt$, 824-11-3; $Cp_2Fe_2(CO)_2(P(OCH_2)_3CEt)_2$, 84848-93-1; $P(OPh)_3$, 101-02-0; $Cp_2Fe_2(CO)_3(P(OCH_2)_3CEt)$, 84848-94-2; $(CpFe(CO)(PMe_3)_2)^+Cp^-$, 84848-95-3.

Preparation of Chloride-Bridged Organopalladium(II) Dimers and Their Role in the Carbonylation of *trans*-[PdClR^1(PR$_3$)$_2$]

Gordon K. Anderson

Department of Chemistry, University of Missouri–St. Louis, St. Louis, Missouri 63121

Received August 19, 1982

Complexes of the type [Pd$_2$(μ-Cl)$_2$R$_2$L$_2$] (R = Ph, C$_6$H$_4$Me-*p*, or CH$_2$Ph; L = PPh$_3$, PMePh$_2$, or PBu$_3$) are prepared by the reaction of R$_2$Hg with [Pd$_2$(μ-Cl)$_2$Cl$_2$L$_2$] in benzene and have been characterized by elemental analysis and NMR spectroscopy. Reaction with L gives the corresponding bis(phosphine)palladium complex, while treatment with CO yields [Pd$_2$(μ-Cl)$_2$(COR)$_2$L$_2$]. Carbonylation of *trans*-[PdClRL$_2$] or bridge cleavage of [Pd$_2$(μ-Cl)$_2$(COR)$_2$L$_2$] with L produces *trans*-[PdCl(COR)L$_2$]. The rates of these processes are considered, and the intermediacy of the dimeric complexes in the carbonylation of *trans*-[PdClRL$_2$] is discussed.

Introduction

Halide-bridged complexes of palladium(II) and platinum(II) are extremely useful as starting materials in the syntheses of organometallic and coordination compounds.[1] Complexes of the type [Pt$_2$(μ-X)$_2$R$_2$L$_2$] (X = halide, R = organic group, and L = neutral ligand) have recently been prepared[2,3] and have been shown to exhibit some interesting chemistry.

A general route to halide-bridged organopalladium(II) complexes, however, has not been described to date, although a few isolated examples of such complexes have been reported. The complex [Pd$_2$(μ-Cl)$_2$(CH$_2$Ph)$_2$(PPh$_3$)$_2$] was somewhat fortuitously obtained upon recrystallization of *trans*-[PdCl(CH$_2$Ph)(PPh$_3$)$_2$] from chloroform/hexane,[4] and a complex described as "[PdI(COPh)(PPh$_3$)]·toluene", which is likely to be dimeric, was obtained by reaction of iodobenzene with [Pd$_3$(CO)$_3$(PPh$_3$)$_4$] in the presence of carbon monoxide.[5] Pentafluorophenyl complexes [Pd$_2$(μ-Cl)$_2$(C$_6$F$_5$)$_2$L$_2$] were obtained by organic group transfer from thallium(III)[6] and Grignard[7] reagents, and reaction of [PdR$_2$L$_2$] (R = C$_6$F$_5$ or C$_6$Cl$_5$) with palladium(II) chloride yielded the corresponding arylpalladium(II) dimer.[8]

This paper describes a general synthetic approach to halide-bridged alkyl- and arylpalladium(II) dimers, using diorganomercurials as the organic group transfer agents, and their reactions with carbon monoxide and other neutral ligands.

Experimental Section

The ^{1}H NMR spectra were recorded at 60.0 MHz on a Varian T-60 spectrometer, and the ^{13}C{^{1}H} and ^{31}P{^{1}H} NMR spectra were obtained at 25.00 and 40.26 MHz, respectively, on a JEOL FX-100 spectrometer operating in the FT mode. Spectra were recorded for CDCl$_3$ solutions at 25 °C; ^{1}H and ^{13}C chemical shifts were measured relative to Me$_4$Si, and ^{31}P chemical shifts were measured relative to external H$_3$PO$_4$, positive shifts representing deshielding.

Infrared spectra were measured in CHCl$_3$ solution by using NaCl cells of 0.5-mm path length and were recorded on a Perkin-Elmer 337 spectrophotometer.

Melting points were determined on a Thomas Hoover capillary melting point apparatus and are uncorrected. Microanalytical data were from Galbraith Laboratories, Inc., Knoxville, TN.

Carbon-13 labeled complexes were prepared by using 90% enriched ^{13}CO obtained from Prochem.

Preparation of [Pd$_2$(μ-Cl)$_2$Ph$_2$(PBu$_3$)$_2$]. Diphenylmercury (1.488 g, 4.20 mmol) and [Pd$_2$(μ-Cl)$_2$Cl$_2$(PBu$_3$)$_2$] (1.592 g, 2.10 mmol) were mixed under nitrogen, and benzene (50 mL) was added. After being stirred for 1 h, the dark brown solution was evaporated to dryness and heated in vacuo (85 °C (0.005 torr)) for 13 h. A small amount of PhHgCl sublimed out, the remaining dark solid was treated with benzene and charcoal, and then the solution was filtered. The volume was reduced, and addition of petroleum ether caused precipitation of pale yellow crystals (0.744 g, 42%).

[Pd$_2$(μ-Cl)$_2$Ph$_2$(PPh$_3$)$_2$] was prepared similarly.

Preparation of [Pd$_2$(μ-Cl)$_2$(C$_6$H$_4$Me-*p*)$_2$(PBu$_3$)$_2$]. To a solution of [Pd$_2$(μ-Cl)$_2$Cl$_2$(PBu$_3$)$_2$] (0.842 g, 1.11 mmol) in benzene (5 mL), under nitrogen, was added a benzene suspension of di-*p*-tolylmercury (0.849 g, 2.22 mmol) over 10 min. The mixture darkened and, after 1.5 h, the precipitated *p*-MeC$_6$H$_4$HgCl was filtered (0.639 g, 88%). Addition of petroleum ether caused precipitation of further *p*-MeC$_6$H$_4$HgCl, and the filtrate was treated with charcoal and filtered to give a clear, yellow solution. This was concentrated, and addition of petroleum ether gave pale yellow crystals (0.412 g, 43%).

[Pd$_2$(μ-Cl)$_2$(CH$_2$Ph)$_2$(PBu$_3$)$_2$] was prepared analogously.

Preparation of [Pd$_2$(μ-Cl)$_2$(CH$_2$Ph)$_2$(PMePh$_2$)$_2$]. Dibenzylmercury (1.021 g, 2.67 mmol), dissolved in benzene (50 mL), was added to a benzene suspension (50 mL), under nitrogen, of [Pd$_2$(μ-Cl)$_2$Cl$_2$(PMePh$_2$)$_2$] (1.007 g, 1.33 mmol) over 2 h. The solvent was evaporated, and the residue was treated at 65 °C (0.005 torr) for 3 h. Some decomposition occurred, but little PhCH$_2$HgCl sublimed, so the solid was washed with warm ethanol to remove PhCH$_2$HgCl. The residue was then treated with charcoal and crystallized from benzene/petroleum ether to give yellow crystals (0.475 g, 41%).

Preparation of [Pd$_2$(μ-Cl)$_2$Ph$_2$(PMePh$_2$)$_2$]. Diphenylmercury (1.907 g, 5.38 mmol) was added, as a solid, to a suspension of [Pd$_2$(μ-Cl)$_2$Cl$_2$(PMePh$_2$)$_2$] (2.029 g, 2.69 mmol) in benzene (100 mL), under nitrogen. The mixture became black, and, after 0.5 h, charcoal was added and filtration yielded a yellow solution. This was evaporated to dryness and the grayish residue was treated at 80 °C (0.005 torr) for 24 h, giving PhHgCl (0.691 g). The residue was dissolved in benzene and again treated with charcoal, and after filtration the addition of pertroleum ether gave the product as colorless crystals (0.500 g, 22%).

The filtrate was evaporated to dryness, and a second crystallization from benzene/petroleum ether yielded colorless crystals of *trans*-[PdClPh(PMePh$_2$)$_2$] (0.233 g). Anal. Calcd for C$_{32}$H$_{31}$ClP$_2$Pd: C, 62.05; H, 5.05. Found: C, 62.39; H, 5.22.

Preparation of [Pd$_2$(μ-Cl)$_2$(COPh)$_2$(PBu$_3$)$_2$]. A CH$_2$Cl$_2$ solution of [Pd$_2$(μ-Cl)$_2$Ph$_2$(PBu$_3$)$_2$] (0.247 g) was stirred under 1 atm of CO for 24 h. The yellow solution was then evaporated to dryness, and the residue was crystallized from benzene/pe-

(1) Hartley, F. R. *Organomet. Chem. Rev., Sect. A* **1970**, *6*, 119.
(2) Eaborn, C.; Odell, K. J.; Pidcock, A. *J. Chem. Soc., Dalton Trans.* **1978**, 1288.
(3) Anderson, G. K.; Cross, R. J. *J. Chem. Soc., Dalton Trans.* **1979**, 1246.
(4) Fitton, P.; McKeon, J. E.; Ream, B. C. *J. Chem. Soc., Chem. Commun.* **1969**, 370.
(5) Hidai, M.; Hikita, T.; Wada, Y.; Fujikura, Y.; Uchida, Y. *Bull. Chem. Soc. Jpn.* **1975**, *48*, 2075.
(6) Uson, R.; Royo, P.; Forniés, J.; Martinez, F. *J. Organomet. Chem.* **1975**, *90*, 367.
(7) Uson, R.; Forniés, J.; Martinez, F. *J. Organomet. Chem.* **1977**, *132*, 429.
(8) Uson, R.; Forniés, J.; Navarro, R.; Garcia, M. P. *Inorg. Chim. Acta* **1979**, *33*, 69.

0276-7333/83/2302-0665$01.50/0

Table I. Characterization Data for the Complexes $[Pd_2(\mu\text{-}Cl)_2R_2L_2]$

R	L	mp, °C	found C	found H	calcd C	calcd H	δ(P)	^{1}H NMR data
Ph	PPh_3	232-233	59.88	4.45	59.89	4.19		
Ph	$PMePh_2$	187	54.25	4.49	54.43	4.33	16.3	δ(CH_3) 1.50 (d, ^2J(P,H) = 10.5 Hz)
CH_2Ph	$PMePh_2$[a]	170	56.90	4.96	57.04	4.79	20.9	δ(CH_3) 1.90 (d, ^2J(P,H) = 10.0 Hz), δ(CH_2) 2.95 (d, ^3J(P,H) = 3.0 Hz)
Ph	PBu_3	149-150	51.24	7.41	51.32	7.66	18.9	
C_6H_4Me-*p*	PBu_3	146-147	52.28	7.73	52.43	7.88		δ(CH_3) 2.20, δ(H) 6.75 (d), 7.15 (d,d, ^3J(H,H^1) = 8.0 Hz, ^4J(P,H) = 2.0 Hz)
CH_2Ph	PBu_3	113-114	52.38	7.91	52.43	7.88	22.4	δ(CH_2) 2.95 (d, ^3J(P,H) = 2.0 Hz)

[a] Contains 0.5 molecule of C_6H_6/dimeric unit, as indicated by integration of the ^{1}H NMR spectrum.

troleum ether to give the product as yellow crystals (0.171 g), mp 150–151 °C. Anal. Calcd for $C_{38}H_{64}Cl_2O_2P_2Pd_2$: C, 50.80; H, 7.19. Found: C, 50.86; H, 7.32.

Other reactions of the organopalladium complexes with carbon monoxide were carried out by stirring a solution of the complex under a ^{13}CO atmosphere or by passing CO through the solution, and the products were examined in situ. Bridge cleavage reactions were performed by addition of the neat ligand to a solution of the complex.

Results and Discussion

Treatment of the complexes $[Pd_2(\mu\text{-}Cl)_2Cl_2L_2]$ (L = PPh_3, $PMePh_2$, or PBu_3) with HgR_2 (R = Ph, C_6H_4Me-*p*, or CH_2Ph) in benzene solution produces the corresponding chloride-bridged organopalladium(II) species $[Pd_2(\mu\text{-}Cl)_2R_2L_2]$ and RHgCl. These new dimeric complexes have been characterized by elemental analysis and, where applicable, ^{1}H NMR spectroscopy (Table I). Their $^{31}P\{^1H\}$ NMR spectra, at ambient temperature, consist of a single line, indicating that only one isomer exists, the cis and trans isomers have coincidental chemical shifts, or, as is most probable, rapid isomerization occurs by a bimolecular process. Indeed, mixing $[Pd_2(\mu\text{-}Cl)_2Ph_2(PBu_3)_2]$ and $[Pd_2(\mu\text{-}Cl)_2(CH_2Ph)_2(PMePh_2)_2]$ in $CDCl_3$ solution caused formation, after 24 h, of an equimolar mixture of the two reactants and $[(Bu_3P)PhPd(\mu\text{-}Cl)_2Pd(CH_2Ph)(PMePh_2)]$ (δ(PBu_3) 19.0, δ($PMePh_2$) 20.8). Phosphine exchange does not take place, since no products of phosphine and organic group mixing were detected. The $^{31}P\{^1H\}$ NMR spectra of the analogous platinum complexes indicate the presence of two isomers.[2,9]

The use of diorganomercury compounds as organic group transfer agents in this context allows the introduction of an alkyl or aryl moiety, whereas the thallium(III) and Grignard reagents mentioned above[6,7] are rather more restrictive. Similarly, the $RSnMe_3$ compounds used in the preparation of the analogous platinum dimers are only suitable where R = aryl.[2] The reactions are accompanied by some decomposition, however. In some cases (see Experimental Section) it is necessary to resort to vacuum sublimation in order to remove the organomercuric chloride byproduct, and the temperatures required to achieve this can lead to further decomposition. Thus the moderate yields are perhaps due in greater measure to the difficulties of product separation than to any inherent instability of the complex involved or to competing side reactions.

The reaction pathways involved in the decomposition of the complexes have not been investigated, but elimination of tertiary phosphine (possibly accompanied by reductive elimination of the organic chloride) seems to be involved, as evidenced by the isolation of *trans*-$[PdClPh(PMePh_2)_2]$ during the preparation of $[Pd_2(\mu\text{-}Cl)_2Ph_2(PMePh_2)_2]$.

The complexes are all colorless or pale yellow crystalline solids, which are stable to air and moisture. They are readily soluble in benzene and halocarbon solvents, with the exception of $[Pd_2(\mu\text{-}Cl)_2Ph_2(PPh_3)_2]$ which is only sparingly soluble, but are insoluble in alcohols and petroleum ether.

The complexes $[Pd_2(\mu\text{-}Cl)_2R_2L_2]$ rapidly undergo bridge cleavage reactions with L to give *trans*-$[PdClRL_2]$. The trans geometry is indicated by the equivalence of the phosphorus nuclei, as evidenced by the single resonance observed in their $^{31}P\{^1H\}$ NMR spectra, the triplet resonance for the benzylic protons in *trans*-$[PdCl(CH_2Ph)(PBu_3)_2]$, and the virtual coupling in *trans*-$[PdClPh(PMePh_2)_2]$, which gives rise to a triplet for the phosphine methyl group. Only *trans*-$[PdCl(CH_2Ph)(PMePh_2)_2]$ exhibits an unexpected ^{1}H NMR spectrum, the very broad benzylic resonance and the broad singlet for the phosphine methyl in $CDCl_3$ or toluene-d_8 solution suggesting that tertiary phosphine exchange occurs at ambient temperature. Such a process has been postulated for *trans*-$[PdCl(CH_2Ph)(PPh_3)_2]$,[4] where a singlet benzylic resonance was observed. Here the resonance at δ 2.55 is very broad, suggesting that phosphine exchange is slower for $PMePh_2$, which might be expected in terms of the relative nucleophilicities of the ligands. Indeed, the more basic PBu_3 does not undergo exchange in *trans*-$[PdCl(CH_2Ph)(PBu_3)_2]$. Tertiary phosphine exchange does not occur with *trans*-$[PdClPhL_2]$ (L = PPh_3, $PMePh_2$, or PBu_3), suggesting that it is the electron-releasing nature of the benzyl group that stabilizes the three-coordinate intermediate that would be formed initially upon ligand dissociation. Consistent with this, the complex *trans*-$[PdCl(COCH_2Ph)(PMePh_2)_2]$ itself (vide infra) shows no sign of exchange, but exchange does occur with excess phosphine, the triplet at δ 2.05 (Table II) being replaced by a singlet resonance at δ 2.00.

A second possible source of the broadening of the ^{1}H NMR signals due to *trans*-$[PdCl(CH_2Ph)(PMePh_2)_2]$ could be the equilibration of this complex with $[Pd(\eta^3\text{-}CH_2Ph)(PMePh_2)_2]^+Cl^-$. Complexes of the latter type have been prepared[10] but only with noncoordinating anions; indeed, addition of lithium chloride to $[Pd(\eta^3\text{-}CH_2Ph)(PEt_3)_2]^+BF_4^-$ caused regeneration of *trans*-$[PdCl(CH_2Ph)(PEt_3)_2]$. Thus, it is not expected that such a rearrangement will occur with a chloride ligand present, and, if it should, the (η^3-benzyl)palladium cation would be best stabilized by the more basic PBu_3 ligand. Since exchange does not occur for *trans*-$[PdCl(CH_2Ph)(PBu_3)_2]$, the evidence seems to point to phosphine exchange as the source of the broadening.

Cleavage of $[Pd_2(\mu\text{-}Cl)_2Ph_2(PMePh_2)_2]$ with triphenylphosphine should, in principle, result in formation of a complex with four different ligands. In fact, within a few

(9) Anderson, G. K.; Cross, R. J. unpublished results.

(10) Becker, Y.; Stille, J. K. *J. Am. Chem. Soc.* **1978**, *100*, 845.

Table II. Spectroscopic Data for Complexes of the Types $[Pd_2(\mu\text{-}Cl)_2(COR)_2L_2]$, *trans*-$[PdClRL_2]$, and *trans*-$[PdCl(COR)L_2]$

complex	ν(CO)/cm^{-1}	δ(P)	δ(^{13}CO)	^2J(P,C)/Hz	^{1}H NMR data
$Pd_2Cl_2(COPh)_2(PPh_3)_2$	1675		216.5	10	
$Pd_2Cl_2(COPh)_2(PMePh_2)_2$	1665		218.1	8	$\delta(CH_3)$ 1.75 (^2J(P,H) = 9.5 Hz)
$Pd_2Cl_2(COCH_2Ph)_2(PMePh_2)_2$	1685				$\delta(CH_3)$ 1.70 (^2J(P,H) = 10.0 Hz) $\delta(CH_2)$ 3.80
$Pd_2Cl_2(COPh)_2(PBu_3)_2$	1650		220.4	9	
			221.4	10	
$Pd_2Cl_2(COC_6H_4Me)_2(PBu_3)_2$	1645, 1670		219.2	9	$\delta(CH_3)$ 2.30, δ(H) 7.05 and 8.00 (^3J(H,H^1) = 8.0 Hz)
$Pd_2Cl_2(COCH_2Ph)_2(PBu_3)_2$	1685				$\delta(CH_2)$ 4.15
$PdClPh(PPh_3)_2$		23.4			
$PdClPh(PMePh_2)_2$		7.2			$\delta(CH_3)$ 1.65 (^2J(P,H) = 3.0 Hz)
$PdCl(CH_2Ph)(PMePh_2)_2$					$\delta(CH_3)$ 2.15 (br), $\delta(CH_2)$ 2.55 (br)
$PdClPh(PBu_3)_2$		4.2			
$PdCl(C_6H_4Me)(PBu_3)_2$					$\delta(CH_3)$ 2.20, δ(H) 6.80 and 7.10 (^3J(H,H^1) = 8.0 Hz)
$PdCl(CH_2Ph)(PBu_3)_2$					$\delta(CH_2)$ 2.60 (^3J(P,H) = 7.0 Hz)
$PdCl(COPh)(PPh_3)_2$	1640	18.5	230.6	3	
$PdCl(COPh)(PMePh_2)_2$	1635	3.0	231.3	3	$\delta(CH_3)$ 1.95 (^2J(P,H) = 3.0 Hz)
$PdCl(COCH_2Ph)(PMePh_2)_2$	1670				$\delta(CH_3)$ 2.05 (^2J(P,H) = 3.5 Hz), $\delta(CH_2)$ 3.25 (^2J(^{13}C,H) = 5.5 Hz)
$PdCl(COPh)(PBu_3)_2$	1625	2.6	234.0	<2	
$PdCl(COC_6H_4Me)(PBu_3)_2$	1625				$\delta(CH_3)$ 2.35, δ(H) 7.05 and 7.90 (^3J(H,H^1) = 7.5 Hz)
$PdCl(COCH_2Ph)(PBu_3)_2$	1655				$\delta(CH_2)$ 3.90

minutes of mixing an almost statistical mixture of *trans*-$[PdClPh(PMePh_2)_2]$, *trans*-$[PdClPh(PPh_3)_2]$, and $[PdClPh(PMePh_2)(PPh_3)]$ ($\delta(PMePh_2)$ 8.5, $\delta(PPh_3)$ 21.9 (^2J(P,P^1) = 430 Hz)) was obtained, as indicated by $^{31}P\{^1H\}$ NMR spectroscopy. The trans arrangement of $PMePh_2$ and PPh_3 in $[PdClPh(PMePh_2)(PPh_3)]$ follows from the magnitude of the two-bond phosphorus–phosphorus coupling constant.[11] The rapid formation of all three products suggests that ready phosphine dissociation also occurs in these phenylpalladium complexes, at least in the presence of free phosphine.

The complexes *trans*-$[PdClRL_2]$ react with carbon monoxide to yield the corresponding acyl or aroyl species, which are characterized by solution infrared, $^{13}C\{^1H\}$ NMR (for samples prepared with ^{13}CO), $^{31}P\{^1H\}$ NMR, and ^{1}H NMR spectroscopies (Table II). The reactions of the benzyl complexes are faster than those of the corresponding phenyl species, the time for complete reaction being less than 1 h in the former case, whereas several hours, at 1 atm of CO, are required for complete carbonylation to *trans*-$[PdCl(COPh)L_2]$. These trends are consistent with the kinetic results of Garrou and Heck[12] for the carbonylation of *trans*-$[PdXRL_2]$ complexes, who found that the reactions proceeded more rapidly for alkylpalladium species.

The dimeric complexes $[Pd_2(\mu\text{-}Cl)_2R_2L_2]$ react with CO to produce the corresponding acyl or aroyl species $[Pd_2(\mu\text{-}Cl)_2(COR)_2L_2]$ that exhibit ν(CO) bands in the range 1645–1685 cm^{-1} in their solution infrared spectra and resonances around 220 ppm in their $^{13}C\{^1H\}$ NMR spectra (Table II). Two isomers are found to exist for $[Pd_2(\mu\text{-}Cl)_2(COPh)_2(PBu_3)_2]$ and $[Pd_2(\mu\text{-}Cl)_2(COC_6H_4Me\text{-}p)_2(PBu_3)_2]$, while a trace of $[PdClPh(CO)(PMePh_2)]$ (δ(C) 168.6 (d, ^2J(P,C) = 8 Hz)) was detected in the carbonylation of $[Pd_2(\mu\text{-}Cl)_2Ph_2(PMePh_2)_2]$.[13] The fact that two separate resonances are observed for $[Pd_2(\mu\text{-}Cl)_2(COR)_2(PBu_3)_2]$ (R = Ph or C_6H_4Me-*p*) suggests that, for these complexes at least, bimolecular exchange processes are slower than for the alkyl- and arylpalladium dimers (vide supra). The solution infrared spectrum of $[Pd_2(\mu\text{-}Cl)_2Ph_2(PBu_3)_1]$ that had been treated with CO for 2 h, in addition to the ν(CO) band at 1650 cm^{-1}, exhibited terminal ν(CO) bands at 1990 and 2015 cm^{-1} that diminished in intensity on standing, but no terminal carbonyl ligands could be detected in the $^{13}C\{^1H\}$ NMR spectrum, and the species involved remain unidentified.

The $[Pd_2(\mu\text{-}Cl)_2Ph_2L_2]$ complexes undergo carbonylation more rapidly than their benzyl analogues, the generation of $[Pd_2(\mu\text{-}Cl)_2(COPh)_2(PPh_3)_2]$ being complete in less than 5 min, despite the low solubility of its precursor. Also, carbonylation of the triphenylphosphine complex is more rapid than for those containing the more nucleophilic ligands.

Addition of tertiary phosphine to solutions of the acyl- and aroylpalladium dimers rapidly and quantitatively produces the corresponding *trans*-$[PdCl(COR)L_2]$ complexes, formed alternatively by carbonylation of *trans*-$[PdClRL_2]$ (vide supra). The latter reaction has been shown[12] to proceed via two pathways involving $[PdClRL_2(CO)]$, one of which requires direct R migration from the five-coordinate intermediate, whereas the other proceeds by initial phosphine dissociation and subsequent R migration from a four-coordinate species. In the case of platinum, it has been found[14] that elimination of tertiary phosphine from $[PtClR(CO)L_2]$[15] yields two isomers of $[PtClR(CO)L]$], A and B, the same two isomers which are produced when $[Pt_2(\mu\text{-}Cl)_2R_2L_2]$ is cleaved by carbon monoxide. The complexes A and B (M = Pt) only isomerize and undergo R migration very slowly, if at all,[3,16] so

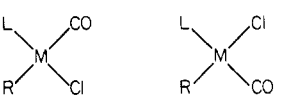

A B

(11) Anderson, G. K.; Clark, H. C.; Davies, J. A. *Inorg. Chem.* **1981**, *20*, 944.
(12) Garrou, P. E.; Heck, R. F. *J. Am. Chem. Soc.* **1976**, *98*, 4115.
(13) The magnitude of ^2J(P,C) indicates a cis arrangement of $PMePh_2$ and CO.
(14) Anderson, G. K.; Cross, R. J. *J. Chem. Soc., Dalton Trans.* **1980**, 1434.
(15) This five-coordinate complex, of unknown geometry, is the initial product of the reaction of *trans*-$[PtClRL_2]$ with carbon monoxide.[12,14]
(16) This probably occurs via reversible dissociation of tertiary phosphine, since it takes place more rapidly with less nucleophilic ligands.[3]

carbonylation of $[Pt_2(\mu\text{-}Cl)_2R_2L_2]$ does not lead to the corresponding acyl or aroyl complexes. On the other hand, the $[Pd_2(\mu\text{-}Cl)_2(COR)_2L_2]$ species are rapidly produced, and, since initial bridge cleavage is likely to occur in analogous fashion to the platinum case, rapid isomerization and R migration from [PdClR(CO)L] species must take place. Thus, in the carbonylations of *trans*-$[MClRL_2]$ (M = Pd or Pt) it is likely that the much greater rates observed for the palladium complexes[12] are due, in large part, to the much faster rearrangement of the [PdClR(CO)L] complexes formed by tertiary phosphine dissociation from the 5-coordinate intermediates.

The relative rates of carbonylation of the phenyl- and benzylpalladium complexes are not readily explained. The reactions of $[Pd_2(\mu\text{-}Cl)_2Ph_2L_2]$ (L = $PMePh_2$ or PBu_3) are faster than those of their benzyl counterparts, whereas the opposite is true for the monomeric complexes.

Acknowledgment. Thanks are expressed to Johnson Matthey and Co. Ltd. for a generous loan of palladium salts and to the University of Missouri–St. Louis for the award of a Faculty Research Fellowship.

Registry No. $[Pd_2(\mu\text{-}Cl)_2Ph_2(PPh_3)_2]$, 84624-47-5; $[Pd_2(\mu\text{-}Cl)_2Ph_2(PMePh_2)_2]$, 84624-48-6; $[Pd_2(\mu\text{-}Cl)_2(CH_2Ph)_2(PMePh_2)_2]$, 84624-49-7; $[Pd_2(\mu\text{-}Cl)_2Ph_2(PBu_3)_2]$, 84624-50-0; $[Pd_2(\mu\text{-}Cl)_2(C_6H_4Me\text{-}P)_2(PBu_3)_2]$, 84624-51-1; $[Pd_2(\mu\text{-}Cl)_2(CH_2Ph)_2(PBu_3)_2]$, 84624-52-2; $[Pd_2(\mu\text{-}Cl)_2(COPh)_2(PPh_3)_2]$, 84624-53-3; $[Pd_2(\mu\text{-}Cl)_2(COPh)_2(PMePh_2)_2]$, 84624-54-4; $[Pd_2(\mu\text{-}Cl)_2(COCH_2Ph)_2(PMePh_2)_2]$, 84624-55-5; $[Pd_2(\mu\text{-}Cl)_2(COPh)_2(PBu_3)_2]$, 84624-56-6; $[Pd_2(\mu\text{-}Cl)_2(COC_6H_4Me)_2(PBu_3)_2]$, 84624-57-7; $[Pd_2(\mu\text{-}Cl)_2(COCH_2Ph)_2(PBu_3)_2]$, 84624-58-8; *trans*-$[PdClPh(PPh_3)_2]$, 22605-84-1; *trans*-$[PdClPh(PMePh_2)_2]$, 84624-59-9; *trans*-$[PdCl(CH_2Ph)(PMePh_2)_2]$, 84642-34-2; *trans*-$[PdClPh(PBu_3)_2]$, 84624-60-2; *trans*-$[PdCl(C_6H_4Me)(PBu_3)_2]$, 84624-61-3; *trans*-$[PdCl(CH_2Ph)(PBu_3)_2]$, 84642-35-3; *trans*-$[PdCl(COPh)(PPh_3)_2$, 50417-59-9; *trans*-$[PdCl(COPh)(PMePh_2)_2]$, 84624-62-4; *trans*-$[PdCl(COCH_2Ph)(PMePh_2)_2]$, 84624-63-5; *trans*-$[PdCl(COPh)(PBu_3)_2]$, 84642-36-4; *trans*-$[PdCl(COC_6H_4Me)(PBu_3)_2]$, 84642-37-5; *trans*-$[PdCl(COCH_2Ph)(PBu_3)_2]$, 84624-64-6; $[Pd_2(\mu\text{-}Cl)_2Cl_2(PBu_3)_2]$, 14882-49-6; $[Pd_2(\mu\text{-}Cl)_2Cl_2(PMePh_2)_2]$, 29887-90-9; $[Pd_2(\mu\text{-}Cl)_2Cl_2(PPh_3)_2]$, 15134-30-2.

Crystal and Molecular Structures of $Mo(CO)_5P(p\text{-tol})_3$ and $Mo_2(CO)_8P(p\text{-tol})_3$ and Spectral Properties of Related σ- and π-Bonded Phosphine Complexes

Elmer C. Alyea,* George Ferguson,* and Arpad Somogyvari

Guelph-Waterloo Centre for Graduate Work in Chemistry, Guelph Campus, University of Guelph, Guelph, Ontario, Canada, N1G 2W1

Received August 4, 1982

Molybdenum complexes of the type $Mo(CO)_5L$ (L = $P(o\text{-tol})_3$, $P(m\text{-tol})_3$, and $P(p\text{-tol})_3$), $Mo(CO)_3L$ (L = $P(p\text{-tol})_3$ and $P(mes)_3$; tol = tolyl) and $Mo_2(CO)_8P(p\text{-tol})_3$ have been prepared and their IR and ^1H, ^{31}P and ^{95}Mo NMR spectra determined. The structure of $Mo_2(CO)_8P(o\text{-tol})_3$ (I) was determined by X-ray crystallography; one Mo atom is coordinated to phosphorus and the other is π bonded to a *p*-tol group. Crystals of I are monoclinic of space group $P2_1/n$ with four molecules in the unit cell of dimensions a = 11.297 (2) Å, b = 20.415 (2) Å, c = 13.016 (2) Å, and β = 100.32 (1)°. Crystals of the related $Mo(CO)_5P(p\text{-tol})_3$ (II) are triclinic of space group $P\bar{1}$ with two independent molecules in the asymmetric unit. Unit-cell dimensions for II are a = 10.908(5) Å, b = 15.281 (8) Å, c = 16.055 (4) Å, α = 106.04 (3)°, β = 95.25 (2), and γ = 91.33 (4)°. Both structures were solved by the heavy-atom method. Refinement was by full-matrix least-squares calculations with anisotropic thermal parameters for I and by blocked-diagonal matrix least-squares calculations with anisotropic thermal parameters for Mo, P, and CO groups for II. R converged to 0.0239 for 5115 observed reflections for I and 0.0388 for 4078 observed reflections for II measured by diffractometer. The crystal structures contain discrete monomeric molecules separated by normal van der Waals distances. Principal dimensions are as follows: for I, Mo(1)–C(carbonyl) = 1.961–1.974 (3) Å, Mo(1)–C(arene) = 2.314–2.370 (2) Å, Mo(2)–P = 2.557 (1) Å, Mo(2)–C(carbonyl) = 1.997 (3) Å (trans to P), 2.038–2.053 (3) Å for others; for II, Mo–P = 2.562 (2) and 2.555 (1), Mo–C(carbonyl) = 1.986 (7) and 1.988 (7) Å (trans to P), 2.001 (6)–2.041 (8) Å for others.

Introduction

Group 6 metal hexacarbonyls are well-known[1] to give mono- and bis-substituted derivatives by reaction with triarylphosphines. However, in the case of tri-*o*-tolylphosphine (tolyl ≡ $CH_3C_6H_4$–, tol) the products of thermal reactions have the stoichiometry $M(CO)_3P(o\text{-tol})_3$ (M = Cr, Mo, W); formulation[2] of these products with π-bonded *o*-tol groups rather than the normal phosphorus coordination was based on infrared, ^1H NMR, and mass spectra data. Further investigations by Bowden and Colton[3] of thermal reactions of triarylphosphines with chromium hexacarbonyl showed that (π-aryl)phosphines are not exclusive to bulky phosphines. Two series of products, formulated as $Cr(CO)_3L$ and $[Cr(CO)_2L]_2$ (L = substituted triarylphosphines), were produced under prolonged reflux at high temperatures. Furthermore, reaction of PPh_2Cl with $(\pi\text{-}C_6H_5Li)_2Cr$ results in a complex containing π-bonded triphenylphosphine groups.[4] This complex may

(1) (a) Magee, T. A.; Matthews, C. N.; Wang, T. S.; Wotiz, J. H. *J. Am. Chem. Soc.* **1961**, *83*, 3200. (b) Poilblanc, R.; Bigorgne, M. *Bull. Soc. Chim. Fr.* **1962**, 1301. (c) Booth, G. *Adv. Inorg. Chem. Radiochem.* **1964**, *6*, 1. (d) Cotton, F. A. *Inorg. Chem.* **1964**, *3*, 702. (e) Angelici, R. J.; Malone, M. D. *Ibid.* **1967**, *6*, 1731. (f) McAuliffe, C. A.; Levason, W. "Phosphine, Arsine, and Stibene Complexes of the Transition Elements"; Elsevier: Amsterdam, 1979.

(2) Bowden, J. A.; Colton, R. *Aust. J. Chem.* **1971**, *24*, 2471.

(3) Bowden, J. A.; Colton, R. *Aust. J. Chem.* **1973**, *26*, 43.

0276-7333/83/2302-0668$01.50/0

carbonylation of $[Pt_2(\mu\text{-}Cl)_2R_2L_2]$ does not lead to the corresponding acyl or aroyl complexes. On the other hand, the $[Pd_2(\mu\text{-}Cl)_2(COR)_2L_2]$ species are rapidly produced, and, since initial bridge cleavage is likely to occur in analogous fashion to the platinum case, rapid isomerization and R migration from [PdClR(CO)L] species must take place. Thus, in the carbonylations of *trans*-$[MClRL_2]$ (M = Pd or Pt) it is likely that the much greater rates observed for the palladium complexes[12] are due, in large part, to the much faster rearrangement of the [PdClR(CO)L] complexes formed by tertiary phosphine dissociation from the 5-coordinate intermediates.

The relative rates of carbonylation of the phenyl- and benzylpalladium complexes are not readily explained. The reactions of $[Pd_2(\mu\text{-}Cl)_2Ph_2L_2]$ (L = $PMePh_2$ or PBu_3) are faster than those of their benzyl counterparts, whereas the opposite is true for the monomeric complexes.

Acknowledgment. Thanks are expressed to Johnson Matthey and Co. Ltd. for a generous loan of palladium salts and to the University of Missouri–St. Louis for the award of a Faculty Research Fellowship.

Registry No. $[Pd_2(\mu\text{-}Cl)_2Ph_2(PPh_3)_2]$, 84624-47-5; $[Pd_2(\mu\text{-}Cl)_2Ph_2(PMePh_2)_2]$, 84624-48-6; $[Pd_2(\mu\text{-}Cl)_2(CH_2Ph)_2(PMePh_2)_2]$, 84624-49-7; $[Pd_2(\mu\text{-}Cl)_2Ph_2(PBu_3)_2]$, 84624-50-0; $[Pd_2(\mu\text{-}Cl)_2(C_6H_4Me\text{-}P)_2(PBu_3)_2]$, 84624-51-1; $[Pd_2(\mu\text{-}Cl)_2(CH_2Ph)_2(PBu_3)_2]$, 84624-52-2; $[Pd_2(\mu\text{-}Cl)_2(COPh)_2(PPh_3)_2]$, 84624-53-3; $[Pd_2(\mu\text{-}Cl)_2(COPh)_2(PMePh_2)_2]$, 84624-54-4; $[Pd_2(\mu\text{-}Cl)_2(COCH_2Ph)_2(PMePh_2)_2]$, 84624-55-5; $[Pd_2(\mu\text{-}Cl)_2(COPh)_2(PBu_3)_2]$, 84624-56-6; $[Pd_2(\mu\text{-}Cl)_2(COC_6H_4Me)_2(PBu_3)_2]$, 84624-57-7; $[Pd_2(\mu\text{-}Cl)_2(COCH_2Ph)_2(PBu_3)_2]$, 84624-58-8; *trans*-$[PdClPh(PPh_3)_2]$, 22605-84-1; *trans*-$[PdClPh(PMePh_2)_2]$, 84624-59-9; *trans*-$[PdCl(CH_2Ph)(PMePh_2)_2]$, 84642-34-2; *trans*-$[PdClPh(PBu_3)_2]$, 84624-60-2; *trans*-$[PdCl(C_6H_4Me)(PBu_3)_2]$, 84624-61-3; *trans*-$[PdCl(CH_2Ph)(PBu_3)_2]$, 84642-35-3; *trans*-$[PdCl(COPh)(PPh_3)_2$, 50417-59-9; *trans*-$[PdCl(COPh)(PMePh_2)_2]$, 84624-62-4; *trans*-$[PdCl(COCH_2Ph)(PMePh_2)_2]$, 84624-63-5; *trans*-$[PdCl(COPh)(PBu_3)_2]$, 84642-36-4; *trans*-$[PdCl(COC_6H_4Me)(PBu_3)_2]$, 84642-37-5; *trans*-$[PdCl(COCH_2Ph)(PBu_3)_2]$, 84624-64-6; $[Pd_2(\mu\text{-}Cl)_2Cl_2(PBu_3)_2]$, 14882-49-6; $[Pd_2(\mu\text{-}Cl)_2Cl_2(PMePh_2)_2]$, 29887-90-9; $[Pd_2(\mu\text{-}Cl)_2Cl_2(PPh_3)_2]$, 15134-30-2.

Crystal and Molecular Structures of $Mo(CO)_5P(p\text{-tol})_3$ and $Mo_2(CO)_8P(p\text{-tol})_3$ and Spectral Properties of Related σ- and π-Bonded Phosphine Complexes

Elmer C. Alyea,* George Ferguson,* and Arpad Somogyvari

Guelph-Waterloo Centre for Graduate Work in Chemistry, Guelph Campus, University of Guelph, Guelph, Ontario, Canada, N1G 2W1

Received August 4, 1982

Molybdenum complexes of the type $Mo(CO)_5L$ (L = $P(o\text{-tol})_3$, $P(m\text{-tol})_3$, and $P(p\text{-tol})_3$), $Mo(CO)_3L$ (L = $P(p\text{-tol})_3$ and $P(mes)_3$; tol = tolyl) and $Mo_2(CO)_8P(p\text{-tol})_3$ have been prepared and their IR and ^1H, ^{31}P and ^{95}Mo NMR spectra determined. The structure of $Mo_2(CO)_8P(o\text{-tol})_3$ (I) was determined by X-ray crystallography; one Mo atom is coordinated to phosphorus and the other is π bonded to a *p*-tol group. Crystals of I are monoclinic of space group $P2_1/n$ with four molecules in the unit cell of dimensions a = 11.297 (2) Å, b = 20.415 (2) Å, c = 13.016 (2) Å, and β = 100.32 (1)°. Crystals of the related $Mo(CO)_5P(p\text{-tol})_3$ (II) are triclinic of space group $P\bar{1}$ with two independent molecules in the asymmetric unit. Unit-cell dimensions for II are a = 10.908(5) Å, b = 15.281 (8) Å, c = 16.055 (4) Å, α = 106.04 (3)°, β = 95.25 (2), and γ = 91.33 (4)°. Both structures were solved by the heavy-atom method. Refinement was by full-matrix least-squares calculations with anisotropic thermal parameters for I and by blocked-diagonal matrix least-squares calculations with anisotropic thermal parameters for Mo, P, and CO groups for II. R converged to 0.0239 for 5115 observed reflections for I and 0.0388 for 4078 observed reflections for II measured by diffractometer. The crystal structures contain discrete monomeric molecules separated by normal van der Waals distances. Principal dimensions are as follows: for I, Mo(1)–C(carbonyl) = 1.961–1.974 (3) Å, Mo(1)–C(arene) = 2.314–2.370 (2) Å, Mo(2)–P = 2.557 (1) Å, Mo(2)–C(carbonyl) = 1.997 (3) Å (trans to P), 2.038–2.053 (3) Å for others; for II, Mo–P = 2.562 (2) and 2.555 (1), Mo–C(carbonyl) = 1.986 (7) and 1.988 (7) Å (trans to P), 2.001 (6)–2.041 (8) Å for others.

Introduction

Group 6 metal hexacarbonyls are well-known[1] to give mono- and bis-substituted derivatives by reaction with triarylphosphines. However, in the case of tri-*o*-tolylphosphine (tolyl ≡ $CH_3C_6H_4$–, tol) the products of thermal reactions have the stoichiometry $M(CO)_3P(o\text{-tol})_3$ (M = Cr, Mo, W); formulation[2] of these products with π-bonded *o*-tol groups rather than the normal phosphorus coordination was based on infrared, ^1H NMR, and mass spectra data. Further investigations by Bowden and Colton[3] of thermal reactions of triarylphosphines with chromium hexacarbonyl showed that (π-aryl)phosphines are not exclusive to bulky phosphines. Two series of products, formulated as $Cr(CO)_3L$ and $[Cr(CO)_2L]_2$ (L = substituted triarylphosphines), were produced under prolonged reflux at high temperatures. Furthermore, reaction of PPh_2Cl with $(\pi\text{-}C_6H_5Li)_2Cr$ results in a complex containing π-bonded triphenylphosphine groups.[4] This complex may

(1) (a) Magee, T. A.; Matthews, C. N.; Wang, T. S.; Wotiz, J. H. *J. Am. Chem. Soc.* **1961**, *83*, 3200. (b) Poilblanc, R.; Bigorgne, M. *Bull. Soc. Chim. Fr.* **1962**, 1301. (c) Booth, G. *Adv. Inorg. Chem. Radiochem.* **1964**, *6*, 1. (d) Cotton, F. A. *Inorg. Chem.* **1964**, *3*, 702. (e) Angelici, R. J.; Malone, M. D. *Ibid.* **1967**, *6*, 1731. (f) McAuliffe, C. A.; Levason, W. "Phosphine, Arsine, and Stibene Complexes of the Transition Elements"; Elsevier: Amsterdam, 1979.

(2) Bowden, J. A.; Colton, R. *Aust. J. Chem.* **1971**, *24*, 2471.

(3) Bowden, J. A.; Colton, R. *Aust. J. Chem.* **1973**, *26*, 43.

0276-7333/83/2302-0668$01.50/0

be used as a precursor in the preparation of an isomer of $[Cr(CO)_2PPh_3]_2$[3] or of complexes containing triphenylphosphine chelating two different metal centers. X-ray analysis[5,6] for the dimeric $[Cr(CO)_2PPh_3]_2$ species has confirmed the existence of a bridging π-bonded triphenylphosphine group. Recent X-ray structural determinations[7] have also proved that $Mo(PMe_2Ph)_4$ and $Cr(CO)_3AsPh_3$ contain π-bonded aryl ligands.

We have reinvestigated the reactions of some triarylphosphines with molybdenum hexacarbonyl with a view toward more complete spectroscopic characterization of the products as well as to extend our interest in the metal complexes of trimesitylphosphine[8] (mes ≡ $(CH_3)_3C_6H_2$). This paper reports the results of the single-crystal X-ray analysis of the novel complex $Mo_2(CO)_8P(p\text{-tol})_3$ (I) and the IR, ^1H, ^{31}P and ^{95}Mo NMR spectra of this complex and of $Mo(CO)_5L$ and $Mo(CO)_3L$ (L = triarylphosphines).

Experimental Section

Proton NMR spectra were obtained with a Varian EM 360 spectrometer operating at 60.00 MHz in the CW mode. All samples were measured at room temperature (298 K) in $CDCl_3$ solvent with chemical shifts referenced to internal Me_4Si. Chemical shifts and coupling constants are believed accurate to 0.50 Hz (0.01 ppm). Phosphorus-31 spectra were recorded on a Bruker WP-60 NMR spectrometer operating at 24.29 MHz in the Fourier transform mode. The spectra were recorded at ambient temperature (306 K) in $CDCl_3$ solvent by using H_3PO_4 as an external reference. Digital resolution was 2.44 Hz (0.10 ppm) per data point. Molybdenum-95 NMR spectra were obtained from naturally abundant samples with a Bruker WH-400 NMR spectrometer in the pulsed Fourier transform mode. The probe was specifically tuned to ^{95}Mo at 26.08 MHz. The samples were measured at 296 K with chemical shifts referenced to aqueous alkaline 2 M K_2MoO_4. Digital resolution was 5.55 Hz (0.21 ppm) per data point.

Infrared spectra were measured on a Perkin-Elmer 180 spectrometer (2200–1750 cm^{-1}) as CH_2Cl_2 solutions between KBr windows. Samples for spectrometric analyses were prepared from dinitrogen-saturated solvents, NMR tubes being sealed with Teflon tape, and the infrared cell with Teflon plugs.

All chemicals were of analytical grade and were used without further purification. Solvents, reagent or spectroanalyzed grade, were saturated with dinitrogen gas for 30 min prior to use. All operations were performed under an atmosphere of dinitrogen gas in a polyethylene glovebag or by use of Schlenk techniques.

Complexes of the type $Mo(CO)_5L$ were prepared either by refluxing excess (mole ratio 2:1) $Mo(CO)_6$ with L in isooctane for 30–60 min[1,9,10] or from $[Et_4N][Mo(CO)_5Cl]$[11] by the method of Connor et al.[12] Complexes of the type $Mo(CO)_3L$ and $Mo_2(CO)_8P(p\text{-tol})_3$ were prepared by refluxing a 5:2 mole ratio of $Mo(CO)_6$ and L in isooctane for 24 h.[2,3] All samples were purified by subliming out $Mo(CO)_6$ in vacuo at 40–50 °C and then recrystallizing the residue from CH_2Cl_2/CH_3OH at 0 °C.

Crystallography. Structure Analysis of I. Slow crystallization of $Mo_2(CO)_8P(p\text{-tol})_3$ from a CH_2Cl_2/CH_3OH solution at 0 °C afforded light orange parallelpiped crystals. A crystal of approximate dimensions 0.16 × 0.40 × 0.68 mm was chosen for X-ray analysis. Preliminary Weissenberg photographs showed the crystal to be of good quality. Accurate unit cell dimensions were obtained by a least-squares procedure applied to the setting angles for 25 general reflections with $10° \le \theta \le 17°$ on an Enraf Nonius Cad-4 diffractometer. Crystal data: $C_{29}H_{21}Mo_2O_8P$, M_r = 720.34, monoclinic, a = 11.297 (2) Å, b = 20.415 (2) Å, c = 13.016 (2) Å, β = 100.32 (1)°, V = 2953.19 Å^3, $F(000)$ = 1432, Z = 4, D_{calcd} = 1.620 g cm^{-3}, λ(Mo Kα) = 0.71069 Å, μ(MoKα) = 9.4 cm^{-1}, space group $P2_1/n$. Systematic absences ($0k0$, $k = 2n + 1$ absent, $h0l$, $h + l = 2n + 1$ absent) uniquely determined the space group to be $P2_1/n$.

The intensities of the unique reflections with $2° \le \theta \le 27°$ were measured on a PDP8 controlled Enraf Nonius Cad-4 diffractometer. Of the 6279 independent reflections measured, the 5115 with $I \ge 3\sigma(I)$ were considered observed; the remainder were excluded from refinement calculations. The data were corrected for Lorentz, polarization, and absorption effects. The transmission coefficients were in the range 0.70–0.86.

The structure was solved by the heavy-atom method from phases originally derived from the coordinates of the molybdenum atoms whose positions in the asymmetric unit were deduced from a three-dimensional Patterson synthesis. Successive difference Fourier synthesis revealed the positions of the remaining non-hydrogen atoms. These were refined with isotropic thermal parameters by full-matrix least-squares calculations to R = 0.0399; a difference Fourier synthesis then revealed the positions of all hydrogen atoms close to those expected on geometrical grounds. These were then positioned geometrically (C–H = 0.95 Å), and only an overall isotropic thermal parameter was refined for the hydrogen atoms in subsequent refinement cycles. Refinement converged to R = 0.0239 and $R_w = (\sum w\Delta^2/\sum wF_o^2)^{1/2}$ = 0.0283 by using anisotropic thermal parameters for all non-hydrogen atoms in full-matrix least-squares calculations. The weights used in the least-squares calculations were derived from counting statistics. The scattering factors[13,14] and anomalous dispersion corrections for Mo and P[15] were taken from the literature.

Structure Analysis of II. Slow crystallization of $Mo(CO)_5P(p\text{-tol})_3$ from isooctane at 0 °C gave well-formed pale yellow prisms. A crystal of approximate dimensions 0.15 × 0.35 × 0.54 mm was chosen for X-ray analysis. Accurate unit-cell dimensions were obtained by a least-squares procedure applied to the setting angles for 25 general reflections on an Enraf Nonius Cad-4 diffractometer. Crystal data: $C_{26}H_{21}MoO_5P$, M_r = 540.37, triclinic, a = 10.908 (5) Å, b = 15.281 (8) Å, c = 16.055 (4) Å, α = 106.04 (3), β = 95.25 (2), γ = 91.33 (4)°, V = 2562.25 Å^3, $F(000)$ = 1096, Z = 4, D_{calcd} = 1.40, λ(Mo Kα) = 0.71069 Å, μ(Mo Kα) = 7.1 cm^{-1}, space group $P1$ or $P\bar{1}$, $P\bar{1}$ from analysis.

The intensities of unique reflections with $2° \le \theta \le 20°$ were measured on a PDP8 controlled Enraf Nonius Cad-4 diffractometer. Of the 4783 independent reflections the 4078 with $I \ge 3\sigma(I)$ were considered observed; the remainder were excluded from refinement calculations. The data were corrected for Lorentz, polarization, and absorption effects. The transmission coefficients were in the range 0.72–0.90.

With Z = 4 there are two independent Mo atoms in the asymmetric unit. The structure was solved by the heavy-atom method from phases originally derived from the coordinates of the molybdenum atoms whose position in the asymmetric unit were deduced from a three-dimensional Patterson synthesis. The non-hydrogen atoms were then refined with isotropic thermal parameters by blocked-diagonal matrix least-squares calculations to R = 0.0893. A difference Fourier revealed the positions of most of the hydrogen atoms close to positions expected on geometrical grounds. These were then positioned geometrically (C–H = 0.95 Å) and an overall isotropic thermal parameter was calculated for each type (i.e., CH_3 and PhH) of hydrogen atom in subsequent refinement cycles. Refinement converged to R = 0.0388 and $R_w = (\sum w\Delta^2/\sum wF_o^2)^{1/2}$ = 0.0479 using anisotropic thermal parameters for molybdenum, phosphorus, and the carbonyl groups in

(4) Elschenbroich, C.; Stohler, F. *Angew. Chem., Int. Ed. Engl.* **1975**, *14*, 174.
(5) Robertson, G. B.; Whimp, P. O.; Colton, R.; Rix, C. J. *J. Chem. Soc., Chem. Commun.* **1971**, 573.
(6) Robertson, G. B.; Whimp, P. O. *J. Organomet. Chem.* **1973**, *60*, C11.
(7) (a) Mason, R.; Thomas, K. M.; Heath, G. A. *J. Organomet. Chem.* **1975**, *90*, 195. (b) Wasserman, H. J.; Wovkulich, M. J.; Atwood, J. D.; Churchill, M. R. *Inorg. Chem.* **1980**, *19*, 2831.
(8) Alyea, E. C.; Ferguson, G.; Somogyvari, A. *Inorg. Chem.* **1982**, *21*, 1369.
(9) Grim, S. O.; Wheatland, D. A.; McFarlane, W. *J. Am. Chem. Soc.* **1967**, *89*, 5573.
(10) Grim, S. O.; Singer, R. M.; Johnson, A. W.; Randall, F. R. *J. Coord. Chem.* **1978**, *8*, 121.
(11) Abel, E. W.; Butler, I. S.; Reid, J. G. *J. Chem. Soc.* **1963**, 2068.
(12) Connor, J. A.; Jones, E. M.; McEwen, G. K. *J. Organomet. Chem.* **1972**, *43*, 357.
(13) Cromer, D. T.; Mann, J. B. *Acta Crystallogr., Sect. A* **1968**, *A24*, 321.
(14) Stewart, R. F.; Davidson, E. R.; Simpson, W. T. *J. Chem. Phys.* **1965**, *42*, 317.
(15) Cromer, D. T. *Acta Crystallogr.* **1965**, *18*, 17.

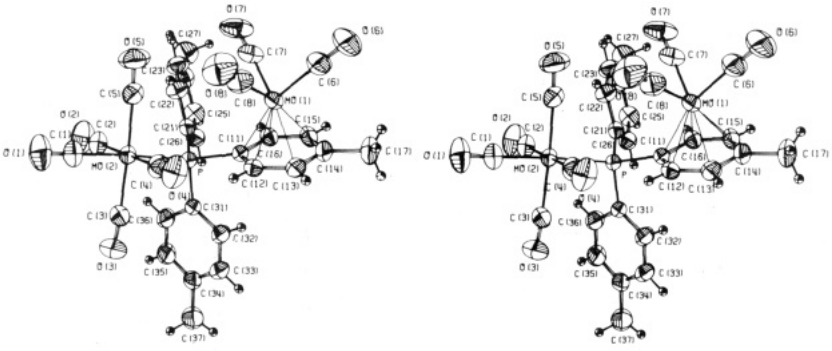

Figure 1. Stereoview of $Mo_2(CO)_8P(p\text{-tol})_3$ (I) with the crystallographic numbering scheme. The thermal ellipsoids are shown at the 50% probability level except the hydrogen atoms which are spheres of arbitrary radius.

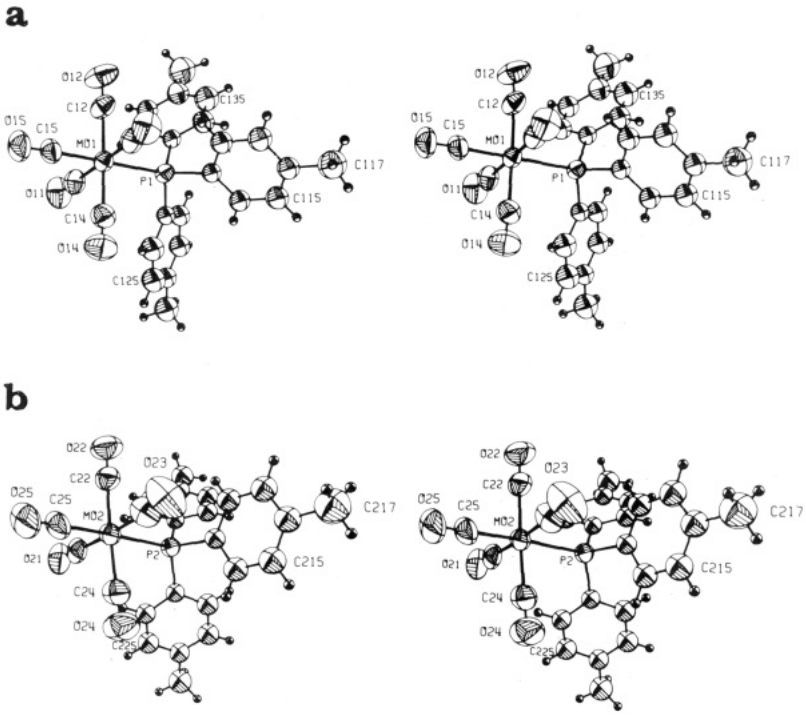

Figure 2. Views of $Mo(CO)_5P(p\text{-tol})_3$ (IIa and IIb) are shown in a and b, respectively, with our numbering scheme. The thermal ellipsoids are shown at the 50% probability level except for the hydrogen atoms which are shown as spheres of arbitrary radius.

blocked-diagonal matrix least-squares calculations.

Atomic coordinates of all non-hydrogen atoms are in Tables I and II, and important interatomic distances and angles are in Tables III and IV. Listings of calculated and observed structure factors and the thermal parameters for all non-hydrogen atoms with their estimated standard deviations as well as Tables V and VI (mean plane data) and hydrogen coordinates and dimensions not given in Tables III and IV have been deposited. Figures 1 and 2a,b show ORTEP[16] views of the molecules with our numbering scheme. Figures 3 and 4, stereoviews of each unit cell contents, have been deposited. Figure 5 shows the $Mo(CO)_3$ unit of I projected on to the plane of the π-bonded p-tolyl ring.

Results and Discussion

Complexes of the type $Mo(CO)_5L$ (L = $P(o\text{-tol})_3$, $P(m\text{-tol})_3$, $P(p\text{-tol})_3$) have been prepared by direct reaction of excess $Mo(CO)_6$ and L for all of the phosphines in this study except $P(mes)_3$, although the complex from $P(o\text{-tol})_3$ is only obtained in low yield and in a crude form. Further high-temperature reflux with both of these bulky phosphines leads to π complexes $Mo(CO)_3L$ (L = $P(o\text{-tol})_3$, $P(mes)_3$),[2,3] which may be readily identified by the two-band carbonyl stretching pattern[1d,17] (Table VII) in the infrared spectrum that is characteristic of (π-arene)M-$(CO)_3$.[18] $Mo_2(CO)_8P(p\text{-tol})_3$ also displays this two-band pattern (Table VII) for the $Mo(CO)_3$ unit albeit superimposed upon the carbonyl stretching vibrations of the $Mo(CO)_5$ moiety (vide infra).

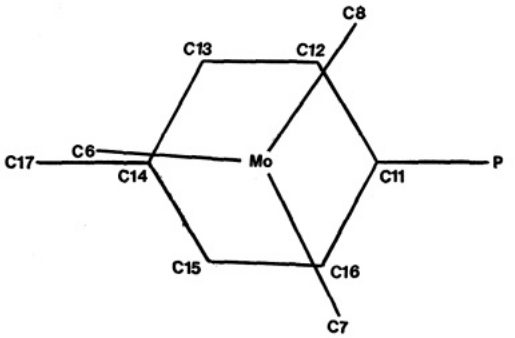

Figure 5. $Mo(CO)_3$ unit of $Mo_2(CO)_8P(p\text{-tol})_3$ projected on the plane of the π-p-tol ring.

(16) Johnson, C. K. ORTEP II, Oak Ridge National Laboratories, Technical Report ORNL-3894—revised, 1971.

(17) Local symmetry (C_{3v}) demands two infrared active bands. Nakamoto, K. "Infrared Spectra of Inorganic and Coordination Compounds"; Wiley-Interscience: New York, 1970; pp 271–273.

(18) Dobson, G. R.; Stolz, I. W.; Sheline, R. K. *Adv. Inorg. Chem. Radiochem.* **1966**, *8*, 1.

Table I. Final Fractional Coordinates (Mo and P, $\times 10^5$; Remainder, $\times 10^4$) with Estimated Standard Deviations in Parentheses for I

atom	x/a	y/b	z/c
Mo(1)	8234 (2)	19781 (1)	43244 (1)
Mo(2)	−6017 (2)	41975 (1)	27858 (1)
P	10645 (5)	34159 (3)	24697 (4)
O(1)	−2563 (2)	5238 (1)	3050 (2)
O(2)	1343 (2)	5325 (1)	2817 (2)
O(3)	−1407 (2)	4365 (1)	328 (2)
O(4)	−2638 (2)	3140 (1)	2875 (2)
O(5)	−29 (3)	4124 (1)	5260 (2)
O(6)	797 (3)	853 (1)	5935 (2)
O(7)	2582 (2)	2771 (1)	5979 (2)
O(8)	−1250 (2)	2612 (2)	5278 (2)
C(1)	−1851 (2)	4861 (1)	2953 (2)
C(2)	654 (2)	4924 (1)	2800 (2)
C(3)	−1103 (3)	4292 (1)	1197 (2)
C(4)	−1889 (2)	3501 (1)	2825 (2)
C(5)	−207 (3)	4135 (1)	4373 (2)
C(6)	803 (3)	1275 (2)	5362 (2)
C(7)	1931 (2)	2469 (2)	5383 (2)
C(8)	−491 (3)	2384 (2)	4923 (2)
C(11)	1016 (2)	2541 (1)	2782 (2)
C(12)	−93 (2)	2209 (1)	2627 (2)
C(13)	−157 (2)	1520 (1)	2731 (2)
C(14)	895 (3)	1152 (1)	3058 (2)
C(15)	2013 (2)	1484 (1)	3229 (2)
C(16)	2068 (2)	2163 (1)	3112 (2)
C(17)	845 (3)	419 (1)	3168 (3)
C(21)	2580 (2)	3647 (1)	3117 (2)
C(22)	2734 (2)	3829 (1)	4163 (2)
C(23)	3874 (3)	3978 (1)	4720 (2)
C(24)	4875 (2)	3968 (1)	4261 (2)
C(25)	4711 (2)	3794 (1)	3208 (2)
C(26)	3580 (2)	3632 (1)	2649 (2)
C(27)	6111 (3)	4116 (2)	4872 (3)
C(31)	1142 (2)	3375 (1)	1078 (2)
C(32)	704 (3)	2841 (1)	476 (2)
C(33)	641 (3)	2850 (1)	−594 (2)
C(34)	1005 (3)	3378 (1)	−1101 (2)
C(35)	1458 (3)	3905 (1)	−503 (2)
C(36)	1515 (3)	3912 (1)	575 (2)
C(37)	919 (4)	3377 (2)	−2269 (2)

Multinuclear NMR data are presented in Table VIII. For known complexes, proton NMR data agree quite well with those reported here, except that for $Mo(CO)_3P(o\text{-}tol)_3$ we do not observe the peak labeled B (δ 2.35 ppm) by Colton;[2] it appears to have shifted under the downfield methyl resonance. Furthermore, the remaining two methyl resonances have shifted upfield by 0.10 ppm. We are unable to account for this discrepancy at this time; however, the remainder of the spectrum agrees with that reported previously.[2] This trend is again observed for $Mo(CO)_3P(mes)_3$. The two methyl peaks expected for the π-bonded aryl group seen to have merged with the remaining methyl resonances. In this regard, we assign the peak at 2.21 ppm to the *o*-methyl groups and the peak at 2.09 ppm to the *p*-methyl groups to be consistent with intensity data. This behavior on coordination is most unusual[8,19] and suggests a degree of rotational freedom (about the P–C bonds) as found for complexes of $As(mes)_3$.[19b,d,e]

The methyl resonances (Table VIII) are well separated in the ^1H NMR spectrum of $Mo_2(CO)_8P(p\text{-}tol)_3$. The upfield methyl resonance is assigned to the π-bonded *p*-tolyl moiety as is the upfield chemical shift in the phenyl region. These assignments are based on intensities as well as the work of others.[2,3,20] It is noted that while the phenyl

Table II. Final Fractional Coordinates (Mo and P, $\times 10^5$; Remainder, $\times 10^4$) with Estimated Standard Deviations in Parentheses for II

atom	x/a	y/b	z/c
Mo(1)	23662 (4)	13233 (3)	45462 (3)
P(1)	13865 (13)	28580 (9)	46848 (9)
O(11)	2008 (5)	1555 (3)	6539 (4)
O(12)	5005 (5)	2337 (4)	4963 (4)
O(13)	2737 (5)	862 (3)	2534 (3)
O(14)	−94 (5)	101 (4)	3965 (4)
O(15)	3598 (5)	−502 (3)	4531 (3)
C(11)	2126 (6)	1491 (4)	5828 (5)
C(12)	4040 (6)	1994 (4)	4832 (4)
C(13)	2597 (6)	1058 (4)	3254 (5)
C(14)	765 (7)	579 (5)	4185 (4)
C(15)	3171 (6)	167 (5)	4531 (4)
C(111)	876 (5)	3123 (3)	3676 (3)
C(112)	1660 (5)	2991 (4)	3023 (4)
C(113)	1337 (5)	3210 (4)	2252 (4)
C(114)	215 (5)	3559 (4)	2124 (4)
C(115)	−563 (6)	3689 (4)	2764 (4)
C(116)	−265 (5)	3474 (4)	3544 (4)
C(117)	−128 (6)	3788 (5)	1280 (4)
C(121)	64 (5)	3078 (3)	5327 (3)
C(122)	−132 (5)	3931 (4)	5871 (4)
C(123)	−1158 (5)	4068 (4)	6353 (4)
C(124)	−2004 (5)	3391 (4)	6308 (4)
C(125)	−1837 (6)	2554 (5)	5757 (4)
C(126)	−808 (6)	2397 (5)	5280 (4)
C(127)	−3099 (6)	3547 (5)	6836 (5)
C(131)	2411 (5)	3842 (3)	5242 (3)
C(132)	2990 (5)	3872 (4)	6057 (4)
C(133)	3730 (5)	4613 (4)	6521 (4)
C(134)	3942 (6)	5326 (4)	6193 (4)
C(135)	3368 (6)	5326 (5)	5398 (5)
C(136)	2604 (5)	4560 (4)	4927 (4)
C(137)	4751 (8)	6162 (6)	6710 (5)
Mo(2)	47384 (4)	130663 (3)	100082 (4)
P(2)	63239 (13)	119470 (9)	93413 (9)
O(21)	6724 (5)	14439 (4)	11270 (4)
O(22)	4300 (6)	12059 (4)	11441 (4)
O(23)	2555 (5)	11772 (4)	8871 (5)
O(24)	4933 (5)	13897 (4)	8425 (4)
O(25)	2774 (5)	14465 (4)	10719 (5)
C(21)	6019 (7)	13938 (5)	10803 (5)
C(22)	4497 (6)	12432 (5)	10940 (5)
C(23)	3364 (7)	12220 (5)	9264 (5)
C(24)	4880 (6)	13615 (5)	9007 (5)
C(25)	3488 (7)	13951 (5)	10468 (5)
C(211)	5536 (5)	11033 (3)	8482 (3)
C(212)	4932 (5)	10331 (4)	8695 (4)
C(213)	4179 (6)	9696 (4)	8081 (4)
C(214)	4008 (6)	9742 (4)	7242 (4)
C(215)	4607 (6)	10437 (4)	7031 (4)
C(216)	5362 (5)	11081 (4)	7641 (4)
C(217)	3168 (7)	9049 (5)	6581 (5)
C(221)	7593 (5)	12378 (3)	8857 (3)
C(222)	8301 (5)	11795 (4)	8283 (4)
C(223)	9356 (6)	12129 (4)	8015 (4)
C(224)	9717 (5)	13029 (4)	8300 (4)
C(225)	9008 (5)	13604 (4)	8870 (4)
C(226)	7940 (5)	13280 (4)	9130 (3)
C(227)	10872 (6)	13398 (4)	8036 (4)
C(231)	7203 (4)	11369 (3)	10030 (3)
C(232)	7610 (5)	11861 (4)	10875 (4)
C(233)	8393 (5)	11472 (4)	11375 (4)
C(234)	8742 (5)	10600 (4)	11082 (4)
C(235)	8342 (6)	10118 (4)	10261 (4)
C(236)	7583 (5)	10493 (4)	9728 (4)
C(237)	9571 (7)	10179 (5)	11658 (5)

(19) (a) Blount, J. F.; Maryanoff, C. A.; Mislow, K. *Tetrahedron Lett.* **1975**, *11*, 913. (b) Alyea, E. C.; Dias, S. A.; Stevens, S. *Inorg. Chim. Acta Lett.* **1980**, *44*, L207. (c) Alyea, E. C.; Dias, S. A.; Ferguson, G.; Parvez, M. *Inorg. Chim. Acta* **1979**, *37*, 45. (d) Dias, S. A.; Alyea, E. C. *Transition Met. Chem. (Weinheim, Ger.)* **1979**, *4*, 209. (e) Alyea, E. C.; Dias, S. A.; Ferguson, G.; Siew, P. Y. *Can. J. Chem.* in press. (f) Alyea, E. C.; Dias, S. A.; Ferguson, G.; Siew, P. Y., manuscript in preparation.

(20) (a) Price, J. T.; Sorenson, T. S. *Can. J. Chem.* **1968**, *46*, 515. (b) Rausch, M. D.; Moser, G. A.; Moser, E. R.; Zaiko, E. J.; Lipman, A. L. Jr. *J. Organomet. Chem.* **1970**, *23*, 185.

Table III. Selected Interatomic Distances (Å) and Angles (deg) with Estimated Standard Deviations in Parentheses for I

(a) Bond Distances

Mo(1)-C(6)	1.974 (3)	Mo(2)-P	2.557 (1)	O(1)-C(1)	1.137 (3)
Mo(1)-C(7)	1.961 (3)	Mo(2)-C(1)	1.997 (3)	O(2)-C(2)	1.128 (3)
Mo(1)-C(8)	1.978 (3)	Mo(2)-C(2)	2.050 (3)	O(3)-C(3)	1.132 (3)
Mo(1)-C(11)	2.358 (2)	Mo(2)-C(3)	2.053 (3)	O(4)-C(4)	1.134 (3)
Mo(1)-C(12)	2.314 (2)	Mo(2)-C(4)	2.040 (3)	O(5)-C(5)	1.136 (3)
Mo(1)-C(13)	2.362 (2)	Mo(2)-C(5)	2.038 (3)	O(6)-C(6)	1.140 (4)
Mo(1)-C(14)	2.370 (2)	P-C(11)	1.834 (2)	O(7)-C(7)	1.150 (3)
Mo(1)-C(15)	2.354 (2)	P-C(11)	1.829 (2)	O(8)-C(8)	1.144 (3)
Mo(1)-C(16)	2.325 (2)	P-C(31)	1.831 (2)		
Mo(1)-R(16)	1.877				

(b) Bond Angles

C(6)-Mo(1)-C(7)	88.6 (1)	C(1)-Mo(2)-C(5)	87.9 (1)	Mo(2)-C(2)-O(2)	179.3 (3)
C(6)-Mo(1)-C(8)	86.2 (1)	C(2)-Mo(2)-C(3)	90.4 (1)	Mo(2)-C(3)-O(3)	177.1 (3)
C(6)-Mo(1)-R(16)[a]	124.9	C(2)-Mo(2)-C(4)	177.1 (1)	Mo(2)-C(4)-O(4)	176.1 (2)
C(7)-Mo(1)-C(8)	86.5 (1)	C(2)-Mo(2)-C(5)	90.6 (1)	Mo(2)-C(5)-O(5)	176.5 (3)
C(7)-Mo(1)-R(16)	127.2	C(3)-Mo(2)-C(4)	91.2 (1)	Mo(1)-C(6)-O(6)	177.5 (3)
C(8)-Mo(1)-R(16)	129.8	C(3)-Mo(2)-C(5)	176.2 (1)	Mo(1)-C(7)-O(7)	177.8 (2)
P-Mo(2)-C(1)	175.2 (1)	C(4)-Mo(2)-C(5)	87.6 (1)	Mo(1)-C(8)-O(8)	179.1 (3)
P-Mo(2)-C(2)	85.7 (1)	Mo(2)-P-C(11)	121.3 (1)	P-C(11)-C(12)	119.9 (2)
P-Mo(2)-C(3)	88.5 (1)	Mo(2)-P-C(21)	114.8 (1)	P-C(11)-C(16)	122.7 (2)
P-Mo(2)-C(4)	96.8 (1)	Mo(2)-P-C(31)	110.8 (1)	P-C(21)-C(22)	117.6 (2)
P-Mo(2)-C(5)	95.2 (1)	C(11)-P-C(21)	102.2 (1)	P-C(21)-C(26)	124.4 (2)
C(1)-Mo(2)-C(2)	90.6 (1)	C(11)-P-C(31)	100.5 (1)	P-C(31)-C(32)	121.5 (2)
C(1)-Mo(2)-C(3)	88.5 (1)	C(21)-P-C(31)	105.1 (1)	P-C(31)-C(36)	120.3 (2)
C(1)-Mo(2)-C(4)	87.1 (1)	Mo(2)-C(1)-O(1)	179.9 (1)		

[a] R(16) = geometric center of the π-bonded ring C(11)-C(16).

resonances for the other complexes reported herein are usually broad and featureless, a single sharp line is observed for each phenyl peak of $Mo_2(CO)_8P(p\text{-tol})_3$ and relatively narrow doublets are observed in the phenyl regions of both $P(mes)_3$ and $Mo(CO)_3P(mes)_3$.

Both ^{31}P and ^{95}Mo NMR offer excellent and complementary techniques for distinguishing between the π-type $Mo(CO)_3L$ complexes and the phosphorous-coordinated $Mo(CO)_5L$ species. As expected, the ^{31}P NMR coordination chemical shift (Δ)[21] for phosphorus-coordinated complexes is large, while only a small shift is observed for the π complexes (Table VIII). The magnitude of the ^{95}Mo NMR chemical shifts and ^{95}Mo–^{31}P coupling constants of the phosphorus-coordinated species are in accord with other $Mo(CO)_5L$ complexes[22] while the chemical shifts of the π complexes resemble those of the respective $Mo(CO)_3L$ (L = xylenes) derivatives[23] and show no coupling to phosphorus. These latter ^{95}Mo chemical shifts are exceedingly low and are most likely affected by the ring currents in the π-bonded arenes.

At first sight, the NMR data for $Mo_2(CO)_8P(p\text{-tol})_3$ (I) appeared anomalous and thus its structure was determined as shown in Figure 1 by X-ray crystallography. ^1H NMR data are consistent with a π complex similar to $Mo(CO)_3P(o\text{-tol})_3$ and $Mo(CO)_3P(mes)_3$. ^{31}P NMR data are consistent with a P atom coordinated to Mo as in $Mo(CO)_5L$ complexes, but there is only one ^{95}Mo NMR resonance which occurs at the chemical shift expected for π-bonded $Mo(CO)_3P(p\text{-tol})_3$ and shows no coupling to phosphorus. The structure determined by our X-ray analysis explain these spectra if one assumes that the ^{95}Mo NMR signal for the $Mo(CO)_5L$ moiety of I is not observed, as was the case for $Mo(CO)_5P(o\text{-tol})_3$. Since molybdenum has a moderately large quadrupolar moment, it is feasible that the more unsymmetrical environments in these cases result in extensive line-broadening.[22]

The structure of $Mo_2(CO)_8P(p\text{-tol})_3$ (I) consists of discrete monomeric molecules separated by normal van der Waals distances (Table III, Figure 3). The molecule has a central molybdenum atom with three carbonyl groups occupying one face of the octahedral geometry. The opposite face is occupied by one p-tol ring of the $P(p\text{-tol})_3$ ligand that is coordinated, through the phosphorus atom, to the molybdenum atom of a pentacarbonylmolybdenum moiety. This complex represents the second X-ray study of an arylphosphine π bonded to molybdenum[7] and the only structure to be completely characterized spectroscopically. We also include the structure of $Mo(CO)_5P(p\text{-tol})_3$ (II) for comparison.

The structure of II consists of discrete monomeric molecules separated by normal van der Waals distances (Table IV, Figure 4). There are two independent molecules IIa and IIb in the asymmetric unit, each containing an octahedrally coordinated central molybdenum atom.

The Mo–P distances (2.557 (1), 2.562 (2), and 2.555 (1) Å, respectively, for I, IIa, and IIb) compare favorably with those found for $Mo(CO)_5PPh_3$ (2.560 (1) Å).[24] The chief difference in the $Mo(CO)_5P(p\text{-tol})_3$ moiety of I and between IIa and IIb lies in the coordination environment about the phosphorus atoms (Tables III and IV; Figures 1 and 2a,b). The Mo–P–C angles range from 110.8 (1) to 121.3 (1)° for I, 114.1 (2) to 116.8 (2)° for IIa, and 108.6 (2) to 118.8 (2)° for IIb while the respective C–P–C angles range from 100.5 (1) to 105.1 (1)°, 101.1 (2) to 104.6 (2)°, and 99.7 (2) to 106.0 (2)°. The corresponding Mo–P–C and C–P–C angles in $Mo(CO)_5PPh_3$[24] range from 111.67 (9) to 118.74 (9)° and 101.9 (1) to 103.2 (1)° and correlate best with IIa. The interplanar angles (Tables V and VI) in neither I nor IIa nor IIb are consistent with a propeller conformation of the aryl groups in contrast to that found for $Mo(CO)_5PPh_3$.[24]

As expected, the Mo–C(carbonyl) bond trans to the phosphorus atom is shorter (1.997 (3) Å in I, 1.986 (7) Å

(21) Δ (ppm) = δ(complex) − δ(ligand).

(22) (a) Dysart, S.; Georgii, E.; Mann, B. E. *J. Organomet. Chem.* **1981**, *213*, C10. (b) Alyea, E. C.; Lenkinski, R. E.; Somogyvari, A. *Polyhedron* **1982**, *1*, 130. (c) Alyea, E. C.; Somogyvari, A. "The Chemistry and Uses of Molybdenum", Proceedings of the Fourth International Conference, Golden, CO, 1982.

(23) Masters, A. F.; Brownlee, R. T. C.; O'Connor, M. J.; Wedd, A. G. *Inorg. Chem.* **1981**, *20*, 4183.

(24) Cotton, F. A.; Darensbourg, D. J.; Ilsley, W. H. *Inorg. Chem.* **1981**, *20*, 578.

Table IV. Selected Interatomic Distances (Å) and Angles (deg) with Estimated Standard Deviations in Parentheses for II

(a) Bond Distances

Mo(1)-P(1)	2.562 (2)	O(11)-C(11)	1.138 (10)	P(2)-C(211)	1.804 (5)
Mo(1)-C(11)	2.044 (8)	O(12)-C(12)	1.141 (9)	P(2)-C(221)	1.841 (6)
Mo(1)-C(12)	2.024 (7)	O(13)-C(13)	1.137 (9)	P(2)-C(231)	1.817 (6)
Mo(1)-C(13)	2.041 (8)	O(14)-C(14)	1.141 (9)	O(21)-C(21)	1.136 (8)
Mo(1)-C(14)	2.010 (7)	O(15)-C(15)	1.134 (9)	O(22)-C(22)	1.140 (11)
Mo(1)-C(15)	1.986 (7)	Mo(2)-P(2)	2.555 (1)	O(23)-C(23)	1.130 (9)
P(1)-C(111)	1.819 (6)	Mo(2)-C(21)	2.001 (6)	O(24)-C(24)	1.138 (11)
P(1)-C(121)	1.833 (5)	Mo(2)-C(22)	2.026 (9)	O(25)-C(25)	1.139 (9)
P(1)-C(131)	1.818 (5)	Mo(2)-C(23)	2.019 (7)		
		Mo(2)-C(24)	2.023 (9)		
		Mo(2)-C(25)	1.988 (7)		

(b) Bond Angles

P(1)-Mo(1)-C(11)	87.6 (2)	C(121)-P(1)-C(131)	101.1 (2)	C(22)-Mo(2)-C(24)	175.1 (3)
P(1)-Mo(1)-C(12)	88.6 (2)	Mo(1)-C(11)-O(11)	177.7 (6)	C(22)-Mo(2)-C(25)	90.4 (3)
P(1)-Mo(1)-C(13)	96.0 (2)	Mo(1)-C(12)-O(12)	176.6 (5)	C(23)-Mo(2)-C(24)	88.1 (3)
P(1)-Mo(1)-C(14)	94.9 (2)	Mo(1)-C(13)-O(13)	176.3 (6)	C(23)-Mo(2)-C(25)	88.8 (3)
P(1)-Mo(1)-C(15)	175.8 (2)	Mo(1)-C(14)-O(14)	174.9 (6)	C(24)-Mo(2)-C(25)	90.3 (3)
C(11)-Mo(1)-C(12)	93.1 (3)	Mo(1)-C(15)-O(15)	177.9 (6)	Mo(2)-P(2)-C(211)	108.6 (2)
C(11)-Mo(1)-C(13)	175.9 (3)	P(1)-C(111)-C(112)	119.2 (4)	Mo(2)-P(2)-C(221)	118.6 (2)
C(11)-Mo(1)-C(14)	90.3 (3)	P(1)-C(111)-C(116)	122.1 (4)	Mo(2)-P(2)-C(231)	118.8 (2)
C(11)-Mo(1)-C(15)	88.7 (3)	P(1)-C(121)-C(122)	122.8 (4)	C(211)-P(2)-C(221)	106.0 (2)
C(12)-Mo(1)-C(13)	88.9 (3)	P(1)-C(121)-C(126)	121.1 (4)	C(211)-P(2)-C(231)	104.2 (2)
C(12)-Mo(1)-C(14)	175.3 (3)	P(2)-Mo(2)-C(21)	93.3 (2)	C(221)-P(2)-C(231)	99.7 (2)
C(12)-Mo(1)-C(15)	89.5 (3)	P(2)-Mo(2)-C(22)	92.4 (2)	Mo(2)-C(21)-O(21)	178.1 (7)
C(13)-Mo(1)-C(14)	87.5 (3)	P(2)-Mo(2)-C(23)	90.2 (2)	Mo(2)-C(22)-O(22)	176.3 (6)
C(13)-Mo(1)-C(15)	87.8 (3)	P(2)-Mo(2)-C(24)	86.9 (2)	Mo(2)-C(23)-O(23)	176.6 (7)
C(14)-Mo(1)-C(15)	87.2 (3)	P(2)-Mo(2)-C(25)	177.0 (3)	Mo(2)-C(24)-O(24)	177.5 (6)
Mo(1)-P(1)-C(111)	116.8 (2)	C(21)-Mo(2)-C(22)	91.1 (3)	Mo(2)-C(25)-O(25)	178.7 (8)
Mo(1)-P(1)-C(121)	116.4 (2)	C(21)-Mo(2)-C(23)	176.2 (3)	P(2)-C(211)-C(212)	119.2 (4)
Mo(1)-P(1)-C(131)	114.1 (2)	C(21)-Mo(2)-C(24)	93.8 (3)	P(2)-C(211)-C(216)	121.6 (4)
C(111)-P(1)-C(121)	104.6 (2)	C(21)-Mo(2)-C(25)	87.8 (3)	P(2)-C(221)-C(222)	122.1 (4)
C(111)-P(1)-C(131)	101.7 (2)	C(22)-Mo(2)-C(23)	87.1 (3)	P(2)-C(221)-C(223)	119.4 (4)

Table VII. Carbonyl Stretching Frequencies

complex[a]	ν(C-O), cm^{-1}
$Mo(CO)_5P(o\text{-tol})_3$	2066 (m), 1937 (vs)
$Mo(CO)_5P(m\text{-tol})_3$	2067 (m), 1938 (vs)
$Mo(CO)_5P(p\text{-tol})_3$	2066 (m), 1942 (vs)
$Mo(CO)_3P(o\text{-tol})_3$	1950 (vs), 1906 (vs)
$Mo(CO)_3P(mes)_3$	1953 (vs), 1873 (vs), 1967 (vs),[b] 1897 (vs)[b]
$Mo_2(CO)_8P(p\text{-tol})_3$	2068 (m), 1972 (vs), 1940 (vs), 1891 (s)

[a] CH_2Cl_2 solutions; abbreviations, (m) medium, (s) strong, (vs) very strong. [b] CCl_4 solutions.

in IIa, and 1.988 (7) in IIb) than the remaining equatorial Mo–C(carbonyl) bonds (2.045 (3), 2.030 (7), and 2.017 (7) Å respectively). This has been observed previously for $Mo(CO)_5PPh_3$,[24] the respective distances (1.995 (3), 2.046 (4) Å) agreeing especially well for I. There is, surprisingly, no difference between the axial (1.137 (3) Å in I, 1.134 (9) Å in IIa, and 1.139 (9) Å in IIb) and equatorial (1.132 (3), 1.139 (9), and 1.136 (9) Å, respectively) C–O distances. The Mo–C–O units are linear (177.8 (3), 176.7 (6), 177.4 (6)° for I, IIa, and IIb, respectively) with bond angles varying very little from those reported (177.3 (3)°) for $Mo(CO)_5PPh_3$.[24]

The Mo–C(carbonyl) distances in the tricarbonyl molybdenum moiety of I are considerably shorter (1.971 (3) Å) than the equatorial distances in the pentacarbonylmolybdenum moiety of I (2.045 (3) Å) or the corresponding distances in IIa (2.030 (7) Å) and IIb (2.017 (7) Å) but compare favorably with the Mo–C(carbonyl) distances found (1.964 (4) Å in (π-mes)$Mo(CO)_3$[25]) for (π-arene)-

Table VIII. Multinuclear NMR Data[a]

complex	δ (^{31}P)	δ (^{95}Mo)	δ (^{1}H)
PPh_3	−6.3		7.63-7.07
$P(o\text{-tol})_3$	−29.8		7.28-6.54, 2.38 [$^4J(^{31}P\text{-}^1H) = 1.7$]
			7.5-7.0, 2.38[b]
$P(m\text{-tol})_3$	−5.3		7.23-6.96, 2.26
	−5.3[c]		7.5-7.0, 2.28[b]
$P(p\text{-tol})_3$	−8.1		7.20-6.93, 2.34
	−8.0[c]		7.5-7.0, 2.32[b]
$P(mes)_3$	−36.6		6.69 [$^4J(^{31}P\text{-}^1H) = 3.0$], 2.20, 2.01
	−39.0[d]		
$Mo(CO)_5P(o\text{-tol})_3$	33.2	...	7.3-7.1, 2.16[b]
$Mo(CO)_5P(m\text{-tol})_3$	36.9	−1739.3	7.24-6.88, 2.29 [$^4J(^{31}P\text{-}^1H) = 2.3$]
	36.7[c]	[$^1J(^{95}Mo\text{-}^{31}P) = 139.5$]	7.3-7.1, 2.31[b]
$Mo(CO)_5P(p\text{-tol})_3$	34.9	−1745.8	7.28-7.02, 2.32
	34.5[c]	[$^1J(^{95}Mo\text{-}^{31}P) = 136.9$]	7.4-7.1, 2.36[b]
$Mo(CO)_3P(o\text{-tol})_3$	−30.4	−1998.9	7.45-7.28, 6.0-5.0, 2.70, 2.07
			7.3-6.8, 5.9-5.0, 2.80, 2.35, 2.20, 2.18[b]
$Mo(CO)_3P(mes)_3$	−31.6	−1832.6	6.76 [$^4J(^{31}P\text{-}^1H) = 3.6$], 5.13 [$^4J(^{31}P\text{-}^1H) = 2.4$]
			2.21, 2.09
$Mo_2(CO)_8P(p\text{-tol})_3$	38.2	−1976.7	7.23, 5.22, 2.33, 2.26

[a] δ (ppm) is positive if downfield from the reference. [b] Reference 2. [c] Reference 10. [d] Reference 19c.

$Mo(CO)_3$ complexes.[26] The C–O distances (1.145 (3) Å) are longer than in the pentacarbonyl moieties (1.133 (3), 1.138 (9) Å, and 1.137 (9) Å for I, IIa, and IIb, respectively), indicating stronger back-bonding to C–O, but only slightly shorter than the C–O distances (1.153 (6) Å) found for (π-mes)$Mo(CO)_3$ (TMB) or (hexamethylbenzene)$Mo(CO)_3$ (HMB).[25] Thus the *p*-tol group is only a slightly poorer π donor/better π acceptor than mesitylene or hexamethylbenzene. This synergism may be examined directly by comparing the C–C distances (1.410 (3) Å) in the π-bonded ring of I with the C–C distances in the remaining two *p*-tol rings (1.387 (3) Å, C(21)–C(26); 1.379 (3) Å, C(31)–C(36)). Similar C–C distances are observed for the rings of IIa and IIb (Table IV). Carbon-carbon distances in TMB (1.410 (6) Å),[25] HMB (1.423 (6) Å),[25] and other (π-arene)$Mo(CO)_3$ complexes[26] support our results. Consistent with the above interpretation, the center of the π-*p*-tol group of I is displaced 1.897 Å from the molybdenum atom, a distance shorter than the 1.908 Å in TMB,[25] 1.923 Å in HMB,[25] or 2.02 Å in $Tl[CpMo(CO)_3]_3$.[27] Consequently, the Mo–C(ring) distances (Table III) are shorter than in complexes previously reported.[25,27]

A slight threefold distortion is observed for the π-bonded ring in I. Alternate bond distances average 1.403 (3) and 1.416 (3) Å (Table III), and there is a slight ruffling of the *p*-tol ring (Table V). Similar distortions have been noted for HMB[25] as well as for a number of (π-arene)chromium tricarbonyls.[28] We feel that in this case the distortion is caused by crystal packing forces (Figure 3, Table III) rather than by electronic effects. These packing forces also account for the severe steric strain experienced at the phosphorus atom of I (Table III). Electronic effects are manifested in the orientation of the carbonyl groups with respect to the aromatic ring.[29] The orientation adopted (Figure 5) indicates a delocalized π system of electrons with the phosphorus atom acting as a stronger electron donor than the methyl group. Also, in accord with previous results,[29] the π-*p*-tol ring plane forms an angle of 2.27° (Table V) with the plane of the carbonyl carbon atoms.

Acknowledgment. The continuing support of the Natural Sciences and Engineering Research Council of Canada in the form of operating grants (E.C.A. and G.F.) is gratefully acknowledged. We thank Dr. Shelton Dias for preliminary investigations of some of the complexes.

Registry No. I, 84473-35-8; II, 36491-12-0; $Mo(CO)_5P(o\text{-tol})_3$, 36491-10-8; $Mo(CO)_5P(m\text{-tol})_3$, 36491-11-9; $Mo(CO)_3P(o\text{-tol})_3$, 36346-24-4; $Mo(CO)_3P(mes)_3$, 84498-67-9; $Mo(CO)_6$, 13939-06-5; $[Et_4N][Mo(CO)_5Cl]$, 14780-96-2; ^{95}Mo, 14392-17-7.

Supplementary Material Available: Tables of mean plane data (Tables V and VI), anisotropic thermal parameters, remaining bond distances and angles, calculated hydrogen coordinates, and structure factor listings for compounds I and II, a table of isotropic thermal parameters for II, and stereoviews of the unit cell for I and II (Figures 3 and 4, respectively) (57 pages). Ordering information is given on any current masthead page.

(25) Koshland, D. E.; Myers, S. E.; Chesick, J. P. *Acta Crystallogr., Sect. B* **1977**, *B33*, 2013.
(26) (a) Anderson, B. F.; Robertson, G. B.; Butler, D. N. *Can. J. Chem.* **1976**, *54*, 1958. (b) McKechnie, J. S.; Paul, I. C. *J. Am. Chem. Soc.* **1966**, *88*, 5927. (c) Dunitz, J. D.; Pauling, P. *Helv. Chim. Acta* **1960**, *43*, 2188. (d) Tremmel, P. O.; Weidenhammer, K.; Wienand, H.; Ziegler, M. L. *Z. Naturforsch., B: Anorg. Chem., Org. Chem.* **1975**, *B30*, 699.
(27) Rajaram, J.; Ibers, J. A. *Inorg. Chem.* **1973**, *12*, 1313.
(28) (a) Bailey, M. F.; Dahl, L. F. *Inorg. Chem.* **1965**, *4*, 1298. (b) *Ibid.* **1965**, *4*, 1306. (c) *Ibid.* **1965**, *4*, 1314.
(29) (a) Carter, O. L.; McPhail, A. T.; Sim, G. A. *Chem. Commun.* **1966**, 212. (b) Muir, K. W.; Ferguson, G.; Sim, G. A. *Ibid.* **1966**, 465. (c) Carter, O. L.; McPhail, A. T.; Sim, G. A. *J. Chem. Soc. A* **1966**, 822. (d) *Ibid.* **1967**, 228. (e) *Ibid.* **1967**, 1619. (f) *Ibid.* **1968**, 1866.

Metal Atom Synthesis of Metallaboron Clusters. 3.[1] Synthesis and Structural Characterization of an (Arene)ferracarborane Complex: 1-(η^6-$CH_3C_6H_5$)Fe-2,3-$(C_2H_5)_2C_2B_4H_4$

Robert P. Micciche and Larry G. Sneddon*[2]

Department of Chemistry and Laboratory for Research on the Structure of Matter, University of Pennsylvania, Philadelphia, Pennsylvania 19104

Received October 22, 1982

The reaction of thermally generated iron atoms with toluene and the small carborane 2,3-$(C_2H_5)_2C_2B_4H_6$ under low-temperature conditions has been found to yield the (arene)ferracarborane complex 1-(η^6-$CH_3C_6H_5$)Fe-2,3-$(C_2H_5)_2C_2B_4H_4$. The molecular structure of the compound has been determined from the single-crystal X-ray diffraction data and confirms the expected sandwich type of configuration found in similar arene complexes. Crystal data: space group $P2_1/c$, $Z = 4$, $a = 8.200$ (7) Å, $b = 12.344$ (4) Å, $c = 14.759$ (11) Å, $\beta = 93.85$ (6)°, $V = 1491$ (3) Å^3. The structure was refined by full-matrix least-squares methods to a final R of 0.071 and R_w of 0.079 for the 1177 reflections that had $F_o^2 > 3\sigma(F_o^2)$.

Introduction

Although an extensive variety of cyclopentadienyl-substituted metallacarborane clusters has been synthesized during the last 20 years, only recently have (π-arene) metallacarborane complexes been reported.[3,4] This is indeed surprising given that a (η-C_5H_5)Co fragment, which is a well-known metallacarborane component, is isoelectronic with a (η^6-arene)Fe unit and suggests that if appropriate synthetic procedures can be developed (ar-

(1) For part 2, see: Zimmerman, G. J.; Sneddon, L. G. *J. Am. Chem. Soc.* **1981**, *103*, 1102.
(2) Alfred P. Sloan Foundation Fellow.
(3) Garcia, M. P.; Green, M.; Stone, F. G. A.; Somerville, R. G.; Welch, A. J. *J. Chem. Soc., Chem. Commun.* **1981**, 871.
(4) Hanusa, T. P.; Huffman, J. C.; Todd, L. J. *Polyhedron* **1982**, *1*, 77.

0276-7333/83/2302-0674$01.50/0

$Mo(CO)_3$ complexes.[26] The C–O distances (1.145 (3) Å) are longer than in the pentacarbonyl moieties (1.133 (3), 1.138 (9) Å, and 1.137 (9) Å for I, IIa, and IIb, respectively), indicating stronger back-bonding to C–O, but only slightly shorter than the C–O distances (1.153 (6) Å) found for (π-mes)$Mo(CO)_3$ (TMB) or (hexamethylbenzene)$Mo(CO)_3$ (HMB).[25] Thus the *p*-tol group is only a slightly poorer π donor/better π acceptor than mesitylene or hexamethylbenzene. This synergism may be examined directly by comparing the C–C distances (1.410 (3) Å) in the π-bonded ring of I with the C–C distances in the remaining two *p*-tol rings (1.387 (3) Å, C(21)–C(26); 1.379 (3) Å, C(31)–C(36)). Similar C–C distances are observed for the rings of IIa and IIb (Table IV). Carbon-carbon distances in TMB (1.410 (6) Å),[25] HMB (1.423 (6) Å),[25] and other (π-arene)$Mo(CO)_3$ complexes[26] support our results. Consistent with the above interpretation, the center of the π-*p*-tol group of I is displaced 1.897 Å from the molybdenum atom, a distance shorter than the 1.908 Å in TMB,[25] 1.923 Å in HMB,[25] or 2.02 Å in $Tl[CpMo(CO)_3]_3$.[27] Consequently, the Mo–C(ring) distances (Table III) are shorter than in complexes previously reported.[25,27]

A slight threefold distortion is observed for the π-bonded ring in I. Alternate bond distances average 1.403 (3) and 1.416 (3) Å (Table III), and there is a slight ruffling of the *p*-tol ring (Table V). Similar distortions have been noted for HMB[25] as well as for a number of (π-arene)chromium tricarbonyls.[28] We feel that in this case the distortion is caused by crystal packing forces (Figure 3, Table III) rather than by electronic effects. These packing forces also account for the severe steric strain experienced at the phosphorus atom of I (Table III). Electronic effects are manifested in the orientation of the carbonyl groups with respect to the aromatic ring.[29] The orientation adopted (Figure 5) indicates a delocalized π system of electrons with the phosphorus atom acting as a stronger electron donor than the methyl group. Also, in accord with previous results,[29] the π-*p*-tol ring plane forms an angle of 2.27° (Table V) with the plane of the carbonyl carbon atoms.

Acknowledgment. The continuing support of the Natural Sciences and Engineering Research Council of Canada in the form of operating grants (E.C.A. and G.F.) is gratefully acknowledged. We thank Dr. Shelton Dias for preliminary investigations of some of the complexes.

Registry No. I, 84473-35-8; II, 36491-12-0; $Mo(CO)_5P(o\text{-tol})_3$, 36491-10-8; $Mo(CO)_5P(m\text{-tol})_3$, 36491-11-9; $Mo(CO)_3P(o\text{-tol})_3$, 36346-24-4; $Mo(CO)_3P(mes)_3$, 84498-67-9; $Mo(CO)_6$, 13939-06-5; $[Et_4N][Mo(CO)_5Cl]$, 14780-96-2; ^{95}Mo, 14392-17-7.

Supplementary Material Available: Tables of mean plane data (Tables V and VI), anisotropic thermal parameters, remaining bond distances and angles, calculated hydrogen coordinates, and structure factor listings for compounds I and II, a table of isotropic thermal parameters for II, and stereoviews of the unit cell for I and II (Figures 3 and 4, respectively) (57 pages). Ordering information is given on any current masthead page.

(25) Koshland, D. E.; Myers, S. E.; Chesick, J. P. *Acta Crystallogr., Sect. B* **1977**, *B33*, 2013.
(26) (a) Anderson, B. F.; Robertson, G. B.; Butler, D. N. *Can. J. Chem.* **1976**, *54*, 1958. (b) McKechnie, J. S.; Paul, I. C. *J. Am. Chem. Soc.* **1966**, *88*, 5927. (c) Dunitz, J. D.; Pauling, P. *Helv. Chim. Acta* **1960**, *43*, 2188. (d) Tremmel, P. O.; Weidenhammer, K.; Wienand, H.; Ziegler, M. L. *Z. Naturforsch., B: Anorg. Chem., Org. Chem.* **1975**, *B30*, 699.
(27) Rajaram, J.; Ibers, J. A. *Inorg. Chem.* **1973**, *12*, 1313.
(28) (a) Bailey, M. F.; Dahl, L. F. *Inorg. Chem.* **1965**, *4*, 1298. (b) *Ibid.* **1965**, *4*, 1306. (c) *Ibid.* **1965**, *4*, 1314.
(29) (a) Carter, O. L.; McPhail, A. T.; Sim, G. A. *Chem. Commun.* **1966**, 212. (b) Muir, K. W.; Ferguson, G.; Sim, G. A. *Ibid.* **1966**, 465. (c) Carter, O. L.; McPhail, A. T.; Sim, G. A. *J. Chem. Soc. A* **1966**, 822. (d) *Ibid.* **1967**, 228. (e) *Ibid.* **1967**, 1619. (f) *Ibid.* **1968**, 1866.

Metal Atom Synthesis of Metallaboron Clusters. 3.[1] Synthesis and Structural Characterization of an (Arene)ferracarborane Complex: 1-(η^6-$CH_3C_6H_5$)Fe-2,3-$(C_2H_5)_2C_2B_4H_4$

Robert P. Micciche and Larry G. Sneddon*[2]

Department of Chemistry and Laboratory for Research on the Structure of Matter, University of Pennsylvania, Philadelphia, Pennsylvania 19104

Received October 22, 1982

The reaction of thermally generated iron atoms with toluene and the small carborane 2,3-$(C_2H_5)_2C_2B_4H_6$ under low-temperature conditions has been found to yield the (arene)ferracarborane complex 1-(η^6-$CH_3C_6H_5$)Fe-2,3-$(C_2H_5)_2C_2B_4H_4$. The molecular structure of the compound has been determined from the single-crystal X-ray diffraction data and confirms the expected sandwich type of configuration found in similar arene complexes. Crystal data: space group $P2_1/c$, $Z = 4$, $a = 8.200$ (7) Å, $b = 12.344$ (4) Å, $c = 14.759$ (11) Å, $\beta = 93.85$ (6)°, $V = 1491$ (3) Å^3. The structure was refined by full-matrix least-squares methods to a final R of 0.071 and R_w of 0.079 for the 1177 reflections that had $F_o^2 > 3\sigma(F_o^2)$.

Introduction

Although an extensive variety of cyclopentadienyl-substituted metallacarborane clusters has been synthesized during the last 20 years, only recently have (π-arene) metallacarborane complexes been reported.[3,4] This is indeed surprising given that a (η-C_5H_5)Co fragment, which is a well-known metallacarborane component, is isoelectronic with a (η^6-arene)Fe unit and suggests that if appropriate synthetic procedures can be developed (ar-

(1) For part 2, see: Zimmerman, G. J.; Sneddon, L. G. *J. Am. Chem. Soc.* **1981**, *103*, 1102.
(2) Alfred P. Sloan Foundation Fellow.
(3) Garcia, M. P.; Green, M.; Stone, F. G. A.; Somerville, R. G.; Welch, A. J. *J. Chem. Soc., Chem. Commun.* **1981**, 871.
(4) Hanusa, T. P.; Huffman, J. C.; Todd, L. J. *Polyhedron* **1982**, *1*, 77.

0276-7333/83/2302-0674$01.50/0

ene)metallacarborane chemistry may exhibit the diversity and scope of their well-known cyclopentadienyl analogues.

We have previously reported[1,5-7] the application of metal atom reaction techniques to the synthesis of metallaboron clusters and have succeeded in using these techniques to produce a number of new cyclopentadienyl-substituted cobaltaborane,[5,7] -carborane,[6,7] and -thiaborane[1] clusters. We have recently initiated studies on the use of metal vapor reactions to generate new metallaboron clusters in which the cage metal atom(s) would be bound to more potentially labile ligands such as π-arenes, thus increasing the possibility for exploitation of cage metal atom reactions. We report here the synthesis and structural characterization of one such compound, 1-(η^6-$CH_3C_6H_5$)Fe-2,3-$(C_2H_5)_2C_2B_4H_4$, formed by the reaction of iron atoms with toluene and the small carborane 2,3-$(C_2H_5)_2C_2B_4H_6$.

Experimental Section

Materials and Procedure. Iron metal (lumps, random) was obtained from Alfa Products/Ventron Division. Toluene (Amend Drug and Chemical Co.) was degassed under vacuum and dried over $CaCl_2$ (Mallinckrodt) with stirring. 2,3-$(C_2H_5)_2C_2B_4H_6$ was synthesized via a modified version of Grimes' procedure.[8] All other reagents were commercially obtained, as directed, and used as received.

Preparative thin-layer chromatography was performed on 0.5 mm (20 × 20 cm) silica gel F-254 plates (Merck). Boron-11 and proton Fourier transform NMR spectra at 32.1 and 100 MHz, respectively, were obtained on a JEOL PS-100 spectrometer equipped with the appropriate decoupling accessories. Proton NMR spectra, at 250 MHz, were obtained on a Bruker WH-250 Fourier transform spectrometer. Boron-11 NMR spectra, at 115.5 MHz, were obtained on a Bruker WH-360 Fourier transform spectrometer located in the Mid-Atlantic Regional NMR Facility. Carbon-13 NMR spectra, at 50.327 MHz, were obtained on an IBM WP200SY Fourier transform spectrometer. All boron-11 chemical shifts were referenced to $BF_3 \cdot O(C_2H_5)_2$ (0.0 ppm) with a negative sign indicating an upfield shift. All proton and carbon-13 chemical shifts were measured relative to internal residual benzene from the lock solvent (99.5% C_6D_6) and then referenced to Me_4Si (0.00 ppm). High- and low-resolution mass spectra were obtained on a Hitachi Perkin-Elmer RMH-2 mass spectrometer and/or a VG Micromass 7070H mass spectrometer interfaced to a Kratos DS50S data system. Infrared spectra were obtained on a Perkin-Elmer 337 spectrophotometer. Elemental analysis was performed by Schwarzkopf Microanalytical Laboratories. The melting point is uncorrected.

The metal atom apparatus employed in these studies was based on a design published by Klabunde[9] and is described elsewhere.[7,10] Approximately 50% of the metal in the crucible is vaporized. Of the vaporized metal it is estimated that only 50% will reach the reaction zone. Therefore yields are calculated under the assumption that only 25% of the metal used actually reacts.

Reaction of Iron Vapor with Toluene and 2,3-$(C_2H_5)_2C_2B_4H_6$. Approximately 1.5 g of iron was placed in an integral tungsten alumina evaporation crucible (Sylvania Emissive Products, CS-1008) and iron vapor (~0.75 g) was generated by electrical heating (~8.0 V, 50 A). The metal vapor was cocondensed with 25 mL of toluene and 3 mL of 2,3-$(C_2H_5)_2C_2B_4H_6$ over a 2-h period onto the walls of the reactor, which were maintained at −196 °C. Upon completion of metal deposition and ligand cocondensation the matrix was warmed to −78 °C and stirred for 40 min. The dark slurry was then warmed to room temperature and stirred for an additional 90 min. Excess ligands were removed in vacuo, and the reactor was flushed with N_2(g). The dark residue was extracted with methylene chloride, filtered through a coarse frit, and then stirred with silica gel (60–200 mesh, VWR Scientific Inc.) for 1 h. The mixture was filtered through a coarse frit and separated by TLC on silica gel by using a 50% hexane in benzene solution. The resulting separation gave as the major product 1-(η^6-$CH_3C_6H_5$)Fe-2,3-$(C_2H_5)_2C_2B_4H_4$: R_f 0.35; yellow; 27.3 mg (1.4%); mp 92.0–92.5 °C, mass measurement calcd for $^{12}C_{13}{}^1H_{22}{}^{11}B_4{}^{56}Fe$ 278.1443, found 278.1463 (17.73%) (also major fragment calcd for $^{12}C_7{}^1H_8{}^{56}Fe$ 147.9975, found 147.9904 (100%)); ^{11}B NMR (ppm, C_6D_6, 115.5 MHz) 8.1 (D, $B_{5(7)}$, J_{BH} = 147 Hz), 5.7 (D, $B_{7(5)}$, J_{BH} = 164 Hz), 2.0 (D, 2, $B_{4,6}$, J_{BH} = 147 Hz); ^1H NMR (δ, C_6D_6, 250 MHz) 4.75 (m, 5, C_6H_5), 2.5 (m, 2, CH_2, J_{CH} = 8 Hz), 2.2 (m, 2, CH_2, J_{CH} = 8 Hz), 2.0 (s, 3, Ph-CH_3), 1.3 (t, 6, CH_3, J_{CH} = 8 Hz); ^1H NMR (δ, C_6D_6, 100 MHz, ^{11}B spin decoupled) 4.2 (s, B_5-H), 3.9 (s, 2, $B_{4,6}$-H), 1.7 (s, B_7-H); ^{13}C NMR (ppm, C_6D_6, 50.3 MHz) 97.8 (C4), 85.0 (C5, C9), 83.3 (C6,C8), 82.7 (C7), 24.6 (C21, C31), 20.8 (C41), 15.2 (C22, C32); IR (KBr pellet, cm^{-1}) 3054 (w), 2954 (s), 2914 (m), 2859 (w), 2534 (sh), 2500 (vs), 2334 (sh), 1734 (w, br), 1634 (w, br), 1520 (w), 1486 (vw), 1444 (s), 1379 (m), 1364 (vw), 1334 (vw), 1228 (w), 1149 (sh), 1143 (w), 1067 (sh), 1060 (w), 1035 (w), 998 (w), 958 (w), 915 (vw), 892 (w), 875 (m), 839 (w), 818 (vw), 788 (w), 733 (w), 673 (w), 662 (vw), 620 (br), 505 (w, br), 466 (w). Anal. Calcd: C, 56.29; H, 7.99; B, 15.59. Found: C, 56.36; H, 8.11; B, 15.32.

In addition to 1-(η^6-$CH_3C_6H_5$)Fe-2,3-$(C_2H_5)_2C_2B_4H_4$, trace amounts of several other (toluene)metallacarboranes were isolated. Possible formulations for these metallacarboranes are as follows: (η^6-$CH_3C_6H_5$)Fe$(C_2H_5)_2C_2B_3H_5$ (R_f 0.91; yellow; 0.7 mg; mass measurement calcd for $^{12}C_{13}{}^1H_{23}{}^{11}B_3{}^{56}Fe$ 268.1428, found 268.1436 (73.31%); ^{11}B NMR (ppm, C_6D_6, 115.5 MHz) 2.8 (D, J_{BH} = 141 Hz), −0.3 (D, 2, J_{BH} = 132 Hz)), (η^6-$CH_3C_6H_5$)Fe$(C_2H_5)_2C_2B_7H_7$ (R_f 0.72; 0.8 mg; mass measurement calcd for $^{12}C_{13}{}^1H_{25}{}^{11}B_7{}^{56}Fe$ 314.1957, found 314.1978 (19.59%)), (η^6-$CH_3C_6H_5$)Fe-$(C_2H_5)_2C_2B_6H_8$ (R_f 0.70; 0.1 mg; mass measurement calcd for $^{12}C_{13}{}^1H_{24}{}^{11}B_6{}^{56}Fe$ 302.1786, found 302.1803(29.70%)), (η^6-$CH_3C_6H_5$)Fe$(C_2H_5)_4C_4B_8H_8$ (R_f 0.51; 0.1 mg; mass measurement calcd for $^{12}C_{19}{}^1H_{36}{}^{11}B_8{}^{56}Fe$ 408.2911, found 408.2954(33.52%)), and (η^6-$CH_3C_6H_5$)Fe$(C_2H_5)_4C_4B_7H_7$ (R_f 0.45; 0.5 mg; mass measurement calcd for $^{12}C_{19}{}^1H_{35}{}^{11}B_7{}^{56}Fe$ 396.2739, found 396.2755 (16.14%)).

Crystallographic Data for 1-(η^6-$CH_3C_6H_5$)Fe-2,3-$(C_2H_5)_2C_2B_4H_4$. Several crystals of the compound were grown overnight by crystallization in a methylene chloride/heptane solution at −3 °C. An irregularly shaped crystal, 0.300 × 0.175 × 0.125 mm, was selected for data collection, mounted on a glass fiber, and then transferred to the diffractometer. The Enraf-Nonius program SEARCH was used to obtain 25 reflections, which were then used in the program INDEX to obtain an orientation matrix for data collection. This orientation matrix was improved by the substitution of new reflections and refined cell dimensions, and their standard deviations were obtained from the least-squares refinement of these 25 accurately centered reflections. Crystal data: $FeC_{13}B_4H_{22}$, mol wt 277.41, space group $P2_1/c$, Z = 4, a = 8.200 (7) Å, b = 12.344 (4) Å, c = 14.759 (11) Å, β = 93.85 (6)°, V = 1491 (3) Å^3, ρ(calcd) = 1.236 g cm^{-3}. The mosaicity of the crystal was judged acceptable on the basis of several θ scans.

Collection and Reduction of Data. The diffraction data were collected at 295 K on an Enraf-Nonius four-circle CAD-4 diffractometer interfaced with a PDP 8/A computer, employing Mo Kα radiation from a highly oriented graphite crystal monochromator. A coupled 2θ–ω scan technique was used to record the intensities of all reflections for which $0° < 2\theta < 55°$ for $\pm h,k,\pm l$ and equivalent reflections averaged. The raw intensities were corrected for Lorentz and polarization effects by using the Enraf-Nonius program DATARD. Of the 3422 measured intensities, 1177 had $F_o^2 > 3\sigma(F_o^2)$ and were used in the analysis.

Solution and Refinement of Structure. All calculations were performed on a PDP 11/60 computer using the Enraf-Nonius structure determination package.[11]

Normalized structure factors were calculated by using a K curve, and the intensity distribution statistics support a centrosymmetric

(5) Zimmerman, G. J.; Hall, L. W.; Sneddon, L. G. *J. Chem. Soc., Chem. Commun.* **1977**, 45.
(6) Zimmerman, G. J.; Wilczynski, R.; Sneddon, L. G. *J. Organomet. Chem.* **1978**, *154*, C-29.
(7) Zimmerman, G. J.; Hall, L. W.; Sneddon, L. G. *Inorg. Chem.* **1980**, *19*, 3642.
(8) Hosmane, N. S.; Grimes, R. N. *Inorg. Chem.* **1979**, *18*, 3294.
(9) Klabunde, K. J.; Efner, H. F. *Inorg. Chem.* **1975**, *14*, 789.
(10) Freeman, M. B.; Hall, L. W.; Sneddon, L. G. *Inorg. Chem.* **1980**, *19*, 1132.
(11) Enraf-Nonius Inc., Garden City Park, NY.

Table I. Positional Parameters and Their Estimated Standard Deviations

atom	x	y	z	atom	x	y	z
Fe	0.7352 (1)	0.1117 (1)	0.36337 (9)	C8	0.645 (1)	0.2632 (9)	0.3879 (10)
C3	0.619 (1)	0.0816 (6)	0.2415 (6)	C22	0.948 (2)	0.0804 (12)	0.1044 (10)
C2	0.793 (1)	0.0742 (6)	0.2369 (6)	C32	0.429 (2)	0.0983 (10)	0.1043 (10)
C31	0.511 (1)	0.1491 (8)	0.1776 (8)	B6	0.871 (1)	−0.0116 (9)	0.3040 (7)
C21	0.882 (1)	0.1298 (9)	0.1662 (8)	B5	0.715 (1)	−0.0584 (9)	0.3551 (8)
C4	0.917 (1)	0.2084 (7)	0.4204 (6)	B4	0.553 (1)	0.0041 (9)	0.3111 (8)
C41	1.094 (2)	0.2170 (11)	0.3998 (9)	B7	0.693 (1)	−0.0500 (9)	0.2392 (8)
C5	0.873 (1)	0.1388 (7)	0.4821 (7)	HB6	1.000 (7)	−0.036 (5)	0.306 (4)
C6	0.714 (1)	0.1291 (9)	0.4978 (7)	HB5	0.716 (7)	−0.113 (4)	0.394 (4)
C9	0.803 (1)	0.2719 (7)	0.3734 (7)	HB4	0.410 (7)	−0.002 (5)	0.306 (4)
C7	0.600 (1)	0.1876 (10)	0.4526 (9)	HB7	0.675 (7)	−0.087 (4)	0.184 (4)

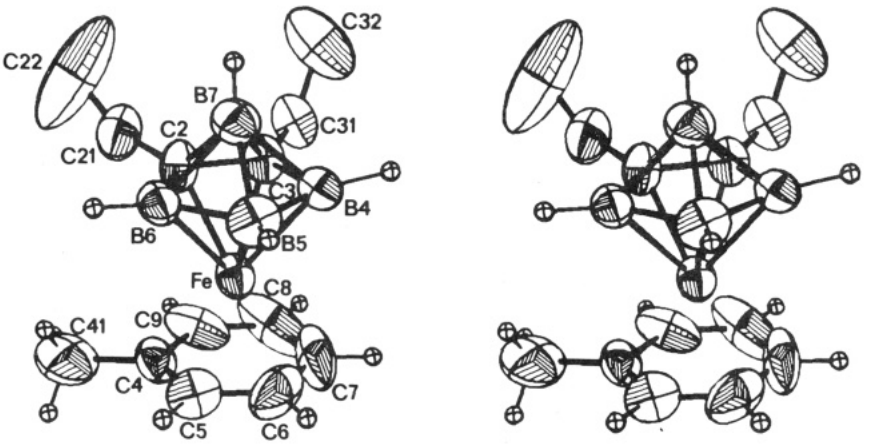

Figure 1. ORTEP stereodrawing of 1-(η^6-$CH_3C_6H_5$)Fe-2,3-$(C_2H_5)_2C_2B_4H_4$. Non-hydrogen atoms are shown as 30% thermal ellipsoids.

space group. A three-dimensional Patterson synthesis gave the coordinates of the iron atom. Full-matrix least-squares refinement of these coordinates, with use of preliminary scale and thermal parameters from the Wilson plot, followed by a subsequent Fourier map phased on these refined coordinates led to the location of the remaining heavy atoms of the complex. Anisotropic least-squares refinement of these atoms followed by a difference Fourier synthesis resulted in the location of the four hydrogen atoms bonded to the boron atoms. The positions of the remaining 18 hydrogen atoms were calculated and included (but not refined) in the structure factor calculations. Final refinement with an absorption correction (transmission coefficient: maximum 87.72%, minimum 84.64%) including anisotropic thermal parameters for non-hydrogen atoms and fixed isotropic thermal parameters (5.00) for the hydrogen atoms yielded the final residual factors $R = 0.071$ and $R_w = 0.079$.

Because of the relatively large thermal vibrations observed for the methyl (C22 and C32) and toluene ring (C6, C7, and C8) carbons, attempts were made to recollect the data at low temperature (−90 °C); however, this proved unsuccessful due to crystal decomposition. It should also be noted that the crystal apparently undergoes a phase change at low temperatures as evidenced by a conversion to an orthorhombic unit cell. This transformation is still under study.

The full-matrix least-squares refinement was based on F, and the function minimized was $\sum w(|F_o| - |F_c|)^2$. The weights (w) were taken as $(4F_o/\sigma(F_o)^2)^2$ where $|F_o|$ and $|F_c|$ are the observed and calculated structure factor amplitudes. The atomic scattering factors for non-hydrogen atoms were taken from Cromer and Waber[12a] and those for hydrogen[12b] from Stewart. The effects of anomalous dispersion were included in F_c by using Cromer and Ibers' values[13] for $\Delta f'$ and $\Delta f''$. Agreement factors are defined as $R = \sum||F_o| - |F_c||/\sum|F_o|$ and $R_w = (\sum w(|F_o| - |F_c|)^2/\sum w|F_o|^2)^{1/2}$.

The final positional parameters are given in Table I. Intramolecular bond distances and selected bond angles are presented in Tables II and III, respectively. Figure 1 shows a stereoscopic view of the complete molecule, while Figure 2 shows a unit cell packing diagram. Listings of final thermal parameters, selected molecular planes, and observed and calculated structure factors are available as supplementary material.

Table II. Bond Distances (Å)

Fe-C2	2.010 (6)	B4-B5	1.633 (10)
Fe-C3	2.011 (6)	B4-B7	1.745 (10)
Fe-B4	2.105 (7)	B4-HB4	1.17 (3)
Fe-B5	2.108 (7)	B5-B6	1.633 (9)
Fe-B6	2.112 (6)	B5-B7	1.710 (10)
Fe-B7	2.716 (8)	B5-HB5	0.89 (4)
Fe-C4	2.047 (6)	B6-B7	1.757 (10)
Fe-C5	2.047 (7)	B6-HB6	1.09 (4)
Fe-C6	2.015 (8)	B7-HB7	0.93 (4)
Fe-C7	2.011 (9)	C21-C22	1.250 (11)
Fe-C8	2.054 (9)	C31-C32	1.387 (9)
Fe-C9	2.056 (6)	C4-C41	1.507 (9)
C2-C3	1.432 (7)	C4-C5	1.321 (8)
C2-C21	1.480 (8)	C4-C9	1.373 (9)
C2-B6	1.559 (8)	C5-C6	1.342 (10)
C2-B7	1.739 (8)	C6-C7	1.328 (14)
C3-C31	1.503 (8)	C7-C8	1.402 (16)
C3-B4	1.528 (8)	C8-C9	1.334 (14)
C3-B7	1.734 (9)		

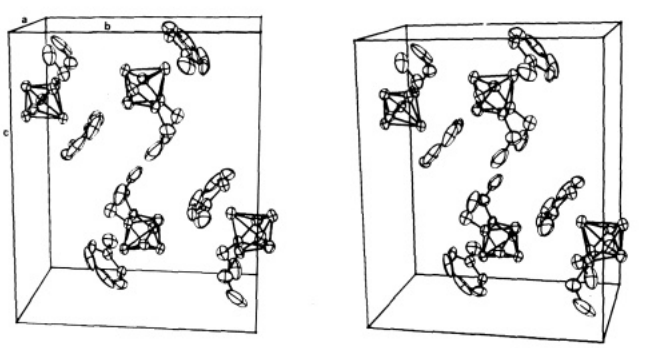

Figure 2. Molecular packing diagram.

(12) (a) Cromer, D. T.; Waber, J. T. "International Tables for X-ray Crystallography"; Kynoch Press: Birmingham, England, 1974; Vol. IV. (b) Stewart, R. F.; Davidson, E. R.; Simpson, W. J. *J. Chem. Phys.* **1965**, *43*, 3175.

(13) Cromer, D. T.; Ibers, J. A. "International Tables for X-ray Crystallography"; Kynoch Press: Birmingham, England, 1974; Vol. IV.

Table III. Selected Bond Angles (Deg)

C2-Fe-C3	41.7 (2)	Fe-B5-B7	90.0 (4)
C2-Fe-B6	44.4 (2)	B4-B5-B6	106.9 (6)
C3-Fe-B4	43.5 (2)	B4-B5-B7	62.9 (5)
B4-Fe-B5	45.6 (3)	B6-B5-B7	63.4 (4)
B5-Fe-B6	45.5 (3)	Fe-B6-C2	64.4 (3)
C4-Fe-C5	37.7 (2)	Fe-B6-B5	67.1 (3)
C4-Fe-C9	39.1 (3)	Fe-B6-B7	88.7 (4)
C5-Fe-C6	38.6 (3)	C2-B6-B5	103.3 (5)
C6-Fe-C7	38.5 (4)	C2-B6-B7	62.9 (4)
C7-Fe-C8	40.3 (5)	B5-B6-B7	60.5 (4)
C8-Fe-C9	37.9 (4)	C2-B7-C3	48.7 (3)
Fe-C2-C21	134.8 (4)	C2-B7-B6	53.0 (4)
Fe-C2-B7	92.5 (4)	C3-B7-B4	52.1 (4)
Fe-C2-C3	69.2 (3)	B4-B7-B5	56.4 (4)
Fe-C2-B6	71.3 (3)	B5-B7-B6	56.2 (4)
C3-C2-B6	112.4 (5)	C2-C21-C22	123.1 (9)
C3-C2-B7	65.5 (4)	C3-C31-C32	118.3 (7)
C3-C2-C21	122.8 (5)	Fe-C4-C41	130.1 (5)
B6-C2-B7	64.1 (4)	Fe-C4-C5	71.2 (4)
B6-C2-C21	124.2 (5)	Fe-C4-C9	70.8 (4)
B7-C2-C21	132.6 (5)	C5-C4-C9	120.6 (7)
Fe-C3-C31	133.0 (4)	C5-C4-C41	119.9 (8)
Fe-C3-B7	92.6 (4)	C9-C4-C41	119.4 (8)
Fe-C3-C2	69.1 (4)	Fe-C5-C4	71.2 (4)
Fe-C3-B4	71.5 (4)	Fe-C5-C6	69.4 (5)
C2-C3-B4	113.0 (5)	C4-C5-C6	119.5 (7)
C2-C3-B7	65.8 (4)	Fe-C6-C5	72.0 (4)
C2-C3-C31	123.5 (5)	Fe-C6-C7	70.6 (6)
B4-C3-B7	64.3 (4)	C5-C6-C7	121.6 (10)
B4-C3-C31	123.2 (5)	Fe-C7-C6	70.9 (5)
B7-C3-C31	134.3 (5)	Fe-C7-C8	71.5 (7)
Fe-B4-C3	65.0 (3)	C6-C7-C8	119.7 (11)
Fe-B4-B5	67.3 (4)	Fe-C8-C7	68.2 (6)
Fe-B4-B7	89.2 (4)	Fe-C8-C9	71.2 (5)
C3-B4-B5	104.3 (5)	C7-C8-C9	117.8 (12)
C3-B4-B7	63.6 (4)	Fe-C9-C4	70.1 (4)
B5-B4-B7	60.7 (4)	Fe-C9-C8	71.0 (5)
Fe-B5-B4	67.1 (4)	C4-C9-C8	120.7 (9)
Fe-B5-B6	67.4 (3)		

Results

The cocondensation at −196 °C of thermally generated iron atoms with toluene and the small carborane 2,3-$(C_2H_5)_2C_2B_4H_6$ followed by reaction at −78 °C was found to produce as the major product 1-(η^6-$CH_3C_6H_5$)Fe-2,3-$(C_2H_5)_2C_2B_4H_4$. The complex was isolated as a yellow, air-stable solid, which based on the spectroscopic data was proposed to have a structure in which the iron atom is sandwiched between an η^6-toluene ring and the open face of a 2,3-$(C_2H_5)_2C_2B_4H_4$ carborane cage. Both the ^{11}B NMR spectrum, which consists of three doublet resonances in the ratio 1:1:2, and the boron-decoupled ^{1}H NMR spectrum, which shows three B–H resonances also in a 1:1:2 ratio, indicate a local C_s symmetry for the ferracarborane cage. Since, as will be discussed below, the molecule does not possess a mirror plane in the solid state, this NMR data implies that the toluene and carborane cage must be freely rotating relative to each other in solution. The ethyl substituents of the carborane give rise to an apparent triplet resonance of intensity six (CH_3) and two multiplet resonances (ABX_3 pattern) arising from the inequivalent methylene protons. The η^6-coordination of the toluene is supported by the observed upfield shift of the aromatic ring protons relative to free toluene and by the ^{13}C NMR spectrum which is similar to those which have been reported for other (toluene)iron complexes,[14] including *closo*-1-(η^6-$CH_3C_6H_5$)-2,4-$(CH_3)_2$-1,2,4-$FeC_2B_9H_9$.[4] A single-crystal X-ray structural determination confirmed the sandwich nature of the complex as can be seen in the ORTEP stereodrawing given in Figure 1.

The structure is similar to those of other (arene)iron complexes derived from 2,3-$(C_2H_5)_2C_2B_4H_6$ such as 1-(η^6-C_6H_6)Fe-2,3-$(C_2H_5)_2C_2B_4H_4$, 1-(η^6-$(CH_3)_6C_6$)Fe-2,3-$(C_2H_5)_2C_2B_4H_4$, and 1-(η^6-$(CH_3)_3C_6H_3$)Fe-2,3-$(C_2H_5)_2C_2B_4H_4$, which have recently been synthesized and structurally characterized by Grimes.[15] The ferracarborane unit 1-Fe-2,3-$(C_2H_5)_2C_2B_4H_4$ has a structure based on a pentagonal bipyramid, consistent with its closo skeletal electron count (seven cage atoms, 16 skeletal electrons). The iron atom is symmetrically located in the open face of the carborane cage with average Fe–B and Fe–C distances of 2.108 (7) and 2.011 (6) Å, respectively. The remaining distances and angles in the ferracarborane cage are normal and similar to those observed in the other (arene)ferracarboranes cited above and with the isoelectronic cobaltacarborane cages in complexes such as 1-(η-C_5H_5)Co-2,3-$(CH_3)_2C_2B_4H_4$.[16] As can be seen in the figure, the methyl groups of the ethyl substituents on the carborane cage, particularly C22, have large thermal vibrations indicative of disordered orientations, and this disorder is undoubtedly the cause of the unrealistically short bond distance observed for C21–C22.

The iron atom is also bound in a symmetrical fashion to the toluene ring with an average Fe–ring carbon distance of 2.038 (9) Å. The average carbon–carbon distance in the η^6-toluene ring is 1.350 (16) Å, which is similar to that observed (room temperature) in other (η^6-toluene)metal complexes such as (η^6-$CH_3C_6H_5$)$Cr(CO)_3$,[17] 1.388 (8) Å, (η^6-$CH_3C_6H_5$)$Co(C_6F_5)_2$,[18] 1.391 (9) Å, and (η^6-$CH_3C_6H_5$)-$Ni(C_6F_5)_2$,[18] 1.387 (8) Å.

The basal ring of the carborane (C2, C3, B4, B5, and B6) and the toluene are parallel (dihedral angle 1.2°) but, as can be observed in the figure, are not oriented in a symmetrical fashion relative to each other. Thus, the plane (B7, B5, Fe) bisecting the ferracarborane cage is rotated 77.8° from the plane (Fe, C41, C4, C7) bisecting the iron–toluene unit. Since there are no serious inter- or intramolecular steric interactions, the reasons for the ring orientations are not apparent.

Also isolated from the reaction were a number of other ferracarborane–toluene complexes in amounts that were insufficient for complete characterization. However, the mass spectrum and ^{11}B NMR data for one of these compounds support its formulation as 1-(η^6-$CH_3C_6H_5$)Fe-2,3-$(C_2H_5)_2C_2B_3H_5$. Isoelectronic metallacarboranes such as 1-$(CO)_3$Fe-2,3-$C_2B_3H_7$[19] and 1-(η-C_5H_5)Co-2,3-$R_2C_2B_3H_5$,[20] R = H or alkyl, which contain a metal atom bound to a cyclic, planar $R_2C_2B_3H_5$ ligand are well-known and have generally been formed as side products of the reaction of organometallic reagents with 2,3-$C_2B_4H_8$. It is therefore reasonable that similar cage degradations during metal atom reactions should give rise to such complexes.

Exact mass measurements on four other complexes isolated in trace amounts are consistent with the formulas (η^6-$CH_3C_6H_5$)Fe$(C_2H_5)_2C_2B_7H_7$, (η^6-$CH_3C_6H_5$)Fe-

(14) Steele, B. R.; Sutherland, R. G.; Lee, C. C. *J. Chem. Soc., Dalton Trans.* **1981**, 529.

(15) Swisher, R. G.; Sinn, E.; Grimes, R. N. *Organometallics* **1983**, *2*, 506.

(16) Weiss, R.; Bryan, R. F. *Acta Crystallogr., Sect. B* **1977**, *B33*, 589.

(17) van Meurs, F.; van Koningsveld, H. *J. Organomet. Chem.* **1977**, *131*, 423.

(18) Radonovich, L. J.; Klabunde, K. J.; Behrens, C. B.; McCollor, D. P.; Anderson, B. B. *Inorg. Chem.* **1980**, *19*, 1221.

(19) (a) Grimes, R. N. *J. Am. Chem. Soc.* **1971**, *93*, 261. (b) Sneddon, L. G.; Beer, D. C.; Grimes, R. N. *Ibid.* **1973**, *95*, 6623. (c) Brennan, J. P.; Grimes, R. N.; Schaeffer, R.; Sneddon, L. G. *Inorg. Chem.* **1973**, *12*, 2266.

(20) Grimes, R. N.; Beer, D. C.; Sneddon, L. G.; Miller, V. R.; Weiss, R. *Inorg. Chem.* **1974**, *13*, 1138.

$(C_2H_5)_2C_2B_6H_6$, $(\eta^6\text{-}CH_3C_6H_5)Fe(C_2H_5)_4C_4B_8H_8$, and $(\eta^6\text{-}CH_3C_6H_5)Fe(C_2H_5)_4C_4B_7H_7$.

Discussion

The synthesis of dibenzene chromium was one of the earliest reported[21] applications of the metal atom technique to synthesis. Since that time these techniques have been used to prepare a wide variety of bis(arene) and mixed arene–ligand organometallic complexes.[22] In addition, it has been shown[23] that the cocondensation of either iron, cobalt, or nickel with toluene results in the formation of weakly bound (toluene)metal complexes which, although not isolable, have proven to be useful organometallic intermediates. For example, potential ligands can be added to these "solvated metal atoms" which can then displace the weakly coordinated toluene(s), yielding either (arene)ML_x or ML_x complexes.

In the present study the metal atom technique was also shown to be a potentially general method for the direct synthesis of (arene)metallacarborane complexes, as illustrated by the production of 1-$(\eta^6\text{-}CH_3C_6H_5)$Fe-2,3-$(C_2H_5)_2C_2B_4H_4$. It is important to note that the reaction procedure involved the cocondensation of iron atoms with the reactants, followed by warming to −78 °C for 40 min, before finally warming the mixture to room temperature. Previous work[23a,d,f] has demonstrated that iron atoms readily react with toluene at low temperatures but that the resulting Fe_x(arene)$_y$ complex is thermally unstable decomposing above −30 °C. Thus, in the reaction described herein the reactants were initially maintained at −78 °C to allow the formation of the (toluene)iron complex and to promote its reaction with the carborane.

The reaction of 2,3-$(C_2H_5)_2C_2B_4H_6$ with the iron–toluene complex may involve the displacement of coordinated toluene(s) followed by oxidative addition of a B–H group at the metal, thereby generating a reactive 16-electron species. This intermediate could then undergo hydrogen elimination accompanied by insertion of the iron into the open face of the carborane cage, yielding the final product.

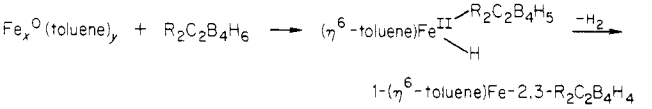

In this regard, Groshens and Klabunde have recently reported[24] that the codeposition of Ni atoms with toluene and $HSiCl_3$, followed by slow warming to room temperature, yields the complex $(\eta^6\text{-toluene})Ni(SiCl_3)_2$ and have proposed that the reaction sequence involves a similar oxidative addition of a Si–H group at the metal as a key step.

Although 1-$(\eta^6\text{-}CH_3C_6H_5)$Fe-2,3-$(C_2H_5)_2C_2B_4H_4$ was the major product of the reaction, several other (toluene)-ferracarborane complexes were formed in only trace amounts. Thus, the relatively mild, low-temperature conditions employed in metal atom reactions apparently minimized the cage degradation reactions which can lead to other products. Minor products of particular interest, however, were two complexes which, based on the high-resolution mass spectral data, were proposed to be $(CH_3C_6H_5)Fe(C_2H_5)_4C_4B_7H_7$ and $(CH_3C_6H_5)Fe(C_2H_5)_4C_4B_8H_8$. These large cage ferracarboranes, which are isoelectronic with the known nido 12- and 13-vertex cobaltacarboranes $(\eta\text{-}C_5H_5)Co(CH_3)_4C_4B_7H_7$[25] and $(\eta\text{-}C_5H_5)Co(CH_3)_4C_4B_8H_8$,[25a] must have been formed by the fusion of two $(C_2H_5)_2C_2B_4H_4$ carborane cages at the iron. These results suggest that by altering the metal atom reaction conditions, it may be possible to use these techniques to synthesize a wide range of larger fused cage systems.

In summary, we feel that metal vapor reactions can provide attractive, one-step synthetic routes to (arene)-metallacarborane complexes, and we are now investigating both the application of these reactions to the synthesis of other such systems and the development of new reaction techniques that will allow the large scale production of these complexes.

Acknowledgment. We thank the National Science Foundation and the Army Research Office for support of this work. We also thank Professor R. N. Grimes for communicating results of his work prior to publication.

Registry No. 1-$(\eta^6\text{-}CH_3C_6H_5)$Fe-2,3-$(C_2H_5)_2C_2B_4H_4$, 84583-02-8; 2,3-$(C_2H_5)_2C_2B_4H_6$, 80583-48-8.

Supplementary Material Available: Listings of selected molecular planes, calculated hydrogen positions, anisotropic temperature factors, and structure factor amplitudes (14 pages). Ordering information is given on any current masthead page.

(21) Timms, P. L. *J. Chem. Soc., Chem. Commun.* **1969**, 1033.

(22) For reviews see: (a) Silverthorn, W. E. *Adv. Organomet. Chem.* **1975**, *13*, 47. (b) Timms, P. L.; Turney, T. W. *Ibid.* **1977**, *15*, 53. (c) Blackborow, J. R.; Young, D. "Metal Vapour Synthesis in Organometallic Chemistry"; Springer-Verlag: Berlin, Heidelberg, New York, 1979. (d) Klabunde, K. J. "Chemistry of Free Atoms and Particles"; Academic Press: New York, 1980. (e) Gastinger, R. G.; Klzbunde, K. J. *Transition Met. Chem.* (Weinheim, Ger.) **1979**, *4*, 1.

(23) (a) Williams-Smith, D. L.; Wolf, L. R.; Skell, P. S. *J. Am. Chem. Soc.* **1972**, *94*, 4042. (b) Klabunde, K. J.; Efner, H. F.; Murdock, T. O.; Ropple, R. *Ibid.* **1976**, *98*, 1021. (c) Anderson, B. B.; Behrens, C. L.; Radonovich, L. J.; Klabunde, K. J. *Ibid.* **1976**, *98*, 5390. (d) Ittel, S. D.; Tolman, C. A. *J. Organomet. Chem.* **1979**, *172*, C47. (e) Gastinger, R. G.; Anderson, B. B.; Klabunde, K. J. *J. Am. Chem. Soc.* **1980**, *102*, 4959. (f) Beard, L. K.; Silvon, M. P.; Skell, P. S. *J. Organomet. Chem.* **1981**, *209*, 245. (g) Groshens, T. G.; Henne, B.; Bartak, D.; Klabunde, K. J. *Inorg. Chem.* **1981**, *20*, 3629.

(24) Groshens, T. J.; Klabunde, K. J. *Organometallics* **1982**, *1*, 564.

(25) (a) Maxwell, W. M.; Grimes, R. N. *Inorg. Chem.* **1979**, *18*, 2174. (b) Grimes, R. N.; Sinn, E.; Pipal, J. R. *Ibid.* **1980**, *19*, 2087. (c) Maynard, R. B.; Sinn, E.; Grimes, R. N. *Ibid.* **1981**, *20*, 1201.

Photochemical preparation of a new complex containing a monodentate dithiocarbamate ligand: tricarbonyl(.eta.5-cyclopentadienyl)(.eta.1-dimethylcarbamodithioato)tungsten(II)

Harmon B. Abrahamson, and Michael L. Freeman

Organometallics, **1983**, 2 (5), 679-681• DOI: 10.1021/om00077a018 • Publication Date (Web): 01 May 2002

Communications

Photochemical Preparation of a New Complex Containing a Monodentate Dithiocarbamate Ligand: Tricarbonyl(η^5-cyclopentadienyl)(η^1-dimethylcarbamodithioato)tungsten(II)

Harmon B. Abrahamson* and Michael L. Freeman

Department of Chemistry, University of Oklahoma Norman, Oklahoma 73019

Received September 14, 1982

Summary: The photolysis of $[(\eta^5\text{-}C_5H_5)(CO)_3W]_2$ in the presence of tetramethylthiuram disulfide, using either visible or ultraviolet irradiation, produces the title complex $(\eta^5\text{-}C_5H_5)(CO)_3WSC(S)N(CH_3)_2$, I, in good yield. This can be transformed to the known bidentate complex $(\eta^5\text{-}C_5H_5)(CO)_2WS_2CN(CH_3)_2$, II, either thermally or photochemically. Photolysis of the tungsten dimer in the presence of other organic disulfides, RSSR, produces in a similar fashion the simple coupling products $(\eta^5\text{-}C_5H_5)(CO)_3WSR$, and preliminary evidence for some of these is included.

Dithiocarbamates are widely used as ligands in transition-metal complexes.[1] Most syntheses result in the dithiocarbamate ligand being bonded to the metal in a symmetrical η^2 fashion, coordinating through both sulfur atoms to form a four-membered chelate ring, A. Very few complexes containing monodentate dithiocarbamate ligands B are known.[2] We would like to report the synthesis

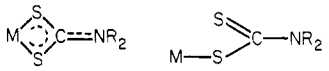

A B

of the title complex I, that is to our knowledge the first example of a monodentate dialkyldithiocarbamate complex of a group 6 metal. Previous attempts[3] to prepare cyclopentadienyl group 6 carbonyl dithiocarbamate complexes via thermal reactions have led to complexes containing a chelating dithiocarbamate ligand. We have discovered a room-temperature photochemical route to I, which appears to be the prototype for a general reaction of metal–metal single bonds and organic disulfides.

Both metal–metal bonded transition-metal carbonyl dimers[7,8] and dithiocarbamate complexes[9] react via apparently radical pathways. In the course of attempting to induce a new metal–metal interaction, we observed[10] that a tricarbonyl complex was the primary photoproduct when $Cp_2W_2(CO)_6$ and $Fe(Me_2dtc)_3$[11] were irradiated in the same solution. We hypothesized this complex to be compound I, since it could be converted easily to the known dicarbonyl chelate II. This assignment has been confirmed by the synthesis of I from $Cp_2W_2(CO)_6$ and the dimer of Me_2dtc—tetramethylthiuram disulfide, Me_4TDS,[12] a preliminary account of which is reported herein.

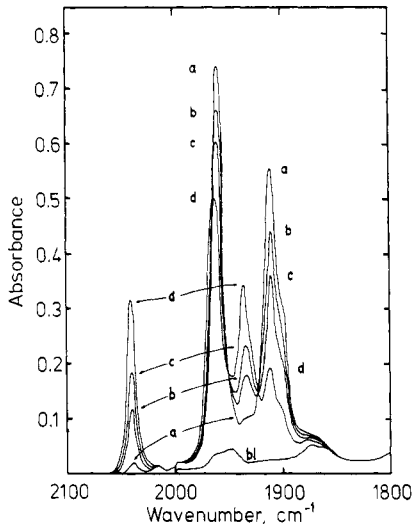

Figure 1. Infrared spectral changes (recorded in linear absorbance mode) resulting from visible light irradiation of a toluene solution of $Cp_2W_2(CO)_6$ and Me_4TDS, each at 7×10^{-3} M, in a 0.10-mm sealed solution cell under a nitrogen atmosphere. Cumulative irradiation times are 0, 15, 30, and 75 s for traces a–d respectively. The base-line absorption by toluene is denoted by bl. The small amount of reaction found at zero irradiation is caused by the visible component of the infrared beam.

When oxygen-free toluene solutions containing $Cp_2W_2(CO)_6$ and tetramethylthiuram disulfide (Me_4TDS) are irradiated with visible light,[13] the color of the solution changes from red to orange with a shift in the visible absorption maximum from 492 to 460 nm with an isosbestic point at 477 nm. At the same time, the carbonyl stretching bands of the metal dimer in the infrared spectrum decrease in intensity and new bands grow in with maintenance of isosbestic points (Figure 1). The product isolated from photolyzed solutions is the tricarbonyl complex **I**, formed

$$[(\eta^5\text{-}C_5H_5)W(CO)_3]_2 + Me_4TDS \xrightarrow{h\nu} \underset{\mathbf{I}}{2(\eta^5\text{-}C_5H_5)(CO)_3WSC(=S)NMe_2} \quad (1)$$

(1) For example, see: Steggerda, J. J.; Cras, J. A.; Willemse, J. *Recl. Trav. Chim. Pays-Bas* **1981**, *100*, 41–48.

(2) (a) Nagao, G.; Tanaka, K.; Tanaka, T. *Inorg. Chim. Acta* **1980**, *42*, 43–48. (b) Robertson, D. R.; Stephenson, T. A. *J. Chem. Soc., Dalton Trans.* **1978**, 486–495. (c) Alison, J. M. C.; Stephenson, T. A. *Ibid.* **1973**, 254–263. (d) Dubrawski, J. V.; Feltham, R. D. *Inorg. Chem.* **1980**, *19*, 355–363. (e) de Croon, M. H. J. M.; van Gaal, H. L. M.; van der Ent, A. *Inorg. Nucl. Chem. Lett.* **1974**, *10*, 1081–1086. (f) Busetto, L.; Palazzi, A.; Foliadis, V. *Inorg. Chim. Acta* **1980**, *40*, 147–152.

(3) This is true whether the reaction is metal carbonyl dimer plus tetraalkylthiuram disulfide[4] or metal carbonyl halide plus the sodium salt[5] or a tin complex[6] of the dialkyldithiocarbamate.

(4) Cotton, F. A.; McCleverty, J. A. *Inorg. Chem.* **1964**, *3*, 1398–1402.

(5) Glass, W. K.; Shiels, A. *J. Organomet. Chem.* **1974**, *67*, 401–405.

(6) Abel, E. W.; Dunster, M. O. *J. Chem. Soc., Dalton Trans.* **1973**, 98–102.

(7) Geoffroy, G. L.; Wrighton, M. S. "Organometallic Photochemistry"; Academic Press: New York, 1979.

(8) Chisolm, M. H.; Rothwell, I. P. *Prog. Inorg. Chem.* **1982**, *29*, 1–72.

(9) (a) Schwendiman, D. P.; Zink, J. I. *J. Am. Chem. Soc.* **1976**, *98*, 1248–1252, 4439–4443. (b) Miessler, G. L.; Zoebisch, E.; Pignolet, L. H. *Inorg. Chem.* **1978**, *17*, 3636–3644.

(10) Abrahamson, H. B. unpublished observations; this is true for both visible and ultraviolet irradiations.

(11) Abbreviations used in this paper: R_2dtc^- = dialkyldithiocarbamate (dialkylcarbamodithioate) $S_2CNR_2^-$; Cp = η^5-cyclopentadienyl.

(12) Me_4TDS = bis(dimethylthiocarbamyl) disulfide, $[SC(S)N(CH_3)_2]_2$.

(13) Visible irradiation source was a GE 40W high intensity desk lamp.

0276-7333/83/2302-0679$01.50/0

Table I. Carbonyl Region Infrared Data for $CpW(CO)_3SR$[a,f]

SR	ν_{CO},[b] cm^{-1}	ref
$SC(=S)N(CH_3)_2$	2040, 1962, 1933	this work
SC_5H_4N[c]	2036, 1958, 1935	this work
SCH_3	2028, 1942	this work
SCH_3	2030, 1943[d]	e
SC_6H_5	2033, 1947	this work
$SC_6H_4CH_3$	2033, 1948[d]	e

[a] Prepared in this work by the visible light photolysis of nitrogen-purged solutions of RSSR and $Cp_2W_2(CO)_6$ in an amalgam-sealed 0.10-mm NaCl cell. [b] In toluene solution unless otherwise noted. [c] 2-pyridyl sulfide. [d] CCl_4 solution. [e] Watkins, D. D.; George, T. A. *J. Organomet. Chem.* **1975**, *102*, 71-77. [f] Crystalline compounds for SR = S_2CNMe_2 and SC_6H_5 have been isolated and give satisfactory elemental analyses.

in the expected ratio of 2:1 (product:tungsten dimer consumed)[14] from the formal cross-coupling of the two dimers. Monochromatic 546-nm irradiation also effects this transformation. Since only the metal dimer and not the disulfide absorbs in this region, the primary photoprocess must involve an excited state of the metal dimer.[16] If traces of oxygen are present during photolysis, only uncharacterized decomposition products are found, as expected for a reaction proceeding through a reactive metal species. Radical species produced by homolysis of the metal–metal bond[7,8] must be viewed as the most likely intermediates, rather than unsaturated species resulting from loss of carbon monoxide,[17] since the dicarbonyl chelate II is not a prompt photoproduct.

The quantum yield for the production of I from the tungsten dimer is 0.36, and the quantum yield for disappearance of the dimer is 0.18.[18] These values are only marginally higher than those reported for the production of $CpW(CO)_3Cl$ from the 550-nm irradiation of the same tungsten dimer in carbon tetrachloride.[20a] The ratio of

Scheme I

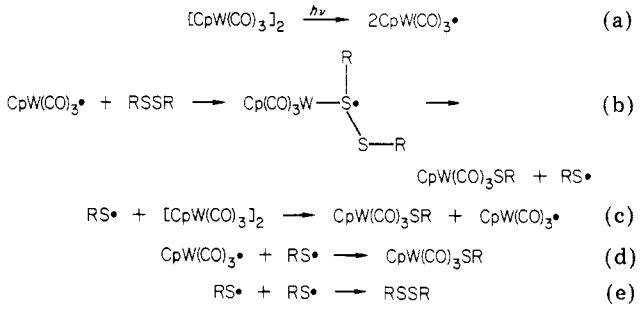

our two quantum yields is 2.0, in good accord with the overall stoichiometry of reaction 1. The fact that this reaction can be driven nearly to completion, even with only a 1:1 ratio of metal dimer and disulfide, demonstrates that both halves of the organic disulfide are used to produce product. No other bands are observed in the carbonyl stretching region of the infrared spectrum, and isosbestic points are maintained in both the infrared and electronic spectra to large conversions.

Ultraviolet irradiation is also effective in inducing reaction 1, but the product tricarbonyl I is photosensitive and with irradiation loses one carbon monoxide ligand to

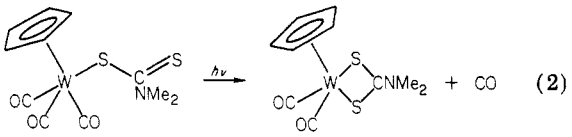

I). the known dicarbonyl chelate II.[21] Visible light is much less efficient in promoting this transformation, and under visible photolysis nearly all of the tungsten dimer can be converted to product I before transformation of I to II begins. Unlike reaction 1, reaction 2 proceeds even in the presence of air with no appreciable decomposition for short irradiation times. Reaction 2 can also be driven by heat as well as light; in fact, attempts to record the melting point of I resulted in decomposition of I to II in the melting point capillary at 106–108 °C.[22]

That the process represented in reaction 1 is a general one can be seen from the results of irradiation of other disulfides with $Cp_2W_2(CO)_6$ (Table I). In every case, the primary photoproduct is the tricarbonyl thiolate complex $CpW(CO)_3SR$ and is formed with the maintenance of isosbestic points in the infrared spectrum.

The detailed mechanism for reaction 1 probably involves attack of the photoproduced metal radical on the organic disulfide to produce an unstable intermediate that would quickly lose RS· to form product I (see Scheme Ib). The fate of the RS· radical so formed is less clear. One possibility is that it may attack a molecule of metal dimer to produce metal radical and product I (Scheme Ic). Since the quantum yields for formation of I are not very different from those for other photoreactions of the tungsten dimer,[20] we feel that a radical chain mechanism such as this is not likely. Another possibility is that the RS· radical is unreactive enough so that it exists in solution until it encounters another radical (metal or sulfur) with which

(14) Pure I can be separated from residual starting material by column chromatography and recrystallization from hexane. A recrystallized sample of I had a satisfactory elemental analysis (Schwarzkopf). Anal. Calcd for $C_{11}H_{11}NO_3S_2W$: C, 29.15; H, 2.45; N, 3.09; S, 14.15; W, 40.57; O (by difference), 10.59. Found: C, 29.15; H, 2.60; N, 3.35; S, 14.62; W, 40.03; O (by difference), 10.25. An infrared spectrum of I has peaks at 2046 (6.1), 1972 (10.0), and 1943 (10.0) cm^{-1} (hexane) and 2040 (8.7), 1962 (10.0), and 1933 (8.7) cm^{-1} (toluene). The electronic spectrum of I has a band at 460 nm (ϵ 1270 mol^{-1} L cm^{-1}) (toluene). The 60-MHz ^1H NMR spectrum (in $CDCl_3$) consists of two singlets, one at δ 3.59 (6 H, methyl) and another at δ 5.78 (5 H, cyclopentadienyl). The monodentate nature of the dithiocarbamate ligand is confirmed[15] by the presence of a doublet (1005 (m), 970 (s) cm^{-1}) for ν(CS) and a relatively low ν(C=N) (1487 (m) cm^{-1}) in a spectrum of the complex in a KBr pellet.

(15) For discussions of infrared evidence for mono- vs. bidentate coordination see: Bonati, F.; Ugo, R. *J. Organomet. Chem.* **1967**, *10*, 257–268. Nakamoto, K. "Infrared and Raman Spectra of Inorganic and Coordination Compounds", 3rd ed.; Wiley-Interscience: New York, 1978; p 339.

(16) Visible light cleaves the tungsten dimer with reasonable efficiency by exciting a $d\pi \rightarrow \sigma^*$ transition, see ref 20.

(17) (a) Tyler, D. R.; Schmidt, M. A.; Gray, H. B. *J. Am. Chem. Soc.* **1979**, *101*, 2753–2755. (b) Caspar, J. V.; Meyer, T. J. *Ibid.* **1980**, *102*, 7794–7795. (c) Fox, A.; Poe, A. *Ibid.* **1980**, *102*, 2497–2499.

(18) Quantum yields were measured on 3 mL of nitrogen-purged toluene solution containing $Cp_2W_2(CO)_6$ and Me_4TDS at the same concentration (4×10^{-4} M) in a 1-cm quartz cuvette capped with a rubber septum. The sample was irradiated with a 546-nm source (filtered medium-pressure Hg lamp), the strength of which was determined by Reineckate actinometry.[19] The concentrations of tungsten dimer and product I as a function of time were calculated from changes in absorbance at 492 and 460 nm. Quantum yields were determined for each irradiation time and extrapolated back to zero time over the first 20% of irradiation to obtain limiting quantum yield. (Some decrease in quantum yield at longer irradiation times was noted due to product absorption at the irradiation wavelength.)

(19) Wegner, E. E.; Adamson, A. W. *J. Am. Chem. Soc.* **1966**, *88*, 394–404.

(20) (a) Wrighton, M. S.; Ginley, D. S. *J. Am. Chem. Soc.* **1975**, *97*, 4246–4251. (b) Laine, R. M.; Ford, P. C. *Inorg. Chem.* **1977**, *16*, 388–391.

(21) The dicarbonyl can be recrystallized from CH_2Cl_2/hexane and displays an infrared spectrum identical with that previously reported: 1943 (10) and 1846 (8.5) cm^{-1} (CH_2Cl_2) and 1943 (10) and 1853 (7.2) cm^{-1} (toluene, this work); 1952 (10) and 1867 (7.3) cm^{-1} (cyclohexane)[6] and 1943 and 1854 cm^{-1} (carbon disulfide).[5]

(22) A sample of I was heated in a Hoover melting point apparatus, and decomposition was noted. The capillary was crushed, and the compound was dissolved in dichloromethane; an infrared spectrum of the resulting solution showed bands for both I and II.

it would combine to form either I or the starting disulfide (Scheme Id,e).[23]

We have found few previous reports of photolytic reactions of metal dimers with disulfides. Irradiation of $(CH_3S)_2$ and $[CpM(CO)_2]_2$, M = Fe[24] and Ru[25] together produces the corresponding $CpM(CO)_2(SR)$ complexes in fair yield; no speculation as to mechanism was advanced, although disulfide cleavage was implied in one case.[25] In other work, metal–metal bonded carbonyl complexes including $[CpM(CO)_3]_2$, M = Mo and W, were reacted with $(CF_3S)_2$[26] under ultraviolet photolysis. The coupling products formed are analogous to those found here (mononuclear MSR complexes) but were postulated to result from the cleavage of the disulfide as the primary photoprocess. Our results demonstrate that this type of reaction arises instead from an initial photoinduced homolytic cleavage of the metal–metal bond of the metal carbonyl dimer. Work is presently underway to ascertain the detailed mechanism of this new mode of metal carbonyl radical reactivity.

Acknowledgment. We wish to thank M. C. Palazzotto for a sample of Me_4TDS. Some initial experiments related to this work were performed at the Massachusetts Institute of Technology while H.B.A. was a Predoctoral Fellow of the National Science Foundation.

Registry No. I, 84693-74-3; II, 39531-00-5; $[(\eta^5\text{-}C_5H_5)(CO)_3W]_2$, 12091-65-5; $CpW(CO)_3SC_5H_4N$, 84680-94-4; $CpW(CO)_3SCH_3$, 12108-26-8; $CpW(CO)_3SC_6H_5$, 12110-93-9; $(CH_3)_2N(S)CSSC(S)N(CH_3)_2$, 137-26-8; $C_5H_4NSSC_5H_4N$, 2127-03-9; CH_3SSCH_3, 624-92-0; $C_6H_5SSC_6H_5$, 882-33-7.

(23) Cross-coupling of photogenerated thiyl radicals has been observed: Gupta, D.; Knight, A. R. *Can. J. Chem.* **1980**, *58*, 1350–1354.
(24) King, R. B.; Bisnette, M. B. *Inorg. Chem* **1965**, *4*, 482–485.
(25) Killops, S. D.; Knox, S. A. R. *J. Chem. Soc., Dalton Trans.* **1978**, 1260–1269. $(C_6H_5S)_2$ and $(C_6H_5CH_2S)_2$ were also used in this case.
(26) (a) Davidson, J. L.; Sharp, D. W. A. *J. Chem. Soc., Dalton Trans.* **1972**, 107–109. (b) Davidson, J. L.; Sharp, D. W. A. *Ibid.* **1973**, 1957–1960. $(C_6F_5S)_2$ was also used in this case.

Occurrence and Origin of a Pronounced Directing Effect of a Hydroxyl Group in Hydrogenation with $[Ir(cod)P\text{-}c\text{-}Hx_3(py)]PF_6$

Robert H. Crabtree* and Mark W. Davis

Sterling Chemistry Laboratory, Department of Chemistry
Yale University, New Haven, Connecticut 06511

Received October 15, 1982

Summary: $[Ir(cod)P\text{-}c\text{-}Hx_3(py)]PF_6$ has been shown to catalyze hydrogenation of an unsaturated alcohol, terpinen-4-ol, with a ca. 1000:1 preference for hydrogen addition to the face of the substrate bearing the OH group. This effect is due to chelation of the alcohol to the catalyst, as evidenced by the detection (^1H NMR, 0 °C) of a catalyst–substrate complex related to the proposed intermediate *cis,trans*-$[IrH_2(endo\text{-}5\text{-norbornen-2-ol})(PPh_3)_2]BF_4$.

The control of stereochemistry in transformations of organic compounds is an important area in which organometallic chemistry has been able to make useful contributions.[1] Since our catalyst[2] $[Ir(cod)P\text{-}c\text{-}Hx_3(py)]PF_6/CH_2Cl_2$ (cod = 1,5-cyclooctadiene; c-Hx = cyclohexyl; py = pyridine) binds ROH strongly, we wondered whether the presence of an OH group on one face of a suitable substrate might steer H_2 addition to that face.

Only rarely have such steering effects been observed in homogeneous hydrogenation. In the best known case,[3] an alkoxide, formed from the substrate, was bound to Wilkinson's catalyst. Under relatively severe conditions (50 °C (7 atm)), H_2 addition took place from the face of the molecule containing the OH group.

In order to be generally useful, first, the catalyst should be able to reduce tri- and tetrasubstituted C=C groups, so that any directing effect would be widely applicable to organic synthesis; the effect can only give distinct stereoisomeric products for tetra-, tri-, and 1,1-disubstituted olefins. Second, a substantial directing effect should be obtained with a common unmodified group such as OH. The catalyst system $[Ir(cod)P\text{-}c\text{-}Hx_3(py)]PF_6$, when dissolved in a noncoordinating solvent, e.g., CH_2Cl_2, fulfills these conditions.

We find that terpinen-4-ol[4] 1, is reduced by Pd/C in EtOH to give a 20:80 ratio of **2a** and **2b** in which H_2 has been preferentially added from the less hindered side of the molecule[5] (eq 1). In cyclohexane, a 53:47 ratio was

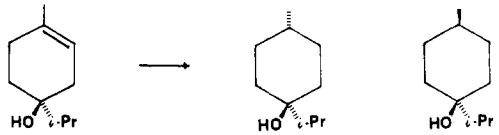

(1)

	1	2a	2b
Pd/C		20	80
$Ir(cod)(PCy_3)(py)^+$		99.9	0.1

found. In contrast, the iridium catalyst gives at least a 1000:1 ratio,[5d] the predominant isomer being the one (**2a**) in which H_2 has been added from the more hindered side of the molecule. (Conditions: 0 °C; CH_2Cl_2, 15 mL; H_2, 1 atm; catalyst, 10 mM; substrate, 0.43 M; reaction time, 90 min.) This degree of selectivity is exceptionally high and is attained neither with heterogeneous catalysts, in which binding to the OH is not as strong, nor among other homogeneous catalysts,[6] where not only is binding usually

(1) Sharpless, K. B.; Yezhoeven, T. R. *Aldrichimica Acta* **1979**, *12*, 63. Kishi Y. *Ibid.* **1980**, *13*, 23.

(2) (a). Crabtree, R. H.; Felkin, H.; Morris, G. E. *J. Organomet. Chem.* **1977**, *141*, 205. (b) Crabtree, R. H.; Demou, P. C. Eden, D.; Mihelcic, J. M.; Parnell, C. A.; Quirk, J. M.; Morris, G. E. *J. Am. Chem. Soc.* **1982**, *104*, 6994.
(3) Thompson, H. W.; McPherson, E. *J. Am. Chem. Soc.* **1974**, *96*, 6232.
(4) Our sample was obtained from Aldrich Chemical Co. and contained no **2**. Minor impurities (~5%) were present in 1, but these did not interfere with our product analyses.
(5) (a) **2a**: mp 51.0–51.5 °C (lit.[5b] 51–52 °C); ^1H NMR (500 MHz, Brucker instrument, $CDCl_3$) δ 0.908 (d, J = 6.8 Hz, Me), 0.918 (d, J = 6.7 Hz, i-Pr); IR ν(OH) 3618 cm^{-1}. Anal. Calcd for $C_{10}H_{20}O$: C, 76.86; H, 12.90. Found: C, 76.93; H, 12.81. **2b**: n^{25}_D 1.459 (lit.[5b] n^{20}_D 1.461); ^1H NMR δ 0.919 (d, J = 6.8 Hz, Me and *i*-Pr) (the overlapping doublets were resolved with $Eu(fod)_3$); IR ν(OH) 3619 cm^{-1}. The stereochemistry of this series of terpenes was first established by Pascual and Coll;[5c] it is still accepted.[5b] (b) Bowman, R. M.; Chambers, A.; Jackson, W. R. *J. Chem. Soc. C* **1966**, 612. Schenk, G. O.; Gollnick, K.; Buchwald, G.; Schroeter, S.; Ohloff, G. *Justus Liebig's Ann. Chem.* **1964**, *674*, 93, 98. (c) Pascual, J.; Coll, C. *An. Quim.* **1953**, *49*, 547, 553. (d) Essentially only **2a** was formed with the Ir catalyst (GC, Perkin-Elmer Model 900, flame ionization detector, $^1/_8$ in. × 13 ft 5% FFAP on Chromosorb P/AW; integration was performed with a Hewlett-Packard 3390A Digital Integrator). Essentially no **2b** was formed with the Ir catalyst. Our 1000:1 ratio arises from a consideration of the probably experimental error and respresents an upper limit for **2b**.

0276-7333/83/2302-0681$01.50/0

Occurrence and origin of a pronounced directing effect of a hydroxyl group in hydrogenation with [Ir(cod)P(C6H11)3(py)]PF6

Robert H. Crabtree, and Mark W. Davis

Organometallics, **1983**, 2 (5), 681-682• DOI: 10.1021/om00077a019 • Publication Date (Web): 01 May 2002

it would combine to form either I or the starting disulfide (Scheme Id,e).[23]

We have found few previous reports of photolytic reactions of metal dimers with disulfides. Irradiation of $(CH_3S)_2$ and $[CpM(CO)_2]_2$, M = Fe[24] and Ru[25] together produces the corresponding $CpM(CO)_2(SR)$ complexes in fair yield; no speculation as to mechanism was advanced, although disulfide cleavage was implied in one case.[25] In other work, metal–metal bonded carbonyl complexes including $[CpM(CO)_3]_2$, M = Mo and W, were reacted with $(CF_3S)_2$[26] under ultraviolet photolysis. The coupling products formed are analogous to those found here (mononuclear MSR complexes) but were postulated to result from the cleavage of the disulfide as the primary photoprocess. Our results demonstrate that this type of reaction arises instead from an initial photoinduced homolytic cleavage of the metal–metal bond of the metal carbonyl dimer. Work is presently underway to ascertain the detailed mechanism of this new mode of metal carbonyl radical reactivity.

Acknowledgment. We wish to thank M. C. Palazzotto for a sample of Me_4TDS. Some initial experiments related to this work were performed at the Massachusetts Institute of Technology while H.B.A. was a Predoctoral Fellow of the National Science Foundation.

Registry No. I, 84693-74-3; II, 39531-00-5; $[(\eta^5\text{-}C_5H_5)(CO)_3W]_2$, 12091-65-5; $CpW(CO)_3SC_5H_4N$, 84680-94-4; $CpW(CO)_3SCH_3$, 12108-26-8; $CpW(CO)_3SC_6H_5$, 12110-93-9; $(CH_3)_2N(S)CSSC(S)N(CH_3)_2$, 137-26-8; $C_5H_4NSSC_5H_4N$, 2127-03-9; CH_3SSCH_3, 624-92-0; $C_6H_5SSC_6H_5$, 882-33-7.

(23) Cross-coupling of photogenerated thiyl radicals has been observed: Gupta, D.; Knight, A. R. *Can. J. Chem.* **1980**, *58*, 1350–1354.
(24) King, R. B.; Bisnette, M. B. *Inorg. Chem* **1965**, *4*, 482–485.
(25) Killops, S. D.; Knox, S. A. R. *J. Chem. Soc., Dalton Trans.* **1978**, 1260–1269. $(C_6H_5S)_2$ and $(C_6H_5CH_2S)_2$ were also used in this case.
(26) (a) Davidson, J. L.; Sharp, D. W. A. *J. Chem. Soc., Dalton Trans.* **1972**, 107–109. (b) Davidson, J. L.; Sharp, D. W. A. *Ibid.* **1973**, 1957–1960. $(C_6F_5S)_2$ was also used in this case.

Occurrence and Origin of a Pronounced Directing Effect of a Hydroxyl Group in Hydrogenation with $[Ir(cod)P\text{-}c\text{-}Hx_3(py)]PF_6$

Robert H. Crabtree* and Mark W. Davis

Sterling Chemistry Laboratory, Department of Chemistry
Yale University, New Haven, Connecticut 06511

Received October 15, 1982

Summary: $[Ir(cod)P\text{-}c\text{-}Hx_3(py)]PF_6$ has been shown to catalyze hydrogenation of an unsaturated alcohol, terpinen-4-ol, with a ca. 1000:1 preference for hydrogen addition to the face of the substrate bearing the OH group. This effect is due to chelation of the alcohol to the catalyst, as evidenced by the detection (^1H NMR, 0 °C) of a catalyst–substrate complex related to the proposed intermediate *cis,trans*-$[IrH_2(endo\text{-}5\text{-norbornen-2-ol})(PPh_3)_2]BF_4$.

The control of stereochemistry in transformations of organic compounds is an important area in which organometallic chemistry has been able to make useful contributions.[1] Since our catalyst[2] $[Ir(cod)P\text{-}c\text{-}Hx_3(py)]PF_6/CH_2Cl_2$ (cod = 1,5-cyclooctadiene; c-Hx = cyclohexyl; py = pyridine) binds ROH strongly, we wondered whether the presence of an OH group on one face of a suitable substrate might steer H_2 addition to that face.

Only rarely have such steering effects been observed in homogeneous hydrogenation. In the best known case,[3] an alkoxide, formed from the substrate, was bound to Wilkinson's catalyst. Under relatively severe conditions (50 °C (7 atm)), H_2 addition took place from the face of the molecule containing the OH group.

In order to be generally useful, first, the catalyst should be able to reduce tri- and tetrasubstituted C=C groups, so that any directing effect would be widely applicable to organic synthesis; the effect can only give distinct stereoisomeric products for tetra-, tri-, and 1,1-disubstituted olefins. Second, a substantial directing effect should be obtained with a common unmodified group such as OH. The catalyst system $[Ir(cod)P\text{-}c\text{-}Hx_3(py)]PF_6$, when dissolved in a noncoordinating solvent, e.g., CH_2Cl_2, fulfills these conditions.

We find that terpinen-4-ol[4] 1, is reduced by Pd/C in EtOH to give a 20:80 ratio of **2a** and **2b** in which H_2 has been preferentially added from the less hindered side of the molecule[5] (eq 1). In cyclohexane, a 53:47 ratio was

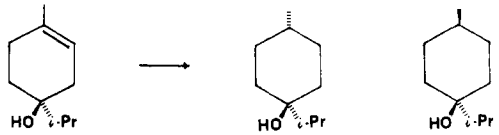

(1)

	1	2a	2b
Pd/C		20	80
$Ir(cod)(PCy_3)(py)^+$		99.9	0.1

found. In contrast, the iridium catalyst gives at least a 1000:1 ratio,[5d] the predominant isomer being the one (**2a**) in which H_2 has been added from the more hindered side of the molecule. (Conditions: 0 °C; CH_2Cl_2, 15 mL; H_2, 1 atm; catalyst, 10 mM; substrate, 0.43 M; reaction time, 90 min.) This degree of selectivity is exceptionally high and is attained neither with heterogeneous catalysts, in which binding to the OH is not as strong, nor among other homogeneous catalysts,[6] where not only is binding usually

(1) Sharpless, K. B.; Yezhoeven, T. R. *Aldrichimica Acta* **1979**, *12*, 63. Kishi Y. *Ibid.* **1980**, *13*, 23.

(2) (a). Crabtree, R. H.; Felkin, H.; Morris, G. E. *J. Organomet. Chem.* **1977**, *141*, 205. (b) Crabtree, R. H.; Demou, P. C. Eden, D.; Mihelcic, J. M.; Parnell, C. A.; Quirk, J. M.; Morris, G. E. *J. Am. Chem. Soc.* **1982**, *104*, 6994.
(3) Thompson, H. W.; McPherson, E. *J. Am. Chem. Soc.* **1974**, *96*, 6232.
(4) Our sample was obtained from Aldrich Chemical Co. and contained no **2**. Minor impurities (~5%) were present in 1, but these did not interfere with our product analyses.
(5) (a) **2a**: mp 51.0–51.5 °C (lit.[5b] 51–52 °C); ^1H NMR (500 MHz, Brucker instrument, $CDCl_3$) δ 0.908 (d, J = 6.8 Hz, Me), 0.918 (d, J = 6.7 Hz, i-Pr); IR ν(OH) 3618 cm^{-1}. Anal. Calcd for $C_{10}H_{20}O$: C, 76.86; H, 12.90. Found: C, 76.93; H, 12.81. **2b**: n^{25}_D 1.459 (lit.[5b] n^{20}_D 1.461); ^1H NMR δ 0.919 (d, J = 6.8 Hz, Me and *i*-Pr) (the overlapping doublets were resolved with $Eu(fod)_3$); IR ν(OH) 3619 cm^{-1}. The stereochemistry of this series of terpenes was first established by Pascual and Coll;[5c] it is still accepted.[5b] (b) Bowman, R. M.; Chambers, A.; Jackson, W. R. *J. Chem. Soc. C* **1966**, 612. Schenk, G. O.; Gollnick, K.; Buchwald, G.; Schroeter, S.; Ohloff, G. *Justus Liebig's Ann. Chem.* **1964**, *674*, 93, 98. (c) Pascual, J.; Coll, C. *An. Quim.* **1953**, *49*, 547, 553. (d) Essentially only **2a** was formed with the Ir catalyst (GC, Perkin-Elmer Model 900, flame ionization detector, $^1/_8$ in. × 13 ft 5% FFAP on Chromosorb P/AW; integration was performed with a Hewlett-Packard 3390A Digital Integrator). Essentially no **2b** was formed with the Ir catalyst. Our 1000:1 ratio arises from a consideration of the probably experimental error and respresents an upper limit for **2b**.

0276-7333/83/2302-0681$01.50/0

weaker but also catalytic activity is usually insufficient to reduce the trisubstituted C=C group. Complex **3** is a

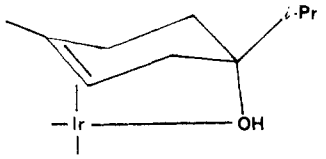

3

plausible intermediate in this process. We wished to try to observe such a species at low temperature. In our previous work in the area we found that the $[Ir(cod)P\text{-}c\text{-}Hx_3(py)]^+$ system, while it was the most active catalyst, did not allow observation of catalytic intermediates. For this we turned to the closely related $[Ir(cod)(PPh_3)_2]^+$ system, a poor catalyst.[7] Our studies[2] have suggested a close mechanistic parallel between the two cases.

A ^1H NMR study of the chemistry of **1** with $[Ir(cod)(PPh_3)_2]^+$ showed that a number of species was formed on hydrogenation. We imagine that the OH group of **1** binds more efficiently than does the C=C group, as we have found[2] in competition experiments between alcohols and olefins. No complex of type **3** could be detected, and it may never be present in other than trace amounts. In order to increase the binding constant of the C=C group so that a chelate could be formed, we used *endo*-5-norbornen-2-ol, **4**. The strain present in the C=C group was expected to lead to a higher binding constant. We did observe a single organometallic product on hydrogenating $[Ir(cod)(PPh_3)_2]^+$ in the presence of **4** or by treating $[IrH_2(Me_2CO)_2(PPh_3)_2]^+$ with **4**. This product was shown by ^1H NMR spectroscopy at 0 °C to be **5** (see eq. 2).

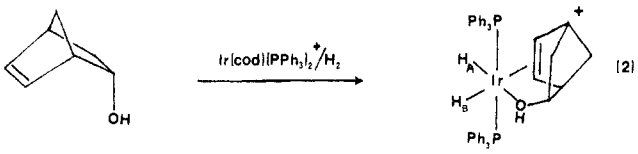

4 5

When **5** was prepared from the acetone complex, it was formed in ca. 70% yield in equilibrium with the acetone complex itself, so the binding is not particularly strong. Indeed, too strong a binding would inhibit catalysis. No other norbornenol complexes can be detected, suggesting this ligand has no significant tendency toward monodentate binding.

Complex **5** is the isomer expected by analogy with the known configuration[2] of nonchelating analogs such as $[IrH_2(C_2H_4)(H_2O)(PPh_3)_2]^+$. Two IrH resonances are observed. One, H_A, has a chemical shift (δ −29.4) characteristic for IrH trans to an oxygen ligand (typical range δ −29 to −32) and the other, H_B, a shift (δ −9.6) characteristic[2] for IrH trans to an olefin (typical range δ −9 to −14). The two resonances arise from the same molecule as coupling is observed between H_A and H_B ($^2J(H,H)$ = 5.5 Hz). The coupling to phosphorus shows that two inequivalent phosphorus nuclei are present, as expected on the basis of structure **5** (e.g., $^2J(H_A, P)$ = 11 and 24 Hz). When being warmed to +30 °C the complex decomposes, apparently by simple loss of H_2.

We propose that the key intermediate in the directing effect observed is of type **5**. Since ROH binds more strongly[2] to the catalyst than does an olefin, we do not expect that binding of the catalyst to the face of compound **1** opposite the OH group is likely, although we cannot rule it out completely. The chemical yield of **2a** was 95%. In contrast, much lower yields are usually observed for the reduction of simple trisubstituted olefins not bearing OH groups, due to deactivation of the catalyst by trimerization. The presence of the OH group does, however, decrease the rate of reduction from ca. 4000 mol of H_2 (mol of Ir)$^{-1}$ h^{-1} for 1-methylcyclohexene to 30 mol of H_2 (mol of Ir)$^{-1}$ h^{-1} for **1**. The OH group therefore protects the catalyst but slows the rate of reduction.

We have shown[8] that a hydroxyl group can direct the stereochemistry of hydrogenation with $[Ir(cod)P\text{-}c\text{-}Hx_3(py)]^+$ and that this probably occurs by a chelated intermediate of type **5**, of which we have studied one example.

Further work is in hand on the effects of different functional groups and substitution patterns.

Acknowledgment. We thank the National Science Foundation, the donors of the Petroleum Research Fund, administered by the American Chemical Society, and the Exxon Educational Foundation for support. M.W.D. gratefully acknowledges support as an F. W. Heyl and Elsie L. Heyl Fellow, and R.H.C. thanks the A.P. Sloan and Henry and Camille Dreyfus Foundations for fellowships.

Registry No. **1**, 562-74-3; **2a**, 3239-02-9; **2b**, 3239-03-0; **4**, 694-97-3; **5**, 84558-26-9; $[Ir(cod)P(c\text{-}Hx_3)(py)]PF_6$, 64536-78-3.

(6) Osborn, J. A.; Jardine, F. H.; Young, J. F.; Wilkinson, G. *J. Chem. Soc. A* **1966**, 1711.
(7) Crabtree, R. H.; Felkin, H.; Fellebeen-Khan, T.; Morris, G. E. *J. Organomet. Chem.* **1979**, *168*, 183.
(8) Stork et al.[9] and Brown and Naik[10] have independently found similar directing effects in the reduction of unsaturated alcohols with $[Ir(cod)Pc\text{-}Hx_3(py)]PF_6/CH_2Cl_2$ and $[Rh(nbd)(PPh_2C_4H_8PPh_2)]BF_4/CH_2Cl_2$, respectively. In the latter case only 1,1-disubstituted olefins were reduced; the iridium catalyst, being more active, is free from this limitation.
(9) Stork, G., personal communication, 1982.
(10) Brown, J. M.; Naik, R. G. *J. Chem. Soc., Chem. Commun.* **1982**, 348.

Stereoselective Formation of Iridium(III) Amides and Ligand-Assisted Heterolytic Splitting of Dihydrogen

Michael D. Fryzuk* and Patricia A. MacNeil
Department of Chemistry
University of British Columbia
Vancouver, British Columbia, Canada V6T 1Y6

Received November 9, 1982

Summary: A series of octahedral iridium(III) amides are formed stereoselectively from four- and five-coordinate precursors. In addition, an unusual ligand-assisted heterolytic splitting of dihydrogen is observed.

We have recently reported[1] that the iridium(I) amido phosphine complex $[Ir(COE)N(SiMe_2CH_2PPh_2)_2]$ (**1**), where COE = η^2-cyclooctene, acts as an efficient catalyst precursor for the homogeneous hydrogenation of simple olefins. In an effort to delineate the mechanism of this process, we investigated a number of stoichiometric oxidative addition and substitution processes to monitor the fate of the square-planar iridium(I) amide precursor. In this communication, we describe (i) the first examples of iridium(III) amides, (ii) a series of completely stereose-

(1) Fryzuk, M. D.; MacNeil, P. A. *Organometallics* **1983**, *2*, 355.

0276-7333/83/2302-0682$01.50/0

weaker but also catalytic activity is usually insufficient to reduce the trisubstituted C=C group. Complex **3** is a

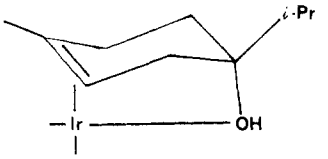

3

plausible intermediate in this process. We wished to try to observe such a species at low temperature. In our previous work in the area we found that the $[Ir(cod)P\text{-}c\text{-}Hx_3(py)]^+$ system, while it was the most active catalyst, did not allow observation of catalytic intermediates. For this we turned to the closely related $[Ir(cod)(PPh_3)_2]^+$ system, a poor catalyst.[7] Our studies[2] have suggested a close mechanistic parallel between the two cases.

A ^1H NMR study of the chemistry of **1** with $[Ir(cod)(PPh_3)_2]^+$ showed that a number of species was formed on hydrogenation. We imagine that the OH group of **1** binds more efficiently than does the C=C group, as we have found[2] in competition experiments between alcohols and olefins. No complex of type **3** could be detected, and it may never be present in other than trace amounts. In order to increase the binding constant of the C=C group so that a chelate could be formed, we used *endo*-5-norbornen-2-ol, **4**. The strain present in the C=C group was expected to lead to a higher binding constant. We did observe a single organometallic product on hydrogenating $[Ir(cod)(PPh_3)_2]^+$ in the presence of **4** or by treating $[IrH_2(Me_2CO)_2(PPh_3)_2]^+$ with **4**. This product was shown by ^1H NMR spectroscopy at 0 °C to be **5** (see eq. 2).

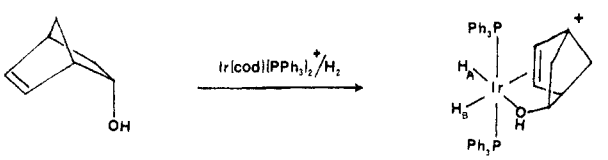

(2)

4 5

When **5** was prepared from the acetone complex, it was formed in ca. 70% yield in equilibrium with the acetone complex itself, so the binding is not particularly strong. Indeed, too strong a binding would inhibit catalysis. No other norbornenol complexes can be detected, suggesting this ligand has no significant tendency toward monodentate binding.

Complex **5** is the isomer expected by analogy with the known configuration[2] of nonchelating analogs such as $[IrH_2(C_2H_4)(H_2O)(PPh_3)_2]^+$. Two IrH resonances are observed. One, H_A, has a chemical shift (δ −29.4) characteristic for IrH trans to an oxygen ligand (typical range δ −29 to −32) and the other, H_B, a shift (δ −9.6) characteristic[2] for IrH trans to an olefin (typical range δ −9 to −14). The two resonances arise from the same molecule as coupling is observed between H_A and H_B ($^2J(H,H)$ = 5.5 Hz). The coupling to phosphorus shows that two inequivalent phosphorus nuclei are present, as expected on the basis of structure **5** (e.g., $^2J(H_A, P)$ = 11 and 24 Hz). When being warmed to +30 °C the complex decomposes, apparently by simple loss of H_2.

We propose that the key intermediate in the directing effect observed is of type **5**. Since ROH binds more strongly[2] to the catalyst than does an olefin, we do not expect that binding of the catalyst to the face of compound **1** opposite the OH group is likely, although we cannot rule it out completely. The chemical yield of **2a** was 95%. In contrast, much lower yields are usually observed for the reduction of simple trisubstituted olefins not bearing OH groups, due to deactivation of the catalyst by trimerization. The presence of the OH group does, however, decrease the rate of reduction from ca. 4000 mol of H_2 (mol of Ir)$^{-1}$ h^{-1} for 1-methylcyclohexene to 30 mol of H_2 (mol of Ir)$^{-1}$ h^{-1} for **1**. The OH group therefore protects the catalyst but slows the rate of reduction.

We have shown[8] that a hydroxyl group can direct the stereochemistry of hydrogenation with $[Ir(cod)P\text{-}c\text{-}Hx_3(py)]^+$ and that this probably occurs by a chelated intermediate of type **5**, of which we have studied one example.

Further work is in hand on the effects of different functional groups and substitution patterns.

Acknowledgment. We thank the National Science Foundation, the donors of the Petroleum Research Fund, administered by the American Chemical Society, and the Exxon Educational Foundation for support. M.W.D. gratefully acknowledges support as an F. W. Heyl and Elsie L. Heyl Fellow, and R.H.C. thanks the A.P. Sloan and Henry and Camille Dreyfus Foundations for fellowships.

Registry No. **1**, 562-74-3; **2a**, 3239-02-9; **2b**, 3239-03-0; **4**, 694-97-3; **5**, 84558-26-9; $[Ir(cod)P(c\text{-}Hx_3)(py)]PF_6$, 64536-78-3.

(6) Osborn, J. A.; Jardine, F. H.; Young, J. F.; Wilkinson, G. *J. Chem. Soc. A* **1966**, 1711.
(7) Crabtree, R. H.; Felkin, H.; Fellebeen-Khan, T.; Morris, G. E. *J. Organomet. Chem.* **1979**, *168*, 183.
(8) Stork et al.[9] and Brown and Naik[10] have independently found similar directing effects in the reduction of unsaturated alcohols with $[Ir(cod)Pc\text{-}Hx_3(py)]PF_6/CH_2Cl_2$ and $[Rh(nbd)(PPh_2C_4H_8PPh_2)]BF_4/CH_2Cl_2$, respectively. In the latter case only 1,1-disubstituted olefins were reduced; the iridium catalyst, being more active, is free from this limitation.
(9) Stork, G., personal communication, 1982.
(10) Brown, J. M.; Naik, R. G. *J. Chem. Soc., Chem. Commun.* **1982**, 348.

Stereoselective Formation of Iridium(III) Amides and Ligand-Assisted Heterolytic Splitting of Dihydrogen

Michael D. Fryzuk* and Patricia A. MacNeil
Department of Chemistry
University of British Columbia
Vancouver, British Columbia, Canada V6T 1Y6

Received November 9, 1982

Summary: A series of octahedral iridium(III) amides are formed stereoselectively from four- and five-coordinate precursors. In addition, an unusual ligand-assisted heterolytic splitting of dihydrogen is observed.

We have recently reported[1] that the iridium(I) amido phosphine complex $[Ir(COE)N(SiMe_2CH_2PPh_2)_2]$ (**1**), where COE = η^2-cyclooctene, acts as an efficient catalyst precursor for the homogeneous hydrogenation of simple olefins. In an effort to delineate the mechanism of this process, we investigated a number of stoichiometric oxidative addition and substitution processes to monitor the fate of the square-planar iridium(I) amide precursor. In this communication, we describe (i) the first examples of iridium(III) amides, (ii) a series of completely stereose-

(1) Fryzuk, M. D.; MacNeil, P. A. *Organometallics* **1983**, *2*, 355.

lective reactions that generate octahedral complexes from four- and five-coordinate starting materials, and (iii) a ligand-assisted heterolytic splitting of dihydrogen (H_2).

When a toluene solution of **1** is allowed to stir under 1 atm of H_2 for 1 h, the coordinatively unsaturated iridium(III) dihydride **2** can be isolated in high yield after removal of solvent and H_2 in vacuo (eq 1). The most

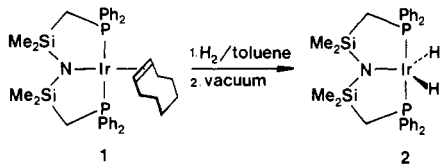

(1)

compelling evidence[2] for **2** is the sharp triplet at −24.9 ppm (^2J_P = 13.2 Hz) in the ^{1}H NMR spectrum for the IrH resonance; in addition, the ^{1}H NMR spectrum is invariant down to −80 °C, suggesting that the proposed trigonal-bipyramidal structure of **2** is stereochemically rigid. Additional evidence for a rigid structure is provided by the stereoselective addition reactions of **2** (vide infra).

If the reaction between **1** and H_2 is monitored (under excess H_2) by ^{1}H NMR spectroscopy, one observes the presence of *free* cyclooctene in the initial stages which is subsequently hydrogenated to cyclooctane. More importantly, no resonances assignable to **2** are observed; in fact, the solution spectroscopic data[3] are consistent with the presence of an iridium(III) amine trihydride, **3** (eq 2). The

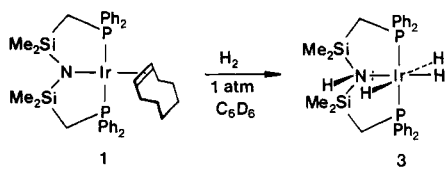

(2)

^{1}H NMR spectrum of a solution of **3** shows three multiplets to high field for the three different Ir–H moieties; in addition the IR (C_6D_6 under H_2) has two moderate intensity bands at 2175 and 1705 cm^{-1} for the Ir–H stretching frequencies, the lower energy absorption characteristic of a trans-H–Ir–H configuration,[4] as well as a weak N–H stretch at 3210 cm^{-1}. All of these absorptions shift appropriately upon deuteration (with D_2). Removal of H_2 from solutions of **3** quantitatively generates the iridium(III) amide dihydride **2**; in fact, when C_6D_6 solutions of **2** are sealed under H_2 (≤1 atm), **3** is formed instantaneously.

In an attempt to isolate **3**, we stirred a concentrated pentane solution of the iridium(I) cyclooctene derivative **1** under H_2 and observed the formation of a fine, yellow precipitate (>70% isolated yield). The spectral and analytical data[5] are consistent with the *facial stereoisomer* of **3**, a new iridium(III) amine trihydride **4** (eq 3). In par-

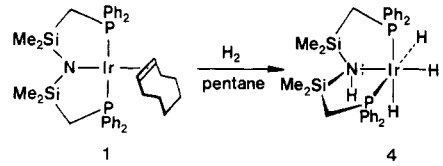

(3)

ticular, the infrared (KBr) shows two Ir–H absorptions at 2180 and 2115 cm^{-1} and a weak N–H stretch at 3200 cm^{-1}. Although stable in the solid state, **4** slowly isomerizes in C_6D_6 solution under H_2, to the meridional isomer **3** (~24 h). Under N_2 in solution, **4** decomposes to give a mixture of **2** and **3**, thus suggesting that the stereoisomerization of **4** to **3** occurs via dissociation of H_2 from the *fac* trihydride **4** to generate the dihydride **2** which, in the presence of H_2, forms the *mer* trihydride **3** (eq 4). The for-

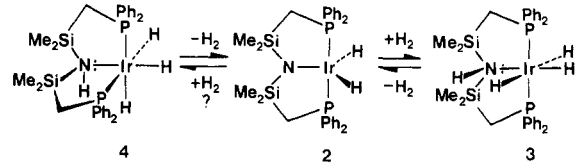

(4)

mation of **3** and **4** from the dihydride **2** is, formally, an intramolecular, ligand-assisted, heterolytic[6] splitting of H_2. Whether this occurs in a concerted process or in a stepwise process involving oxidative addition to generate an Ir(V) intermediate, followed by reductive elimination, is unknown.

The iridium(III) amide dihydride **2** easily adds simple ligands such as PMe_3 and CO in a completely stereoselective fashion to generate the isomerically pure meridional-cis dihydride complexes **5** (L = PMe_3) and **6** (L = CO) (eq 5). The formation of the *mer*-cis stereochemistry

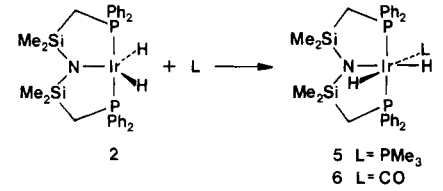

(5)

requires that the ligand L approach **2** cis to the iridium–amide bond and coordinate to either of the N–Ir–H edges. For reasons that are obscure at present, approach of L trans to the iridium–amide bond of **2**, to generate the unobserved *mer*-trans isomer, is completely inhibited. Furthermore, isomerization of the unobserved *mer*-trans isomer to the observed *mer*-cis isomer (**5** or **6**) can be ruled out on the basis of the following experiment:[8] if paraformaldehyde $(HCHO)_n$ is stirred with the iridium cyclooctene complex **1**, the isomerically pure meridional-trans

(2) **2**: ^{1}H NMR (C_6D_6, ppm) $SiCH_3$ 0.24 (s), CH_2P 1.89 (t, J_{app} = 5.2 Hz), $P(C_6H_5)_2$ 7.02 (m, para/meta), 7.92 (m, ortho), IrH −24.86 (t, $^2J_{H,P}$ = 13.2 Hz); $^{31}P\{^1H\}$ NMR (C_6D_6, $P(OMe)_3$ internal reference, ppm) 23.9 (s); IR (KBr, cm^{-1}) ν_{Ir-H} 2200 (m). Anal. Calcd for $C_{30}H_{38}IrNP_2Si_2$: C, 49.86; H, 5.26; N, 1.94. Found: C, 50.20; H, 5.56; N, 2.00.

(3) **3**: ^{1}H NMR (C_6D_6, ppm) $SiCH_3$ −0.02 (s), 0.05 (s), CH_2P, 1.70 (dt, J_{app} = 4.9 Hz, J_{gem} = 14.1 Hz), 2.36 (dt, J_{app} = 4.1 Hz), $P(C_6H_5)_2$ 6.99, 7.12 (m, para/meta), 8.20, 8.35 (m, ortho), IrH, −8.97 (td, $^2J_{P,H}$ = 19.5 Hz, $^2J_{H,H}$ = 5.0 Hz), −9.69 (td, $^2J_{P,H}$ = 18.0 Hz), −24.6 (tt, $^2J_{P,H}$ = 15.5 Hz); $^{31}P\{^1H\}$ NMR (C_6D_6, $P(OMe)_3$ external reference, ppm) 11.44 (s); IR (C_6D_6, cm^{-1}) ν_{N-H} 3210 (w), ν_{Ir-H} 2175 (m), 1705 (m).

(4) Adams, D. M. "Metal-Ligand and Related Vibrations"; Edward Arnold (Publishers) Ltd.: London, 1967; p 6.

(5) **4**: ^{1}H NMR (C_6D_6, ppm) $SiCH_3$ 0.23 (s), 0.25 (s), CH_2P 1.91 (dd, $^2J_{H,P}$ = 9.00 Hz, J_{gem} = 14.1 Hz), 2.09 (dd, $^2J_{H,P}$ = 11.00 Hz), $P(C_6H_5)_2$ 6.98 (m), 8.28 (m), IrH_A (trans to PPh_2), −8.5 (m, from spectral simulation of AA′MXX′ pattern, $^2J_{A,A'}$ = 2.2 Hz, $^2J_{A,M}$ = $^2J_{A',M}$ = 5.5 Hz, $^2J_{A,X}$ = $^2J_{A',X'}$ = −19.0 Hz, $^2J_{M,X}$ = $^2J_{M,X'}$ = 14.0 Hz, $^2J_{A,X'}$ = $^2J_{A',X}$ = 130.0 Hz, $^2J_{X,X'}$ = 1.0 Hz), IrH_M (trans to NH) −24.3 (tt); IR (KBr, cm^{-1}) ν_{N-H} 3200 (w), ν_{Ir-H} 2115 (m), 2180 (w). Anal. Calcd for $C_{30}H_{40}IrNP_2Si_2$: C, 49.72; H, 5.52; N, 1.93. Found: C, 49.86; H, 5.66; N, 1.97.

(6) Halpern, J. *J. Organomet. Chem.* **1980**, *200*, 133.

(7) **5**: ^{1}H NMR (C_6D_6, ppm) $SiCH_3$ 0.18 (s), 0.53 (s), $P(CH_3)_3$ 0.76 (d, $^2J_{H,P}$ = 8.0 Hz), CH_2P 1.79 (dt, J_{app} = 5.2 Hz, J_{gem} = 13.0 Hz), 2.22 (dt, J_{app} = 5.2 Hz), $P(C_6H_5)_2$ 6.95, 7.05 (m, para/meta), 7.83, 8.14 (m, ortho), IrH (trans to PPh_2) −10.21 (ddt, $^2J_{H,P}$(cis) = 17.6 Hz, $^2J_{H,P}$(trans) = 135.0 Hz, $^2J_{H,H}$ = 5.1 Hz), IrH (trans to N) −19.96 (dquart, $^2J_{H,P}$ = 19.5 Hz); $^{31}P\{^1H\}$ NMR (C_6D_6, $P(OMe)_3$ internal reference, ppm) PPh_2 11.00 (d, $^2J_{PMe_3,PPh_2}$ = 19.0 Hz), PMe_3 −56.83 (br t); IR (KBr, cm^{-1}) ν_{Ir-H} 2110 (s, br). Anal. Calcd for $C_{33}H_{47}IrNP_3Si_2$: C, 49.62; H, 5.89; N, 1.75. Found: C, 50.00; H, 6.00; N, 1.74. **6**: ^{1}H NMR (C_6D_6, ppm) $SiCH_3$ 0.31 (s), 0.34 (s), CH_2P 1.80 (dt, J_{app} = 5.4 Hz, J_{gem} = 13.8 Hz), 2.09 (dt, J_{app} = 6.5 Hz), $P(C_6H_5)_2$ 6.96, 7.04 (m, para/meta), 7.70, 7.95 (m, ortho), IrH (trans to CO) −7.86 (dt, $^2J_{H,P}$ = 17.6 Hz, $^2J_{H,H}$ = 4.4 Hz), IrH (trans to N), −16.09 (dt, $^2J_{H,P}$ = 12.5 Hz); $^{31}P\{^1H\}$ NMR (C_6D_6, $P(OMe)_3$ internal reference, ppm) 24.3 (s); IR (KBr, cm^{-1}) ν_{Ir-H} 2075 (s), 1925 (s), ν_{CO} 1965 (s). Anal. Calcd for $C_{31}H_{38}IrNOP_2Si_2$: C, 49.60; H, 5.07; N, 1.87. Found: C, 49.90; H, 5.13; N, 1.90.

(8) Thorn, D. L. *Organometallics* **1982**, *1*, 927.

dihydride derivative[9] **7** is formed in virtually quantitative yield (eq 6). Although the intermediate cis formyl hydride

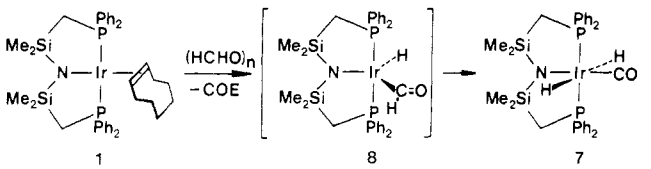

(6)

8 was not detected, it is reasonable to suggest that a stereoselective migratory deinsertion process[10] occurs to generate the *mer*-trans complex **7**. Solutions of **7** do not isomerize to the *mer*-cis complex **6** even under 1 atm of CO.

Both oxidative additions of H_2 and paraformaldehyde to **1** have similar features; in each case, dissociation of cyclooctene accompanies oxidative addition to generate a rigid, five-coordinate derivative, **2** or **8**, which undergoes further reaction to **3** and **7**, respectively, depending on the reaction conditions. In the absence of dissociation, straightforward oxidative addition is observed; thus the reaction of H_2 with the analogous iridium(I) complex[1] $[Ir(PMe_3)N(SiMe_2CH_2PPh_2)_2]$ (**9**) proceeds with complete stereoselectivity to generate the facial-cis dihydride **10** in quantitative yield (eq 7). The IrH resonance[11] appears

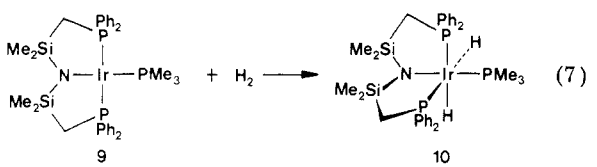

(7)

as a second-order, symmetrical multiplet at −11.04 ppm, which can be simulated as an AA′XX′Y spin system. In addition, confirmation of the *fac*-cis stereochemistry was provided by an X-ray crystal structure[12] of **10**. That **9** does not undergo dissociation of PMe_3 is presumably the reason it is not a catalyst precursor for hydrogenation reactions.[1] The related iridium(I) carbonyl[1] $[Ir(CO)N(SiMe_2CH_2PPh_2)_2]$ does not oxidatively add dihydrogen.

This study has shown that a number of heretofore unknown[13] iridium(III) amides (complexes **2**, **5**, **6**, **7**, and **10**) can be isolated by a series of completely stereoselective reactions. In addition, the formation of both **3** and **4** is an example of a novel ligand-assisted heterolytic splitting of H_2. Further studies to determine the importance of these reactions to the mechanism of hydrogenation are underway.

Acknowledgment. Financial support for this research was generously provided by the UBC Department of Chemistry and the Natural Sciences and Engineering Research Council of Canada. We also thank Johnson Matthey for the loan of $IrCl_3$. P.A.M. acknowledges the Walter C. Sumner Memorial Foundation for a graduate scholarship.

Registry No. **1**, 84074-30-6; **2**, 84751-23-5; **3**, 84751-24-6; **4**, 84799-44-0; **5**, 84751-25-7; **6**, 84751-26-8; **7**, 84799-45-1; **9**, 84074-32-8; **10**, 84799-46-2; H_2, 1333-74-0.

(9) **7**: ^1H NMR (C_6D_6, ppm) $SiCH_3$ 0.18 (s), CH_2P 2.04 (t, J_{app} = 5.7 Hz), $P(C_6H_5)_2$ 6.98 (m, para/meta), 7.87, (m, ortho), IrH −6.00 (t, $^2J_{H,P}$ = 14.7 Hz), $^{31}P\{^1H\}$ NMR (C_6D_6, $P(OMe)_3$ internal reference, ppm) 9.68 (s); IR (KBr, cm^{-1}) ν_{CO} 1990 (s), ν_{Ir-H} 1725 (s). Anal. Calcd for $C_{31}H_{38}IrNOP_2Si_2$: C, 49.60; H, 5.07; N, 1.87. Found: C, 50.00; H, 5.15; N, 1.88.

(10) Gladysz, J. A.; Johnson, D. L.; Tam, W.; Williams, G. M. *J. Organomet. Chem.* **1977**, *140*, C1.

(11) **9**: ^1H NMR (C_6D_6, ppm) $SiCH_3$ 0.32 (s), 0.72 (s), CH_2P 1.95 (m), 2.05 (m), $P(C_6H_5)_2$ 6.89 (m), 7.08 (m), IrH (m, from spectral simulation of AA′XX′Y pattern: $^2J_{A,X}$ = $^2J_{A',X'}$ = −21.0 Hz, $^2J_{A,Y}$ = $^2J_{A'Y}$ = 21.0 Hz, $^2J_{A,X'}$ = 147.0 Hz, $^2J_{A,A'}$ = 4.0 Hz, $^2J_{X,Y}$ = 9.0 Hz, $^2J_{X,X'}$ = 4.0 Hz); $^{31}P\{^1H\}$ NMR (C_6D_6, $P(OMe)_3$ internal reference, ppm) PPh_2 −1.67 (br d, $^2J_{PMe_3,PPh_2}$ = 9.0 Hz), PMe_3 −51.62 (t); IR (KBr, cm^{-1}) ν_{Ir-H} 2065 (s), 2020 (s). Anal. Calcd for $C_{33}H_{47}IrNP_3Si_2$: C, 49.62; H, 5.89; N, 1.75. Found: C, 49.91; H, 5.87; N, 1.84.

(12) Rettig, S. J., personal communication.

(13) Lappert, M. F.; Power, P. P.; Sanger, A. R.; Srivastava, R. C. "Metal and Metalloid Amides"; Horwood-Wiley: Chichester-New York, 1980; p 488.

Photochemical Synthesis and Structure of (μ-η^4-*syn*-1,3-Butadiene)(μ-carbonyl)bis(η^5-cyclopentadienyl)dicobalt(*Co–Co*), a Dinuclear Butadiene Complex

Joseph A. King, Jr., and K. Peter C. Vollhardt[*,†]

Department of Chemistry, University of California and the Materials and Molecular Research Division Lawrence Berkeley Laboratory Berkeley, California 94720

Received November 16, 1982

Summary: Irradiation of (η^4-1,3-butadiene)(η^5-C_5H_5)Co in the presence of (η^5-C_5H_5)Co(CO)$_2$ results in the title compound, the first dinuclear parent η^4-butadiene complex adopting a syn configuration to be characterized by X-ray crystallography.

Transition-metal-mediated transformations involving butadiene are of considerable current academic and industrial interest.[1] Whereas there are a number of structurally characterized mononuclear diene complexes known, molecules in which the diene unit is bound to more than one metal are scarce,[2] a possible reflection of the lack of facile synthetic approaches to such compounds. Nevertheless, their bonding characteristics should command attention as potential indicators of ligand-surface interactions,[3] of relevance to heterogeneous catalysis, and as key structures with which to investigate the organometallic chemistry of higher nuclear clusters.[4] We wish to report the synthesis of the title compound **3** by a novel route, which promises to be general, and its X-ray structural features. Complex **3** is the first μ-η^4-*syn*-1,3-butadiene complex to be unambiguously characterized in this fashion.

Our approach to **3** was modeled after the photochemical addition of CpCoCO (Cp = η^5-C_5H_5) to CpCo(CO)$_2$ (**1**), which furnishes $Cp_2Co_2(CO)_3$ containing one bridging and two terminal carbonyl ligands.[5] It was of interest to de-

† University of California.

(1) G. W. Parshall, "Homogeneous Catalysis. The Applications and Chemistry of Catalysis by Soluble Transition Metal Complexes", Wiley-Interscience, New York, 1980. P. W. Jolly and G. Wilke, "The Organic Chemistry of Nickel", Vol. 2, Academic Press, New York, 1975.

(2) (a) K. A. Klandermann, *Diss. Abstr.*, **25**, 6253 (1964/1965); (b) K. K. Cheung, R. J. Cross, K. P. Forrest, R. Wardle, and M. Mercer, *Chem. Commun.*, 875 (1971); (c) H. E. Sasse and M. L. Ziegler, *Z. Anorg. Allg. Chem.*, **392**, 167 (1972); (d) M. Tachikawa, J. R. Shapley, R. C. Haltiwanger, and C. G. Pierpont, *J. Am. Chem. Soc.*, **98**, 4651 (1976); C. G. Pierpont, *Inorg. Chem.*, **17**, 1976 (1978); (e) P. F. Jackson, B. F. G. Johnson, J. Lewis, P. R. Raithby, G. J. Will, M. PcPartlin, and W. J. H. Nelson, *J. Chem. Soc., Chem. Commun.*, 1190 (1980); (f) Y. N. Al-Obaidi, M. Green, N. D.White, J.-M. Bassett, and A. J. Welch, *ibid.*, 494 (1981); (g) K.-H. Franzreb and C. G. Kreiter, *Z. Naturforsch., B: Anorg. Chem., Org. Chem.* **37B**, 1058 (1982).

(3) E. L. Muetterties, *Angew. Chem.*, **90**, 577 (1978); *Angew. Chem., Int. Ed. Engl.*, **17**, 545 (1978).

(4) E. L. Muetterties, *Bull. Soc. Chim. Belg.*, **85**, 451 (1976); *Science (Washington, D.C.)*, **196**, 839 (1977); R. G. Bergman, *Acc. Chem. Res.*, **13**, 113 (1980).

(5) K. P. C. Vollhardt, J. E. Bercaw, and R. G. Bergman, *J. Organomet. Chem.*, **97**, 283 (1975).

0276-7333/83/2302-0684$01.50/0

dihydride derivative[9] **7** is formed in virtually quantitative yield (eq 6). Although the intermediate cis formyl hydride

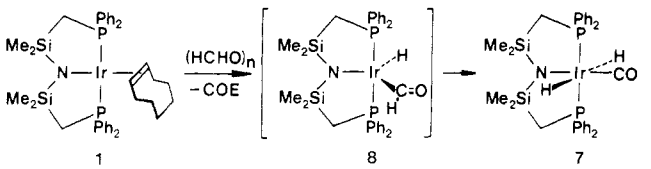

(6)

8 was not detected, it is reasonable to suggest that a stereoselective migratory deinsertion process[10] occurs to generate the *mer*-trans complex **7**. Solutions of **7** do not isomerize to the *mer*-cis complex **6** even under 1 atm of CO.

Both oxidative additions of H_2 and paraformaldehyde to **1** have similar features; in each case, dissociation of cyclooctene accompanies oxidative addition to generate a rigid, five-coordinate derivative, **2** or **8**, which undergoes further reaction to **3** and **7**, respectively, depending on the reaction conditions. In the absence of dissociation, straightforward oxidative addition is observed; thus the reaction of H_2 with the analogous iridium(I) complex[1] $[Ir(PMe_3)N(SiMe_2CH_2PPh_2)_2]$ (**9**) proceeds with complete stereoselectivity to generate the facial-cis dihydride **10** in quantitative yield (eq 7). The IrH resonance[11] appears

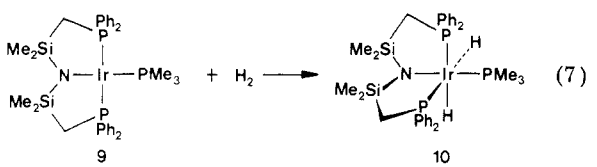

(7)

as a second-order, symmetrical multiplet at −11.04 ppm, which can be simulated as an AA′XX′Y spin system. In addition, confirmation of the *fac*-cis stereochemistry was provided by an X-ray crystal structure[12] of **10**. That **9** does not undergo dissociation of PMe_3 is presumably the reason it is not a catalyst precursor for hydrogenation reactions.[1] The related iridium(I) carbonyl[1] $[Ir(CO)N(SiMe_2CH_2PPh_2)_2]$ does not oxidatively add dihydrogen.

This study has shown that a number of heretofore unknown[13] iridium(III) amides (complexes **2**, **5**, **6**, **7**, and **10**) can be isolated by a series of completely stereoselective reactions. In addition, the formation of both **3** and **4** is an example of a novel ligand-assisted heterolytic splitting of H_2. Further studies to determine the importance of these reactions to the mechanism of hydrogenation are underway.

Acknowledgment. Financial support for this research was generously provided by the UBC Department of Chemistry and the Natural Sciences and Engineering Research Council of Canada. We also thank Johnson Matthey for the loan of $IrCl_3$. P.A.M. acknowledges the Walter C. Sumner Memorial Foundation for a graduate scholarship.

Registry No. **1**, 84074-30-6; **2**, 84751-23-5; **3**, 84751-24-6; **4**, 84799-44-0; **5**, 84751-25-7; **6**, 84751-26-8; **7**, 84799-45-1; **9**, 84074-32-8; **10**, 84799-46-2; H_2, 1333-74-0.

(9) **7**: ^1H NMR (C_6D_6, ppm) $SiCH_3$ 0.18 (s), CH_2P 2.04 (t, J_{app} = 5.7 Hz), $P(C_6H_5)_2$ 6.98 (m, para/meta), 7.87, (m, ortho), IrH −6.00 (t, $^2J_{H,P}$ = 14.7 Hz), $^{31}P\{^1H\}$ NMR (C_6D_6, $P(OMe)_3$ internal reference, ppm) 9.68 (s); IR (KBr, cm^{-1}) ν_{CO} 1990 (s), ν_{Ir-H} 1725 (s). Anal. Calcd for $C_{31}H_{38}IrNOP_2Si_2$: C, 49.60; H, 5.07; N, 1.87. Found: C, 50.00; H, 5.15; N, 1.88.

(10) Gladysz, J. A.; Johnson, D. L.; Tam, W.; Williams, G. M. *J. Organomet. Chem.* **1977**, *140*, C1.

(11) **9**: ^1H NMR (C_6D_6, ppm) $SiCH_3$ 0.32 (s), 0.72 (s), CH_2P 1.95 (m), 2.05 (m), $P(C_6H_5)_2$ 6.89 (m), 7.08 (m), IrH (m, from spectral simulation of AA′XX′Y pattern: $^2J_{A,X}$ = $^2J_{A',X'}$ = −21.0 Hz, $^2J_{A,Y}$ = $^2J_{A'Y}$ = 21.0 Hz, $^2J_{A,X'}$ = 147.0 Hz, $^2J_{A,A'}$ = 4.0 Hz, $^2J_{X,Y}$ = 9.0 Hz, $^2J_{X,X'}$ = 4.0 Hz); $^{31}P\{^1H\}$ NMR (C_6D_6, $P(OMe)_3$ internal reference, ppm) PPh_2 −1.67 (br d, $^2J_{PMe_3,PPh_2}$ = 9.0 Hz), PMe_3 −51.62 (t); IR (KBr, cm^{-1}) ν_{Ir-H} 2065 (s), 2020 (s). Anal. Calcd for $C_{33}H_{47}IrNP_3Si_2$: C, 49.62; H, 5.89; N, 1.75. Found: C, 49.91; H, 5.87; N, 1.84.

(12) Rettig, S. J., personal communication.

(13) Lappert, M. F.; Power, P. P.; Sanger, A. R.; Srivastava, R. C. "Metal and Metalloid Amides"; Horwood-Wiley: Chichester-New York, 1980; p 488.

Photochemical Synthesis and Structure of (μ-η^4-*syn*-1,3-Butadiene)(μ-carbonyl)bis(η^5-cyclopentadienyl)dicobalt(*Co–Co*), a Dinuclear Butadiene Complex

Joseph A. King, Jr., and K. Peter C. Vollhardt[*,†]

Department of Chemistry, University of California and the Materials and Molecular Research Division Lawrence Berkeley Laboratory Berkeley, California 94720

Received November 16, 1982

Summary: Irradiation of (η^4-1,3-butadiene)(η^5-C_5H_5)Co in the presence of (η^5-C_5H_5)Co(CO)$_2$ results in the title compound, the first dinuclear parent η^4-butadiene complex adopting a syn configuration to be characterized by X-ray crystallography.

Transition-metal-mediated transformations involving butadiene are of considerable current academic and industrial interest.[1] Whereas there are a number of structurally characterized mononuclear diene complexes known, molecules in which the diene unit is bound to more than one metal are scarce,[2] a possible reflection of the lack of facile synthetic approaches to such compounds. Nevertheless, their bonding characteristics should command attention as potential indicators of ligand-surface interactions,[3] of relevance to heterogeneous catalysis, and as key structures with which to investigate the organometallic chemistry of higher nuclear clusters.[4] We wish to report the synthesis of the title compound **3** by a novel route, which promises to be general, and its X-ray structural features. Complex **3** is the first μ-η^4-*syn*-1,3-butadiene complex to be unambiguously characterized in this fashion.

Our approach to **3** was modeled after the photochemical addition of CpCoCO (Cp = η^5-C_5H_5) to CpCo(CO)$_2$ (**1**), which furnishes $Cp_2Co_2(CO)_3$ containing one bridging and two terminal carbonyl ligands.[5] It was of interest to de-

† University of California.

(1) G. W. Parshall, "Homogeneous Catalysis. The Applications and Chemistry of Catalysis by Soluble Transition Metal Complexes", Wiley-Interscience, New York, 1980. P. W. Jolly and G. Wilke, "The Organic Chemistry of Nickel", Vol. 2, Academic Press, New York, 1975.

(2) (a) K. A. Klandermann, *Diss. Abstr.*, **25**, 6253 (1964/1965); (b) K. K. Cheung, R. J. Cross, K. P. Forrest, R. Wardle, and M. Mercer, *Chem. Commun.*, 875 (1971); (c) H. E. Sasse and M. L. Ziegler, *Z. Anorg. Allg. Chem.*, **392**, 167 (1972); (d) M. Tachikawa, J. R. Shapley, R. C. Haltiwanger, and C. G. Pierpont, *J. Am. Chem. Soc.*, **98**, 4651 (1976); C. G. Pierpont, *Inorg. Chem.*, **17**, 1976 (1978); (e) P. F. Jackson, B. F. G. Johnson, J. Lewis, P. R. Raithby, G. J. Will, M. PcPartlin, and W. J. H. Nelson, *J. Chem. Soc., Chem. Commun.*, 1190 (1980); (f) Y. N. Al-Obaidi, M. Green, N. D.White, J.-M. Bassett, and A. J. Welch, *ibid.*, 494 (1981); (g) K.-H. Franzreb and C. G. Kreiter, *Z. Naturforsch., B: Anorg. Chem., Org. Chem.* **37B**, 1058 (1982).

(3) E. L. Muetterties, *Angew. Chem.*, **90**, 577 (1978); *Angew. Chem., Int. Ed. Engl.*, **17**, 545 (1978).

(4) E. L. Muetterties, *Bull. Soc. Chim. Belg.*, **85**, 451 (1976); *Science (Washington, D.C.)*, **196**, 839 (1977); R. G. Bergman, *Acc. Chem. Res.*, **13**, 113 (1980).

(5) K. P. C. Vollhardt, J. E. Bercaw, and R. G. Bergman, *J. Organomet. Chem.*, **97**, 283 (1975).

0276-7333/83/2302-0684$01.50/0

Table I. ^{1}H and ^{13}C NMR Spectra for Complexes 2 and 3 (δ Values in ppm from Me_4Si in C_6D_6)

nucleus	2	3
H_1	−0.23 (dd, J = 8.3, 0.9 Hz)	−0.78 (dd, J = 11.7, 1.8 Hz)
H_2	1.82 (ddd, J = 6.8, 1.5, 0.9 Hz)	1.94 (ddd, J = 7.2, 1.8, 1.8 Hz)
H_3	5.01 (m)	4.79 (m)
Cp-^{1}H	4.67 (s)	4.69 (s)
C_1	30.4	23.6
C_2	77.6	48.8
Cp-^{13}C	78.8	85.1

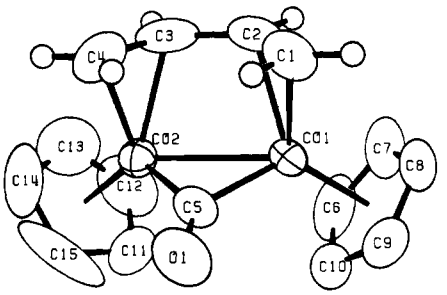

Figure 1. ORTEP diagram of 3. Ellipsoids are scaled to represent the 50% probability surface.

termine whether CpCo(η^4-1,3-butadiene) (2)[6] would function as a $CpCo(CO)_2$ equivalent in this reaction. Indeed, irradiation of the very air-sensitive 2 (30 mmol) in the presence of 1 (1.1 equiv) at 5 °C in THF for 5 h (N_2 purge) with a 250-W medium pressure Hg lamp, followed by chromatography (1, Al_2O_3 neutral, activity 2.5, pentane; 2, HPLC, ODS reverse phase, CH_3CN[7]) gave the desired product 3 as dark green relatively air-stable crystals (46%, mp 174–176 °C dec from CH_3CN), in addition to starting material 2 (38%).

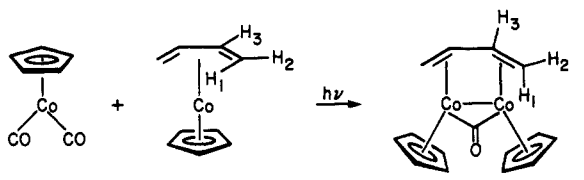

1 2 3

The structural assignment of 3 is consistent with its analytical (C, H, Co) and spectral data. The mass spectrum exhibits a molecular ion at m/e 330 (relative intensity 24.3) and prominent fragments at m/e 300 (62.9), 189 (90.3), 178 (76), 124 (100), and 98 (51.9). The IR spectrum exhibits the anticipated[2f] bridging carbonyl stretching absorption at 1782 cm^{-1}.

The ^{1}H and ^{13}C NMR spectra of 3 are compared to those of 2 in Table I. The most pronounced differences are noted in the chemical shifts for H_1, H_3, and C_2. Although the overall trends are compatible with the presence of a more tightly bound ligand in 3 (involving stronger donation from the ligand HOMO and back-coordination into the LUMO)[8] relative to 2, they could also be interpreted either as a reflection of the anisotropy effect[9] of the additional cobalt or as being due to the presence of a structural alternative, e.g., the anti[2a,c–e,10] or dimetallacyclohexene[11] isomer. For clarification of these points and because of the novelty of the proposed structure, a single-crystal X-ray diffraction study was carried out (Figure 1, Table II).

Table II. Selected Bond Lengths (Å) and Angles (Deg) for 3[a]

Bond Lengths			
Co_1-Co_2	2.485 (1)	C_1-C_2	1.381 (4)
Co_1-C_1	2.024 (3)	C_2-C_3	1.438 (4)
Co_1-C_2	2.038 (3)		
Co_1-C_5	1.870 (2)	C_3-C_4	1.407 (4)
Co_1-Cp_1	1.720[b]	C_5-O	1.178 (3)
Bond Angles			
Co_2-Co_1-C_1	97.22 (9)	C_5-Co_1-C_1	89.84 (11)
Co_2-Co_1-C_2	75.87 (9)	C_1-Co_1-C_2	39.76 (12)
Co_2-Co_1-C_5	48.07 (7)	C_1-C_2-C_3	124.1 (3)
Co_2-Co_1-Cp_1	134.05[b]	C_2-C_3-C_4	123.8 (3)
Cp_1-Co_1-C_1	127.91[b]	Co_1-C_5-Co_2	83.5 (1)
Cp_1-Co_1-C_2	132.15[b]		

[a] Estimated standard deviations in parentheses. [b] Cp_1 is the centroid of the cyclopentadienyl ring.

Figure 1 clearly establishes the structural identity of 3. The complex is seen to contain an η^4-bound 1,3-butadiene ligand in which the two double bonds appear to be independently bound, in an η^2 fashion, to the two metal centers. The vinylic protons are found to be located in the ligand plane, the latter being arranged at a 12.1° angle with respect to the plane incorporating the Co_2CO fragment. The open side of the ligand is orientated syn relative to the bridging carbonyl group. The diene ligand shows bond alternation as in free butadiene,[13] unlike many other di-[2a–e] and mononuclear[14] diene complexes in which significant C_1–C_2 bond elongation and C_2–C_3 shortening are observed. The only exception is found in a recently structurally characterized (η^4-cyclohexadiene)bis(η^5-indenyl)dirhodium system,[2f] which adopts an arrangement similar to 3. In this compound the relatively small perturbation of the (cyclic) diene unit on complexation was interpreted as indicative of weakened bonding, possibly operating also in the parent

(6) This compound is most readily and efficiently prepared by irradiation of excess butadiene in the presence of $CpCo(CO)_2$ in THF (N_2 purge) at 0 °C for several hours (95% yield). For a summary of other, less efficient syntheses, see: "Gmelins Handbuch der Anorganischen Chemie", Supplement to the 8th edition, Vol. 5, Part 1, 1973, p 314.

(7) J. M. Huggins, J. A. King, Jr., K. P. C. Vollhardt, and M. J. Winter, *J. Organomet. Chem.*, **208**, 73 (1981).

(8) For some recent bonding considerations in metal diene complexes: M. Elian and R. Hoffmann, *Inorg. Chem.*, **14**, 1058 (1975); D. M. P. Mingos, *J. Chem. Soc., Dalton Trans.*, 20 (1977); A. J. Pearson and P. R. Raithby, *ibid.*, 884 (1981).

(9) For ^{1}H NMR spectral data of CpCo dienes see: E. D. Sternberg and K. P. C. Vollhardt, *J. Am. Chem. Soc.*, **102**, 4839 (1980); T. R. Gadek and K. P. C. Vollhardt, *Angew. Chem.*, **93**, 801 (1981); *Angew. Chem., Int. Ed. Engl.*, **20**, 802 (1981). "Gmelins Handbuch der Anorganischen Chemie", Supplement to the 8th edition; Vol. 5, Part 1, 1973, p 340.

(10) G. Erker, J. Wicher, K. Engel, and C. Krüger, *Chem. Ber.*, **115**, 3300 (1982); Y. Kai, N. Kanehisa, K. Miki, N. Kasai, K. Mashima, K. Nagasuna, H. Yasuda, and A. Nakamura, *J. Chem. Soc., Chem. Commun.*, 191 (1982).

(11) W. H. Hersh and R. G. Bergman, *J. Am. Chem. Soc.*, **103**, 6992 (1981).

(12) F. J. Hollander, U.C. Berkeley College of Chemistry X-ray Crystallographic Facility (CHEXRAY). Compound 3: $[\mu\text{-}\eta^4\text{-}C_4H_6][\mu\text{-}CO][\eta^5\text{-}C_5H_5Co]_2$, monoclinic; space group $P2_1/n$, a = 7.4696 (9) Å, b = 11.1916 (15) Å, c = 15.5375 (14) Å, β = 93.686 (9)°, V = 1296.2 (5) Å^3 at 25 °C; formula weight 330.16 amu; Z = 4, d_{calcd} = 1.692 g cm^{-3}; μ_{calcd} = 25.4 cm^{-1}; size 0.21 × 0.25 × 0.35 mm. Data were measured in the hemisphere + h,+k,±l, 2θ = 3→45°, using monochromatized Mo Kα radiation (λ = 0.71073 Å) and a θ–2θ scan mode. Data were corrected for absorption (T_{max} = 0.63, T_{min} = 0.55). The structure was solved by Patterson and Fourier techniques and refined via full-matrix least-squares procedures: R = 2.48% and R_w = 3.80% using 1688 observations with $F^2 > 3\sigma(F^2)$ out of a total of 1941; weights were proportional to $\sigma^{-2}(F)$ esd's with a p factor of 0.03 [$\sigma(F^2) = \sigma_o^2(F^2) + (pF^2)^2$].

(13) D. J. Marais, N. Sheppard, and B. P. Stoicheff, *Tetrahedron*, **17**, 163 (1962).

(14) For structures of mononuclear CpCo diene complexes, see: M. R. Churchill and R. Mason, *Proc. R. Soc. London, Ser. A* **279**, 191 (1964); N. El Murr, Y. Dusausoy, J. E. Sheats, and M. Agnew, *J. Chem. Soc., Dalton Trans.*, 901 (1979); Y. Wakatsuki, K. Aoki, and H. Yamazaki, *ibid.*, 89 (1982).

(15) W. S. Lee and H. H. Brintzinger, *J. Organomet. Chem.*, **127**, 87 (1977); N. E. Schore, C. S. Ilenda, and R. G. Bergman, *J. Am. Chem. Soc.*, **99**, 1781 (1977).

system **3**. Interestingly, while **3** is found to be less air-sensitive than **2**, preliminary data show that **3** is thermally labile, converting completely to **2** and the reactive blue $(CpCoCO)_2$ (C_6H_6, 100 °C, 22 h). The latter has been prepared previously,[15] but never cleanly and/or efficiently, and the present route offers a potential entry into the exploratory chemistry of this compound.

In summary, this work reports a new method for the preparation of dinuclear butadiene cobalt complexes[16] and the structural and some preliminary chemical details of **3**, the parent compound in the series.

Acknowledgment. This work was supported by the NSF (Grant CHE-82-00049). K.P.C.V. is a Camille and Henry Dreyfus Teacher-Scholar (1978–1983).

Registry No. **1**, 12078-25-0; **2**, 1271-08-5; **3**, 84802-74-4; Co, 7440-48-4.

Supplementary Material Available: An experimental description of the structure determination, a listing of observed and calculated structure factors, and tables of positional and thermal parameters and bond lengths and angles (20 pages). Ordering information is given on any current masthead page.

(16) This method appears to be general also for substituted systems: J. A. King, Jr., and K. P. C. Vollhardt, in preparation.

Preparation and Reactions of New Isocyanide Complexes of Rhodium and Their Role in Carbon–Hydrogen Bond Activation

William D. Jones* and Frank J. Feher
Department of Chemistry, University of Rochester
Rochester, New York 14627

Received September 7, 1982

Summary: The compounds $[C_5(CH_3)_5]Rh[CNCH_2C(CH_3)_3]X_2$ (X = Cl, Br) can be mono arylated with Grignard reagents to give $[C_5(CH_3)_5]Rh[CNCH_2C(CH_3)_3](p\text{-}C_6H_4CH_3)X$ or, after addition of NH_4X, the carbenes $[C_5(CH_3)_5]Rh\{C(p\text{-}C_6H_4CH_3)[NHCH_2C(CH_3)_3]\}X_2$. Facile isocyanide insertion into the rhodium–tolyl bond occurs upon addition of PMe_3. Reduction of $[C_5(CH_3)_5]Rh[CNCH_2C(CH_3)_3]I_2$ in the presence of isocyanide gives $[C_5(CH_3)_5]Rh[CNCH_2(CH_3)_3]_2$, which produces the imine $C_6H_5CHNCH_2C(CH_3)_3$ upon irradiation in benzene.

There has been a recent resurgence of activity in the activation of carbon–hydrogen bonds by homogeneous transition-metal complexes. While most of these reports involve intermolecular oxidative addition of C–H bonds to metal centers,[1] some also include the functionalization

Scheme I

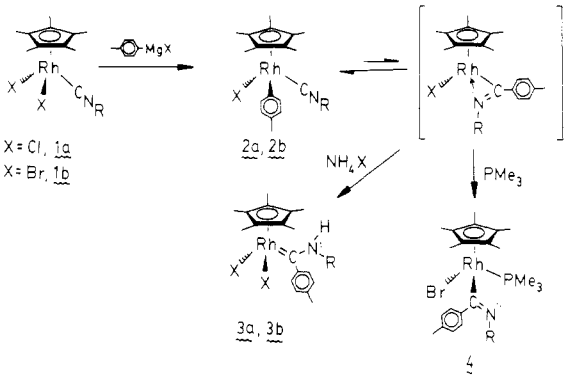

Scheme II

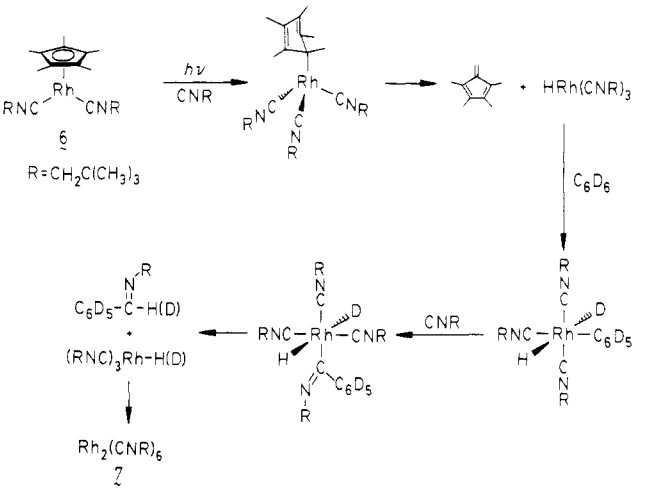

of the carbon attached to the metal center.[2] We wish to report here the preparation of new isocyanide complexes of rhodium(III) and their reduction to rhodium(I) species capable of activating arene C–H bonds under photolytic conditions.

The bridging halide complexes $\{[C_5(CH_3)_5]RhX\}_2(\mu\text{-}X)_2$ (X = Cl, Br, I)[3] can be easily cleaved by addition of 1 equiv of $CNCH_2C(CH_3)_3$ in CH_2Cl_2 solution, producing air-stable, monomeric $[C_5(CH_3)_5]Rh[CNCH_2C(CH_3)_3]X_2$ (**1a**, X = Cl; **1b**, X = Br; **1c**, X = I)[4] in >95% yield after recrystallization from CH_2Cl_2/hexane. Addition of 1 equiv of $p\text{-}CH_3C_6H_4Li$ or $p\text{-}CH_3C_6H_4MgBr$ to a 0.025 M THF solution of **1b** produces quantitatively (NMR) a new species whose ^1H NMR spectrum (THF-d_8, 400 MHz) shows singlets at δ 1.643 (15 H), 0.999 (9 H), and 2.179 (3 H) and doublets at δ 6.697 (J = 8 Hz, 2 H) and 7.301 (J = 8 Hz, 2 H). The compound exhibits a terminal isocyanide stretch at 2190

(1) (a) Janowicz, A. H.; Bergman, R. G. *J. Am. Chem. Soc.* **1982**, *104*, 352. (b) Green, M. L. *Pure Appl. Chem.* **1978**, *50*, 27–35. (c) Rausch, M. D.; Gastinger, R. C.; Gardner, S. A.; Brown, R. K.; Wood, J. S. *J. Am. Chem. Soc.* **1977**, *99*, 7870–7876. (d) Crabtree, R. H.; Mellea, M. F.; Mihelcic, J. M.; Quirk, J. M. *Ibid.* **1982**, *104*, 107–113. (e) Grebenik, P. D.; Green, M. L. H.; Izquierdo, A. *J. Chem. Soc., Chem. Commun.* **1981**, 186–187. (f) Gell, K. I.; Schwartz, J. *J. Am. Chem. Soc.* **1981**, *103*, 2687–2695. (g) Bradley, M. G.; Roberts, D. A.; Geoffroy, G. L. *Ibid.* **1981**, *103*, 379–384. (h) Baudry, D.; Ephritikhine, M.; Felkin, H. *J. Chem. Soc., Chem. Commun.* **1980**, 1243–1244. (i) Hoyano, J. K.; Graham, W. A. G. *J. Am. Chem. Soc.* **1982**, *104*, 3723–3725.

(2) (a) Parshall, G. W. *Acc. Chem. Res.* **1975**, *8*, 113–117. (b) Gustavson, W. A.; Epstein, P. S.; Curtis, M. D. *Organometallics* **1982**, *1*, 884–885. (c) Diamond, W. E.; Szalkiewicz, A.; Mares, F. *J. Am. Chem. Soc.* **1979**, *101*, 490–491. (d) Horino, H.; Inoue, N. *Tetrahedron Lett.* **1979**, *26*, 2403–2406. (e) Fujiwara, Y.; Kawauchi, T.; Taniguchi, H. *J. Chem. Soc., Chem. Commun.* **1980**, 220–221.

(3) Kang, J. W.; Moseley, K.; Maitlis, P. M. *J. Am. Chem. Soc.* **1969**, *91*, 5970–5977.

(4) All NMR spectra were recorded at 400 MHz. For **1a**: ^1H NMR (C_6D_6) δ 0.728, (s, 9 H), 1.438 (s, 15 H), 2.652 (s, 2 H); IR ($CHCl_3$) 2221 cm^{-1}. Anal. Calcd for $C_{16}H_{26}Cl_2NRh$: C, 47.31; H, 6.45; N, 3.45. Found: C, 47.25; H, 6.58; N, 3.36. For **1b**: ^1H NMR (C_6D_6) δ 0.700 (s, 9 H); 1.541 (s, 15 H), 2.521 (s, 2 H); IR ($CHCl_3$) 2216 cm^{-1}. For **1c**: ^1H NMR (C_6D_6) δ 0.710 (s, 9 H), 1.767 (s, 15 H), 2.579 (s, 2 H); IR ($CHCl_3$) 2210 cm^{-1}. Cf. Faraone, F.; Marsala, V.; Tresoldi, G. *J. Organomet. Chem.* **1978**, *152*, 337–345.

0276-7333/83/2302-0686$01.50/0

Preparation and reactions of new isocyanide complexes of rhodium and their role in carbon-hydrogen bond activation

William D. Jones, and Frank J. Feher

Organometallics, **1983**, 2 (5), 686-687• DOI: 10.1021/om00077a022 • Publication Date (Web): 01 May 2002

system **3**. Interestingly, while **3** is found to be less air-sensitive than **2**, preliminary data show that **3** is thermally labile, converting completely to **2** and the reactive blue $(CpCoCO)_2$ (C_6H_6, 100 °C, 22 h). The latter has been prepared previously,[15] but never cleanly and/or efficiently, and the present route offers a potential entry into the exploratory chemistry of this compound.

In summary, this work reports a new method for the preparation of dinuclear butadiene cobalt complexes[16] and the structural and some preliminary chemical details of **3**, the parent compound in the series.

Acknowledgment. This work was supported by the NSF (Grant CHE-82-00049). K.P.C.V. is a Camille and Henry Dreyfus Teacher-Scholar (1978–1983).

Registry No. **1**, 12078-25-0; **2**, 1271-08-5; **3**, 84802-74-4; Co, 7440-48-4.

Supplementary Material Available: An experimental description of the structure determination, a listing of observed and calculated structure factors, and tables of positional and thermal parameters and bond lengths and angles (20 pages). Ordering information is given on any current masthead page.

(16) This method appears to be general also for substituted systems: J. A. King, Jr., and K. P. C. Vollhardt, in preparation.

Preparation and Reactions of New Isocyanide Complexes of Rhodium and Their Role in Carbon–Hydrogen Bond Activation

William D. Jones* and Frank J. Feher
Department of Chemistry, University of Rochester
Rochester, New York 14627

Received September 7, 1982

Summary: The compounds $[C_5(CH_3)_5]Rh[CNCH_2C(CH_3)_3]X_2$ (X = Cl, Br) can be mono arylated with Grignard reagents to give $[C_5(CH_3)_5]Rh[CNCH_2C(CH_3)_3](p\text{-}C_6H_4CH_3)X$ or, after addition of NH_4X, the carbenes $[C_5(CH_3)_5]Rh\{C(p\text{-}C_6H_4CH_3)[NHCH_2C(CH_3)_3]\}X_2$. Facile isocyanide insertion into the rhodium–tolyl bond occurs upon addition of PMe_3. Reduction of $[C_5(CH_3)_5]Rh[CNCH_2C(CH_3)_3]I_2$ in the presence of isocyanide gives $[C_5(CH_3)_5]Rh[CNCH_2(CH_3)_3]_2$, which produces the imine $C_6H_5CHNCH_2C(CH_3)_3$ upon irradiation in benzene.

There has been a recent resurgence of activity in the activation of carbon–hydrogen bonds by homogeneous transition-metal complexes. While most of these reports involve intermolecular oxidative addition of C–H bonds to metal centers,[1] some also include the functionalization

Scheme I

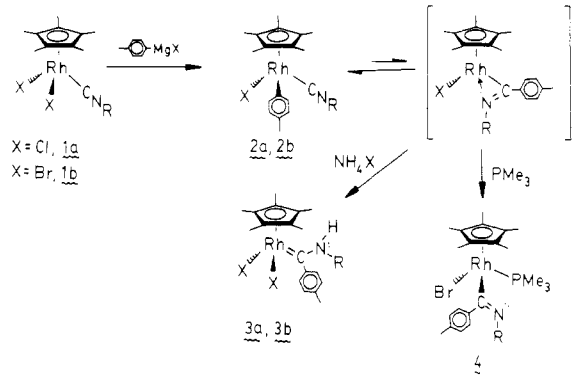

Scheme II

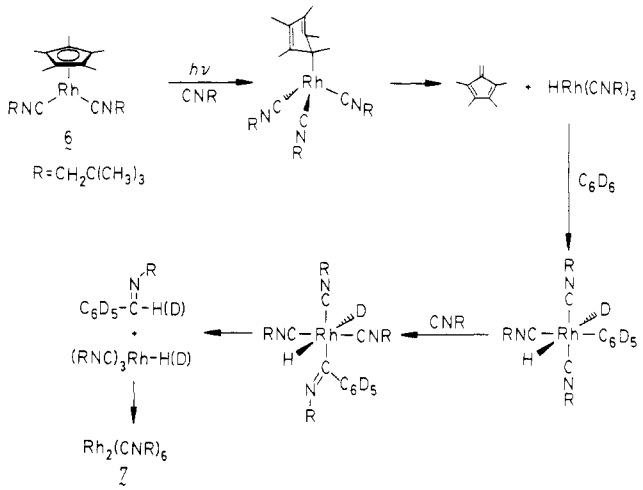

of the carbon attached to the metal center.[2] We wish to report here the preparation of new isocyanide complexes of rhodium(III) and their reduction to rhodium(I) species capable of activating arene C–H bonds under photolytic conditions.

The bridging halide complexes $\{[C_5(CH_3)_5]RhX\}_2(\mu\text{-}X)_2$ (X = Cl, Br, I)[3] can be easily cleaved by addition of 1 equiv of $CNCH_2C(CH_3)_3$ in CH_2Cl_2 solution, producing air-stable, monomeric $[C_5(CH_3)_5]Rh[CNCH_2C(CH_3)_3]X_2$ (**1a**, X = Cl; **1b**, X = Br; **1c**, X = I)[4] in >95% yield after recrystallization from CH_2Cl_2/hexane. Addition of 1 equiv of $p\text{-}CH_3C_6H_4Li$ or $p\text{-}CH_3C_6H_4MgBr$ to a 0.025 M THF solution of **1b** produces quantitatively (NMR) a new species whose ^1H NMR spectrum (THF-d_8, 400 MHz) shows singlets at δ 1.643 (15 H), 0.999 (9 H), and 2.179 (3 H) and doublets at δ 6.697 (J = 8 Hz, 2 H) and 7.301 (J = 8 Hz, 2 H). The compound exhibits a terminal isocyanide stretch at 2190

(1) (a) Janowicz, A. H.; Bergman, R. G. *J. Am. Chem. Soc.* **1982**, *104*, 352. (b) Green, M. L. *Pure Appl. Chem.* **1978**, *50*, 27–35. (c) Rausch, M. D.; Gastinger, R. C.; Gardner, S. A.; Brown, R. K.; Wood, J. S. *J. Am. Chem. Soc.* **1977**, *99*, 7870–7876. (d) Crabtree, R. H.; Mellea, M. F.; Mihelcic, J. M.; Quirk, J. M. *Ibid.* **1982**, *104*, 107–113. (e) Grebenik, P. D.; Green, M. L. H.; Izquierdo, A. *J. Chem. Soc., Chem. Commun.* **1981**, 186–187. (f) Gell, K. I.; Schwartz, J. *J. Am. Chem. Soc.* **1981**, *103*, 2687–2695. (g) Bradley, M. G.; Roberts, D. A.; Geoffroy, G. L. *Ibid.* **1981**, *103*, 379–384. (h) Baudry, D.; Ephritikhine, M.; Felkin, H. *J. Chem. Soc., Chem. Commun.* **1980**, 1243–1244. (i) Hoyano, J. K.; Graham, W. A. G. *J. Am. Chem. Soc.* **1982**, *104*, 3723–3725.

(2) (a) Parshall, G. W. *Acc. Chem. Res.* **1975**, *8*, 113–117. (b) Gustavson, W. A.; Epstein, P. S.; Curtis, M. D. *Organometallics* **1982**, *1*, 884–885. (c) Diamond, W. E.; Szalkiewicz, A.; Mares, F. *J. Am. Chem. Soc.* **1979**, *101*, 490–491. (d) Horino, H.; Inoue, N. *Tetrahedron Lett.* **1979**, *26*, 2403–2406. (e) Fujiwara, Y.; Kawauchi, T.; Taniguchi, H. *J. Chem. Soc., Chem. Commun.* **1980**, 220–221.

(3) Kang, J. W.; Moseley, K.; Maitlis, P. M. *J. Am. Chem. Soc.* **1969**, *91*, 5970–5977.

(4) All NMR spectra were recorded at 400 MHz. For **1a**: ^1H NMR (C_6D_6) δ 0.728, (s, 9 H), 1.438 (s, 15 H), 2.652 (s, 2 H); IR ($CHCl_3$) 2221 cm^{-1}. Anal. Calcd for $C_{16}H_{26}Cl_2NRh$: C, 47.31; H, 6.45; N, 3.45. Found: C, 47.25; H, 6.58; N, 3.36. For **1b**: ^1H NMR (C_6D_6) δ 0.700 (s, 9 H); 1.541 (s, 15 H), 2.521 (s, 2 H); IR ($CHCl_3$) 2216 cm^{-1}. For **1c**: ^1H NMR (C_6D_6) δ 0.710 (s, 9 H), 1.767 (s, 15 H), 2.579 (s, 2 H); IR ($CHCl_3$) 2210 cm^{-1}. Cf. Faraone, F.; Marsala, V.; Tresoldi, G. *J. Organomet. Chem.* **1978**, *152*, 337–345.

0276-7333/83/2302-0686$01.50/0

cm^{-1} (THF) and can be assigned the structure $[C_5(CH_3)_5]Rh[CNCH_2C(CH_3)_3](p\text{-}C_6H_4CH_3)Br$, **2b**.[5] Its extreme air sensitivity has thus far precluded its isolation in analytically pure form.

Treatment of a THF solution of **2a** or **2b** with saturated aqueous NH_4Cl or NH_4Br, respectively, produces the new carbene complexes $[C_5(CH_3)_5]Rh\{C(p\text{-}C_6H_4CH_3)[NHCH_2C(CH_3)_3]\}X_2$ (**3a**, X = Cl; **3b**, X = Br) in 90% yield after preparative thin-layer chromatography (SiO_2, 2% THF/CH_2Cl_2) and recrystallization from benzene/hexane. The complexes are believed to form by insertion of the isocyanide into the rhodium–tolyl bond, protonation of the iminoacyl nitrogen, and coordination of halide ion to the vacant Rh(III) site (Scheme I).[6,7] Further evidence for the facile insertion of the isocyanide into a rhodium–tolyl bond was obtained by treating a 0.025 M solution of **2b** with 1 equiv of PMe_3 at room temperature. An immediate reaction produces the iminoacyl species $[C_5(CH_3)_5]Rh[P(CH_3)_3][C(p\text{-}C_6H_4CH_3)NCH_2C(CH_3)_3]Br$, **4**, identified on the basis of its NMR, IR, mass spectrum and elemental analysis.[8] Reduction of **1c** with 0.47% Na/Hg in 2:1 THF/benzene (v:v) or with sodium napthalide in THF produces a deep blue solution from which dark blue crystals of a complex assigned structure **5** are obtained.[9]

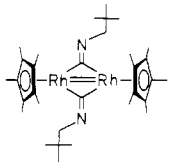

5

Similar reductions of **1a** and **1b** lead to decomposition. However, reduction of **1c** in the presence of excess $CNCH_2(CH_3)_3$ leads to the mononuclear complex $[C_5(CH_3)_5]Rh[CNCH_2(CH_3)_3]_2$, **6**, obtained as air-sensitive red-orange crystals in >85% isolated yield after recrystallization from hexane at −78 °C.[10]

Compound **6** is stable to thermolysis in C_6D_6 at 200 °C for 3 h. However, UV irradiation of **6** in C_6D_6 results in the formation of traces (~1%) of the imine $C_6D_5CD{=}NCH_2C(CH_3)_3$ at the expense of **6**. Irradiation of **6** in the presence of 2 equiv of $CNCH_2(CH_3)_3$ increases the yield of imine to 26% (GC) as all of **6** is consumed (eq 1). ^1H NMR and mass spectral analysis of the imine reveals a 1:1 ratio of d_5 and d_6 imine.

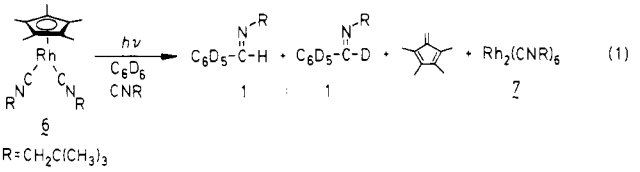

The detailed fate of the metal in these irradiations is not exactly known, but we suspect that a photoprocess in which the $C_5(CH_3)_5$ ring is cleaved from the metal is occurring. The isolation of 2,3,4,5-tetramethylfulvene[12] and $Rh_2[CNCH_2C(CH_3)_3]_6$,[13] **7**, from the photolysis solution in yields similar to that of the imine supports this hypothesis. Other workers have also proposed a decrease in hapticity of η^5-coordinated cyclopentadienyl rings upon irradiation.[14]

A possible mechanism accounting for these observations is shown in Scheme II. Simple loss of isocyanide followed by oxidative addition of a benzene C–D bond does not appear to be occurring here. Irradiation of **6** in toluene produces a 2:1 mixture of the meta- and para-methyl-substituted imines in low yield (~1%), consistent with a step involving arene C–H oxidative addition to a low valent metal center.[15] Further work investigating the chemistry of complex **7** and its role in C–H bond activation is under way.

Acknowledgment is made to the donors of the Petroleum Research Fund, administered by the American Chemical Society, and to the Camille and Henry Dreyfus Foundation for support of this research. We also wish to thank Johnson Matthey, Inc., for a generous loan of rhodium trichloride.

Registry No. **1a**, 85028-72-4; **1b**, 85028-73-5; **1c**, 85028-74-6; **2a**, 85028-76-8; **2b**, 85028-75-7; **3a**, 85028-77-9; **3b**, 85028-78-0; **4**, 85028-79-1; **5**, 85028-80-4; **6**, 85028-81-5; **7**, 85028-82-6; $\langle[C_5(CH_3)_5]RhCl\rangle_2(\mu\text{-}Cl)_2$, 12354-85-7; $\langle[(C_5CH_3)_5]RhBr\rangle_2(\mu\text{-}Br)_2$, 36484-11-4; $\langle[C_5(CH_3)_5]RhI\rangle_2(\mu\text{-}I)_2$, 67841-74-1; $C_6D_5CD{=}NCH_2C(CH_3)_3$, 85028-83-7; $C_6D_5CH{=}NCH_2C(CH_3)_3$, 85028-84-8; 2,3,4,5-tetramethylfulvene, 76089-59-3.

(5) For the chloro derivative $[C_5(CH_3)_5]Rh[CNCH_2C(CH_3)_3](p\text{-}C_6H_4CH_3)Cl$, **2a**: ^1H NMR ($CDCl_3$) δ 1.555 (s, 15 H), 0.629 (s, 9 H), 2.489 (s, 2 H), 2.289 (s, 3 H), 7.059 (d, J = 8 Hz, 2 H), 7.787 (d, J = 8 Hz, 2 H); IR (THF) 2180 cm^{-1}. In contrast to Adams studies,[6] we do not observe an η^2-iminoacyl species.

(6) Cf. Adams, R. D.; Chodosh, D. F. *J. Am. Chem. Soc.* **1982**, *99*, 6544–6550.

(7) For **3a**: ^1H NMR ($CDCl_3$) δ 0.939 (s, 9 H) 1.371 (s, 15 H), 2.406 (s, 3 H), 3.192 (d, J = 6 Hz, 2 H), 7.224 (d, J = 8 Hz, 2 H), 7.307 (d, J = 8 Hz, 2 H), 11.389 (br s, 1 H) (coupled to δ 3.192 resonance); IR ($CHCl_3$) 3155 (m), 1573 (s), 1562 (sh) cm^{-1}. Anal. Calcd for $C_{23}H_{34}Cl_2NRh$: C, 55.43; H, 6.82; N, 2.81. Found: C, 54.99; H, 6.98; N, 2.86. For **3b**: ^1H NMR (C_6D_6) δ 0.787 (s, 9 H), 1.293 (s, 15 H), 2.035 (s, 3 H), 2.838 (d, J = 6 Hz, 2 H), 6.903 (d, J = 8 Hz, 2 H), 7.377 (d, J = 8 Hz, 2 H), 11.625 (br s, 1 H) (coupled to δ 2.838 resonance); ^{13}C NMR ($CDCl_3$) δ 9.35 (q, J = 129.0 Hz), 21.19 (q, J = 126.7 Hz), 27.68 (q, J = 123.8 Hz), 32.30 (s), 61.74 (t, J = 145.0 Hz), 97.89 (d, J = 6.6 Hz), 124.72 (d, J = 160.8 Hz), δ 128.21 (d, J = 158.2 Hz), 138.74 (s), 139.77 (s), 233.84 (d, J = 39.7 Hz); IR ($CHCl_3$) 3160 (m), 1568 (sh), 1558 (s) cm^{-1}; mass spectrum (75 eV), m/e 585, 587, 589 (M^+). Anal. Calcd for $C_{23}H_{34}Br_2NRh$: C, 47.04; H, 5.84; N, 2.39. Found: C, 46.87; H, 5.82; N, 2.45. An X-ray structure determination of **3a** is in progress.

(8) For **4**: ^1H NMR (C_6D_6) δ 1.056 (s, 9 H), 1.346 (dd, J = 11, 1 Hz, 9 H), 1.583 (d, J = 3 Hz, 15 H), 2.144 (s, 3 H), 2.961 (dd, J = 14, 3 Hz, 1 H), 3.347 (d, J = 14 Hz, 1 H); 7.120 (d, J = 8 Hz, 2 H), 6.962 (d, J = 8 Hz, 2 H); IR (THF) 1560 cm^{-1}; mass spectrum (75 eV), m/e 505, 507 (M^+ − 76). Anal. Calcd for $C_{26}H_{42}BrNPRh$: C, 53.61; H, 7.27; N, 2.42. Found: C, 53.91; H, 7.49; N, 2.36.

(9) For **5**: ^1H NMR (C_6D_6) δ 1.259 (s, 18 H), 1.663 (s, 30 H), 4.178 (s, 4 H); ^{13}C NMR ($CDCl_3$) δ 11.31 (q, J = 126 Hz), 28.31 (q, J = 127 Hz), 32.73 (s), 68.70 (t, J = 128 Hz), 100.14 (s), 234.95 (t, J = 53 Hz); IR (THF) 1690 cm^{-1}. A structurally similar complex, $Cp_2Rh_2(CO)_2$, has been reported: Nutton, A.; Maitlis, P. M. *J. Organomet. Chem.* **1979**, *166*, C21–C22.

(10) For **6**: ^1H NMR (C_6D_6) δ 0.805 (s, 18 H), 2.234 (s, 15 H), 2.803 (d, J = 1 Hz, 4 H); ^{13}C NMR ($CDCl_3$) δ 11.84 (q, J = 125 Hz), 26.73 (q, J = 127 Hz), 32.24 (s), 56.51 (t, J = 128 Hz), 97.66 (s), 166.92 (d, J = 82 Hz). IR (KBr) 2073(s), 1977(m) cm^{-1}; mass spectrum (75 eV), m/e 432 (M^+). Traces of **6** are also produced in the reductions of **1a**, **1b**, and **1c** in the absence of added isocyanide.

(11) The imine was identified by gas chromatographic coinjection with an authentic sample on a 10 ft × $^1/_8$ in. 5% SE-30/Chromosorb WAW column (125 °C, 20 mL/min), by its mass spectrum (75 eV, m/e 180, 181), and by its ^1H NMR spectrum ((C_6D_6) δ 1.021 (s, 9 H), 3.244 (s, 2 H), 7.999 (br s, 0.5 H)). Irradiations were performed with a 500-W Hanovia lamp (no. 679A10) filtered through quartz at a distance of 15 cm. An air jet maintained the sample at 25 °C (±5 °C).

(12) Identified by ^1H NMR ((C_6D_6) δ 1.683 (s, 6 H), 1.845 (s, 6 H), 5.337 (s, 2 H) and mass spectroscopy (75 eV, m/e 134) and by gas chromatographic coinjection with an authentic sample.

(13) $Rh_2[CNCH_2C(CH_3)_3]_6$ can be recrystallized from benzene/hexane: ^1H NMR (C_6D_6) δ 2.529 (s, 4 H), 2.472 (s, 8 H), 0.694 (s, 36 H), 0.678 (s, 18 H); IR (KBr) 2214 (m), 2156 (vs), 2015 (s) cm^{-1}. Traces of added isocyanide scramble the isocyanide resonances on the NMR time scale. The related palladium derivative $[Pd_2(CNR)_6]^{2+}$ has been reported: Doonan, D. J.; Balch, A. L.; Goldberg, S. Z.; Eisenberg, R.; Miller, J. S. *J. Am. Chem. Soc.* **1975**, *97*, 1961–1962. Goldberg, S. Z.; Eisenberg, R. *Inorg. Chem.* **1976**, *15*, 535–541.

(14) Crichton, O.; Rest, A. J.; Taylor, D. J. *J. Chem. Soc., Dalton Trans.* **1980**, 167–173. Green, M. L. H. *Pure Appl. Chem.* **1978**, *50*, 27–35.

(15) Cf. Jones, W. D.; Feher, F. J. *J. Am. Chem. Soc.* **1982**, *104*, 4240–4242. Tolman, C. A.; Ittel, S. D.; English, A. D.; Jesson, J. P. *Ibid.* **1979**, *101*, 1742–1751.

Direct Observation of Metastable Organometallic Cation Radicals from Group 4B Alkyls

B. W. Walther,[1a] F. Williams,*[1a] W. Lau,[1b] and J. K. Kochi*[1b]

Departments of Chemistry, University of Tennessee Knoxville, Tennessee 37996 and Indiana University Bloomington, Indiana 47405[1]

Summary: Transient organometallic cations are generated by electron detachment from various tetrahedral group 4B alkyls. Analyses of the ESR spectra of the lead and tin analogs (Me_4Pb^+, Me_4Sn^+, and t-$BuSnMe_3^+$) are in accord with unusual trigonal-pyramidal structures of C_{3V} symmetry.

The homoleptic organometals, particularly of the group 4B metals (silicon, germanium, tin, and lead), are excellent electron donors.[2] For example, the permethyl derivatives are all readily oxidized by outer-sphere electron transfer to various oxidants in solution or at an electrode surface.[3] Although the kinetics of the chemical and electrochemical oxidations involve a rate-limiting, one-electron process, i.e.

$$Me_4M \xrightarrow{[-e]} Me_4M^+ \quad (1)$$

$$M = Si, Ge, Sn, Pb$$

the existence of the cations Me_4M^+ etc. as *direct* products has merely been inferred, owing to their extremely short lifetimes. Coupled with the relevance to organometallic reaction mechanisms of the ubiquitous charge transfer (CT) interactions extant between such alkylmetals and various electrophiles,[4] e.g.

$$Me_4M\,Br_2 \xrightarrow{h\nu_{CT}} Me_4M^+Br_2^- \quad (2)$$

we have felt that it is important to establish unambiguously the existence of organometal cations by direct observation and to determine the structure of these transient species as viable intermediates.

Indeed, recent developments in the γ irradiation of solid solutions have allowed the tetramethylsilane and tetramethylgermane cation radicals to be detected by electron spin resonance (ESR) spectroscopy.[5] In the course of completing the study with the important lead and tin analogues, we have discovered unusual structural effects which we report herein, since they provide unique insight into these novel organometal cations.

The first-derivative ESR spectrum obtained from a dilute solution of Me_4Pb in trichlorofluoromethane at 90 K after γ irradiation is shown in Figure 1a (upper). The ESR spectrum derived from Me_4Sn under the same conditions is shown in Figure 1b. While these studies were 4B metals (silicon, germanium, tin, and lead), are excellent in progress, Symons also reported an independent observation of Me_4Sn^+.[6] The ESR spectra of Me_4Pb^+ (I) and Me_4Sn^+ (II) are characterized by well-resolved (1:3:3:1) quartet splittings of 14.7 and 13.7 G, respectively, arising from *one unique methyl ligand*. It is noteworthy that the

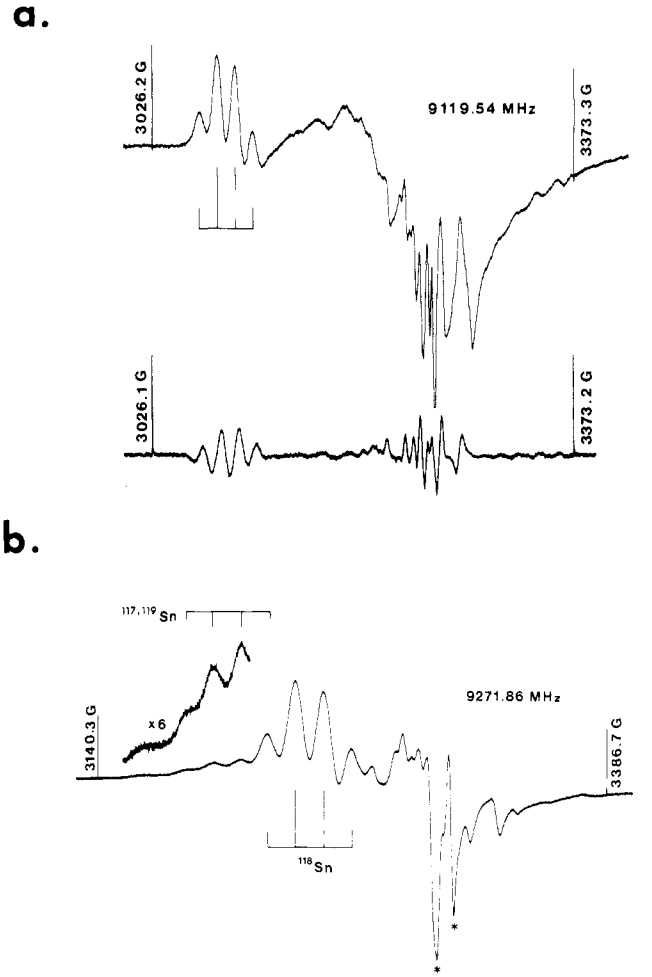

Figure 1. (a) X-band ESR spectrum of a γ-irradiated solution of 3 mol % tetramethyllead in trichlorofluoromethane at 85 K shown in first derivative (upper) and second derivative (lower). (b) First derivative ESR spectrum derived from tetramethyltin under similar conditions. The features marked with the asterisk are photobleached by visible light.

Table I. ESR Parameters of the Organometal Cations of Group 4B Alkyls[a]

cation	proton hfs, G	$^{117,119}Sn$ hfs, G	g value	ref
$H_3CPbMe_3^+$	$A_\perp$(3 H)[b] 14.7		2.111	f
$H_3CSnMe_3^+$	$A_\perp$(3 H)[b] 13.7	77 (⊥)	2.044	f
	13–14	78 (⊥)	2.044	g
$(H_3C)_3CSnMe_3^+$	$A_\perp$(9 H)[c] 7.6	88 (⊥)	2.046	f
$Me_3SnSnMe_3^+$	$A_\perp$(18 H) 3.4	100 (⊥)	2.110 (⊥)	h
$Me_3SnGeMe_3^+$	d	115 (⊥)	2.077 (⊥)	f
$Me_3GeGeMe_3^+$	$A_\perp$((18 H) 5.18		2.0441 (⊥)	i
$Me_3GeSiMe_3^+$	$A_\perp$(18 H)[e] 5.37		2.0274 (⊥)	f
$Me_3SiSiMe_3^+$	$A_\perp$(18 H) 5.55		2.0086[j]	i
	A (18 H) 5.65			k

[a] In trichlorofluoromethane matrix at <90 K. [b] Three protons from a single methyl group. [c] Nine protons from the *tert*-butyl group, $A_\perp$ (^{13}C), 187 G. [d] Not resolved. [e] 18 protons are equivalent within the spectral resolution. [f] This work. [g] From ref 6. [h] From ref 8. [i] From ref 16. [j] g value was recalculated. [k] From ref 17.

(1) (a) University of Tennessee. (b) Indiana University.

(2) Jonas, A. E.; Schweitzer, G. K.; Grimm, F. A.; Carlson, T. A. *J. Electron Spectrosc. Relat. Phenom.* **1972**, *1*, 29. Evans, S.; Green, J. C.; Joachim. P. J.; Orchard, A. F.; Turner, D. W.; Maier, J. P. *J. Chem. Soc., Faraday Trans. 2* **1972**, *68*, 905. Boschi, R.; Lappert, M. R.; Pedley, M. B.; Schmidt, W.; Wilkins, B. T. *J. Organomet. Chem.* **1973**, *50*, 69.

(3) Wong, C. L.; Kochi, J. K. *J. Am. Chem. Soc.* **1979**, *101*, 5593. Klingler, R. J.; Kochi, J. K. *Ibid.* **1980**, *102*, 4790.

(4) (a) Kochi, J. K. "Organometallic Mechanisms and Catalysis"; Academic Press: New York, 1978; Part III. (b) Fukuzumi, S.; Mochida, K.; Kochi, J. K. *J. Am. Chem. Soc.* **1979**, *101*, 5961; **1980**, *102*, 2141; *J. Phys. Chem.* **1980**, *84*, 2246, 2254.

(5) Walther, B. W.; Williams, F. *J. Chem. Soc., Chem. Commun.* **1982**, 270.

(6) Symons, M. C. R. *J. Chem. Soc., Chem. Commun.* **1982**, 869.

0276-7333/83/2302-0688$01.50/0

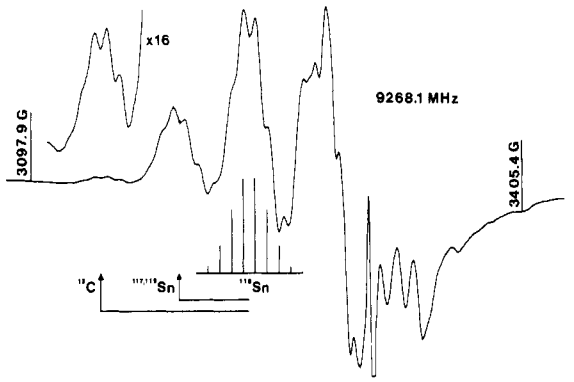

Figure 2. First derivative ESR spectrum obtained from a solution of *tert*-butyltrimethyltin in trichlorofluoromethane under conditions similar to those in Figure 1.

proton hyperfine splittings from the three remaining methyl ligands are less than the spectral resolution of 2–3 G. Furthermore in the tin analogue, the perpendicular component of the hyperfine coupling to the naturally abundant magnetic isotopes of ^{117}Sn and ^{119}Sn with $I = {}^1/_2$ is clearly delineated in the inset recorded at higher gain in Figure 1b. The remarkably small splitting of only 77 G in Table I is consistent with a small degree of s character in the singly occupied molecular orbital (SOMO) and indicative of a planar or near planar metal center.[6] Taken together, these ESR results suggest that the organometal undergoes a dramatic change in configuration from T_d to C_{3V} symmetry attendant upon oxidation. Judging from the similarity of the ^{1}H splitting and the expected larger positive g shift for the perpendicular components of Me_4Pb^+, we surmise that a similar structural reorganization occurs in tetramethyllead. Accordingly, the cations I and II are both envisaged as approximating the trigonal-pyramidal structures in which the SOMO is largely localized in the dashed vertical metal–carbon bond.

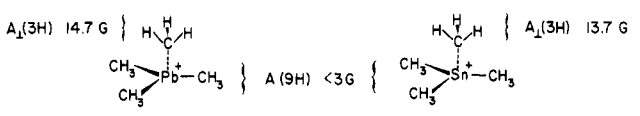

I. II.

In order to focus on the unique methyl ligand in the cation II, we examined the series of monoalkyl analogues $RSnMe_3$ with increasing α-methyl substitution, i.e., R = ethyl, isopropyl, and *tert*-butyl. The ESR spectrum in Figure 2 obtained from *t*-$BuSnMe_3$ is particularly informative. First, the *tert*-butyl ligand is clearly identified by the binomial decet splitting of 7.6 G in the spectrum. Second, the tin splitting of 88 G and the g value of 2.046 are essentially the same as that observed in the parent cation Me_4Sn^+. Third, the weaker feature at lowest field (shown in the inset of Figure 2) is assigned to the $M_I = +{}^1/_2$ perpendicular component of the ^{13}C satellite.[7] The magnitude of the ^{13}C splitting ($A_\perp$ 187 G) is consistent with the pyramidal configuration at the central carbon, similar to that presented for I and II (vide supra).[9] Interestingly, the ESR spectrum obtained from the ethyl derivative $EtSnMe_3$ (under the standard conditions described above) consisted solely of the ethyl radical. Likewise, attempts to observe the cationic *i*-$PrSnMe_3^+$ led only to the ESR spectrum of the isopropyl radical.

The observation of ethyl and isopropyl radicals from $EtSnMe_3$ and *i*-$PrSnMe_3$, respectively, is in direct accord with the chemical and electrochemical studies that have previously established the rapid homolytic fragmentation of these organometal cations, i.e.[3,4]

$$RSnMe_3^+ \xrightarrow{\text{fast}} R\cdot + SnMe_3^+ \qquad (3)$$

The differences in the rates of the facile homolysis in eq 3 can relate to the driving forces, which arise mainly from the stability of the alkyl radical (R·). If so, it is reasonable to formulate the parent Me_4Sn^+ as being sufficiently persistent to allow its ESR observation, owing to the relatively high heat of formation of the methyl radical.[10] Such a thermodynamic explanation, however, is not completely adequate since the *tert*-butyl radical is 19 kcal mol^{-1} more stable than the ethyl radical—yet *t*-$BuSnMe_3^+$ is apparently less prone to homolytic fragmentation than $EtSnMe_3^+$.[11] It is interesting to note that the same unexpected behavior has been recently observed by Skell and May[12] in the homolytic decarboxylation of acyloxy radicals, *t*-$BuCO_2\cdot$ being actually more persistent than $EtCO_2\cdot$. We believe that both phenomena are related and follow their explanation that attributes this difference in homolytic behavior to kinetic instability arising from steric effects.[13]

The transient organometallic cations described above also relate to a series of kindred dimetallic species $Me_3MMMe_3^+$ and heterobimetallic analogues

(7) The relative intensity of the ^{117,119}Sn satellite to the main feature is ~0.35 although the ratio based on the natural abundance (16.4%) of these magnetic isotopes should be only about 0.10. This enhancement can be explained if the spread in the anisotropy of the low-field ($M_I = -{}^1/_2$) ^{117,119}Sn component is significantly less than that of the main feature (cf. ref 8), and this is very likely to be the case here with $A_\parallel > A_\perp$ and $g_\perp > g_\parallel$. A similar argument can be made for the signal enhancement of the low-field ($M_I = {}^1/_2$] ^{13}C satellite feature, and the intensity ratio of the two satellites is close to that (16) of their natural abundances. (Note that the spectral variations in the ^{13}C satellite of *t*-$BuSnMe_3^+$ with alterations in the microwave power, the temperature, and the preferred sample orientation always paralleled the changes in the main features of the spectrum. The ^{13}C splitting in the ESR spectrum of Me_4Sn^+ is presently under study with a highly ^{13}C-enriched sample.)

(8) Symons, M. C. R. *J. Chem. Soc., Chem. Commun.* **1981**, 1251.

(9) (a) For example, the ^{13}C hfs for a tetrahedral configuration is expected to be 204 G if the spin density on carbon is 0.8, which seems to be a reasonable estimate. Syntheses are in progress for tetramethyltin-$^{13}C_4$ and -d_{12}. (b) Note that the structures I and II differ from the C_{2V} distortions in the silicon and germanium analogues.[5] We tentatively suggest that the preferred C_{3V} distortions in Me_4Pb^+ and Me_4Sn^+ results from a tendency of the Me_3M^+ moiety to be more planar and the Me·M bonds to be longer than those in the silicon and germanium structures. Note that the first vertical ionization potentials decrease in the order $Me_4Si > Me_4Ge > Me_4Sn > Me_4Pb$ as 9.42, 9.38, 8.85, 8.38 eV. The same order is probably maintained for the inner d subshells of these metals.[2] For the Jahn–Teller effect on the photoelectron spectra of the series of Me_4M, see ref 2a.

(10) For example the heats of formation of methyl, ethyl, isopropyl, and *tert*-butyl radicals decrease progressively as 34, 26, 17.5 and 7 kcal mol^{-1}, respectively, at 25 °C. Streitwieser, A., Jr.; Heathcock, C. H. "Introduction to Organic Chemistry", 2nd ed.; Macmillan: New York, 1981; p 103. For recent measurements, see: Castelhano, A. L.; Marriot, P. R.; Griller, D. *J. Am. Chem. Soc.* **1981**, *103*, 4262.

(11) It is noteworthy that the ESR spectrum of *tert*-butyl radical is not observed even when the temperature of the matrix is raised to 140 K, and there is a significant decay of the cation. Similarly, the ESR spectrum of the methyl radical is not observed when the matrix temperature of Me_4Sn^+ is raised to 155 K. In this regard, our results differ from those reported by Symons,[6] who managed to trap methyl radicals in his system. Unfortunately, we have not yet been able to repeat this result.

(12) May, D. D.; Skell, P. S. *J. Am. Chem. Soc.* **1982**, *104*, 4500.

(13) For example, steric inhibition to the attainment of planarity in the Me_3Sn moiety during fragmentation of *t*-$BuSnMe_3^+$ is conceptually analogous to the explanation put forth by May and Skell[12] for the relatively slow loss of carbon dioxide from *t*-$BuCO_2\cdot$. Alternatively, a reviewer has suggested an explanation for the apparent persistence of *t*-$BuSnMe_3^+$ compared to the other analogues which is based on polar effects. For example, the relatively low ionization potential of the *tert*-butyl radical [IP (eV): Me· (9.84), Et· (8.51), *i*-Pr· (7.69), *t*-Bu· (6.92) by Houle, F. A.; Beauchamp, J. L. *J. Am. Chem. Soc.* **1979**, *101*, 4067 and discussion by Rollick, K. L.; Kochi, J. K. *Ibid.* **1982**, *104*, 1319] indicates that the *tert*-butyl ligand can lead to an enhanced charge stabilization in the cation radical.

$Me_3M'MMe_3^+$, which can be generated from their neutral diamagnetic precursors by a similar procedure.[14] Pertinent to the structure of the trimethyltin moiety in II, the perpendicular component of the tin splitting in the ESR spectrum of the ditin species $Me_3SnSnMe_3^+$ was found to be 100 G, suggesting that the configuration about each tin center is nearly planar as in II.[8] Similarly, we found the tin splitting in the heterobimetallic species $Me_3GeSnMe_3^+$ to be of the same order of magnitude. The ESR parameters listed in Table I thus relate the tetraalkylmetal cations to the family of hexaalkyldimetal cations in a single consistent pattern.[15]

Acknowledgment. We thank the Division of Chemical Sciences, Office of Basic Energy Sciences, U.S. Department of Energy, and the National Science Foundation for financial support of the research carried out at Tennessee and Indiana, respectively, and Dr. K. Mochida for a sample of $Me_3SnGeMe_3$.

Registry No. $H_3CPbMe_3^+$, 85080-92-8; $H_3CSnMe_3^+$, 84494-88-2; $(H_3C)_3CSnMe_3^+$, 85005-13-6; $Me_3SnSnMe_3^+$, 81419-26-3; $Me_3SnGeMe_3^+$, 85005-14-7; $Me_3GeGeMe_3^+$, 79644-92-1; $Me_3GeSiMe_3^+$, 85005-15-8; $Me_3SiSiMe_3^+$, 77958-47-5.

(14) For the donor properties of these dimetallic systems, see: Szepes, L.; Korányi, T.; Náray-Szabó, G.; Modelli, A.; Distefano, G. *J. Organomet. Chem.* **1981**, *217*, 35.

(15) (a) For the related charge-transfer reactions see ref 4. (b) The sizeable configurational changes incurred during cation formation in these donor systems is no doubt related to the large reorganizational energies λ observed during electron transfer. See: Klingler, R. J.; Kochi, J. K. *J. Am. Chem. Soc. 1981, 103*, 5839.

(16) Wang, J. T.; Williams, F. *J. Chem. Soc., Chem. Commun.* **1981**, 666.

(17) Shida, T.; Kubodera, H.; Egawa, Y. *Chem. Phys. Lett.* **1981**, *79*, 179.

Hydrocarbon–Hydrogen Interactions with Metals. A Molecular Orbital Analysis of $HFe_4(CO)_{12}(\eta^2\text{-CH})$

Catherine E. Housecroft and Thomas P. Fehlner*

Department of Chemistry, University of Notre Dame Notre Dame, Indiana 46556

Received November 3, 1982

Summary: The electronic structure of $HFe_4(CO)_{12}(\eta^2\text{-CH})$ has been examined by using the Fenske–Hall quantum chemical approach with a fragment analysis in terms of the butterfly metal cluster $HFe_4(CO)_{12}^+$ and the ligand CH^-. The preference for the tilted (η^2) orientation of the CH^- ligand over a symmetric vertical orientation can be explained in terms of the unusual properties of the frontier orbitals of the butterfly fragment. The η^2 orientation causes the CH bond to be weakened in the complex because of the mixing of an empty CH antibonding orbital with a filled metal cluster orbital.

While characterizing the electronic structure of $HFe_4(CO)_{12}BH_2$[1] using the Fenske–Hall quantum chemical approach,[2] we had cause to examine the isoelectronic compound $HFe_4(CO)_{12}CH$, Ib.[3] In doing so we observed

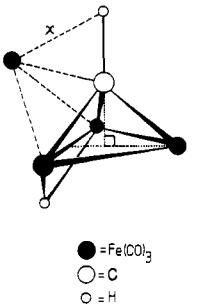

Figure 1. Generation of $HFe_4(CO)_{12}(\eta^2\text{-CH})$ by the capping of an alkylidyne triiron complex, $[HFe_3(CO)_9CH]^{2-}$, with a $Fe(CO)_3^{2+}$ fragment: X(calcd) = 1.82 Å, X(measd) = 1.75 Å.[3] $[HFe_3(CO)_9CH]^{2-}$ geometry was obtained from the known structure of $H_3Fe_3(CO)_9CCH_3$.[8]

the properties of a tetrametal "butterfly" fragment that facilitate the binding of a CH ligand in a tilted (η^2) geometry. Thus, not only does the nature of the ligand bonding generated by this multinuclear array of metal atoms provide a mechanism for B-H bond weakening,[1] but also it suggests one for CH as well.[4,5] Compounds containing transition-metal borane–hydrogen interactions are common;[6] however, those with metal hydrocarbon–hydrogen interactions are not. Ib has been proposed as a reasonable model for C–H bond activation on a metal surface.[7] A comparison of the bonding in the observed (tilted) structure with the hypothetical more symmetric (vertical) structure Ia reveals the orbital properties of a tetrametal "butterfly" fragment that permit the η^2 binding of CH.

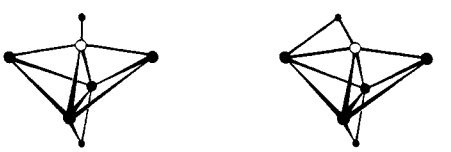

Ia Ib

The primary expression of electronic structure is the geometrical relationship between the observed nuclear positions. A fragment analysis of Ib that is very revealing in this regard is shown in Figure 1. The observed geometry of Ib is quantitatively generated by capping a Fe_2C face of a doubly deprotonated (μ_3-methylidyne)triiron nonacarbonyl complex[8] with a $Fe(CO)_3^{2+}$ fragment. The CH axis in the experimental geometry lies close to a C_3 axis of one metal triangle of the butterfly. Unless fortuitous,

(1) Wong, K. W.; Scheidt, W. R.; Fehlner, T. P. *J. Am. Chem. Soc.* **1982**, *104*, 1111. Fehlner, T. P.; Housecroft, C. E.; Scheidt, W. R.; Wong, K. S. *Organometallics*, in press.

(2) Hall, M. B.; Fenske, R. F. *Inorg. Chem.* **1972**, *11*, 768. Hall, M. B. Ph.D. Thesis, University of Wisconsin, Madison, WI, 1971. Fenske, R. F. *Pure Appl. Chem.* **1971**, *27*, 61.

(3) The synthesis and structural characterization of the compound $HFe_4(CO)_{12}CH$ has been reported in detail. Tachikawa, M.; Muetterties, E. L. *J. Am. Chem. Soc.* **1980**, *102*, 4541. Beno, M. A.; Williams, J. M.; Tachikawa, M.; Muetterties, E. L. *Ibid.* **1980**, *102*, 4542. Beno, M. A.; Williams, J. M.; Tachikawa, M.; Muetterties, E. L. *Ibid.* **1981**, *103*, 1485.

(4) The C–H bond distance in Ia is significantly longer than the accepted value for hydrocarbons (1.19 viz. 1.09 Å).[3]

(5) M–H–C interactions in mononuclear complexes can lead to C–H bond weakening, but apparently to a lesser degree than is accomplished by binding to a multinuclear metal fragment: Goddard, R. J.; Hoffmann, R.; Jemmis, E. D. *J. Am. Chem. Soc.* **1980**, *102*, 7667. A reported interaction between a β-CH and a single metal center actually leads to C–H bond shortening: Dawoodi, Z.; Green, M. L. H.; Mtetwa, V. S. B.; Prout, K. *J. Chem. Soc., Chem. Commun.* **1982**, 802.

(6) Housecroft, C. E.; Fehlner, T. P. *Adv. Organomet. Chem.* **1982**, *21*, 57.

(7) Muetterties, E. L.; Rhodin, T. N.; Band, E.; Brucker, C. F.; Pretzer, W. R. *Chem. Rev.* **1979**, *79*, 91. Gavin, R. M., Jr.; Reutt, J.; Muetterties, E. L. *Proc. Natl. Acad. Sci. U.S.A.* **1981**, *78*, 3981.

(8) Wong, K. W.; Haller, K. J.; Dutta, T. K.; Chipman, D. M.; Fehlner, T. P. *Inorg. Chem.* **1982**, *21*, 3197.

0276-7333/83/2302-0690$01.50/0

$Me_3M'MMe_3^+$, which can be generated from their neutral diamagnetic precursors by a similar procedure.[14] Pertinent to the structure of the trimethyltin moiety in II, the perpendicular component of the tin splitting in the ESR spectrum of the ditin species $Me_3SnSnMe_3^+$ was found to be 100 G, suggesting that the configuration about each tin center is nearly planar as in II.[8] Similarly, we found the tin splitting in the heterobimetallic species $Me_3GeSnMe_3^+$ to be of the same order of magnitude. The ESR parameters listed in Table I thus relate the tetraalkylmetal cations to the family of hexaalkyldimetal cations in a single consistent pattern.[15]

Acknowledgment. We thank the Division of Chemical Sciences, Office of Basic Energy Sciences, U.S. Department of Energy, and the National Science Foundation for financial support of the research carried out at Tennessee and Indiana, respectively, and Dr. K. Mochida for a sample of $Me_3SnGeMe_3$.

Registry No. $H_3CPbMe_3^+$, 85080-92-8; $H_3CSnMe_3^+$, 84494-88-2; $(H_3C)_3CSnMe_3^+$, 85005-13-6; $Me_3SnSnMe_3^+$, 81419-26-3; $Me_3SnGeMe_3^+$, 85005-14-7; $Me_3GeGeMe_3^+$, 79644-92-1; $Me_3GeSiMe_3^+$, 85005-15-8; $Me_3SiSiMe_3^+$, 77958-47-5.

(14) For the donor properties of these dimetallic systems, see: Szepes, L.; Korányi, T.; Náray-Szabó, G.; Modelli, A.; Distefano, G. *J. Organomet. Chem.* **1981**, *217*, 35.

(15) (a) For the related charge-transfer reactions see ref 4. (b) The sizeable configurational changes incurred during cation formation in these donor systems is no doubt related to the large reorganizational energies λ observed during electron transfer. See: Klingler, R. J.; Kochi, J. K. *J. Am. Chem. Soc. 1981, 103*, 5839.

(16) Wang, J. T.; Williams, F. *J. Chem. Soc., Chem. Commun.* **1981**, 666.

(17) Shida, T.; Kubodera, H.; Egawa, Y. *Chem. Phys. Lett.* **1981**, *79*, 179.

Hydrocarbon–Hydrogen Interactions with Metals. A Molecular Orbital Analysis of $HFe_4(CO)_{12}(\eta^2\text{-CH})$

Catherine E. Housecroft and Thomas P. Fehlner*

Department of Chemistry, University of Notre Dame Notre Dame, Indiana 46556

Received November 3, 1982

Summary: The electronic structure of $HFe_4(CO)_{12}(\eta^2\text{-CH})$ has been examined by using the Fenske–Hall quantum chemical approach with a fragment analysis in terms of the butterfly metal cluster $HFe_4(CO)_{12}^+$ and the ligand CH^-. The preference for the tilted (η^2) orientation of the CH^- ligand over a symmetric vertical orientation can be explained in terms of the unusual properties of the frontier orbitals of the butterfly fragment. The η^2 orientation causes the CH bond to be weakened in the complex because of the mixing of an empty CH antibonding orbital with a filled metal cluster orbital.

While characterizing the electronic structure of $HFe_4(CO)_{12}BH_2$[1] using the Fenske–Hall quantum chemical approach,[2] we had cause to examine the isoelectronic compound $HFe_4(CO)_{12}CH$, Ib.[3] In doing so we observed

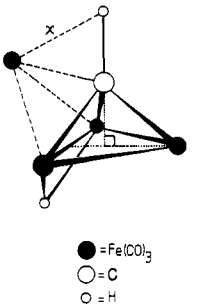

Figure 1. Generation of $HFe_4(CO)_{12}(\eta^2\text{-CH})$ by the capping of an alkylidyne triiron complex, $[HFe_3(CO)_9CH]^{2-}$, with a $Fe(CO)_3^{2+}$ fragment: X(calcd) = 1.82 Å, X(measd) = 1.75 Å.[3] $[HFe_3(CO)_9CH]^{2-}$ geometry was obtained from the known structure of $H_3Fe_3(CO)_9CCH_3$.[8]

the properties of a tetrametal "butterfly" fragment that facilitate the binding of a CH ligand in a tilted (η^2) geometry. Thus, not only does the nature of the ligand bonding generated by this multinuclear array of metal atoms provide a mechanism for B-H bond weakening,[1] but also it suggests one for CH as well.[4,5] Compounds containing transition-metal borane–hydrogen interactions are common;[6] however, those with metal hydrocarbon–hydrogen interactions are not. Ib has been proposed as a reasonable model for C–H bond activation on a metal surface.[7] A comparison of the bonding in the observed (tilted) structure with the hypothetical more symmetric (vertical) structure Ia reveals the orbital properties of a tetrametal "butterfly" fragment that permit the η^2 binding of CH.

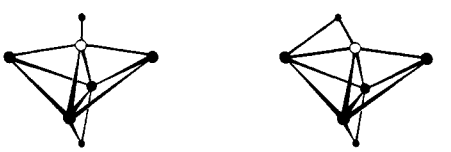

Ia Ib

The primary expression of electronic structure is the geometrical relationship between the observed nuclear positions. A fragment analysis of Ib that is very revealing in this regard is shown in Figure 1. The observed geometry of Ib is quantitatively generated by capping a Fe_2C face of a doubly deprotonated (μ_3-methylidyne)triiron nonacarbonyl complex[8] with a $Fe(CO)_3^{2+}$ fragment. The CH axis in the experimental geometry lies close to a C_3 axis of one metal triangle of the butterfly. Unless fortuitous,

(1) Wong, K. W.; Scheidt, W. R.; Fehlner, T. P. *J. Am. Chem. Soc.* **1982**, *104*, 1111. Fehlner, T. P.; Housecroft, C. E.; Scheidt, W. R.; Wong, K. S. *Organometallics*, in press.

(2) Hall, M. B.; Fenske, R. F. *Inorg. Chem.* **1972**, *11*, 768. Hall, M. B. Ph.D. Thesis, University of Wisconsin, Madison, WI, 1971. Fenske, R. F. *Pure Appl. Chem.* **1971**, *27*, 61.

(3) The synthesis and structural characterization of the compound $HFe_4(CO)_{12}CH$ has been reported in detail. Tachikawa, M.; Muetterties, E. L. *J. Am. Chem. Soc.* **1980**, *102*, 4541. Beno, M. A.; Williams, J. M.; Tachikawa, M.; Muetterties, E. L. *Ibid.* **1980**, *102*, 4542. Beno, M. A.; Williams, J. M.; Tachikawa, M.; Muetterties, E. L. *Ibid.* **1981**, *103*, 1485.

(4) The C–H bond distance in Ia is significantly longer than the accepted value for hydrocarbons (1.19 viz. 1.09 Å).[3]

(5) M–H–C interactions in mononuclear complexes can lead to C–H bond weakening, but apparently to a lesser degree than is accomplished by binding to a multinuclear metal fragment: Goddard, R. J.; Hoffmann, R.; Jemmis, E. D. *J. Am. Chem. Soc.* **1980**, *102*, 7667. A reported interaction between a β-CH and a single metal center actually leads to C–H bond shortening: Dawoodi, Z.; Green, M. L. H.; Mtetwa, V. S. B.; Prout, K. *J. Chem. Soc., Chem. Commun.* **1982**, 802.

(6) Housecroft, C. E.; Fehlner, T. P. *Adv. Organomet. Chem.* **1982**, *21*, 57.

(7) Muetterties, E. L.; Rhodin, T. N.; Band, E.; Brucker, C. F.; Pretzer, W. R. *Chem. Rev.* **1979**, *79*, 91. Gavin, R. M., Jr.; Reutt, J.; Muetterties, E. L. *Proc. Natl. Acad. Sci. U.S.A.* **1981**, *78*, 3981.

(8) Wong, K. W.; Haller, K. J.; Dutta, T. K.; Chipman, D. M.; Fehlner, T. P. *Inorg. Chem.* **1982**, *21*, 3197.

0276-7333/83/2302-0690$01.50/0

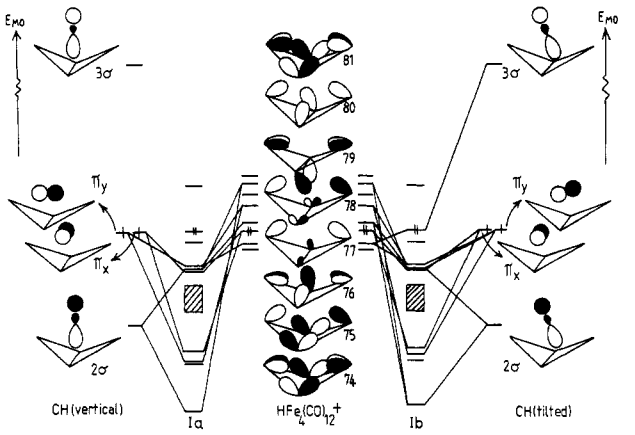

Figure 2. Correlation of MO's of $HFe_4(CO)_{12}^+$ and CH^-. The center column shows a schematic representation of the frontier orbitals of the $HFe_4(CO)_{12}^+$ fragment. The left-hand side of the figure shows how these fragment orbitals interact with those of CH^- when the ligand is in a vertical orientation, Ia. (Note that although π_x only interacts with 76, the interaction leads to *two* MO's in the complex Ia. In all there are six MO's of the complex with major metal ligand character.) The right-hand side of the figure shows additional orbital interactions that are a consequence of tilting the ligand into geometry Ib. Orbital 76 is the HOMO of $HFe_4(CO)_{12}^+$. Orbitals 74, 79, and 81 do not interact significantly with the CH^- fragment.

this geometrical analysis implies that the demonstrated affinity for C–R to be bound perpendicularly to a trimetal fragment[9] is important in stabilizing Ib over Ia.[10] The geometrical analysis reveals nothing concerning the nature of the Fe–H–C interaction (bonding, nonbonding, antibonding). Hence, molecular orbital (MO) calculations[11] on both Ia and Ib are compared below and provide a more detailed understanding of the preference for structure Ib.

In contrast to the above geometrical analysis, the calculations are analyzed in terms of the $HFe_4(CO)_{12}^+$ and CH^- fragments as this provides a straightforward method of exploring the differences between Ia and Ib. The orbitals of the CH^- fragment are simple and may be found in standard texts; however, those of the $HFe_4(CO)_{12}^+$ fragment are complex and are briefly described here. The set of eight frontier orbitals of this fragment are illustrated in Figure 2; however, only five of these (75, 76, 77, 78, and 80) are of interest here since these are the principal orbitals involved in binding the CH^- ligand (see the correlation diagram in Figure 2). Hence, only the changes in these interactions in going from Ia to Ib are examined. The major changes diagramatically illustrated in Figure 2 are described in the following.

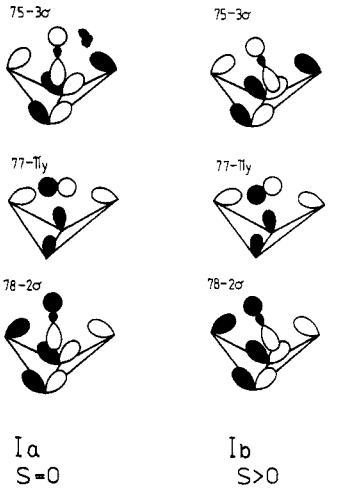

Figure 3. The three principal orbital interactions that lead to increased overlap, S, between the fragments when the CH^- ligand is tilted with respect to the tetrairon fragment. The left-hand column emphasizes that these orbital combinations are symmetry disallowed before tilting.

Complex Ia possesses six MO's containing the major fragment–fragment interactions. With respect to the C_2 axis of the butterfly fragment, two have σ symmetry, two have π_x symmetry, and two have π_y symmetry. In going to Ib the distinction between σ and π_y symmetry is lost and the four MO's having these symmetries in Ia are substantially altered in Ib. In terms of relative metal–ligand Mulliken overlap populations the σ MO's of Ia become more bonding in going to Ib; i.e., tilting favors the Ib structure. In contrast the π_y MO's of Ia experience a substantial loss of metal–ligand overlap population on going to Ib; i.e. tilting favors structure Ia. The balance between these two opposing interactions is a delicate one;[14] however, the net fragment–fragment overlap populations do suggest a small preference for the observed structure Ib.

In terms of qualitative understanding it is profitable to examine the fragment orbitals of $HFe_4(CO)_{12}^+$ that experience significant perturbation on tilting the CH^- ligand. As judged by changes in Mulliken populations between Ia and Ib, only orbitals 77 and 78 (Figure 2) qualify in this regard. Specifically the symmetry disallowed interaction ($77-\pi_y$) in Ia becomes allowed in Ib (Figure 3) but takes place at the expense of the ($78-\pi_y$) interaction. As shown in Figure 3, the π_y orbital of CH interacts with one triangular array of iron atoms in Ib in the same fashion as the $2p\pi$ orbitals of CH interact with the cobalt atoms in $Co_3(CO)_9CH$.[15] Likewise the ($78-\sigma$) interaction that is disallowed in Ia becomes important in Ib. Note that although tilting perturbs the ($80-\sigma$) interaction, the symmetry of the fragment orbital suggests and the net overlaps confirm little change in the strength of the bonding interaction. Thus, the factor that favors the Ib structure is the strong CH σ and π_y interactions with the iron atoms

(9) A large number of compounds of this type have been structurally characterized. See for example: Raithby, P. R. In "Transition Metal Clusters"; Johnson, B. F. G., Ed.; John Wiley: New York, 1980; p 5. The fact that this system exists under metal fragment "redistribution" conditions suggests considerable thermodynamic stability for the RCM_3 unit. Beurich, H.; Vahrenkamp, H. *Angew. Chem., Int. Ed. Engl.* **1981**, *93*, 128.

(10) A recent report of the structure of $HOs_3(CO)_{10}CH$ demonstrates that preference of CH for a capping position on a trimetal fragment can be overridden. Shapley, J. R.; Cree-Uchiyama, M. E.; St. George, G. M.; Churchill, M. R.; Bueno, C. *J. Am. Chem. Soc.* **1983**, *105*, 140.

(11) Calculations have been carried out on a total of eight isoelectronic compounds; however, the results on Ia and Ib are sufficient to establish the qualitative points. The Fenske–Hall technique allows the solutions of the SCF problem in an atomic orbital basis set to be explicitly transformed into a basis set of the fragment orbitals.[12] Not only does this simplify the development of a correlation between fragments and molecule but also allows the examination of Mulliken populations related to fragment–fragment bonding. The geometry of Ib was derived from that of $HFe_4(CO)_{12}BH_2$[1] and the experimental structure.[3] Calculations were carried out for structures with the CH carbon centered between the wing-tip irons as well as off center as found experimentally. The geometry of Ia was the same as that of Ib except the CH hydrogen was placed on the C_2 axis. The basis functions used have been described previously.[13] There are no adjustable parameters in Fenske–Hall method. Results of extended Hückel calculations on the same system may be found in ref 7. We have also completed extended Hückel calculations on Ia and Ib with results that support the conclusions derived from the Fenske–Hall method.

(12) See for example: Kostic, N. M.; Fenske, R. F. *Organometallics* **1982**, *1*, 974.

(13) DeKock, R. L.; Wong, K. W.; Fehlner, T. P. *Inorg. Chem.* **1982**, *21*, 3203.

(14) In fact the total energy is only 3 kcal more negative for Ib vs. Ia in the extended Hückel methods.

of one of the butterfly's triangular wings. But these (plus the π_x interaction which is unchanged by tilting) are exactly the ones that account for the bonding of the CH fragment to the $Co_3(CO)_9$ fragment in $Co_3(CO)_9CH$.[15] Thus, the geometrical arguments are confirmed in the calculations.

The calculations show that a consequence of tilting the CH ligand is the involvement of the high-lying CH 3σ antibonding orbital in the interaction with the metal fragment (Figure 2). In going from Ia to Ib, a previously symmetry-disallowed interaction develops between the filled fragment MO 75[16] and the empty 3σ orbital (Figure 3). A net bonding interaction develops between the carbon atom and the same iron triangle emphasized above as well as between the hydrogen atom and the remaining wing-tip iron. This further stabilizes the tilted geometry. The 3σ orbital is empty both in the free CH^- and in Ia. Since the 3σ orbital is C–H antibonding, acceptance of electronic charge from the metal fragment will necessarily weaken the CH bond on forming Ib. Hence the appearance of such an interaction in the HOMO of Ib provides a satisfying mechanism for the known lengthening of the CH bond in Ib.[3] It is the availability of a special cluster fragment orbital inherent in the butterfly fragment that permits this phenomenon to occur.[17]

In summary, the CH^- ligand prefers to be bound perpendicularly to a triangle of iron atoms contained within the $HFe_4(CO)_{12}^+$ butterfly. In attaining this orientation, an otherwise disallowed interaction between an empty, CH antibonding orbital and a filled metal cluster orbital occurs. Consequently, the carbon is bound more strongly to the triiron triangle, the hydrogen is bound to the unused wing-tip metal, and the carbon–hydrogen bonding decreases; i.e., the butterfly becomes the "rack" upon which the CH bond is stretched.

Acknowledgment. The support of the National Science Foundation under Grant No. CHE 81-09503 is gratefully acknowledged. We also thank the Notre Dame Computing Center for computing time and Professor Roger DeKock for his help with the transformations.

Registry No. Ib, 74792-06-6; Fe, 7439-89-6.

(15) (a) Evans, J. *J. Chem. Soc., Dalton Trans.* **1980**, 1980. (b) Chesky, P. T.; Hall, M. B. *Inorg. Chem.* **1981**, *20*, 4419. (c) Granozzi, G.; Tondello, E.; Ajö, D.; Casarin, M.; Aime, S.; Osella, D. *Ibid.* **1982**, *21*, 1081. (d) Xiang, S. F.; Bakke, A. A.; Chen, H.-W.; Eyermann, C. J.; Hoskins, J. L.; Lee, T. H.; Seyferth, D.; Withers, H. P., Jr.; Jolly, W. L. *Organometallics*, **1982**, *1*, 699. (e) DeKock, R. L.; Deshmukh, P.; Dutta, T. K.; Fehlner, T. P.; Housecroft, C. E.; Hwang, J. L.-S. *Organometallics*, in press.

(16) Note that like 77 orbital 75 has neither σ nor π symmetry with respect to the C_2 axis of the metal butterfly.

(17) The calculations on Ib with the carbon of the CH slipped towards a wingtip iron, as found in the known structure,[3] support these conclusions and reveal a greater net CH–cluster overlap population as well as greater population of the CH 3σ orbital in the complex.

1,2-Silaoxetane. An Alternative View

Thomas J. Barton* and Gregory P. Hussmann

Department of Chemistry, Iowa State University
Ames, Iowa 50011

Received January 10, 1983

Summary: The NMR and IR spectral data recently reported by Ando in support of their claim of the first isolation of a 1,2-silaoxetane are reinterpreted as most consistent with six-membered-ring ketene acetal.

In the decade since we first proposed[1] that silenes (1) reacted with carbonyl compounds to afford olefins and silanones (3) through the intermediacy of 2-silaoxetanes (2) (eq 1), many unsuccessful attempts[2] have been made to prepare isolable 2-silaoxetanes to test this often utilized[3] mechanistic rational.

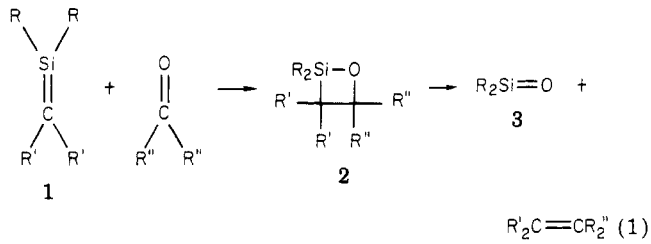

Thus, it was of considerable interest to read the recent report[4] that cothermolysis of ethyl pentamethyldisilanyldiazoacetate (4) and 2-norbornanone produced isolable 2-silaoxetane 7 in 38% yield. The suggested mechanism was addition of silene 5 to generate zwitterion 6 which closes to 7 (eq 2).

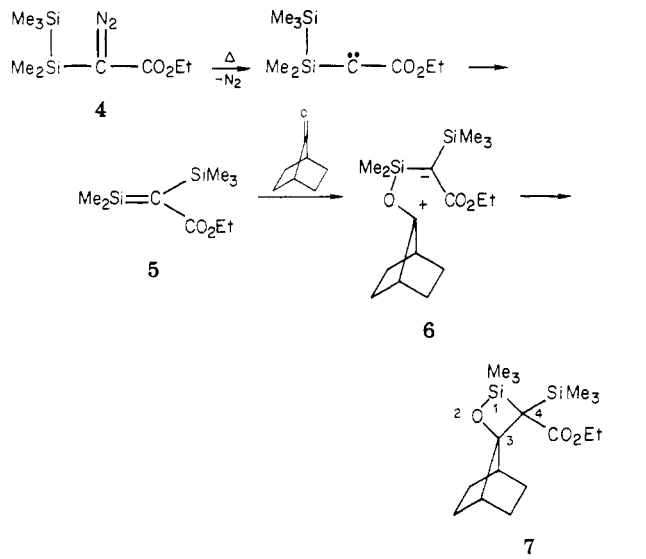

Two strange spectroscopic features were noted for 7: "an unusual chemical shift of ^{13}C at C_3 (113.8 ppm) and an abnormal stretching vibration of the ester carbonyl (1560 cm^{-1})".[4] In addition, although not commented upon, was the unusual low-field chemical shift (58.9 ppm) of C_4. We would submit that these spectral values are *not* abnormal for the correct structure of adduct 7, namely, ketene acetal 8—not an unexpected cyclization product from zwitterion 6.

(1) Barton, T. J.; Kline, E. A.; Garvey, P. M., 3rd International Symposium on Organosilicon Chemistry, Madison, WI, 1972.

(2) (a) Gusel'nikov, L. E.; Nametkin, N. S. *Chem. Rev.* **1979**, *79*, 529. (b) Barton, T. J. *Pure Appl. Chem.* **1980**, *52*, 615.

(3) (a) Ando, W.; Sekiguchi, A.; Migita, T. *J. Am. Chem. Soc.* **1975**, *97*, 7159. (b) Barton, T. J.; Kilgour, J. A. *Ibid.* **1976**, *98*, 7231. (c) Ando, W.; Ikeno, M.; Sekiguchi, A. *Ibid.* **1977**, *99*, 6447. (d) Golino, C. M.; Bush, R. D.; Sommer, L. H. *Ibid.* **1975**, *97*, 7371. (e) Reference 2.

(4) Ando, W.; Sekiguchi, A.; Sato, T. *J. Am. Chem. Soc.* **1982**, *104*, 6830.

0276-7333/83/2302-0692$01.50/0

of one of the butterfly's triangular wings. But these (plus the π_x interaction which is unchanged by tilting) are exactly the ones that account for the bonding of the CH fragment to the $Co_3(CO)_9$ fragment in $Co_3(CO)_9CH$.[15] Thus, the geometrical arguments are confirmed in the calculations.

The calculations show that a consequence of tilting the CH ligand is the involvement of the high-lying CH 3σ antibonding orbital in the interaction with the metal fragment (Figure 2). In going from Ia to Ib, a previously symmetry-disallowed interaction develops between the filled fragment MO 75[16] and the empty 3σ orbital (Figure 3). A net bonding interaction develops between the carbon atom and the same iron triangle emphasized above as well as between the hydrogen atom and the remaining wing-tip iron. This further stabilizes the tilted geometry. The 3σ orbital is empty both in the free CH^- and in Ia. Since the 3σ orbital is C–H antibonding, acceptance of electronic charge from the metal fragment will necessarily weaken the CH bond on forming Ib. Hence the appearance of such an interaction in the HOMO of Ib provides a satisfying mechanism for the known lengthening of the CH bond in Ib.[3] It is the availability of a special cluster fragment orbital inherent in the butterfly fragment that permits this phenomenon to occur.[17]

In summary, the CH^- ligand prefers to be bound perpendicularly to a triangle of iron atoms contained within the $HFe_4(CO)_{12}^+$ butterfly. In attaining this orientation, an otherwise disallowed interaction between an empty, CH antibonding orbital and a filled metal cluster orbital occurs. Consequently, the carbon is bound more strongly to the triiron triangle, the hydrogen is bound to the unused wing-tip metal, and the carbon–hydrogen bonding decreases; i.e., the butterfly becomes the "rack" upon which the CH bond is stretched.

Acknowledgment. The support of the National Science Foundation under Grant No. CHE 81-09503 is gratefully acknowledged. We also thank the Notre Dame Computing Center for computing time and Professor Roger DeKock for his help with the transformations.

Registry No. Ib, 74792-06-6; Fe, 7439-89-6.

(15) (a) Evans, J. *J. Chem. Soc., Dalton Trans.* **1980**, 1980. (b) Chesky, P. T.; Hall, M. B. *Inorg. Chem.* **1981**, *20*, 4419. (c) Granozzi, G.; Tondello, E.; Ajö, D.; Casarin, M.; Aime, S.; Osella, D. *Ibid.* **1982**, *21*, 1081. (d) Xiang, S. F.; Bakke, A. A.; Chen, H.-W.; Eyermann, C. J.; Hoskins, J. L.; Lee, T. H.; Seyferth, D.; Withers, H. P., Jr.; Jolly, W. L. *Organometallics*, **1982**, *1*, 699. (e) DeKock, R. L.; Deshmukh, P.; Dutta, T. K.; Fehlner, T. P.; Housecroft, C. E.; Hwang, J. L.-S. *Organometallics*, in press.

(16) Note that like 77 orbital 75 has neither σ nor π symmetry with respect to the C_2 axis of the metal butterfly.

(17) The calculations on Ib with the carbon of the CH slipped towards a wingtip iron, as found in the known structure,[3] support these conclusions and reveal a greater net CH–cluster overlap population as well as greater population of the CH 3σ orbital in the complex.

1,2-Silaoxetane. An Alternative View

Thomas J. Barton* and Gregory P. Hussmann

Department of Chemistry, Iowa State University
Ames, Iowa 50011

Received January 10, 1983

Summary: The NMR and IR spectral data recently reported by Ando in support of their claim of the first isolation of a 1,2-silaoxetane are reinterpreted as most consistent with six-membered-ring ketene acetal.

In the decade since we first proposed[1] that silenes (1) reacted with carbonyl compounds to afford olefins and silanones (3) through the intermediacy of 2-silaoxetanes (2) (eq 1), many unsuccessful attempts[2] have been made to prepare isolable 2-silaoxetanes to test this often utilized[3] mechanistic rational.

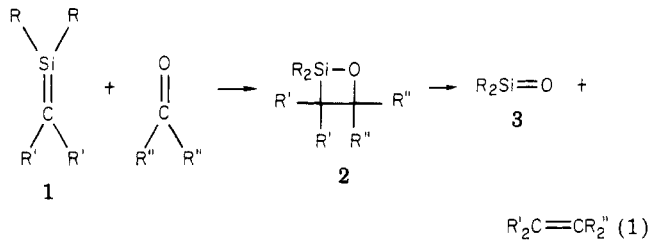

Thus, it was of considerable interest to read the recent report[4] that cothermolysis of ethyl pentamethyldisilanyldiazoacetate (4) and 2-norbornanone produced isolable 2-silaoxetane 7 in 38% yield. The suggested mechanism was addition of silene 5 to generate zwitterion 6 which closes to 7 (eq 2).

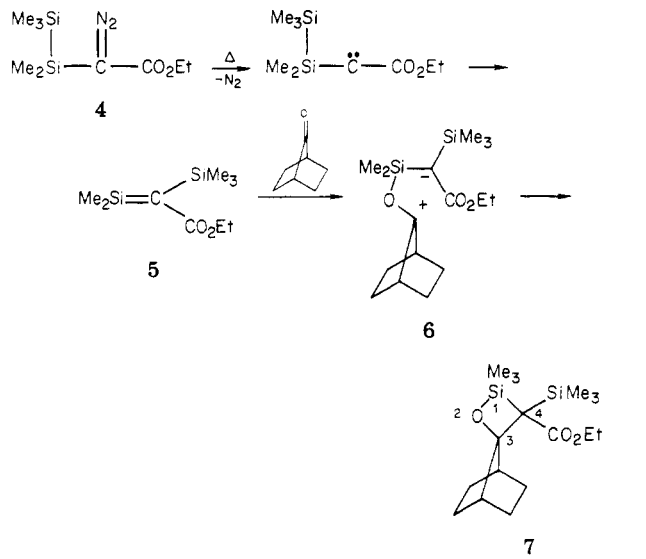

Two strange spectroscopic features were noted for 7: "an unusual chemical shift of ^{13}C at C_3 (113.8 ppm) and an abnormal stretching vibration of the ester carbonyl (1560 cm^{-1})".[4] In addition, although not commented upon, was the unusual low-field chemical shift (58.9 ppm) of C_4. We would submit that these spectral values are *not* abnormal for the correct structure of adduct 7, namely, ketene acetal 8—not an unexpected cyclization product from zwitterion 6.

(1) Barton, T. J.; Kline, E. A.; Garvey, P. M., 3rd International Symposium on Organosilicon Chemistry, Madison, WI, 1972.

(2) (a) Gusel'nikov, L. E.; Nametkin, N. S. *Chem. Rev.* **1979**, *79*, 529. (b) Barton, T. J. *Pure Appl. Chem.* **1980**, *52*, 615.

(3) (a) Ando, W.; Sekiguchi, A.; Migita, T. *J. Am. Chem. Soc.* **1975**, *97*, 7159. (b) Barton, T. J.; Kilgour, J. A. *Ibid.* **1976**, *98*, 7231. (c) Ando, W.; Ikeno, M.; Sekiguchi, A. *Ibid.* **1977**, *99*, 6447. (d) Golino, C. M.; Bush, R. D.; Sommer, L. H. *Ibid.* **1975**, *97*, 7371. (e) Reference 2.

(4) Ando, W.; Sekiguchi, A.; Sato, T. *J. Am. Chem. Soc.* **1982**, *104*, 6830.

0276-7333/83/2302-0692$01.50/0

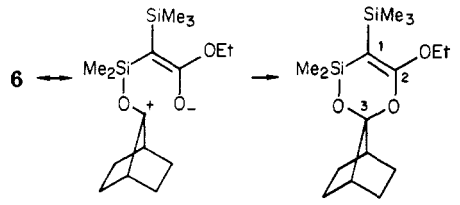

We assign the CMR absorptions at δ 58.9 and 164.7 (assumed carbonyl) to C_1 and C_2 of **8**. Indeed, these values are remarkably close to those observed for dimethylketene acetal (**9**).[5] The ^{13}C NMR absorption at δ 113.8 we assign to C_3. The methylene carbons of oxetane[6] (**10**) are found at δ 72.6, while ketal carbons are usually around δ 100 (e.g., 1,1-diethoxyethane (**11**).[7] Lastly, one must contend with the IR band at 1560 cm^{-1} that is clearly too low to be an ester carbonyl. That this band is the olefinic stretching vibration in **8** is not immediately obvious since the C=C stretching frequency of enol ethers does not usually differ much from normal olefins.[8] However, it has long been known that silyl substitution produces dramatic bathochromic shifts of $\nu_{C=C}$ as can be dramatically seen for the olefinic sequence **12**, **13**, and **14**.[9] Thus, a strong IR band at 1560 cm^{-1} is not unexpected for **8**.

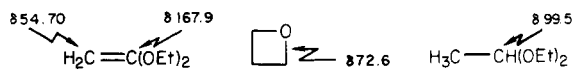

9, $\nu_{C=C}$ 1639 cm^{-1} **10** **11**

$H_2C{=}CH_2$
12, $\nu_{C=C}$ 1623 cm^{-1}

$Me_3SiCH{=}CH_2$
13, $\nu_{C=C}$ 1592 cm^{-1}

$(Me_3Si)_2C{=}CH_2$
14, $\nu_{C=C}$ 1569 cm^{-1}

Adduct **8** also provides an excellent rational for the reported observations[4] (surprising for **7**) that both thermolysis and methanolysis of **7** regenerated norbornanone as the major product. While it is certainly possible that **7** is involved in formation of the minor thermolysis product **15**, that explanation is not demanded.

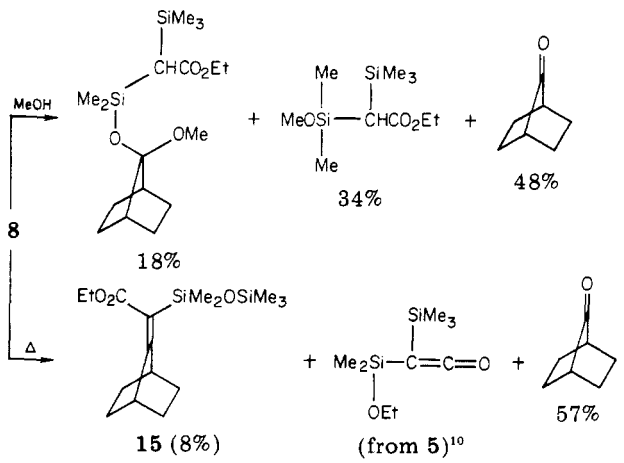

Registry No. **7**, 83547-74-4; **8**, 85185-51-9.

(5) Herberhold, M.; Wiedersatz, G. O.; Kreiter, C. B. *Z. Naturforsch., B: Anorg. Chem., Org. Chem.* **1976**, *31B*, 35.
(6) Silverstein, R. M.; Bassler, G. C.; Morrill, T. C. "Spectrometric Identification of Organic Compounds", 4th ed.; Wiley: New York, 1981; p. 269.
(7) Johnson, L. F.; Jankowski "Carbon-13 NMR spectra", Wiley-Interscience: New York, 1972; p 217.
(8) Dolphin, D.; Wick, A. "Tabulation of Infrared Spectral Data"; Wiley-Interscience: New York, 1977; pp 96–112.
(9) Bock, H.; Seidl, H. *J. Organomet. Chem.* **1968**, *13*, 87.
(10) Ando, W.; Sekiguchi, A.; Sato, T. *J. Am. Chem. Soc.* **1981**, *103*, 5573.

Properties of the Pentacarbonyls of Ruthenium and Osmium

Paul Rushman, Gilbert N. van Buuren, Mahmoud Shiralian, and Roland K. Pomeroy*

Department of Chemistry, Simon Fraser University Burnaby, British Columbia, Canada V5A 1S6

Received December 28, 1982

Summary: The pentacarbonyls of ruthenium and osmium have been prepared by the action of high-pressure carbon monoxide on the corresponding solid trimetal dodecarbonyls at elevated temperatures. Physical data for the pentacarbonyls are reported along with some chemical properties of the osmium compound.

The pentacarbonyls of ruthenium and osmium have been known for several decades.[1,2] However, except for the work of Calderazzo and L'Eplattenier,[3] they have been little studied, presumably because of the difficulty involved in their preparation. We have developed a useful method for the routine synthesis of these important compounds in a pure form. This has allowed their spectral and physical characteristics to be accurately determined.

Pure $Ru(CO)_5$ was formed nearly quantitatively by the reaction of solid $Ru_3(CO)_{12}$ with CO (ca. 200 atm) at 160 °C.[4] When freshly prepared, $Ru(CO)_5$ was a colorless liquid at room temperature (mp −17 to −16 °C) which rapidly developed a yellow-orange coloration due to the formation of $Ru_3(CO)_{12}$. It was extremely sensitive to heat and light and had to be handled in the dark to prevent decomposition. Pure $Os(CO)_5$ was formed (in ca. 60% yield) from the corresponding reaction of $Os_3(CO)_{12}$ and CO (200 atm) only at much higher temperatures (280–290 °C).[5] The much more forcing conditions required are consistent with the view that the osmium–osmium bonds are stronger than ruthenium–ruthenium bonds.[7] As isolated, $Os(CO)_5$ formed large, colorless to pale yellow crystals that melted at 2–2.5 °C to give a mobile yellow liquid. It was far more robust than its ruthenium congener and only formed $Os_3(CO)_{12}$ at a significant rate at 80 °C or above (in solution under normal laboratory lighting). It may be stored indefinitely at −15 °C without any special precautions.

If the reactions were carried out in hexane, solutions of the pentacarbonyls were produced. However, the conditions used to prepare $Os(CO)_5$ were sufficiently extreme to cause the formation of some hexenes by dehydrogenation of the solvent. (Control experiments have shown that

(1) Manchot, W.; Manchot, W. J. *Z. Anorg. Allg. Chem.* **1936**, *226*, 385.
(2) Heiber, W.; Stallmann, H. *Z. Elektrochem.* **1943**, *49*, 288.
(3) Calderazzo, F.; L'Eplattenier, F. *Inorg. Chem.* **1967**, *6*, 1220; **1968**, *7*, 1290.
(4) The trimetal dodecacarbonyl, $M_3(CO)_{12}$ (1.0–2.0 g), was placed in a high-pressure autoclave (500 mL) and the vessel pressurized with CO (ca. 200 atm). It was sealed and heated (M = Ru, 160 °C; M = Os, 280 °C) for 48 h after which the autoclave was cooled to −78 °C and the gas vented. The autoclave was connected to a vacuum line, and, as the autoclave warmed to room temperature, the $M(CO)_5$ product was vacuum distilled (<5 × 10^{-3} mmHg) into a trap cooled to −196 °C (M = Ru, quantitative yield; M = Os, yield ca. 60%). The ruthenium compound was collected with the strict exclusion of light.
(5) This method of preparation is reminiscent of the original synthesis of $Os(CO)_5$[2]: treatment of OsO_4 with CO (200–300 atm) at 150–300 °C. Dodecacarbonyltriosmium is usually prepared from OsO_4 and CO under milder conditions (100 atm, 150 °C).[6]
(6) Johnson, B. F. G.; Lewis, J.; Kilty, P. A. *J. Chem. Soc. A* **1968**, 2859.
(7) Cotton, F. A.; Wilkinson, G. "Advanced Inorganic Chemistry"; 4th ed.; Wiley: New York, 1980; p 1082.

0276-7333/83/2302-0693$01.50/0

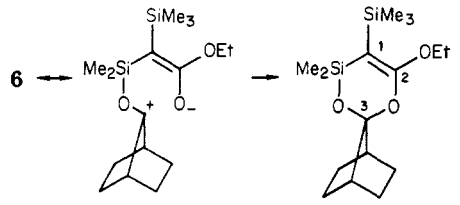

We assign the CMR absorptions at δ 58.9 and 164.7 (assumed carbonyl) to C_1 and C_2 of **8**. Indeed, these values are remarkably close to those observed for dimethylketene acetal (**9**).[5] The ^{13}C NMR absorption at δ 113.8 we assign to C_3. The methylene carbons of oxetane[6] (**10**) are found at δ 72.6, while ketal carbons are usually around δ 100 (e.g., 1,1-diethoxyethane (**11**).[7] Lastly, one must contend with the IR band at 1560 cm^{-1} that is clearly too low to be an ester carbonyl. That this band is the olefinic stretching vibration in **8** is not immediately obvious since the C=C stretching frequency of enol ethers does not usually differ much from normal olefins.[8] However, it has long been known that silyl substitution produces dramatic bathochromic shifts of $\nu_{C=C}$ as can be dramatically seen for the olefinic sequence **12**, **13**, and **14**.[9] Thus, a strong IR band at 1560 cm^{-1} is not unexpected for **8**.

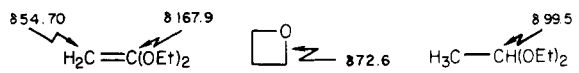

9, $\nu_{C=C}$ 1639 cm^{-1} **10** **11**

$H_2C{=}CH_2$
12, $\nu_{C=C}$ 1623 cm^{-1}

$Me_3SiCH{=}CH_2$
13, $\nu_{C=C}$ 1592 cm^{-1}

$(Me_3Si)_2C{=}CH_2$
14, $\nu_{C=C}$ 1569 cm^{-1}

Adduct **8** also provides an excellent rational for the reported observations[4] (surprising for **7**) that both thermolysis and methanolysis of **7** regenerated norbornanone as the major product. While it is certainly possible that **7** is involved in formation of the minor thermolysis product **15**, that explanation is not demanded.

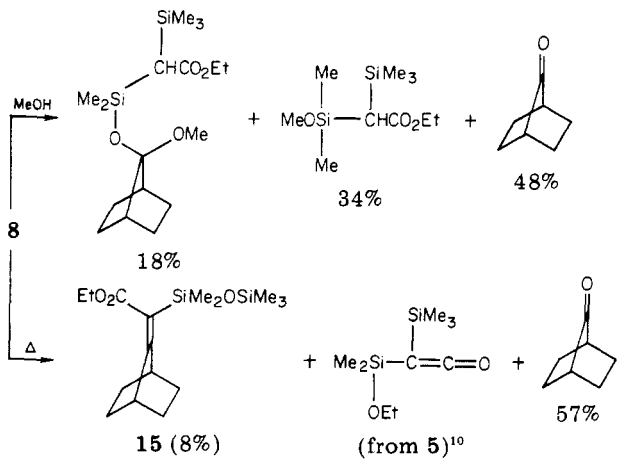

Registry No. **7**, 83547-74-4; **8**, 85185-51-9.

(5) Herberhold, M.; Wiedersatz, G. O.; Kreiter, C. B. *Z. Naturforsch., B: Anorg. Chem., Org. Chem.* **1976**, *31B*, 35.
(6) Silverstein, R. M.; Bassler, G. C.; Morrill, T. C. "Spectrometric Identification of Organic Compounds", 4th ed.; Wiley: New York, 1981; p. 269.
(7) Johnson, L. F.; Jankowski "Carbon-13 NMR spectra", Wiley-Interscience: New York, 1972; p 217.
(8) Dolphin, D.; Wick, A. "Tabulation of Infrared Spectral Data"; Wiley-Interscience: New York, 1977; pp 96–112.
(9) Bock, H.; Seidl, H. *J. Organomet. Chem.* **1968**, *13*, 87.
(10) Ando, W.; Sekiguchi, A.; Sato, T. *J. Am. Chem. Soc.* **1981**, *103*, 5573.

Properties of the Pentacarbonyls of Ruthenium and Osmium

Paul Rushman, Gilbert N. van Buuren, Mahmoud Shiralian, and Roland K. Pomeroy*

Department of Chemistry, Simon Fraser University Burnaby, British Columbia, Canada V5A 1S6

Received December 28, 1982

Summary: The pentacarbonyls of ruthenium and osmium have been prepared by the action of high-pressure carbon monoxide on the corresponding solid trimetal dodecarbonyls at elevated temperatures. Physical data for the pentacarbonyls are reported along with some chemical properties of the osmium compound.

The pentacarbonyls of ruthenium and osmium have been known for several decades.[1,2] However, except for the work of Calderazzo and L'Eplattenier,[3] they have been little studied, presumably because of the difficulty involved in their preparation. We have developed a useful method for the routine synthesis of these important compounds in a pure form. This has allowed their spectral and physical characteristics to be accurately determined.

Pure $Ru(CO)_5$ was formed nearly quantitatively by the reaction of solid $Ru_3(CO)_{12}$ with CO (ca. 200 atm) at 160 °C.[4] When freshly prepared, $Ru(CO)_5$ was a colorless liquid at room temperature (mp −17 to −16 °C) which rapidly developed a yellow-orange coloration due to the formation of $Ru_3(CO)_{12}$. It was extremely sensitive to heat and light and had to be handled in the dark to prevent decomposition. Pure $Os(CO)_5$ was formed (in ca. 60% yield) from the corresponding reaction of $Os_3(CO)_{12}$ and CO (200 atm) only at much higher temperatures (280–290 °C).[5] The much more forcing conditions required are consistent with the view that the osmium–osmium bonds are stronger than ruthenium–ruthenium bonds.[7] As isolated, $Os(CO)_5$ formed large, colorless to pale yellow crystals that melted at 2–2.5 °C to give a mobile yellow liquid. It was far more robust than its ruthenium congener and only formed $Os_3(CO)_{12}$ at a significant rate at 80 °C or above (in solution under normal laboratory lighting). It may be stored indefinitely at −15 °C without any special precautions.

If the reactions were carried out in hexane, solutions of the pentacarbonyls were produced. However, the conditions used to prepare $Os(CO)_5$ were sufficiently extreme to cause the formation of some hexenes by dehydrogenation of the solvent. (Control experiments have shown that

(1) Manchot, W.; Manchot, W. J. *Z. Anorg. Allg. Chem.* **1936**, *226*, 385.
(2) Heiber, W.; Stallmann, H. *Z. Elektrochem.* **1943**, *49*, 288.
(3) Calderazzo, F.; L'Eplattenier, F. *Inorg. Chem.* **1967**, *6*, 1220; **1968**, *7*, 1290.
(4) The trimetal dodecacarbonyl, $M_3(CO)_{12}$ (1.0–2.0 g), was placed in a high-pressure autoclave (500 mL) and the vessel pressurized with CO (ca. 200 atm). It was sealed and heated (M = Ru, 160 °C; M = Os, 280 °C) for 48 h after which the autoclave was cooled to −78 °C and the gas vented. The autoclave was connected to a vacuum line, and, as the autoclave warmed to room temperature, the $M(CO)_5$ product was vacuum distilled (<5 × 10^{-3} mmHg) into a trap cooled to −196 °C (M = Ru, quantitative yield; M = Os, yield ca. 60%). The ruthenium compound was collected with the strict exclusion of light.
(5) This method of preparation is reminiscent of the original synthesis of $Os(CO)_5$[2]: treatment of OsO_4 with CO (200–300 atm) at 150–300 °C. Dodecacarbonyltriosmium is usually prepared from OsO_4 and CO under milder conditions (100 atm, 150 °C).[6]
(6) Johnson, B. F. G.; Lewis, J.; Kilty, P. A. *J. Chem. Soc. A* **1968**, 2859.
(7) Cotton, F. A.; Wilkinson, G. "Advanced Inorganic Chemistry"; 4th ed.; Wiley: New York, 1980; p 1082.

0276-7333/83/2302-0693$01.50/0

Table I. Physical and Spectroscopic Properties of the Pentacarbonyls

	mp, °C	ν(CO),[a] cm^{-1}	^{13}C NMR,[b] ppm
$Fe(CO)_5$	−20.5[c]	2022.5 2000.5	210.6
$Ru(CO)_5$	−17 to −16	2036.5 2001.5	200.4
$Os(CO)_5$[d]	2 to 2.5	2035.0 1993.0	182.6

[a] Hexane solution. [b] Recorded at 100.6 MHz, $CDCl_3$ solution at −40 °C. [c] Wender, I.; Pino, P., Eds. "Organic Syntheses via Metal Carbonyls"; Wiley: New York, 1968; p 39. [d] Calcd: C, 18.17, H, 0.0. Found: C, 18.37; H, 0.0.

this dehydrogenation was independent of the presence of osmium carbonyls.) A very minor byproduct using this method was $Os(CO)_4H_2$ presumably formed by the reaction of $Os(CO)_5$ with the hydrogen liberated from the solvent.[8] In most cases, the presence of the hexenes does not interfere with the chemistry of $Os(CO)_5$ although it was not possible to prepare $Os_2(CO)_9$[9] from such solutions since the low-temperature photolysis yielded the olefin complex $Os(CO)_4(\eta^2$-hexene).

The ^{13}C NMR spectrum of each pentacarbonyl recorded in $CDCl_3$ at −40 °C showed a singlet. For $Os(CO)_5$, the singlet remained sharp at −110 °C ($CFCl_2H$ solution), indicating, as expected,[10] rapid exchange between axial and equatorial ligands. The ^{13}C chemical shifts along with other physical data for the compounds are collected in Table I.

The mass spectrum showed a parent ion with the expected isotopic distribution for each case. Successive loss of five carbonyl groups from the parent ion, and the carbide-containing ions $[OsC(CO)]^+$ and $[MC]^+$ (M = Ru, Os), was also clearly observed. No higher molecular weight ions of significant abundance were detected.

The chemistry of $Os(CO)_5$ is currently under investigation.[11] As expected it undergoes the oxidative elimination reaction with a variety of substrates. In some cases ionic intermediates have been isolated. For example, from the reaction with Cl_2 in solution at −78 °C a white compound was isolated (in quantitative yield) that had properties[12] consistent with the formulation $[Os(CO)_5(Cl)][Cl]$.[13] The compound was stable at room temperature unlike similar iron derivatives;[14] when a suspension of it was refluxed in hexane, the known[15] dimer $[Os(CO)_3Cl_2]_2$ was produced.

The olefin complex $Os(CO)_4(\eta^2$-dimethyl fumarate) has also been synthesized, from the UV irradiation of a solution of $Os(CO)_5$ and dimethyl fumarate under a CO atmosphere.[16] The two signals observed in the ^{13}C NMR spectrum of the compound (in $CDCl_3$) that are assigned to the carbonyl ligands were sharp at room temperature. When the solution was warmed, the peaks broadened, but even at 105 °C (toluene-d_8 solution, 100.6 MHz operating frequency) they still had not quite collapsed. By assuming a collapse temperature of 115 °C, a barrier to rearrangement, $\Delta G^{\ddagger}_{388}$, of 18.8 kcal mol^{-1} may be estimated. This barrier is higher than that found for $Ru(CO)_4(\eta^2$-diethyl fumarate) ($\Delta G^{\ddagger}_{298}$ = 15.4 kcal mol^{-1}) which in turn is higher than that in $Fe(CO)_4(\eta^2$-diethyl fumarate) ($\Delta G^{\ddagger}_{298}$ = 12.8 kcal mol^{-1}).[17]

Acknowledgment. We are grateful to the Natural Sciences and Engineering Research Council of Canada for financial support.

Registry No. $[Os(CO)_5(Cl)][Cl]$, 85097-37-6; $Os(CO)_4B$ (B = η^2-dimethyl fumarate), 85097-38-7; $Ru(CO)_5$, 16406-48-7; $Os(CO)_5$, 16406-49-8; $Ru_3(CO)_{12}$, 15243-33-1; $Os_3(CO)_{12}$, 15696-40-9; CO, 630-08-0.

(8) L'Eplattenier, F.; Calderazzo, F. *Inorg. Chem.* **1967**, *6*, 2092.
(9) Moss, J. R.; Graham, W. A. G. *J. Chem. Soc., Dalton Trans.* **1977**, 95.
(10) Jesson, J. P.; Meakin, P. *J. Am. Chem. Soc.* **1973**, *95*, 1344.
(11) A crystal structure determination of $Os(CO)_5$ by X-ray diffraction techniques will be attempted in the near future.
(12) Calcd for $OsC_5O_5Cl_2$: C, 15.11, H, 0.0. Found: C, 14.96; H, 0.0 Insoluble in hexane, sparingly soluble in CH_2Cl_2. IR (CH_2Cl_2): ν(CO) 2175 (w), 2104 (vs), 2084 (m), 2075 (sh), 2055 (s) cm^{-1}.
(13) The compound is not the known[8] *cis*-$Os(CO)_4Cl_2$ that we have prepared from the reaction of $Os(CO)_5$ with CCl_4.
(14) Noack, K. *J. Organomet. Chem.* **1968**, *13*, 411.
(15) Bruce, M. I.; Cooke, M.; Green, M.; Westlake, D. J. *J. Chem. Soc. A* **1969**, 897.
(16) Calcd for $OsC_{10}H_8O_8$: C, 26.91; H, 1.81. Found: C, 27.01; H, 1.81. IR (hexane): ν(CO) 2136.5 (w), 2062.5 (s), 2045 (m), 2008.5 (s) cm^{-1}. ^{13}C NMR ($CDCl_3$): δ 25.3 (=C<), 51.9 (−CH_3), 172.2, 173.2 (−CO), 176.8 (−C(O)−). MS: m/e 446 w (P^+), 418 s [$(P - CO)^+$].
(17) Kruczynski, L.; Martin, J. L.; Takats, J. *J. Organomet. Chem.* **1974**, *80*, C9.